



Abstract Volume and Field Guide of the Fifth International Volcano Geology Workshop

Edited by
Károly Németh and Szabolcs Kósik



Palmerston North, New Zealand
25 February - 4 March 2019



1VGW - Madeira

2VGW - Prague

3VGW - Etna and Aeolian Islands

4VGW - Eastern Transylvania



International Association of Volcanology
and Chemistry of the Earth's Interior

Commission on
Volcano Geology





Fifth International Volcano Geology Workshop

Volcanism in a rapidly changing environment relating to an atypical plate margin

Palmerston North, New Zealand

25th February – 4th March 2019

Abstract Volume and Field Guide

Edited by

Károly Németh and Szabolcs Kósik

Geoscience Society of New Zealand Miscellaneous Publication 152

ISBN (print) 978-0-473-47041-8

ISBN (online) 978-0-473-47042-5

Previous VGWs

First International Volcano Geology Workshop
Madeira, Portugal, 2014

Second International Volcano Geology Workshop
Prague, Czech Republic, 2015

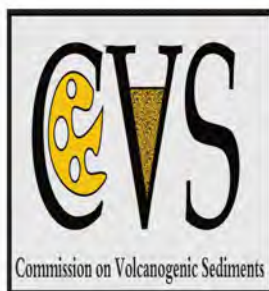
Third International Volcano Geology Workshop
Etna and Aeolian Islands, Italy, 2016

Fourth International Volcano Geology Workshop
Eastern Transylvania, Romania, 2017

Workshop Supporters



Commission on
Volcano Geology





Organizing Committee

Károly Németh (*Massey University, Palmerston North, New Zealand*)
Shane J. Cronin (*The University of Auckland, Auckland, New Zealand*)
Jonathan Procter (*Massey University, Palmerston North, New Zealand*)
Szabolcs Kósik (*Massey University, Palmerston North, New Zealand*)

Scientific Advisory Group

Nobuo Geshi (*AIST, Japan Geological Survey, Tsukuba, Japan*)
Gianluca Groppelli (*CNR, Milan, Italy*)
José Luis Macias (*Instituto de Geofísica, UNAM, Morelia, Mexico*)
Joan Marti (*Institute of Earth Science Jaume Almera, Barcelona, Spain*)
Natalia Pardo (*Universidad de Los Andes, Bogota, Colombia*)
Roberto Sulpizio (*University of Bari, Bari, Italy*)
Alexandru Szakács (*Sapientia University, Cluj, Romania*)

Preface

Dear Participants of the 5VGW,

We welcome you to the IAVCEI 5th Volcano Geology Workshop (5VGW) organised by the Massey University and The University of Auckland. The single day workshop is at the Massey University's Turitea Campus in Palmerston North. The field trip will take the participants to iconic volcanic sites of New Zealand, including the Ruapehu, Tongariro Volcanic Complex, Taupo and Taranaki volcano. The 5VGW is a special event of the IAVCEI Commission of Volcano Geology, with a focus on field-based workshops with a central theme in every 2nd or 3rd Years.

As Volcanology has made great advances in the last three decades and gradually become a modern interdisciplinary science that has learned how to quantify volcanic processes, their associated hazards and resources, there was a need to create a formal IAVCEI Commission. In addition, the scientific and technological revolution undertaken by modern volcanology created a remarkable explosion of physical and mathematical modelling as a necessary tool to undertake a comprehensive approach on volcanic processes. The IAVCEI Commission on Volcano Geology was established by the global need to coordinate scientific effort to understand volcano geology from ancient volcanic terrains to modern and active volcanoes. The Commission uses the workshops to provide a snapshot on the current state of art of volcano science that is field geology based and commonly function as a link between volcano researches to other geological subject areas.

The IAVCEI First International Workshop on Volcano Geology was held in Madeira [Portugal] between 7 and 11 July, 2014. A desire to strengthen the importance of geology in modern volcanology triggered the organisation of the 1st International Workshop on Volcano Geology in order to provide a forum for discussion among researchers on the state of the art of geological studies in volcanology as the basis for understanding the behaviour of volcanoes and their future activity, and to encourage multidisciplinary research in the geological fields involved in volcanological studies.

The IAVCEI Second International Volcano Geology Workshop was held as a scientific session and panel discussion during the IUGG General Assembly in Prague in 2015. The main aim of this workshop (after a scientific session) was to be a forum in which discussions on the current topics of volcano geology was facilitated. This workshop also represented a benchmarking event to see the global community reaction to formalize the action on volcano geology especially around volcano stratigraphy and geological mapping issues. The workshop was focused on discussing the state of the art of geological studies in volcanology, which are the baseline for the understanding of volcanic activity behaviour. The workshop operated as invited lectures on selected topics leading to guided discussions. Part of these discussions provided an interactive platform to discuss further those presentations presented during the same conference's volcano geology session. At the end of this workshop a preliminary draft of guidelines in Volcano Geology themes and techniques for geological mapping was provided that functioned as a foundation of scientific discussions for the next, IAVCEI Third International Volcano Geology Workshop.

The IAVCEI Third International Volcano Geology Workshop was held in southern Italy, at Mount Etna and in the Aeolian (Lipari) Islands (hosted in Vulcano) between 3 and 10 July 2016. The aim of this workshop was to present and discuss the current topics of the geological studies in modern Volcanology, and to examine the first achievements of the just established IAVCEI Commission on Volcano Geology. The workshop was particularly focused on discussing the state of the art of geological fieldwork and mapping in volcanic areas, which are the baseline for understanding the volcano behaviour and its associated hazards.

Some keynote lectures followed by a poster session was arranged with an aim to promote a wide discussion on main topics of Volcano Geology. This workshop day was followed by a combined fieldtrip on iconic outcrops of Mt Etna (including Valle del Bove depression and NE Rift) and Vulcano, Lipari and Stromboli volcanoes (Aeolian Islands) comprising the ascent to the Stromboli active craters. This workshop was particularly focused on volcano stratigraphy and geological mapping techniques in

a volcanic region still active. The workshop provided a good working draft of a guideline that was further developed during the next workshop

The IAVCEI Fourth International Volcano Geology Workshop was hosted by the Romanian Academy of Sciences', Institute of Geology and the workshop took the participants across Transylvania's iconic volcanic landforms such as the Ciomadul (Csomad) volcano with Lake St Anna (Lake Sfânta Ana) Crater lake in Romania between 8 and 14 October 2017. The concept of this workshop was very different from the previous workshops' concepts as it was planned on a region that is old (Miocene to Pleistocene) and hence it was to provide an ideal place where participants can see and discuss geological mapping problems commonly occur in older volcanic terrains. This workshop therefore acted as a venue where ideas derived from active volcanic terrains can be tested and developed further for geological mapping context. This concept worked well, and also triggered to take the Fifth International Volcano Geology Workshop to New Zealand.

While previous VGWs in Madeira and Italy took the participants to active or at least young volcanic terrains where exposures were abundant and young volcanic products were preserved well, both locations represent a rather unique scenario either by having lava flow dominated terrains or provide sites that expose only proximal volcanic edifice-building successions. In this perspective, the Fifth Workshop in New Zealand offer a new vantage point for the participants by visiting compound and complex stratovolcanic sequences where volcanic successions can be traced from the proximal edifice-building zones to the distal ring plain-forming volcanoclastic sedimentary units. The Fifth Workshop also intends to provide an insight to see together composite, landscape forming stratovolcanic systems hand in hand with small-volume monogenetic volcanic systems as well as landscape-forming silicic caldera-dominated volcanoclastic sedimentary assemblages. This unique experience may help the participants to better understand volcanic processes, understand them from special references and be able to link modern processes and their sedimentary records to ancient sites.

The Fifth Workshop also plans to show clear evidence that utilizes the results of tephrostratigraphy with traditional geological mapping in volcanic terrains and highlights the role of understanding the ring plain versus edifice building effusive and explosive eruptive products. This workshop will also take the participants to iconic sites in an atypical arc settings, where hyperactive silicic systems interlinked with compound stratovolcanoes that suffered numerous collapse events and regrowth. The workshop will provide practical experiences to see volcanology in action and to demonstrate the importance to have volcanic edifices, their proximal to distal facies of their eruptive products and the "host" sedimentary environment linked together to see the co-evolution of volcanism and landscape or the role of landscape forming elements of large scale eruptions.

We hope that this workshop also help to move the draft guideline on volcano stratigraphy principals to be presentable for the International Stratigraphy Union.

Kia ora, Welcome to New Zealand,

Prof Karoly Nemeth (Massey University)

A/Prof Jon Procter (Massey University)

Prof Shane J Cronin (The University of Auckland)

List of Participants

(in alphabetical order)

Mark Bebbington

Massey University, New Zealand
(*m.bebbington@massey.ac.nz*)

Shane J. Cronin

The University of Auckland, New Zealand
(*s.cronin@auckland.ac.nz*)

Nessa D'Mello

Massey University, New Zealand
(*n.d'mello@massey.ac.nz*)

Elicier Duarte

Observatorio Vulcanológico y Sismológico
de Costa Rica (OVSICORI), Costa Rica
(*e.duarte@una.ac.cr*)

Michael Garcia

University of Hawaii, United States
(*garcia@soest.hawaii.edu*)

Nobuo Geshi

Geological Survey of Japan, AIST, Japan
(*geshi-nob@aist.go.jp*)

Amy Gilmer

U.S. Geological Survey (USGS), United States
(*agilmer@usgs.gov*)

Satoshi Goto

University of Yamanashi, Japan
(*goto@yamanashi.ac.jp*)

Gianluca Groppelli

Consiglio Nazionale delle Ricerche (CNR), Italy
(*gianluca.groppelli@unimi.it*)

Roberto Isaia

Istituto Nazionale di Geofisica e
Vulcanologia (INGV), Italy
(*roberto.isaia@ingv.it*)

Gábor Kereszturi

Massey University, New Zealand
(*g.kereszturi@massey.ac.nz*)

Szabolcs Kósik

Massey University, New Zealand
(*s.kosik@massey.ac.nz*)

Marinel Kovacs

Technical University of Cluj-Napoca, Romania
(*marinel.kovacs@cunbm.utcluj.ro*)

David Kuentz

Miami University, United States
(*kuentzdc@miamioh.edu*)

Brandi Lawler

University of Wyoming, United States
(*blawler@uwyo.edu*)

Graham S. Leonard

GNS Science, New Zealand
(*g.leonard@gns.cri.nz*)

Geoffrey A. Lerner

The University of Auckland, New Zealand
(*g.lerner@auckland.ac.nz*)

Boxin Li

Massey University, New Zealand
(*doomlee1216@hotmail.com*)

Charline Lormand

Massey University, New Zealand
(*c.lormand@massey.ac.nz*)

Gert Lube

Massey University, New Zealand
(*g.lube@massey.ac.nz*)

Federico Lucchi

Università degli Studi di Bologna, Italy
(*federico.lucchi@unibo.it*)

Peter Luffi

Romanian Academy, Romania
(*peter.luffi@gmail.com*)

Justine Magson

University of the Free State,
Republic of South Africa
(*markramj1@ufs.ac.za*)

Kate Mauriohooho

Victoria University of Wellington
(*kate.mauriohooho@vuw.ac.nz*)

Oliver E. McLeod

The University of Waikato, New Zealand
(*oliveremcleod@gmail.com*)

Gerhard Meintjes

University of the Free State,
Republic of South Africa
(*pgm@pgmmanagement.co.za*)

Viorel Mirea

Romanian Academy, Romania
(*vmirea@geodin.ro*)

Yasuo Miyabuchi

Kumamoto University, Japan
(*miyabuchi@gmail.com*)

Sizah Nawzad

University of New South Wales, Australia
(*sizahnawzad@yahoo.com*)

Linus Nche

Ibaraki University, Japan
(*ncheanye2002@gmail.com*)

Károly Németh

Massey University, New Zealand
(k.nemeth@massey.ac.nz)

Alan S. Palmer

Massey University, New Zealand
(a.s.palmer@massey.ac.nz)

Julie Palmer

Massey University, New Zealand
(j.palmer@massey.ac.nz)

Zoltán Pécskay

Hungarian Academy of Sciences, Hungary
(zoltan.pecskay@gmail.com)

Estefanía Pedró

YPF Tecnología S.A, Argentina
(estefania.pedro@ypftecnologia.com)

Donna Pohlmann-Lawler

University of Wyoming, United States
(lawl0068@umn.edu)

Jonathan N. Procter

Massey University, New Zealand
(j.n.procter@massey.ac.nz)

Callum Rees

Massey University, New Zealand
(callumjrees@gmail.com)

Frederick Roelofse

University of the Free State,
Republic of South Africa
(roelofsef@ufs.ac.za)

Matteo Roverato

Yachay Tech University, Ecuador
(matteoroverato1809@gmail.com)

Ioan Seghedi

Romanian Academy, Romania
(seggedi@geodin.ro)

Alina Shevchenko

GFZ German Research Centre for
Geosciences, Germany
(alinash@gfz-potsdam.de)

Ian E.M. Smith

The University of Auckland, New Zealand
(ie.smith@auckland.ac.nz)

Ildikó Soós

Eötvös Loránd University, Hungary
(ildiko.soos14@gmail.com)

Grace Stanford

University of Wyoming, United States
(gstanford1999@gmail.com)

Roberto Sulpizio

Università degli Studi di Bari, Italy
(roberto.sulpizio@uniba.it)

Alexandru Szakács

Romanian Academy, Romania
(szakacs@sapientia.ro)

János Szepesi

Hungarian Academy of Sciences, Hungary
(szepeja@gmail.com)

Sarah Tapscott

Massey University, New Zealand
(sarahj.tapscott@gmail.com)

Ren Thompson

U.S. Geological Survey (USGS), United States
(rathomps@usgs.gov)

Olaf Tietz

Senckenberg Museum of Natural
History, Görlitz, Germany
(olaf.tietz@senckenberg.de)

Andrea Todde

Massey University, New Zealand
(a.todde@massey.ac.nz)

Ingrid Ukstins Peate

University of Iowa, United States
(ingrid-peate@uiowa.edu)

Gabriel Ureta

Universidad Católica del Norte, Chile
(gabriel.ureta@ucn.cl)

Marija Voloschina

Massey University, New Zealand
(m.voloschina@massey.ac.nz)

Willem van der Westhuizen

University of the Free State,
Republic of South Africa
(vdWestWA@ufs.ac.za)

Alan Whittington

University of Missouri, United States
(whittingtona@missouri.edu)

Elisabeth Widom

Miami University, United States
(widome@miamioh.edu)

Georg F. Zellmer

Massey University, New Zealand
(g.f.zellmer@massey.ac.nz)

Aliz Zemeny

Massey University, New Zealand
(a.zemeny@massey.ac.nz)

Anke V. Zernack

Massey University, New Zealand
(a.v.zernack@massey.ac.nz)

Lynn Zimek

University of Wyoming, United States
(lzimek@hotmail.com)

Detailed Program

Monday, February 25th – Participants Arrival and Ice Breaker

All day	Participants arrive to Palmerston North
16:30	Registration and Ice Breaker (Wharerata Function Centre)
17:30	DINNER with traditional Hāngī

Tuesday, February 26th – Campus Workshop hosted in the Massey University Sport and Rugby Institute

9:00	BREAKFAST
9:30	Introduction to Volcano Geology - Purpose of the Workshop. Károly Németh
9:45	Welcome by IAVCEI. Roberto Sulpizio
10:10	Commission on Volcano Geology - New Stratigraphy Framework Document (Keynote Lecture). Gianluca Groppelli
10:35	An integrated stratigraphic platform for volcanic fieldwork and mapping (Keynote Lecture). Frederico Lucchi
11:00	SHORT COFFEE BREAK
11:15	Mapping hydrothermal alteration on Mt Ruapehu (New Zealand) using field, laboratory, and hyperspectral imaging measurements. Gábor Kereszturi
11:20	Paleomagnetic insights into mapping deposits of eruptive periods. Geoffrey A. Lerner
11:25	Map representation of volcanic areas at regional scale in the Carpathian-Pannonian Region (Eastern Europe): Challenges and dilemmas. Alexandru Szakács
11:30	Geological mapping of monogenetic volcanic fields. Károly Németh
11:35	Volcano regrowth after sector collapse studied for Kamchatkan andesitic volcanoes. Alina Shevchenko
11:40	Flow mapping of Mt. Taranaki through aerial photography: constraining sampling sites for petrographic and geochemical work. Nessa G. D'Mello
11:45	Change of map representation of volcanic rocks of Balaton Highland (Hungary, Europe) from 19th century to nowadays. Csilla Galambos
11:50	POSTER/PC PRESENTATIONS AND LUNCH BREAK
13:20	New Zealand perspective in geological mapping in volcanic terrains (Keynote Lecture). Graham S. Leonard
13:45	The joy and sorrow of fieldwork in the 2.0-1.88 Ga Paleoproterozoic Amazonian Craton (Brazil). Matteo Roverato
13:50	Unraveling a Miocene rhyolite dome field stratigraphy using porosity and water content data, Tokaj Mts, Hungary. János Szepesi
13:55	Frequent cycles of growth and catastrophic collapse at Mt. Taranaki. Anke Zernack
14:00	Definition of internal horizons by litho-chemostratigraphic characterization for The Serie Tobífera, Austral Basin. Estefanía Pedró

- 14:05 Perspectives on the structure, vent distribution and composition of Pirongia, the North Island's largest basaltic volcano.
Oliver McLeod
- 14:10 Discoveries of pre-rift diatremes in the Lausitz Volcanic Field, Bohemian Massif – clues for landscape evolution and re-use of diatremes. **Olaf Tietz**
- 14:15 Physical volcanology studies in the Perşani Mountains monogenetic volcanic field (Southeastern Carpathians, Romania). **Ildikó Soós**
- 14:30 Quaternary Volcanism in the Itasy and Ankaratra Volcanic Fields, Madagascar: vent density, eruptive ages, and magmatic sources.
Elisabeth Widom
- 14:35 Particular features of the Oaş-Gutâi Volcanic Zone, Eastern Carpathians, Romania: Implications for understanding and reconstructing volcanic geology.
Marinel Kovacs
- 14:40 Newly identified debris avalanche deposits (DADs) in the North Harghita Mts. (Romania): emplacement history and tectonic significance. **Ioan Seghedi**
- 14:45 Structure and evolution of the most active sector of Campi Flegrei caldera (southern Italy). **Roberto Isaia**
- 14:50 A window into magmatic time (340 – 25 ka): How magma systems reorganised between supereruptions in the north Taupō area.
Kate Mauriohooho
- 15:00 **POSTER/PC PRESENTATIONS AND COFFEE BREAK**
(coffee and light snack will be served during this time)
- 16:00 Distal silicic tephra horizons provide chronostratigraphic control on the sedimentary record of an emergent Mid Quaternary coastline in SW North Island, New Zealand (Keynote Lecture). **Alan S. Palmer**
- 16:25 A rich archive of our volcanic past: Tephrostratigraphy in the Whanganui Basin, New Zealand. **Callum Rees**
- 16:30 Reconstruction of the eruption history of Miyakejima Volcano based on the detailed stratigraphic investigation and ¹⁴C dating. **Nobuo Geshi**
- 16:35 Explosive volcanism triggered by superslow ascent of hot andesites.
Charline Lormand
- 16:40 A violent phreatomagmatic volcano in Arxan-Chaihe Volcanic Field, NE China. **Boxin Li**
- 16:45 The September 14, 2015 explosive eruption at Nakadake first crater, Aso Volcano, SW Japan. **Yasuo Miyabuchi**
- 16:50 Mapping of dispersed small-volume volcanism of the silicic caldera system of the Taupo Volcanic Zone, New Zealand: results and limitations.
Szabolcs Kósik
- 16:55 From Pumiceous Obsidian to Lithoidal Rhyolite: Mapping textural variations in rhyolite lava flows and domes, and what we can learn about emplacement processes. **Alan Whittington**
- 17:00 Stratigraphy of pyroclastic deposits associated with multiple vent activity of rhyolite eruptions at Tarawera, New Zealand: the case of the ca. 1314 ± 12 AD Kaharoa eruption. **Andrea Todde**
- 17:05 Scoria cones of the Quaternary Ollagüe Volcanic Field, Central Andean Volcanic Zone, northern Chile. **Gabriel Ureta**
- 17:10 Petrographic and geochemical characteristics of the Kamo monogenetic volcanic field, Southern Kyushu, Japan.
Linus A. Nche

- 17:15 Detailed tephrostratigraphy as a tool to identify small-volume multi-stage eruptions: a field approach from the 1800 yrs eruptive record of Mt. Ruapehu, New Zealand. ***Marija Voloschina***
- 17:20 Medial volcanoclastic mass flow deposit apron of Mt. Taranaki (New Zealand); Recording stratovolcano construction and associated chemical changes of the magmatic system. ***Aliz Zemeny***
- 17:25 ***POSTER/PC PRESENTATIONS AND COFFEE BREAK***
(coffee and light snack will be served during this time)
- 18:25 Building integrated records of volcanic activity by combining on and off-volcano sequences, lessons from Mts. Ruapehu, Tongariro and Taranaki, New Zealand: An introduction to the field workshop. ***Shane J. Cronin***
- 19:25 ***PLENARY DISCUSSION: IAVCEI Commission on Volcano Geology, Location of 6th IAVCEI VGW***
- 20:00 ***DINNER (Wharerata Function Centre)***

Wednesday February 27th – Field Day 1 –Southern ring plain of Mt. Ruapehu

- 9:00 Departure from the Square, Palmerston North
- 11:00 ***Stop 1-1:*** Mataroa Formation overview
- 12:30 ***Stop 1-2:*** Introduction, Whagaehu Valley, Ruapehu Graben
- 14:00 ***Stop 1-3:*** Tangiwai Disaster Memorial
- 15:00 ***Stop 1-4:*** Ohakune Volcanic Complex
- 17:30 Arrival to accomodation (Hobbit Motorlodge, Ohakune)

Thursday February 28th – Field Day 2 –Eastern ring plain of Mt. Ruapehu

- 9:00 Departure from Hobbit Motorlodge
- 10:00 ***Stop 2-1:*** Tufa Trig Formation – Young tephra and landscape overview; inception of Crater Lake and movement of vents
- 12:30 ***Stop 2-2:*** 60 ky slice through the ring plain – sedimentation in relation to volcanic activity and the last glaciation, fluvio-glacial cycles
- 14:00 ***Stop 2-3:*** Bullot Formation type section – major explosive phase at Ruapehu before termination of this eruption style at 10 ka
- 15:30 ***Stop 2-4:*** Waihohonu – Tongariro tephra – sudden onset of Tongariro eruptions as Ruapehu changed eruption style – tectonic triggers
- 17:00 *Marae visit and DINNER at Tiorangi*
- 19:00 Return to accomodation

Friday March 1st – Field Day 3 –Western side of Mt. Ruapehu and Tongariro

9:00	Departure from Hobbit Motorlodge
10:00	Stop 3-1: Whakapapa Skifield – Scoria Flat; Pinnacle Ridge, collapse and debris avalanches, unconformity, Whakapapa Formation – new lava flows, change in eruptive and sedimentary regime
11:00	Stop 3-2: Murimotu debris avalanche – Mounds walk, off-volcano expression of the Pinnacle Ridge/Whakapapa Fm. unconformity
13:00	Stop 3-3: Mangetepopo Valley, growth of Ngauruhoe, Eruptive styles of Tongariro volcanism, tectonics, glacial history
17:00	Return to accommodation

Saturday March 2nd – Field Day 4 –Option A: Southern and Western ring plain of Mt. Ruapehu

9:00	Departure from Hobbit Motorlodge
10:00	Stop 4-1A: Onetapu lahars near Tiorangi Marae
11:00	Stop 4-2A: Whangaehu Valley Formation – older debris avalanche sequence
14:30	Stop 4-3A: Raurimu Spiral road section – Age sequence, depositional types, changes due to topography (pumice rich units, channel forms)
16:00	Stop 4-4A: Te Whaiarau debris avalanche, Taupo Pumice Formation
17:30	Stop 4-5A: Overview to the central TVZ on lookout above Tokaanu – Tongariro delta, Taupo Volcanic Centre and central TVZ volcanism
19:00	Stop 4-6: Sunset view from Turoa Skifield – recapping the Ruapehu experience
20:00	Return to accommodation

Saturday March 2nd – Field Day 4 –Option B: Central Taupo Volcanic Zone

8:50	Departure from Hobbit Motorlodge
10:00	Stop 4-1B: Oruanui Formation, accretional lapilli-bearing ignimbrite section
11:30	Stop 4-2B: Taupo Pumice Formation
12:30	Stop 4-3B: Five Mile Bay of Lake Taupo, Post-eruption lake sedimentation Horomatangi Reef, <i>LUNCH</i>
13:45	Stop 4-4B: Punatekahi Complex – small-volume mafic volcanism (scoria cones and tuff rings) of the Taupo Volcanic Centre
15:00	Stop 4-5B: Small-volume silicic volcanism in the central TVZ (tuff rings, maars and lava domes at Puketerata, Maroa Volcanic Centre)
16:00	Beach time at Whakaipo Bay of Lake Taupo with view to silicic domes
19:00	Stop 4-6: Sunset view from Turoa Skifield – recapping the Ruapehu experience
20:00	Return to accommodation

Sunday March 3rd – Field Day 5 –Travel to Taranaki Penisula, northern ring plain of Mt. Taranaki

8:30	Departure from Hobbit Motorlodge
10:00	Stop 5-1: Taupo ignimbrite valley ponded facies
12:00	<i>LUNCH at Whangamomena</i>
16:30	Stop 5-2: Maitahi debris avalanche at Oakura
18:00	Arrival to accomodation in New Plymouth
18:30	<i>DINNER and winery visit at Okurukuru</i>

Monday March 4th – Field Day 6 –Southwestern ring plain of Mt. Taranaki

8:30	Departure from Flamingo Hotel
9:00	Stop 6-1: Pungarehu debris avalanche and Warea lahar deposit
10:00	Stop 6-2: Drive up through Pungarehu mounds from Parihaka Road to Wiremu Road, western ring plain of Mt. Taranki
11:00	Stop 6-3: Mass flow facies associated to a growing ring plain – Middleton Bay, Opunake paleoriver system
12:00	Stop 6-4: Lizzie Bell paleochannel system – distal sedimentation during volcanic destruction and regrowth cycle
17:30	Arrival to Palmerston North Airport
18:00	Arrival to Palmerston North CBD (The Square)

PART A



Charles Blomfield 1886

Abstract Volume

Contents

(Abstracts are listed in alphabetical order of first author. The presenting author bolded)

- Page 17 – **Shane J. Cronin**, Jonathan N. Procter and Károly Németh: Building integrated records of volcanic activity by combining on and off-volcano sequences, lessons from Mts. Ruapehu, Tongariro and Taranaki, New Zealand: An introduction to the field workshop (**KEYNOTE**)
- Page 19 – **Nessa G. D’Mello**, Gabor Kereszturi, Georg F. Zellmer, Jonathan Procter and Robert B. Stewart: Flow mapping of Mt. Taranaki through aerial photography: constraining sampling sites for petrographic and geochemical work
- Page 21 – **Elicier Duarte**: Eight Years of Summit Transformations at Turrialba Volcano: Costa Rica
- Page 23 – Csilla Galambos, **Károly Németh**, Gábor Timár and László Bereczki: Change of map representation of volcanic rocks of Balaton Highland (Hungary, Europe) from 19th century to nowadays
- Page 25 – **Nobuo Geshi** and Teruki Oikawa: Reconstruction of the eruption history of Miyakejima Volcano based on the detailed stratigraphic investigation and 14C dating
- Page 27 – **Amy K. Gilmer** and Ren A. Thompson: The volcanic-plutonic connection at the Platoro caldera complex, Southern Rocky Mountains Volcanic Field, Colorado
- Page 29 – **Gianluca Groppelli**: Guidelines for mapping volcanic areas. State of art and perspectives (**KEYNOTE**)
- Page 33 – **Roberto Isaia**, Maria G. Di Giuseppe, Francesco D’Assisi Tramparulo, Antonio Troiano, and Stefano Vitale: Structure and evolution of the most active sector of Campi Flegrei caldera (southern Italy)
- Page 35 – **Gabor Kereszturi**, Lauren Schaefer, Reddy Pullanagari, Craig Miller, Stuart Mead, Ben Kennedy and Jonathan Procter: Mapping hydrothermal alteration on Mt Ruapehu (New Zealand) using field, laboratory, and hyperspectral imaging measurements
- Page 37 – **Szabolcs Kósik**, Károly Németh, and Mark Bebbington: Mapping of dispersed small-volume volcanism of the silicic caldera system of the Taupo Volcanic Zone, New Zealand: results and limitations
- Page 39 – **Marinel Kovacs**, Alexandrina Fulop, Zoltán Pécskay: Particular features of the Oaş-Gutâi Volcanic Zone, Eastern Carpathians, Romania: Implications for understanding and reconstructing volcanic geology
- Page 41 – **Graham S. Leonard**, Dougal B. Townsend and Colin J.N. Wilson: New Zealand perspectives in geological mapping of volcanic terrains (**KEYNOTE**)
- Page 47 – **Geoffrey A. Lerner**, Shane J. Cronin and Gillian M. Turner: Paleomagnetic insights into mapping deposits of eruptive periods
- Page 49 – **Boxin Li**, Károly Németh, Julie Palmer, Alan S. Palmer, Jonathan N. Procter: A violent phreatomagmatic volcano in Arxan-Chaihe Volcanic Field, NE China
- Page 51 – **Charline Lormand**, Georg F. Zellmer, Geoff Kilgour, Károly Németh, Alan S. Palmer, Naoya Sakamoto, Hisayoshi Yurimoto, Takeshi Kuritani, Yoshi Iizuka, Anja Moebis: Explosive volcanism triggered by superslow ascent of hot andesites
- Page 53 – **Federico Lucchi**: An integrated stratigraphic platform for volcanic fieldwork and mapping (**KEYNOTE**)
- Page 59 – **Kate Mauriohoho**, Colin J.N. Wilson, Graham S. Leonard and Isabelle Chambefort: A window into magmatic time (340 – 25 ka): How magma systems reorganised between supereruptions in the north Taupō area

- Page 61 – **Oliver McLeod**, *Adrian Pittari, Marco Brenna and Roger Briggs*: Perspectives on the structure, vent distribution and composition of Pirongia, the North Island's largest basaltic volcano
- Page 63 – **Gerhard Meintjes** and *Willem van der Westhuizen*: Late-Archaean felsic LIPs of the Ventersdorp Supergroup, South Africa
- Page 65 – **Yasuo Miyabuchi**, *Yoshiyuki Iizuka, Chihoko Hara, Akihiko Yokoo and Takahiro Ohkura*: The September 14, 2015 explosive eruption at Nakadake first crater, Aso Volcano, SW Japan
- Page 67 – **Linus A. Nche**, *Takeshi Hasegawa, Károly Németh, Tetsuo Kobayashi³ and Festus T. Aka*: Petrographic and geochemical characteristics of the Kamo monogenetic volcanic field, Southern Kyushu, Japan
- Page 69 – **Károly Németh**, *Gábor Csillag*: *Geological mapping of monogenetic volcanic fields*
- Page 71 – **Alan S. Palmer**, *Julie Palmer, Callum Rees and Károly Németh*: Distal silicic tephra horizons provide chronostratigraphic control on the sedimentary record of an emergent Mid Quaternary coastline in SW North Island, New Zealand (**KEYNOTE**)
- Page 73 – **Estefanía Pedró**, *Leonardo Tórtora, Guillermo Azpiroz and Graciela Covellone*: Definition of internal horizons by litho-chemostratigraphic characterization for The Serie Tobífera, Austral Basin
- Page 75 – **Callum Rees**, *Alan S. Palmer and Julie Palmer*: *A rich archive of our volcanic past: Tephrostratigraphy in the Whanganui Basin, New Zealand*
- Page 77 – **Matteo Roverato**, *Caetano Juliani, Carlos M. Dias Fernandes, Daniele Giordano, Tommaso Giovanardi*: The joy and sorrow of fieldwork in the 2.0-1.88 Ga Paleoproterozoic Amazonian Craton (Brazil)
- Page 79 – **Ioan Seghedi**, *Viorel Mirea and Péter Luffi*: Newly identified debris avalanche deposits (DADs) in the North Harghita Mts. (Romania): emplacement history and tectonic significance
- Page 81 – **Alina Shevchenko**, *Viktor Dvigalo, Thomas R. Walter, René Mania and Ilya Svirid*: Volcano regrowth after sector collapse studied for Kamchatkan andesitic volcanoes
- Page 83 – **Ildikó Soós**, *Szabolcs Harangi, Károly Németh and Alexandru Szakács*: Physical volcanology studies in the Perşani Mountains monogenetic volcanic field (Southeastern Carpathians, Romania)
- Page 85 – **Alexandru Szakács**, *Jaroslav Lexa, Károly Németh, Ioan Seghedi, Marinel Kovacs, Vlastimil Konecny, Zoltán Pécskay and Alexandrina Fülöp*: Map representation of volcanic areas at regional scale in the Carpathian-Pannonian Region (Eastern Europe): Challenges and dilemmas
- Page 87 – **János Szepesi**, *Réka Lukács, Tamás Buday, Zoltán Pécskay, Andrea Di Capua, Gianluca Gropelli, Gianluca Norini, Roberto Sulpizio and Szabolcs Harangi*: Unraveling a Miocene rhyolite dome field stratigraphy using porosity and water content data, Tokaj Mts, Hungary
- Page 89 – **Ren A. Thompson** and *Amy K. Gilmer*: Reconstructing the Pliocene magmatic and tectonic history of the Taos Plateau volcanic field region, northern Rio Grande rift, USA
- Page 91 – **Olaf Tietz**, *Jörg Büchner and Erik Wenger*: Discoveries of pre-rift diatremes in the Lausitz Volcanic Field, Bohemian Massif – clues for landscape evolution and re-use of diatremes
- Page 93 – **Andrea Todde**, *Károly Németh and Jonathan N. Procter*: Stratigraphy of pyroclastic deposits associated with multiple vent activity of rhyolite eruptions at Tarawera, New Zealand: the case of the ca. 1314 ± 12 AD Kaharoa eruption
- Page 95 – **Gabriel Ureta**, *Károly Németh, Felipe Aguilera and Szabolcs Kósik*: Scoria cones of the Quaternary Ollagüe Volcanic Field, Central Andean Volcanic Zone, northern Chile

- Page 97 – **Marija Voloschina**, Gert Lube, Jonathan N. Procter, Anja Moebis: Detailed tephrostratigraphy as a tool to identify small-volume multi-stage eruptions: a field approach from the 1800 yrs eruptive record of Mt. Ruapehu, New Zealand
- Page 99 – **Alan Whittington**, Stuart Kenderes, Graham Andrews, Shelby Isom, Kenny Befus, and Tyler Leggett: From Pumiceous Obsidian to Lithoidal Rhyolite: Mapping textural variations in rhyolite lava flows and domes, and what we can learn about emplacement processes
- Page 101 – **Elisabeth Widom**, C. Rasoazanamparany, A. Rakotondrazafy, T. Raharimahefa, K. Rakotondravelo and Dave Kuentz: Quaternary Volcanism in the Itasy and Ankaratra Volcanic Fields, Madagascar: vent density, eruptive ages, and magmatic sources
- Page 103 – **Aliz Zemeny**, Jonathan N. Procter, Károly Németh, Georg Zellmer and Shane J. Cronin: Medial volcanoclastic mass flow deposit apron of Mt. Taranaki (New Zealand); Recording stratovolcano construction and associated chemical changes of the magmatic system
- Page 105 – **Anke Zernack**, Shane J. Cronin, Mark Bebbington, Richard Price, Ian Smith, Bob Stewart and Jonathan N. Procter: Frequent cycles of growth and catastrophic collapse at Mt. Taranaki

The bibliographic reference for the abstracts is:

Author, A., Author, B., 2019. Title of abstract. In: Németh, K., and Kósik, S. (Eds): *Abstract Volume and Field Guide of the IAVCEI Fifth International Volcano Geology Workshop. Palmerston North, New Zealand, 25 February to 4 March 2019. Geoscience Society of New Zealand Miscellaneous Publication 152: p. x.* [ISBN (print): 978-0-473-47041-8; ISBN (online): 978-0-473-47042-5]

Building integrated records of volcanic activity by combining on and off-volcano sequences, lessons from Mts. Ruapehu, Tongariro and Taranaki, New Zealand: An introduction to the field workshop

Shane J. Cronin¹, Jonathan Procter² and Károly Németh²

¹ School of Environment, The University of Auckland, Auckland, New Zealand; s.cronin@auckland.ac.nz

² School of Agriculture and Environment, Massey University, Palmerston North, New Zealand

Keywords: ring plain, cone growth and collapse, sedimentary record

One of the greatest challenges facing the development of an integrated volcanic geological history of a volcano is combining records of dominantly effusive growth and collapse/unconformities on volcano flanks, with the sedimentary record of the ringplain. During this field trip we will examine the challenges and advantages of integrating on and off-cone records. In three contrasting stratovolcano cases, it is clear that while general stratigraphic and sedimentology approaches apply, different tools and techniques are needed.

At Mt. Ruapehu (2797 m), generally erupting a two-pyroxene andesite magma, large lava flows are produced during effusive phases, building a long-lived and relatively stable edifice over the last ~320 ka. Major debris avalanches are generated by hydrothermal weakening of parts of the edifice, but each collapse removes only a sector, leaving records of many of the earliest periods of growth on parts of the edifice, unconformably underlying more recent growth periods. Not all periods of volcanism are represented on the current edifice, with some seen only in the ring plain records of debris avalanche deposits, or long run-out mass flow sequences. Tracking the distal Ruapehu record requires interpreting the deposition of volcanic mass flows through a complex deeply eroded Tertiary mudstone terrain. The volcanic units are resistant to erosion and thus armor many of the oldest surfaces in these river valley systems. The ring plain surrounding Ruapehu also records some periods of growth and explosive volcanic activity at very high resolution, with sedimentation strongly influenced by periods of explosive volcanism (pyroclastic deposits and pumice-rich lahar deposits), as well as volcanic-glacier interactions. The latest phases of Ruapehu volcanism record an interplay between changing styles and locations of eruption, brought about by two major collapses: at ~10 ka a flank collapse and debris avalanche to the north-west terminated a 25 kyr-long period of highly explosive volcanism, and at ~4.5 ka a debris avalanche to the east resulted in shifting of the vent area to its present location and the subsequent dominance of Crater Lake on small-explosive eruptions.

At Tongariro volcano (~1900 m), a central stratovolcano edifice never developed because the volcano has grown within a rapidly spreading active graben system and is cut by numerous normal faults. This created conditions for formation of at least 14 major vent areas, with effusive and explosive volcanism shifting from site to site. Magmas erupted in these phases may reflect the rapid supply of magma from mantle depths with less storage and recharge than the Ruapehu system. The eruptive history of Tongariro appears also to be largely episodic, in contrast to the more regular eruptions of Ruapehu. This has led to the volcano forming a series of partially overlapping, separate edifices. The last highly explosive phase at this volcano at ~10 ka produced six plinian eruptions within a 200 year period from a dispersed chain of at least 6 vents. At least two major debris avalanches punctuated Tongariro's growth, but because it was not creating as large a central edifice as Ruapehu, the collapses were fewer and more isolated. Ngauruhoe (~2200 m) is the youngest and best described of these, having formed by a sustained period of mainly effusive and mildly explosive growth since ~7 ka. The last Glaciation strongly influenced volcanic sedimentation around Ruapehu and Tongariro, and erased many of the pre-15 ka sequences on the volcano. Due to the complex range of processes influencing sedimentation of this region, the chronostratigraphic markers that are very useful for integrating the volcanic sequences in this area include andesitic tephra, paleosols, last-glacial-maximum fluvial/aeolian reworked deposits along with ignimbrites and rhyolitic tephra from the Taupo and Okataina Calderas to the north.

Mt. Taranaki (2518 m) in the Western North Island erupts a more hydrous basaltic andesite to trachyandesite magma (hornblende rich) that produces dominantly domes and a very unstable edifice constructed of block-and-ash flow deposits intercalated with thin flows. Thus the current edifice above ~1200 m is entirely <14 ka in age. By contrast, the ring-plain constructed around the edifice contains a record of 170 ka of volcanism from Taranaki, with debris avalanches recording

TIME (ka)	LAHARIC, RIVER AND LAVA FORMATIONS	ANDESITIC TEPHRA	RHYOLITIC TEPHRA	
HOLOCENE	Onetapu 2 cal ka BP-present (Hodgson et al. 2007)	Tufa Trig Formation 1.72 ± 0.03 cal ka BP-present (Donoghue et al. 1997)	Kaharoa tephra (Ok) 1.314 ± 0.012 ka AD (Hogg et al. 2003)	WAHIAHOA FAULT AREA UPPER WAIKATO STREAM
	Mangalo 4.6 cal ka BP (Donoghue & Neall 2001)	Mangatawai Tephra (Ng) 3.52 cal ka BP (Moebis et al. 2011)	Taupo pumice 1.718 ± 0.005 cal ka BP (232 AD) (Hogg et al. 2012)	
	Manutahi 5.37-3.2 cal ka BP (Lecointre et al. 2004)	Ngauruhoe Formation 7 cal ka BP (Moebis et al. 2011)	Mapara tephra (Tp) 2.059 ± 0.12 cal ka BP (Wilson 1995)	
Murimotu 10.5 cal ka BP (Eaves et al. 2015)	Upper Papakai Formation (Tg) 3.7 cal ka BP (Donoghue et al. 1995)	Stent tephra (Tp) 4.322 cal ka BP (Alloway et al. 1994)		
10	Tangatu 17.7-5.37 cal ka BP (Hodgson 1993)	Lower Papakai Formation (Ru) 11.1 cal ka BP (Donoghue et al. 1995)	Hinemaia tephra (Tp) 5.225 ± 0.05 ka (Wilson 1993)	
			Whakatane tephra (Ok) 5.53 ± 0.02 cal ka BP (Hajdas et al. 2006)	
			Motutere tephra (Tp) 6.9 ± 0.25 cal ka BP (Moebis et al. 2011)	
PLEISTOCENE	Whakapapa 10.6 ka (Eaves 2015) (lava)	Mangamate Formation (Tg) 11-12 cal ka BP (Hitchcock & Cole 2007)	Poronui tephra (Tp) 11.2 ± 0.08 cal ka BP (Hajdas et al. 2006)	
	Ohakean Terrace Last glacial maximum period 13-14 ka (Hajdas et al. 2015)	Poutu lapilli 11 cal ka BP (Hitchcock & Cole 2007)		
		Fahoka Tephra 11 cal ka BP (Nairn et al. 1998)		
		Bullit Formation (Ru) 25-11 ka (Pardo et al. 2012)	Karapiti tephra (Tp) 11.4 ± 0.2 cal ka BP (Hajdas et al. 2006)	
		Okupata-Pourahu 11.77 ± 0.19 cal ka BP (Hajdas et al. 2006)		
		Ohinewairua eruptive period (Akurangi, Oruanui, Shawcross)	Waiohau tephra (Ok) 13.64 ± 0.17 cal ka BP (Lowe et al. 2008)	
	Te Heuheu >25.4-17.7 ka BP (Hodgson 1993) (R8)	Kariol eruptive period 15 ka	Rotorua tephra (Ok) 15.6 cal ka BP (Hajdas et al. 2006)	
	Last glacial maximum period 13-14 ka (Hajdas et al. 2015)	Tukino eruptive period 17-13.63 ± 0.17 cal ka BP (Topping 1973)		
		Rotoaira lapilli 17 cal ka BP (Shane et al. 2008)		
		Rangipo eruptive period 17-21.8 ± 0.5 cal ka BP	Rerewhakaaitu tephra (Ok) 17.7 ± 0.56 cal ka BP (Martin 2005)	
20	Mangawhero 50-20 ka (Gamble et al. 2003) (lava)	Hokey Pokey eruptive period 25.4-21.8 ± 0.5 cal ka BP	Okareka tephra (Ok) 21.8 ± 0.5 cal ka BP (Shane et al. 2008)	
25	(R9)		Oruanui tephra (Tp) 25.36 ± 0.16 cal ka BP (Vandergoes et al. 2013)	
30	Ratan Terrace 32 ka (R11)	Marker unit 1 (olive tephra) (Cronin 1996)	Okiaia tephra 28.6 cal ka BP (Molloy et al. 2009)	
35	(R12)		Omataroa tephra (Ok) 28.2 cal ka BP (Froggatt & Lowe 1990)	
45	Horopito 45-25.4 ka (R13)*	Orange lapilli	Hauaparua tephra (Ok) 36.1 cal ka BP (Shane et al. 2005)	
55	Te Whalau 45-36.1 ka (Lecointre et al. 2002)*	Elephant surge (marker unit 2) (Cronin 1996)		
	Waimarino 80-45 ka (R14)*	Orange lapilli (marker unit 3) (Cronin 1996)	Rotoehu ash (Ok) 45.16 ± 3 ka (Danisik et al. 2012)	
65	Whangapehu 180-45 ka (Keigler et al. 2011) (R15)*			
	Wahianoa 134-45 ka (Gamble et al. 2003) (lava)*			
	Porewan Terrace >45 ka*			
	Te Herenga >200 ka (Hodgson et al. 2007) (lava)			

Fig. 1. Chronological stratigraphic summary of the laharic and lava formations and andesitic tephtras from the Tongariro Volcanic Centre interbedded with distal rhyolitic tephtras from the Taupo Volcanic Zone calderas from Gómez-Vasconcelos et al. (2016).

episodes of cone growth and collapse on 14 occasions. Petrological studies show that each collapse removed at least half the paleo edifice, with collapses heralding growth a new edifice with a distinct composition. Off volcanic records of tephtras within swamp and lake records show evidence of >220 eruptions over the last 30 ka, with the largest being plinian in size and involving long-runnout pyroclastic flows and the smallest (<0.01 km³) alternating between explosive and effusive styles. Combining on-cone records of lava flows and Block-and-ash flow deposits and off-cone tephtra sequences is challenging and depends on collection of many radiocarbon dates and detailed chemistry. This is only possible so far for the last ~5 ka with high resolution.



Fig. 2. The glaciated summit of Mt. Ruapehu

In all three cases, a comparison of on and off cone records requires a long-term and multidiscip-

linary approach. A range of relative and absolute dating methods are required and the character of each volcano is important to factor in to the expected combination of deposit types. Regional influences, such as global glaciation cycles and the rhyolitic eruptions of the Central North Island help provide additional correlation potential, but in many cases, the correlation of off and on volcano records remains highly speculative.

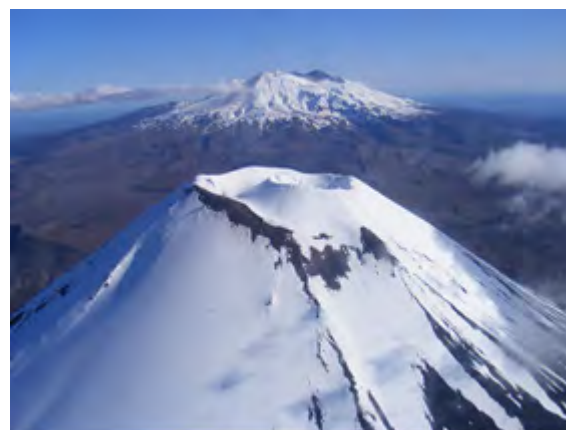


Fig. 3. Aerial image of the summit of Ngauruhoe volcano with Mt. Ruapehu in the background.

References

Gómez-Vasconcelos, M.G., Villamor, P., Cronin, S.J., Procter, J., Kereszturi, G., Palmer, A., Townsend, D., Leonard, G., Berryman, K., Ashraf, S. (2016). Earthquake history at the eastern boundary of the South Taupo Volcanic Zone, New Zealand. *New Zealand Journal of Geology and Geophysics*: 1-22.

Flow mapping of Mt. Taranaki through aerial photography: constraining sampling sites for petrographic and geochemical work

Nessa G. D'Mello¹, Gabor Kereszturi¹, Georg F. Zellmer¹, Jonathan N. Procter¹ and Robert B. Stewart¹

¹ School of Agriculture and Environment, Massey University, Palmerston North, New Zealand; n.d'mello@massey.ac.nz

Keywords: Taranaki, flow mapping, ascent rates.

Mt. Taranaki / Mt. Egmont is an active stratovolcano located in the west of the North Island, New Zealand (Stewart et al., 1996). Mt. Taranaki displays a range of eruption styles (from effusive to sub-Plinian) as well as eruptive products (basaltic to dacitic). Taranaki is one of the most economically productive regions of New Zealand and petrographical and geochemical studies of the volcano can provide important insight into the working of this volcano that would contribute to volcanic hazard mitigation of the region.

An approach using high resolution aerial photography was chosen to aid the petrographical and geochemical work of this study. The digitized map created distinguishes the products of different eruptive episodes over the last 10,000 years that form the current edifice. With the data obtained, the geological map of the region can be updated and volumes of the eruptions can be estimated- which is key to hazard mitigation. In addition, the map will also be used for sampling site selection. Intensive field mapping of the mountain can be quite tedious considering the mountains immense size, the 335km² region of dense rainforest and native bush of the Egmont National Park that covers the lower flanks of the volcano, the steep faces of the upper cone, and the constantly changing weather on the mountain.

Recently, we have completed a low-flying airborne hyperspectral and digital photography survey using a Cessna 185 aircraft. The airborne GPS-tagged photographs were used to construct a Digital Surface Model (DSM) using the structure-from-motion technique. This resulted in true-coloured mosaicked imagery and a DSM with a spatial resolution of 0.3 m. We used this DSM and photo mosaicked to trace the deposits of effusive activity of Mt. Taranaki. The high-resolution image data made it possible to identify individual lava flows and lobes from previous eruptions and to trace their extent, and morphology. The DSM will be used to calculate thicknesses and volumes of lava flows to gain insights into the magma extrusion rates during each effusive period, thereby constraining magma supply from the plumbing system beneath Mt. Taranaki.

Fig 1 is the map created from the DSM of Mt. Taranaki. The lava flows have been grouped into eruptive events that were determined previously (J. N. Procter, pers. comm.). Geochemical analysis and field correlation will be required to determine the stratigraphic succession of the flows and delineate the flows from phases of the same eruptive episode as well as deposits such as pyroclastic and alluvial deposits.

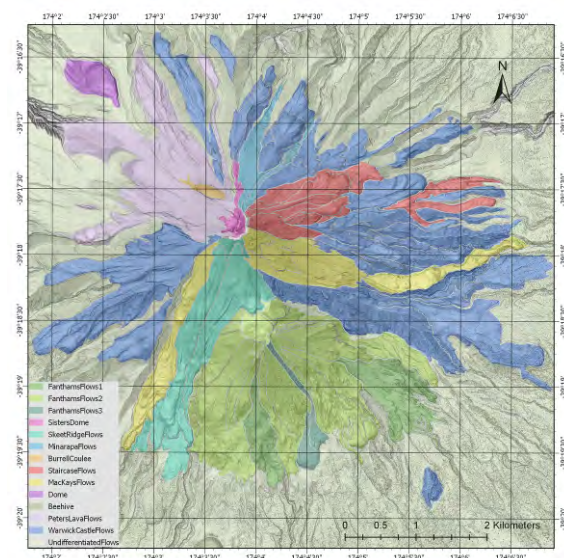


Fig. 1 – Preliminary map of the lava flows of Mt. Taranaki created from the DSM.

Magma Ascent Rates through Petrographic Observations:

Magma ascent rates can help determine whether magma has the potential to erupt explosively, and changes in ascent rates can be observed through petrological studies of hydrous minerals such as hornblende (Rutherford, 2008). During ascent, decompression induced exsolution of volatiles triggers breakdown of the hornblende crystals resulting in the formation of a reaction rim. The thickness of this rim is a function of the time the crystal has spent outside its stability field before eruption, and is indicative of magma ascent rates (Rutherford, 2008; Rutherford and Hill, 1993; Foden and Green, 1992).

Steady state ascent experiments of dacitic magmas from Mount St. Helens at 900°C (Rutherford and Hill, 1993) and andesitic magmas from the Soufrière Hills at 830°C, 845°C and 860°C (Rutherford and Devine, 2003) correlated rim thicknesses to ascent rates. However, factors such as temperature, composition, pressure, viscosity and water content, of melt and mineral affect the thicknesses of the rims and consequently the calculated ascent rate (Devine et al. 1998; Browne and Gardner 2006) that must be taken into consideration before calculating ascent rates for Taranaki lavas using these calibrations. Hornblendes from Taranaki's andesitic lavas show a great variation in the oxidized rim thicknesses from 0-80µm. Previous mineral chemistry work (Stewart et al. 1996) shows a temperature of 860-965°C for the groundmass, and Al concentrations of amphiboles indicate crystallization over a wide range of pressures. It is clear, that further work that will help constrain other variables is required to calculate the ascent rates of the effusive eruptions of Mt. Taranaki.

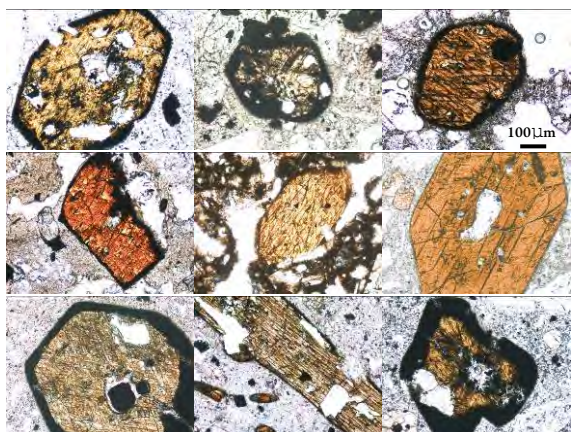


Fig. 2 Variations in the reaction rim thicknesses of the hornblende mineral grains sampled from Taranaki.

References

- Foden JD and Green DH (1992), Possible role of amphibole in the origin of andesite: some experimental and natural evidence. *Contrib. Mineral. Petrol*, 109, pp. 479-493
- Rutherford MJ and Hill PM (1993), Magma ascent rates from amphibole breakdown: An experimental study applied to the 1980–1986 Mt St. Helens eruptions, *J. Geophys. Res.*, 98(B11), 19667–19685
- Stewart RB, Price RC and Smith IEM (1996), Evolution of high- K arc magma, Egmont Volcano, Taranaki, New Zealand: evidence from mineral chemistry *J. Vol. and Geotherm Research* 74, pp. 275-295
- Devine JD, Rutherford MJ, Gardner JE (1998), Petrologic determination of ascent rates for the 1995-1997 Soufrière Hills Volcano andesite magma, *Geophys. Res.*, Vol 25 (19) pp. 3673-3676
- Rutherford MJ and Devine JD (2003), Magmatic conditions and magma ascent as indicated by hornblende phase equilibria and reactions in the 1995–2002 Soufrière Hills magma. *Journal of Petrology* Vol 44, pp. 1433-1454
- Browne BL and Gardner JE (2006), The influence of magma ascent path on the texture, mineralogy and formation of hornblende reaction rims, *Earth and Planetary Science* 246 pp. 161-176
- Rutherford MJ, (2008), Magma ascent rates *Reviews in Mineralogy and Geochemistry* VOL. 69, pp. 241-271
- Procter, J.N., Cronin, S.J. and Zernack, A.V., 2009. Landscape and sedimentary response to catastrophic debris avalanches, western Taranaki, New Zealand. *Sedimentary Geology*, 220(3-4): 271-287.
- Wilson, C.J.N., 2001. The 26.5 ka Oruanui eruption, New Zealand: an introduction and overview. *Journal of Volcanology and Geothermal Research*, 112(1-4): 133-174.
- Zernack, A.V., Procter, J.N. and Cronin, S.J., 2009. Sedimentary signatures of cyclic growth and destruction of stratovolcanoes: A case study from Mt. Taranaki, New Zealand. *Sedimentary Geology*, 220(3-4):288-305.

Eight Years of Summit Transformations at Turrialba Volcano: Costa Rica

Elicier Duarte¹

¹*Volcanological and Seismological Observatory of Costa Rica (OVSICORI), Universidad Nacional. P. O. Box. P.O.Box 2346-3000 Heredia-Costa Rica; eduarte@una.ac.cr*

Keywords: Turrialba volcano, Costa Rica, geomorphology, tephra, summit.

Turrialba volcano (10° 01' 03" N, 83° 45' 52" W) is located some 50 kms E of San Jose, Capital city of Costa Rica. Due to its steepness, altitude and location related to the most populated area in this country (the Central Valley) it poses a serious threat to its surroundings. This volcano has produced numerous eruptions historically and pre-historically and only within the recent 22 years its last eruptive period started. Reagan, M et al 2006. The current summit shows 3 main craters: West or active (1), Central (2) and east (3). (Fig. 1).

Ejection and deposition of air-borne fragmental volcanic material, from explosive and passive eruptions, constitute the thicker layers of deposits around the emitting point combining juvenile and accidental products. Erupted material has reached up to 3 kms (above the summit) and it has blanketed the slopes several square kms around the active crater.



Fig. 1 – Turrialba volcano viewed from east to west (aerial). Numbers depict craters. E. Duarte

Since 1996 Turrialba volcano showed its first seismic swarms escalating slowly to erratic

degassing on new areas at the summit; 9 years later. After this; effects on vegetation produced the first and most notorious changes.

Major geomorphological changes occurred after January 2010 when the first vent opened SW of the west crater (a), another smaller vent opened at the bottom of that active crater in the middle of 2011 (b) and finally the third vent formed in January 2012; SE (c) of that mentioned crater. (Fig. 2). Duarte, E. 2014.

Proximal zones (0-3 kms) of potential hazards have been affected by direct impact of bulky products. In the near future this same area can be impacted by backflood of numerous deep valleys, river bank collapse and inundation by lahar deposits in distal lowlands.

It is possible that newly deposited pyroclastic material, along with an important volume of mobilized old deposits (charged with recently accumulated organic material) will be eroded and rapidly transported down the slopes and abundant basins.

After the opening of vents the most dramatic change occurred at the end of October 2014 when destructive eruptions widened and deepened the west crater. Emplacement of mainly ash and larger pyroclasts has been documented 360° around the west crater showing: edges, inner structures, nearby hills and other features. Special emphasis is given to the east and west; where most of the deposition occurred. To the east because of the infilling of central crater and potential implications for the future activity of this feature. To the west due to the potential of the area to accumulate voluminous materials becoming ready to conform lahars down the northern distant plains.

Spatially, changes documented, will not exceed 500 horizontal meters from the active crater, in all directions. Ash and pre-existent sediments range from few micras to 2mm. Ballistics, scoria and blocks range from several cms. to several meters.

Sequential photos from several key points depict surface changes from the very beginning (vegetated surroundings) to actuality (total devastation). Despite rapid erosion (due to heavy rain) and gravity; thickness in most locations, remain above

several meters. Images show rapid topographical changes that in some cases occurred within weeks or even days.



Fig. 2 – West crater viewed from the northeast. Letters depict original site of opened vents. E. Duarte

Most of the thick deposition occurred from 2014 to January 2017 nonetheless nowadays small ash eruptions (low volume, fine grained) are produced intermittently.

Beyond the horizontal area, offered in this essay, lie up to 4 kms of total and partial devastation; mainly to the west and southwest. Diminishing layers of tephra cemented the once rich slopes of this green volcano to convert it in a desert like landscape.

Eight years of accumulative changes on the summit have changed more than half of the bigger summit caldera. Topographical and geomorphological transformations will be detailed in this work in order to understand those dramatic

changes documented during routine volcano monitoring duties. Duarte 2015.

So far only pyroclasts, ash, gases and vapor have impacted the area nonetheless other eruptive modalities may trigger (vg. Pyroclastic flows and lava tongues or domes) in the near future thus increase the impact already observed and documented; more importantly affecting nearby communities already broken.

Acknowledgements

To authorities of Universidad Nacional and to CONICIT-MICIT for moral and economical support. To OVSICORI co-workers that daily, in one way or another, push me at work.

To organizers for economical and logistic support.

References

- Reagan, M. Duarte, E. Soto, G. Fernández, E. 2006. The eruptive history of Turrialba volcano, Costa Rica and potential hazards from future eruptions. Geological Society of America. Special Paper 412.
- Duarte, E. Enero-Junio 2014. Las cuatro erupciones freáticas recientes del volcán Turrialba (2010-2013): Una por año. Revista Geográfica de América Central. No 52. ISSN 1011-48X. Pp 139-161.
- Duarte, E. June 2015. Impacto ambiental y socioeconómico del volcán Turrialba según monitoreo realizado entre 1980 2015. ISSS 1409-214X. Ambientico 254, Artículo 1. Pp 4-16.

Change of map representation of volcanic rocks of Balaton Highland (Hungary, Europe) from 19th century to nowadays

Csilla Galambos¹, Károly Németh², Gábor Timár³ and László Bereczki¹

¹ Mining and Geological Survey of Hungary

² School of Agriculture and Environment, Massey University, Palmerston North, New Zealand; k.nemeth@massey.ac.nz

³ Dept. of Geophysics and Space Science, Eötvös University, Hungary

Keywords: historical maps, geological maps, Balaton Highland

The Balaton Highland, an area of cca 1000 km² in the Pannonian Basin, Central Europe, is a nice example of the Neogene (Pliocene) intracontinental basaltic volcanism. Its geological character was identified quite early, in the early 19th century. Smaller and larger basalt plateaus, covering, thus protecting older, mostly siliciclastic sediments were mapped as early as 1818, by Beudant (1822). The very first systematic geological mapping was conducted in 1840s, and the results were hand-drawn on the 1:144,000 scale survey sheets of the Second Military Survey of the Habsburg Monarchy (cf. Timár, 2006). Present study is a comparison of the mapped outlines of the basaltic outcrop occurrences in the 1840s map and the present-day digital maps provided by the Hungarian Geological Survey, basically conducted in 1:100,000 scale (Gyalog, 2005). It is important to underline that the scale of the two survey maps are not differing significantly. The old map products cover significant (cca. one half) parts of the historical Hungary, which are now lay mostly in the territory of the present day Hungary, Slovakia and Austria. Our study area is only a small part of its full extents.

The working method consists of two steps. First, the historical maps were geo-referred and reprojected to the modern map grid system(s) – practically the WGS84 of *Google Earth* and *OpenStreetMaps*. Completing this task enables us to fit the two cartographic data sets into overlaying layers and describe the characteristic differences between the outline of the basaltic products on the two maps. The geo-reference is based on the exact knowledge of the map projection and geodetic datum of the historical maps. Reference ellipsoid was the hybrid ones of Oriani and Zách (semimajor axis=6,376,130 m; flattening=1/310). Its spatial displacement was controlled by the southern tower of the Vienna Cathedral (Stephansdom) in Austria. This point was also the center of the applied Cassini projection of the old map products. Knowing the terrain extents of the sheets enables us to define only the sheet corner points as GCPs (ground control points), without seeking identified terrain objects. Accuracy of this method is around 30-40 meters

(Timár et al., 2006), which is pretty acceptable for an 1:144,000 scale map. The modern geological database is originally geo-referred in the Hungarian National Grid System (EOV) and can be reprojected into e.g. WGS84 with sub-meter error.

Results of two typical parts of the Balaton Highland are shown in Figs 1 & 2. Fig. 1 shows the western cluster of the basaltic occurrences. In general, we detect that the outline of the basaltic area (including all the basaltic eruptive products of pyroclastic and effusive origin) is larger in the historic map with only one notable exception. The inner side of the westernmost patch (Mt. Tátika) is missing and indicated as alluvium. All of the other patches are larger in the old map. Explanation is quite obvious: while surveying the old map, the dense basaltic debris were mapped also as coherent, in situ basalt, while in the modern interpretation, only the basaltic base rocks are mapped. This explains the smaller extents of the basalt in the modern map, systematically surrounded by basaltic area in the old map but alluvium in the modern one. Some indications of the extent mining activity can also be found; where the solid, compact basalt plateaus were indeed there 160 years ago. Mining broke them to fragments; that is found of the modern map. Coupling of the old and new mapped extents leads to a more complex pattern in Fig. 2, showing the eastern patch group, the most elevated basaltic hills of the area. In the NE (Mt. Kab) zone, it was one of the densest forest in this part of the country in the 19th century. Less accurate field survey can be assumed in case of the old map, as the outline is more or less the envelope of the much more detailed modern result. We also find two ‘shifted’ patches. According to the topographic checking of old map fitting accuracy, we can exclude the geodetic/topographic error but assume some misplacement during the hand drawing. Other patches are more or less following the ‘rule’ detected in Fig. 1, as old patches are a bit more extended than modern ones, in most cases.

We can conclude that geo-reference is a powerful tool to place our old geological knowledge into the modern databases. This allows us to make

qualitative, territorial and even quantitative comparisons between the data from old and modern geological maps. In the specific case of the Balaton Highland, all volcanic patches are represented in both maps, however their extents are different. The old maps are shown larger basaltic areas supposedly because of the slope debris misinterpretation, and less basaltic area where mining activity obscured the volcanic bodies in the past century. In rough terrains, the old outlines of the mapped volcanic bodies are much less complex, following rather the envelopes, assumedly the less accurate field survey.

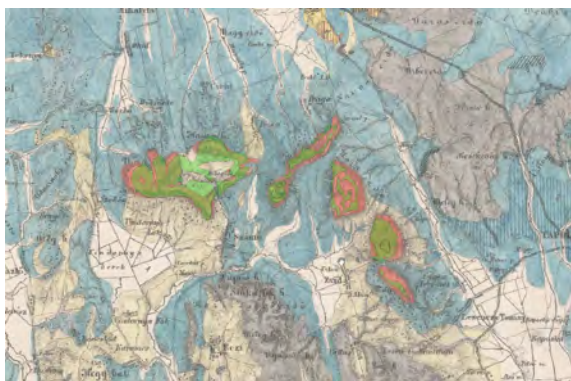


Fig. 1 – Western cluster of the Balaton Highland. Background image: the mid-1800s geological maps; basaltic area is shown by reddish hue. The outline of the volcanic bodies by the modern map database is shown by partially transparent greenish patches.

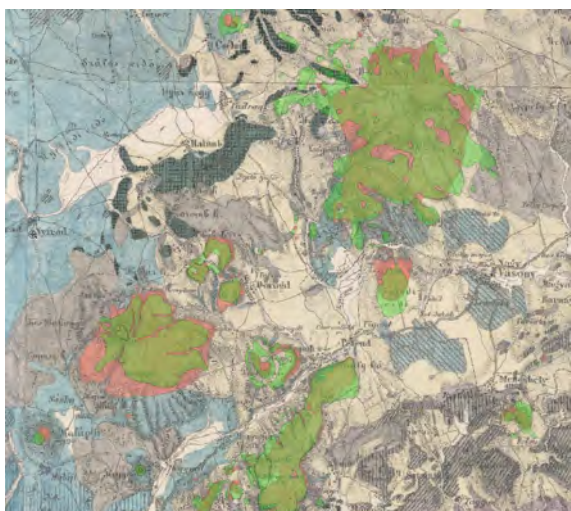


Fig. 2 – Eastern group of the volcanic plateaus of the Balaton Highland, color scheme is the same as in Fig. 1. Differences in the extents are because of the slope debris interpretation, the less accurate old survey and the mining activity between the two surveys.

References

- Beudant, F. S. (1822) Voyage minéralogique et géologique, en Hongrie: pendant l'année 1818. Verdière, Paris, 614 p.
- Gyalog, L. (2005): Explanation to the Geological Map of Hungary, with the short description of the units (in Hungarian). Magyar Állami Földtani Intézet, Budapest, 188 p.
- Timár, G., Molnár, G., Székely, B., Biszak, S. Varga, J., Jankó, A. (2006): Digitized maps of the Habsburg Empire - The map sheets of the second military survey and their georeferenced version. Arcanum, Budapest, 59 p.

Reconstruction of the eruption history of Miyakejima Volcano based on the detailed stratigraphic investigation and ¹⁴C dating

Nobuo Geshi¹ and Teruki Oikawa¹

¹ *Research Institute of Earthquake and Geology, Geological Surv. Japan, AIST, Japan; geshi-nob@aist.go.jp*

Keywords: ¹⁴C dating, flank fissure eruptions

Identification and mapping of the eruption vents and the products of recent eruptions are a fundamental approach to reconstruction of the eruption history of an active volcano. It will tell us the evolution of the volcanic system, the knowledges of the distributions of vents and the tendency of the styles of the past eruptions are also critical for the proper and efficient plan for hazard mitigation.

Our project in Miyakejima Volcano, Japan, aims to re-build the detailed history of the eruption activities of the volcano. Though some previous studies already presented the model of eruption history of this volcanoes (e.g., Tsukui and Suzuki, 1998), dramatical improvement of the exposure by the wiping out of the forest and creation of new outcrops by the 2000 AD eruption requires the revise of these previous results. The recent progress of the detailed digital elevation model of the islands also reveals the detailed distributions of the vents, cones and lava flows, some of which are unknown or hidden by the vegetation.

Miyakejima is a basaltic-andesitic volcano, sitting on the northernmost part of the Izu-Mariana volcanic arc. Miyakejima is one of the most active volcanoes in Japan, with four magmatic eruptions within the last 100 years. The edifice of Miyakejima shows a conical shape with ~12 km at its submarine base, and a height of ~1.2 km, including its submarine part. The subaerial part of the edifice forms a volcanic island, which has a semi-circular shape, ~8 km in diameter and ~750 m in height above sea level.

The subaerial part of the volcanic edifice of Miyakejima can be divided into three parts, bordered by two concentric caldera structures, the outer and older “Kuwanokidaira” caldera, and the inner and younger “Hatchodaira” caldera. The collapsed Hatchodaira caldera, approximately 2 km in diameter, formed at the top of the volcanic edifice, around 2.5 ka (Tsukui et al., 2005). Post-Hatchodaira volcanic activity from the inside of the caldera buried the caldera by ~1 ka. Many lateral fissure eruptions also occurred during the post-Hatchodaira period. Withdrawal of magma, by the lateral-intrusion during the 2000 AD eruption, again caused caldera collapse.

Our project particularly focuses on the period within the last 1,400 years, because of the ideal exposure of the structure and products of the eruptions of this period. The eruption history was reconstructed based on the stratigraphy of the erupted materials with the constraint with the ¹⁴C age, owing to the limitation of the reliable documental records of the eruptions except for the period after 19th century.

In our project, distribution of the vents and associated structures (cones, lava flows, and tephra aprons) are identified based on the relief maps which were created from the 1-meter-mesh digital elevation model. We confirm the distributions of the structures by detailed field surveys. Many new outcrops formed by the rapid gully erosion and the sabo-works after the 2000 eruption provide the stratigraphy of the erupted materials.

The tephra units were identified by the field occurrence, internal depositional sequence and structure, and the petrographical and petrochemical signatures. The identified tephra units were dated using the carbonized plant materials obtained from the base of the tephra. The fragments of fine branch and skins of tree were selected for dating to avoid the “old-tree effect” on the ¹⁴C age. We subsidiary use the radiocarbon ages of the paleosol beneath the tephra layer because the age of soil can be deviated from the real age of the tephra owing to the effect of the contamination of new and old organic materials.

Our result reconstructed the history of the eruptions within the last 1,400 years since the 7th century. Our study identified three unknown eruptions, revised the sequential position and eruption site of eight eruptions. We concluded at least 20 eruptions occurred from the 7th century to 1983 AD. The eruptions concentrated in the northeastern sector (5 eruptions) and the southwestern sector (9 eruptions) of the volcano (Fig. 1). No fissure eruption was recognized in the northwestern and southern sectors of the volcano during the last 1400 years. Two fissure eruptions occurred in the eastern flank in the 9th and 16th century. At least two eruptions were identified in the western upper slope of the volcano, possibly in the 19th century. Beside these flank fissure eruptions, two summit activities are recognized.

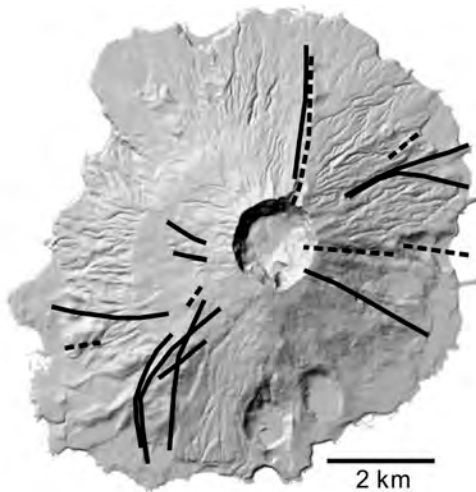


Fig. 1 – distribution of the eruption fissures of Miyakejima within the last 1400 years. Broken lines show the eruption fissures between the 7th and 15 th century. Solid lines show the eruption fissures since the 16th century.

We identified two major eruptions in the 7th century (Suoana-Kazahaya eruption), and the 9th century (Oyama eruption), both of which produced $\sim 10^8$ m³ of tephra and lavas. Suoana-Kazahaya eruption occurred from a 3-km-long fissure in the northern slope of the volcano and is characterized by the phreatomagmatic explosive activity. The Oyama eruption is one of the largest eruptions in this period with complex evolution from the lava effusion from the summit, shifted to a fissure eruption, and lasted by explosive phreatomagmatic activities in the costal area.

The result of our study indicates that the average interval of the eruptions within the last 1400 years is ~ 70 years. This value is clearly longer than the average interval (~ 30 years) of the well-documented eruptions since 1835 AD. The numbers of eruptions in the 19th and 20th century are 3, whereas one or two eruptions are identified in the previous centuries.

It is debatable the both possibilities of the presence of several unknown eruptions and the possibility of the increase of eruption frequency. The counting loss of the eruption events is possible cause of the decrease of the eruption frequency. Because of the relatively-small magnitude and moderate

explosivity of the fissure eruptions of Miyakejima, the distribution of fall-out tephra is limited in the vicinity of the eruption site. Frequent eruptions particularly in the southwestern sector of the volcano can cover the products of previous eruption. Therefore, the field survey with limited number of outcrops may result the overlooking of some minor eruptions.

Change of the eruption frequency is also possible model. In the southwestern flank, the layers of scoria-fall deposits before the 16th century were interbedded by relatively thick paleosol, whereas the younger scoria-fall deposits have thinner paleosol. The difference of the development of paleosol can indicate the increase of the eruption frequency in the last ~ 400 years.

The quality of geological surveys strongly depends on the field condition. Destruction of the forest by the 2000 AD eruptions offered an idea exposure of the eruption products. With the developing of the new technic of the detailed DEM mapping, the accuracy of the geological investigations of the eruption history of Miyakejima has been integrated. However, our result also suggests the limitation of the geological fieldwork to identify the past minor eruptions. The eruption history of a volcano based on the geological field survey is the fundamental data for the mitigation of eruption disasters. Therefore, increasing of the accuracy of the field survey and the reducing of counting loss of the past eruptions are crucial for the evaluation of the volcanic activities.

Acknowledgements

Our field survey in Miyakejima was supported by the government of Miyake Village and the Japan Meteorological Agency.

References

- Tsukui, M., and Suzuki, Y., 1998. Eruptive history of Miyakejima Volcano during the last 7000 years. *Bulletin of the Volcanological Society of Japan*, 43, 149-166.
- Tsukui, M., Niihori, K., and Kawanabe, Y., 2005. *Geological Map of Miyakejima Volcano*. Geological

The volcanic-plutonic connection at the Platoro caldera complex, Southern Rocky Mountains Volcanic Field, Colorado

Amy K. Gilmer¹ and Ren A. Thompson¹

¹ U.S. Geological Survey, Denver, CO USA; agilmer@usgs.gov

Keywords: geochronology, intrusion, magmatic system.

The connection between volcanic and plutonic rocks has received significant attention, yet it is often difficult to assess because the intrusive rocks may not be exposed. The polycyclic Platoro caldera in the Southern Rocky Mountain volcanic field has exceptional exposures of both ignimbrites and plutons within and adjacent to the caldera. Previous mapping delineated these plutons and dikes (Lipman, 1974; Lipman, 1975), but geochronologic and petrologic constraints were minimal.

The Platoro caldera complex is in the southeastern part of the San Juan volcanic region (SJVR), the erosional remnant of the central locus of the mid-Tertiary aged Southern Rocky Mountain Volcanic Field (SRMVF) (Fig. 1). Volcanic activity in the SJVR lasted from 38 to 23 Ma and generated 25 large-volume ignimbrites from multiple calderas (Lipman, 2007; Lipman and Bachmann, 2015; Steven and Lipman, 1976). The Platoro caldera itself sourced seven major ignimbrites between 30.1 and 28.8 Ma including the last and largest, the Chiquito Peak Tuff (Lipman et al., 1996).

A series of plutons, laccoliths, and dikes associated with the post-caldera magmatic activity at Platoro intrude pre-caldera lavas and volcanoclastic deposits of the Conejos Formation, the La Jara Canyon and Chiquito Peak Tuffs and the caldera-filling Summitville basaltic andesite lavas. The plutons range in composition from diorite to quartz monzonite with minor occurrences of aplitic granite.

New zircon U-Pb SHRIMP ages and trace-element compositions document continued epizonal magma emplacement after the ignimbrite eruptions. Zircons from fourteen intrusions and the final crystal-rich dacitic ignimbrite, the Chiquito Peak Tuff record magma emplacement until ca. 27 Ma. The Chiquito Peak Tuff yielded a mean $^{206}\text{Pb}/^{238}\text{U}$ date of 28.92 ± 0.50 Ma, within uncertainty of an existing $^{40}\text{Ar}/^{39}\text{Ar}$ sanidine eruption age, 28.77 ± 0.03 Ma (Lipman and Zimmerer, *in review*). The larger intrusions within the caldera range from ca. 29.0 Ma to 27.4 Ma. Intrusions beyond the western margin of the caldera are younger, ranging in age from ca. 27.1 to 26.9 Ma. A series of dacite porphyry dikes that have ages from ca. 28.3 to 27.5 Ma intrude the caldera and radiate westward beyond the caldera margin.

The bulk compositions of these intrusions range from 55.6 to 69.8 wt.% SiO_2 with the youngest sanidine-quartz dacite porphyry dikes being the most evolved. The Chiquito Peak Tuff ranges from 63.9 to 68.4 wt.% SiO_2 .

Modally, all intrusions contain plagioclase clinopyroxene, biotite, orthoclase, and quartz. One striking difference between the intrusions within the caldera and the intrusions and dikes on the western caldera margin is the presence of hornblende phenocrysts and much less clinopyroxene.

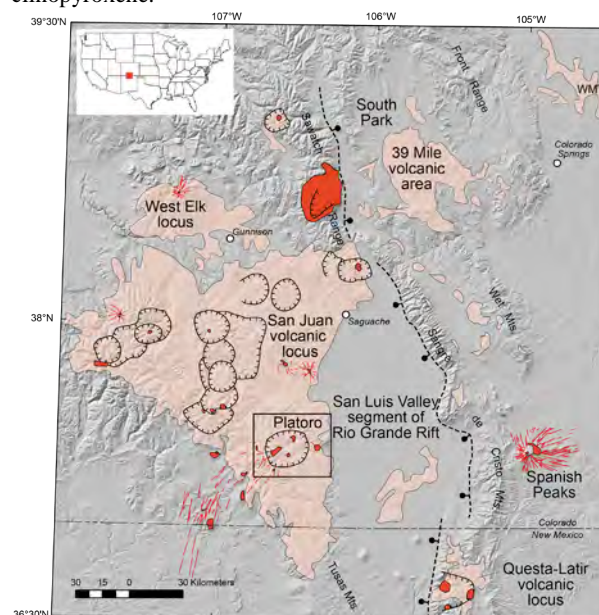


Fig. 1 – Map of Southern Rocky Mountain volcanic field, showing ignimbrite calderas, major erosional remnants mid-Tertiary volcanic cover and intrusions. The Platoro caldera complex is denoted by the black box. Modified Lipman et al 2015.

Electron microprobe analysis of the amphiboles in the dikes and western margin intrusions suggests polybaric differentiation for these magmas. Comparison with experimental data suggests that crystallization of amphibole in the system may have begun in the mid- to lower crust and continued to shallow levels. The presence of abundant amphibole in these magmas also suggests a higher water content compared with Chiquito Peak Tuff and the intrusions emplaced within the caldera and on the eastern margin.

Plagioclase compositions were also analyzed by electron microprobe. For the Chiquito Peak Tuff and the intrusion closest in age, the Alamosa River monzonite, plagioclase anorthite values are An_{29-82} and An_{27-65} , respectively. Sr in plagioclase ranges from 1230 to 2950 ppm in the tuff and 560 to 1400 ppm in the monzonite. Additionally, biotite in the Chiquito Peak Tuff is distinctly different in composition from of the similarly aged intrusions.



Fig. 2 – Hydrothermally altered Alum Creek quartz monzonite porphyry. This intrusion is part of the post-caldera magmatism in the Platoro caldera complex.

Zircon trace elements suggest distinct compositional differences between the older and younger magmas. The Chiquito Peak Tuff zircons have Eu/Eu^* values than that of the Alamosa River monzonite while zircons from younger intrusions from the western margin of the caldera have even higher Eu/Eu^* values. Ti-in-zircon temperature estimates are higher for the Alamosa River, Cat Creek, and Jasper plutons ($\sim 1000-800^\circ\text{C}$), in comparison with the other intrusions and dikes and the Chiquito Peak Tuff (mostly $<800^\circ\text{C}$).

Based on the zircon U-Pb ages, zircon trace element compositions and plagioclase and biotite compositions, it is unlikely that these intrusions

represent residual magma of the ignimbrite magma reservoir. Magmatism spatially associated with Platoro spans too much time ($\gg 1\text{ Ma}$) to represent a single upper crustal mush zone, and more likely reflects mush that was remobilized from different depths in the trans-crustal magmatic system.

Acknowledgements

This work was supported by the USGS National Cooperative Geologic Mapping Program and the Mineral Resources Program.

References

- Lipman, P.W., 1974, Geologic map of the Platoro caldera area, southeastern San Juan Mountains, Colorado: U.S. Geological Survey Miscellaneous Investigations Series Map I-828, scale 1:48,000.
- Lipman, P.W., 1975, Evolution of the Platoro caldera complex and related volcanic rocks, southeastern San Juan Mountains, Colorado: U.S. Geological Survey Professional Paper 852: 128 p.
- Lipman, P.W., 2007, Incremental assembly and prolonged consolidation of Cordilleran magma chambers: evidence from the Southern Rocky Mountain volcanic field: *Geosphere*, 3(1): 42-70.
- Lipman, P. W., and Bachmann, O., 2015, Ignimbrites to batholiths: Integrating perspectives from geological, geophysical, and geochronological data: *Geosphere*, 11(3): 705-743.
- Lipman, P.W., Dungan, M.A., Brown, L.D., and Deino, A., 1996, Recurrent eruption and subsidence at the Platoro caldera complex, southeastern San Juan volcanic field, Colorado: *New tales from old tuffs: Geological Society of America Bulletin*, 108(8): 1039-1055.
- Lipman, P.W., Zimmerer, M.J., McIntosh, W.W., 2015. An ignimbrite caldera from the bottom up: Exhumed floor and fill of the resurgent Bonanza caldera, Southern Rocky Mountain volcanic field, Colorado: *Geosphere*, 11(6): 1902-1947.
- Lipman, P.W., Zimmerer, M.J., *in review*. Magmato-Tectonic Links: Ignimbrite Calderas, Regional Dike Swarms, and the Transition from Arc to Rift in the Southern Rocky Mountains. *Geosphere*.
- Steven, T.A., and Lipman, P.W., 1976, Calderas of the San Juan volcanic field, southwestern Colorado: U.S. Geological Survey Professional Paper 958: 35 p.

Guidelines for mapping volcanic areas State of art and perspectives

Gianluca Groppelli¹ on behalf of the working group

¹ *Consiglio Nazionale delle Ricerche, Istituto per la Dinamica dei Processi Ambientali, sezione di Milano, Italy;*
gianluca.groppelli@gmail.com

Keywords: Geological Map, Volcanic Stratigraphy, Guidelines

The IAVCEI Commission on Volcano Geology began its activity in 2015 and one of the main aims of the Commission is the preparation of a common and as much as possible shared methodology to prepare geological map in volcanic areas. In fact, geological maps (Fig. 1) represent

- 1) the fundamental document for understanding the evolution of an area (Fig. 2),
- 2) the warehouse where to store in the objective way all the field data, including past eruptions and inter-eruptive phenomena,
- 3) the basis for further and in depth studies (e.g. physical volcanology, petrography, geochemistry and petrology, geophysical modeling, analogue and numerical modeling, volcanic hazard constraints, ore geology, geothermal resources, etc.).

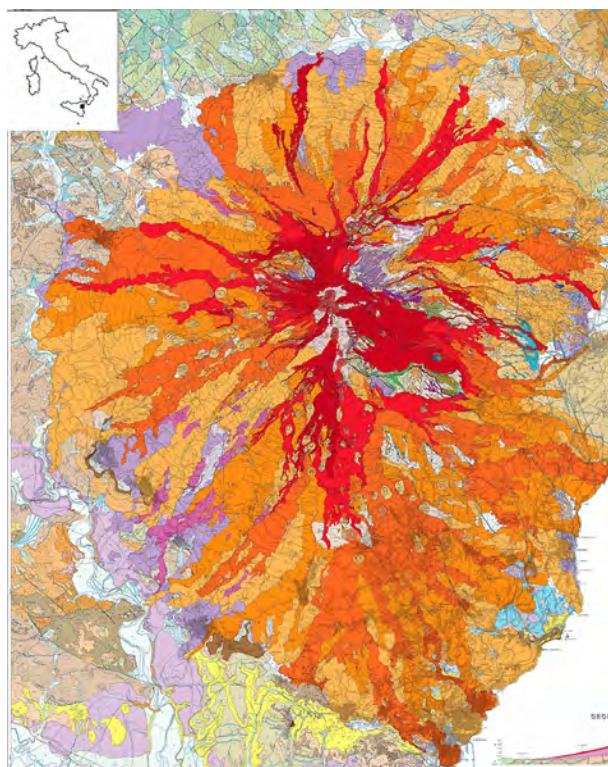


Fig. 1 – Geological map of Mount Etna (Branca et al. 2011)



Fig. 2 – La Reforma Caldera Complex, Mexico (modified from Garcia et al., submitted)

During the previous workshops organized by the IAVCEI Commission on Volcano Geology we had the opportunity to discuss different methodologies applied to various geological settings and exposures. At the same time, there was the request from numerous participants to share a common methodology during field survey. For this reason, the preparation of guidelines for mapping volcanoes and volcanic regions (ancient and modern) is in progress and in these days we present and discuss the first draft.

The original structure of the guidelines follows the structure listed below, even if not all the chapters have been completed and discussed enough:

- the explanation of a basic geological map, map organization and information inside the map, scale
- scale of field survey
- historical overview on mapping volcanoes during last two centuries (Fig. 3), from the first geological maps based on the volcanic center definition to maps based on petrographic-geochemical units, to the recent stratigraphic units (e.g. volcanic activity units, lithostratigraphic units, synthemic units, eruptive units, etc.)
- use of the lithostratigraphic unit to map volcanic terrains and to realize an objective geological map
- lithosomes, their definition and practical usage in volcanic regions
- synthems in volcanic terrains, their applications and their conceptual link to non-volcanic frameworks

- eruptive units: their definition, practical aspects and useful aspects in understanding a volcanic system, either ancient or modern and in assessing volcanic hazard
- recent volcanic activity and the problem of representing tephra successions and frequent narrow lava flows in a geological map of an active volcano

- peculiar features mapping old volcanic terranes and the pitfalls of applying the same methodology of recent volcanic terrains
- volcanic geomorphology and their practical utility mapping volcanic units
- mapping structures and volcano-tectonic features, a link between structural geology, tectonics and volcanism.

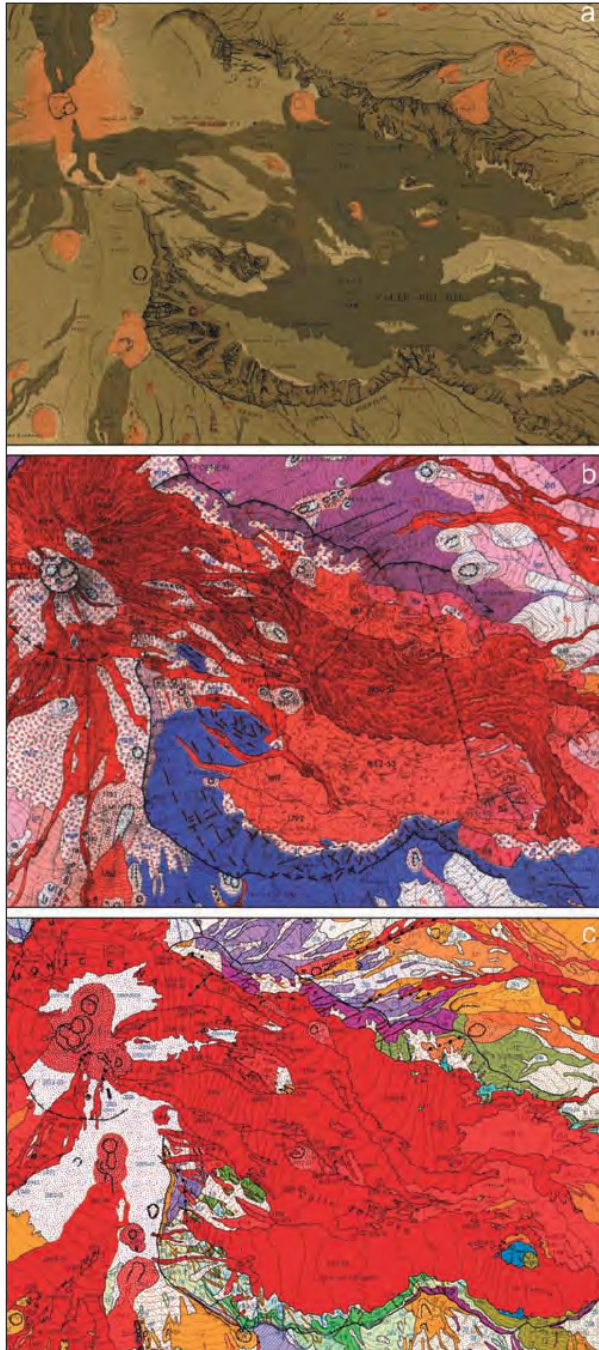


Fig. 3 – The summit region of Mt Etna and the Valle del Bove as reported in the geological maps at 1:50,000 scale of: (a) Waltershausen (1844-59); (b) Romano et al. (1979) and (c) Branca et al. (2011)

Most of the recent geological maps of volcanic areas apply stratigraphic units of different kinds during field survey and the final realization of map. The use of stratigraphic units is fundamental because it is the only way to define the geological time and hence to recognize the evolution of an area based only on the stratigraphic position of the different rock bodies. Some geological maps are characterized by the use of different stratigraphic units, often in parallel, with the aim to better define the evolution of a volcanic area and to show the spatial and temporal changes in the feeding system (Fig. 4).

STRATIGRAPHIC RELATIONSHIPS SCHEME OF MOUNT ETNA VOLCANIC DISTRICT

Synthetic Unit	Lithostratigraphic Unit	Lithostratigraphic Unit	Stratigraphic relationships		
Supersystem	Synthem	Subunit (code)	Stratigraphic relationships		
Stratovolcano	Il Piano Synthem	Torre del Filosofo formation: 3-19th AD - Present 2-1100 AD - 3971 AD 1-122 BC - 1669 AD			
		Pietrascanna formation Upper member 3/9 ka - 122 BC (4) Lower member 15 ka - 3/9 ka (2) Cubana member (5) Alto member (1) Orincole member (3)			
	Concazze Synthem	Portella Guverna formation Casanaleone zivoo member (6) Ragato member (7) Brancavia-Altroldo gronoleto member (8)			
		Monte Catalano formation			
		Simeto formation Piano D'Aragona member (9) Concazze Ragaglia member (1)			
		Piano Provenzana formation: Tropic member (2) Tulliozoo member (4)			
		Pizzi Denari formation: Upper member (3) Lower member (5)			
		Serra della Concazze formation			
		Valle del Bove		Cuvigghiu Synthem	Concazze della Montagnola formation Serra Cuvigghiu formation: Laghetto member (1)
					Acqua della Pesca formation
Zappia Synthem	Serra di Salfizzo formation Valle degli Zappia formation				
	Serra Gianicola Grande formation: Albeckino member (4)				
	Monte Fiori di Codomo formation				
	Monte Scorsone formation				

Fig. 4 – Stratigraphic relationship scheme of geological map of Mount Etna (Branca et al. 2011)

The basic unit is the lithostratigraphy, used during the field survey and also in the display of the final map, because the lithologic properties and stratigraphic relationships of rock bodies are the only characteristics immediately recognizable. Laboratory data (e.g. petrographic, geochemical, radiometric analyses) only allow a subsequent, more

comprehensive definition of a field-identified lithostratigraphic unit. In parallel to the lithostratigraphic units, lithosomatic and synthemic ones are applied to synthesize the volcanic evolution of the area and to distinguish major phases based on field (“objective”) characteristics (fig. 5). However, the application of the lithostratigraphic and synthemic units to volcanic areas faces problems of scale (temporal and spatial) respect to their application mapping large sedimentary basins, as usually hiatuses are of short duration (days to 10 000 years), and the limited areal extent of units (restrictions to few kilometers as individual volcanic bodies or a volcano). On the other side the synthemic units allow distinguishing in objective way the main phases of volcanism and to relate them with the variation of the regional tectonic regime and other regional events, as eustatic sea level changes.

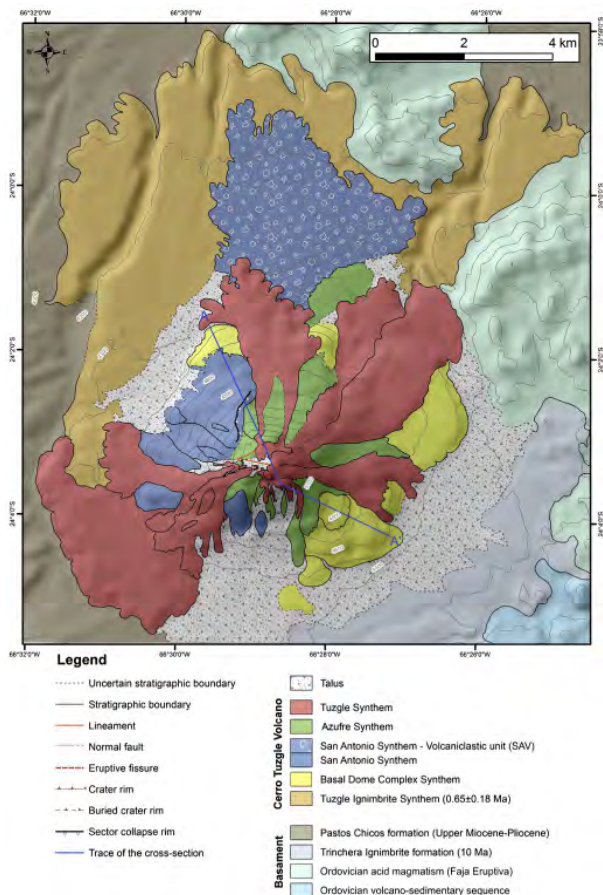


Fig. 5 – Geological map of Tuzgle volcano, Argentina (Norini et al. 2014)

After the current IAVCEI 5th Volcano Geology Workshop we plan to share the draft guidelines among all members of the IAVCEI Commission on Volcano Geology and also intend to involve

traditional stratigraphers in the final review process to:

- 1) share the proposed methodology as much as possible with the hope that the guidelines will be applied in future,
- 2) validate our guidelines among earth scientists working in various geological settings and using the same kinds of stratigraphic units,
- 3) make geological maps of volcanic areas that are easy to understand even for non-volcanologists, and
- 4) place the evolution of a volcanic area into the wider geological context.



Fig. 6 – Mayon Volcano (Philippines)

For these reasons we plan to present the final version of the guidelines to the STRATI 2019 conference (July 2019, Milan, Italy) to the IUGG 2019 (July 2019, Montreal, Canada) and to other important international conferences, as the Geological World Congress in New Delhi (2020).

Of course during the current workshop, we will discuss how to finalize the guidelines, once it has been approved by the IAVCEI Commission on Volcano Geology. In fact, it is fundamental that 1) the International Stratigraphy Commission is embedded and hence approves this guide, 2) the guidelines will be widely distributed and hence used by geologists mapping volcanic terrains, and 3) the final guide is planned to be published in the Episodes or similar journals, which deals with the stratigraphy, stratigraphical nomenclature and their applications, and strongly aligned with geological surveys doing the state financed geological maps.

References

- Branca, S., Coltelli, M. and Groppelli, G., 2011. Geological evolution of a complex basaltic

- stratovolcano: Mount Etna, Italy. *Italian Journal of Geosciences*, 130(3): 306-317.
- Norini, G., Cogliati, S., Baez, W., Amosio, M., Bustos, E., Viramonte, J. and Groppelli, G., 2014. The geological and structural evolution of the Cerro Tuzgle Quaternary stratovolcano in the back-arc region of the Central Andes, Argentina. *Journal of Volcanology and Geothermal Research*, 285: 214-228.
- Romano, R., Sturiale, C. and Lentini, F., 1979. Geological Map of Mt. Etna. CNR, Progetto Finalizzato Geodinamica, Istituto Internazionale di Vulcanologia (Catania). 1:50.000 scale.
- Walterhausen, W., 1844-59. *Atlas des Aetna*. Berlin, Göttingen, Weimar.

Structure and evolution of the most active sector of Campi Flegrei caldera (southern Italy)

Roberto Isaia¹, Maria G. Di Giuseppe¹, Francesco D'Assisi Tramparulo¹, Antonio Troiano¹ and Stefano Vitale^{1,2}

¹Istituto Nazionale di Geofisica e Vulcanologia, sezione di Napoli Osservatorio Vesuviano; roberto.isaia@ingv.it

²Dipartimento di Scienze della Terra, dell'Ambiente e delle Risorse (DiSTAR), Università di Napoli Federico II.

Keywords: maar volcano, Campi Flegrei, Electrical Resistivity Tomography

The central sector of the Campi Flegrei, including the Solfatara maar and Pisciarelli fumarolic field, is currently the most active part of the caldera as regards seismicity and gaseous emissions and it plays a major role in the recent unrest crises of the volcano. Just few of the volcanic features part of this sector are known also in their deep structure, while a more general reconstruction of the entire sector is still missing.

The volcanological investigation allowed us to define the succession of the eruptive events and their characteristics as well as the structural data permit to better understand the volcano-tectonic evolution of the area. Furthermore, we present an application of deep Electrical Resistivity Tomography that resulted in the reconstruction of a three-dimensional resistivity model for the entire sector.

The most active area of CF caldera is mainly concentrated around the Solfatara volcano. It is a maar-diatreme structure erupted contemporaneously to the Averno volcano at about 4.2 ka, characterized by a shallow crater, cut in the pre-eruptive basement, and a deep diatreme (down to 2-3 km). The Solfatara area is presently the site of most intense fumarolic and hydrothermal manifestation within the caldera. The first phase of the Solfatara eruption emplaced massive to plane-parallel beds stratified ash/lapilli deposits, with no clear juvenile material. Within proximal area the centimetre thick, basal coarse cohesive ash layer contains many imprints of leaves. The ash fraction (<2 mm) of the Solfatara deposits is mainly composed of tuff fragments and pumice clasts covered by fine ash. Many clasts are deeply altered. This material could represent the host rock (La Pietra Tuff).

In the second phase discrete explosions involving a juvenile component formed wavy to plane-parallel beds from PDCs distributed around the vent area and ash fallout from low eruptive column. Juvenile material includes grey pumice fragments. Lithic clasts, made up mainly by fresh and altered lavas, often rounded, and minor green and yellow tuffs, reach up to 75% of the total rock volume in the breccia-like layers.

The first phase of the eruption was likely triggered by the explosion of the hydrothermal system located below the crater, involving a great contribution of hydrothermal fluids very scarce amount of magma. Eruptive dynamics generated small dispersed pyroclastic flows by low eruptive column. Discrete explosions produced PDC and low eruptive column during the second phase of the eruption, characterized also by a greater involvement of the magma. Deposits dispersed mainly toward NNE, with the PDC strongly controlled by paleotopography. The area covered by deposits is of about 55 km² with a volume of 0.05 km³.

The volcanological and geophysical results highlight the anatomy of the volcano-tectonic characteristics, providing valuable elements for the evaluation of both the current state of the system and the possible evolution of volcanic activity and a solid basis for any attempt to develop physical-mathematical models that can explain the ongoing phenomena.

The resolved details of the diatreme of the Solfatara, of the degassing area of Pisciarelli, of the Agnano Plain and of other significant structures of the sector represent elements of novelty in the framework of the structural knowledge of the caldera, a study area so far somewhat neglected but essential to achieve an adequate basic knowledge of the volcano. Type volcanism as occurred in the Solfatara area should be taken into account for the construction of future eruptive scenario in relation to possible small magnitude eruptive events at Campi Flegrei, including phreatic activity.

Acknowledgements

This work has benefited from funding provided by the Italian Presidenza del Consiglio dei Ministri – Dipartimento della Protezione Civile (DPC), agreement INGV-DPC. This paper not necessarily represent the DPC official opinion and policies.

Mapping hydrothermal alteration on Mt Ruapehu (New Zealand) using field, laboratory, and hyperspectral imaging measurements

Gabor Kereszturi¹, Lauren Schaefer², Reddy Pullanagari¹, Craig Miller³, Stuart Mead¹, Ben Kennedy² and Jonathan N. Procter¹

¹ School of Agriculture and Environment, Massey University, Palmerston North, New Zealand; g.kereszturi@massey.ac.nz

² Department of Geological Sciences, University of Canterbury, Christchurch, New Zealand

³ GNS Science, Wairakei Research Centre, Taupo, New Zealand

Keywords: hydrothermal alteration, composite volcano, imaging spectroscopy.

In active volcanic systems, primary lava and volcanoclastic deposits progressively weaken through hydrothermal alteration, which may lead to collapse without warning. The resultant mass flows, such as landslides, debris flows and debris avalanches, are hazardous to communities and lifeline infrastructure up to 100 km from volcanoes. These dangerous mass wasting processes have occurred on every large-volume volcano in New Zealand. Currently, New Zealand does not have a model in place to delineate likely source zones and forecast these volcanic hazards. Moreover, volcano collapses are often multi-hazard events, with even small-scale landslides capable of triggering decompression-driven phreatic eruptions, such as Te Maari in a 2012 (Pardo et al. 2014), or creating break-out lahars, such as Crater Lake in 2007 (Procter et al. 2010). Hence, identifying susceptible weak-zones on composite volcano is an important part of the long-term land-use planning, monitoring, and natural hazard mitigation. To better identify areas that are more susceptible to generate mass flows, we propose a novel methodology combining field, laboratory, and surface imaging measurements of the chemical, physical, and mechanical properties of volcanic rocks and sediments to identify areas of hydrothermal alteration around the volcanic edifice.

Mt. Ruapehu is an andesitic to dacitic composite volcano (Fig. 1), associated with the westward subduction of the Pacific Plate beneath the Australian Plate. Mt. Ruapehu has also produced numerous small to large scale hydrothermal, magmatic, and phreatomagmatic eruptions, recently, such in 1945, 1969, 1971, 1977, 1995-96, and 2007 (e.g. Procter et al. 2010). In its geological past, it has suffered several large-scale flank collapses and many smaller collapses of the crater rim that have resulted in debris avalanches, landslides, and lahars (e.g. Palmer & Neall 1989, Procter et al. 2010). Therefore, Mt. Ruapehu, with its well-developed hydrothermal alteration zones, is prone to instabilities across a range of scales, making it an excellent case study for developing new approaches for hazard assessment and mitigation.

To identify the degree of hydrothermal alteration at the surface, this study utilized airborne hyperspectral imaging. The hyperspectral image was acquired from a low-flying fixed-wing aircraft, mounted with an AisaFENIX pushbroom sensor. Hyperspectral imaging detects the visible to shortwave infrared parts of the electromagnetic spectrum (370-2500 nm), at many narrow and slightly overlapping spectral channels. The image has been radiometrically and atmospherically corrected, and geocoded, before image mosaicking to provide a seamless map of surface reflectance. The surface reflectance is sensitive to a range of minerals, such as clay (e.g. Kruse 2012, Kereszturi et al. 2018).

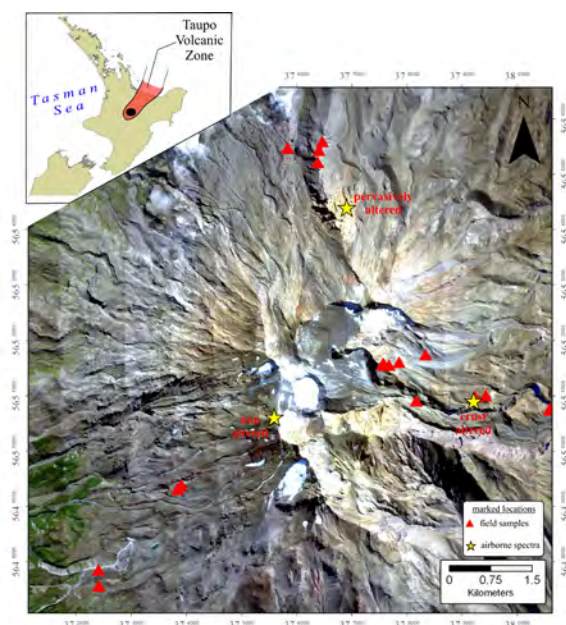


Fig. 1 – Hyperspectral image of Mt Ruapehu, and its location within the Taupo Volcanic Zone (inset).

The field campaigns were focused on sampling lithologies of different ages and hydrothermal alteration (Fig. 1). The samples have been analysed to determine the chemical, such as surface mineralogy, alteration types, and physical properties, such as density, permeability, uniaxial strength, and

magnetic susceptibility. This study presents the surface mineralogy established through spectroscopy (Fig. 2).

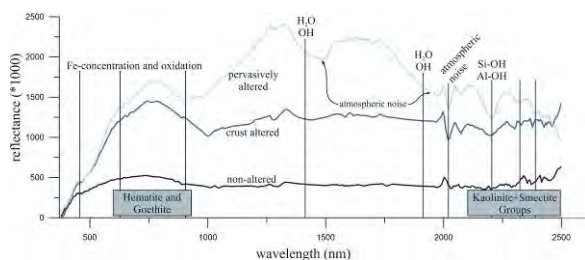


Fig. 2 – Airborne spectral readings of fresh (dark blue), crust-altered (blue) and pervasively altered lithologies (light blue). For locations see Fig. 1.

The main mineral phase detected, using USGS spectral libraries and spectral matching algorithms, is consistent with kaolinite and montmorillonite, using absorption feature located around 2120 nm (Fig. 2). Other absorption features, in the visible part of the spectra (370-700 nm), suggests the presence of hematite and goethite. Based on the spectral information from the hyperspectral image, such end-member mineral associations occur as systematic linear mixtures on the surface. The surface mineralogy is consistent with a low-temperature (≤ 80 °C), hydrothermal-fluid driven argillic alteration (e.g. Kereszturi et al. 2018).

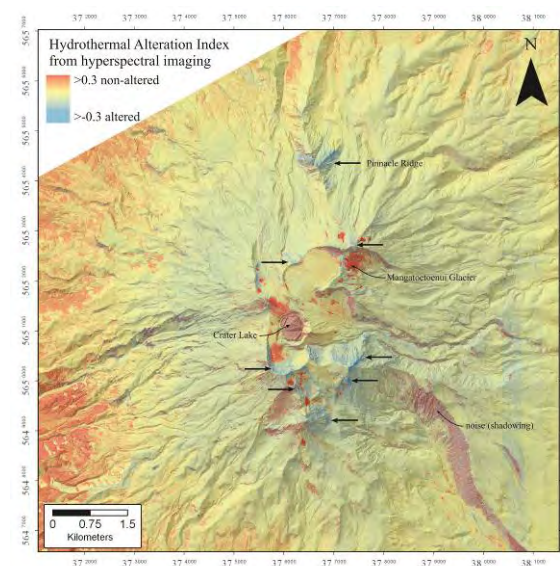


Fig. 3 – Hydrothermal alteration zones of Mt Ruapehu. The arrows show the main surface alteration zones (blue tones).

The strong sensitivity of the spectral regions centred at 2120 nm allows spatial mapping of the distribution of surface clay minerals, using band ratios. The normalized clay index was calculated as: $(B1-B2)/(B1+B2)$, where B1 and B2 are the spectral wavelengths of 2118.8 nm and 2207.1 nm, respectively. The resultant map highlights the areas

of hydrothermal alteration on Mt Ruapehu, including Te Herenga and Wahianoa Formations. These are the oldest parts (≥ 80 ky) of Mt Ruapehu with (e.g. Conway et al. 2016).

The distribution of surface hydrothermal alteration using hyperspectral imaging can highlight potential source areas for mass flows (e.g. debris avalanches and landslides). However, alteration can change with the stratigraphy, and surface alteration may not represent properties at depth. This will be overcome in the future with the newly acquired aero-magnetic survey data that allows us to model the sub-surface distribution of hydrothermal alteration. The mapped source areas will provide inputs for future numerical simulations of mass flows hazards, contributing to long-term land-use planning, volcano monitoring, and natural hazard mitigation at Mt. Ruapehu.

Acknowledgements

This research is supported by Natural Hazards Research Platform (“Too big to fail? – A multidisciplinary approach to predict collapse and debris flow hazards from Mt. Ruapehu”) and by the GK’s Early Career Researchers Fund from Massey University.

References

- Conway, C.E., Leonard, G.S., Townsend, D.B., Calvert, A.T., Wilson, C.J.N., Gamble, J.A. and Eaves, S.R., 2016. A high-resolution $40\text{Ar}/39\text{Ar}$ lava chronology and edifice construction history for Ruapehu volcano, New Zealand. *Journal of Volcanology and Geothermal Research*, 327: 152-179.
- Kereszturi, G., Schaefer, L.N., Schleiffarth, W.K., Procter, J., Pullanagari, R.R., Mead, S. and Kennedy, B., 2018. Integrating airborne hyperspectral imagery and LiDAR for volcano mapping and monitoring through image classification. *International Journal of Applied Earth Observation and Geoinformation*, 73: 323-339.
- Kruse, F.A., 2012. Mapping surface mineralogy using imaging spectrometry. *Geomorphology*, 137(1): 41-56.
- Palmer, B.A. and Neall, V.E., 1989. The Murimotu Formation—9500 year old deposits of a debris avalanche and associated lahars, Mount Ruapehu, North Island, New Zealand. *New Zealand Journal of Geology and Geophysics*, 32(4): 477-486.
- Pardo, N., et al. 2014. Perils in distinguishing phreatic from phreatomagmatic ash; insights into the eruption mechanisms of the 6 August 2012 Mt. Tongariro eruption, New Zealand. *Journal of Volcanology and Geothermal Research*, 286: 397-414.
- Procter, J., Cronin, S.J., Fuller, I.C., Lube, G. and Manville, V., 2010. Quantifying the geomorphic impacts of a lake-breakout lahar, Mount Ruapehu, New Zealand. *Geology*, 38(1): 67-70.

Mapping of dispersed small-volume volcanism of the silicic caldera system of the Taupo Volcanic Zone, New Zealand: results and limitations

Szabolcs Kósik¹, Károly Németh¹, and Mark Bebbington¹

¹ School of Agriculture and Environment, Massey University, Palmerston North, New Zealand; s.kosik@massey.ac.nz

Keywords: spatio-temporal and volumetric distribution, digital terrain analysis, explosiveness of lava extrusions

The Taupo Volcanic Zone (TVZ) is one of the most productive silicic volcanic regions on Earth, and was established about 2 Ma due to the oblique subduction of Hikurangi Plateau of Pacific Plate at the southern end of the Tonga-Kermadec arc (Fig. 1). Its estimated mass magma output of 4000 km³ is dominated by 12 caldera-forming eruptions in the past 350 ky (Gualda et al., 2018), however at least 300 other significant eruptions have occurred, with considerably smaller eruptive volumes comprising a minimum total of 260 km³ DRE volcanic material in the same period (Kósik, 2018).

Caldera volcanism is generally considered to be polygenetic. From the point of view of magmatic plumbing systems, neither the small-volume eruptions nor the caldera-forming eruptions of large silicic systems match perfectly to the “polygenetic” criteria (e.g. Smith and Németh, 2017). There are no long-lived settled magma chambers envisioned in association with many of TVZ’s silicic volcanoes of any size. Instead there are rather newly-formed separate melt packages forming lenses in the upper crust which slowly crystallised or are evacuated in a short geological time (Allan et al. 2013; Shane and Smith, 2013). Most eruptions establish a new eruptive vent in a similar manner to basaltic monogenetic fields; these vents rarely function as the loci of subsequent eruptions due to their infill with solidified magma. For these reasons, the silicic caldera system of TVZ can be interpreted as a high-flux volcanic field with frequent small (but larger on average than those at basaltic monogenetic fields) volume eruptions, as well as large-volume (VEI 7 and 8) “accidental” events associated with caldera formation and widespread deposition of ignimbrite. These latter events were most likely triggered by external factors, such as regional tectonism.

These characteristics of the magma reservoir are reflected in the spatial, temporal and volumetric distribution of TVZ’s small-volume volcanism.

Spatially, only two thirds of the vents are located inside the known or inferred caldera boundaries, and there is little evidence that subsequent vent locations were controlled by the margins of calderas. However, vents of small-volume eruptions are spatially over-represented near rift-parallel faults,

and often form lava dome complexes by the extrusion of magma from closely spaced vents (e.g. Tarawera).

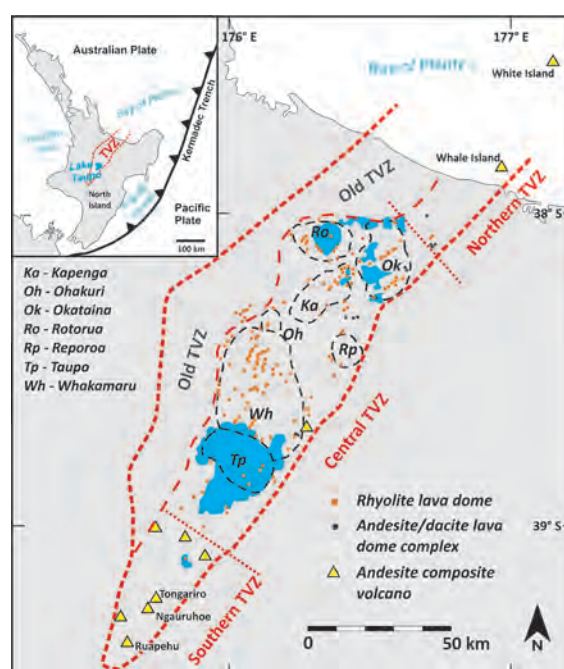


Fig. 1 – Location of silicic extrusive vents and calderas. Regional map shows the geographic location of the TVZ and its relative position to the plate boundary (inset map). The border (bold red dashed lines) between the Old TVZ and the Young TVZ and the present-day compositional divisions (red dotted lines) between the more andesitic Southern and Northern TVZ and the rhyolitic Central TVZ are from Wilson et al. (1995). Outlines of rhyolitic calderas (black dashed lines) are from Houghton et al. (1995).

Temporally, four periods with different magma output rate were distinguished in the past 350 ky. However, the earliest period which coincides with the ignimbrite flare-up between 350 ka to 280 ka (Gravley et al. 2016) has significantly fewer events and total erupted volume (12.2 km³) than the following periods (Kósik et al., 2018). Moreover, only 35 extrusive bodies of small-volume eruptions known from the preceding ~700 ky that are located in a high topographic position and at the margins or further off the active rift of TVZ. The small number of events strongly suggests that the inventory of

extrusive small-volume activity is substantially deficient prior to the ignimbrite flare-up. For this reason, only the past 350 ky is suitable for the quantitative evaluation of small-volume volcanism. We consider three kinds of processes affecting the geologic observations; caldera formation, burial (e.g. extensive ignimbrite deposition) and erosion.

Pre-caldera structures within the caldera margins are destroyed or subside during the formation of caldera; the material may then have partially been incorporated to the evolving ignimbrite deposits (e.g. lithic lag breccias).

Extensive ignimbrite sheets are one of the main causes of burial along with lacustrine deposition of subsiding areas of the TVZ. A large number of completely buried edifices relating to post-350 ka small-volume activity have been discovered from drill cores (e.g. Downs et al., 2014) and volcanoclastic deposits associated with deep-seated phreatomagmatic activity (Kósik et al., 2017).

The evaluation of the preservation potential of thin tephra blankets is an important factor in characterizing the full picture of small-volume volcanism. A part of these were formed by pure explosive activity, while others are associated with lava extrusion; The younger and thoroughly examined dome eruptions (e.g. Okataina) were associated with significant explosive activity. However, pyroclastic deposits or morphologic features relating to explosive activity are only recognized in a few cases for older lava extrusions, which suggests either that the role and frequency of explosive activity associated with dome-forming eruptions may be larger than is currently apparent, or to alter now and then.

Besides the above limitations of geologic observations, the scale of geologic mapping is an important factor in recognition and basic characterization of small-volume activity. For young volcanic terrains with diverse and dispersed volcanic structures, such as the TVZ, the scale of 1 to 250,000 (e.g. Leonard et al, 2010) cannot cope with the discrimination and representation of distinctive units, such as coherent lava, block-and-ash flow breccias, diatreme infills and fine tephra with magmatic or phreatomagmatic origin.

Further, geologic mapping may have been fostered by geomorphologic characterisation at young volcanic terrains using DEMs with the aim of better understanding the genetic perspectives of the landscape structures, such as is the case with the small-volume volcanoes of the TVZ (Kósik, 2018).

Acknowledgements

This research was funded by School of Agriculture and Environment, Massey University through the doctoral scholarship awarded to SK.

References

- Allan, A.S., Morgan, D.J., Wilson, C.J. and Millet, M.-A., 2013. From mush to eruption in centuries: assembly of the super-sized Oruanui magma body. *Contributions to Mineralogy and Petrology*, 166(1): 143-164.
- Downs, D.T., Rowland, J.V., Wilson, C.J.N., Rosenberg, M.D., Leonard, G.S. and Calvert, A.T., 2014. Evolution of the intra-arc Taupo-Reporoa Basin within the Taupo Volcanic Zone of New Zealand. *Geosphere*, 10(1): 185-206.
- Gravley, D.M., Deering, C.D., Leonard, G.S., Rowland, J.V., 2016. Ignimbrite flare-ups and their drivers: A New Zealand perspective. *Earth-Science Reviews*, 162: 65-82.
- Gualda, G.A.R., Gravley, D.M., Connor, M., Hollmann, B., Pamukcu, A.S., Bégué, F., Ghiorso, M.S., Deering, C.D., 2018. Climbing the crustal ladder: Magma storage-depth evolution during a volcanic flare-up. *Science Advances*, 4: eaap7567.
- Houghton, B., Wilson, C., McWilliams, M., Lanphere, M., Weaver, S., Briggs, R. and Pringle, M., 1995. Chronology and dynamics of a large silicic magmatic system: central Taupo Volcanic Zone, New Zealand. *Geology*, 23(1): 13-16.
- Kósik, S., 2018. Small-volume volcanism associated with polygenetic volcanoes, Taupo Volcanic Zone, New Zealand. Unpublished PhD thesis, Massey University, Palmerston North, 304 p.
- Kósik, S., Németh, K., Gravley, D.M., Procter, J.N., 2018. Temporal-volumetric pattern of small-volume volcanism of the Taupo Volcanic Zone, New Zealand. Program and Abstracts, 7th International Workshop on Collapse Calderas Toba Caldera, Sumatra, Indonesia: 31-32.
- Kósik, S., Németh, K., Procter, J. and Zellmer, G., 2017. Maar-diatreme volcanism relating to the pyroclastic sequence of a newly discovered high-alumina basalt in the Maroa Volcanic Centre, Taupo Volcanic Zone, New Zealand. *Journal of Volcanology and Geothermal Research*, 341: 363-370.
- Leonard, G.S., Begg, J.G. and Wilson, C.J.N., 2010. Geology of the Rotorua area. Institute of Geological and Nuclear Sciences 1:250,000 geological map 5. sheet + 102 p. Lower Hutt, New Zealand. GNS Science.
- Shane, P. and Smith, V.C., 2013. Using amphibole crystals to reconstruct magma storage temperatures and pressures for the post-caldera collapse volcanism at Okataina volcano. *Lithos*, 156: 159-170.
- Smith, I.E.M. and Németh, K., 2017. Source to surface model of monogenetic volcanism: a critical review. Geological Society, London, Special Publications, 446(1): 1-28.
- Wilson, C.J.N., Houghton, B.F., McWilliams, M.O., Lanphere, M.A., Weaver, S.D. and Briggs, R.M., 1995. Volcanic and structural evolution of Taupo Volcanic Zone, New Zealand: a review. *Journal of Volcanology and Geothermal Research*, 68(1-3): 1-28.

Particular features of the Oaş-Gutâi Volcanic Zone, Eastern Carpathians, Romania: Implications for understanding and reconstructing volcanic geology

Marinel Kovacs¹, Alexandrina Fulop² and Zoltán Pécskay³

¹*Tech.Univ.Cluj-Napoca, North Univ.Centre Baia Mare, Baia Mare, Romania; marinel.kovacs@cunbm.utcluj.ro*

²*De Beers Canada-Exploration, Toronto, Ontario, Canada;*

³*Institute of Nuclear Research of the Hungarian Academy of Sciences, Debrecen, Hungary*

Keywords: Carpathians, Miocene volcanism, volcano geology

The Oaş-Gutâi Volcanic Zone (OGVZ), situated in the North-West part of Romania, lies within the Neogene-Quaternary volcanic range of the Carpathian-Pannonian region (CPR), in Central-Eastern Europe. OGVZ is located in the eastern part of the Transcarpathian Basin, where post-collisional magmatism has been generated at the mantle lithosphere/crust level building up several volcanic areas (Seghedi and Downes, 2011).

Sub-alkaline volcanism developed in OGVZ during Miocene, within a large time-interval of approximately 8 Myr, between 15.4 and 7.0 Ma, (Pécskay et al., 2006) and generated a variety of volcanic rocks ranging from basalts to rhyolites, but dominantly andesites. Three types of volcanic activity were defined (Kovacs et al., 2017) as follows: 1) Felsic (i.e. rhyolitic), caldera-related volcanism (its onset dated at 15.4 Ma, Fülöp 2002) forming a complex assemblage of ignimbrites, co-ignimbrite fallout tuffs, and ignimbrite-related resedimented volcanoclastics interlayered with sedimentary deposits. The felsic volcanic rocks are widespread in the southern part of Gutâi Mountains, but dominantly covered by younger volcanics. 2) Intermediate (i.e. andesitic) volcanism, developed along the 13.4-7.0 Ma time-interval in OGVZ, but was shorter in Oaş Mountains (approximately 2.5 Ma, between 12-9.5 Ma). 3) Small-volume andesitic-rhyolitic volcanism (11.3-9.5 Ma), comprising several monogenetic andesitic-dacitic domes and a rhyolitic dome-coulée structure exclusively developed in the southwestern part of Oaş Mts. The intermediate (andesitic) volcanic activity produced more than 90% of the volcanic rocks of OGVZ. The multiphase activity, with its climax between 11-9 Ma, groups four different stages based on temporal evolution (Kovacs et al., 2017). The first two volcanic stages were the most voluminous. They include numerous volcanic complexes, which group volcanic products with temporal, spatial, and compositional affinities. Assigned to these two stages, numerous shallow sub-volcanic intrusive bodies (dykes, sills, small-sized laccoliths) lie mainly in the southeastern part

of Gutâi Mts. (11.9-9.0 Ma, Kovacs et al., 2013). The third and the fourth volcanic stages comprise small volumes of volcanic rocks, such as a small-sized composite andesitic-dacitic structure, 8.5-8.0 Ma age in the third stage, and small basaltic intrusions, 8.1-7.0 Ma age in the fourth stage.

Important metallogenetic activity, (polymetallic and gold-silver epithermal mineralizations), took place in the southern part of Gutâi Mts. and the northern part of Oaş Mts., in connection with the intermediate/andesitic volcanism (11.5-7.9 Ma, Lang et al., 1994).

OGVZ represents one of the most complex volcanic areas of CPR, due to a number of particular features that influenced the volcanic evolution. The volcanic activity mostly took place simultaneously with tectonic events related to the geotectonic evolution of the area. OGVZ occurs near the edges of the two tectonic blocks/microplates, ALCAPA and TISZA-DACIA, and along the W-E-striking Bogdan-Dragoş Vodă fault system (BDVS), an extension of the Mid-Hungarian Fault Zone. A series of volcano-tectonic depressions developed along, or parallel to the BDVS infilled with large volumes of volcanic products (e.g. Gutâi Mts., Lexa et al., 2010).

The OGVZ volcanism was influenced by the local paleogeography consisting of intra-volcanic and marginal basins. The volcanic activity evolved mostly in shallow to deep submarine setting. The volcanic products were emplaced both on land and subaqueously. Submarine deposited sequences bear the fingerprint of explosive and non-explosive quench fragmentation, combining primary deposition with re-deposition. Because of the large-scale reworking processes it is difficult to recognize the primary volcanic facies and to assign the volcanic rocks to particular volcanic sources.

Another feature of the OGVZ consists in the overlapping of the volcanic products belonging to different stages and/or to different coeval volcanic structures hindering identification and reconstruction of individual edifices. Thus, only a few composite volcanic structures were identified in Gutâi Mts. In

contrast, the dominant monogenetic domes and dome complexes developed in Oaş Mts. are readily identifiable by the typical topographic features of individual, isolated bodies crosscutting the sedimentary cover of the Oaş Depression of the Transcarpathian Basin.

OGVZ represents an ancient, extinct and poorly-exposed volcanic area, with heavy soil and vegetation coverage, and only scattered outcrops. Thus, the recently proposed methodologies - i.e. the UBU lithostratigraphic concept (Branca et al., 2011), or the Master events concept (Szakács and Canon-Tapia, 2010) cannot be applied to mapping the volcano geology in OGVZ. However, in order to understand and reconstruct the volcano geology, multiple methodologies have been used and integrated: 1:5000 scale detailed geological mapping, petrography and geochemical studies, sequential analysis of volcanoclastic and sedimentary sequences (e.g. facies analysis of the felsic ignimbrite volcanism with resedimented counterparts and dome growth related intermediate products). Logging of hundreds of exploration drill cores (300-1400 m deep) enabled the recognition and description of the old volcanic products buried under younger formations, and their correlation across OGVZ. The radiometric dating (more than 130 K-Ar age determinations on the majority of rock-types) and paleomagnetic studies essentially contributed to understanding volcanic evolution in OGVZ. Nevertheless, numerous questions and challenges still arise about the volcano geology of OGVZ, as an old and poorly-exposed volcanic region, with a complex volcanic history.

References

- Branca, S., Coltelli, M., Gropelli, G., 2011. Geologic evolution of a complex basaltic stratovolcano, Mount Etna, Italy. *Ital. J. Geosci.*, 130, 3:306-317.
- Fülöp, A., 2002. Transport and emplacement of the 15.4 Ma rhyolitic ignimbrites from Gutâi Mts., Eastern Carpathians, Romania. *Studia Universitatis Babeş-Bolyai, Geologia*, XLVII, 1: 65-75.
- Kovacs, M., Pécskay, Z., Fülöp, A., Jurje, M., Edelstein, O., 2013. Geochronology of the Neogene intrusive magmatism of the Oaş-Gutâi Mts., Eastern Carpathians, NW Romania. *Geologica Carpathica* 64: 483-496.
- Kovacs, M., Seghedi, I., Yamamoto, M., Fülöp, A., Pécskay, Z., Jurje, M. 2017. Miocene volcanism in the Oaş-Gutâi Volcanic Zone, Eastern Carpathians, Romania: Relationship to geodynamic processes in the Transcarpathian Basin. *Lithos*, 294-295: 304-318.
- Lang, B., Edelstein, O., Steinitz, G., Kovacs, M., Halga, S., 1994. Ar-Ar dating of adularia - a tool in understanding genetic relations between volcanism and mineralization: Baia Mare area (Gutâi Mountains), northwestern Romania. *Economic Geology*, 89: 174-180.
- Lexa, J., Seghedi, I., Németh, K., Szakács, A., Konečný, V., Pécskay, Z., Fülöp, A., Kovacs, M., 2010. Neogene-Quaternary volcanic forms in the Carpathian-Pannonian Region: a review. *Central European Journal of Geosciences* 2 (3): 207-270.
- Pécskay, Z., Lexa, J., Szakács, A., Seghedi, I., Balogh, K., Konečný, V., Zelenka, T., Kovacs, M., Póka, T., Fülöp, A., Márton, E., Panaiotu, C., Cvetković, V., 2006. Geochronology of Neogene-Quaternary magmatism in the Carpathian arc and Intra-Carpathian area: a review. *Geologica Carpathica* 57: 511-530.
- Seghedi, I., Downes, H., 2011. Geochemistry and tectonic development of Cenozoic magmatism in the Carpathian-Pannonian region. *Gondwana Research* 20: 655-672.
- Szakács, A., Canon-Tapia, E., 2010. Some challenging new perspectives of volcanology. In Canon-Tapia, E. and Szakacs, A., eds., *What is a Volcano?* Geological Society of America Special Paper 470.

New Zealand perspectives in geological mapping of volcanic terrains

Graham S. Leonard¹, Dougal B. Townsend¹ and Colin J.N. Wilson²

¹ GNS Science, 1 Fairway Drive, Lower Hutt 5010, New Zealand; G.Leonard@gns.cri.nz

² School of Geography, Environment and Earth Sciences, Victoria University of Wellington, PO Box 600, Wellington 6140, New Zealand.

Keywords: Mapping, Stratigraphy, Volcanic.

Experiences and observations in the mapping of New Zealand volcanic geology in New Zealand are discussed here in the context of two recently published maps (a regional geology tile that includes all of the caldera volcanoes, and a volcano-specific map for Ruapehu and Tongariro stratovolcanoes), a map in progress (volcano-specific map for the whole Taupo Volcano Zone) and a map under revision with the work just beginning (the basaltic Auckland Volcanic Field).

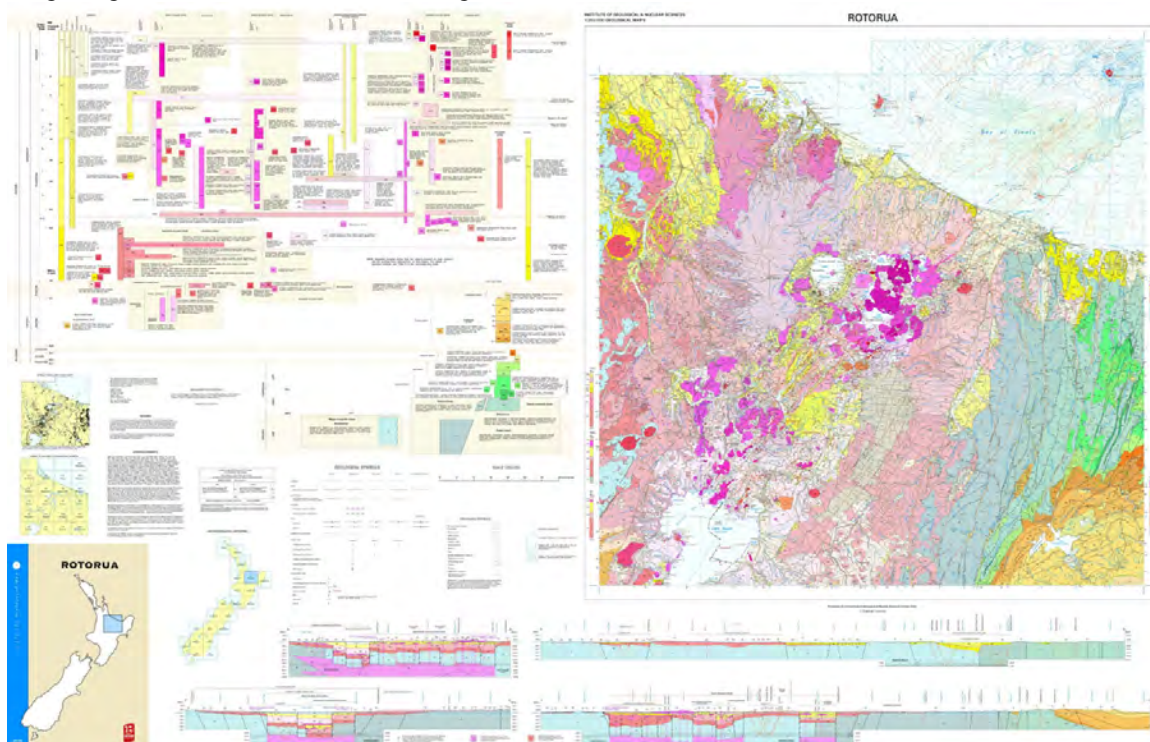
New Zealand case studies:

Quarter-million Map (QMAP) 5: Rotorua

The regional QMAP series is the highest detail national-coverage of New Zealand's geology, mapped at a scale of 1:250,000. It is not volcano-focussed. However, it gives excellent context for future, more specific work. QMAP Rotorua (Leonard et al., 2010) includes all the known calderas of the Taupo Volcanic Zone (TVZ) and was one of the final maps to be completed within a 16-year national geological mapping programme. Together with an ongoing Ar-Ar dating program we have: (a) drawn a unified spatial-temporal picture of migrating volcanism from the waning Miocene

Coromandel Volcanic Zone through the Tauranga-Kaimai area to the present day TVZ; (b) further resolved episodic events within the history of the TVZ and Taupo Rift; and (c) correlated major sedimentation events with those episodes. The central TVZ is notable for its high frequency of caldera-forming ignimbrite eruptions and voluminous output (>6,000 cubic kilometres of magma over 2 million years), i.e. it is an ignimbrite 'flare-up'. The history of this area can also be subdivided into episodes of escalated volcanism followed by periods of relative quiescence. We have newly identified a burst of activity around 550 ka. In addition, we now separately date and map distinct deposits of the largest single episode, which lasted 100 thousand years (from ca. 350 to 250 ka) and erupted more than 3,000 cubic kilometres of magma (half of the total output) from 7 caldera sources that, together, encompass most of the central TVZ. We also detail a series of volcanic and tectonic events that represent the build-up to that largest burst of activity, including a major shift in the TVZ volcano-tectonic regime just prior to the largest episode, and a smaller earlier shift.

Fig. 1 – QMAP Rotorua (Leonard et al., 2010)



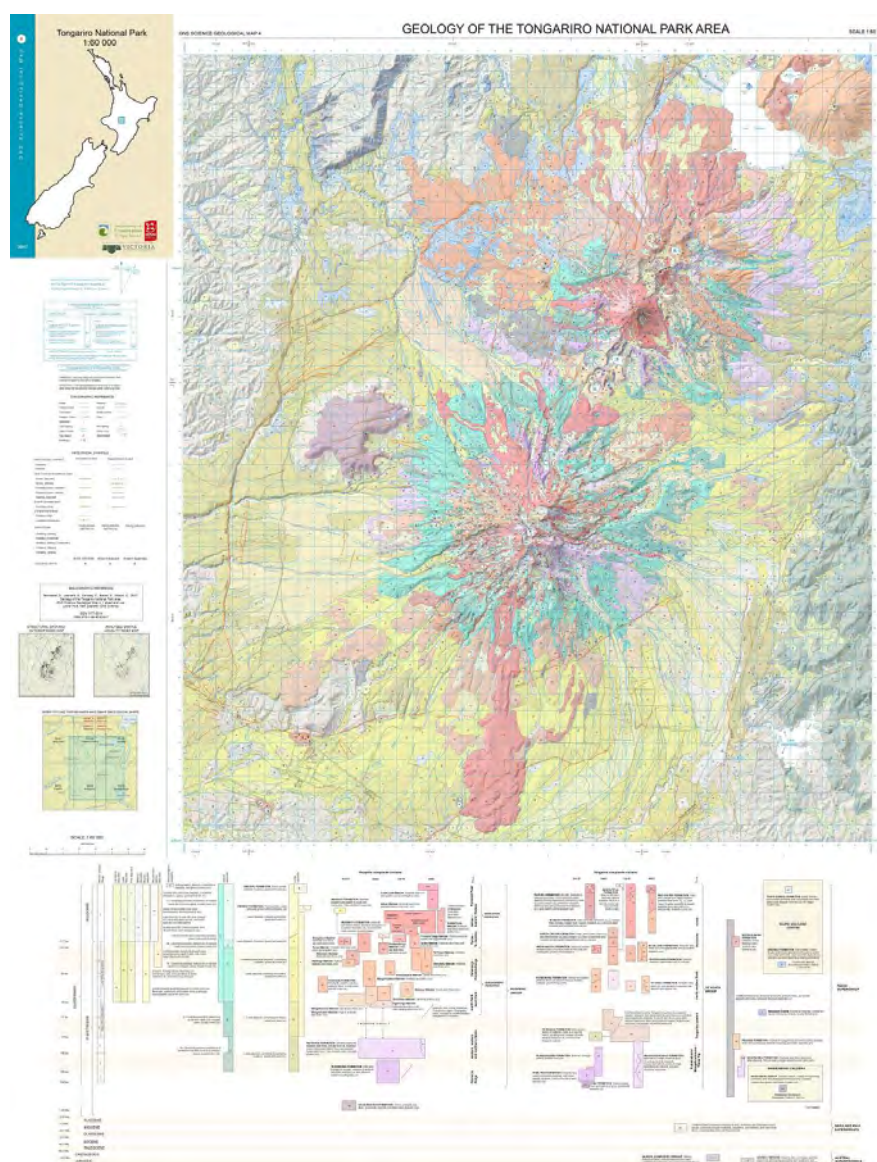
All of the QMAP tiles have been merged into the QMAP seamless GIS coverage for New Zealand (Heron, 2018). This coverage is now the main 1:250,000 geological map for the country, being updated incrementally at specific locations within individual 'sheets'.

Geology of the Tongariro National Park Area

Research for the first detailed (1:60,000) volcanic geological map (Townsend et al., 2017) of Tongariro National Park (Ruapehu and Tongariro andesite-dacite volcanoes) has led to new insights into their evolution. Both stratovolcanoes have hosted ice caps through much of their eruptive histories, and lava-ice interactions have strongly influenced the landform development. Mapping included field work analysing deposits and contacts, collecting samples over the volcanoes, and checking geomorphology mapped from aerial photos and a new high resolution Digital Surface Model. New geochemical analyses, combined with Ar-Ar dating, paleomagnetic data and previously published geochemical data allow for correlation of eruptive units and the development of comprehensive eruption stratigraphies linking both effusive and explosive phases. New high-precision (± 1 ka) groundmass Ar-Ar age dates show Ruapehu has been persistently active from 50 ka to present. Paleomagnetic study of flows dated between 45 and 39 ka bracket anomalous magnetizations consistent with the Laschamp excursion. There are extensive complex moraine and lava sequences over much of both volcanoes. The distributions of lava flows and pyroclastic deposits have been heavily controlled by ice distributions at the time of eruption. We now recognise widespread features of volcano-ice interaction including fine lava margin jointing, intercalated stacked moraines and perched lavas,

sub-glacial lavas, Holocene valley-floor lavas mantling glacial features, and features apparently due to sub-glacial lacustrine volcanism. The tephra cover on moraines is being studied: stratigraphic constraints are being combined with cosmogenic ^3He surface exposure dating of moraines to ascertain the relative and absolute timing of volcanic events and their relationships to past ice configurations. The results of these varied dating techniques shed new light on the timing of growth of late Pleistocene cones, the Holocene lavas and their relationships to the regional fall and flow deposits previously documented from the ring plains of both major cones.

Fig. 2 – Geology of the Tongariro National Park Area (Townsend et al., 2017)



Volcanic Geology of the Taupo Volcanic Zone

Work began in 2014 on a multi-year programme to publish a volcanic ‘special sheet’ map of the Taupo Volcanic Zone (TVZ) including all TVZ calderas, accompanied by a comprehensive bulletin detailing the eruptive history. This detailed history narrative is new compared to the QMAP, and will be complemented by a more detailed 1:120,000 scale (intermediate between QMAP and TNP map), and the opportunity to use a full colour and stipple pallet for the volcano units.

This new map will build substantially on regional mapping for QMAP Rotorua (2010), and the new volcanic geology map of Tongariro National Park. The special sheet will also integrate results from >150 new Ar-Ar ages, interpretation of new fieldwork and LiDAR elevation data, and the findings of new research since 2010.

Geology of the Auckland Urban Area - update

The original 1:50,000 urban map sheet and bulletin (Kermode, 1992) lays out the geology of the basaltic Auckland Volcanic Field along with Quaternary sediments and underlying Tertiary sediments. A large amount of new research has been undertaken in this field since 1992, however, along with the advent of LiDAR elevation data and significant growth of the Auckland City urban area.

The updated map and bulletin will include new understanding of the field relationships and eruptive histories of individual volcanic vents (of which there are about 53 known), their ages, and new detailed geomorphic mapping of all geological units. The map and bulletin will be linked to 3D subsurface geology models under development in the region, and the bulletin and descriptions will target the current needs of the city council and other companies and agencies. It may also be able to present an enhanced summary of the evolution of the volcanic field, akin to the content of the TNP and TVZ maps. New aerial photography will capture the volcanoes in relation to the substantially changed urban footprint.

Stratigraphic unit approaches

All GNS Science maps (including QMAP seamless, TNP, TVZ and the future Auckland map) now conform to GeoSciML, a global data model and data transfer standard for geological data. Volcanic stratigraphers in New Zealand have traditionally attempted a compromise across a range of variables to most-usefully distinguish map units. In a volcanic context, these are primarily:

- When was it deposited? (Stratigraphic control, radiometric age, fossils etc.)
- What’s the eruption/deposition process? What are the external environmental factors, such as presence of ice/glaciers? (is it lava, pyroclastic, sediment, till etc.)
- Where did it erupt from (vent location, volcano, volcanic centre, ‘caldera’ or other spatial eruption clustering).
- What is the petrology/chemistry of magma erupted? (basalts lying next to rhyolites would be separately named units even if their vent and age were virtually the same).

The breakdown into groups, formations, members and any sub-units should ideally make the most meaning from at least one, but preferably all of these variables, roughly in decreasing order of priority. Generally, groups are reserved for units at the caldera-related volcanic centre level, or the whole of a stratovolcano. However, the spatial distribution of two groups may occupy an overlapping footprint if separated by a major unconformity or other distinction (e.g. two calderas or stratovolcanoes of markedly different age). Formation, member and other sub-units have been applied to packages of variable spatial or chronological coverage depending on the group. In some cases, sub-groups have been used (e.g. where a particularly large supereruption in a short period of time has buried a large area and the second-order subsets are generally of a larger-than-formation scale). The use of formations for fallout/airfall tephra units has had a variable application over many decades. In some cases, these have included the deposits of single fall events without any unconformity, but in other cases many fall units and even intervening paleosols. Nearly always, such ‘formations’ are not of a mappable scale or thickness, but the linkage between mapped stratigraphic units and tephra units is usually depicted in a comparison table in the accompanying bulletin. Stratigraphic legends in some cases include lines marking the most widespread marker tephra’s ages and linkages to coeval map unit(s).

Map purpose

Generally, the map, legend, and especially the bulletin, take into account as much of the range of expected users as possible, and will include content to help with:

- Resource discovery and use,
- geotechnical investigations,

- volcano monitoring basis (past activity of the volcano),
- hazard and risk mapping (volcanic and tectonic),
- Emergency management decision-making,
- Public interest/education and earth science literacy.

Specific points of consideration

There are several aspects that we have found to require specific attention and decisions before and during the compilation of each map:

Data sources – for each of the case study maps these referenced sources number in the dozens of main source maps and hundreds of total maps, theses and map-related publications. In some areas there are many, overlapping sources. The challenge is to determine the most useful or correct one(s), especially if they are incompatible in their interpretations. Additional petrographic, geochemical, radiometric age, geomorphic, satellite, air photo and LiDAR datasets are integrated with, more recently, input from hyperspectral remote sensing looking promising. In all cases map compilation drafts are field checked, and in areas where there is no existing data or mapping primary field work is conducted. For areas of incompatible published interpretations, fieldwork and (often also) lab work are used to determine the preferred interpretation. Studies resulting in substantial new stratigraphic units, interpretive models, or geochemical/age data are preferably also published in peer reviewed journals as well as being presented in the map and bulletin.

Interpolation - especially with sparse exposure is a major challenge throughout most of New Zealand's volcanoes due to the temperate climate and substantial rainfall leading to dense vegetation cover. This iteratively becomes easier with an understanding of the wider geological/volcanic context, but often means there are a range of possible interpretations with inferred and concealed contacts being more common than precise observed contacts. Above the bush line in TNP is a marked exception, where there is excellent exposure.

Handling erosion and burial – to allow for this we usually map the landscape-forming unit. This is a judgement call but often correlates to the order of 10 m thick or thicker top layer(s) at 1:250,000 and perhaps half of this at 1:50,000. However, thickness is less important when compared to geomorphic interpretation. If the geomorphic nature of a landform in terms of its deposition process is visible in the deposit, then this is the mapped unit. If that landform represents the nature of an underlying

deposit within the 10 or so meters of the surface, then that is instead the mapped deposit. With cases of widespread landscape-mantling fallout/airfall tephra of more than 10 m thickness (e.g. the Mangaone Subgroup in the Bay of Plenty) a stipple has been used allowing the underlying unit to also be shown by colour. Many volcanic contacts, especially in the central TVZ and in Auckland Volcanic Field, are vertical or inclined, so use of stippling, or thickness cut-offs, and classical stratigraphic succession representations are of limited value. In places where stream erosion, or remnant razor-back ridges, expose very narrow but long outcrops, symbolised lines have been used to represent key units. This symbol (including a line segment in the legend) has been borrowed from the 'horizon' feature in sedimentology (e.g. a limestone bed in a sandy unit) but the application is not strictly consistent with that definition.

Inter-relationships of map, legend, and bulletin text – much consideration is given in New Zealand to geological map legends and the case study maps (and most maps in general in recent decades) have a large spatio-temporal legend that symbolises relative location in space from left to right (flattened from radial sector for the cone volcanoes), and age on the vertical axis. The size, spacing and shape of the legend 'swatches' are all varied to maximise the explanation of stratigraphic relationships. Long sentence or sometimes multi-sentence descriptions are attempted where space permits. There is an emphasis on relatively long bulletins rich with color figures and text to explain the units, geomorphology, hazards, resources, tectonics and, in the case of volcano-specific maps like TNP and TVZ, cartoons that explain the eruption history. These are printed in soft-cover to keep costs down and also to allow for more frequent reprinting. This then allows for more frequent updates of both the map/legend and the bulletin at the time of reprinting (as often as every 5-10 years).

Physical map compilation – GNS Science have (like many map makers) moved from pencil on mylar to heads-up topologically-correct mapping in ArcMap. For volcano maps this is true from TNP map onwards. Record sheets (physical or digital) are usually compiled at a scale 4-6 times more detailed than the final product, with a target minimum polygon print width of 5 mm at publication scale, but allowing for narrowing in places (especially valley bottoms) to less than this.

Description vs interpretation – there is an emphasis on description in map units themselves, along with a separate statement as to the interpreted deposit type. The classification into group/formation/member etc., requires an interpreted model and so the balance of description and interpretation is always a challenge. Ideally, if



Fig. 3 – View looking southwest over the Taupo super-volcano (now partly infilled by Lake Taupo), towards the snow-capped stratovolcanoes of Tongariro National Park. GNS Science photograph by Dougal Townsend.

descriptive units would still be independent enough that many could be re-applied in the new interpretation, but this cannot be guaranteed. In the case of TNP map, the constructional model for both Ruapehu and Tongariro volcanoes has changed markedly with the new map to recognise that both volcanoes have spent the majority of their construction under and next to substantial volumes of glacial ice. Formations and some members from previous research and thesis publications were able to be retained, but not all.

The use of proper nouns and physical volcanology – in the case studies here a departure from some previous published map and research uses was made. Proper nouns had in many cases included technical interpretive terms such as Ignimbrite, Breccia or Pyroclastics. In many cases these were simplifications of formations that also included other deposits (e.g. fallout/airfall tephra) or for which the process was ambiguous (e.g. breccia) and they have been formalised as groups, formations and members. Un-capitalised physical volcanology descriptors are still used in interpretations regularly. For example, ignimbrite (acceptably differentiated in text as ‘Whakamaru ignimbrite’) is a substantial component of the Whakamaru Group, but the presence in the Group of fallout/airfall tephra and other deposits means that previous use of Whakamaru Ignimbrite for the whole suite of deposits was misleading.

Emphasis: Colour, stipple, digital terrain models – the QMAP series uses a standard national colour scheme that allocates pink-red tones to volcanic rocks. Ad-hoc maps such as TNP and TVZ in contrast can use a full topic-specific internal colour

palette. For the TVZ map we continue previous volcano map conventions for New Zealand of using a range of blues and greens for rhyolite lava and ignimbrite, reserving pinks and reds for andesites through basalts. The TNP map, being mostly andesite, mostly kept to this scheme but did venture more widely than simply red through pink. Colour and stipple are generally applied to maximise the clarity of the volcanic evolution and differences in the map, generally linked to both eruptive vent and petrological affinities, with tone (darker vs. lighter) adding emphasis for age variation. The TNP map uses an underlying shaded relief digital terrain model to enhance public readability.

Paper vs. digital products – paper maps and bulletins continue to be produced and the TVZ map is planned to be published this way. However, full digital GIS datasets for these case study maps are also available and are perhaps equally or even more frequently used by academics. The QMAP seamless coverage for New Zealand is digital only, but individual ‘sheets’ are still re-printed from it, as stocks of the original independent sheets run out.

Acknowledgements

We highlight and thank the many dozens of New Zealand volcanic geologists and international collaborators that have directly contributed to the map case studies discussed here, along with the authors of hundreds of source maps compiled or updated into these example maps. We refer the reader to the Acknowledgements and References lists in the individual map bulletins of Leonard et al. (2010) and Townsend et al. (2017).

References

- Heron DW (custodian) (2018) Geological map of New Zealand 1:250,000 (2nd ed.). Lower Hutt, NZ: GNS Science. GNS Science geological map 1. 1 CD
- Kermode L (1992) Geology of the Auckland Urban Area: Sheet R11: 1:50 000. Institute of Geological & Nuclear Sciences, Lower Hutt.
- Leonard GS, Begg, JG, Wilson CJN (compilers) (2010) Geology of the Rotorua area. Institute of Geological & Nuclear Sciences 1:250 000 geological map 5. 1 sheet + 102 p. Lower Hutt, New Zealand. GNS Science.
- Townsend DB, Leonard GS, Conway CE, Eaves SR, Wilson CJN (compilers) (2017) Geology of the Tongariro National Park area [map]. Lower Hutt (NZ): GNS Science. 1 sheet + 109 p., scale 1:60 000. (GNS Science geological map 4).

Paleomagnetic insights into mapping deposits of eruptive periods

Geoffrey A. Lerner¹, Shane J. Cronin¹ and Gillian M. Turner²

¹ School of Environment, The University of Auckland, Auckland, New Zealand; g.lerner@auckland.ac.nz

² School of Chemical and Physical Sciences, Victoria University of Wellington, Wellington, New Zealand

Keywords: paleomagnetism, pyroclastic flows, Taranaki

Understanding the type and temperature of mass flows from stratovolcanoes is necessary for properly mapping volcanic deposits. Volcanic sequences frequently contain a variety of deposit types resulting from varying styles and sizes of eruptions. These deposits are not necessarily always easily distinguishable in the field based on outcrop characteristics like fabric, color, sorting, and clast description. This is particularly the case at distal outcrops where clast material is frequently rare.

Paleomagnetism provides a valuable tool in the volcanologist's toolbox for distinguishing high temperature (>500 °C) pyroclastic density current (PDC) deposits from cold (ambient temperature) debris flow and hyperconcentrated flow units. By analyzing the direction of thermoremanent magnetization (TRM) of the clasts or the matrix of a deposit, it is possible to distinguish between deposits emplaced above and below the Curie temperature of

the magnetic minerals in the deposit (frequently ~580 °C). Further, for deposits emplaced at intermediate temperatures (~100-580 °C), analysis of vector component diagrams can allow a precise estimation of emplacement temperature.

These methods were employed at Mt Taranaki, an active stratovolcano on the North Island of New Zealand, in order to evaluate both the recent activity of the past 1000 years as well as older, larger eruptions from the volcano.

Deposits from the Maero Formation, representing activity at Taranaki from c. AD 960-1800 were found to represent primarily a series of >500 °C deposits emplaced in medial distances from the volcano (~5-15 km). This sequence contains 11 temporally distinct episodes, mostly resulting from the collapse of hot lava domes, resulting in hot block-and-ash flow (BAF) deposits, with rare reworked, low-temperature units. The TRM analysis

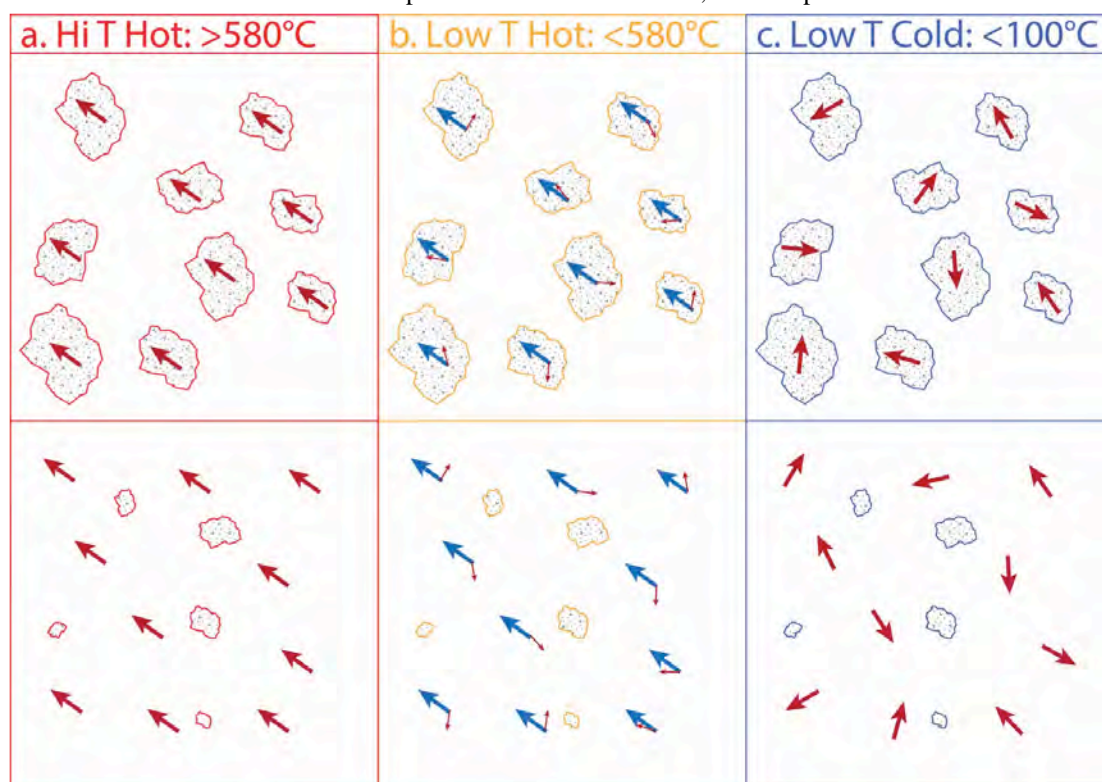


Fig. 1 – Conceptual diagram of paleomagnetic emplacement temperature method. Three scenarios are possible: a) deposit emplaced at high temperature (PDC), resulting in alignment of single component of TRM, b) deposit emplaced at intermediate temperature (low temperature PDC), resulting in multi-component TRM with alignment of the post-emplacement component, c) deposit emplaced at ambient temperature (lahar or reworked deposit), resulting in randomization of TRM direction.

provided a way to distinguish between these primary and reworked deposits which appeared virtually identical in the field, showing that additional laboratory analysis can be valuable when attempting to map deposits of different type and origin.

Matrix material from the distal deposits of the ~11,500 BP Warea Formation was also analyzed, with alignment of TRM directions and analysis of vector component diagrams showing an intermediate emplacement of most deposits around 300-400 °C. These deposits, located up to 24 km from the volcano, show significantly longer runout of PDCs than previously mapped high temperature deposits at Taranaki (~15 km). This shows the largest possible PDC hazard at Taranaki and has impact on hazard mapping and mitigation at the volcano.

This comparison of the size and type of deposits emplaced during recent activity with older deposits representing the full range of activity types at a stratovolcano allows for the analysis of activity at during the current period of activity. Activity types of the last 1000 years at Taranaki do not represent the full range of activity seen over the last 30,000 years at the volcano (e.g. the large-scale eruption represented by the Warea deposits), thus hazard in the current regime of activity may not represent the same range of hazard presented over Taranaki's entire history.

Acknowledgements

The authors would like to acknowledge numerous field assistants who aided in sample collection. GL would like to thank AINSE Ltd for providing financial assistance (Award - PGRA) to enable work on this project and to the George Mason Charitable Trust for providing financial assistance towards fieldwork

References

- Aramaki, S. and Akimoto, S.-i., 1957. Temperature estimation of pyroclastic deposits by natural remanent magnetism, *American Journal of Science*, 255:619-627.
- Damaschke, M., Cronin, S., Holt, K., Bebbington, M., and Hogg, A., 2017. A 30,000 yr high-precision eruption history for the andesitic Mt. Taranaki, North Island, New Zealand, *Quaternary Research*, 87:1-23.
- Hoblitt, R.P. and Kellogg, K.S., 1979. Emplacement temperatures of unsorted and unstratified deposits of volcanic rock debris as determined by paleomagnetic techniques. *Geol Soc Am Bull*, 90:633-642.
- Kent, D.V., Ninkovich, D., Pescatore, T. and Sparks, R.S.J., 1981. Paleomagnetic determination of emplacement temperature of the Vesuvius AD 79 pyroclastic deposits, *Nature*, 290:393-396.
- Lerner, G.A., Cronin, S.J., Bebbington, M.S. and Platz, T., in review, The characteristics of a multi-episode volcanic period; the post-AD800 Maero eruptive period of Mt. Taranaki (New Zealand), *Bulletin of Volcanology*
- Lerner, G.A., Cronin, S.J., Turner, G.M. and Piispa, E.J., in review, Recognizing long-runout pyroclastic flow deposits using paleomagnetism of ash, *GSA Bulletin*
- Neall, V.E., Stewart, R.B. and Smith I.E.M., 1986. History and Petrology of the Taranaki Volcanoes, in Smith, I.E.M., ed., *Late Cenozoic Volcanism in New Zealand: Wellington, New Zealand, Royal Society of New Zealand*, 251-263.
- Paterson, G.A., Roberts, A.P., Mac Niocaill, C., Muxworthy, A.R., Gurioli, L., Viramonté, J.G., Navarro, C., and Weider, S., 2010. Paleomagnetic determination of emplacement temperatures of pyroclastic deposits: an under-utilized tool, *Bulletin of Volcanology*, 72:309-330
- Platz, T., 2001. Mapping and characterisation of the volcanoclastic Maero formation deposits on the northwestern sector of Egmont volcano (Mt. Taranaki), New Zealand. Diploma mapping thesis. Ernst-Moritz-Arndt Univ., Greifswald, Germany
- Platz, T., 2007. Understanding Aspects of Andesitic Dome-forming Eruptions Through the Last 1000 yrs of Volcanism at Mt. Taranaki, New Zealand, PhD Thesis, Massey University
- Procter, J.N., Cronin, S.J. and Zernack, A.V., 2009. Landscape and sedimentary response to catastrophic debris avalanches, western Taranaki, New Zealand. *Sedimentary Geology*, 220(3-4): 271-287.
- Schnepf, E., Worm, K. and Scholger, R., 2008. Improved sampling techniques for baked clay and soft sediments, *Physics and Chemistry of the Earth Parts A/B/C*, 33:407-413.
- Uehara, D., Cas, R.A.F., Folkes, C., Takarada, S., Oda, H. and Porreca, M., 2015. Using thermal remanent magnetisation (TRM) to distinguish block and ash flow and debris flow deposits, and to estimate their emplacement temperature: 1991-1995 lava dome eruption at Mt. Unzen, *Journal of Volcanology and Geothermal Research*, 303:92-111.

A violent phreatomagmatic volcano in Arxan-Chaihe Volcanic Field, NE China

Boxin Li¹, Károly Németh¹, Julie Palmer¹, Alan S. Palmer¹ and Jonathan N. Procter¹

¹School of Agriculture and Environment, Massey University, Palmerston North, New Zealand; doomlee1216@hotmail.com

Keywords: intra-plate, phreatomagmatic, pyroclastic beddings

The geology of Northeast China is complex. Not because it has the varieties of landscape ranging from the plain to the mountain ranges, but has numerous mafic volcanic fields many of them with historic and post-Pleistocene activity. The regional tectonic and geological settings have distinctively defined this area in terms of intra-plate continental settings. Much like the East Africa Rift, Northeast China has experienced a series of rifting and extensional tectonic movements since the Mesozoic. The monogenetic volcanic field, Arxan-Chaihe Volcanic Field (AVCF) is a typical small volcano cluster that formed post-Pliocene and last erupted less than 2000 years ago. At least 24 vents have been discovered in a 3000 km² area. Post-eruptive precipitation and ground-water recharge has filled many of the phreatomagmatic volcanoes forming crater lakes.



Fig. 1 – A view of the Tongxin Lake, from the west.

One such lake, Tongxin Lake, is located at the northeastern-most part of the AVCF. This lake, interpreted as a maar lake by previous researchers, covers an area of approximately 0.4 km² (Fig 1). In September 2018 a group of scientists from Massey University and Institute of Geology and Geophysics, Chinese Academy of Sciences, Beijing undertook a preliminary study of the proximal, median and distal volcanoclastic facies and their distributions (Fig 2).



Fig. 2 – Location of the field sites visited and documented.. At the contact between the bedrock and initial pyroclastic units is exposed. This is the inferred location of the first eruption phase.



Fig. 3 –At Site 1, located on the west flank of the rim, interbedded fine to coarse pyroclastic beds displaying distinctive dune and cross-bedding structures.

Figure 3 shows the proximal units composed of pure pyroclasts (eg. ash, lapilli, tuff breccia) dominated by sub-horizontal, plane parallel bedding. Typical cross beds and dune structures indicate pyroclastic density current transport direction. Ballistic volcanic bombs are intercalated with clast supported lapilli and coarse ash forming distinct laterally continuous horizons. Reverse grading dominates the succession, however, normal grading and symmetric grading are also present. Site 2 has the best preserved sedimentary structures including cross-beds, dunes and chute-and-pool structures (Fig 4). Almost all the beds are supported by very fine to fine ash matrix with intermittent coarse lapilli strings. The componentry of Site 2 is slightly different from Site 1 in respect to the percentages of

each rock type, mineral occurrence and general grain size while the bedding structures are the same.



Fig. 4 – The Site 2 general view, comparing with Site 1, the clasts are finer than the one within the Site 1, this is assumed as shock wave in which the pyroclastic materials transport with tremendous velocity and contain highly devastating energy.

Documenting surface textures of juvenile and bedrock clasts together with grain size analysis and point counting were undertaken to determine the likely magnitude of the eruptive events as well as the involvement between juvenile material and bedrock during the eruptions (Fig 5).

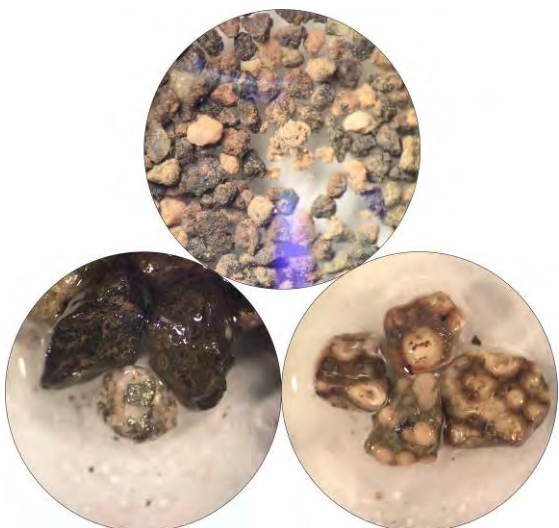


Fig. 5 –Microscopy reveals the presence of angular lithics and juvenile scoriaceous lapilli sized particles .Ppyrite on the surface of a granitoid bedrock clast and “teeth-like” granitoid accidental lithics are also present.

Preliminary results suggest Tongxin Lake experienced repeated eruption phases with various eruption styles that appear to be dominated by intensive phreatomagmatic explosions. These results point to the presence of a distinct monogenetic volcanic field in NE China.

Acknowledgements

The author wishes to thank all the members of supervision board who provide the precious opinions, especially for Dr Alan Palmer who accompanied during the very first field trip and brought the invaluable fieldwork experiences. Also, many thanks to the Massey University provided the scholarship which reinforced this research, and two Chinese colleagues Dr Wu and Dr Sun to be the field guides during the entire trip.

References

- Li, B., 2018. Violent phreatomagmatic eruptions that formed maars in an intra-mountain basin at Arxan-Chaihe Volcanic Field, Inner Mongolia, China (unpublished Master's thesis). Massey University, Palmerston North, NZ. p. 163
- Németh, K. and Kereszturi, G., 2015. Monogenetic volcanism: personal views and discussion. *International Journal of Earth Sciences*, 104(8): 2131-2146.
- Németh, K., Wu, J., Sun, C. and Liu, J., 2017. Update on the Volcanic Geoheritage Values of the Pliocene to Quaternary Arxan–Chaihe Volcanic Field, Inner Mongolia, China. *Geoheritage*, 9(3): 279-297.
- Németh, K., 2010a. Monogenetic volcanic fields: Origin, sedimentary record, and relationship with polygenetic volcanism, *What Is a Volcano? Geological Society of America Special Papers*, pp. 43-66.
- Wilson, C.J.N., 2001. The 26.5 ka Oruanui eruption, New Zealand: an introduction and overview. *Journal of Volcanology and Geothermal Research*, 112(1-4): 133-174.
- Zernack, A.V., Procter, J.N. and Cronin, S.J., 2009. Sedimentary signatures of cyclic growth and destruction of stratovolcanoes: A case study from Mt. Taranaki, New Zealand. *Sedimentary Geology*, 220(3-4):288-305.

Explosive volcanism triggered by superslow ascent of hot andesites

Charline Lormand¹, Georg F. Zellmer¹, Geoff Kilgour², Karoly Németh¹, Alan S. Palmer³, Naoya Sakamoto⁴, Hisayoshi Yurimoto⁴, Takeshi Kuritani⁵, Yoshi Iizuka⁶ and Anja Moebis³

¹ School of Agriculture and Environment, Volcanic Risk Solutions, Massey University, PO Box 11222, Palmerston North 4442, New Zealand; charline.lormand@massey.ac.nz

² GNS Science, Wairakei Research Centre, PO Box 2000, Taupo 3352, New Zealand

³ School of Agriculture and Environment, Department of Soil Science, Massey University, PO Box 11222, Palmerston North 4442, New Zealand

⁴ Isotope Imaging Laboratory, Hokkaido University, Sapporo 060-0810, Japan

⁵ Graduate School of Science, Hokkaido University, Sapporo 060-0810, Japan

⁶ Institute of Earth Sciences, Academia Sinica, 128 Academia Road Sec. 2, Nankang, Taipei 11529, Taiwan

Keywords: magma ascent, microlites, crystal size distributions

Deciphering timescales and rates of eruptive processes such as magma residence time and magma ascent rate is critical to the volcanology research community to understand volcano behaviours, and to improve evacuation plans and hazard maps mitigation in anticipation of future eruptions. Several techniques have been used to estimate it such as using the thickness of breakdown rims around amphiboles (Hammer and Rutherford, 2002; Rutherford and Hill, 1993), modelling elemental diffusion (e.g., Chen et al., 2013; Demouchy et al., 2006; Humphreys et al., 2008) or based on seismicity (Aki and Koyanagi, 1981; Endo et al., 1996). Microlite textures and growth measurements compared with data from decompression experiments (Cashman, 1992; Geschwind and Rutherford, 1995) also allow to infer processes of magma ascent.

The Tongariro Volcanic Centre (TgVC) located at the southern end of the Taupo Volcanic Zone in the North Island of New Zealand is part of an active volcanic arc and is composed of two major volcanic centres, namely Ruapehu and Tongariro, with several vent sites such as for instance the Ngauruhoe stratovolcano, part of the TgVC. Historical eruptions from the TgVC have been Strombolian to Plinian style and their deposits have been preserved as tephra formations. The last eleven thousand years of the TgVC's activity has produced frequent, well-documented volcanic events of differing intensities and styles. Complete stratigraphy of these volcanic events were thoroughly described in several previous works (Auer et al., 2015; Donoghue and Neall, 1996; Donoghue et al., 1995a; Moebis et al., 2011; Nairn et al., 1998; Nakagawa et al., 1998; Topping, 1973).

A semi-automatic segmentation method was used to outline microlites of pyroxene and plagioclase from BSE images of 118 glassy tephra from (Lormand et al., accepted). The larger

microlites (>30 µm) display complex growth zoning (see Figure), and only the smallest crystals have formed during magma ascent in the conduit. A combination of orthopyroxene geothermometry (Putirka, 2008), plagioclase hygrometry (Waters and Lange, 2015), and MELTS modelling is used to determine constraints on pressure, temperature and water content during crystallisation.

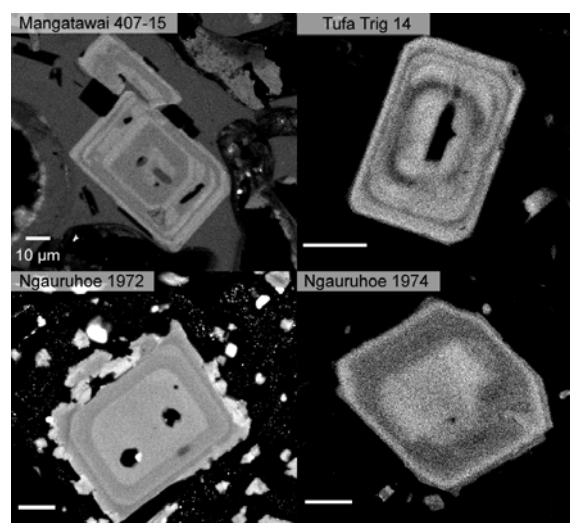


Figure – Fe-maps of orthopyroxene microlites obtained using the FE-SEM JEOL JSM-7000F at the Isotope Imaging Laboratory of Hokkaido University in Sapporo, Japan. Note the resorbed cores and the complex zonations in iron. The scale of 10 microns is represented by a white lamella at the left bottom corner of each image.

Size distributions of a total of 228 CSDs including >60,000 microlites yield concave-up curves with similar slopes of the smallest size irrespective of eruption style. Combining a well-constrained orthopyroxene crystal growth rate from one typical tephra (Zellmer et al., 2016) and the CSD slopes yield to timescales of microlite formation ranging from 10 to 30 hours. Hygrothermobarometry and MELTS both indicate

that these microlites began to grow at maximum pressures of 5.5 kbar from hot magmas (1010-1130 °C) with low H₂O content (0-1.5 wt. %). The low crystallinity of the tephras is consistent with the low water content and the high temperature. These data imply that microlites form in response to cooling of melts ascending at velocities of <20 cm/s prior to H₂O exsolution, which only occurs at <330 bars. Water exsolution during final decompression yields maximum ascent rates of <30 m/s, still more than an order of magnitude lower than the supersonic vent velocities typical of Vulcanian or sub-Plinian eruptions. This implies that most of the magma ascending from depth occurs in dikes, and that vent velocities at the surface are controlled by a reduction of conduit in size towards the surface, possibly modulated by phreatomagmatic processes. The constraints on depths and timescales of magma ascent provided by this data should be key to future volcano monitoring and hazard mitigation efforts in the southern Taupo Volcanic Zone, and the methods employed here will be useful in assessing volcanic hazards globally.

References

- Aki, K. and Koyanagi, R.Y., 1981. Deep volcanic tremor and magma ascent mechanism under Kilauea, Hawaii. *Journal of Geophysical Research*, 86: 7095-7110.
- Auer, A., Martin, C.E., Palin, J.M., White, J.D.L., Nakagawa, M. and Stirling, C., 2015. The evolution of hydrous magmas in the Tongariro Volcanic Centre: the 10 ka Pahoka-Mangamate eruptions. *New Zealand Journal of Geology and Geophysics*, 58(4): 364-384.
- Cashman, K.V., 1992. Groundmass crystallization of Mount St. Helens dacite, 1980-1986: a tool for interpreting shallow magmatic processes. *Contrib Mineral Petrol*, 109(4): 431-449.
- Chen, Y., Provost, A., Schiano, P. and Cluzel, N., 2013. Magma ascent rate and initial water concentration inferred from diffusive water loss from olivine-hosted melt inclusions. *Contributions to Mineralogy and Petrology*, 165: 525-541.
- Demouchy, S., Jacobsen, S.D., Gaillard, F. and Stem, C.R., 2006. Rapid magma ascent recorded by water diffusion profiles in mantle olivine. *Geology*, 34: 429-432.
- Donoghue, S.L. and Neall, V.E., 1996. Tephrostratigraphic studies at Tongariro Volcanic Centre, New Zealand: an overview. *Quaternary International*, 34-36: 13-20.
- Donoghue, S.L., Neall, V.E. and Palmer, A.S., 1995a. Stratigraphy and chronology of late Quaternary andesitic tephra deposits, Tongariro Volcanic Centre, New Zealand. *Journal of the Royal Society of New Zealand*, 25: 115-206.
- Endo, E.T., Murray, T.L. and Power, J.A., 1996. A comparison of pre-eruption, real-time seismic amplitude measurements for eruptions at Mount St. Helens, Redoubt Volcano, Mount Spurr, and Mount Pinatubo. In: C.G. Newhall and R.S. Punongbayan (Editors), *Eruptions and Lahars of Mount Pinatubo, Philippines*, University of Washington press, pp. 233-246.
- Geschwind, C.H. and Rutherford, M.J., 1995. Crystallisation of microlites during magma ascent - the fluid-mechanics of 1980-1986 eruptions at Mount-St.-Helens. *Bulletin of Volcanology*, 57: 356-370.
- Hammer, J.E. and Rutherford, M.J., 2002. An experimental study of the kinetics of decompression-induced crystallization in silicic melt. *Journal of Geophysical Research: Solid Earth*, 107(B1): ECV8-1 - ECV8-24.
- Humphreys, M.C.S., Menand, T., Blundy, J.D. and Klimm, K., 2008. Magma ascent rates in explosive eruptions: Constraints from H₂O diffusion in melt inclusions. *Earth and Planetary Science Letters*, 270: 25-40.
- Lormand, C., Zellmer, G.F., Nemeth, K., Kilgour, G., Mead, S., Palmer, A.S., Sakamoto, N., Yurimoto, H. and Moebis, A., accepted. Weka Trainable Segmentation plugin in ImageJ: a semi-automatic tool applied to crystal size distributions of microlites in volcanic rocks. *Microscopy and Microanalysis*.
- Moebis, A., Cronin, S.J., Neall, V.E. and Smith, I.E., 2011. Unravelling a complex volcanic history from fine-grained, intricate Holocene ash sequences at the Tongariro Volcanic Centre, New Zealand. *Quaternary International*, 246: 352-363.
- Nairn, I.A., Kobayashi, T. and Nakagawa, M., 1998. The ~10 ka multiple vent pyroclastic eruption sequence at Tongariro Volcanic Centre, Taupo Volcanic Zone, New Zealand: Part 1. Eruptive processes during regional extension. *Journal of Volcanology and Geothermal Research*, 86: 19-44.
- Nakagawa, M., Nairn, I.A. and Kobayashi, T., 1998. The ~10 ka multiple vent pyroclastic eruption sequence at Tongariro Volcanic Centre, Taupo Volcanic Zone, New Zealand: Part 2. Petrological insight into magma storage and transport during regional extension. *Journal of Volcanology and Geothermal Research*, 86: 45-65.
- Putirka, K.D., 2008. Thermometers and barometers for volcanic systems. In: K.D. Putirka and F. Tepley (Editors), *Reviews in Mineralogy and Geochemistry*, pp. 61-120.
- Rutherford, M.J. and Hill, P.M., 1993. Magma ascent rates from amphibole breakdown: An experimental study applied to the 1980-1986 Mount St. Helens eruptions. *Journal of Geophysical Research*, 98(B11): 19667-19685.
- Topping, W.W., 1973. Tephrostratigraphy and chronology of late quaternary eruptives from the Tongariro Volcanic Centre, New Zealand. *New Zealand Journal of Geology and Geophysics*, 16(3): 397-423.
- Waters, L.E. and Lange, R.A., 2015. An updated calibration of the plagioclase-liquid hygrometer-thermometer applicable to basalts through rhyolites. *American Mineralogist*, 100(10): 2172-2184.
- Zellmer, G.F., Sakamoto, N., Matsuda, N., Iizuka, Y., Moebis, A. and Yurimoto, H., 2016. On progress and rate of the peritectic reaction Fo + SiO₂ → En in natural andesitic arc magmas. *Geochimica et Cosmochimica Acta*, 185: 383-393.

An integrated stratigraphic platform for volcanic fieldwork and mapping

Federico Lucchi¹

¹ *Dipartimento di Scienze Biologiche, Geologiche e Ambientali, Università degli Studi di Bologna, Italy; federico.lucchi@unibo.it*

Keywords: lithostratigraphy, unconformity-bounded units, eruptive history

Volcanic fieldwork and mapping must face a much more complex geological nature than any other sedimentary settings, arising from a great diversity of rock types, components and grain sizes, extremely dynamic transport and depositional regimes and multiple (often simultaneous) vents of variable geometry and location. The episodic nature of eruptive events may result in a rapid and catastrophic supply of volcanic products interrupted by quiescence periods of variable duration. Caldera and lateral (flank/sector) collapses commonly lead (together with dykes and intrusive bodies) to complex stratigraphic and structural patterns, posing serious challenges for geological mapping and stratigraphic correlation. The purpose here is to provide insights on a widely acceptable procedure for stratigraphic analysis in field volcanology on which objective and largely acceptable geological maps and stratigraphic frameworks are built up as

essential datasets to best support petrological studies, physical volcanology and modeling, hazard evaluation, resource-exploration analyses, and territorial planning. This methodology mostly follows the guidelines of the International Stratigraphic Guide (ISG) (Salvador 1994), with a few departures aimed at adequately taking into account some special features of volcanic successions (Pasquarè et al., 1992; Lucchi, 2013, 2018). Such suggestions are proposed in order to improve the communication with regional stratigraphers and geologists working in other geological environments. The integrated use of different rock-stratigraphic units (lithostratigraphic units, lithofacies, lithosomes, unconformity-bounded units), combined with time-stratigraphic units (Tab. 1), provide (para)objective and complete stratigraphic and geological data for any volcanic terrain. The concepts and practice of this

Table 1 - Summary of rock-stratigraphic and time-stratigraphic units adopted for volcanic fieldwork and mapping (see the text for references)

	CATEGORY	DEFINITION	UNIT-TERMS	PURPOSE OF STUDY
ROCK- STRATIGRAPHY (objective or para- objective)	Lithostratigraphic Units	Rock bodies defined and recognized on the basis of observable and distinctive lithologic properties and stratigraphic relations in a vertical succession	<i>Group</i> Formation (<i>primary unit</i>) Member	Basic units of geological mapping. Description of rock types and reconstruction of (vertical) rock successions
	Lithofacies	Subdivisions of a lithostratigraphic unit based on distinctive lithologic characters (stratification, grain size, components, grain shape, sorting, fabric)	near-vent, proximal, intermediate, distal facies	Lateral or vertical variations induced by i) time, ii) paleo-topography and iii) increasing distance from the source
	Lithosomes (<i>informal</i>)	Rock bodies with distinctive 3D geometry	lithosome (<i>dimensionless</i>)	Identification of eruptive vents and volcanic edifices (or other sedimentary bodies)
	Unconformity-Bounded Units	Rock bodies bounded below and above by significant and demonstrable unconformities representing a considerable stratigraphic hiatus	<i>Supersynthem</i> Synthem Subsynthem Minor Subsynthem	Stratigraphic correlation and synthesis on a local to regional scale (not mappable)
TIME- STRATIGRAPHY (interpretative - not mappable)	Eruption Units	Volcanic material emplaced during a single eruption, eruptive phase or pulse	Lava flow, fallout, pyroclastic density current, lahar (...) eruption units	Internal architecture of a volcanic succession and information on its eruptive and depositional behaviour
	Volcanic Activity Units	Periods of relatively continuous volcanic activity separated by intervals of quiescence of varying time duration	Eruptive period - <i>ka to Ma</i> Eruptive Epoch - <i>tens years to ka</i> Eruption - <i>days to years</i> Eruptive phase - <i>min. to days</i> Eruptive pulse - <i>sec. to min.</i>	Determination of the main steps of eruptive history

methodology, as well as arguments *pro et contra* the use of the different stratigraphic units, are discussed mostly, but not uniquely, on the basis of the twenty-year working experience in the stratigraphy and mapping of the Aeolian Islands volcanoes (Lucchi et al., 2013). This approach includes the following steps: (1) describing and documenting the different rock/deposit types (using lithostratigraphic units); (2) recognizing the main source areas and distribution of active eruptive vents (using lithosomes); (3) establishing correlations and deciphering the main building and destruction stages of a volcano (using unconformity bounded units); (4) interpreting the eruptive history of a volcano and its distinctive eruption styles (and vents) through time (combining rock-stratigraphic units and volcanic activity units).

Lithostratigraphic units (in order of decreasing rank: group, formation, member) are the basic units of geological mapping and stratigraphy in volcanic terrains, as in any other geological environments. “Formations” and “members” are introduced to describe and map the main lava bodies and volcanoclastic units (and non-volcanic rock bodies) on the basis of their distinctive lithological features and stratigraphic position (and age) in a vertical succession of rocks. The number of mapped units depends on the age and exposure of a volcanic area (ancient vs recent), the fieldwork scale and aims of the study. “Flows” may be subordinately introduced for distinctive (and widespread) lava bodies. “Beds” and “laminae” are instead applied to distinct layers of variable thickness in a stratified volcanoclastic unit according to the nomenclature of Ingram (1954). The aggregation of formations with common lithologic properties into “groups” is considered less useful than other merging criteria (e.g. lithosomes and unconformity-bounded units).

Lithofacies criteria are adopted to describe the mapped lithostratigraphic units based on their physical characteristics, such as colour, nature and abundance of the juvenile components, grain size characteristics and sorting, thickness variations and depositional features (see Branney and Kokelaar, 2002; Sulpizio and Dellino, 2008 for reviews). Lithofacies are particularly useful to describe the lateral (near-vent to distal) or vertical variations of the physical features of some volcanic units related to time, paleo-topography, and increasing distance from the source, and provide strong constraints on transport and emplacement mechanisms.

Lithosomes are originally defined as (informal) rock-stratigraphic units with variable lithologic properties that are defined and characterized on the basis of their geometrical features and specific physico-chemical environment (Wheeler and Mallory, 1953, 1956; Weller, 1960). In volcanic stratigraphy and mapping, lithosomes may identify

eruptive vents or volcanic edifices with a distinctive 3D geometry (e.g. tuff ring/tuff cone, scoria cone, lava dome/coulee, composite volcano or stratovolcano), independently of their dimensions, mono- or polygenesis, eruptive style and type and volume of erupted products (Lucchi, 2013). A volcanic lithosome can correspond to a number of aligned scoria cones or lava domes erupted (almost) contemporaneously from an eruptive fissure or even a volcanic body (e.g. lava flow field or pyroclastic deposit) with geometry and thickness variations clearly indicative of an adjacent, spatially connected or disconnected, external source area. The definition of lithosomes is objective to semi-objective, based on the interpretation of the geometric features of a volcanic rock body in relation to its provenance source. This allows to put emphasis on the morphological factor and its fundamental role in the definition of the eruptive vents and their localization through time, particularly in recent to active volcanic areas. Lithosomes are generally not directly mapped, and are suggested to be used only in association to lithostratigraphic units. Their use is warmly supported when lithosomes group together two or more lithostratigraphic units with a common volcanic source. The intertonguing between distinct adjacent lithosomes may be useful to recognize the relative chronology of volcanic rock bodies originated from different and alternating source areas, resulting in articulated vertical successions of lithostratigraphic units. By doing so, lithosomes allow definition of the vertico-lateral relationships between distinct rock bodies (which is generally not accurately possible using lithostratigraphic subdivisions alone), thus contributing to the purpose of a broader stratigraphic synthesis and correlation.

Unconformity-Bounded Units (UBU) are rock bodies bounded below and above by significant and demonstrable unconformities representing evident gaps in the stratigraphic record (Chang, 1987; Salvador, 1994). The basic UBU is the “synthem”, which can be subdivided into two or more “subsynthems” or aggregated with other synthems into a “supersynthem”. The synthem stratigraphy is suggested here as the preferred terminology to be used in volcanic areas (Lucchi, 2018), although other (partly different) schemes of nomenclature for stratigraphic units essentially bounded by unconformities exist in the literature (i.e., allostratigraphic units, sequences). UBUs are differentiated only by the presence or absence of the bounding unconformities, being independent of the lithological features of the content and its genetic significance. Thus, they can be objectively identified as far as the bounding unconformities are significant and identifiable in the field or readily inferred from one outcrop to another. Several unconformities of variable duration, character and areal distribution

occur in volcanic areas reflecting the strongly episodic nature of eruptive activity and the occurrence of caldera and lateral collapses. They correspond to erosive and/or collapse unconformities formed during periods of volcanic quiescence, mostly in response to processes of internal modification of a volcano (Lucchi, 2013; 2018). Most of the erosive unconformities are angular unconformities, and are frequently associated with paleosols and interlayered epiclastic deposits. In volcanic areas angular unconformities typically vary from proximal to distal areas, with higher angles between the bedding planes along the steeper flanks of a volcano passing to low-angle unconformities to disconformities towards the flattish areas at its foot. “Angular unconformities” must be carefully distinguished from “angular discordances” formed during fairly continuous volcanic activity, which are not representative of a significant erosional gap. In volcanic areas angular discordances may form in relation to a variable localization of eruptive vents or specific transport and depositional mechanisms of volcanic products, or even along the rims of crater structures (i.e. crater discordances). Collapse unconformities are related to calderas and lateral collapses, if associated to a quiescent phase of the volcano. These unconformities typically change their character from proximal towards distal areas, passing from sub-vertical faults (within the collapse) to high-angle unconformities (along the flanks of the volcano outside the collapse) to low-angle unconformities or disconformities (along the surrounding ring-plains). In any case, the identification of an effective stratigraphic hiatus is necessary to identify an unconformity. This is frequently mirrored in different lithological features of the products below and above the unconformity as a consequence of shifts of the eruptive vents or changes of magma composition or eruptive style occurred during the corresponding stratigraphic hiatus. Correlation of volcanic unconformities can be not straightforward, and not all of them are equally recognizable in outcrop on large geographic extents. However, the working experience in the Aeolian Islands (Lucchi et al., 2013) and other volcanic areas (e.g. Pardo et al., 2018) has shown that unconformities and UBUs can be generally extended laterally if a careful stratigraphic analysis (and dating) is carried out in different points of observations. The correlation of unconformities with a certain chronostratigraphic significance is particularly useful in volcanic stratigraphy, where lithocorrelations, usually more direct and intuitive, are not easily applied. Such difficulty is commonly due to a great diversity of rock/deposit types, sudden lithofacies variation and frequent lithology repetition in different stratigraphic positions, together with a (relatively) limited areal extension of most volcanic

units (except for large-scale ignimbrites and lava flow fields or plinian fallout layers). UBUs allow correlation of geographically distant (vertical) stratigraphic successions characterized by the occurrence of lithologically-different rock bodies, thus displaying a general, synthetic stratigraphic framework on a scale from local to regional. Lithostratigraphic units (and lithofacies) remarkably continue to be the preferred units to be used in volcanic stratigraphy and mapping. However, UBUs can be an additional tool of stratigraphic analysis in volcanic terrains, and should be established when they fulfill the need of subdividing the stratigraphic succession into groups of distinct lithostratigraphic units (and lithosomes) that are recognizable over large areas. Therefore, UBUs allow to establish correlations on different scales and provide a space-time stratigraphic framework into which the description (and interpretation) of the rock bodies in a greater detail can be oriented, as a fundamental contribution to the mapping procedures.

The application of UBUs in volcanic areas suffers from the problem of ranking the unconformities and establishing the hierarchy of the relative UBUs. The rank (or magnitude) of an unconformity is usually evaluated on the basis of i) the time duration of the stratigraphic hiatus, ii) the degree of erosional truncation or structural angularity across an unconformity, and iii) the areal extent of an unconformity (local to regional/interregional). In volcanic areas these criteria are not necessarily dependent on each other, and can be fundamental elements of hierarchy in any one case study. This concept is typified by the collapse unconformities that may be characterized by high-angle surfaces of structural truncation but generally have a limited areal extent and don't necessarily reflect a prolonged stratigraphic hiatus. The classification of UBUs thus depends strictly on the context in which it is proposed, the sediment types, the amount of data available for the stratigraphic analysis and the scale of observation. However, the magnitude of the area involved by the bounding unconformities is suggested as the optimum approach to define the hierarchy of UBUs in volcanic areas, with the purpose of emphasizing the potential use of unconformities for correlations. On this, it is notable that unconformities related to sea level variations can be stratigraphically significant on a regional to interregional scale (given their link with a “global” process), being extended to adjacent volcanic areas characterized by independent genetic processes and eruptive histories. The time duration of stratigraphic hiatus corresponding to an unconformity can be taken into account as a secondary criterion for ranking UBUs, whereas the degree of erosional truncation or structural angularity of an unconformity is considered less

important because too much variable from one location to another and from proximal to distal areas. Also, the importance of the causative geologic process of an unconformity in the volcanic history of an area (e.g. a caldera unconformity) may be adopted to rank unconformities with a similar geographic extent. In terms of nomenclature, synthems are originally defined for mobile belts or stable cratonic sedimentary settings as units bounded by unconformities of regional to interregional areal extent (Salvador, 1994). This would make UBUs substantially impractical in volcanic stratigraphy, where the great majority of unconformities are regionally insignificant. Yet, the adoption of UBUs can be really useful in certain volcanic areas, where even local (lower-rank) unconformities can be equally important to provide stratigraphic subdivision at the scale of individual volcanic edifices subdivided into successive built-up portions. To make appropriate the concept of UBUs to volcanic areas, it is necessary to amend the formal hierarchy proposed in the ISG (Salvador, 1994), and expand their classification. A ninefold rank classification can be obtained if the original terms of supersynthem, synthem and subsynthem are preceded by "major" and "minor". However, the practice of fieldwork in volcanic areas makes it clear that three different orders of rank of UBUs are commonly useful to provide a meaningful stratigraphic framework of classification and correlations at different scales. It is recommendable that synthems are adopted as major-rank UBUs bounded by (first-order) unconformities with a regional to inter-regional significance, conforming with the ISG, in order to promote correlation with adjacent volcanic terrains or other sedimentary environments. Further subdivisions of a synthem on a local scale can be established by means of unconformities with a minor areal extent. Second-order unconformities recognized in most of a volcanic area or a whole volcanic complex, but regionally insignificant, are adopted to define "subsynthems", whereas third-order unconformities recognizable over a limited sector of a volcanic area delimit "minor subsynthems" (Fig. 1). This can provide a practical tool of stratigraphic subdivision and correlation of a volcanic area on a scale from regional to local, and, combined with lithostratigraphic units and lithosomes, a rational approach to the understanding of volcanic stratigraphy.

Field stratigraphy and mapping in volcanic terrains are primarily devoted to the reconstruction of the eruptive history, with a fundamental outcome on hazard assessment in active or recent volcanoes. Volcanic activity units are commonly adopted for the purpose of describing the evolution of volcanic activity (Fisher and Schmincke, 1984; Oerton,

1996). They are time-stratigraphic units defined on the basis of the time duration and eruption types (and location of eruptive vents) through the volcanic successions. Volcanic activity units represent periods of relatively continuous eruptive activity of varying duration, separated by intervals of variable quiescence lapses. It is recommended that volcanic activity units are adopted in volcanic stratigraphy conforming to their original definition, and different terminologies occasionally proposed for volcanic products by modifying the original schemes of nomenclature are considered of little use (e.g. De Rita et al., 2004). The "eruption" is the basic unit corresponding to a relatively continuous period of volcanic activity lasting from days to years, eventually subdivided in "phases" or "pulses". Different eruptions can be aggregated in an "eruptive epoch", lasting tens to thousands of years, or an "eruptive period", developing over thousands to millions of years (Fisher and Schmincke, 1984). A useful link between rock-stratigraphy and time-stratigraphy can be established by interpreting the UBUs recognized in a volcanic area (combined with lithostratigraphic units and lithosomes) in terms of volcanic activity units (Fig. 2). UBUs can be readily interpreted as distinct volcanic activity units, corresponding to the erupted volcanic deposits, separated by intervals of quiescence (and collapses) between eruptions, recorded in the main unconformities (Lucchi, 2013, 2018). The main difficulty in putting this concept into the practice of volcanic stratigraphy is that volcanic activity units are typically classified according to the time duration, which is not easily extractable from the volcanic successions. This may create an obstacle in linking the stratigraphic unconformities with the time duration of the quiescence periods between eruptions. It may be suggested that the major unconformities corresponding to caldera and lateral collapses, long erosional and/or epiclastic deposition intervals or major compositional changes of erupted products are adopted to define different eruptive epochs, as longer units of volcanic activity referred

	First-order unconformities (regional)	Second-order unconformities (island)	Third-order unconformities (island-sectors)
			
1	Synthems	Subsynthems	Minor subsynthems
2	Supersynthems	Synthems	Subsynthems

Fig. 1 - Proposed hierarchy of unconformities and UBUs in volcanic areas based on their areal extent following the Aeolian Islands case study: (1) present work; (2) Lucchi, 2013

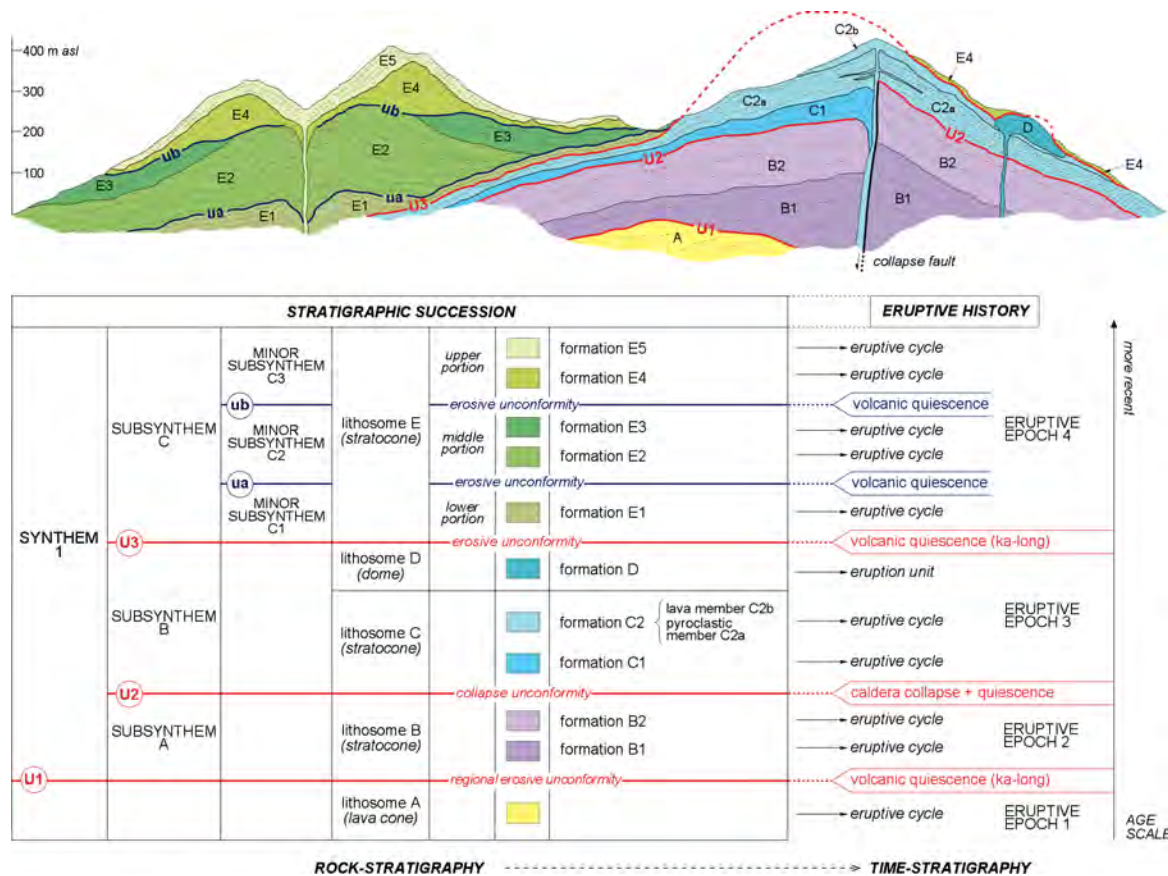


Fig. 2 - Generalized cross-section of a volcanic area and related stratigraphic succession based on UBUs combined with lithosomes and lithostratigraphic units (formations and members). The UBUs are bounded by erosive and collapse unconformities that separate distinct lithosomes (defining the eruptive centres) and lithostratigraphic units (describing the mappable rock bodies). The unconformities have a different rank depending on their areal extension, and the corresponding UBUs are classified according to Fig.1, with synthems being correlated on a regional scale, subsynthems over the whole volcanic area and minor subsynthems recognized in a specific sector of it. A direct relationship between rock-stratigraphic units (UBUs, lithosomes and lithostratigraphic units) and time-stratigraphic units (eruptive epochs, eruptive cycles, eruption units) is also established (see the text for further explanation), providing a scan of the main eruptive, erosional and collapse instability events in the history of the volcanic area on the grounds of the reconstructed stratigraphic succession.

to the construction of independent volcanoes. The epochs are then subdivided in distinct eruptions separated by shorter depositional gaps recorded in minor-rank unconformities. A sequence of eruptions close in time can be defined “eruptive cycle”. These periods of activity are characterized by distinctive location and types of eruptive vents (defined by lithosomes), and lithology and chemical composition of the erupted products (described in the mapped lithostratigraphic units). It is recommended that volcanic activity units are used at the level of interpretation, after that rock classification and correlation of a volcanic succession has been provided by means of rock-stratigraphic units. Volcanic activity units are in fact far too conceptual and of less practical use in geological fieldwork and mapping (Fisher and Schmincke, 1984), especially for older volcanic successions.

On this, “eruption units” are frequently used in volcanic stratigraphy to identify the volcanic deposits emplaced during single eruptions, eruptive

phases or pulses (Fisher and Schmincke, 1984), thus providing a link between rock stratigraphy and time stratigraphy. However, a mappable lithologically-distinctive volcanic unit (formation or member) corresponding to a succession of lava flow units or a pyroclastic succession can be the result of an individual eruption, namely an eruption unit, or even derive from a sequence of eruptions separated by short-lived interruptions of deposition at the considered time scale. This makes difficult to recognize objectively the number of eruption units that constitute a volcanic unit. It is thus recommended that lithostratigraphic units are used as the mappable units at the 1:5,000 to 1:100,000 scales typical of most volcanic fields. The interpretation of the mapped volcanic rock bodies in terms of distinct eruption units of fallout, pyroclastic density currents, lava flows or other eruptive and post-eruption phenomena (e.g. debris avalanche, lahar) can give information on the eruption behaviour and depositional mechanisms in a

volcanic area. Eruption units can be used directly in the field for more detailed volcanic stratigraphy, when the purpose is to understand the internal structure of a pyroclastic succession (possibly lithologically homogeneous) and its eruption dynamics for hazard assessment. Distinct eruption units are delimited by features indicative of interruptions of deposition at the time scale of the considered eruptive process, e.g. erosive surfaces, paleosoils, angular discordances and/or detrital horizons or even changes in components or petrochemical composition. These internal unconformable contacts generally have a time and spatial magnitude smaller than the unconformities used to bound UBUs.

Summarizing, a stratigraphic approach to volcanic fieldwork and mapping based on the integrated use of different rock-stratigraphic units and time-stratigraphic units allows to extract from the field stratigraphy and mapping the fundamental elements for the interpretation of the geologic history of a volcanic area in terms of volcanic, collapse and erosional events (event stratigraphy) and eruptive behaviour. This procedure is mostly based on the common rules of stratigraphic nomenclature at the level of fieldwork and mapping, thus promoting communication and understanding between stratigraphers working in different geological environments and scales.

Acknowledgements

N. Pardo, R. Sulpizio, G. Gropelli, G. Giordano, K. Nemeth and many other colleagues participating to the IAVCEI Commission on Volcano Geology are warmly thanked for having discussed in different occasions the main topics of the presented procedure of stratigraphic analysis and mapping in volcanic terrains.

References

- Branney, M.J., Kokelaar, P., 2002. Pyroclastic density currents and the sedimentation of ignimbrites. *Geological Society of London, Memoirs*, 27, pp. 143.
- de Rita, D., Giordano, G., Fabbri, M., Rodani, S., 2004. Cartography of syn-eruption and inter-eruption deposits: the example of Roccamonfina Volcano. In: Pasquare`, G., Venturini, C., Gropelli, G., (eds), 2004. *Mapping Geology in Italy*. APAT (Agenzia per la Protezione dell'Ambiente e per i servizi Tecnici), Dipartimento difesa del suolo, Geological Survey of Italy, SELCA, Firenze, pp. 131-136.
- Fisher, R.V., Schmincke, H.-U., 1984. *Pyroclastic Rocks*. Berlin, Springer Verlag, pp. 472.
- Ingram, R.L., 1954. Terminology for the thickness of stratification and parting units in sedimentary rocks. *Geological Society of America Bulletin*, 65: 937-938.
- Lucchi, F., 2013. Stratigraphic methodology for the geological mapping of volcanic areas: insights from the Aeolian archipelago (southern Italy). *Geological Society of London, Memoirs*, 37: 37-53.
- Lucchi, F., 2018. On the use of unconformities in volcanic stratigraphy and mapping: insights from the Aeolian Islands (southern Italy). *Journal of Volcanology and Geothermal Research* accepted to press.
- Lucchi, F., Peccerillo, A., Keller, J., Tranne, C.A., Rossi, P.L. (eds.), 2013. *The Aeolian Islands Volcanoes*. Geological Society of London, Memoirs, 37, pp. 510.
- Orton, G.J., 1996. Volcanic environments. In: Reading, H.G. (ed.), *Sedimentary Environments: Processes, Facies and Stratigraphy*. Blackwell Science, Oxford, pp. 485-567.
- Pardo, N., Pulgarín, B., Betancourt, V., Lucchi, F., Valencia, L.J., 2018. Facing geological mapping at low-latitude volcanoes: The Doña Juana Volcanic Complex study-case, SW-Colombia. *Journal of Volcanology and Geothermal Research, VOLGEO-06359*, pp. 21.
- Pasquare`, G., Abbate, E., Bosi, C., Castiglioni, G.B., Merenda, L., Mutti, E., Orombelli, G., Ortolani, F., Parotto, M., Pignone, R., Polino, R., Premoli Silva, I., Sassi, F.P., 1992. *Carta Geologica d'Italia 1:50 000, Guida al rilevamento*. Servizio Geologico Nazionale, Quaderni, ser. III, 1, Istituto Poligrafico e Zecca dello Stato, Roma.
- Salvador, A. (ed.), 1994. *International Stratigraphic Guide – A Guide to Stratigraphic Classification, Terminology, and Procedure (2nd Edition)*. International Subcommission on Stratigraphic Classification, The International Union of Geological Sciences and The Geological Society of America, The Geological Society of America, Boulder, Colorado, pp. 214.
- Sulpizio, R., Dellino, P., 2008. Sedimentology, depositional mechanisms and pulsating behaviour of pyroclastic density currents. *Developments in Volcanology*, 10: 57-96.
- Weller, J.M., 1960. *Stratigraphic Principles and Practice*. Harper, New York.
- Wheeler, H.E., Mallory, V.S., 1953. Designation of stratigraphic units. *American Association of Petroleum Geologists Bulletin*, 37: 2407-2421.
- Wheeler, H.E., Mallory, V.S., 1956. Factors in lithostratigraphy. *American Association of Petroleum Geologists Bulletin*, 40: 2711-2723.

A window into magmatic time (340 – 25 ka): How magma systems reorganised between supereruptions in the north Taupō area

Kate Mauriohooho¹, Colin J.N. Wilson¹, Graham S. Leonard², and Isabelle Chambefort³

¹ School of Geography, Environment and Earth Sciences, Victoria University, PO Box 600, Wellington 6140; kate.mauriohooho@vuw.ac.nz

² GNS Science, Avalon Research Centre, PO Box 30-368, Lower Hutt 5040

³ GNS Science, Wairakei Research Centre, Private Bag 2000, Taupo 3352

Keywords: Taupō, Maroa, supervolcano, magma systems.

A surficial volcanic record from Taupō volcano extends from ~1.7 ka back to the Whakamaru Group super- and other eruptions at 349-339 ka (Leonard et al., 2010). During this time period at some stage what we now call Taupō volcano began erupting, in conjunction with the Maroa volcanic centre just to the north. But how many “volcanoes” were in existence then? Burial by younger deposits and insufficient age data means that much of this history is obscured (Barker et al., 2014). An exact definition as to when Taupō volcano became Taupō volcano is elusive in the literature. In general terms, it is suggested that the modern Taupō volcano and its magmatic system post-dates the 25.4 ka Oruanui caldera-forming supereruption (e.g. Sutton et al., 2000; Barker et al., 2015: Figs. 1, 2). Sutton et al. (1995) presented a detailed petrological study of eruptions from Taupō volcano and the surrounding areas. They reported that chemical and isotopic compositional variations in the pre-Oruanui rhyolites indicated that they did not originate from a single magma system or chamber, instead suggesting that geographically and/or temporally distinct batches of magma were tapped.

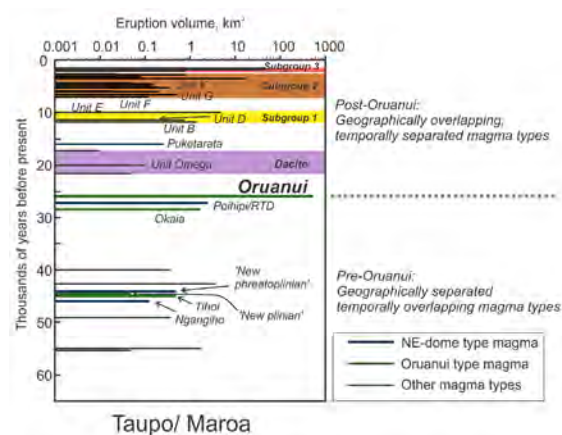


Fig. 1. Pre and Post Oruanui magma types (Wilson & Charlier, 2009). Why did their geographic and temporal relationships change at the time of the Oruanui eruption? What was the regional magmatic architecture further back in time?

How magma systems evolve and assemble magma to supply supereruptions is still an unresolved question (Sutton et al., 2000; Charlier et al., 2005; Allan et al., 2017). This research focuses on this topic using a defined time bracket in between the two youngest supereruptions from the central Taupo Volcanic Zone (TVZ). This area has hosted four of the ten Quaternary supereruptions (>450 km³, magma) known worldwide. How magmatic/volcanic systems behaved in between these vast events is not well constrained, yet is important in determining the factors that lead to supereruptions. We are using the volcanic products erupted between the Whakamaru and Oruanui supereruptions to understand how magma systems in the north Taupō-Maroa area were organized in time and space. This new research builds on existing tephrostratigraphic data and localities (Vucetich & Howorth, 1976; CJNW unpubl. data) with new analytical data, improved geochronological constraints (Houghton et al., 1991; Leonard, 2003; Wilson et al., 2006) by dating of eruption units (Fig. 3), and extension of pre-existing geochemical datasets. Surficial eruption products will also be correlated to drillhole formations in geothermal fields in the area (Wairakei-Tauhara, Ngatamariki, Rotokawa) to look at patterns of rift-related subsidence in the area.

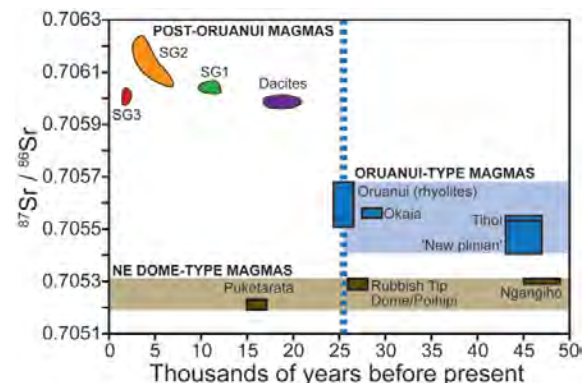


Fig. 2. The ⁸⁷Sr / ⁸⁶Sr values for Post Oruanui magmas, Oruanui type magmas and NE dome type magmas (Barker et al., 2014). What geochemical differences do older eruption deposits exhibit? What similarities or differences will be seen in deposits > 60 ka?

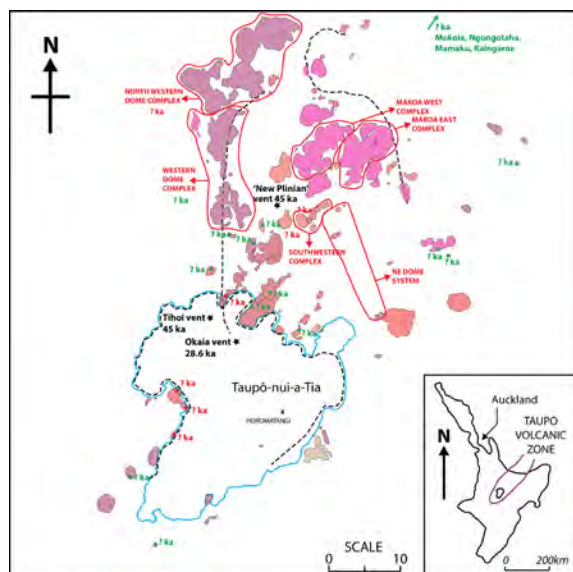


Fig. 3. Distribution of surficial post-Whakamaru rhyolite lavas. Green question marks are samples dated or being processed. Red question marks are areas sampled recently or will be sampled shortly. Geological map information taken from Leonard et al. (2010).

The project is using two approaches. 1) A field observation-based approach identifying and analysing pyroclastic deposits beginning with the Oruanui 25.4 ka eruption products down to the Rotoehu-Rotoiti eruption products (~ 60 ka) and extending where feasible with larger units back to ~340 ka. 2) A laboratory-based approach utilising $^{40}\text{Ar}/^{39}\text{Ar}$ dating, petrography, and electron microprobe, x-ray fluorescence and plasma mass spectrometry (for major elements, trace elements, new glass and mineral chemistry and [if time permits] Sr, Nd and Pb isotopes). The data generated will provide an understanding of how the sub-surface magmatic systems and root zones between the Whakamaru, Maroa and Taupo areas were organised prior to the Oruanui eruption and how they have behaved and evolved over time to account for their different chemistries. Why should smaller eruptions precede or follow a larger supereruption? The volumes and diversity of the magmas produced in this limited area over a ~300 kyr period is unusual globally (see also Gravley et al., 2016), and the results of this work have global implications. An understanding of how magma systems operated through numerous but relatively small eruptions before and during the onset of the Oruanui magma system will provide new insights into the workings of large rhyolitic volcanoes.

Acknowledgements

We thank Joseph Mauriohooho for field assistance and use of his ute. We would also like to

thank Kinleith Forestry, and Waipapa, Tūwharetoa, Tuaropaki and Tauhara North No 2 trusts for land access. EQC for funds to perform analytical work and Victoria University for a Victoria University Doctoral Scholarship.

References

- Allan, A.S.R., Barker, S.J., Millet, M.-A., Morgan, D.J., Rooyackers, S.J., Schipper, C.I., Wilson, C.J.N. (2017). A cascade of magmatic events during the assembly and eruption of a super-sized magma body. *Contrib Mineral Petrol* 172, 49.
- Barker, S.J., Wilson, C.J.N., Smith, E.G.C., Charlier, B.L.A., Wooden, J.L., Hiess, J., & Ireland, T.R. (2014). Post-supereruption magmatic reconstruction of Taupo Volcano (New Zealand), as reflected in zircon ages and trace elements. *J Petrol* 55, 1511-1533.
- Barker, S.J., Wilson, C.J.N., Allan, A.S.R., & Schipper, C.I. (2015). Fine-scale temporal recovery, reconstruction and evolution of a post-supereruption magmatic system. *Contrib Mineral Petrol* 170, 5.
- Charlier, B.L.A., Wilson, C.J.N., Lowenstern, J.B., Blake, S., Van Calsteren, P.W., & Davidson, J.P. (2005). Magma generation at a large, hyperactive silicic volcano (Taupo, New Zealand) revealed by U–Th and U–Pb systematics in zircons. *J Petrol* 46, 3-32.
- Gravley, D.M., Deering, C.D., Leonard, G.S., Rowland, J.V., 2016. Ignimbrite flare-ups and their drivers: a New Zealand perspective. *Earth-Sci Rev* 162, 65-82.
- Houghton, B.F., Lloyd, E.F., Wilson, C.J.N., Lanphere, M.A., (1991). K-Ar ages from the Western Dome Belt and associated rhyolitic lavas in the Maroa-Taupo area, Taupo Volcanic Zone, New Zealand. *NZ J Geol Geophys* 34, 99-101.
- Leonard, G.S. (2003). The evolution of Maroa Volcanic Centre, Taupo Volcanic Zone, New Zealand. Unpublished PhD thesis, University of Canterbury, Christchurch.
- Leonard, G.S., Begg, J.G., Wilson, C.J.N. (compilers) 2010: Geology of the Rotorua area. Institute of Geological & Nuclear Sciences 1:250 000 geological map 5. 1 sheet + 102 p. Lower Hutt, New Zealand.
- Sutton, A.N., Blake, S., Wilson, C.J.N. (1995). An outline geochemistry of rhyolite eruptives from Taupo volcanic centre, New Zealand. *J Volcanol Geotherm Res* 69, 153-175.
- Sutton, A.N., Blake, S., Wilson, C.J.N., Charlier, B.L.A. (2000). Late Quaternary evolution of a hyperactive rhyolite magmatic system; Taupo volcanic centre, New Zealand. *J Geol Soc Lond* 157, 537-552.
- Vucetich, C.G., Howarth, R. (1976). Late Pleistocene tephrostratigraphy in the Taupo District, New Zealand. *NZ J Geol Geophys* 19, 51-69.
- Wilson, C.J.N., Blake, S., Charlier, B.L.A., Sutton, A.N. (2006). The 26.5 ka Oruanui eruption, Taupo Volcano, New Zealand: Development, characteristics and evacuation of a large rhyolitic magma body. *J Petrol* 47, 35-69.
- Wilson, C.J.N., Charlier, B.L.A. (2009). Rapid rates of magma generation at contemporaneous magma systems, Taupo Volcano, New Zealand: insights from U–Th model-age spectra in zircons. *J Petrol* 50, 875-907.

The inherent difficulty of unit correlation in heavily forested terrane was made easier by the high degree of textural diversity between volcanic lithologies, which range from fine-grained basalts, to extremely coarse-grained ankaramites, hornblende-basaltic-andesites and andesites. In some cases, field correlation of lavas was possible over large (1-3 km) distances where a distinct identifying mineral was present (e.g. skeletal hornblende). Petrographic correlation was useful where field correlation was ambiguous (e.g. fine-grained basaltic-andesite lavas). Dikes were mapped based on their morphological expression in aerial photographs, measured strike and correlated into groups based on spatial distribution, stratigraphic position, orientation pattern (e.g. sub-parallel or radial) and other field characteristics (e.g. rock texture, presence of inclusions).

The map presents thirty-five new volcanic units with a proposed stratigraphic order that is consistent with existing K/Ar age data for the volcano. The map uncovers the post-erosional distribution of lava fields, dike swarms, volcanoclastic breccias and ring plain deposits produced over a period of 1 Myr.

Vent facies, dominated by andesitic dikes (at least 50 are exposed) and fragmental material are dispersed within a ~ 1.6 km radius of Pirongia summit. The dikes form spatially distinct groups with localized emplacement patterns that each mark the source of magmas that fed a major cone-building eruptive phase. Prominent dike swarms occur near three of Pirongia's major peaks: the summit (959 m), The Cone (953m) and Mahaukura (902 m). Andesitic deposits are intercalated with basaltic scoria, lavas and dikes.

The flank facies consist of thick successions of autobrecciated basaltic to basaltic-andesite lava flows (1-2 m thick) and associated volcanoclastic breccias. Typical flank lavas dip $15-20^\circ$ and steepen to $25-28^\circ$ at upper elevations.

Flank vents are situated within two zones ~ 2.4 km and ~ 6 km from the radius of Pirongia summit. Erupted compositions are primarily basaltic with textures ranging from fine-grained to coarsely porphyritic, and are typically abundant in augite and olivine phenocrysts. Vent proximal deposits are scoriaceous and form eroded mounds cross cut by dikes or doleritic plugs of similar composition. Associated lava flow fields are typically expansive and reach 3-4 km in length.

Ring plain facies occupy most of the gentle lower flanks of Pirongia (with slopes of $5-10^\circ$). Deposits include diamictons associated with large volume debris avalanches (length >12 km), as well as basaltic block and ash flows, andesitic ignimbrites, and bouldery laharic material.

The Pirongia Volcano is a stratigraphically complex, long-lived compound volcanic system that produced large volumes of basaltic magma of diverse texture and composition. The new geological map illustrates the spatial and temporal association of its main volcanic units. The mapped deposits imply that the volcanic edifice was formed through multiple stages of cone-building (and collapse) within a dispersed area of its present summit zone. Each central vent produced a thick succession of basaltic lavas that evolved in composition and eruption style towards vulcanian andesitic volcanism. The edifice was progressively broadened by Hawaiian-type fissure eruptions of lava on the flanks of Pirongia, and the continual aggradation of debris to its ring plain. Erosion in the post-volcanic period has removed most of the unconsolidated upper sections of the cones ($\sim 300-400$ m eroded vertically) and exposed their feeder dikes.

Acknowledgements

This research is supported by a University of Waikato Doctoral Scholarship. The author thanks members of the Pirongia Te Aroaro o Kahu Restoration Society and his colleagues at the university for assistance with field work.

References

- Briggs, R.M., 1983. Distribution, form and structural control of the Alexandra Group, North Island, New Zealand. *New Zealand Journal of Geology and Geophysics*, 26(1):47-55.
- Briggs, R.M., Itaya, T., Lowe, D.J. and Keane, A.J., 1989. Ages of the Pliocene-Pleistocene Alexandra and Ngatutura Volcanics, western North Island, and some geological implications. *New Zealand Journal of Geology and Geophysics*, 32(4): 417-427.
- Briggs, R.M. and McDonough, W.F., 1990. Contemporaneous Convergent Margin and Intraplate Magmatism, North Island, New Zealand. *Journal of Petrology*, 31(4):813-851.
- Kear, D. and Schofield, J.C., 1978. Geology of the Ngaruawahia Subdivision. *New Zealand Geological Survey bulletin* 88, 168 p.

Late-Archaean felsic LIPs of the Ventersdorp Supergroup, South Africa

Gerhard Meintjes¹ and Willem van der Westhuizen¹

¹University of the Free State, Bloemfontein, South Africa; pgm@pgmmanagement.co.za

Keywords: Ventersdorp, Late-Archaean, LIPs.

We have unique access to thousands of cored exploration boreholes allowing detailed study of the Ventersdorp Supergroup, a volcanic-sedimentary sequence overlying the auriferous Witwatersrand Supergroup. Some of these boreholes are over 5000 m deep. Despite a wealth of exploration data, e.g. drill holes, aeromagnetic data, deep seismic surveys and geochemical analyses, this major Kaapvaal Craton sequence has been poorly studied.

The Ventersdorp Supergroup is exceptionally well preserved, being largely only affected by regional burial metamorphism (up to greenschist facies) and non-destructive tectonic deformation. The strata are still in-situ, as it was deposited 2780 to 2720 million years ago. The sequence is composed of three major LIPs: a basal flood basalt sequence (Klipriviersberg Group), a middle intermediate to felsic sequence (Platberg Group) and an upper flood basalt sequence (Allanridge Formation), each with relative minor associated sediments (Figure 1; Van der Westhuizen et al., 2006).

	Group	Formation	Main Rock Types
Ventersdorp Supergroup	Pniel	Allanridge	lava
		Bothaville	sediments
	Platberg	Rietgat	lava
		Makwassie	quartz porphyries & lava
		Goedgenoeg	feldspar porphyries & lava
		Kameeldoorns	sediments
		Edenville	lava
	Klipriviersberg	Loralne	lava
		Jeanette	lava
		Orkney	lava
		Alberton	lava
		Westonaria	lava & sediments
		Venterspost	sediments & lava

Fig. 1 – Stratigraphy of the Ventersdorp Supergroup.

The Klipriviersberg Group LIP is a continental tholeiitic flood basalt sequence and was emplaced as viscous lava flows, decreasing in viscosity from the base to the top, from komatiite lavas, pahoehoe and aa to block lavas. Tuffs and sediments are extremely rare in the succession.

The middle and upper Ventersdorp sequences have especially been under-studied. The middle Platberg Group LIP is poorly exposed and the full sequence can only be realised from borehole

intersections, being composed of sediments, andesites, dacites and rhyolites (Figure 2). A basal sedimentary unit (Kameeldoorns Formation) occur localised as result of onset of rifting, with further minor sediments being interbedded with the rest of the overlying volcanic successions (Goedgenoeg, Makwassie and Rietgat Formations).

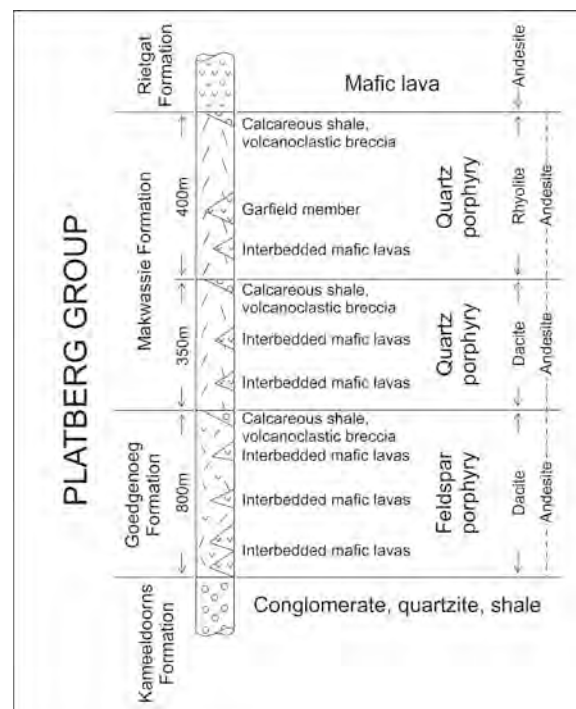


Fig. 2 – Generalised stratigraphy of the Platberg Group.

Geochemical fingerprinting of the Platberg Group volcanics has established that six distinct magma types erupted (Meintjes and Van der Westhuizen, 2018), which enables correlation of the individual units across the Platberg Group depository of about 300 x 600 km.

The andesites were emplaced as viscous lava flows and forms the base of the Goedgenoeg Formation. This magma has consistent geochemical composition and continued to co-erupt with the rest of the overlying dacite-rhyolite succession, occurring widespread in the depository as interbedded lavas with the dacites and rhyolites,

The rest of the Goedgenoeg Formation is composed of feldspar-porphyry dacites that were mainly deposited as highly welded ignimbrites (Figure 3). Two magma compositions can be distinguished, based on Zr concentrations: a low-Zr dacite (~450 ppm) and a high-Zr dacite (~650 ppm), each with distinct distribution ranges. These dacites are considered to be the mixed product of crustal melt and the andesite magma (Figure 4).

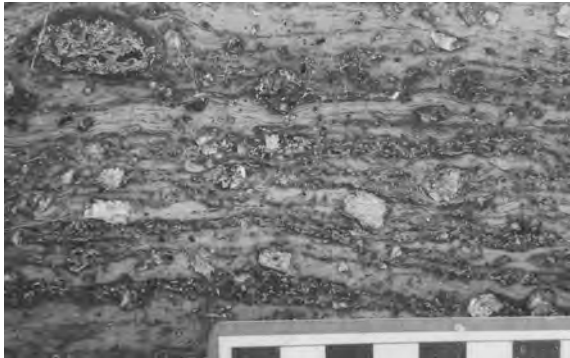


Fig. 3 – Feldspar porphyry of the Goedgenoeg Formation in outcrop (scale bar in centimetres).

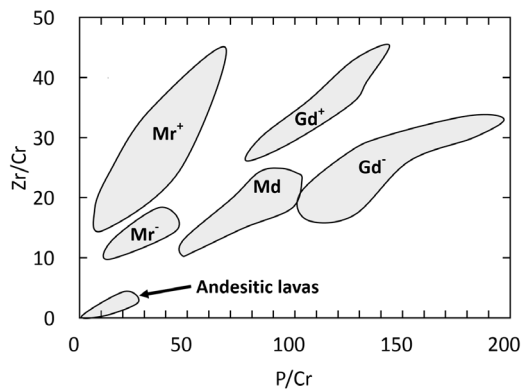


Fig. 4 – Geochemical magma groups of the Platberg Group: Goedgenoeg Fm. low-Zr and high-Zr (Gd- and Gd+) dacites; Makwassie Fm. dacites (Md), low-Zr/Cr and high-Zr/Cr rhyolites; andesitic lavas co-erupted with the rest.

The overlying Makwassie Formation is composed of a basal dacitic quartz porphyry and an upper rhyolitic quartz porphyry, deposited mainly as highly welded ignimbrites (Figures 5) and ash flows. Rarely rhyolites lava flows are also encountered. The dacite is a mixed product of the andesitic magma and crustal melt, similar to the Goedgenoeg Formation dacites but less evolved. The overlying rhyolites are crustal melts, contaminated by the andesitic magma. Two groups can be recognised in the rhyolites based on Zr/Cr ratios, which are related to the crustal sources of the melts. Resurgent eruption of the andesitic magma created a localised sequence of andesitic lavas (the Rietgat Formation), overlying the Makwassie Formation and forming the final formation of the Platberg Group.

It is remarkable that such persistent magmas of Late-Archaean age were erupting over such widespread areas of the Kaapvaal Craton, signifying the maturity of the Kaapvaal Craton early after earth formation.

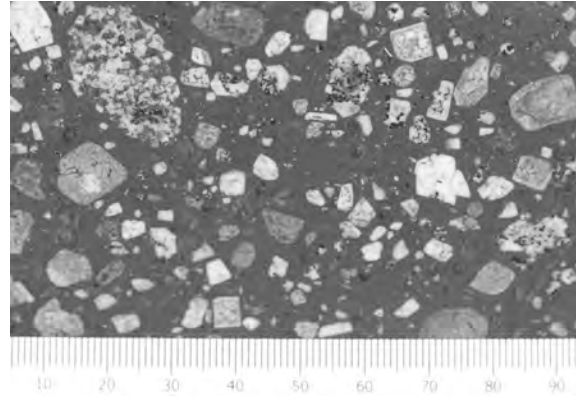


Fig. 5 – Quartz porphyry of the Makwassie Formation.

New ages for the Makwassie Formation rhyolites was established at 2720 ± 2 Ma and for the Goedgenoeg dacites at 2746 ± 9 Ma, but the latter is still poorly constrained.

The Platberg Group is overlain by a regional quartzite and conglomerate formation (Bothaville Formation), which is capped by a major flood basalt LIP (Allanridge Formation), together forming the Pniel Group.

Our research program will continue to investigate the detailed stratigraphy of the Ventersdorp Supergroup and correlation of the individual units across the Kaapvaal Craton. Structural study of the Ventersdorp Supergroup has also largely been neglected and will receive attention, as it has direct relation to the structure of the underlying Witwatersrand Supergroup. Of concern is that most of the historic exploration drill core and data is presently of low value to the Witwatersrand gold mining industry, which has been in a waning phase for the last two decades. This core and data are unique, never to be repeated, and must urgently be preserved.

References

- Meintjes, P.G. and Van der Westhuizen, W.A., 2018. Stratigraphy and Geochemistry of the Goedgenoeg and Makwassie Formations, Ventersdorp Supergroup, in the Bothaville area of South Africa. *South African Journal of Geology*, (in press).
- Van der Westhuizen, W.A., de Bruijn, H. and Meintjes, P.G., 2006. The Ventersdorp Supergroup. In: Johnson, M.R., Anhaeusser, C.R. and Thomas, R.J. (Eds.). *The Geology of South Africa*. The Geological Society of South Africa, Johannesburg/Council for Geoscience, Pretoria, 187-208.

The September 14, 2015 explosive eruption at Nakadake first crater, Aso Volcano, SW Japan

Yasuo Miyabuchi¹, Yoshiyuki Iizuka², Chihoko Hara³, Akihiko Yokoo⁴ and Takahiro Ohkura⁴

¹ Faculty of Advanced Science and Technology, Kumamoto University, Kumamoto, Japan; miyabuchi@gmail.com

² Institute of Earth Sciences, Academia Sinica, Taipei, Taiwan

³ Nishikokubu Elementary School, Fukuoka, Japan

⁴ Aso Volcanological Laboratory, Institute for Geothermal Sciences, Kyoto University, Kumamoto, Japan

Keywords: phreatomagmatic eruption, ballistic clasts, pyroclastic density currents

Nakadake Volcano, which is the only active central cone inside the Aso caldera, is one of the most active volcanoes in Japan. The active crater (first crater) of Nakadake is occupied by a hot, hyperacidic (pH=0.43) crater lake during its calm periods (Miyabuchi and Terada, 2009; Ohsawa et al., 2010). During active periods, volcanic activity of Nakadake first crater is characterized by continuous fallout of black sandy ash from a dark eruption plume (Ono et al., 1995). In more active periods, strombolian eruptions have scattered red-hot scoriaceous clasts around the vent. Moreover, phreatic or phreatomagmatic eruptions occurred in September 1979 and April 1990, ejecting coarse lithic blocks and generating small low-temperature pyroclastic density currents around the crater (Ono et al., 1982; Ikebe et al., 2008).

Following the November 2014–May 2015 magmatic activity including ash emissions and strombolian eruptions (Yokoo and Miyabuchi, 2015), an explosive eruption occurred at Nakadake first crater on September 14, 2015. The amplitude of short period tremor began to increase at 09:18 (Japan Standard Time; GMT+9 h), and explosive activity started at 09:43 (Fig. 1). Rising ash plumes, showers of ballistic ejecta and emergence of pyroclastic density currents (PDCs) during the



Fig. 1 – Photograph of the September 14, 2015, eruption of Nakadake first crater taken at a site 3 km west of the crater (photo credit: Yuka Matsushima).

eruption were recorded by a video camera operated by Nippon Hoso Kyokai (NHK; Japan Broadcasting Corporation) at about 1.1 km SW of the crater.

We performed fieldwork for observing and sampling of deposits immediately after the September 14, 2015 eruption. The eruptive deposits are divided into ballistics, PDC and ash-fall deposits (Miyabuchi et al., 2018). A large number of ballistic clasts (mostly <10 cm in diameter; maximum size 1.6 m) are scattered within about 500 m from the center of the crater. The ballistic clasts are dominated by basaltic andesite fragments of lavas or pyroclastic rocks, and show varying degree of alteration. Almost half of the ballistics appear as fresh and unaltered basaltic andesite rocks interpreted to be derived from a fresh batch of magma, while the rest is weakly to highly altered clasts. The surface of weight covered with a sheet of low-density, cement-filled polyethylene inside an ash sampler was ignited by the clast, indicating that parts of ballistic clasts were over 350°C during the eruption.

A relatively thin ash derived from PDCs covered an area of 2.3 km² with the SE-trending main axis and two minor axes to the NE and NW. The PDC deposit (maximum thickness <10 cm even at the crater rim) is wholly fine grained, containing no block-sized clasts, and could be divided into three units by grain-size and sorting characteristics. The temperature of the PDCs was much lower than the melting point of polyethylene (100–115°C) because plastic bags covering ash samplers suffered with no damage. Based on the isopach map, the mass of the PDC deposit was estimated at approximately 5.2×10⁴ tons.

The ash-fall deposit is finer grained and clearly distributed to about 8 km west of the source crater. The dispersal axis extends about 4 km to the northwest, then changes to west-southwest. The ash fall was recognized in the southern part of Fukuoka prefecture (~60 km NW of crater). The mass of the ash-fall deposit was calculated at about 2.7×10⁴ tons. Adding the mass of the PDC deposit, the total discharged mass of the September 14, 2015 eruption was 7.9×10⁴ tons.

The September 14 PDC and ash-fall deposits consist of glass shards (ca. 30%), crystals (20-30%) and lithic (40-50%) grains. Most glass shards are unaltered poorly crystallized pale brown glasses which probably resulted from quenching of juvenile magma (Fig. 2). This suggests that the September 14, 2015 event at the Nakadake first crater was a phreatomagmatic eruption although the eruption is one order of magnitude smaller in eruptive volume than the September 6, 1979 and April 20, 1990 eruptions at the same crater.

The proximate cause of the September 14, 2015 eruption was that the magma came in contact directly with an aquifer. The resulting combined burst of gas and entrained particulate materials broke the semi-solidified magma head, hydrothermally altered materials surrounding the conduit, consequently generating ballistic ejecta apron and PDCs around the crater.

Phreatic or phreatomagmatic eruptions frequently occur at crater-lake volcanoes worldwide. This type of eruption is potentially energetic and hazardous for areas within a few km of the active crater. These eruptions occasionally occur without clear precursor signals. In the case of the September 14, 2015 Nakadake eruption, the amplitude of short-period tremor began to increase four days prior to the eruption, and then seismicity levels remained elevated until the eruption. Moreover, another gradual increase of amplitude of short-period tremors, which probably indicates magma and water interactions, was observed about 25 min before the onset of eruption. These seismic records are thought to be precursor phenomena of the September 14 eruption. Therefore, seismic monitoring is very important for predicting these phreatic or phreatomagmatic eruptions at the Nakadake first crater. This study highlights the potential hazard

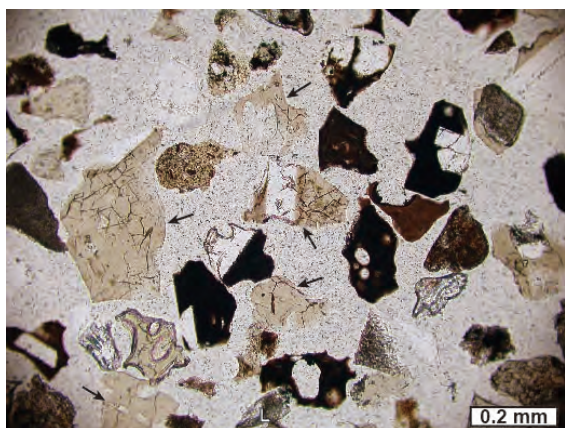


Fig. 2 – Polarizing microscope photograph of the September 14, 2015 ash-fall deposit. Arrows show unaltered poorly crystallized pale brown glass shards.

from phreatic or phreatomagmatic eruptions at Nakadake first crater, and provides useful information that will assist in preventing or mitigating future disasters at other similar volcanoes worldwide.

Acknowledgements

Parts of fieldwork were undertaken with Hideho Inoue, Shin-ichi Matsusue and Mitsuru Utsugi. Video record provided by the NHK Kumamoto Broadcasting station was very useful to understand the detailed sequence of the September 14, 2015 Nakadake eruption. The Aso Summit Office (Aso City) gave us permission for our field survey. The eruption photograph was provided by Yuka Matsushima. This study was supported by the Ministry of Education, Culture, Sports, Science and Technology (MEXT) of Japan, under its Earthquake and Volcano Hazards Observation and Research Program (No. 1802).

References

- Ikebe, S., Watanabe, K. and Miyabuchi, Y., 2008. The sequence and style of the 1988-1995 eruptions of Nakadake, Aso Volcano, Kyushu, Japan. *Bulletin of the Volcanological Society of Japan*, 53: 15-33.
- Miyabuchi, Y. and Terada, A., 2009. Subaqueous geothermal activity revealed by lacustrine sediments of the acidic Nakadake crater lake, Aso Volcano, Japan. *Journal of Volcanology and Geothermal Research*, 187: 140-145.
- Miyabuchi, Y., Iizuka, Y., Hara, C., Yokoo, A. and Ohkura, T., 2018. The September 14, 2015 phreatomagmatic eruption of Nakadake first crater, Aso Volcano, Japan: Eruption sequence inferred from ballistic, pyroclastic density current and fallout deposits. *Journal of Volcanology and Geothermal Research*, 351: 41-56.
- Ohsawa, S., Saito, T., Yoshikawa, S., Mawatari, H., Yamada, M., Amata, K., Takamatsu, N., Sudo, Y. and Kagiya, T., 2010. Color change of lake water at the active crater lake of Aso volcano, Yudamari, Japan: is it in response to change in water quality induced by volcanic activity? *Limnology*, 11: 207-215.
- Ono, K., Shimokawa, K., Soya, T. and Watanabe, K., 1982. Geological and petrological study on the ejecta of 1979 eruption of Nakadake, Aso volcano, Japan. Report on an urgent study of 1979 eruption of Ontake and Aso volcano, Science and Technology Agency, 167-189.
- Ono, K., Watanabe, K., Hoshizumi, H. and Ikebe, S., 1995. Ash eruption of the Naka-dake crater, Aso volcano, southwestern Japan. *Journal of Volcanology and Geothermal Research*, 66: 137-148.
- Yokoo, A. and Miyabuchi, Y., 2015. Eruption at the Nakadake 1st crater of Aso Volcano started in November 2014. *Bulletin of the Volcanological Society of Japan*, 60: 275-278.

Petrographic and geochemical characteristics of the Kamo monogenetic volcanic field, Southern Kyushu, Japan.

Linus A. Nche¹, Takeshi Hasegawa¹, Károly Németh², Tetsuo Kobayashi³ and Festus T. Aka⁴

¹ Department of Earth Science, Ibaraki University, Mito, Japan; ncheanye2002@gmail.com

² School of Agriculture and Environment, Massey University, Palmerston North, New Zealand

³ Graduate school of Science and Technology, Kagoshima University, Japan

⁴ Institute of Geological and Mining Research, Yaounde, Cameroon

Keywords: monogenetic, maars, Kagoshima graben

Kamo monogenetic volcanic field (KMVF) consists of small-volume basaltic volcanoes forming part of the volcanic front of Southern Kyushu that extend to the Southern Island of Japan. These volcanoes include the late Pleistocene Aojiki (scoria cone and lava field) formed at about ~100ka and two Holocene maar volcanoes, the Sumiyoshiike and Yonemaru that erupted at 8.2ka and 8.1ka respectively (Nagaoka, 1988; Nagaoka et al., 2001; Morikawi et al., 2016). These two maars were formed through phreatomagmatic eruptions during sea level high stand along the northern edge of the Kagoshima graben, where large caldera forming volcanism has been concentrated, leading to the accumulation of widespread dacitic and rhyolitic tephra (Nagaoka, 1988). Eruptions of basaltic volcanoes in this area are rare. While the volume of erupted basaltic magma is low, they have played a significant role in the evolution of the felsic magmas in the Kagoshima graben (Kimura et al., 2015).

The physical attributes of these maar deposits have been described in Morikawi et al. (1986) and Morikawi (1992). In this study, we present preliminary petrological and geochemical examinations of the juvenile pyroclasts in order to understand the mafic magma genesis. In addition, we also provide data for the Aojiki volcano identified in between the two maars.

Field investigations indicate that the tephra ring of both maars is stratified and consists of thin beds of volcanic ash, scoriaceous lapilli and bombs. These tephra deposits are generally rich in accidental lithic clasts, made up of brown pumice and laminated silts sediments, especially at the proximal part of the maar crater, which will be referred in this study as lower outcrops. These accidental lithic are also seen widely distributed around the Aojiki volcano and the two maars. The brown pumice clasts are the product of Ito Ignimbrites coming from the Aira caldera that erupted ~29ka covering a vast area around Southern Kyushu (Aramaki, 1984).

While sediments formally grouped into the Kamo Formation, is considered to be the basement

rock of the area (Kobayashi et al., 2004; Kagawa and Otsuka, 2000).

At Yonemaru, the lower outcrop consists of alternating thin beds of ash and lapilli of base surge origin. Cross and planar laminated structures are common in this section.

The upper outcrops for both maars are richer in juvenile pyroclasts especially at Sumiyoshiike.

Bulk and large juvenile sampling was done where exposures allowed. However, it is important to point out that, both outcrops are likely to represent a single continuous sequence as suggested by Moriwaki et al. (1986) and Moriwaki (1999).

The scoria cone of Aojiki volcano, at attitude of 213m, consists of variable pyroclast sizes ranging from ash to bomb and block. Meanwhile, the Aojiki lava found below the cone and it is characterized by clinkery aa lava surface textures and massive blocky lava structure

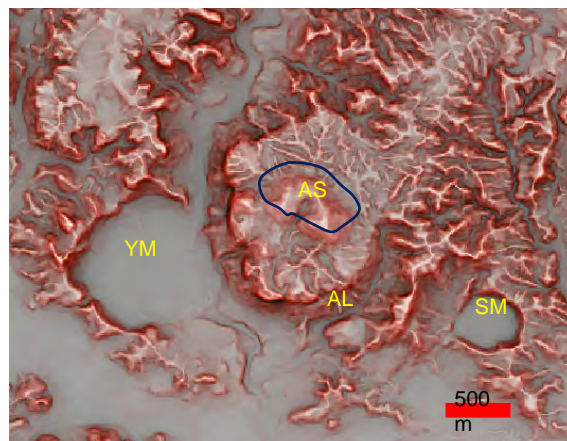


Fig.1 Topographic Relief map showing the position of the two Holocene maars: SM=Sumiyoshiike maar, YM=Yonemaru maar, and the Aojiki volcano AS=Aojiki scoria, AL= Aojiki lava (Geospatial Information Authority of Japan).

Petrographically, the juvenile pyroclasts consist of plagioclase and clinopyroxene as major phenocrysts and microphenocryst of olivine set within a glassy groundmass of same minerals exhibiting mostly hyalo-ophitic texture. Honey comb texture defined by numerous small melt

inclusions in plagioclase phenocrysts are common from the Yonemaru maar products.

Whole rock geochemical data indicates that the juvenile pyroclasts are composed of mostly basalts and minor basaltic andesites showing little compositional variations (SiO_2 : 46.17 wt.% -52.10 wt.%, MgO : 4.26-7.21 wt.%). All the juvenile pyroclasts can be defined as tholeiitic magma series of mainly medium K characteristic. Based on looking at individual volcanoes, distinct chemical trends can be inferred with a narrow compositional range for the Sumiyoshiike and for both Aojiki scoria and lava, while a wide compositional range can be recognized in the Yonemaru, suggesting independent magmatic evolution within each volcano. The eruptive products of the upper section of the Yonemaru volcano are more evolved with SiO_2 content ranging from 49.80 wt.% to 52.10 wt.% with low concentration of Ni, Cr, Co. Major and trace elements variation diagrams suggests crystal fractionation of olivine, clinopyroxene and plagioclase during melt evolution. This observation is consistent with petrographic descriptions of representative samples for each of these volcanoes. Ratios of different trace elements such as Ba versus Nb or Y(LILE/HFSE), Nb versus Y(HFSE) indicate compositional variation for the Yonemaru upper and lower products and for the Aojiki scoria and lava. The variations between the lower and upper products, which form a linear trend, inferred to be due to mixing of two magma batches leading to such varied compositions.

Acknowledgements

This work is still on-going and form part of the PhD research which focuses on the “*Volcanology and geochemistry of basaltic maar volcanoes of Cameroon and Japan*”. Special thanks to MEXT for the scholarship offered. Much gratitude to Ibaraki University for sponsoring part of the field trip to Kagoshima and my supervisors.

References

- Aramaki, S. (1984). Formation of the Aira caldera, southern Kyushu, -22,000 years ago. *Journal of Geophysical Research*. **89**, 8485–8501.
- Kagawa, A. and Otsuka, H. (2000). Stratigraphic sequence and volcano-tectonic event deposits of the middle Pleistocene Kokubu Group on the coastal area of the north Kagoshima Bay, South Kyushu, Japan. *Journal of the Geological Society of Japan*, vol. 106, 762–782 (in Japanese with English abstract).
- Kimura, J.-I., Nagahashi, Y., Satoguchi, Y. and Chang, Q. (2015). Origins of felsic magmas in Japanese subduction zone: Geochemical characterizations of tephra from caldera-forming eruptions <5 Ma, *Geochemistry Geophysics Geosystem* 16, 2147-2174, doi:10.1002/2015GC005854.
- Kobayashi, T., Iwamoto, Y., and Okuno, M. (2004). Ages and mode of eruption of Kamo monogenetic volcano group, Southern Kyushu, Japan. Programme and Abstracts of the Volcanological Society of Japan 2004 Meeting, Page 26, A26.
- Moriwaki, H., Machida, H., Hatsumi, Y. and Matsushima, Y., (1986). Phreatomagmatic eruptions affected by postglacial transgression in the northern coastal area of Kagoshima bay, southern Kyushu, Japan. *Chigaku Zasshi (Journal of Geography)* 95, 24-43, in Japanese with English abstract.
- Moriwaki, H. (1992). Late Quaternary phreatomagmatic tephra layers and their relation to paleo-sea levels in the area of Aira caldera, southern Kyushu, Japan. *Quaternary International* 13/14, 195-200.
- Moriwaki, H., Nakamura, N., Nagasako, T. and Lowe, D.J. (2016). The role of tephra in developing a high - precision chronostratigraphy for Paleoenvironmental reconstruction and archaeology in southern Kyushu, Japan, since 30,000 cal. BP: An integration. *Quaternary International* 397,79-92
- Nagaoka, S. (1988) Late Quaternary tephra layers from the caldera volcanoes in and around Kagoshima Bay, southern Kyushu, Japan. *Geography. Report. Tokyo Metropolitan University.*, **23**, 49–122.
- Nagaoka, S., Okuno, M., Arai, F. 2001. Tephra-stratigraphy and eruptive history of the Aira caldera volcano during 100-30 ka, Kyushu, Japan (in Japanese with English abstract). *Journal of the Geological Society of Japan* 107, 432-450.

Geological mapping of monogenetic volcanic fields

Károly Németh¹ and Gábor Csillag^{2,3}

¹ School of Agriculture and Environment, Massey University, Palmerston North, New Zealand; k.nemeth@massey.ac.nz

² Research Centre for Astronomy and Earth Sciences, Hungarian Academy of Sciences (MTA), Budaörsi út 45, 1112, Budapest, Hungary

³ MTA-ELTE Geological, Geophysical and Space Science Research, Pázmány Péter sétány 1/C, 1117, Budapest, Hungary

Keywords: monogenetic, scoria, phreatomagmatic

Monogenetic volcanoes are those that erupt shortly and produce small volume of eruption products, typically far less than 1 km³ DRE (Smith and Németh 2017). The small eruptive volume of this type of volcanism reflected in the small edifice volumes and narrow dispersal rate of pyroclastic deposits associated with them (Kereszturi et al. 2013). This fact hinders the proper representation of monogenetic volcanoes in any geological maps. Monogenetic volcanoes commonly appear on geological maps single dots in scale 1 to 50,000 or less, with a common denomination of a single lithological unit (eg. basalt).

In current development in understanding of monogenetic volcanism delivered several key aspects of this type of volcanism that need to be represented in a geological map. As geological maps should “tell a story” to the reader, these new conceptual views need to be represented on such maps. Monogenetic volcanic fields and their volcanoes are the product of an interplay between the magmatic conditions of the eruptions and their interaction with the eruptive environment (Smith and Németh 2017). In volcanic fields where external hydrogeological conditions are dominated by the presence of water-saturated country rocks, fissure and cavity filling ground water bodies or surface water, the eruption styles of the resulting monogenetic volcanoes can be dominated by eruptive products derived from phreatomagmatic explosive eruptions hence their eruptive products will be strikingly different than those where no external water influence occurred. These conditions can be reflected in the volcanic rock record that can be mapped. Explosive phreatomagmatic eruptions commonly occur in the early stage of the growth of a small-volume volcano and this is reflected in the initial eruptive products (Kereszturi et al. 2017). Basal phreatomagmatic eruptive products are commonly overlain by subsequent magmatic explosive and effusive products producing a specific stratigraphy. This stratigraphy holds key information on the style of volcanism characteristics for a volcanic field. This information has even volcanic hazard aspects as reflects the eruptive nature of the volcanic field and this information is vital for

potential future eruption scenario studies of such dispersed volcanic fields that are considered to be active (Kereszturi et al. 2014).

While the phreatomagmatic to magmatic explosive and effusive path of eruptive events in the life of a single monogenetic volcano is commonly taken as a rule, there are reversal orders and even repeated eruption styles that can create complex nested volcanoes (Gutmann 2002).

Due to the significance to recognize some sort of basic order of eruption style changes in an individual monogenetic volcano it is important somehow to reflect these variations even in geological maps.



Fig. 1 – Details of a 1 to 50,000 scale geological map of the Bakony- Balaton Highland Volcanic Field, Hungary showing distribution pattern of basaltic volcanic rocks in various tones of green as part of the Tapolca Basalt Formation (Budai et al. 1999, Németh and Csillag, 1999). Volcanic rocks have been separated and mapped as 1) Intrusive and Lava rocks (taPa2β) – dark green; 2) Basaltic Scoria Pyroclastic Rocks (taPa2βt) – light green. Short side of the image frame represents about 5 km. (taPa2βs) – bright green; 3) Volcanogenic or Fine

On the Bakony- Balaton Highland Volcanic Field (BBHVF) in Hungary where monogenetic volcanism was active about 6 millions of years and produced at least 35 small-volume volcanoes such as maars surrounded by tuff rings, scoria cones and associated lava fields (Németh and Martin 1999). The eruptive products were grouped in a single formation (Tapolca Basalt Formation) with three distinct volcanic units: “*basalt*”, “*basaltic scoria*” and “*volcanoclastic rocks*” (Németh and Csillag, 1999). In addition, “hot spring: deposits as a post-eruptive lacustrine unit were also mapped separately. In the explanatory booklet (Budai et al., 1999) the definition of this lithological mapping units were give such as 1) “*basalt*” reflects any coherent volcanic rocks regardless if they are effusive or intrusive in origin, 2) “*basaltic scoria*” referred to fragmented magmatic explosive eruptive products, and 3) “*volcanoclastic rocks*” indicated primarily tuff, lapilli tuff and tuff breccia with phreatomagmatic explosive eruption origin. This lithology-based mapping unit distinction worked well, as the produced geological map offered a visually attractive medium to see directly the mappable rock types that provide strong indication to their volcanic eruptive origin. This triplicate distinction of lithologies potentially could be applied to any mafic volcanic fields in a mapping scale ranges between 1 to 50,000 to 1 to 250,000 scale (Figs 2 & 3). Potentially the lithological units could be renamed to *phreatomagmatic* to *magmatic pyroclastic rocks* with a documentation of their common nature in the field in the explanatory booklet. To apply additional lithological units such as *crater lake deposits* accumulated in volcanic craters or *reworked volcanoclastic aprons* around eroded edifices, if they are preserved and large enough to the given mapping scale are advisable to distinguish in the map to get the full picture of the volcanic landscape.



Fig. 2 – Mappable phreatomagmatic pyroclastic unit (light, bedded) covered by a thin magmatic explosive unit (reddish black, bedded) and a coherent lava (dark on top) at Wiri Mtn, Auckland Volcanic Field, New Zealand.

Approaching toward smaller scale mapping goals if basal phreatomagmatic pyroclastic units are not large enough to be able to represent them on the map, a single poly-line solution should be followed. For instance, “*scoria*” or magmatic explosive eruptive products could be partially outlined with a

specific line type to indicate, if it is underlined by a thin phreatomagmatic pyroclastic rock unit or not. This is a vital information that could help the reader to locate key sections or get an overall impression on the nature of the volcanic field eruption styles. Polyline solution also could be applied in sections where intercalated or repeated sequences are known to document their exact locations on the map.



Fig. 3 Mappable thick magmatic explosive unit (reddish black, bedded) and a coherent lava (dark on top) at Wiri Mtn, Auckland Volcanic Field, New Zealand.

References

- Budai T, Csillag G, Dudko A, Koloszar L (1999) A Balaton-felvidék földtani térképe 1: 50,000 [Geological map of the Balaton Highland], Budapest
- Gutmann JT (2002) Strombolian and effusive activity as precursors to phreatomagmatism: eruptive sequence at maars of the Pinacate volcanic field, Sonora, Mexico. *J Volc Geotherm Res* 113(1-2):345-356
- Kereszturi G, Bebbington M, Németh K (2017) Forecasting transitions in monogenetic eruptions using the geologic record. *Geology* 45(3):283-286
- Kereszturi G, Németh K, Cronin SJ, Agustin-Flores J, Smith IEM, Lindsay J (2013) A model for calculating eruptive volumes for monogenetic volcanoes - Implication for the Quaternary Auckland Volcanic Field, New Zealand. *J Volc Geotherm Res* 266:16-33
- Kereszturi G, Németh K, Cronin SJ, Procter J, Agustin-Flores J (2014) Influences on the variability of eruption sequences and style transitions in the Auckland Volcanic Field, New Zealand. *J Volc Geotherm Res* 286:101-115
- Németh K, Martin U (1999) Late Miocene paleogeomorphology of the Bakony-Balaton Highland Volcanic Field (Hungary) using physical volcanology data. *Zeitschrift Geomorph* 43(4):417-438
- Németh, K and Csillag, G. (1999) Tapolca Basalt Formation. In: Budai et al., A Balaton-felvidék földtana: Magyarázó a Balaton-felvidék földtani térképéhez, 1:50 000 [Geology of the Balaton Highland: explanatory booklet for the geology map of the Balaton Highland, scale 1:50 000]. Occasional Papers of the Geological Institute of Hungary. Vol 197, Budapest, 114-122.
- Smith IEM, Németh K (2017) Source to surface model of monogenetic volcanism: a critical review In: Németh K, Carrasco-Nuñez G, Aranda-Gomez JJ, Smith IEM (eds) Monogenetic Volcanism, Geological Society of London, Special Publications, 446, pp 1-28.

Distal silicic tephra horizons provide chronostratigraphic control on the sedimentary record of an emergent Mid Quaternary coastline in SW North Island, New Zealand

Alan S. Palmer¹, Julie Palmer¹, Callum Rees¹ and Károly Németh¹

¹ School of Agriculture and Environment, Massey University, Palmerston North, New Zealand; a.s.palmer@massey.ac.nz

Keywords: Tephra, Quaternary, New Zealand.

During the Mid Quaternary, from about 350 ka to 280 ka, after a period of quiescence, there was a flair up of rhyolitic explosive volcanism during which over 2500 km³ of tephra and ignimbrite was erupted from the Taupo Volcanic Zone in the Central North Island (Downs et al., 2014; Gravley et al., 2016). Tephra, some related to large ignimbrite bearing eruptions, form valuable marker beds in Whanganui Basin over 200 km to the south of the eruption sources.

Whanganui Basin is a 40,000 km², NE-SW orientated fluctuating marine to terrestrial sedimentary basin in SW North Island, New Zealand. It occupies a back-arc position in the current Pacific-Australia plate boundary, west of an axial ridge of Mesozoic greywacke-argillite. Subsidence from the latest Miocene–Pleistocene has progressed in a NE-SW direction, so that the current depo-centre is west of the lower North Island, and 4–5 km of sediment has accumulated. Throughout the Quaternary sedimentation has matched subsidence resulting in the accumulation of shelf muds through to nearshore or coastal sands and occasional terrestrial deposits on a low lying broad coastal plain. The sedimentary record is preserved as 58 cyclothem resulting from Quaternary climate fluctuation on 41 ka (2.58–1 Ma) and then 100 ka cycles (1 Ma–0.125 Ma).

During the Quaternary (last 2.58 million years), Whanganui Basin has emerged from the sea and the coastline has steadily retreated towards the south and southwest. During interglacials in the western side of the basin, marine terraces were carved across Early Quaternary to Pliocene marine sediments. Central and Eastern parts of the basin filled with nearshore sands and shelf muds. Today these nearshore sands are preserved as marine terraces. During glacial cycles, the coastline retreated exposing a continental shelf at least 100 km wide. N-S flowing rivers at first entrenched into the marine terraces, but then aggraded with gravels and sands to form river aggradation surfaces. This was driven by increased erosion rates in the hinterland as forests gave way to a grass and shrub-land

vegetation as a response to the cooler climate. Older terraces were covered in loess derived from the aggradation surfaces. Each of the rivers became more confined with time as uplift, matched by river down-cutting isolated each river between interfluvies. This process was abetted by growth of NNE-SSW orientated anticlines and attendant fault zones, and rapid uplift of the Mesozoic greywacke-argillite axial ranges.

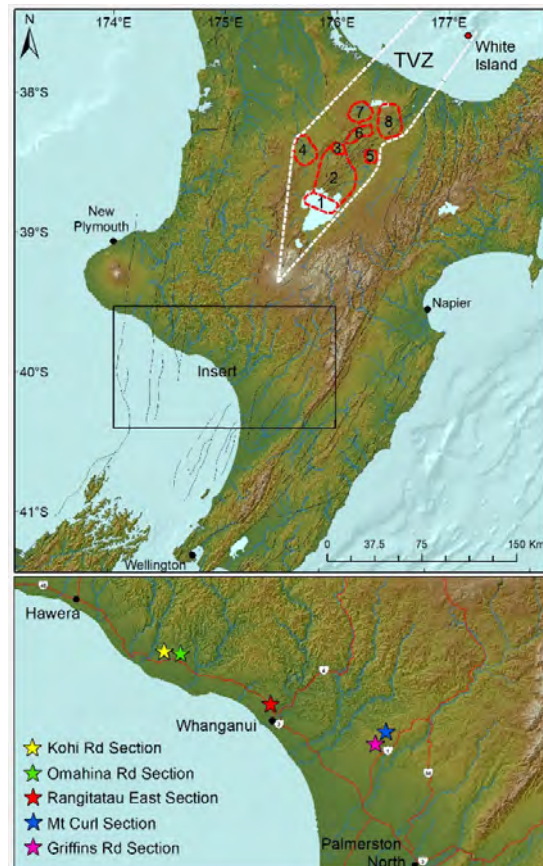


Fig. 1 – Map of the North Island showing study area in relation to the Whanganui Basin (WB) and Taupo Volcanic Zone (TVZ). Red outlines represent the eight major calderas within the TVZ: 1 = Taupo, 2 = Whakamaru, 3 = Ohakuri, 4 = Mangakino, 5 = Reporoa, 6 = Kapenga, 7 = Rotorua, 8 = Okataina. Black lines indicate faults. Some of the main sections studied are shown in the insert.

Five major tephras are common in the landscape, in order of decreasing age:

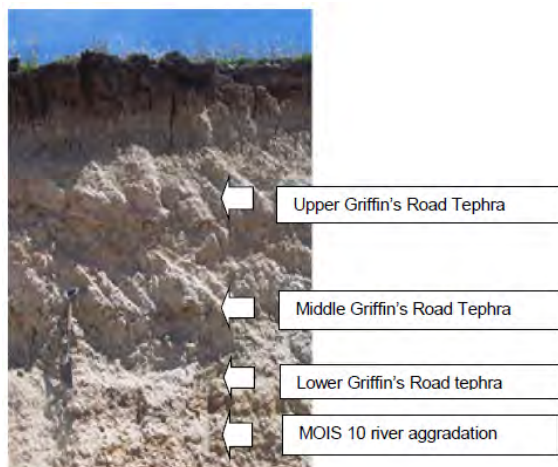


Fig. 2 – Griffin's Road tephras in a Quarry on Griffin's Road, Marton.

1. **Rangitawa Tephra** is well dated by Isothermal Plateau Fission Track dating (IPFT) at approximately 350 ka and is correlated with Whakamaru Ignimbrite erupted from just North of the present Lake Taupo. It is the most widespread, thickest and coarsest tephra, being 30-50 cm thick across the study area. The tephra is most commonly preserved within loess correlated to Marine Oxygen Isotope Stage (MOIS) 10.

2. **Lower Griffin's Road Tephra** is found directly overlying MOIS 10 river aggradation gravels and in dune-sands on the MOIS 11 marine terrace. Its source is unknown, and it is not directly dated but is thought to be approximately 320 ka based on its stratigraphic position.

3. **Middle Griffin's Road Tephra** is tentatively correlated to Matahina Ignimbrite in the Okataina Volcanic Centre. It is not directly dated but is found in alluvial over-bank deposits and dune-sands in the study area. It probably fell about 310 ka within MOIS 9c.

4. **Upper Griffin's Road Tephra** is distinctive for it forming a duripan (silica cemented pan) and thus being prominent in exposures. It is generally found in overbank alluvial deposits, possibly loess and dune-sands. It probably fell in MOIS 9c or 9b about 300 ka. Its volcanic glass chemistry tentatively correlates with Kaingaroa Ignimbrite erupted from Reporoa caldera in the Taupo Volcanic Zone.

5. **Fordell Tephra** is found in the western part of the area and has distinctive glass chemistry. It has yet to be correlated to any major eruption from the Taupo Volcanic Zone and fell approximately 290 ka during MOIS 9a.

These tephras are readily identifiable and correlated using volcanic glass chemistry. The tephras enable aggradation and marine terraces and other landscapes to be aged, and they provide a relative chronology for the emergence of the southwestern part of the North Island from the sea. The region studied here provides a unique opportunity to see the interplay of the climate change-forced sea level fluctuation and regional tectonic processes as the distal tephra horizons provide excellent chronostratigraphic markers. In addition, these tephras also show the widespread nature of silicic ash associated with major ignimbrite-forming eruptions from distal (200 km+) sources. There is scope to use them to correlate to adjacent on-shore and off-shore sedimentary basins.

References

- Downs, D.T., Rowland, J.V., Wilson, C.J.N., Rosenberg, M.D., Leonard, G.S. and Calvert, A.T., 2014. Evolution of the intra-arc Taupo-Reporoa Basin within the Taupo Volcanic Zone of New Zealand. *Geosphere*, 10(1): 185-206.
- Gravley, D., Deering, C., Leonard, G. and Rowland, J., 2016. Ignimbrite flare-ups and their drivers: A New Zealand perspective. *Earth-Science Reviews*, 162: 65-82.

Definition of internal horizons by litho-chemostratigraphic characterization for The Serie Tobífera, Austral Basin

Estefanía Pedró¹, Leonardo Tórtora¹, Guillermo Azpiroz² and Graciela Covellone²

¹ YPF Tecnología S.A, Argentina; estefania.pedro@ypftecnologia.com

² YPF S.A, Argentina.

Keywords: Serie Tobífera, chemostratigraphy, sedimentology.

The evolution of the Austral Basin includes an early rifting stage (Jurassic - Early Cretaceous) related with Gondwanian break out, filled with volcanic and volcanoclastic rocks, known as “Bahia Laura Group” in the Deseado Masif, “El Quemado Complex” in the Patagonian Andes and “Lemaire Fm.” in Tierra del Fuego Province; all of these stratigraphic units are englobed in the subsurface denomination “Serie Tobífera” (Cortiñas et al., 2005).

The difficulty to establish a regional correlation relies on: a strong compositional heterogeneity, complex areal distribution of facies and difficulties on individualizing volcanic events. Using a detailed description of lithofacies and chemical facies (chemofacies), we tried to contribute to the understanding of this volcanic and volcanoclastic rocks.

Analysis of XR fluorescence (XRF) were made altogether with thin section, cutting and plug descriptions of ten wells including Lago Fuego field (Tierra del Fuego, Argentina) and San Sebastian block (Tierra del Fuego, Chile).

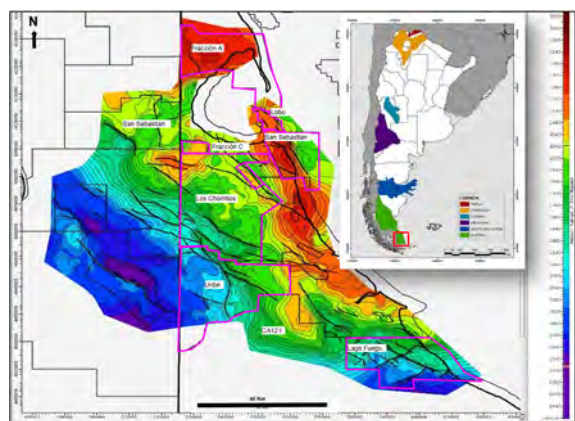


Fig. 1 – Ubiacion map, different fields and top Serie Tobífera structural map. Azpiroz et al. (2018).

Chemofacies are rock associations that have chemical signatures that not always match with the lithofacies. Chemofacies associations, called *chemosequences*, might be made and they can represent different paleoenvironmental, diagenetic, eustatic and tectonic conditions. In this work

chemofacies were defined by using *K-Means Cluster Analysis* (Davis, 2002). The number of classes/chemofacies is determined before making the calculation by an iterative procedure and depends on the heterogeneity of the stratigraphic column under study.

For Lago Fuego field 4 chemofacies were obtained: 1) volcanic rocks of intermediate composition (andesites), 2) volcanic rocks of silicic composition (vitrophyres), 3) pyroclastic deposits (tuffs and ignimbrites) and 4) siliciclastic rocks with an important influence of volcanoclastic sediments (volcanoclastic sands). The difference between the last two facies is simply compositional, so an *ad hoc* classification was established: dacitic affinity and rhyolitic affinity. This association contributes to identify different pyroclastic and volcanogenic/volcanoclastic sin-eruptive events with different origins. This association matches well with stratigraphic markers previously established using well logs such as GR, Resistivity, Density and Sonic.

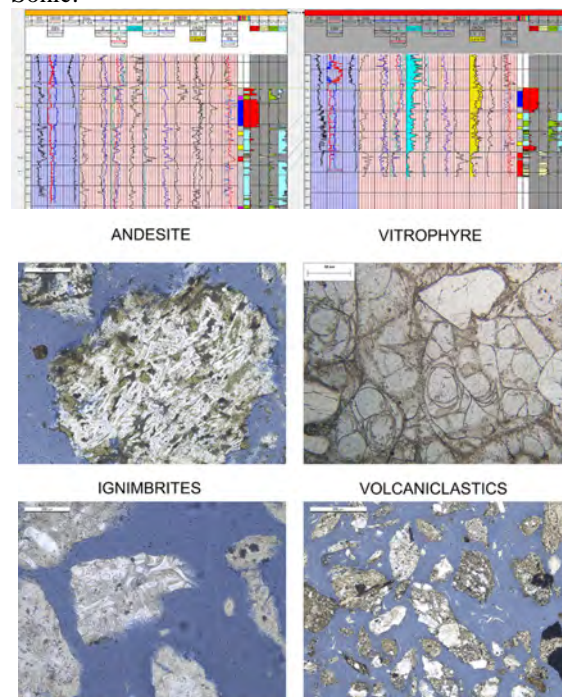


Fig. 2 – Upper: Well to well chemofacies correlation. Lower: Facies characterization using thin sections.

For San Sebastian field 4 chemofacies were calculated that match with different lithologies observed in the core plug descriptions. This helped to define an explosive volcanic interval dominated with vitric tuffs (ignimbrites), probably dacitic in composition and following upwards an effusive series composed by lava deposits of mesosilicic composition (andesites) and locally rhyolitic.

The results presented in this work contributed to improve precision in order to characterize both reservoir fields, refining intra-formational surfaces and reservoir thicknesses previously established. On the other hand, remarks XRF chemostratigraphic studies as a very important complementary tool to lithological descriptions in wells with scarce information, such as uncored wells or older ones with only drilling cutting samples.

Acknowledgements

All the Authors kindly thanked YPF S.A for allowing us to present the results of the studies.

References

- Bravo, P., Herrero, C., 1997. Reservorios naturalmente fracturados en rocas volcánicas Jurásicas, Cuenca de Magallanes, Chile. Asociación Colombiana de Geólogos y Geofísicos del Petróleo.
- Cortiñas, J., Homoc, J., Lucero, M., Gobbo, E., Laffitte, G. y Viera, A. 2005. Las cuencas de la región del Deseado. En Chebli, G. (ed.) Frontera exploratoria de la Argentina. Instituto Argentino del Petróleo y Gas 14: 289-306, Buenos Aires.
- Davis, J., 2002. Statistics and data analysis in Geology. John Wiley & Sons, Inc. New York.
- Hinterwimmer, G., 2002. Los reservorios de la Serie Tobífera. V Congreso de Exploración y Desarrollo de Hidrocarburos, pp. 36-56.
- Thomas, C., 1949. Geology and petroleum exploration in Magallanes province, Chile. AAPG. Geol. Bull., 33, 9: 1553-1578.
- Zilli, N., Pedrazzini, M. y Peroni, G., 2002. La Cuenca Austral, Capítulo III-3, pp 607-642, en M.J. Haller (Edit); Geología y Recursos Naturales de Santa Cruz. Relatorio del XV Congreso Geológico Argentino, El Calafate.

A rich archive of our volcanic past: Tephrostratigraphy in the Whanganui Basin, New Zealand

Callum Rees¹, Alan Palmer¹ and Julie Palmer¹

¹ School of Agriculture and Environment, Massey University, Palmerston North, New Zealand; callumrees@gmail.com

Keywords: Whanganui Basin, Quaternary, Tephrostratigraphy, Taupo Volcanic Zone, Tephrochronology

Whanganui Basin in the lower North Island of New Zealand (Fig. 1) provides one of the most complete Quaternary sedimentary records, exposed onland, anywhere in the world.

Positioned conveniently southwest of the modern day Taupo Volcanic Zone, the basin has acted as an important sedimentary archive, preserving the volcanic evolution of the Central Volcanic Region through space and time.

Beautifully preserved volcanic (Fig. 2) and biotic facies, remnant paleomagnetic signatures and carefully conducted fieldwork have been used in combination to develop a basin-wide, Late Miocene to Holocene chronostratigraphic framework, with direct implications to the geographic, tectonic and volcanic evolution of New Zealand and widely appreciated importance to global ice and sea level reconstructions.

Mapping and dating tephra and reworked volcanoclastic deposits has played a critical role in construction of the basin framework over the past 100+ yrs. Development and application of isothermal plateau fission-track dating and electron microprobe ‘fingerprinting’ techniques has resulted in collation of a library of geochemical datasets, enabling correlation of texturally complex units to known eruptive events.

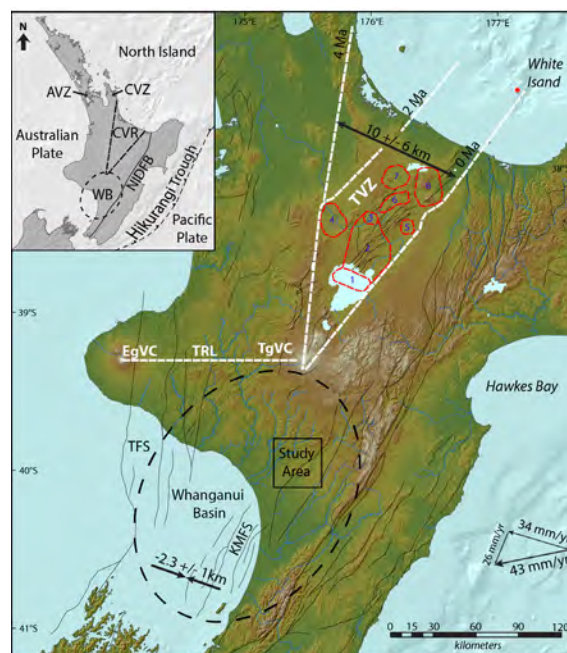
Here, we present our experience mapping in the eastern Whanganui Basin (Fig. 1), applying modern digital techniques together with traditional tephrostratigraphy to correlate marker horizons across the landscape. Rapid lateral facies variation within the Whanganui Basin’s Pleistocene succession has led to historic difficulties and misidentification during mapping. Tremendous benefits are gained from our improved ability to date and geochemically fingerprint tephra and pumice preserved within these sedimentary units.

We present important basin wide chronohorizons related to initiation of voluminous rhyolitic eruptions within the Taupo Volcanic Zone at the Mangakino Volcanic Centre c. 1.6 Ma.

Our work draws from decades of existing literature and unpublished datasets, contributing

sections from less frequented side tributaries and interfluves between the key river sections, to augment and refine existing stratigraphic correlations.

A unique glimpse into Pleistocene basin history is provided through the assessment and correlation of volcanic and siliciclastic units within the field area. We place constraint on the timing of uplift in the main axial range and document the evolution of drainage networks, landscape features and major regional geological structures.



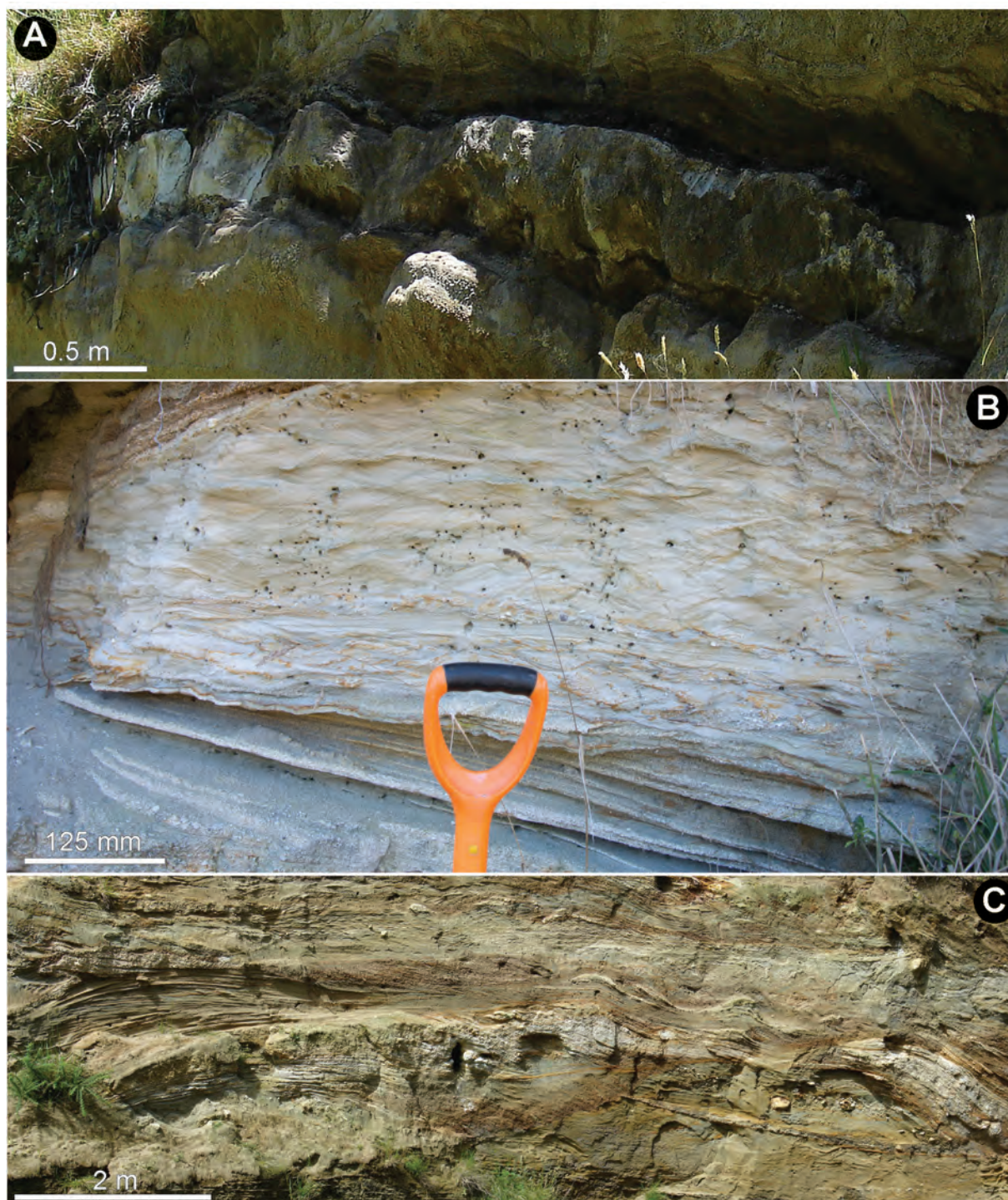


Fig. 2 – A) Mangapipi Tephra, c. 1.51 Ma. B) Potaka Pumice (Kidnappers) c. 1 Ma, displaying exquisite trough crossbeds. C) The first influx of Potaka Pumice into the Whanganui Basin, a nationally significant isochronous marker horizon, indicating emplacement of the Cape Kidnappers and Rocky Hill ignimbrites within the headwaters of rivers draining the central North Island.

The joy and sorrow of fieldwork in the 2.0-1.88 Ga Paleoproterozoic Amazonian Craton (Brazil)

Matteo Roverato^{1,2}, Caetano Juliani², Carlos M. Dias Fernandes³, Daniele Giordano⁴, Tommaso Giovanardi⁵

¹ School of Earth Sciences, Energy and Environment, Yachay Tech University, Ecuador. matteoroverato1809@gmail.com

² Instituto de Geociências, Universidade de São Paulo (USP), INCT-Geociam, SP, Brazil.

³ Instituto de Geociências, Universidade Federal do Pará, (UFPA), Belém, Brazil.

⁴ Università degli studi di Torino, Dipartimento di Scienze de la Terra, Torino, Italy.

⁵ Università di Modena e Reggio Emilia, Dip. di Scienze Chimiche e Geologiche, Modena, Italy.

Keywords: Amazonian craton, paleoproterozoic volcanism, lithofacies analyses

The Proterozoic Eon (2500 – 541 Ma) is the longest and youngest part of the Precambrian Supereon. This period was likely the most tectonically active in Earth's history. The Proterozoic volcanism acting during this Eon, played an important role in the geological evolution and formation of new crust (Eriksson et al., 2010; Strand and Köykkä, 2012). The subaerial volcanic rocks cropping out in the Amazonian craton (AC), as a whole, record one of the most complete and best-preserved Paleoproterozoic magmatic episodes on Earth.

The AC (Almeida et al., 1981) is located in the northern part of South America and is divided into two Precambrian shields, the Central-Brazil (or Guaporé, southern portion) and Guiana Shields (northern portion), which are separated by the Phanerozoic Amazonian Sedimentary Basin (Fig. 1) (Almeida et al., 1981).

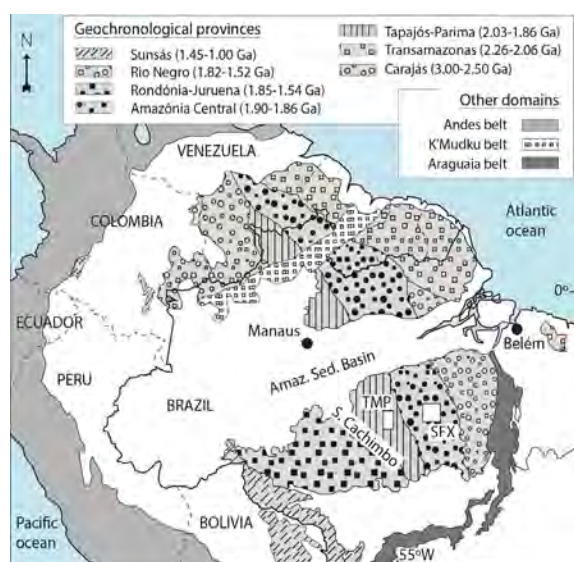


Fig. 1 - Location map of the northern South America and the Amazonian Craton with its geochronological provinces and other domains (according to Santos et al., 2000); TMP = Tapajós Mineral Province, SFX = São Felix do Xingú Region

Based on geochronological and isotopic data (Teixeira et al., 1989; Tassinari and Macambira, 1999; Santos et al., 2000) the AC is divided into several, NW-oriented geochronological provinces (Fig. 1), which have been interpreted as successive continental accretionary events, followed by granitic magmatism and tectonic reworking (Santos et al., 2000; Vasquez et al., 2008).

The subaerial volcanic rocks in Proterozoic and Archean volcano-sedimentary successions are often considered to be poorly preserved due to erosive/weathering processes (Muller et al., 2000). Of course, this is truthful, but at the same time the late Paleoproterozoic rocks here described, seems to be one of the rare exceptions to the rule. In fact, the superb preservation of the rock-textures allowed us to better understand the genetic processes that form these deposits and the geotectonic implication from the volcanoclastic sequences.

The title “The joy and sorrow of fieldwork in the 2.0-1.88 Ga Paleoproterozoic Amazonian Craton (Brazil)” is emblematic. In fact, whilst the extremely well-preserved architecture of the volcanic rocks found in the AC allows for better characterization of these rocks, the territory where these rocks crop out is not always easily accessible. Ancient volcanic regions represent a challenge for the understanding of emplacement dynamics especially when the stratigraphic relationships are difficult to decipher or blurred by erosion or vegetation cover. In the AC, the main task is not related to the weathering of the outcrops, in fact the rocks, as already mentioned before, are very well preserved, the main challenge is tracking down the outcrops in this wide territory. Difficulty in accessing the outcrops, due to dense forest cover and the presence of extensive water basins together with, in most cases, the lack of preservation of the outcrops with frequently obliterated structures and textures, significantly complicate this task.

In this presentation we report on the lithofacies analysis of rocks recognized during long field campaigns at the Tapajós Mineral Province (TMP)

and São Felix do Xingú Region (SFX) (Juliani et al., 2010; Fernandes et al., 2011; Roverato et al., 2017, Roverato et al., 2019). Within the study area, massive (felsic and intermediate) to banded lava flows and rheo-ignimbrites as well as felsic and intermediate primary volcanoclastic rocks of various origin are frequently found. Reworked (secondary) volcanoclastic rocks and sedimentary alluvial/coastal clastic deposits (epiclastic) are also widely distributed in both TMP and SFX areas (Fig. 2).

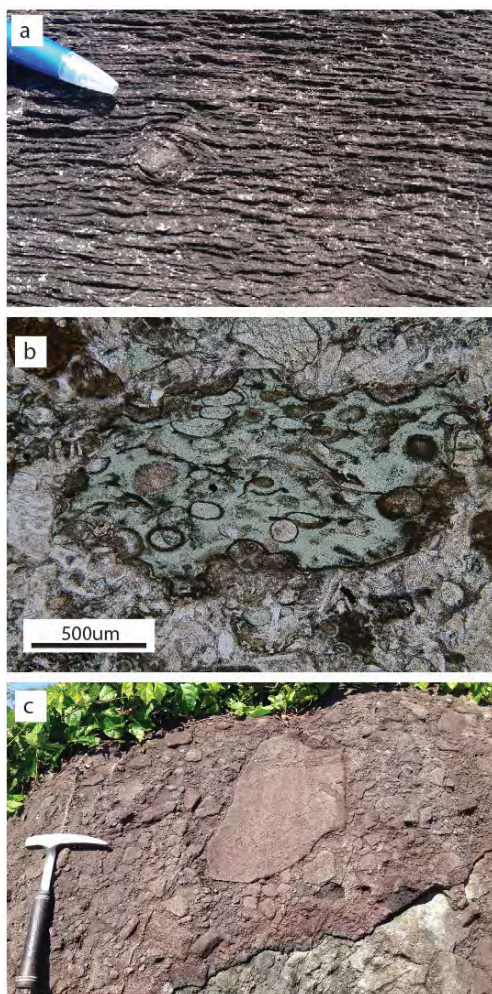


Fig. 2 - Examples of rocks cropping out in the studied area. a) High-grade welded felsic ignimbrite, b) detail of a pumice in an andesitic PDC deposit, c) secondary volcanoclastic deposit.

Finally, in terms of depositional panorama we could image very active volcanic environments characterized by large production of volcanic flows, pyroclastic density currents, and volcanoclastic debris, similar to the modern volcanic settings.

Acknowledgements

We would like to thank Jeovaci Jr. Martins da Rocha, Diego Felipe Gomez Gutierrez, Lucas

Villela Cassini and Carlos Marcelo Echeverri Misas for the help in the field and for the interesting discussions.

References

- Almeida, F.F.M., Hasui, Y., Brito Neves, B.B., Fuck, R.A., 1981. Brazilian structural provinces: an introduction, *Earth Science Reviews* 17, 1-29.
- Eriksson, P.G., Catuneanu, O., Nelson, D.R., Rigby, M.J., Bandopadhyay, P.C., Altermann, W., 2010. Events in the Precambrian history of the Earth: challenges in discriminating their global significance. *Marine and Petroleum Geology*.
- Fernandes, C.M.D., Juliani, C., Monteiro, L.V.S., Lagler, B., Misas, C.M.E., 2011. High-K calc-alkaline to A-type fissure-controlled volcano-plutonism of the São Félix do Xingu region, Amazonian craton, Brazil: Exclusively crustal sources or only mixed Nd model ages? *Journal of South America Earth Science* 32 (4), 351-368.
- Juliani, C., Fernandez C.M.D., 2010. Well-preserved Late Paleoproterozoic volcanic centers in the São Félix do Xingu region, Amazonian Craton, Brazil, *Journal of Volcanology and Geothermal Research* 191, 167-179.
- Mueller, W.U., Chown, E.H., Thurston, P.C., 2000. Processes in physical volcanology and volcanoclastic sedimentation: modern and ancient, *Precambrian Research* 101, 81-85.
- Roverato, M., Juliani, C., Marcelo Dias-Fernandes, C., Capra, L., 2017. Paleoproterozoic andesitic volcanism in the southern Amazonian craton, the Sobreiro Formation: new insights from lithofacies analysis of the volcanoclastic sequences, *Precambrian Research* 289, 18-30.
- Roverato, M., Giordano, D., Giovanardi, T., Juliani, C., Polo, L., (IN PRESS). The 2.0-1.88 Ga Paleoproterozoic evolution of the southern Amazonian Craton (Brazil): an interpretation inferred by lithofaciological, geochemical and geochronological data, *Gondwana research*.
- Santos, J.O.S., Hartmann, L.A., Gaudette, H.E., Groves, D.I., McNaughton, N.J., Fletcher, I.R., 2000. A new understanding of the provinces of the Amazon craton based on integration of field mapping and U/Pb and Sm/Nd geochronology. *Gondwana Research* 3, 453-488.
- Strand, K., Köykkä, J., 2012. Early Paleoproterozoic rift volcanism in the eastern Fennoscandian Shield related to the breakup of the Kenorland supercontinent, *Precambrian Res.*, 214-215, 95-105.
- Tassinari, C.C.G., Macambira, M.J.B., 1999. Geochronological provinces of the Amazonian craton, *Episodes* 22, 174-182.
- Teixeira, W., Tassinari, C.C.G., Cordani, U.G., Kawashita, K., 1989. A review of the geochronology of the Amazonian craton: tectonic implications, *Precambrian Res.* 42, 213-227.
- Vasquez, M.L., Sousa, C.S., Carvalho, J.M.A., 2008. Mapa Geológico e de Recursos Minerais do Estado do Pará, escala 1:1.000.000. Programa Geologia do Brasil, Belém, CPRM.

Newly identified debris avalanche deposits (DADs) in the North Harghita Mts. (Romania): emplacement history and tectonic significance

Ioan Seghedi¹, Viorel Mirea¹ and Péter Luffi^{1,2}

¹ Institute of Geodynamics, Romanian Academy, 19-21, J.-L. Calderon str., 020032 Bucharest, Romania; seghedi@geodin.ro

² Geological Institute of Romania, 1, Caransebeş str., 12271 Bucharest, Romania

Keywords: Flank collapse, debris-avalanche deposits, North Harghita Mts.

Geological mapping in old, poorly exposed volcanic areas has been recently improved by using digital elevation models (DEM). Here we document two old debris avalanche deposits (DADs) belonging to two adjacent volcanoes, Ostoros̄ and Ivo-Cocoizaş located in the North Harghita Mountains of the Călimani-Gurghiu-Harghita volcanic range (CGH) in the East Carpathians, Romania (Fig. 1).

CGH consists of twelve juxtaposed medium-sized composite volcanoes as well as several close-by isolated monogenetic cones. Volcanological observations and K/Ar geochronology attest that CGH is the result of a nearly continuous eruptive activity that migrated from NNW to SSE between 10.2 and 0.03 Ma (e.g., Pécskay et al., 2006 and references therein). Detailed geological mapping, petrographic observations, and K-Ar geochronology carried out in the past two decades led to the identification of a series of major edifice failure (e.g., Szakács & Seghedi, 1995, 2000). Several SSW-oriented DADs have been identified in association with the main volcanic edifices: Rusca-Tihu at ~7.8 Ma in Călimani Ma, Fâncel-Lăpuşna (~6.8 Ma) in Gurghiu, Vârghiş (~4.8 Ma) in North Harghita, as well as Luci-Lazu (~4.0 Ma) and Pilişca (~1.7 Ma) in South Harghita.

A series of new volcanological, petrographic, and geomorphic observations reveal two previously unidentified DADs generated close to each other at the Ostoros̄ and Ivo-Cocoizaş composite edifices at ~5Ma. The main difference from the other CGH DADs is their E-SE-directed displacement.

The Ostoros̄ (O) and Ivo-Cocoizaş (IC) composite volcanoes initiated their activity by phreatomagmatic eruptions, and continued as effusive cones delivering amphibole-pyroxene and pyroxene-bearing andesites in O and chiefly pyroxene andesites in IC. The two edifices form a buttressed system along with the Vârghiş volcano (Fig. 2). The activity of both volcanoes ended with major sector collapse events in the eastern part of their edifices, toward the Upper Ciuc Basin that developed in the same time (Mureşan & Szakács, 1996). The magmatic feeding systems of the volcanoes are indicated by hydrothermally altered

volcanic rocks and associated small intrusions (red circles in the figure 2).

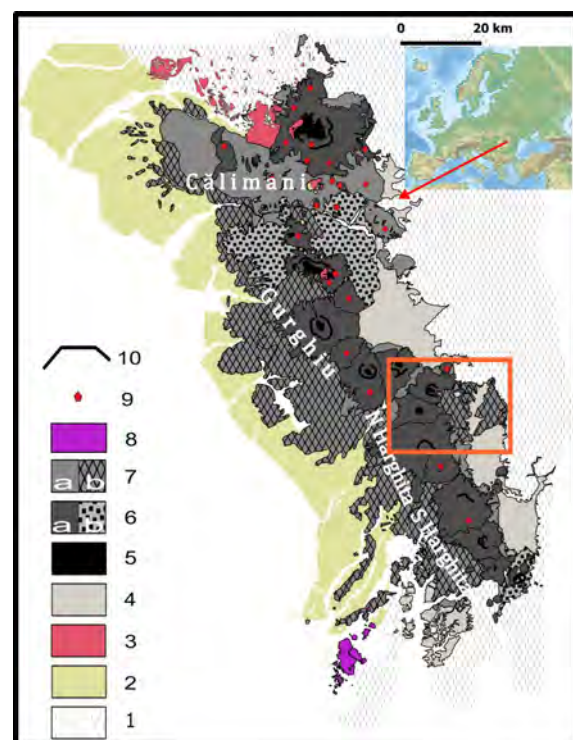


Fig. 1 – Simplified volcanic facies map of CGH. Inset shows location in Europe, frame indicates the studied area. Legend: 1. East Carpathian basement; 2. Transylvanian Basin formations; 3. Subvolcanic intrusions; 4. Intra-mountain Basins; Volcanic edifices: 5. Central facies; 6. Proximal facies: a. dominantly effusive; b. dominantly explosive; 7. a. medial-distal facies; b. debris avalanche deposits; 8. Perşani Mts. alkali basaltic field; 9. Caldera/crater/edifice failure rim.

The collapse scars are morphologically well exposed, being larger at IC; they are filled with toreva block, especially at IC. The original scars are now disrupted by subsequent degradation processes, soil formation and vegetation growth.

DADs deposits within the amphitheater are best observed in the O edifice, where tilted, hydrothermally altered amphibole-pyroxene lava blocks of several cubic meters (toreva) are

associated with monogenetic clast-supported lithic breccia. Outside amphitheaters, in the medial area, DEMs indicate numerous hummocks and various mound-shaped topographic features; these are well preserved, suggesting that no significant erosional processes occurred in the past 5 Ma. They are mostly covered by thin Quaternary deposits and soil, but are available to observations in several quarries. The two DADs tend to overlap and are thus difficult to distinguish in their medial sections.

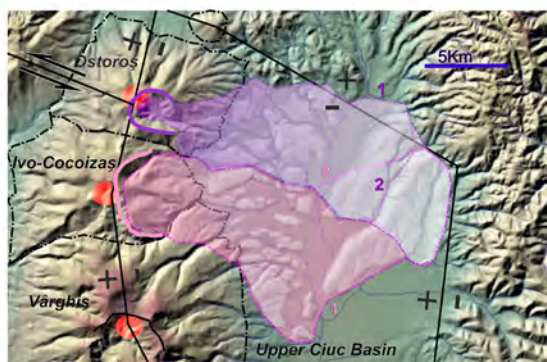


Fig. 2 – DEM of the studied area showing the distribution of hummocks as well as ridges in the distal DADs. The outline of volcanoes, their collapse scars, their inferred central feeding systems (red circles) are highlighted; normal and strike-slip faults are shown as black lines. Contours 1 and 2 mark two alternative DAD models discussed in the text.

In the medial section of DADs hummocks show various shapes. In the block facies dominated IC-DAD they appear as 60m high, ~500m wide, and 150-2000m long E-W elongated ellipsoids, and are locally associated with debris flows. Medial hummocks in O-DAD are dominated by matrix facies commonly associated with debris flow deposits; they too are E-W elongated, but display larger front widths up to ~2000m.

In the distal zone, both DADs show large hummocks oriented normal to the transport direction. There is a middle ridge between two N-S oriented hummocks in the front of O; the ridge in the front of IC displays a slight shift in orientation toward SW. If the two ridges and hummocky deposits developed simultaneously, but involved different lithologies, it is possible that the resulting contrasting mechanical behaviors have led to dissimilar emplacement dynamics (Valderrama et al., 2016).

The existing data allow us to formulate two depositional models (Fig. 2). The first model (M1) proposes that all the northern hummock groups including large volume of hydrothermally altered rocks belong to O, whereas the southern hummock groups dominated by block facies belong to IC. In this case, volume estimates for O-DAD and IC-DAD are 8.6 km³ and 10 km³, respectively. The second model (M2) proposes that the entire frontal ridge

belongs to IC-DAD, which has formed first, whereas the spreading of the subsequent O-DAD has been limited by the IC-DAD frontal ridge. In this scenario, O-DAD and IC-DAD mobilized 6.1 km³ and respectively 12.6 km³ material. Further observations are required to test these models.

The edifice failure events affecting O and IC appear to be closely related to a series of tectonic processes that followed the along-range growth of new volcanoes and the opening of intra-mountain basins in a post-collisional setting (Fielitz and Seghedi, 2005). After the concurrent formation of the Upper Ciuc Basin and activation of volcanism in North Harghita (6.5-5Ma), the initial strike-slip faults continued operating as normal faults, thereby facilitating edifice failures at O and IC as well as the displacement of their DADs toward E-SE. This situation represents an exception from the other DADs in CGH, which are displaced toward the SSW from their source volcanoes, most likely following the preexisting topographic slope toward the Transylvanian Basin (Seghedi et al., 2017).

Acknowledgements

This work was supported by grant of Ministry of Research and Innovation, CNCS – UEFISCDI, project number PN-III-P4-ID-PCCF-2016-4-0014, within PNCDI III.

References

- Fielitz W., Seghedi I. (2005) Late Miocene-Quaternary volcanism, tectonics and drainage system evolution in the East Carpathians, Romania. *Tectonophysics* 410, 111-136
- Mureşan M., Szakács A. (1998). The Ciuc formation: a Miocene pre-volcanic detritic deposit east of Harghita Mts (East Carpathians). *Rev Roum Géol*, 42, 17-27
- Pécskay Z., Lexa J., Szakács A., Seghedi I., Balogh K., Konečný V., Zelenka T., Kovacs M., Póka T., Fülöp A., Márton E., Panaiotu C. and Cvetković V. (2006). Geochronology of Neogene-Quaternary magmatism in the Carpathian arc and Intra-Carpathian area: a Review. *Geologica Carpathica* 57, 6, 511-530
- Seghedi I., Szakács A., Mirea V., Vişan M., Luffi P., (2017) Challenges of mapping in poorly-exposed volcanic areas. *Romanian Journal of Earth Sciences* 91 Special Issue, 90 pp
- Szakács A., Seghedi I. (2000) Large volume volcanic debris avalanche in the East Carpathians, Romania. in H. Leyrit & C. Montenat (eds) "Volcaniclastic rocks, from magma to sediments", H., Gordon Breach Science Publishers, p. 131-151.
- Valderrama et al., (2016) Dynamic implications of ridges on a debris avalanche deposit at Tutupaca volcano (southern Peru) *Bull Volc* 78:14

Volcano regrowth after sector collapse studied for Kamchatkan andesitic volcanoes

Alina Shevchenko^{1,2}, Viktor Dvigalo², Thomas R. Walter¹, René Mania¹ and Ilya Svirid²

¹GFZ German Research Centre for Geosciences, Potsdam, Germany; alinash@gfz-potsdam.de

²Institute of Volcanology and Seismology FEB RAS, Petropavlovsk-Kamchatsky, Russia.

Keywords: sector collapse, lava dome, stratocone.

Edifices of active andesitic volcanoes are subject to frequent destruction due to explosive or gravitational processes. However, after large-scale destruction many andesitic volcanoes begin to regrow. Usually, this process begins with the formation of lava domes in newly formed craters or collapse scars, such as at Mount St. Helens, Soufriere Hills, Merapi volcano, amongst others. In the case of continued activity and the predominance of constructional over destructive processes, the collapsed volcanic edifice may develop into a conical morphology; a process of collapse and regrowth that has been identified to be recurrent (Begét and Kienle, 1992). However, details on the regrowth, such as the transition from dome to cone building have been suspected but barely investigated. Here, we present morphologic observations of edifice regrowth at Shiveluch, Bezymianny, and Avachinsky volcanoes in Kamchatka, Russia. We integrate oblique and vertical aerial photogrammetry as well as high resolution satellite data to derive and compare topographic changes at the three andesitic volcanoes and identify different stages and locations of volcanic regrowth after sector collapse (Fig. 1).

At the present time, Shiveluch is the most active volcano of the Kamchatka Peninsula. During the 1964 catastrophic eruption, the edifice of the volcano, which comprised several merged domes, was destroyed by a southward directed sector collapse (Belousov, 1995). A collapse amphitheater 1.8×3.5 km in size formed. Since 1980, gradual regrowth of a new lava dome has been observed in the amphitheater. Our compilation of aerial photo data shows that in the first two stages of formation (1980–1981 and 1993–1995), endogenous dome growth prevailed. At the current stage (2001–present), the dome grows predominantly exogenously, identified by extrusion of lava lobes, coulées, and formation of crease structures. Although dome growth was accompanied by small-scale collapses, the volume of Shiveluch's dome gradually increased that increasingly filled the 1964 amphitheater (Shevchenko et al., 2015).

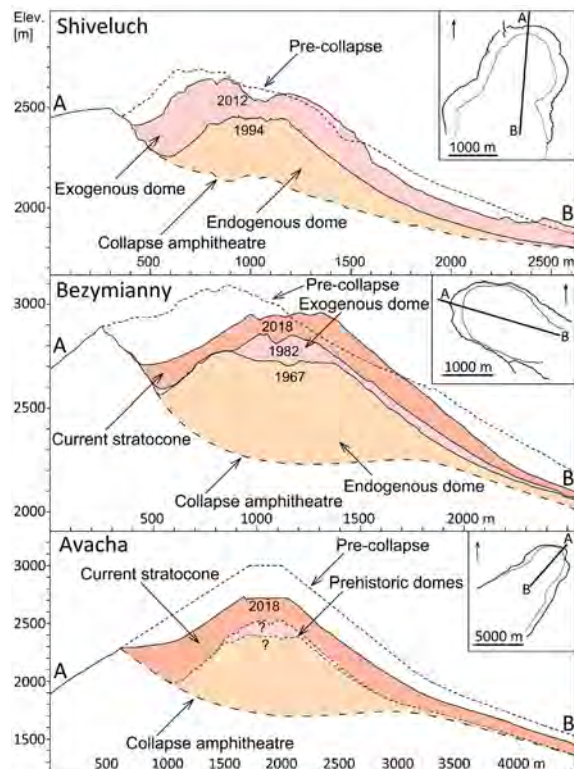


Fig. 1 Profiles of Shiveluch, Bezymianny, and Avachinsky volcanoes at the different stages of their regrowth after sector collapse.

In 1956, Bezymianny had a cataclysmic eruption followed by a major sector collapse that formed a 1.3×2.7 km amphitheater. Almost immediately after that, the amphitheater was replaced by new dome material. The dome growth at Bezymianny was marked by the consecutive emergence of three endogenous domes with distinct eruptive centers that merged together until 1969. Then, the character of growth changed to exogenous with the beginning of ductile lava extrusions on the slopes of the dome (Kirsanov et al., 1971). Since 1977, eruptions were frequently accompanied by lava flow emplacements (e.g., Bogoyavlenskaya et al., 1991; Girina, 2013). Our aerial data reveals that by 2009, the dome surface was completely covered by lava and pyroclastic flows that formed a conical shaped edifice, and a summit crater established in its current

position. Our satellite data shows that after the 2017 eruption series, large amounts of pyroclastic deposits filled most of the northern amphitheater so that the cone now incorporates parts of the northern 1956 crater rim. Therefore, our topographic data suggest that the dome at Bezymianny gradually converted into a conical morphology that strongly resembles that of a stratocone.

As the least active of the three volcanoes, Avachinsky had its last magmatic eruption in 1991. Catastrophic collapse of the Avachinsky edifice occurred at approx. 30 ka (Melekestsev et al., 1994), leaving behind a southwest facing horseshoe-shaped amphitheater measuring 4×4.5 km in size. Volcano regrowth began inside this amphitheater at approx. 3.8 ka (Melekestsev et al., 1994) with the formation of andesitic lava domes, as evidenced by deposits of pyroclastic flows, which supposedly descended during extrusive-explosive domes growth period (Masurenkov et al., 1991). Currently, the amphitheater accommodates a classic stratocone with a summit crater plugged by lava of the 1991 eruption.

Thus, using the observations of three active andesitic volcanoes of Kamchatka, we can distinguish three stages of volcanic regrowth after significant destruction. All three volcanoes were characterized by initial dome growth activity. Shiveluch currently shows the transition from endogenous to exogenous dome growth. At Bezymianny, the ongoing transition from exogenous dome to a stratocone hosting a summit crater is evident. In this case, we have a unique opportunity to trace this process from the very beginning. Avachinsky is an already regrown stratovolcano.

Close comparison of these volcanoes reveals that the stages of volcanic regrowth may be present at single volcanoes in chronology. In this, volcano growth is interrupted by partial or complete collapse of a sector, decapitating the central conduit with summit region. This leaves a morphology with a pronounced amphitheater geometry. New magmatic activity resumes inside this amphitheater, either off-centered or at the approximate location of the former alleged conduit zone. This new magmatic activity is initially in the form of endogenous dome growth, gradually changing to a more dominantly exogenous

dome growth. As the morphology of the new cone builds up, it gradually develops into a morphology that is characteristic for stratocones, with short lava flows, pyroclastic deposition and formation of a central apical crater system. When this new cone has reached a volume approaching the earlier protocone, it may produce again partial or complete collapse of a sector, so that the cycle restarts. This scenario has been observed at different stages at Shiveluch, Bezymianny, and Avachinsky, but bears strong similarities also to Soufriere Hills, Merapi, and Santa Maria volcanoes.

References

- Begét, J.E. and Kienle, J., 1992. Cyclic formation of debris avalanches at Mount St Augustine volcano. *Nature*, 356: 701-704.
- Belousov, A.B., 1995. The Shiveluch volcanic eruption of 12 November 1964-explosive eruption provoked by failure of the edifice. *J. Volcanol. Geotherm. Res.*, 66: 357-365.
- Bogoyavlenskaya, G.E., Braitseva, O.A., Melekestsev, I.V., Maksimov, A.P. and Ivanov, B.V., 1991. Bezymianny Volcano. In: Fedotov, S.A. and Masurenkov, Yu.P. (Eds.). *Active Volcanoes of Kamchatka*. Nauka Publishers, Moscow, 1: 168-197.
- Girina, O.A., 2013. Chronology of Bezymianny Volcano activity, 1956-2010. *J. Volcanol. Geotherm. Res.*, 263: 22-41.
- Kirsanov, I.T., Studenikin, B.Yu., Rozhkov, A.M., Chirkov, A.M., Kirsanova, T.P. and Markov, I.A., 1971. New stage of Bezymianny volcano eruption. *Bull. of Volcanol. Stat.*, 47: 8-14 (in Russian).
- Masurenkov, Yu.P., Yegorova, I.A., Puzankov, M.Yu., Balesta, S.T. and Zubin, M.I., 1991. Bezymianny Volcano. In: Fedotov, S.A. and Masurenkov, Yu.P. (Eds.), *Active Volcanoes of Kamchatka*. Nauka Publishers, Moscow, 2: 246-273.
- Melekestsev, I.V., Braitseva, O.A., Dvigalo, V.N. and Bazanova, L.I., 1994. Historical Eruptions of the Avachinsky Volcano on Kamchatka. Part 1. *Vulkanol. Seismol.*, 15: 649-667.
- Shevchenko, A.V., Dvigalo, V.N. and Svirid, I.Y., 2015. Airborne photogrammetry and geomorphological analysis of the 2001-2012 exogenous dome growth at Molodoy Shiveluch Volcano, Kamchatka. *J. Volcanol. Geotherm. Res.*, 304: 94-107.

Physical volcanology studies in the Perșani Mountains monogenetic volcanic Field (Southeastern Carpathians, Romania)

Ildikó Soós^{1,2}, Szabolcs Harangi^{1,2}, Károly Németh³ and Alexandru Szakács⁴

¹ Department of Petrology and Geochemistry, Eötvös University H-1117 Budapest, Hungary; ildiko.sooos14@gmail.com

² MTA-ELTE Volcanology Research Group, H-1117 Budapest, Pázmány Péter sétány 1/C, Budapest, Hungary

³ Institute of Agriculture and Environment, Massey University, Palmerston North, New Zealand.

⁴ Institute of Geodynamics, Romanian Academy, 19-21 Jean Louis Calderon, Bucharest, Romania

Keywords: geological mapping, ancient volcano, monogenetic volcanism.

The Pleistocene Na-alkaline basaltic volcanic area in the Perșani Mts. (Perșani Mountains Volcanic Field; PMVF) is located at the interior of the Carpathian bend area, at the junction between the Carpathian fold-and-thrust belt and the Transylvanian Basin. It is a small (>176 km²) field of monogenetic volcanoes, one of the smallest and youngest in the Carpathian-Pannonian Region (Seghedi and Szakács, 1994, Seghedi et al., 2016, Harangi et al. 2015) (Fig. 1). Melt generation from a variously depleted MORB mantle-source occurred by decompression melting under relatively thin continental lithosphere in the depth range from 85–90 km to 60 km (Harangi et al., 2013). Volcanic activity developed in at least five short-duration eruptive episodes in the time interval between ca. 680 and 1220 ka through 21 volcanic centers (Panaiotu et al., 2016, Seghedi et al., 2016). It is coeval with the waning phase of the Miocene to Pleistocene calc-alkaline volcanic activity in the East Carpathians. The principal volcanological features were presented on modern grounds by Seghedi and Szakács (1994) and Seghedi et al. 2016. Eruptive products associated with explosive volcanic eruptions include pyroclastic successions of maar/tuff ring type phreatomagmatic centers and Strombolian scoria cones. Lava fields and a shield-like volcano resulted from effusive activity are also present. Some of the structures, scoria cones and lava fields in particular, are well preserved and expressed in readily recognizable topographic features. Phreatic/phreatomagmatic centers of maar and tuff-ring type having little or no topographic expressions are more difficult to identify. A few of them have been tentatively inferred by studying the spatial distribution of phreatomagmatic deposits and their features (Seghedi and Szakács, 1994, Seghedi et al. 2016). Others, although hints of their existence were obtained, remain elusive concerning their actual location.

Although, the PVF has a limited areal extent, it shows a remarkable geodiversity in volcanic features led to an initiation of a volcano heritage study. For assessment of the geosites and their principal volcanic features, a reexamination using physical

volcanological approach is necessary. In particular, interpretation of the phreatomagmatic formations, based on detailed documentation of the sedimentological features and stratigraphic successions of various primary and reworked volcaniclastic rock units supported by grain-size distribution studies, has not been carried out so far.

The main goal of a recently started investigation is to better understand the eruptive conditions including the governing factors of fragmentation, the dominant eruptive and depositional mechanisms, and the range of the eruptive products created by different eruptive mechanisms.

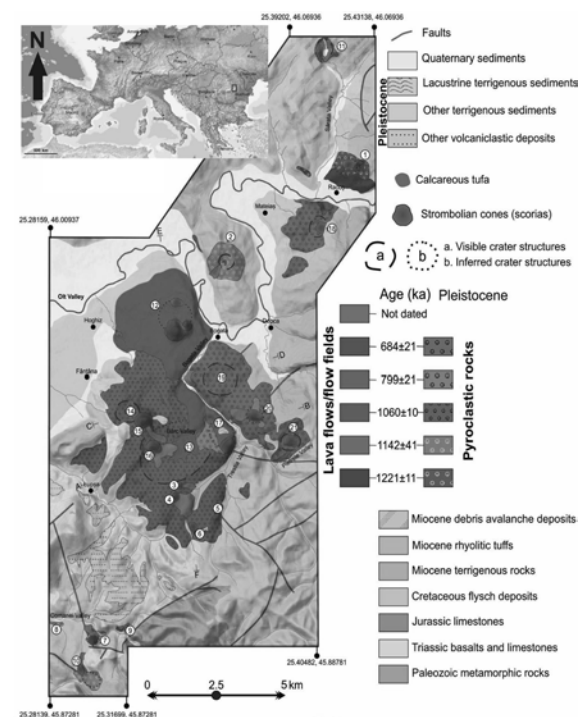


Fig. 1 – Volcanological map of the Perșani Mountains Volcanic Field with the different volcanic rocks and structures (modified after Seghedi et al. 2016). Circled numbers represent eruptive centers.

The volcanic assemblage of a complex volcanic edifice is well-exposed in the Racoș area (#1 in Fig.

1) due to intense quarrying allowing a detailed lithostratigraphic investigation. In the Hegheş scoria cone facies transition of the edifice-forming scoriaceous succession of the volcano can be studied along a proximal to distal cross-section. In the Brazi quarry a complex succession of pre-scoria cone volcanic deposits can be studied. At the base a shallow intrusive body with subhorizontal and vertical injection features penetrating into the > 30 m thick pyroclastic sequence can be followed. The pyroclastic unit, containing unconformities and faults (Fig. 2), is characterized by dark-colored beds alternating with light-colored beds rich in accidental lithic clasts. At the top of the sequence the contact with the scoria lapilli deposits of the overlying Hegheş Scoria cone is exposed (Fig. 2).



Fig. 2 – Alternating light and dark colored (black line) pyroclastic succession with lava intrusion in the Brazi quarry, Perşani Mountains Volcanic Field (L – lava, white dotted line – faults, white dashed line – boundary between lava and pyroclastic succession)

There are numerous exposures in the small-sized Perşani Mts. monogenetic volcanic field in which the study of the phreatomagmatic products allows to infer the types and the varying levels of magma-water interaction occurred during the volcanic activities. Among the various features, numerous ballistic impact structures such as plastically deformed bomb sags, soft sediment deformations and pyroclastic density current deposits are present in two areas (Mateiaş, Bogata) of the field (Soós and Szakács, 2013) indicating the water-saturated nature of the subsurface host-rocks (Németh et al., 2001); they were identified as maar-related phreatomagmatic deposits (Seghedi et al. 1994, 2016).

Our planned investigations intend to define the grain-size distribution of the matrix-supported pyroclastic units, the componentry and the morphological characteristics of the juvenile and lithic clasts using stereomicroscopy and Scanning Electron Microscopy. By defining clasts densities and vesicle characteristics (e.g. vesicle size, shape and density) relevant information will be obtained

allowing the understanding of the conditions and mechanisms of magma ascent and degassing which can also elucidate the changing conditions within the conduit between consecutive eruptive phases. We also plan a detailed examination of the compositional variations through time by plotting petrochemical data of the juvenile components found in consecutive units. By carrying out a detailed study of the most representative outcrops in the Perşani Mountains Volcanic Field we will contribute to the understanding of the monogenetic volcanism in the Carpathian-Pannonian Region and provide a base for the volcanic geoheritage assessment.

Acknowledgements

This research is supported by a Doctoral Scholarship of Eötvös Loránd University, Hungary. I am grateful for Erasmus + and Campus Mundi Grant for a 3-month research work in New Zealand and by this making also possible to attend the IAVCEI 5th Volcano Geology Workshop.

References

- Harangi, Sz., Jankovics, M.E., Sági, T., Kiss, B., Lukács, R., Soós, I. 2015. Origin and geodynamic relationships of the Late Miocene to Quaternary alkaline basalt volcanism in the Pannonian basin, eastern–central Europe. *Int J Earth Sci* 104(8):2007-2032.
- Harangi S., Sági T., Seghedi I., Ntaflos T. 2013. Origin of basaltic magmas of Perşani volcanic field, Romania: A combined whole rock and mineral scale investigation. *Lithos* 180–181, 43–57.
- Németh, K., Martin, U. and Harangi, S., 2001. Miocene phreatomagmatic volcanism at Tihany (Pannonian Basin, Hungary). *Journal of Volcanology and Geothermal Research*, 111(1-4):111-135.
- Panaiotu C.G., Dimofte D., Necula C., Dumitru A., Seghedi I., Popa R-G. 2016. Revised paleosecular variation from Quaternary lava flows from the east Carpathians. Romania. *Reports in Physics* 68(1):416–424.
- Seghedi, I., Popa, R-G., Panaiotu, C. G., Szakacs, A., Pecsikai, Z. 2016. Short-lived eruptive episodes during the construction of a Na-alkalic basaltic field (Perşani Mountains, SE Transylvania, Romania). *Bull Volc* 78:69.
- Seghedi, I., Szakács, A., 1994. The Upper Pliocene-Pleistocene effusive and explosive basaltic volcanism from the Perşani Mountains. *Rom. J. Petrology* 76, 101-107.
- Soós I., Szakács A. 2013. Tentative location of maar type phreatomagmatic alkali-basaltic volcanic centers in the Mateias area (Persani Mts., Romania). In: Büchner J., Rappich V., Tietz O. *Basalt 2013. Cenozoic Magmatism in Central Europe: Abstract and Excursion Guides*, Czech Geological Survey, p. 144.

Map representation of volcanic areas at regional scale in the Carpathian-Pannonian Region (Eastern Europe): Challenges and dilemmas

Alexandru Szakács¹, Jaroslav Lexa², Károly Németh³, Ioan Seghedi¹, Marinel Kovacs⁴, Vlastimil Konecny†², Zoltán Pécskay⁵ and Alexandrina Fülöp⁶

¹ Institute of Geodynamics, Romanian Academy, Bucharest, Romania; szakacs@sapientia.ro

² Geological Institute of the Slovak Academy of Sciences, Bratislava, Slovakia

³ School of Agriculture and Environment, Massey University, Palmerston North, New Zealand

⁴ Technical University, Cluj-Napoca, North Univ. Baia Mare Centre, Baia Mare, Romania

⁵ Institute of Nuclear Research, Hungarian Academy of Sciences, Debrecen, Hungary

⁶ De Beers Canada-Exploration, Toronto, Ontario, Canada

Keywords: volcanic areas, mapping, Carpathian-Pannonian region.

Miocene to Pleistocene volcanic areas are represented on classical geological maps at regional scale (e.g. 1: 1,000,000 or 1: 200,000) in the Carpathian-Pannonian Region (CPR) as patches of different colors according to the dominant rock type and age; actually they are petrographic maps (Fig. 1). Volcanic features are represented, if so, only as symbols indicating major volcanic centers (crater, stratovolcano, caldera, mostly their erosional remnants) and major lithostratigraphic units (distinguishing, for instance, between larger intrusions and lava-dominated areas from volcanoclastic sequences). Distal volcanic products, such as tuffs, are summarily represented only if they occur on wide surfaces. Buried or partially buried volcanic rocks (frequently present in the CPR) are not represented at all.

An international team is involved for decades in devising a CPR-scale volcanological map of the Neogene-Quaternary volcanic areas, the most important in Europe in terms of space (a region of ca. 600x300 km) and time (21 to 0.03 Ma) coverage. A synthesis on what we know about the Neogene volcanic forms in the CPR is given in Lexa et al. (2010), as part of this project. The major challenge in devising such a map arises from the fact that the area to be covered is located on the territories of seven different countries (Czech Republic, Slovakia, Ukraine, Austria, Slovenia, Hungary and Romania). The available cartographic information to be compiled in a unique regional map is extremely uneven in terms of map representation style of volcanic areas, scales and type of information included. Many of them, in particular those published before 1990, actually do not contain relevant volcanological information. Therefore their usage is limited. Moreover, a large volume of new (i.e. post-1990) data resulted from volcanological studies, petrological investigation, regional to local tectonic investigation and radiometric dating are not

yet integrated in a common database to be used in a modern approach to map representation of volcanic formations. However, there first important steps were already done, by arriving to an agreement among the international participants in this informal project regarding the major map representation approach (i.e. one based on the volcanic facies concept in which central, proximal, medial and distal facies are distinguished and map-represented) and new local (country-wide or individual volcanic areas-wide) volcanological maps were created (and some old ones re-interpreted) according to this principle. Moreover, a first attempt of regional (i.e. CPR-wide) volcanological map of the Neogene volcanism in the area has been completed, but not yet finished in a publishable form.

The main dilemmas of how to represent volcanic features on a regional scale are related to the following issues: 1) what kind of geological-tectonic background features be represented (e.g. which fracture zones/fault relevant from the viewpoint of volcanic evolution to be included and to what detail); 2) how to combine map symbols representing areas large enough to be included as outlined “patches” with those too small to be represented as so (e.g. as in Fig. 1); 3) how to represent in the same uniform and coherent manner large composite volcanic structures and small-sized monogenetic edifices; 4) how to represent buried volcanic areas covering large territories in CPR; although buried formations are not shown on standard geological maps, in the particular case of CPR, where large volumes of volcanic rock assemblages (including whole composite volcanic edifices are buried beneath thick younger sediments of the Pannonian Basin (Zelenka et al., 2004), their map representation is important and necessary to understand the space distribution and evolution of volcanism on the regional scale (Pécskay et al., 2006); 5) how to represent areas covered by distal

pyroclastic sequences, some occurring in a laterally-extensive fashion while some only locally, but wearing important information on the volcanic evolution of the area; 6) how to distinguish between primary and reworked volcanic rocks of any type in the map representation; 7) how to include major age and petrographic/ptrogenetic information on the volcanic facies-based regional map in a simply visualized and easily understandable manner; and more?

We are aware that the solution to the major challenge and to the above dilemmas resides in profiting from the newly available modern IT and GIS-based technologies. For that purpose, a comprehensive database is needed enclosing all the available relevant and validated information related to the Neogene volcanism in the CPR. Still, a CPR-wide volcanological map is needed as a most general regional map representation of the volcanic features and, as so, this map should include the most relevant general information available. Then, any user of the map and of the database may go to details by zooming on any of the particular Neogene volcanic areas of CPR or on particular parts of the volcanism (e.g. only the alkaline monogenetic volcanic fields). However, the user has to have access also to detailed map representations of all zones wherever the zooming is focused equally presented in terms of geological details and legend. That needs uniformization/standardization of map units and

scientists, including volcanologists, has to be actively involved.

Acknowledgements

Many colleagues from the seven countries covering the Neogene-Quaternary volcanic areas of CPR, who cannot be enumerated here individually, contributed with their published or unpublished data to the present-day knowledge on the Neogene volcanism in the CPR. Too, numerous national and international projects, which cannot be enumerated here individually, contributed to the same. We acknowledge all of them here.

References

- Lexa J., Seghedi I., Németh K., Szakács A., Konecny V., Pécskay Z., Fülöp A., Kovacs M. (2010). Neogene-quaternary volcanic forms in the Carpathian-Pannonian region: A review. *Central European Journal of Geosciences*, 2 (3): 207-270
- Pécskay Z., Lexa J., Szakács A., Seghedi I., Balogh K., Konecny V., Zelenka T., Kovacs M., Póka T., Fülöp A., Márton E., Panaiotu C., Cvetkovic V. (2006). Geochronology of Neogene magmatism in the Carpathian arc and intra-Carpathian area. *Geologica Carpathica*, 57 (6): 511-530
- Zelenka T., Kiss B., Kiss J., Nemesi L. (2004) Buried Neogene volcanic structures in Hungary. *Acta Geologica Hungarica*, 47 (2-3): 177-219

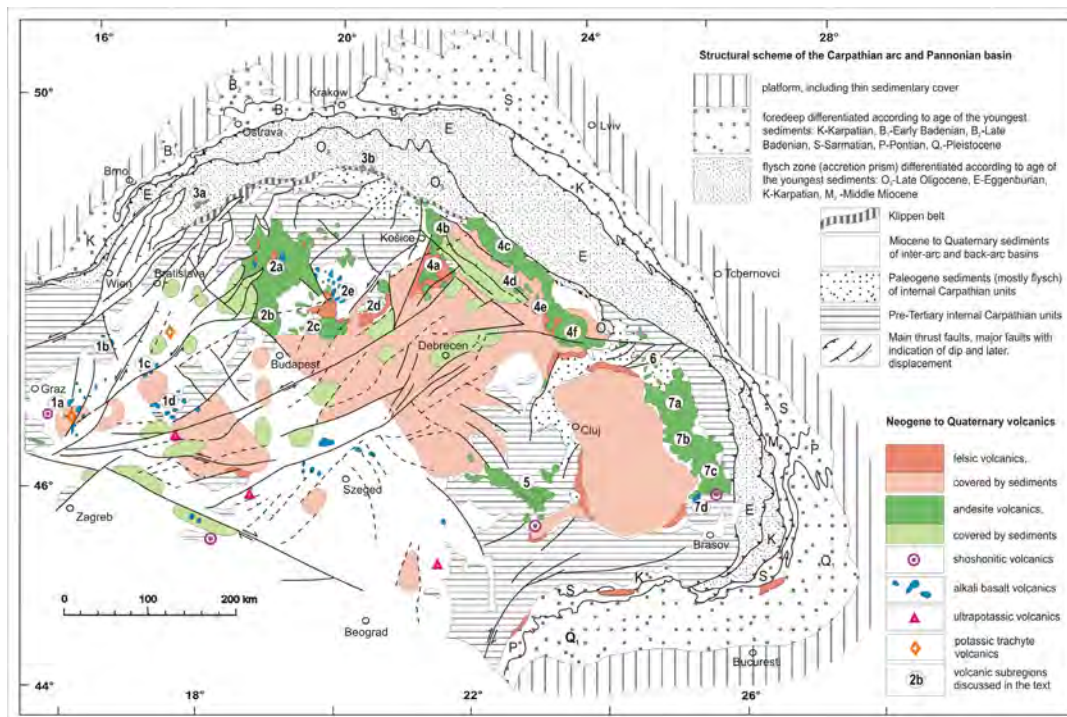


Fig. 1 General space distribution of Neogene-Pleistocene volcanic formations in the Carpathian-Pannonian Region (from Lexa et al., 2010)

achieve this goal a new generation of young

Unraveling a Miocene rhyolite dome field stratigraphy using porosity and water content data, Tokaj Mts, Hungary

János Szepesi¹, Réka Lukács¹, Tamás Buday², Zoltán Pécskay³, Andrea Di Capua⁴, Gianluca Groppelli⁴, Gianluca Norini⁴, Roberto Sulpizio^{4,5} and Szabolcs Harangi^{1,6}

¹ MTA-ELTE Volcanology Research Group, Budapest, Hungary; szepeja@gmail.com

² University of Debrecen Department of Mineralogy and Geology, Debrecen, Hungary

³ Isotope Climatology and Environmental Research Centre (ICER), Institute for Nuclear Research, Hungarian Academy of Sciences, Debrecen, Hungary

⁴ CNR-Istituto per la Dinamica dei Processi Ambientali, Milano, Italy

⁵ Dipartimento di Scienze della Terra e Geoambientali, Università degli Studi di Bari, Bari, Italy

⁶ Department of Petrology and Geochemistry, Eötvös University, Budapest, Hungary

Keywords: perlite, rhyolite, stratigraphy

Introduction

Effusive silicic volcanism produces extreme textural heterogeneity within flows and domes from their inner coherent core to autoclastic carapace (Calder et al. 2015, Fink and Manley 1987). The quantitative textural markers identify every lithofacies zones and allow comparisons between different lava/dome successions. Well exposed and drilled palaeovolcanic areas could give an excellent possibility to describe this internal lithological diversity.

Geological setting

The Telkibanya Lava Dome Field (TLDF, Tokaj Mts, Carpathian-Pannonian region) represents the final stage of the silicic explosive-effusive succession (ca 11.6 Ma, Szepesi et al. 2016, 2017). Perlite related projects drilled 30 boreholes with a dissected total depth reaching 2500 meters (Ilkey-Perlaky 1972; Gyarmati 1981). Our new facies oriented geological mapping started in 2013 and aimed to identify the evolutionary stages of the sequence. The internal lithofacies architecture of the dome/flow units comprises coherent (microcrystalline and glassy) and autoclastic (mainly glassy) lithofacies associations representing distinct parts (proximal, medial and distal) of the edifices.

Methods

From every major lithofacies zones density and total volatile content data were reported (Ilkey-Perlaky, 1972; Gyarmati 1981). The dense rock equivalent (ρ_{DRE}), bulk density (ρ_{BULK}) measurements (70 samples), which were further used for porosity calculations (ϕ_{dens} %) based on the equation of Shea et al., 2010:

$$\phi_{dens} = \frac{\rho_{DRE} - \rho_{BULK}}{\rho_{DRE}} \times 100$$

The volatile content dataset has been re-evaluated by comparing them with new thermogravimetry measurements (University of Debrecen, MOM

Derivatograph C, TGA: 25-1000°C, heating rate: 5°C min⁻¹) on fieldwork samples from every lithofacies zones (20 samples). quantifying the sample weight loss and total volatile content.

Results

The TLDF lavas display highly diverse textural characteristics, which grouped into 4 major lithofacies associations. The *micro crystalline core* (massive and fluidal rhyolite) and *transition zone* (perlitic rhyolite/) exhibit the highest density ($\rho_{bulk} = 2.3 \text{ g/cm}^3$) and usually have the least porosity ($\phi_{dens} < 15\%$), except for the lithophysae rich and highly vesicular zones (>40%). The *coherent glass* lithofacies association comprises the typical and pumiceous perlite. The typical perlite has also high density ($\rho_{bulk} = 2.3 \text{ g/cm}^3$) and poorly vesicular ($\phi_{dens} \sim 5\%$) character. The pumiceous perlite lithofacies zone shows diverse textural characteristics with sheared alternation of dense and highly vesicular domains. The decreasing density ($\rho_{bulk} = 2.2-1.9 \text{ g/cm}^3$) coupled with variable porosity values ($\phi_{dens} = 10-50\%$). The same trend developed in the *fragmented carapace*. The porosity increases from the perlite breccia ($\rho_{bulk} = 2.1 \text{ g/cm}^3$, $\phi_{dens} = 5-25\%$) through the red and black breccia ($\rho_{bulk} = 2.0 \text{ g/cm}^3$, ϕ_{dens} up to 30%) to pumiceous perlite breccia ($\rho_{bulk} = 1.78 \text{ g/cm}^3$, $\phi_{dens} = 12-38\%$) lithofacies, showing systematic negative correlation. Density of basal breccias is similar to coherent lithofacies associations, however it shows locally elevated porosity (>10%).

Generally, water contents decrease inwards from the carapace breccia to coherent core facies and correlate well with the porosity. The highest water content was measured in the pumiceous perlite and in the red and black breccia, especially in their matrix (up to 7 wt%). The mean water contents of the pumiceous perlitites and the fragmented lava samples are usually above 4 wt%. In the coherent perlite samples H₂O contents show only 3.1 wt%, and in the spherulitic perlite zone 2.2-3.6 wt% in the

perlitic zones but only 0.6 wt% in the spherulitic domains. In the crystalline rhyolite zone water content is usually decreased to 1 wt%.

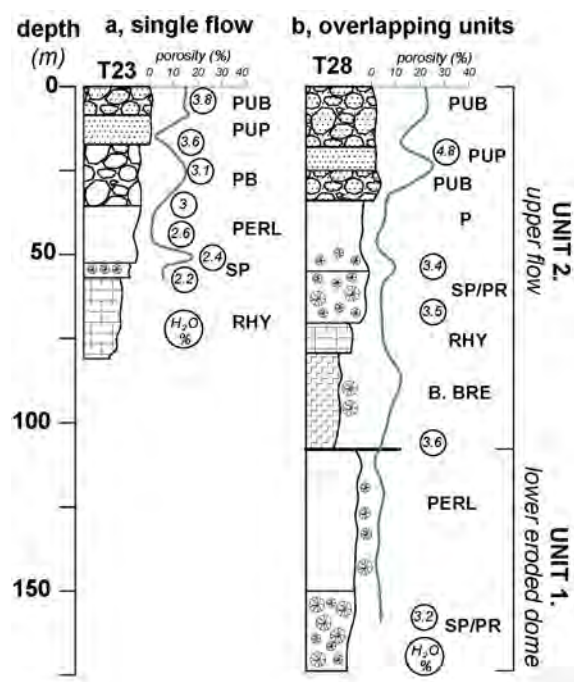


Fig. 1 – Borehole profiles of Telkibanya Lava Dome Field. with porosity and water content data a) single flow unit b) overlapping flow over an eroded dome Lithofacies abbreviations: *microcrystalline core*: rhyolite (RHY), *transition zone*: spherulitic perlitic (SP), perlitic rhyolite (PR), coherent glass: perlitic (PERL), pumiceous perlitic (PUP), *fragmented carapace*: perlitic breccia (PB), pumiceous perlitic breccia (PUB), basal breccia (B.BRE)

Discussion

The exceptionally exposed and drilled bodies of TLDF exhibit a regular textural zonation similar to Holocene rhyolite flows (Little Glass Mountain, Fink 1983; Obsidian Dome, Manley and Fink 1987; Ben Lomond, New Zealand, Stevenson et al. 1994). The subsurface lithofacies distributions indicate alternation of coherent and autoclastic zones building a complex stratigraphy. The water content changes revealed a porosity dependent variation tendency (Fig. 1). Elevated vesicularity of the groundmass in the outer fragmented and coherent lithologies could foster hydration (reaching ~5 wt% water contents). This is continuously decreased inward with increasing density (~3 wt% in perlitic) reaching the minimum in the rhyolite (<2%).

The drillings revealed a complete flow profile (Fig 1a) The deeper boreholes with recurring changes in porosity and water content indicate overlapping bodies (Fig. 1b). In this case the dominance of high density/low porosity coherent facies zones under basal breccia reinforces that erosion event occurred before development of upper flow unit. The TLDF lavas erupted in subaerial environment and suffered comprehensive hydration

right after or during deposition by meteoric water. Our results show a porosity-controlled hydration rate pattern, which determined the formation of economically important perlitic stock.

Acknowledgements

This study belongs to the Hungarian–Italian MTA-CNR bilateral research project 2016–2018.. The research is supported by the European Union and the State of Hungary, co-financed by the European Regional Development Fund in the project of GINOP-2.3.2-15-2016-00009 ‘ICER’.

References

- Calder, E.S., Lavallée, Y., Kendrick, J.E., Bernstein, M., 2015. Lava Dome Eruptions In: Sigurdsson H. (Ed.), The Encyclopedia of Volcanoes 2nd edition, Academic Press 343-362.
- Fink, J.H., 1983. Structure and emplacement of a Rhyolite Obsidian Flow: Little Glass Mountain, Medicine Lake Highland, Northern California. *Geol. Soc. Am. Bull.* 94, 362-380.
- Fink, J.H., Manley, C.R., 1987. Origin of pumiceous and glassy textures in rhyolite domes and flows in the emplacement of silicic domes and lava flows. *Geol. Soc. Am. S.* 212. 77-89.
- Gyarmati, P., 1981. Perlite exploration of the Tokaj-mountains Comprehensive report of the research between 1978-80 Manuscript OFG Data Storage Budapest, No. 9476. (in Hungarian)
- Ilkeyné Perlaki, E. 1972b Final report and reserve calculation of exploratory research of Telkibánya-Kőgát perlitic occurrence Archives of Hungarian Geological Survey, manuscript 1-311 (in Hungarian).
- Shea, T., Houghton, B.F., Gurioli, L., Cashman, K.M., Hammer, J.E., Hobden, B-J., 2010. Textural studies of vesicles in volcanic rocks: an integrated methodology. *J. Volcanol. Geoth. Res.*, 190, 271-289.
- Stevenson, R.J., Briggs, R.M., Hodder, A.P.W., 1994 Physical volcanology and emplacement history of the Ben Lomond rhyolite lava flow, Taupo Volcanic Centre, New Zealand. *New Zeal. J. Geol. Geop.* 37, 345-358.
- Szepesi, J., Harangi, Sz., Lukács, R., Pál-Molnár, E., 2016. Facies analysis of a Late Miocene lava dome field in the Tokaj Mts. (Carpathian-Pannonian Region): Implication for a silicic caldera structure? In: Branca S., Groppelli G., Lucchi F., Sulpizio R. (Eds.), Geological fieldwork in volcanic areas: mapping techniques and applications III. Workshop on Volcano Geology Abstract book 60-63.
- Szepesi, J. Soós I., Lukács, R. Sulpizio, R., Groppelli G., Harangi, Sz. 2017. Reconstructing the facies architecture and depositional settings of Miocene pyroclastic sequence, Tokaj - Slanske Mountains, Carpathian-Pannonian region *Rom. J. Earth Sci.* 91, 84-85.

Reconstructing the Pliocene magmatic and tectonic history of the Taos Plateau volcanic field region, northern Rio Grande rift, USA

Ren A. Thompson¹ and Amy K. Gilmer¹

¹ United States Geological Survey, Denver, CO, 80225, USA; rathomps@usgs.gov

Keywords: Rio Grande, rift, volcanism

Continental rifting is the dynamic process responsible for thinning of the sub-continental lithosphere, extension and rupture of the overlying crust, and eventual formation of a mid-ocean ridge and new plate boundaries. Most intra-continental rifts become inactive long before plate boundary formation and preserve the time-integrated record of tectonic and magmatic components of rifting, often spanning tens of millions of years. Linking the evolution of rift magmatism to extensional tectonism and associated basin formation in active intracontinental rifts is still problematic due to uncertainties in the 3D spatial distribution of volcanic deposits and the time transgressive nature of intra-basin extensional faulting.

The Rio Grande rift is North America's only active continental rift. It extends from Chihuahua, Mexico in the south to at least northern Colorado, structurally separating the North American craton to the east from the Colorado Plateau and Great Basin to the west (Fig. 1). The rift is considered the easternmost component of western North America's Basin and Range extensional terrane. Pliocene to Pleistocene rift basins and associated volcanic deposits are superposed on eroded deposits of regionally extensive Oligocene to Miocene arc volcanism related to the subduction of the Pacific and Farallon plates beneath the North-American continent (Christiansen and Lipman, 1972; Lipman, 1980; Chapin and Cather, 1994; Baldrige et al., 1995).

In the northern rift, the transition from arc to rift volcanism is temporally and spatially complex (Ricketts et al., 2016), with the dominant magmatic shift associated with the migration from large intermediate to silicic caldera-forming systems to dominantly basaltic to intermediate composition monogenetic volcanic fields erupted within north-trending, right-stepping, en-echelon, half grabens separated by strike-slip accommodation zones. The largest half graben delineating the geomorphic San Luis Valley is structurally bound to the east along a master range bounding fault system against the Sangre de Cristo Mountains. Subsurface interpretations based on gravity inversion modeling reveal north-south elongate sub-basins adjacent to the range bounding fault (Drenth et al., 2016).

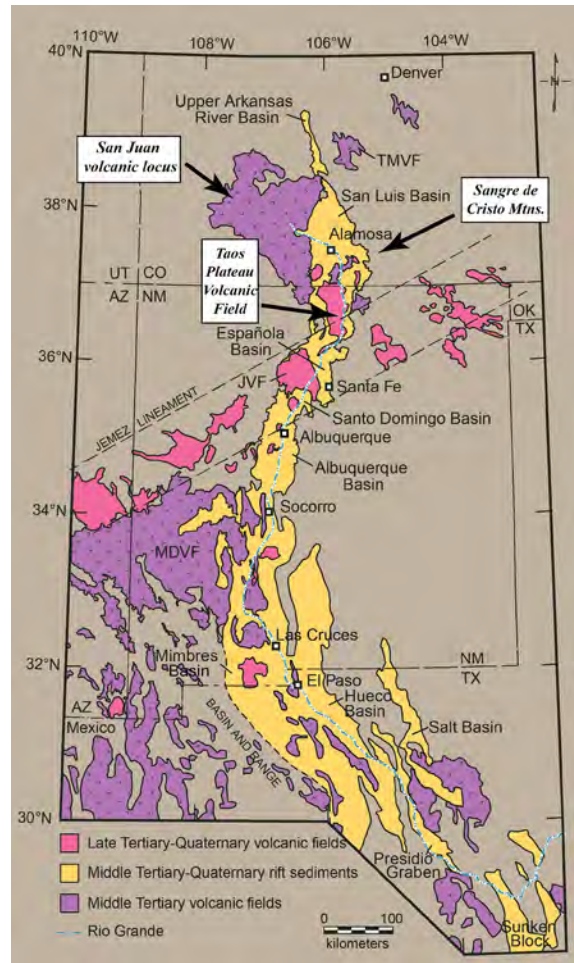


Fig. 1 – Simplified regional geologic map of Rio Grande rift basins, basaltic volcanic fields of the Jemez Lineament, and the eastern extent of Oligocene volcanic deposits of the mid-Tertiary ignimbrite flare-up. The San Juan locus of the southern Rocky Mountain Volcanic Field extends beneath the Taos Plateau and is preserved in the Questa area of the Sangre de Cristo Mountains, east of the basin. Miocene and Pliocene volcanic deposits are locally a dominant component of the basin-fill of the San Luis Basin. The TPVF spans the compositional range of other Pliocene to Pleistocene volcanic fields of the Jemez Lineament but shares a temporal and spatial association with active Pliocene and Pleistocene extension in the basin.

New geologic mapping of the Taos Plateau volcanic field in the San Luis Basin of northern New Mexico, combined with ~ 150 $^{40}\text{Ar}/^{39}\text{Ar}$ age

determinations, delineate >60 eruptive centers ranging in composition from basalt to rhyolite erupted episodically from 5.2-2.95 Ma (Thompson et al., *in press*). Volcanic and interbedded clastic deposits exposed in ~170 m deep gorges of the Rio Grande, its tributaries and surrounding areas encompass ~4500 km² of the southern San Luis Valley.

Eruptive volume, estimated from geologic map data, geophysical modeling of basin geometry and subsurface distribution of basaltic deposits, is ~300 km³; comprising 66% Servilleta Basalt, 17% dacite, 12% andesite, 3% trachybasalt & trachyandesite, and <1% rhyolite. The dominantly basaltic field records three main eruptive sequences (5.2-4.5 Ma; 4.1-4.0 Ma; 3.7-3.5 Ma).

Sedimentary interbeds deposited during 200-300 ka intervals between basaltic flow packages reflect local magmatic hiatuses during which basin deposition is dominated by prograding fan deposits sourced in the Sangre de Cristo Mountains. These interbeds reflect relative tectonic quiescence along the range bounding Sangre de Cristo fault. Conversely, rapid infilling of basin lows by lava flows is linked to intrabasin fault displacement along western margins of sub-basins.



Fig. 2 – View north toward Ute Mtn. from approximately 20 km south along the course of the Rio Grande. Ute Mtn is an andesite-dacite volcanic dome complex ranging in age from approximately 3.9-3.5 Ma and locally preserves 3.17 Ma basaltic andesite satellite vents along the southeastern flanks (likely more related to local extensional faulting than the Ute Mtn. magmatic plumbing system). The foreground is occupied by basaltic lava flows of the Servilleta Formation, here approximately 3.5-3.3 Ma. Ute Mtn. rises to elevations

of approximately 3070 m, nearly 800 meters above the valley floor.

Basalt erupted from north-trending fissures and small shields was coincident with faulting. Dacite dome complexes up to 21 km³ erupted volume (~5 Ma Guadalupe Mountain/Cerro Negro, ~3.9 Ma Ute Mountain, ~3 Ma San Antonio Mountain) reach elevations of ~770 m above the valley floor (Fig. 2). Each is spatially coincident with fault-bounded sub-basins superposed on the broader structural valley. Monogenetic andesitic shield volcanoes (~5-4.4 Ma and each ~15 km³ erupted volume) are distributed along the north-trending mapped intra-basin faults. Pliocene fault-slip rates are ~2.5 times the long-term rates determined for the valley, confirming the temporal link between local intra-basin extensional faults and the eruptive centers.

References

- Baldrige, W.S., Keller, G.R., Haak, V., Wendlandt, E., Jiracek, G.R., and Olsen, K.H., 1995, The Rio Grande rift, *in* Olsen, K.H., ed., *Continental Rifts—Evolution, Structure, and Tectonics*: Amsterdam, Elsevier Publishing: 233-275.
- Chapin, C.E., and Cather, S., 1994, Tectonic setting of the axial basins of the northern and central Rio Grande rift, *in* Keller, G.R., and Cather, S.M., eds., *Basins of the Rio Grande rift—Structure, stratigraphy, and tectonic setting*: Geological Society of America Special Paper 291: 5-23.
- Christiansen, R.L., and Lipman, P.W., 1972, Cenozoic volcanism and plate-tectonic evolution of the western United States, Part 2, late Cenozoic: *Proceedings of the Royal Society of London*, 271: 249-284.
- Drenth, B.J., Grauch, V.J.S., Thompson, R.A., Rodriguez, B.D., Bauer, P.W., and Turner, K.J., 2016, Preliminary 3D model of the San Luis Basin, northern Rio Grande rift, Colorado and New Mexico: *Geological Society of America Abstracts with Programs*: 48(7).
- Lipman, P.W., 1980, Cenozoic volcanism in the western United States—Implications for continental tectonics: *Studies in geophysics—Continental Tectonics*, National Academy of Sciences, Washington: 161-174.
- Lipman, P.W., 2007, Incremental assembly and prolonged consolidation of Cordilleran magma chambers: evidence from the Southern Rocky Mountain volcanic field: *Geosphere*, 3(1): 42-70.
- Ricketts, J.W., Kelley, S.A., Karlstrom, K.E., Schmandt, B., Donahue, M.S., van Wijk, J., 2016, Synchronous opening of the Rio Grande rift along its entire length at 25-10 Ma supported by apatite (U–Th)/He and fission-track thermochronology, and evaluation of possible driving mechanisms: *Geological Society of America Bulletin*, 128: 397–424.
- Thompson, R.A., Turner, K.J., Lipman, P.W., Wolff, J.A., and Dungan, M.A., (*in press*), Continental arc to rift volcanism of the southern Rocky Mountain-Southern Rocky Mountain, Taos Plateau and Jemez Mountains volcanic fields of southern Colorado and northern New Mexico: USGS Scientific Investigations Report 2017-5022-R.

Discoveries of pre-rift diatremes in the Lausitz Volcanic Field, Bohemian Massif – clues for landscape evolution and re-use of diatremes

Olaf Tietz¹, Jörg Büchner¹ and Erik Wenger¹

¹ Senckenberg Museum of Natural History Görlitz, Görlitz, Germany; olaf.tietz@senckenberg.de

Keywords: Melilithite, Ar-Ar ages, diatreme evolution.

The study area is located near the boundary to the České středohoří Volcanic Complex at the southern margin of the Lausitz Volcanic Field (LVF). Both volcanic areas are part of the Central European Volcanic Province (CEVP) and are genetically connected to the Ohře/Eger Rift, a prominent Cenozoic rift zone of the Bohemian Massif.

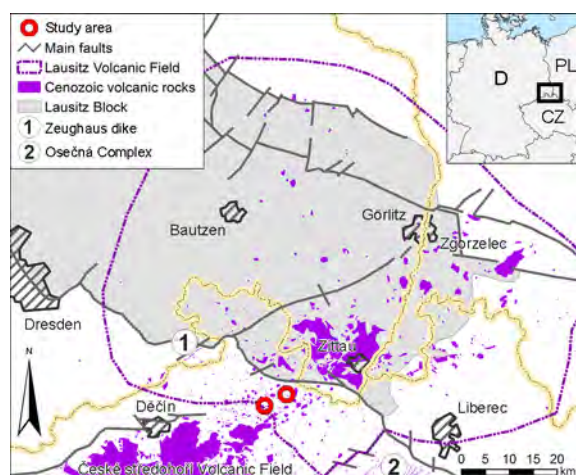


Fig. 1 – Map of the Lausitz Volcanic Field including the study area (modified from Büchner et al. 2015).

The LVF (Fig. 1) covers a transborder area encompassing parts of Eastern Saxony (Germany), Lower Silesia (Poland) and Northern Bohemia (Czech Republic). The Ar/Ar isotopic ages of its volcanic rocks range from 35 to 27 Ma but mostly centred around 32–29 Ma, indicating a climax stage of volcanism in the LVF during the Lower Oligocene (Büchner et al. 2015). The appearance of basaltoids (nephelinites, basanites, tephrites) as well as geochemically more differentiated volcanics (trachytes, phonolites) indicates petrographic bimodality of the lavas within the LVF. Mafic magmas typically formed scoria cone volcanoes or, less commonly, maar-diatreme volcanoes, whereas evolved rock melts formed crypto or lava domes. Today, major parts of most volcanic edifices are removed and their erosional relics – massive lava rocks of former lava lakes, lava flows, dykes, plugs and domes – mainly form hills and ridges.

This study focuses on two diatreme structures with ultramafic melilite-bearing lava intrusions (Fig. 1). Such silica undersaturated lavas are rare in the wider study region and are concentrated at the 8 km long Zeughaus dyke in Saxon Switzerland at the southeastern margin of the LVF (Seifert et al. 2008) and the Osečná Complex, near Liberec northeast of the České středohoří Volcanic Complex (Ulrych et al. 2008; 2014). Aside from these well-known areas, at least eight hitherto neglected occurrences are present in a small belt between both main distributions of the melilithic volcanic rocks in the southern margin of the LVF (Fig. 1). Only two of these melilithic localities are definitely located within diatreme structures (Fig. 1): these are the Stožec diatreme 4 km south of Jiřetín pod Jedlovou (North 50.837947, East 14.586664) and the Dolní Falknov diatreme in Kytlice (North 50.816581, East 14.520664). Both diatreme structures are surrounded by Cretaceous (Upper Cenomanian-Middle Coniacian) sandstones of the northern part of the North Bohemian Cretaceous Basin and are mapped by Valečka et al. (2006).

Both diatreme structures are filled by diatreme breccias, even cliffs occur in the case of Dolní Falknov. The lapilli-bearing tuff at both sites contains about 30% juvenile clasts and 10% host rock material, such as sandstone and quartz grains. Furthermore, well rounded gravel, cobble and boulder clasts of 1–50 cm in size are typical components in the breccia of both diatremes. These unique inclusions could be of Permian origin (Valečka et al. 2006). The diameters of the Stožec and Dolní Falknov diatremes are 175 m and 225 m, respectively. Therefore, the diatreme root zones reach 650 m and 850 m below the present earth's surface and consequently do not touch the Cadomian granitic basement, which lies respectively at depths of 730 m and 945 m (Valečka et al. 2006). Furthermore, bore holes of this area did not uncover Permian deposits between Cretaceous strata and the Cadomian basement. The Permian pebbles enclosed by the diatreme breccias therefore remain an unsolved enigma.

In both diatreme structures, three lava intrusions were dated with the ⁴⁰Ar/³⁹Ar isotopic age

method by Kathleen Zanetti, Nevada Isotope Geochronology Lab (University of Nevada, Las Vegas, U.S.A.). According to these analyses, the Stožec diatreme is penetrated by an olivine melilitite/vesecite of 68.80 ± 0.85 Ma (pseudo isochron age) and a basanite–olivine basalt of 30.49 ± 0.11 Ma (total gas age). The olivine melilitite nephelinite of the Dolní Falknov diatreme was dated at $\leq 68.34 \pm 0.33$ Ma (maximum age without statistically valid plateau or isochron). A similar K/Ar age, 60.5 ± 3.3 Ma, already exists for the Stožek melilitite (Skála et al. 2015).

Both ultramafic melilitite-bearing volcanic rocks indicate a start of volcanism at the southern margin of the LVF at the end of the Cretaceous period, confirming their affinity to the pre-rift melilitic magmatism of the Bohemian Massif (Skála et al. 2015, Ulrych et al. 2008; 2014). Additionally, the evidence for diatreme-related magmatism in connection with melilitic rocks is new for the Lausitz Volcanic Field. Furthermore, the younger basanite intrusion in the Stožec diatreme suggests a later re-use of the diatreme structure after about 40 Ma. This is remarkable, as lava intrusions in diatremes do not usually persist over such long-time spans. A particularly long example, 8 Ma, is the Hammerunterwiesenthal maar-diatreme volcano (Rapprich et al. 2017).

The Late Cretaceous (Maastrichtian) age of both diatreme structures enables interpretation of the origin of Permian pebbles for the first time. The new possibility is that the pebbles represent redeposited Permian rocks derived from the Lausitz Block which has been uplifted since around 100 Ma. These Permian materials (rhyolites and stable components from coarse breccias, such as quartzites) were rounded off to beach pebbles in Upper Cretaceous coastal areas at the southern margin of the Lausitz Island, subsequently becoming incorporated into the Maastrichtian diatremes. While all younger Late Cretaceous sediments have since been denudated, the Permian pebbles remain preserved in this sheltered subsurface position today. We therefore cannot find such coarse Cretaceous deposits with boulders up to 0.5 m in diameter, not even at the base of Oligocene volcanoes which overlie the remnants of Upper Cretaceous deposits of Cenomanian–Coniacian ages. This indicates the existence of younger Cretaceous strata (Coniacian to Maastrichtian; 86–68 Ma) and requires denudation off these younger sediments between early diatreme (pre-rift) volcanism (ca. 68 Ma) and the main Lower Oligocene volcanism (32–29 Ma). This denudation is confirmed by apatite fission-track analyses, which show greater uplift of Cretaceous sandstones prior to ca. 62 Ma (Kořínková et al. 2013). Vitrinite

reflectance measurements of Turonian bituminous coal deposits, which suggest a 3.3 to 4.2 km thick sediment packet once covered the now preserved Cretaceous sediments, (Tietz et al. 2018) provide additional evidence for such a former covering.

References

- Büchner J., Tietz O., Viereck L., Suhr P. and Abratis M., 2015. Volcanology, geochemistry and age of the Lausitz Volcanic Field. *International Journal of Earth Sciences*, 104: 2057-2083
- Kořínková, D., Adamovič, J., Svojtka, M. and Filip, J., 2013. Reconstruction of low time-temperature history of the crystalline blocks and sedimentary rocks along Lusatian Fault, Bohemian Massif. Poster abstract, 11th Meeting of the Central European Tectonic Studies Groups. *Geological and Geophysical Institute of Hungary, Várgesztes*: 30-31
- Rapprich, V., Suhr, P., Magna, T. and Pécskay Z., 2017. Basalt2017 Pre-conference fieldtrip: rift-flank volcanism in the Krusne hory/Erzgebirge Mts. area. Basalt2017 conference 18th to 22nd September 2017 in Kadaň/Czech Republic, Abstract & Excursion guides: 63-85
- Seifert, W., J. Büchner and O. Tietz, 2008. Der „Melilithbasalt“ von Görlitz im Vergleich mit dem Melilithit vom Zeughausgang: Retrospektive und neue mineralchemische Ergebnisse. *Zeitschrift für geologische Wissenschaften*, 36(3): 155-176
- Skála R., Ulrych J., Ackerman L., Krmiček L., Fediuk F., Balogh K., & Hegner E., 2015. Upper Cretaceous to Pleistocene melilitic volcanic rocks of the Bohemian Massif: Petrology and mineral chemistry. *Geologica Carpathica* 66(3): 197-216
- Tietz, O. and J. Büchner, 2015. The landscape evolution of the Lausitz Block since the Paleozoic – with special emphasis to the neovolcanic edifices in the Lausitz Volcanic Field (Eastern Germany). *German Journal of Geoscience*, 166(2): 125-147
- Tietz, O., Lange, W., Volkmann N., Gerschel H., Wenger E., Wilmsen M., Svobodová M. and Büchner J., 2018. Steinkohle in den Oberkreide-Sandsteinen von Waltersdorf im Zittauer Gebirge, Sachsen. *Berichte der Naturforschenden Gesellschaft der Oberlausitz*, 26: 77-105
- Ulrych J., Dostal J., Hegner E., Balogh, K. and Ackerman L., 2008. Late Cretaceous to Paleocene melilitic rocks of the Ohře/Eger Rift in northern Bohemia, Czech Republic: insights into the initial stages of continental rifting. *Lithos* 101: 141-161
- Ulrych J., Adamovič J., Krmiček L., Ackerman L., Balogh K. 2014. Revision of Scheumann's classification of melilitic lamprophyres and related melilitic rocks in light of new analytical data. *Journal of Geoscience*, 59: 3-22
- Valečka, J. (and 12 co-workers), 2006. Geological base map of the Czech Republic, sheet 02-242 Dolní Podluží. Czech Geological Survey, Prague: 1 map sheet and Explanation booklet: 1-57

Stratigraphy of pyroclastic deposits associated with multiple vent activity of rhyolite eruptions at Tarawera, New Zealand: the case of the ca. 1314 ± 12 AD Kaharoa eruption

Andrea Todde¹, Károly Németh¹ and Jonathan N. Procter¹

School of Agriculture and Environment, Massey University, Palmerston North, New Zealand; a.todde@massey.ac.nz

Keywords: Tarawera, rhyolite eruptions, stratigraphy.

We present here some aspects of an ongoing research that aims to understand the depositional patterns, eruptive dynamics and possible eruption scenarios for rhyolite eruptions at Tarawera, New Zealand. In this study, we characterized the pyroclastic deposits emplaced during the ca. 1314 ± 12 AD Kaharoa eruption, the youngest rhyolitic event in New Zealand, chose as case study, and for which no written chronicles are available.

Mid- to large-scale eruptions typically consist in a composite succession of individual eruptive phases, characterized by: (i) quantifiable intensities and magnitudes, (ii) specific dynamics involving magma ascent in the volcanic conduit, and (iii) styles of the resulting eruptive activity. Similar eruptive phases may repeat during an eruption or may alternate with phases of different activity. In addition, several vents can be sequentially and/or simultaneously active, generating very complex proximal stratigraphy. Given these complexities, difficulties arise to link medial deposits to the proximal products of deposition and therefore to the source vent(s). This makes also the time-variant evolution of eruption hard to constrain, particularly at active volcanoes with limited or not available historical records.

All the four rhyolitic eruptions occurred along the Tarawera Volcanic Complex in the past ca. 22 ka, shared three common complexities: (i) the multi-vent nature of the eruption; (ii) a long-lasting activity with possible period of quiescence between eruptive events; (iii) changing in style, magnitude and intensity during the explosive activity, that precede or alternate with the extrusion of lava domes and flows.

The AD 1314 ± 12 Kaharoa eruption developed at seven different vents aligned on an 8-km-long lineament across Mt. Tarawera. The eruption encompassed a wide spectrum of rhyolite activity and exhibited a complex succession of events. The first part of the eruption consisted in a series of individual sub-Plinian to Plinian events, and progressed towards the extrusions of lava domes, with block-and-ash flows accompanying dome growth (Nairn et al., 2001). A medial to distal stratigraphic framework have been proposed by

Sahetapy-Engel et al. 2014, in which the isopach maps of 13 sub-Plinian to Plinian fall units have been traced, and for those a total DRE volume was estimated at 7.3 km³. Each fall unit was dispersed into discrete lobes within two main directions, SE and N from Mt. Tarawera.

In this study, the deposits of the explosive phases of the Kaharoa eruption distributed SE and N from eruptive vents in proximal to medial sites (up to 10-15 km from Mt. Tarawera's summit at Ruawahia Dome) have been analysed and reinterpreted. The overall stratigraphic architecture of the Kaharoa tephra sequence consists in several cm- to dm-thick, coarse-grained pumiceous lapilli beds, separated by cm-thick beds of fine ash. A remarkable characteristic of the deposit in regard to the relationship between lapilli and ash beds can be summed up as follow: in medial sites, a single or more adjacent, dm-thick, lapilli beds is capped by a well sorted cm-thick massive ash layer, having >50 wt% of the layer finer than 63 µm.

This pattern repeated with stratigraphic height, along with the lithological and sedimentological features of the deposit, has enabled us to subdivide the SE succession of tephra beds into seven lapilli-bearing units (L-1S to L-7S), three main ash-bearing unit (A-1S to A-3S) and four inter-beds of fine ash between the lapilli units (AX-1S to AX-4S). Note that here we use the term unit to define a bed or group of beds recognizable in the field for a distinct pattern of sedimentological and lithological characteristics, distinguishable from the over- and underlying units, that occupies a precise stratigraphic interval in the tephra sequence.

The northern succession of tephra beds resembles the one of the SE sector, however less units can be identified, being at least three lapilli-bearing units (L-1N to L-3N), two ash-bearing units (A-1N to A-2N) and two inter-beds of fine ash (AX-1N and AX-2N).

The presence of inter-beds of fine ash helped to subdivide the whole stratigraphy (SE and N sectors) into units and interpreted them in term of eruptive events. However, reliable correlations of units among different outcrops are possible only within 10-15 km from the vents, as the threefold division of

the stratigraphy in lapilli and ash units, and interbeds of fine ash, is not maintained, due to the limited dispersal of the ash deposits. In addition, within 10 km from the vents, the interbeds of fine ash have a narrow dispersion making the overall architecture of the Kaharoa deposit to pass from ash-dominated to an interbedded lapilli and ash deposit, and to lapilli-dominated within outcrops few km apart. We tentatively interpreted these relative rapid outcrop-scale variations as possibly due to the combined effects of the slightly different dispersal of individual units and the migration of the eruptive vent position from the SE to the N units.

The dispersal, thickness and sedimentological characteristics of the lapilli-bearing units are consistent with fallout from explosive events of sub-Plinian activity. Deposits characteristics of individual units suggest different evolutions for each sub-Plinian event, characterized by different fluctuations in mass discharge rate: stratified units are associated with unsteady event, while units characterized by size grading of the pumice clasts are possibly associated with quasi-steady events.

Three main types of ash-bearing units have been recognized on the field. (i) Layer of well-sorted coarse ash to fine lapilli. (ii) Stratified layer alternating massive, well-sorted coarse ash beds and damp, cohesive fine ash beds. (iii) Thick cross-stratified coarse ash dominated deposit with dune structures. The first type forms the bottom of both the SE and N successions and is interpreted as the low-intensity opening phases of the explosive vents, whereas the last two types mark significant changes in the eruptive dynamics within the sequence of sub-Plinian events.

The interbeds of fine ash at the top of most of the lapilli-bearing units are interpreted as the results of (i) the delayed sedimentation from the umbrella region of individual columns and (ii) as small volume pyroclastic density currents.

Only few field evidences of time brakes have been found within the tephra sequence, being two erosional gullies at different stratigraphic positions in the SE successions, at the contact between lapilli-bearing and ash-bearing units, and are interpreted as short hiatus in the eruptive activity.

This study shows the complexity of the Kaharoa deposit and the need to achieve a comprehensive stratigraphic framework of proximal and medial areas. Units identified in the field can be then placed into eruptive phases of dominant eruptive dynamics and style, for which individual volcanic hazards can be evaluated.

Acknowledgements

This research is supported by the “Quantifying Exposure to Specific and Multiple Volcanic Hazards” programme of the New Zealand Natural Hazards Research Platform, funded by the Ministry of Business, Innovation and Employment.

References

- Nairn, I. A., Self, S., Cole, J. W., Leonard, G. S., & Scutter, C. (2001). Distribution, stratigraphy, and history of proximal deposits from the c. AD 1305 Kaharoa eruptive episode at Tarawera Volcano, New Zealand. *New Zealand Journal of Geology and Geophysics*, 44(3), 467-484.
- Sahetapy-Engel, S., Self, S., Carey, R. J., & Nairn, I. A. (2014). Deposition and generation of multiple widespread fall units from the c. AD 1314 Kaharoa rhyolitic eruption, Tarawera, New Zealand. *Bulletin of Volcanology*, 76(8), 836.

Scoria cones of the Quaternary Ollagüe Volcanic Field, Central Andean Volcanic Zone, northern Chile

Gabriel Ureta^{1,2}, Károly Németh⁴, Felipe Aguilera^{2,3} and Szabolcs Kósik⁴

¹ Programa de Doctorado en Ciencias Mención Geología, Universidad Católica del Norte, Av. Angamos 0610, Antofagasta Chile; gabriel.ureta@ucn.cl

² Centro Nacional de Investigación para la Gestión Integrada del Riesgo de Desastres (CIGIDEN), Chile.

³ Departamento de Ciencias Geológicas, Universidad Católica del Norte, Av. Angamos 0610, Antofagasta, Chile

⁴ School of Agriculture and Environment, Massey University, Palmerston North, New Zealand.

Keywords: monogenetic volcanism, Salar de Carcote, cinder cone.

Monogenetic volcanism produces small volume volcanoes with a wide range of eruptive styles, lithological features and geomorphic architectures (Németh and Kereszturi, 2015). Scoria cones, also known as cinder cones, are formed by the accumulation of tephra due to periodic mild explosive eruptions of mafic to intermediate magma. They are characterized by conical geometry commonly with a crater on top. Eruption that fed from small-volume magma batch or several magma batches may go through a variety of eruptive styles (e.g. Hawaiian, Strombolian, and violent Strombolian eruptions), including magma-water interactions (phreatomagmatism), especially after the initial stages if they are dominated by relatively high magma flux (Kereszturi and Németh, 2012).

Scoria cone formation is controlled by (1) pre-existing condition as topography and environmental conditions; (2) syn-eruptive processes as tectonics that drive magmatic eruptions, the eruptive dynamics, the sedimentary features of the fallout deposit, and environmental factors; and (3) post-eruptive processes as weathering, erosion and the re-deposition (Wood 1980a, b, Kereszturi and Németh, 2012). Scoria cones are also commonly associated with stratovolcanoes and tend to form on their flanks following some sort of rift zones. This study presents the preliminary results of the integrated use of the volcanic stratigraphy, petrography, petrology and the morphometric analysis to understand the evolution of low-magma output rate magmatic systems from a perspective of spatial, temporal, volumetric, and of eruption style patterns on the scoria cones from the Ollagüe Volcanic Field, northern Chile.

Ollagüe volcano (21°18'S - 68°11'W; 5,868 m a.s.l.) is a composite stratovolcano of Quaternary age with a summit lava dome and a persistent fumarolic activity at east from Salar de Carcote (Fig. 1). Quaternary volcanism on Ollagüe area was developed during extensional event during relaxation times of the crust (Tibaldi et al., 2009). Ollagüe volcano hosts multistage effusive and explosive eruptive products with an age range from

1.2 ± 80 Ma to 130 ± 40 ka, and a range from basaltic andesites to andesites and dacites as well as two debris avalanche deposits (Vezolli et al., 2008). The basaltic andesite centers are represented by Poruñita, SC2, Luna de Tierra and some other scattered strongly eroded and/or salar deposit submerged unnamed scoria cones in the northern part of the Salar de Carcote (Fig. 1). In this work, the first three monogenetic centers have been described in terms of location, morphology, volcanology, petrography and geochemistry.

Poruñita (21°19'7.11"S - 68°17'40.79"W; 3,932 m a.s.l.) is located towards northeast border of the Salar de Carcote, in the same latitude that Ollagüe volcano (Fig. 1). This monogenetic center presents at less two evolution stages characterized by a pyroclastic deposit with a horseshoe shaped and a well-preserved but truncated cone with a symmetrical profile with a shallow, debris-filled crater. This cone profile would be classified closest to be a perfect cone. The edifice is built up mainly by angular, moderately vesicular scoriaceous lapilli of basaltic andesite composition, characterized by a succession of non-welded scoria beds forming loose, grain-supported lensoid shape wedges indicating modified grain flow origin. Vesicle shapes of the scoria ash and lapilli indicate vesicle collapses due to sudden cooling contraction. Wörner et al. (2000) have dated dense lapilli by ⁴⁰K/⁴⁰Ar in whole rock method and its age yielded to be in a range of 420 ± 200 ka to 680 ± 200 ka.

SC2 (21°17'20.42"S - 68°18'42.14"W; 3,723 m a.s.l.) is situated towards north border of the Salar de Carcote (Fig. 1). The cone is characterized by three distinct flank zones delineating an open crater closely resembling a typical horseshoe cones. The edifice is characterized by andesite lapilli with smooth, billowy and ropy surfaces. Mattioli et al. (2006) described the SC2 lavas as black, aphanitic rock that shows some flow textures. However, SC2 is also composed by red aphyric andesite lavas inferred to be associated with thermal oxidation and high temperature in the core of the cone. These products are characterized by skeletal olivine

microphenocrysts that they in some cases present breakdown rim width. In addition, quartz xenocrysts were commonly rimmed by a network of clinopyroxene microlites.

Luna de Tierra (21°18'23.02"S - 68°19'51.67"W; 3,712 m a.s.l.) is located at the northwest border of the Salar de Carcote (Fig. 1). It is defined by three-sided flanks with an open crater, which correspond to tuff ring. The edifice is built up mainly by lapilli, bomb and block of andesite that are weakly to moderately vesicular. The products are characterized by gray to black and red andesite pyroclasts with 1 – 4 mm thick intercalating black andesite ash. Juvenile pyroclasts are composed of plagioclases phenocrysts and microphenocrysts with resorption rims, dendritic textures, and skeletal olivine microphenocrysts.

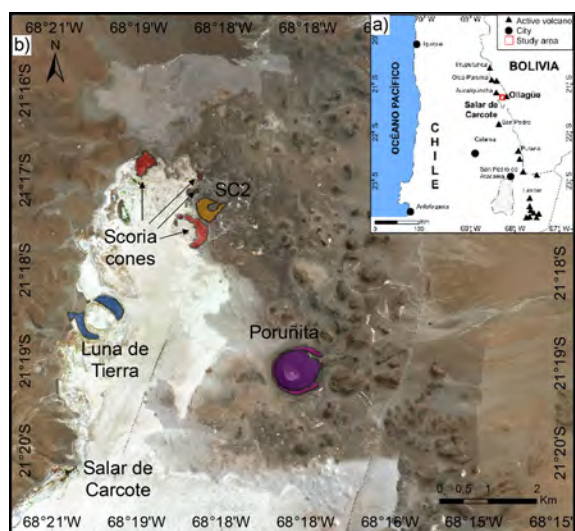


Fig. 1 – a) Location map of Ollagüe Volcanic Field, northern Chile. b) Location map of scoria cones based on a satellite image.

On the base of the morphology, petrographic and geochemistry, we can infer that the formation of these monogenetic centers corresponds to a normal Strombolian style explosive eruption styles, which would have slightly influenced by ground water (as evidenced from vesicle and pyroclast shapes and textures) due to the proximity to the water saturated sediment infill of Salar de Carcote, especially on Poruñita and Luna de Tierra. On the other hand, decompression processes from multiple magma batches and extensive fine scale magma mixing/mingling that can operate during quick magma ascent are evidenced on the different disequilibrium textures. The eruptive products from these small volcanoes present an enrichment of incompatible components, with low concentrations of Y and high values of Sr/Y. This geochemical signature can be linked to magma sourced from partial melting of the mafic continental lower crust (depths > 70 km) in the presence of residual garnet,

suffered stalling and formation of upper crustal melt packets to form. With respect to the spatial distribution, other four possible small monogenetic centers (Fig. 1) have been recognized recently that are aligned with Poruñita and SC2 located at the north border of Salar de Carcote. Thus, we propose that monogenetic volcanism on Salar de Carcote region would correspond to a volcanic field generated by multiple magma batches of high temperature from upper mantle or lower continental crust going through of a rapid crystallization associated to decompression and cooling processes.

Acknowledgements

This work is supported by the PhD Grant of GU “Becas de Doctorado Nacional CONICYT (Comisión Nacional de Investigación Científica y Tecnología) - PCHA / Doctorado Nacional / 2016-21161286”. We also thank to Cristóbal González, Ian Del Río and Diego Jaldin for their support during fieldworks.

References

- Kereszturi, G., and Németh, K., 2012. Monogenetic basaltic volcanoes: genetic classification, growth, geomorphology and degradation. In: K. Németh (Editor), *Updates in Volcanology – New Advances in Understanding Volcanic Systems*, InTech, pp. 3-88.
- Mattioli, M., Renzulli, A., Menna, M., and Holm, P. M., 2006. Rapid ascent and contamination of magmas through the thick crust of the CVZ (Andes, Ollagüe region): Evidence from a nearly aphyric high-K andesite with skeletal olivines. *Journal of Volcanology and Geothermal Research* 158(1): 87-105.
- Németh, K., and Kereszturi, G., 2015. Monogenetic volcanism: personal views and discussion. *Int. J. Earth Sci* 104(8): 2131-2146.
- Tibaldi, A., Corazzato, C., and Rovida, A., 2009. Miocene–Quaternary structural evolution of the Uyuni–Atacama region, Andes of Chile and Bolivia. *Tectonophysics* 471(1-2): 114-135.
- Vezzoli, L., Tibaldi, A., Renzulli, A., Menna, M., and Flude, S., 2008. Faulting-assisted lateral collapses and influence on shallow magma feeding system at Ollagüe volcano (Central Volcanic Zone, Chile-Bolivia Andes). *Journal of Volcanology and Geothermal Research* 171(1): 137-159.
- Wood, C.A., 1980a. Morphometric evolution of cinder cones. *J Volcanol Geotherm Res*, 7(3-4): 387-413.
- Wood, C.A. 1980b. Morphometric analysis of cinder cone degradation. *J Volcanol Geotherm Res*, 8(2-4): 137-160.
- Wörner, G., Hammerschmidt, K., Henjes-Kunst, F., Lezaun, J., and Wilke, H., 2000. Geochronology (40Ar/39Ar, K-Ar and He-exposure ages) of Cenozoic magmatic rocks from northern Chile (18-22 S): implications for magmatism and tectonic evolution of the central Andes. *Revista geológica de Chile* 27(2): 205-240.

Detailed tephrostratigraphy as a tool to identify small-volume multi-stage eruptions: a field approach from the 1800 yrs eruptive record of Mt. Ruapehu, New Zealand

Marija Voloschina¹, Gert Lube¹, Jon Procter¹ and Anja Moebis¹

¹ School of Agriculture and Environment, Massey University, Palmerston North, New Zealand; m.voloschina@massey.ac.nz

Keywords: multi-stage eruption, ash-rich, tephra.

Recent studies and observations of historical eruptions suggest that the vast majority of historically documented eruptions involve relatively small erupted volumes ($<10^8$ m³) and VEIs less than 3 (Siebert et al., 2015a, b). According to an analysis of the catalogue of the Smithsonian Institution's Global Volcanism Program (Global Volcanism Program 2013), >50% of the historical events contain more than one eruption stage (Jenkins et al., 2007). Nonetheless, understanding the dynamic changes in eruption behavior between and within eruption stages remains a major challenge in volcanology. While for ongoing eruptions, additional information is obtained from geophysical monitoring and in-situ observations and sampling, this is more problematic for prehistorical eruptions. They can be accessed only through the study of more or less well-preserved tephra deposits.

Mt. Ruapehu is a 2797 m high composite andesitic volcano on the southernmost tip of the Taupo Volcanic Zone. Its extensive Ring Plain preserves a tephra record which witnesses a wide range of eruption styles and magnitudes, ranging from the large Plinian eruptions of the Bullot Formation (~27,000-10,000 cal yrs BP, Pardo et al., 2011) to the small volume phreatomagmatic-strombolian eruptions of the Tufa Trig Formation (~1800 cal yrs BP- present, Donoghue et al., 1995, 1997).

The here presented research uses the tephra record of the Tufa Trig Formation to discuss how detailed tephrostratigraphy can be used to infer eruption dynamics from small-volume, ash-dominated eruptions from andesitic volcanoes.

We distinguish between stage units and eruption unit, with the stage unit being the smallest identifiable unit. The term "stage" is used in agreement with the definition of Jenkins et al., (2007) relating to an eruption event characterized by a predominant eruption style and durations from hours to months. Eruption unit boundaries are marked by soil with thicknesses ≥ 1 mm and can comprise one or more stage units (Fig. 1). Eruption units that contain one stage unit are interpreted to represent a single-stage eruption event while eruption units that are composed of multiple stage

units are interpreted as multi-stage events (e.g. Fig. 1).

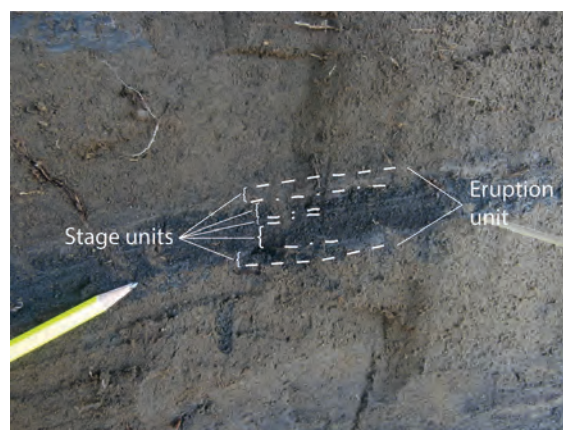


Fig. 1 – Example of the characterization of an ash-rich Ruapehu Tephra. Boundaries of individual stage units are marked by line-dots while eruption boundaries are marked by dashed line.

Using this approach, the Tufa Trig Formation can be re-defined to contain at least 29 eruption units, increasing the existing frequency record from one eruption every ~100 years (Donoghue et al., 1997) to one every ~60 years. Three dominant eruption types can be distinguished: (1) pumiceous eruptions, (2) single-stage ash eruptions and (3) multi-stage ash eruptions. About 2/3 of the eruptive record of the past 1800 yrs consist in multi-stage ash eruptions (Fig. 2). This has important implications for the existing eruption scenarios of Mt. Ruapehu: ash fall from multi-stage eruptions could potentially affect larger areas due to potential changes in wind directions, acting over longer time spans. Similarly, abrupt changes in eruption style could lead to different types of volcanic hazards and areas at risk would be exposed to these hazards and the resulting economic or health consequences for longer time periods. As a comparison, the most recent eruption episodes of 1995/1996 which erupted ~0.1 km³ of magma (Johnston et al., 2000) resulted in an economic loss of \$130 million (New Zealand Dollars), heavily affecting the alpine tourist industry (Johnston et al., 2000). This highlights the

From Pumiceous Obsidian to Lithoidal Rhyolite: Mapping textural variations in rhyolite lava flows and domes, and what we can learn about emplacement processes

Alan Whittington¹, Stuart Kenderes¹, Graham Andrews², Shelby Isom², Kenny Befus³ and Tyler Leggett³

¹ Department of Geological Sciences, University of Missouri, Columbia MO 65211, USA; whittingtona@missouri.edu

² West Virginia University, Morgantown WV, USA

³ Baylor University, Waco TX, USA

Keywords: obsidian, rhyolite, lava flow emplacement

High-silica rhyolite lava flows and domes are one compositional and morphological end-member of terrestrial lava flows. Commonly 50m to 100m thick, with steep sides and flow-fronts, the emplacement mechanisms of these silicic flows remain a matter of debate.

devitrification of lava (Manley and Fink, 1987), emplaced by primarily exogenous processes.

Recent observations of active silicic lavas in Chile contradict existing models of emplacement and suggest endogenous emplacement processes more similar to basaltic lavas (e.g. Bernstein et al. 2013; Pallister et al. 2013; Tuffen et al. 2013; Farquharson et al. 2015; Magnall et al. 2017), but only the surfaces of active lavas can be observed.

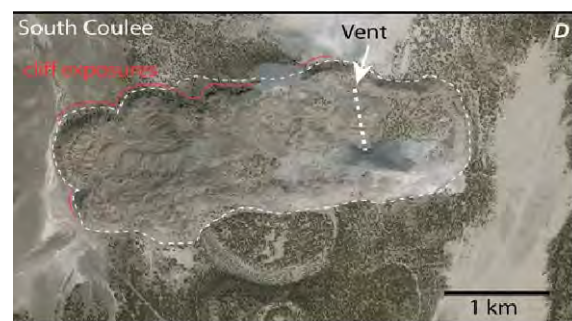
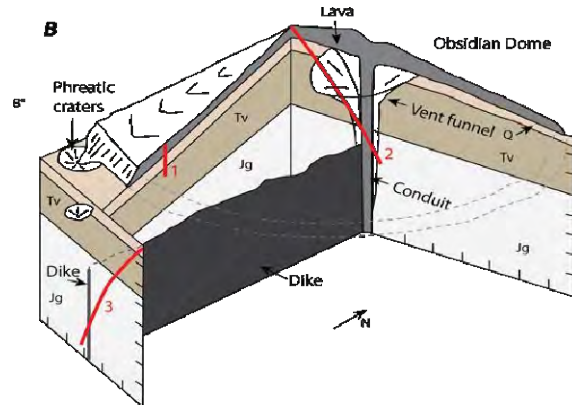
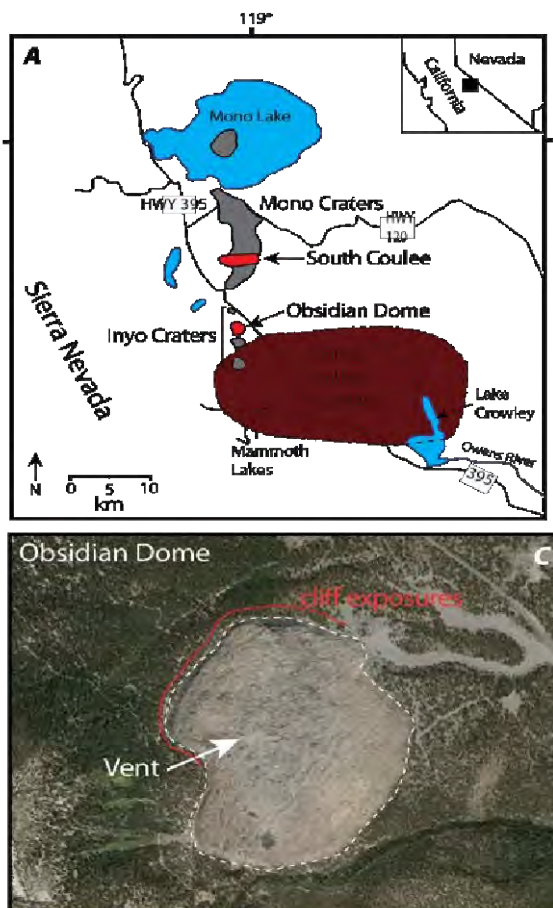


Fig. 1 – A – Location of Obsidian Dome and South Coulee within the Mono-Inyo volcanic chain on the NW margin of Long Valley caldera (Castro et al. 2002). B – cut-away diagram through Obsidian Dome based on drilling results (Yunker et al. 1988). Drill holes RDO-2A and -2B are shown as 1 and 2. C & D – Google Earth images of Obsidian Dome and South Coulee, respectively.

Obsidian Dome and South Coulee are two silicic lavas, erupted in California about 1000 years ago. Scientific drilling at Obsidian Dome has revealed its internal structure and textures (Yunker et al. 1988). Variations in vesicularity and crystallinity have been correlated with observations at older dissected flows, and interpreted as recording cooling, degassing, and

Mapping of the different textural units (fine vesicular pumice [FVP], dense obsidian, coarse vesicular pumice [CVP] and foliated rhyolite) has

revealed a complex set of field relationships that can, in principle be used to determine the thermal and deformation history during emplacement. Contrasting mechanical behavior of compositionally similar materials results from textural differences during deformation (e.g. glassy vs microcrystalline rhyolite, Fig 2).



Fig. 2 – Boudinaged lithoidal rhyolite blocks enveloped by dense obsidian at the western margin of Obsidian Dome

Flow banding in the Mono-Inyo domes and coulees is almost always sub-vertical in the field (exposures at or close to the flow surface), indicating that it is inherited from the conduit. At greater depth, in drill core and in diapirs that have exhumed deeper material (Fig 3), this banding commonly rotates into a sub-horizontal orientation.



Fig. 3 – Recumbent isoclinal fold in coarse vesicular pumice, exposed in sub-vertical wall of “crease structure”

Isoclinal and recumbent folds in coarse vesicular pumice layers, exposed in the axial cleft of “crease structures” strongly suggest that the coarse vesicular texture post-dated folding. We suggest that the CVP formed, not through the accumulation of ascending bubbles under a strong cap later, but rather by decompression and *in situ* vesiculation, resulting from brittle fractures propagating downwards into the ductile flow core. On the timescale of fracture

propagation, this core would behave in a brittle fashion, but rapid decompression could trigger bubble growth in lava that was still above its glass transition. The bubbles could not rise through the viscous melt, but generated enough buoyancy for the bulk lava to ascend upwards through the crack, forming an upwelling at the surface with radial patterns reminiscent of diapiric ascent.

In this interpretation, diapiric masses of CVP are the consequence of brittle fracture of the cold outer carapace, not the cause. This in turn means that CVP layers should not be used as stratigraphic sub-units when mapping thick lava flows, as they are unlikely to be laterally continuous and the boundaries of the CVP texture may truncate and obscure structural layering.

Acknowledgements

This work supported by National Science Foundation awards EAR-1725131 (Andrews), EAR-1725003 (Befus), and EAR-1724581 (Whittington).

References

- Bernstein, M., Pavez, A., Varley, N., Whelley, P., and Calder, E.S., 2013. Rhyolite lava dome growth styles at Chaitén Volcano, Chile (2008-2009): Interpretation of thermal imagery. *Andean Geology*, 40:295-309.
- Farquharson, J.I., James, M.R., and Tuffen, H., 2015. Examining rhyolite lava flow dynamics through photo-based 3D reconstructions of the 2011-2012 lava flowfield at Cordón-Caulle, Chile. *Journal of Volcanology and Geothermal Research*, 304:336-348.
- Magnall, N., James, M.R., Tuffen, H., and Vye-Brown, C., 2017. Emplacing a cooling-limited rhyolite lava flow: similarities with basaltic lava flows. *Frontiers in Earth Science*, 5: 44.
- Manley, C.R., and Fink, J.H., 1987. Internal textures of rhyolite flows as revealed by research drilling. *Geology* 15:549-552.
- Pallister, J.S., Diefenbach, A.K., Burton, W.C., Munoz, J., Griswold, J.P., Lara, L.E., Lowenstern, J.B., and Valenzuela, C.E., 2013. The Chaitén rhyolite lava dome-eruption sequence, lava dome volumes, rapid effusion rates and source of the rhyolite magma. *Andean Geology*, 40: 277–294.
- Tuffen, H., James, M.R., Castro, J.M., and Schipper, C.I., 2013. Exceptional mobility of a rhyolitic obsidian flow: observations from Cordón Caulle, Chile, 2011–2013. *Nature Communications*, 2709.
- Younker, L.W., Eichelberger, J.C., Kasameyer, P.W., Newmark, R.L., and Vogel, T.A., 1988. Results from shallow research drilling at Inyo Domes, Long Valley Caldera, California and the Salton Sea geothermal field, Salton Trough, California. In Boden, A., et al. eds, *Deep Drilling in Crystalline Bedrock*, 172-188.

Quaternary Volcanism in the Itasy and Ankaratra Volcanic Fields, Madagascar: vent density, eruptive ages, and magmatic sources

Elisabeth Widom¹, C. Rasoazanamparany¹, A. Rakotondrazafy², T. Raharimahefa³, K. Rakotondravelo² and Dave Kuentz¹

¹ Department of Geology & Environmental Earth Science, Miami University, Oxford, Ohio, USA; widome@miamioh.edu

² Département de Géologie, Université d'Antananarivo, Ambohitsaina, Madagascar.

³ Department of Geology, University of Regina, Regina, Canada.

Keywords: monogenetic volcanism, Madagascar,

The Quaternary Itasy and Ankaratra volcanic fields, the most recently active volcanic fields in Madagascar, are located within ~50 - 100 km of the capital city, Antananarivo. Despite their proximity to Antananarivo, these volcanic fields have been relatively little studied with respect to eruptive ages, number or distribution of vents, or causes and sources of volcanism. In this study, we have performed field work and GIS mapping of vent locations and associated lava flows, Ar-Ar age dating of select samples spanning the recent eruptive history, and petrographic and geochemical analyses to better constrain the sources of volcanism and the likelihood of future eruptions.

The Itasy and Ankaratra volcanic fields are characterized by mafic monogenetic volcanism, including explosive maar volcanoes, which have been active in the late Pleistocene and – at least in the case of Itasy – the Holocene, with the youngest recorded eruption at 8.5 ka (Vogel, 1970; Rufer et al., 2014). Our new mapping and Ar-Ar ages indicate that these volcanic fields have been highly active, both recently and simultaneously, with ages in the two volcanic fields ranging primarily from ~110 to 30 ka. Vent densities in the Itasy volcanic field are $\sim 1.6 \times 10^{-7}$ vents/m² (180 vents/1100 km²), similar to that of the Auckland volcanic field, and ~3 to 5 times the vent densities of the Sierra Chichinautzin and Michoacán-Guanajuato volcanic fields, respectively. Frequent seismicity beneath both volcanic fields further supports the possibility of future eruptions (Bertil and Regnault, 1998).

Major and trace element and isotopic analyses of lavas from the Itasy and Ankaratra volcanic fields show that both volcanic fields exhibit significant compositional diversity. The Itasy eruptive products range in composition from foidite to phonotephrite, whereas Ankaratra lavas range from basanite to trachybasalt. Trace element signatures of samples from both volcanic fields are very similar to those of ocean island basalts (OIB), with significant enrichment in Nb and Ta, depletion in Rb, Cs, and K, and relatively high Nb/U and Ce/Pb. However, the Itasy volcanic rocks show enrichment relative to

those of Ankaratra in most incompatible elements, indicative of a more enriched source and/or lower degrees of partial melting.

Significant inter- and intra-volcanic field heterogeneity is also observed in Sr, Nd, Pb and Os isotope signatures. The Itasy volcanic rocks generally have less radiogenic Sr and Nd isotopic ratios but more radiogenic Pb isotopic signatures than the Ankaratra volcanic field. The lack of correlation between isotopes and indices of crustal contamination (e.g. MgO and Nb/U) are inconsistent with crustal contamination, and instead suggest mixing between compositionally distinct mantle sources. A single trend in Pb-Pb isotope space, but distinct trends in Sr vs. Nd isotopes displayed by samples from Itasy and Ankaratra, respectively, argue for complex source mixing involving three or more sources. Anomalously radiogenic Os isotope signatures and a wide range in Th isotope ratios and ²³⁰Th/²³⁸U activity ratios are tentatively interpreted to reflect mixing between Indian Ocean MORB and enriched sub-continental lithospheric mantle containing pyroxenite and/or mica-rich veins. Although the cause of melting remains unknown, the presence of highly metasomatized mantle, combined with local extensional tectonics, likely plays an important role.

Acknowledgements

This research has been funded by NSF EAR grant #1523442, and the Janet and Elliot Baines Professorship, both awarded to E. Widom.

References

- Bertil, D. & Regnault, J.M. (1998). Seismotectonics of Madagascar. *Tectonophysics* 294, 57-74.
- Rufer, D., Preusser, F., Schreurs, G., Gnos, E. & Berger, A. (2014). Late Quaternary history of the Vakinankaratra volcanic field (central Madagascar): insights from luminescence dating of phreatomagmatic eruption deposits. *Bulletin of Volcanology* 76, 817.
- Vogel, 1970. Groningen radiocarbon dates IX. *Radiocarbon* 12, 444-471.

Medial volcanoclastic mass flow deposit apron of Mt. Taranaki (New Zealand); Recording stratovolcano construction and associated chemical changes of the magmatic system

Aliz Zemeny¹, Jonathan N. Procter¹, Karoly Nemeth¹, Georg F. Zellmer¹ and Shane J. Cronin²

¹ School of Agriculture and Environment, Massey University, Palmerston North, New Zealand; a.zemeny@massey.ac.nz

² School of Environment, The University of Auckland, Auckland, New Zealand.

Keywords: construction phase, mass flow, geochemistry

Andesitic stratovolcanoes are characterised by periodic edifice growth (construction) followed by volcano collapse events (destruction phases; Zernack et al., 2009). The cyclic behaviour results in the deposition and accumulation of syn- and post-eruptive primary and secondary volcanoclastic successions accumulating around the volcanic edifice, commonly defined as the ring-plain. The ring-plain of Mt. Taranaki offers a nearly complete lithostratigraphic and chronostratigraphic record of volcanic evolution. The identification of lithostratigraphic units or packages of like lithologies (with similar genetic properties) has proved to be very useful in medial facies to understand the evolution of the volcano as these volcanoclastic successions preserve volcanic deposits that cannot be examined in proximal sites.

The aim of the research is to characterize the evolution of the volcano, in particular the construction phases by developing sedimentology frameworks and facies categorization of medial volcanoclastic deposits in order to track magmatic changes through their geochemical fingerprint.

Field investigations in the ring-plain around Mt. Taranaki have focussed on volcanoclastic mass flows between the Te Namu (29 ka), Rama (35 ka) and Otakeho (55 ka) debris avalanche deposits that represent destruction phases. Successions along the shoreline were mapped and correlated by the identification of paleochannels and unconformities in cross-section, based on sedimentological and lithofacies classifications. We constructed a stratigraphic model for the investigated time period that pointed out the stratigraphic positions of characteristic hyperconcentrated flows which were lithic-rich and mappable for kilometres in longitudinal extensions along the coastline. Major lithology is represented as dense lithics (75 – 90 surf. %), thus, pumice clasts are also present (between 5 – 25 surf. %) in each pulse. Presence of pumice constitutes eruptive material that was rapidly remobilised from pyroclastic flows of significant eruptive periods during construction. In order to characterize the changes of the magmatic system in growth phases, pumice clasts were sampled from

three selected representative sites of lithic-rich hyperconcentrated flows of the studied construction phases (Fig. 1).

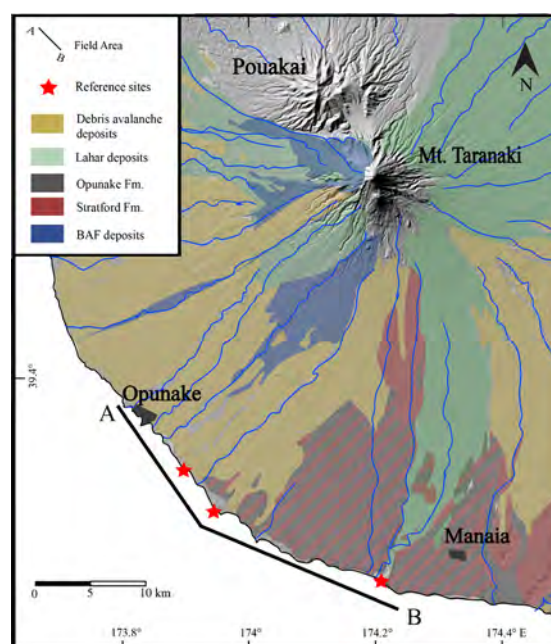


Fig. 1 – Quaternary Geological Map of the south, south-western part of Taranaki showing the distribution of volcanic and volcanoclastic deposits (modified after Neall, 1979; Neall and Alloway, 2004; Alloway et al., 2005) and the coastal region that were examined during this study (indicated with A-B black line; red stars indicate sampled and investigated reference sections). Note that the composite deposits involve Stratford and Opunake Formations that characterise the studied time-period.

Whole-rock geochemical analysis of pumices (> 55 ka) have SiO₂ contents that vary from 48.3 wt. % for the most primitive to 54.5 wt. % for the most evolved rocks. However, the following collapse event that provided the Otakeho debris avalanche deposit represents SiO₂ contents of clasts that range from 53.25 wt. % to 59.75 wt. %.

In the next construction phase, pumice clasts (>35 ka) represent SiO₂ compositions between 47 wt. % to 58 wt. % of which are distinct according to the composition of clasts from the following Rama

debris avalanche deposit that represent SiO_2 contents between 53.5 wt. % to 60.5 wt. %.

The following construction phase characterizes SiO_2 composition in-between 43 wt. % to 56 wt. % in spite of compositions of the Te Namu debris avalanche that is associated to the next destruction phase characterizing SiO_2 contents that range from 52.5 wt. % to 59.25 wt. %.

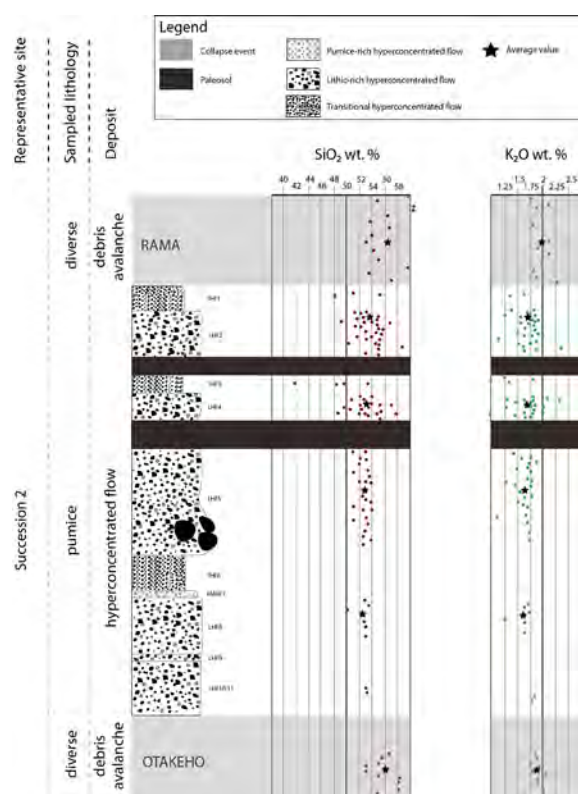


Fig. 2 – Geochemical evolution by time of the construction phase between 35 – 55 ka (Succession 2). Schematic stratigraphic figure represents the SiO_2 and K_2O compositions of pumice clasts from individual pulses of volcanoclastic hyperconcentrated mass flow deposits.

Thus, not only SiO_2 contents deputize lower values of edifice growth, K_2O also indicates lower compositions in the construction phases. Moreover,

focusing on individual construction phases, pumice clast compositions of volcanoclastic mass flow pulses represent increasing values in relation to time with interbedded paleosols or fluvial deposits as time-break signatures respectively (see composition variations in the construction phase between 35 – 55 ka as an example in Fig. 2).

This increase in major element compositions by time reflects the edifice growth and the associated magmatic behavior. Geochemical variations of pumice clasts, which represent the certain magmatic conditions at that time when those mass flows were deposited, correspond to the outcomes that the growing edifice inflicts by time.

Our data of the construction phases show significant differences relating to compositions of debris avalanche deposits proving a cyclic pattern in magmatic behaviour indicating multiple edifice growth of Mt. Taranaki between 30 – 60 ka.

References

- Alloway B, McComb P, Neall V, Vucetich C, Gibb J, Sherburn S, Stirling M., 2005. Stratigraphy, age, and correlation of voluminous debris avalanche events from an ancestral Egmont volcano: implications for coastal plain construction and regional hazard assessment – *Journal of the Royal Society of New Zealand*, 35: 229-267.
- Neall V.E., 1979. Sheets p19, p20 and p21. New Plymouth, Egmont and Manaia – Geological map of New Zealand 1:50,000. 3 maps and notes, 36 p. New Zealand Department of Science and Industrial Research,
- Neall Ve, Alloway B.E., 2004. Quaternary Geological Map of Taranaki. Institute of Natural Resources – Massey University, Soil & Earth Sciences Occasional Publication No. 4.
- Zernack, A.V., Procter, J.N. and Cronin, S.J., 2009. Sedimentary signatures of cyclic growth and destruction of stratovolcanoes: A case study from Mt. Taranaki, New Zealand. *Sedimentary Geology*, 220 (3-4):288-305.

Frequent cycles of growth and catastrophic collapse at Mt. Taranaki

Anke Zernack¹, Shane J. Cronin², Mark Bebbington¹, Richard Price³, Ian Smith², Bob Stewart¹ and Jon Procter¹

¹ School of Agriculture and Environment, Massey University, Palmerston North, New Zealand; a.v.zernack@massey.ac.nz

² School of Environment, The University of Auckland, Auckland, New Zealand.

³ Faculty of Sciences, University of Waikato, Hamilton, New Zealand.

Keywords: Mt. Taranaki, volcanic debris avalanche, cyclic edifice failure

Regular large-scale edifice collapse and regrowth is a common pattern during the lifespans of andesitic stratovolcanoes worldwide. Most long-lived composite edifices experience multiple failures on various magnitudes and timescales, ranging from hundreds to thousands or thousands to tens of thousands of years in the case of Mt. Taranaki (Zernack et al. 2011). Edifice collapse and regrowth cycles are reflected in geomorphic features, such as scarps and caldera-like depressions, and in volcanoclastic ring-plain sequences (e.g. Zernack et al. 2009). The Mt. Taranaki ring-plain succession displays a recurring sedimentary pattern (Fig. 1) with each cycle comprising deposits of: (1) cone collapse, (2) re-adjustment of drainage channels, and (3) renewed volcanism and cone growth (Procter et al. 2009; Zernack et al. 2009). Massive sequences of mainly monolithologic debris-flow and pumice-rich hyperconcentrated-flow deposits with interbedded tephra layers were formed during phases of active volcanism and edifice construction. Periods of repose separating eruption episodes are characterised by landscape adjustment through fluvial and aeolian processes, peat accumulation and soil development.

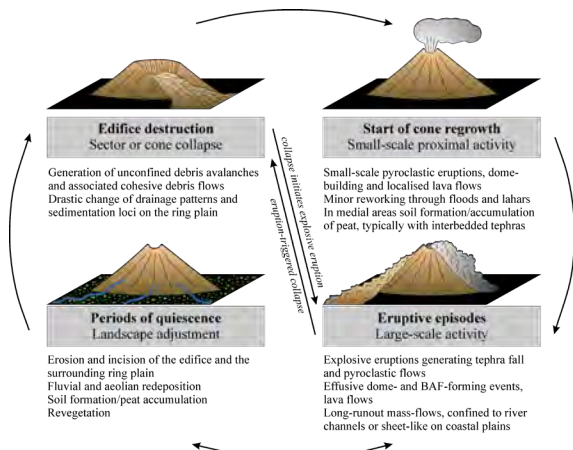


Figure 1 – Simplified sketch of growth and collapse cycles at Mt. Taranaki (from Zernack et al. 2009)

Edifice failures generated debris avalanches with minimum run-out distances of 26–45 km onshore, extending at least a further 8 km offshore (Neall 1979; Alloway et al. 2005).

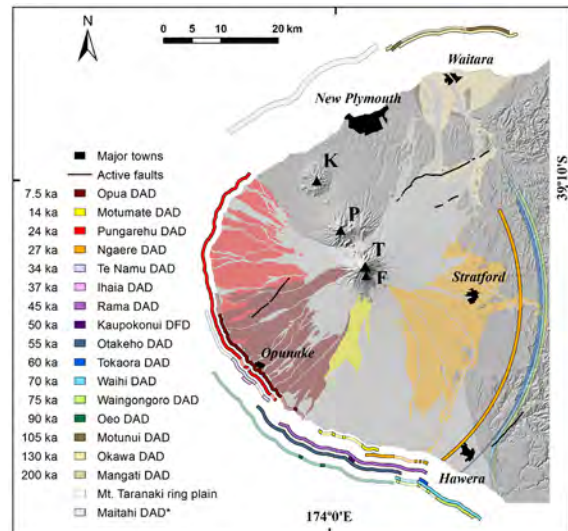


Figure 2 – Map of the Taranaki Peninsula highlighting ages of Mt. Taranaki-sourced debris avalanche deposits and their dispersal in coastal cliffs and the ring-plain.

The >200 ka history of Mt. Taranaki is punctuated by at least 15 catastrophic and 4 smaller collapses, producing debris avalanche deposits of 1 to >7.5 km³ and 0.1–0.2 km³ respectively (Neall 1979; Alloway et al. 2005; Zernack et al. 2011). These were sourced from all sectors of the volcano (Fig. 2) with the largest events removing as much as one third of the present-day equivalent cone. Thus, debris avalanche deposits are the main landscape-forming element of the Taranaki ring plain, forming distinctive fans of hummocky terrain, variously covered by superficial tephra, loess and lahar deposits. The deposits exhibit classic sedimentary characteristics, including jigsaw-cracked clasts, megaclasts, and large rip-up clasts (e.g., Zernack et al. 2009), and gradational marginal transformation into debris flow deposits, reflecting the low-relief, unconfined nature of the terrain.

Similar sedimentary and geomorphic features suggest similar proto-edifice characteristics, failure trigger mechanisms and runout path conditions. Each collapse was followed by sustained renewed volcanism and cone regrowth, although there are no matching stepwise geochemical changes in the magma erupted (Fig. 3); instead a stable, slowly evolving magmatic system has prevailed (Price et al.

1999; Zernack et al. 2012b). Last Glacial climatic variations are also uncorrelated with the timing or magnitudes of collapse. Given the steady-state behaviour of the volcanic system over time, i.e. invariant physical properties of the edifice due to similar eruptive styles and magmatic compositions, and stable basement geology conditions, large-scale edifice failure and the generation of catastrophic debris avalanches at Mt. Taranaki was primarily governed by a fairly constant magma-supply rate driving edifice growth rates (Zernack et al. 2012a).

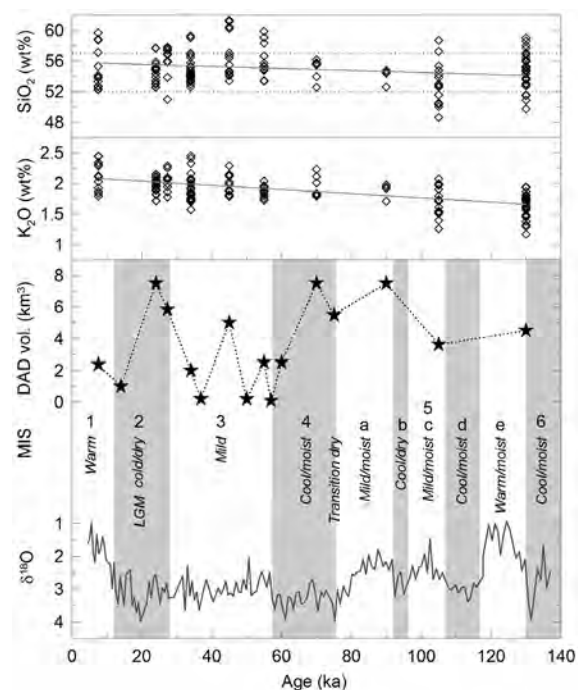


Figure 3 – Age-volume plot of Mt. Taranaki debris avalanche deposits, SiO₂- and K₂O-trends and local climate conditions during marine isotope stages (MIS) 1-6 (from Zernack et al. 2012a). LGM=Last Glacial Maximum.

The Mt. Taranaki example illustrates that edifice construction and large-scale failure follows a natural mass balance relationship between magma supply and degradation through erosion. The observed semi-regular recurrence pattern of collapse cycles appears to be the result of a long-term steady growth process punctuated by random triggering of edifice failures with collapse frequency and size being influenced by both, the nature of the triggering event and the precondition of the edifice at the time.

Typically, a weak disturbance has little effect on a stable edifice whereas a stronger one may trigger a small flank collapse. Over time as eruption rates and episodic edifice growth exceed the rate of normal fluvial, aeolian and glacial mass-wasting processes, the volcano becomes increasingly metastable with edifice dimensions ultimately becoming closer to their natural stability limit. As this limit is approached, a range of ongoing background

processes that could trigger collapse (such as earthquakes, magma intrusion, hydrothermal processes, rapid climatic changes and rain storms) become more effective. At this stage, a similar weak disturbance might generate a small- to medium-sized collapse. However, when a strong disturbance coincides with a weak, destabilised edifice that has exceeded its critical stable dimension, it has the potential to trigger large-scale gravitational sector collapse, thereby restoring edifice equilibrium conditions (Zernack et al. 2012a).

Acknowledgements

This work was supported by Massey University and German Academic Exchange Service (DAAD) doctoral scholarships, FRST contract MAUX0401 to SC and the NZ Natural Hazards Research Platform.

References

- Alloway, B., McComb, P., Neall, V., Vucetich, C., Gibb, J., Sherburn, S., and Stirling, M., 2005, Stratigraphy, age, and correlation of voluminous debris-avalanche events from an ancestral Egmont Volcano: Implications for coastal plain construction and regional hazard assessment: *Journal of the Royal Society of New Zealand*, 35: 229-267.
- Neall, V.E., 1979, Geological map of New Zealand, sheets P19, P20 and P21, New Plymouth, Egmont and Manaia: New Zealand Dept. of Science and Industrial Research, Wellington, scale 1:50,000, 3 sheets, 36 p.
- Price, R.C., Stewart, R.B., Woodhead, J.D., and Smith, I.E., 1999, Petrogenesis of high-K arc magmas: Evidence from Egmont Volcano, North Island, New Zealand: *Journal of Petrology*, 40: 167-197.
- Procter, J.N., Cronin, S.J. and Zernack, A.V., 2009. Landscape and sedimentary response to catastrophic debris avalanches, western Taranaki, New Zealand. *Sedimentary Geology*, 220(3-4): 271-287.
- Zernack, A.V., Procter, J.N. and Cronin, S.J., 2009. Sedimentary signatures of cyclic growth and destruction of stratovolcanoes: A case study from Mt. Taranaki, New Zealand. *Sedimentary Geology*, 220(3-4): 288-305.
- Zernack, A.V., Cronin, S.J., Neall, V.E., and Procter, J.N., 2011, A medial to distal volcanoclastic record of an andesitic stratovolcano: Detailed stratigraphy of the ring-plain succession of south-west Taranaki, New Zealand: *International Journal of Earth Sciences*, 100: 1937-1966.
- Zernack, A.V., Cronin, S.J., Bebbington, M.S., Price, R.C., Smith, I.E.M., Stewart, R.B., and Procter, J.N., 2012a, Forecasting catastrophic stratovolcano collapse: A model based on Mount Taranaki, New Zealand. *Geology* 40 (11): 983-986.
- Zernack, A.V., Price, R.C., Smith, I.E.M., Cronin, S.J., and Stewart, R.B., 2012b, Temporal evolution of a high-K andesitic magmatic system: Taranaki Volcano, New Zealand: *Journal of Petrology*, 53: 325-363.

PART B



Field Guide

Field Trip Guide for the Fifth International Volcano Geology Workshop

26 February – 4 March, 2019

Volcanism in a rapidly changing environment relating to an atypical plate margin

Szabolcs Kósik¹, Marija Voloschina¹, Aliz Zemeny¹, Shane J. Cronin², Károly Németh¹, Jonathan N. Procter¹ and Anke Zernack¹

¹ School of Agriculture and Environment, Massey University, Palmerston North, New Zealand; ² School of Environment, The University of Auckland, Auckland, New Zealand



Introduction

The choice of the North Island of New Zealand for the 5th International Volcano Geology Workshop allows the participants to discover a dynamic and varied volcanic landscape from small to large composite volcanoes, silicic caldera systems and monogenetic volcanoes with the wide variety of eruptive styles, transport and depositional processes. This unique volcanic environment evolving on a rapidly changing plate boundary has volcanism interacting with the underlying terrestrial to marine sediments of Zealandia providing interrelated unique depositional sequences. The workshop takes the participants to world class sites of volcanic facies from the central volcanic edifice to the distal part of the surrounding area (commonly referred to as ring plain). The field workshop will provide a quick overview of a great variety of eruptive products formed through all known volcanic eruption styles and produced deposits easily accessible and ready to explore. The

fieldtrip intends to reinforce the scientific discussions to answer key questions and outline basic rules experts may need to follow in geological mapping of volcanic terrains regardless of the age the rocks formed.

This field guide is divided into two sections. The first section gives a general overview about the tectonic settings and volcanism of the southernmost part of a ~2800 km long subduction zone following a convergent plate margin between the subducting Pacific Plate and the eastern margin of the Australia-India Plate. This subduction front and its volcanic arc initiates at 15°S latitude near islands of Tonga and ends near the southeastern shore of North Island of New Zealand where the subduction direction becomes near parallel to the plate margin. The active volcanic arc established due to the subduction of the Pacific Plate under the Indo-Australian Plate, and formed a volcanically very active modern rifted arc formally named the Taupo Volcanic Zone (TVZ).

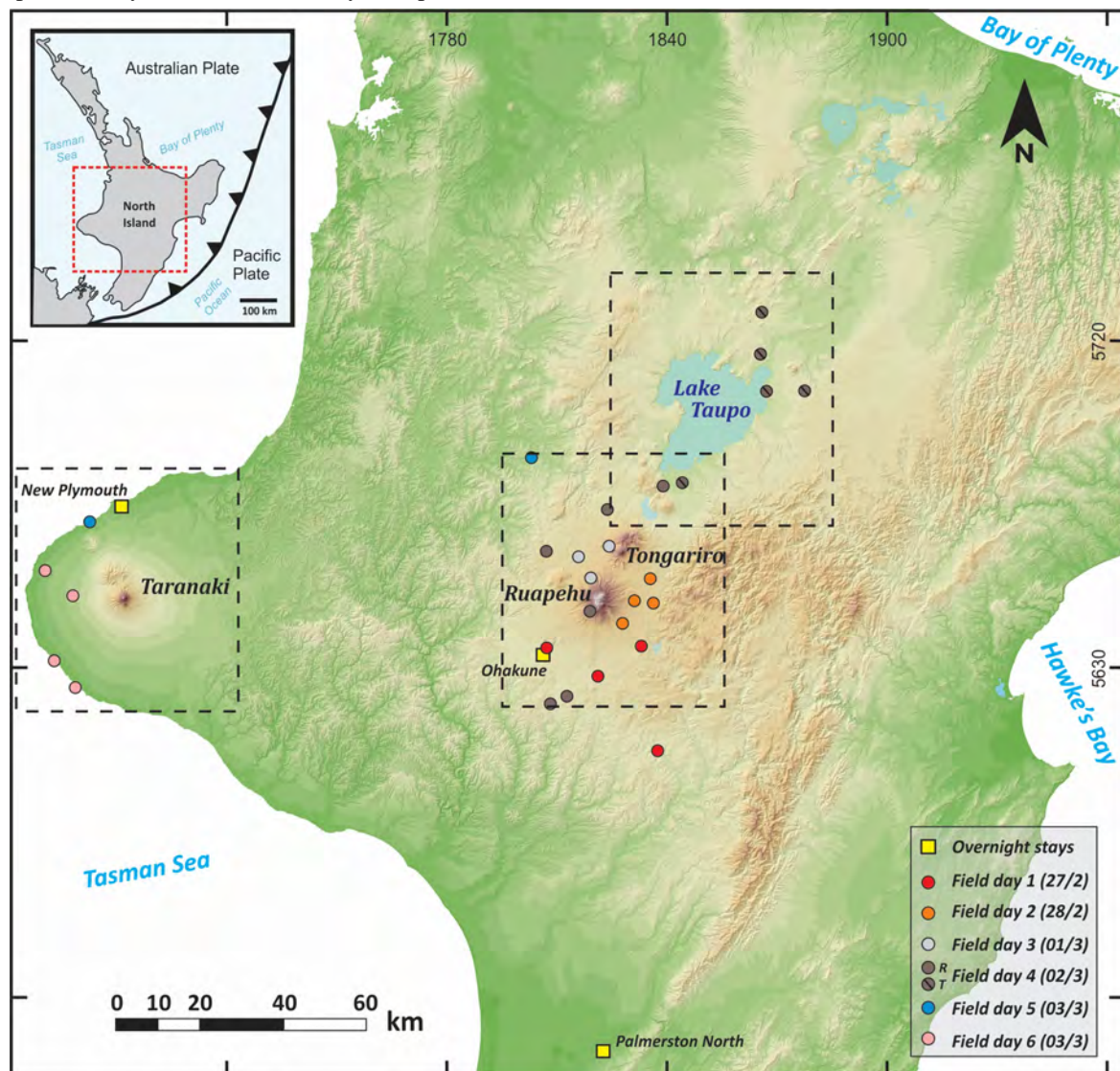


Fig. 1. – Overview of the geographic position of the planned stops with the extents of regional maps (Figs. 15, 46, 62)

1-3	Tangiwai Disaster Memorial	State Highway 49 (near Waiouru)	39.466°S, 175.576°E	1821566 mE, 5628331 mN
1-4	Ohakune Volcanic Complex	Old Station Road, Ohakune	39.432°S, 175.410°E	1807407 mE, 5632556 mN
DAY 2 (28 February)				
2-1	Tufa Trig Formation	Forestry Road (near Waiouru)	39.335°S, 175.645°E	1827946 mE, 5642710 mN
2-2	Waikato Stream site, 60 ky slice of the ring plain	State Highway 1 -Desert Road	39.281°S, 175.744°E	1836653 mE, 5648391 mN
2-3	Bullot Formation	Tukino Road	39.276°S, 175.684°E	1831513 mE, 5649108 mN
2-4	Waihohonu - Tongariro tephra	State Highway 1 - Desert Road	39.221°S, 175.734°E	1836018 mE, 5655181 mN
DAY 3 (1 March)				
3-1	Volcano destruction, Whakapapa Formation	Whakapapa Skifield, Scoria Flat	39.224°S, 175.541°E	1819352 mE, 5655234 mN
3-2	Murimoto debris avalanche	State Highway 48 (Mounds walk)	39.170°S, 175.503°E	1816218 mE, 5661348 mN
3-3	Eruptive styles and glacial history of the Tongariro volcano	Tongariro Crossing (Mangetepopo V.)	39.145°S, 175.597°E	1824440 mE, 5663884 mN
DAY 4 Option A (2 March)				
4A-1	Onetapu lahars	Whangaehu Valley Road	39.496°S, 175.479°E	1813182 mE, 5625238 mN
4A-2	Whangaehu Valley Formation	Old Fields Track	39.539°S, 175.426°E	1808451 mE, 5620644 mN
4A-3	Raurimu Spiral road section	State Highway 4 (near National Park)	39.134°S, 175.399°E	1807317 mE, 5665567 mN
4A-4	Te Whaihu debris avalanche and Taupo Pumice Fm.	State Highway 47 (Mangetepopo Sect.)	39.057°S, 175.582°E	1823430 mE, 5673700 mN
4A-5	Overview of the volcanism central TVZ and Taupo volcano	Te Ponanga Saddle View Point	38.990°S, 175.764°E	1839432 mE, 5680645 mN
4-6	Turoa Skifield – recapping the Ruapehu experience	Turoa Skifield	39.305°S, 175.527°E	1817887 mE, 5646337 mN
DAY 4 Option B (2 March)				
4-1	Oruanui Fm. - accretionary lapilli-bearing ignimbrite	State Highway 1, Turangi	38.986°S, 175.820°E	1844246 mE, 5680943 mN
4-2	Taupo Pumice Formation - medial full sequence	State Highway 5 (near Taupo)	38.748°S, 176.200°E	1878092 mE, 5706357 mN
4-3	Post-eruption lake sedimentation	5 Mile Beach (near Taupo)	38.748°S, 176.072°E	1866816 mE, 5707044 mN
4-4	Punetekahi - K-Trig Basalt Formation	Poihipi Road (near Taupo)	38.659°S, 176.035°E	1864095 mE, 5716674 mN
4-4	Puketerata Volcanic Complex	State Highway 1	38.555°S, 176.058°E	1866512 mE, 5728218 mN
DAY 5 (3 March)				
5-1	Taupo Pumice Fm. Valley-ponded ignimbrite facies	Te Maire Bluff, SH43 (near Taumarunui)	38.943°S, 175.189°E	1789688 mE, 5687268 mN
5-4	Maitahi debris avalanche	Oakura	39.109°S, 173.958°E	1682853 mE, 5670724 mN
DAY 6 (4 March)				
6-1	Pungarehu debris avalanche and Warea deposits	State Highway 45, Warea	39.230°S, 173.817°E	1670484 mE, 5657371 mN
6-2	Pungarehu debris avalanche mounds	Parihaka Road, Wiremu road	39.292°S, 173.904°E	1677936 mE, 5650400 mN
6-3	Middleton Bay, Opunake paleoriver system	Middleton Bay, Opunake	39.455°S, 173.849°E	1673074 mE, 5632364 mN
6-4	Lizzie Bell paleochannel system	Puketapu road (near Pihama)	39.520°S, 173.916°E	1678723 mE, 5625135 mN

Table 1. – Stops of the field workshop in the order of visit with coordinates given in geographic coordinate system and in New Zealand National metric system (New Zealand Transverse Mercator – NZTM2000).

The TVZ is in many volcanological aspects among the most unique on Earth being the site of the largest Holocene silicic eruption. The workshop will also show iconic volcanic sites slightly offset from the TVZ and will take the group to the Taranaki Peninsula just about ~100 km to west from the southern end of Taupo Volcanic Zone.

This section continues with the introduction to the volcanism of the Tongariro Volcanic Centre (TgVC) and finishes with the geological overview of the Taranaki Peninsula. The two volcanic areas are dominated by large composite, polygenetic volcanoes with broad ring plains. In addition, as an alternative for the participants, an introduction to the volcano-sedimentary system of large silicic, caldera-dominated volcanism of the Taupo Volcanic Zone will be provided by visiting iconic volcanic products of the Taupo Volcano. This part of the trip will demonstrate the landscape forming effects of these large eruptions, the significance of the remobilisation of pumiceous pyroclasts through re-establishing fluvial networks and the impacts of high frequency silicic eruptions that created

multiple caldera systems in the past 1.6 millions of years and produced thousands of cubic kilometres of volcanic material.

The second part of the field guide includes overall 28 stops that were planned to be visited during the field workshop (Fig. 1, Table 1). The field guide provides an overview map with the localities of geological stops for all the visited volcanic regions (Fig. 15, 46, 62). Each field stop descriptions begin with a hill-shaded topographic map (New Zealand Topo50 map series, LINZ - Land Information New Zealand) of the surroundings of the location supplemented with a hillshade inset map (derived from the New Zealand 8 m DEM, (LINZ - Land Information New Zealand, 2012) with the boundaries and names of geologic units and active faults (black-yellow dashed lines) from QMAP (Rattenbury and Isaac, 2014) that occur in vicinity of the stops. Figure numbers are not assigned to these maps that largely support the finding of visited locations and give an easy to use guide for planning of future trips. A colour code was also

used for the signs of different stop helping to understand the field program.

Structural settings and evolution of the TVZ

The TVZ is the southernmost section of the 2800 km long Tonga-Kermadec arc-back-arc system established at the convergent plate boundary between the Pacific and Australian plates at 2 Ma. From the early Miocene the tectonic regime and volcanic activity of the broader area of North Island were strongly linked to and influenced by complex subductional settings. The first subduction related to a SE-NW trending volcanic arc was established along the Three Kings Ridge southwards to Northland in the Early Miocene (23-18 Ma) (Fig. 2) (Herzer, 1995; Mortimer et al., 2010), comprising small to medium-sized basaltic to andesitic shield and cone structures (Smith et al., 1989). From 17 Ma, subduction ceased in at Northland and began along the ENE trending Colville-Lau volcanic arc associated with the convergent plate boundary between the Australian and Pacific plates. The associated Middle Miocene to Early Pleistocene (~18-2 Ma) andesitic to rhyolitic products are mostly preserved onshore in the Coromandel Peninsula and nearby islands, referred to as the Coromandel Volcanic Zone (CVZ) (Fig. 3) (Mortimer et al., 2010; Booden et al., 2012). As a result of the rifting of the Colville-Lau arc from ~5.5 Ma due to the changes of pole rotation of the Pacific Plate, the arc was transferred to the east, forming the Kermadec Arc and opening the Havre Trough back-arc basin in between (Fig. 2) (Herzer, 1995; Ballance et al., 1999; King, 2000; Mortimer et al., 2007; Mortimer et al., 2010).

The current configuration is determined by the westward subduction of a 15-25 km thick oceanic crust segment called the Hikurangi Plateau located offshore of the east coast of the North Island (Ballance, 1976; Cole and Lewis, 1981; Mortimer et al., 2010; Reyners, 2013; Timm et al., 2014) (Fig. 2). The Hikurangi Plateau is one of the piece of the fragmented Ontong Java Nui Large Igneous Province (LIP), formed as a result of mantle plume magmatism at 125-117 Ma (Timm et al., 2014; Zhang and Li, 2016; Hochmuth and Gohl, 2017). The difference in thickness between the Hikurangi Plateau and the 4-6 km thick crust underneath the Pacific Ocean to the north, as well as the altered and buoyant nature of the LIP-related crust, must have a strong effect on tectonic erosion and the local plate stress regime, as well as being a contributor of volatile components to the overlying mantle (Timm et al., 2014). As a result, the convergence along the Hikurangi Trench is

characterised by a shallow-angle oblique (~20°) subduction with a rate of motion of 47-55 mm/yr in the north and 38 mm/yr in the south (Figs. 2 and 4) (Henrys et al., 2003; Reyners, 2013). As a consequence, the fore-arc is either characterised by extensive shortening due to the reverse faulting of the accretionary prism and dextral strike-slip movements, which are mostly restricted to the eastern margin of the Axial Ranges, or is being induced rotation-like in a clockwise direction as several discrete blocks in the east coast of the North Island (Fig. 3) (Davey et al., 1986; Cashman et al., 1992; Barnes and Lépinay, 1997; Beanland and Haines, 1998; Reyners, 1998; Wallace et al., 2004).

The basement of the central North Island consists of Late Paleozoic to Early Mesozoic weakly metamorphosed sandstones and mudstones (greywacke), which are exposed at the thrust-faulted Axial Ranges. Within the fore-arc basins the greywacke is overlain by Early Cretaceous to Late Pliocene calcareous marine sediments (Mortimer, 1994; Lee et al., 2011). The volcanic arc is located about 250 km west of the Hikurangi Trench and coincides with an intra-arc rifting, which is accommodated on a highly-thinned crust up to 15-20 km (Bibby et al., 1995; Harrison and White, 2004; Stratford and Stern, 2006; Reyners et al., 2007; Davey, 2010) and a dense system of predominantly NNE-SSW trending, steeply-dipping normal faults of the Taupo rift (Fig. 4) (Rowland and Sibson, 2001; Villamor and Berryman, 2001). The fault slip data of the TVZ indicates that rates of rifting increase from 3mm/yr in the SW to 15 mm in the NE (Villamor and Berryman, 2001; Wallace et al., 2004), together with a dextral shear of 2.6 mm/yr (Acocella et al., 2003).

The fluids originating from the metasomatised subducting slab induce partial melting in the mantle wedge that is overlapped by decompression-driven melting beneath the TVZ due to an active intra-arc extension, which together provides a vast magma source for calc-alkaline volcanism (Price et al., 1992; Gamble et al., 1993b). The generation of most primitive erupted magmas is related to a low degree of partial melting (<10%) of the mantle peridotite, which also indicates chemical enrichment due to the likely contribution of slab components and the further effects of lithospheric contributions (Gamble et al., 1993a; Graham et al., 1995; Hiess et al., 2007). Most commonly, mafic magma is fractionating and assimilating the greywacke basement while migrating through the

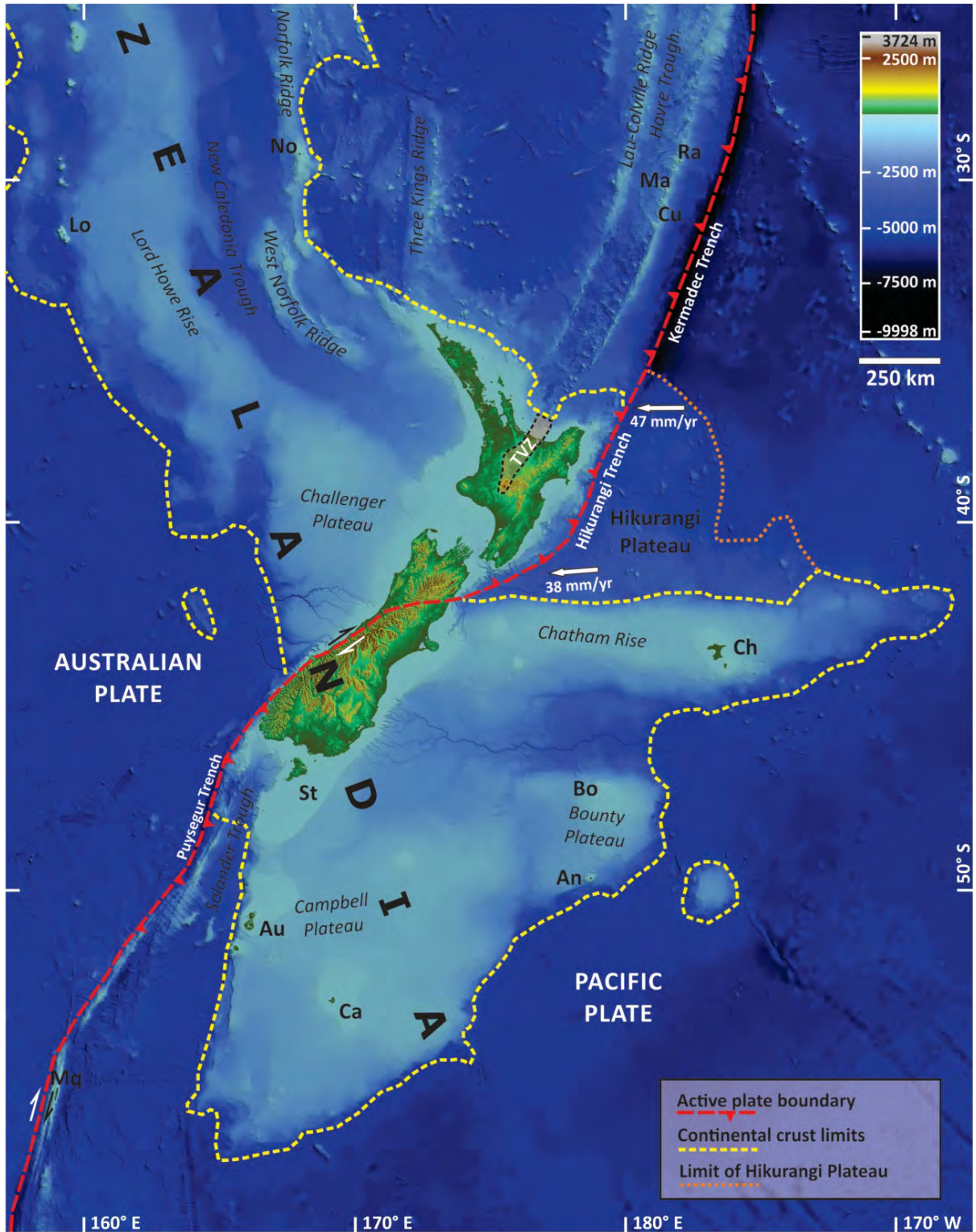


Fig. 2. – Topographic and tectonic settings of the broader environment of New Zealand (Zealandia), with respect to the position of the TVZ. Topographic information was derived from 250 m resolution gridded bathymetric data, National Institute of Water and Atmospheric Research (NIWA) (New Zealand Regional Bathymetry 2016). Tectonic and structural information from Mortimer et al. (2017). Au – Auckland Islands; An – Antipodes Islands; Bo – Bounty Islands; Ca – Campbell Island; Ch – Chatham Islands; Cu – Curtis Island; Lo – Lord Howe Island; Ma – Macauley Island; Mq – Macquaire Island; No – Norfolk Island; Ra – Raoul Island; St – Stewart Island.

crust, (Harrison and White, 2004; Charlier et al., 2008) or interacting with melt-dominated plutonic bodies (Blake et al., 1992; Leonard et al., 2002; Shane et al., 2007; Kósik et al., 2017b). Rarely mafic magma may reach the surface via dykes (Nairn and Cole, 1981), demonstrated by the few dozen basaltic occurrences spread over the TVZ (Houghton et al., 1987; Hiess et al., 2007). Evolved melts have an upper crustal origin as a result of a combination of fractionation from mafic mantle-derived magmas and crustal anatexis (Graham et al., 1995; Charlier et al., 2004). Evolved magmas may also go through multiple mixing events of different magmas prior to their eruption (Blake et al., 1992; Graham et al., 1995; Leonard et al., 2002; Charlier et al., 2004).

The TVZ volcanic activity began around 2 Ma with predominantly andesitic activity, which marks the start of the transition of the volcanic activity from the CVZ to the TVZ (Wilson et al., 1995; Briggs et al., 2005; Gravley et al., 2016). The transition between the two arcs is considered to be completed by the first large silicic eruption of the modern arc (Ngaroma ignimbrite, dense rock equivalent (DRE) volume: ~100 km³), indicating a substantial shift in back-arc rifting and associated caldera volcanism at 1.55 Ma (Briggs et al., 2005; Wilson et al., 2009).

The volcanism of the TVZ is divided into two time periods representing different vent localisations and the geochemistry of the erupted magmas. From 2 Ma to 0.7 Ma activity was characterised by andesite-dominated volcanism, whereas the second period from 0.7 to the present is dominated by rhyolitic volcanism in the central part of the TVZ (Deering et al., 2011). There is another subdivision of the history of the TVZ based on the spatial and temporal distribution of eruptive vents. Here, an 'old' TVZ (2 Ma to 0.35 Ma) is separated from the 'young' TVZ by the initiation of the ignimbrite flare-up at the Whakamaru caldera at 0.35 Ma (Wilson et al., 1995; Gravley et al., 2016). The latter subdivision is somewhat controversial, because there is a large-scale spatial and temporal overlap between the old and the young TVZ activity (Fig. 3).

The early andesitic activity of the TVZ is not very well known, and is only represented by two poorly-exposed andesitic stratovolcanoes (Titirapunga and Pureora, Fig. 3) and a few submerged andesite/dacite lava bodies intersected by geothermal drillholes (Graham et al., 1995; Leonard et al., 2010). Recent findings indicate that minor rhyolitic activity was also occurring from 1.9 Ma (Gravley et al., 2016), however the large-volume andesitic-rhyolitic volcanism in the TVZ was initiated by two ignimbrite eruptions at 1.55

and 1.53 Ma (Table 2) after a ~0.5 Ma quiescence since the formation of the 2.09 Ma Waiteariki Ignimbrite (Kaimai Volcanic Centre, CVZ) (Briggs et al., 2005; Wilson et al., 2009). The western part of the TVZ, which is mostly buried by younger ignimbrites (e.g. the Whakamaru and Mamaku Plateau Ignimbrites), was identified as the source of these earliest TVZ ignimbrites, where the only recognised caldera structure is the Mangakino Volcanic Centre (Houghton et al., 1995; Wilson et al., 1995). Besides the several small to moderate-sized (30-100 km³) ignimbrite eruptions, three large-volume ignimbrite sequences (Ongatiti, Kidnappers and Rocky Hill) were emplaced between 1.2 and 1.0 Ma (Houghton et al., 1995; Wilson et al., 2009; Deering et al., 2011) (Table 2). At this time, the volcanic activity was migrating to the east, which is presumed to be the reason for the progression or acceleration of the rifting of the TVZ (Wilson et al., 1995). By 0.9 Ma, the western TVZ became inactive and the volcanic activity continued at the east side of the Mangakino Volcanic Centre, characterised by predominantly less explosive andesitic volcanism until 0.7 Ma (Cole, 1981; Wilson et al., 1995; Deering et al., 2011). Simultaneously, typical arc-related volcanism had appeared in the south (e.g. Hauhungatahi, Cameron et al., 2010) (Fig. 3), which indicates an additional southward development of the rift during this period. The evolved andesitic composite cones lying near the axis of the rift subsided and have been found at 1-2 km depth, except the deeply-eroded Rolles Peak that is located on the eastern margin of the rift (Wilson et al., 1995; Deering et al., 2011) (Fig. 3). By the time of the eruption of Waiotapu Ignimbrite (0.71 Ma) (Table 2) the caldera volcanism had shifted to the Kapenga Volcanic Centre, indicating the waning conditions for arc-specific andesitic activity within the central part of the TVZ.

The first half of the second period (0.7 Ma to 0.34) is mostly characterised by dome-building episodes, interrupted by the eruption of the Utu Ignimbrite (~90 km³) at 0.55 Ma (Deering et al., 2010; Deering et al., 2011) (Table 2). Large-scale rhyolitic activity initiated at ~0.35 Ma resulted in the eruption of at least 2300 km³ of ignimbrite (Whakamaru Group) by a series of events within a 10 ky period (Houghton et al., 1995; Wilson et al., 2009; Gravley et al., 2016). The source of the flare-up was the Whakamaru Volcanic Centre (Fig. 3), which indicates the southward advancement of caldera volcanism. In the following 60-80 ky, another six caldera-forming events occurred, producing more than 600 km³ of ignimbrite erupted from various sources

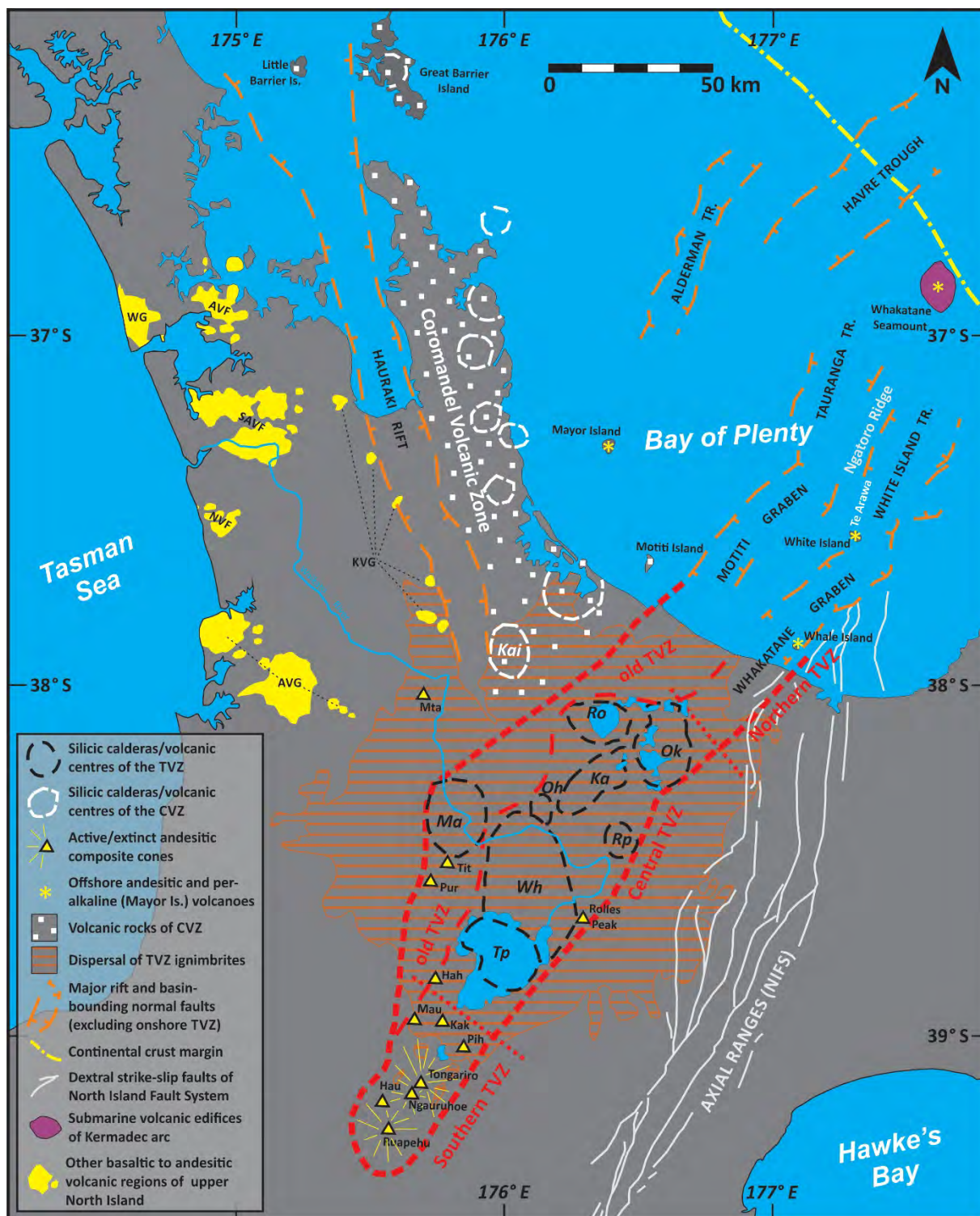


Fig. 3. – Map of the upper North Island of New Zealand indicating the margin and main volcanic structures (calderas: Ma – Mangakino; Ka – Kapenga; Wh – Whakamaru; Oh – Ohakuri; Ro – Rotorua; Rp – Reporoa; Ok – Okataina; Tp – Taupo; and andesitic composite cones: Mta – Maungatautari; Tit – Tītirāupenga; Pur – Pureora; Hah – Hauhungaroa; Hau – Hauhungatahi; Mau – Maungakatote; Kak – Kakaramea; Pih – Pihanga) of the old and young TVZ in relation to the CVZ, Kermadec arc, Havre Trough and other Neogene volcanic fields of the North Island; WG – Waitakere Group; AVF – Auckland Volcanic Field; SAVF – South Auckland Volcanic Field; NVF – Ngatutura Volcanic Field; KVG – Kīwitahi Volcanic Group; AVG – Alexandra Volcanic Group; Kai – Kaimai Volcanic Centre (CVZ). Map modified from Briggs et al. (2005) and Rowland et al. (2010), complemented with data from the GNS 1:250000 map series (Edbrooke, 2001; Edbrooke, 2005; Townsend et al., 2008; Leonard et al., 2010; Lee et al., 2011). Offshore Bay of Plenty structures after Wright (1992), TVZ delineation after Wilson et al. (1995)

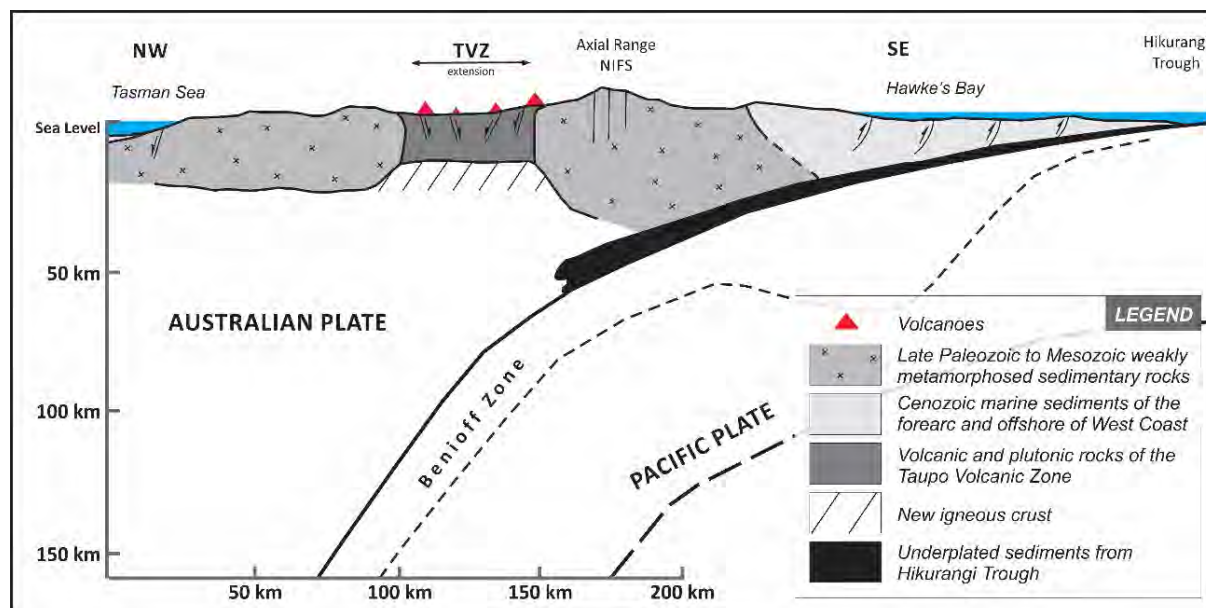


Fig. 4 Schematic SE-NW trending cross-section of the central North Island, with the main structural elements of the crust and upper mantle as determined by seismology modified after Cole and Spinks (2009).

(Gravley et al., 2006; Gravley et al., 2007; Wilson et al., 2009; Gravley et al., 2016) (Table 2). This intense explosive episode was followed by mostly effusive volcanism producing a large number of lava domes and associated smaller-volume ignimbrites up to the combined volume of 5-6 km³ (Wilson et al., 1986; Leonard, 2003; Leonard et al., 2010).

Simultaneously, the southern part of the TVZ was characterised by cyclic cone-building and destructive periods at Tongariro and Ruapehu volcanoes (Gamble et al., 2003; Tost and Cronin, 2015). The geological record of the last ~50 ka evolution of the TVZ (usually referred to as the modern TVZ; Wilson et al., 1995) is more detailed, with about 70 notable eruptions spread throughout the central part of the TVZ (Wilson et al., 2009; Ashwell et al., 2013). Three of these eruptions involved by caldera-forming activity, producing widespread ignimbrites (Rotoiti, Oruanui, Taupo Pumice) with a combined total volume of 645 km³ (Wilson et al., 2009) (Table 2).

Historically, andesitic volcanic activity occurred regularly at White Island (Houghton and Nairn, 1991) and at the stratovolcanoes of the southern TVZ. The last major activity occurred in 1974-1975 at Ngauruhoe (Nairn and Self, 1978), and in 1995-1996 at Ruapehu (Cronin et al., 1998), while the latest, but minor activity was initiated at the Te Maari craters on the northern slopes of Tongariro in 2012 (Breard et al., 2014; Pardo et al., 2014). The 1886 basaltic fissure eruption of Tarawera (Okataina Volcanic Centre) is the only historical

magmatic eruption from the central TVZ, which produced ~1 km³ of basaltic ejecta (Walker et al., 1984; Nairn, 2002; Leonard et al., 2010) (Fig. 3).

Structural settings of the Taranaki Peninsula

The Taranaki Peninsula located well separately from the TVZ on the west coast of North Island. Beneath the region of Taranaki the depth of subduction and the emplacement of the slab is c. 250 km (Fig. 4) (Boddington et al., 2004; Reyners et al., 2006), whereas the volcanoes are located about 400 km west of the Hikurangi trench and overlie 25 – 35 km thick continental crust (Stern and Davey, 1987).

The western part of the North Island is the onshore component of the Taranaki Basin that is cut by several active and inactive Quaternary faults that determine its boundaries. The Cape Egmont Fault Zone (CEFZ) to the west of the peninsula subdivides the basin into two regions, the tectonically inactive Western Stable Platform and the active Eastern Mobile Belt dominated by extension and compression related tectonic processes (Fig. 4, King, 1991; King and Thrasher, 1996). The Taranaki Fault (TF) marks the eastern boundary of Taranaki Basin that vertically offset the basement by 6 km and has accommodated a dip-slip displacement of 12-15 km since the last Cretaceous (King and Thrasher, 1996; Nicol and Wallace, 2007). The Taranaki Basin was formed during the extension and faulting of the basement due to the formation of the Tasman Sea in the middle Cretaceous.

Name	Source caldera	Age (ka)	Age error	Dating method	DRE volume (km ³)	Reference
Taupo Pumice F	Taupo	1.8	0.05	C14	35	1
Oruanui Formation	Taupo	25.4	0.2	C14	530	5
Rotoiti Formation	Okataina	45	1.4		80	4
Mokai	uncertain	210	6	Ar/Ar	40	1
Kaingaroa Formation	Reporoa	281	21	Ar/Ar	100	1
Ohakuri Formation	Ohakuri	~280-290		Ar/Ar	100	1, 5
Mamaku Plateau F.	Rotorua	~280-290		Ar/Ar	145	1, 5
Pokai Formation	Kapenga	~300		Ar/Ar	100	1, 5
Chimpanzee Formation	Kapenga	uncertain			50	1, 5
Matahina Formation	Okataina	322	7	Ar/Ar	150	1, 5
Whakamaru Group, Paeroa Subgroup	Whakamaru	339	5	Ar/Ar	110	5, 6
Whakamaru Group F.	Whakamaru	349	4	Ar/Ar	2200	5, 6
Utu ignimbrite	Okataina	~549		Ar/Ar	90	3
Waiotapu Formation	Kapenga	710	60	K/Ar	100	1
Rahopaka	?Kapenga	720	30	K/Ar	30	1
Tikorangi	?Kapenga	890	40	K/Ar	30	1
Marshall Formation	?Mangakino	950	30	K/Ar	50	1
Akatarewa ignimbrite	uncertain	950	50	K/Ar		5
Rocky Hill ignimbrite	Mangakino	1000	50	K/Ar	200	1
Kidnappers ignimbrite	Mangakino	1010	10	K/Ar	1200	1
Ahuroa ignimbrite	Mangakino	1180	20	K/Ar	100	1
Unit D	?Mangakino	1200	40	K/Ar	100	1
Ongatiti Formation	Mangakino	1210	40	K/Ar	400	1
Unit C (Pouakani F.)	Mangakino	1400	100	K/Ar	50	1, 2
Unit B (Tolley F.)	?Mangakino	1530	40	K/Ar	100	1, 2
Ngaroma Formation	?Mangakino	1550	50	K/Ar	100	1
Unit F (Link Formation)	uncertain	1600	90	K/Ar	30	1,2
Torlesse Subgroup (metasedimentary basement rocks)		Late Jurassic				5

Table 2 Stratigraphic relationship, source and estimated volumes of large-volume, caldera-forming eruptions of the TVZ. DRE volume estimates for most deposits are based on known mapped extents and recorded thicknesses that are converted, assuming that bulk volumes are equivalent to magma volumes when erosion and co-eruptive fall deposits now missing are taken into account (Wilson et al. 2009). The age of eruptions was compiled from: 1 – Wilson et al. (2009); 2 – Leonard et al. (2010); 3 – Deering et al. (2010); 4 – Danišik et al. (2012); 5 – Downs et al. (2014b); 6 – Gravley et al. (2016).

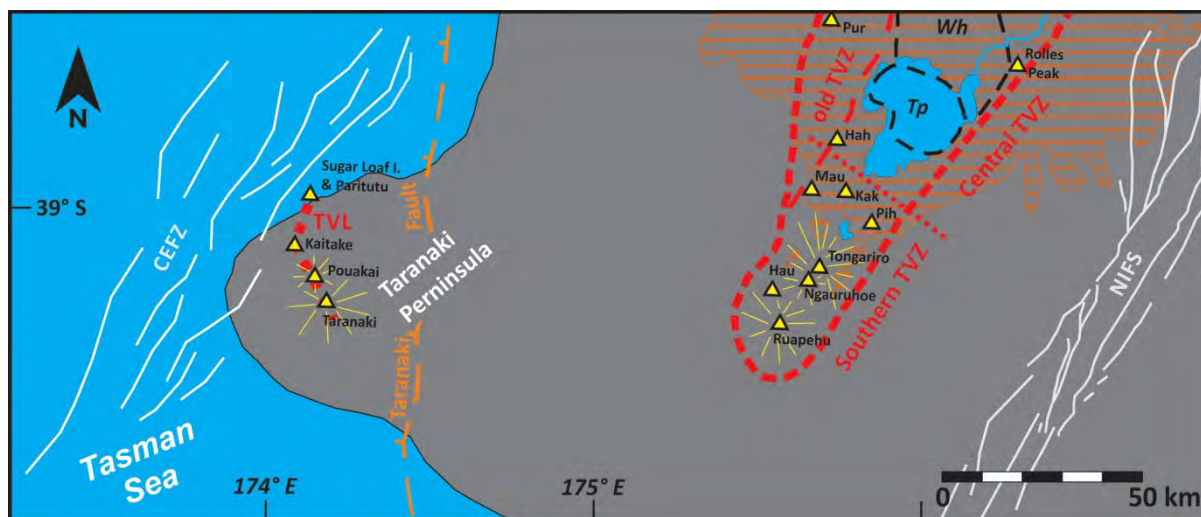


Fig. 5 Geographic location and main structural elements and volcanic centres of the Taranaki Peninsula and its relative position to the TVZ. Volcanic activity occurred along the Taranaki Volcanic Lineament (TVL). The Taranaki Basin bounded by the Cape Egmont Fault Zone (CEFZ) and the Taranaki Fault.

Volcanic architecture of the young TVZ

The TVZ is a rifting arc running across the North Island through 280 km from Ohakune (Rangataua craters) located on the southern ring plain of Ruapehu volcano (Figs. 3 and 6) to the continental margin north from White Island in the Bay of Plenty (Fig. 3). The maximum width of the young TVZ is about 50 km at the central part marked off by the vent locations of the past 0.34 Ma (Wilson et al., 1995). From a geomorphic point of view, the extent of the volcanic region of the TVZ is significantly larger than the area enclosed by vents due to the ignimbrite plateaus extending over the Taupo rift at the eastern (Kaingaroa Plateau) and the western (Mamaku Plateau) sides (Leonard et al., 2010) (Fig. 2). Due to the extensive and thick ignimbrite coverage at the NW margin of the TVZ, the volcanic structures of the old TVZ may have been obscured, thus the structural boundary of both the TVZ and CVZ is poorly defined.

The activity of the southern TVZ and the eastern margin of the central TVZ more resemble the characteristics of arc volcanism in terms of the chemical composition of rocks and volcanic architecture, while other parts are defined by caldera structures relating to a volcanism more controlled by the intra-arc extension (Spinks et al., 2005; Downs et al., 2014a). Due to this dichotomy, the young TVZ is spatially partitioned into three different parts based on the volcanic architecture and the characteristics of volcanism; the northern and southern TVZ are dominated by long-lived stratovolcanoes with predominantly andesitic volcanism, while the central TVZ is characterised predominantly by rhyolitic activity (Fig.2) (Wilson et al., 1995). Eruptions with andesitic/dacitic compositions are very rare in the central TVZ and

their volcanic structures are mostly restricted to the eastern margin of the central TVZ. These dome complexes, previously referred to as polygenetic volcanoes, represent most the conventional arc magmatism within the central TVZ (Cole, 1990; Wilson et al., 1995). These conical-shaped lava dome complexes, with associated pyroclastic fans (such as Edgecumbe, Puhipuhi, Maungakakamea/Rainbow Mountains and Tauhara), are most likely characterised by a single eruption period that lasted no longer than a few hundred to several hundreds of years (Lewis, 1968; Duncan, 1970; Carroll et al., 1997; Nairn, 2002) (Fig. 6), which brings into question their polygenetic origin and similarities with the long-lived arc-type massifs of the southern TVZ. The usual volume of these largest dome complexes do not exceed 3-4 km³, which complies with the largest rhyolitic dome eruptions of the TVZ.

Southern TVZ - Local geological framework

The southern TVZ, often referred to as the Tongariro Volcanic Centre (TgVC) comprises two large active composite volcanoes, Mt. Ruapehu and Mt. Tongariro, as well as other extinct composite cones and monogenetic structures of varying sizes and ages (Figs. 3 and 6). Mt. Ruapehu (from Te Reo Māori language: Rua- pit, pehu- to explode) is the highest peak (2797 m asl) of the North Island and the largest of the Tongariro Volcanic Centre (110 km³, Hackett and Houghton, 1989). The composite Mt. Tongariro (from Te Reo Māori language: Riro- carried away, Tonga- south wind) comprises multiple nested volcanic cones, which are roughly aligned in NE-SW direction (Fig. 7b). Both volcano complexes are surrounded by extensive overlapping ring plains, which are

strongly shaped by glaciation and the deposition of debris avalanches, pyroclastic material and

reworked lahar and fluvial sequences (Cole, 1978; Hackett and Houghton, 1989).

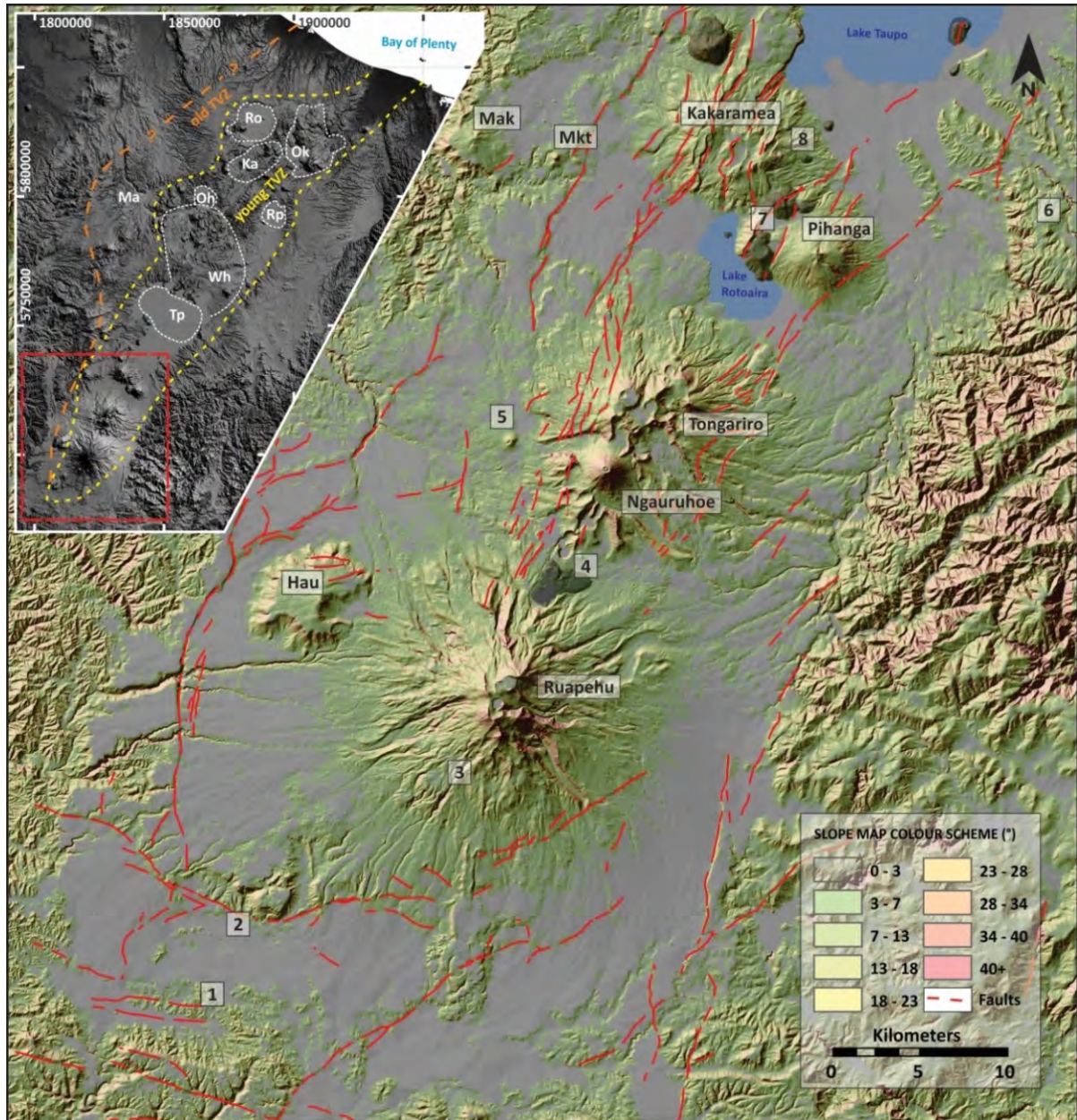


Fig. 6. – Topography of the southern TgVC as displayed on a shaded slope map derived from an 8 m DEM (LINZ - Land Information New Zealand, 2012). The inset map shows its geographic position and extent within the TVZ, coordinates are in NZTM2000. The vent locations mentioned in the text are labelled: Hau – Hauhungatahi; Mak – Maungaku; Mkt – Maungakatoke; 1 – Rangataua Craters; 2 – OhVC; 3 – inferred source vent of Rangataua lava flow; 4 – Saddle Cone and Tama Lakes; 5 – Pukeonake; 6 – Waimarino; 7 – vents in the Rotopounamu Graben (from the south: Puketopo, Pukemohono, Lake Rotopounamu and Onepotu); 8 – Te Ponanga.

The basement below the TgVC consists mainly in greywacke and argillite of the Mesozoic Torlesse Terrane and, to the west, of the volcanic arc basement of the mafic Waipapa terrane (Price et al., 2012). Compared to the central TVZ, the crust beneath Ruapehu is thicker (40 km, Price et al., 2012, and references therein) and extension rates

are lower (Villamor et al., 2007, and references therein).

Mt. Ruapehu is located within the 40 km wide Ruapehu graben, filled by tertiary sediments (Price et al., 2012) and limited by the Rangipo fault to the east and the Raurimu fault to the west (Villamor et al., 2007). The oldest dated eruptive products at Mt.

Ruapehu suggest that eruptive activity commenced ~200 ka ago (Tanaka et al., 1997; Gamble et al., 2003; Conway et al., 2016). However, lava clasts from distal mass flows have been geochemically linked to Mt. Ruapehu and yield an age of ~340 ka (Tost and Cronin, 2015). Four major cone-forming episodes sourced from at least six summit and flank vents (Fig. 7a) are defined in Hackett and Houghton (1989), Tanaka et al. (1997), Gamble et al. (2003) and Price et al. (2012), with recently

published new dates and redefined formation members after Conway et al. (2016) and Conway et al. (2018);

- Te Herenga Fm. (205 ± 27 to 159 ± 8 ka)
- Wahianoa Fm. (~160 to 88.1 ± 6.4 ka)
- Mangawhero Fm. (earlier eruptive package 50-35 ka, middle 35-26 ka, late eruptive package 36-15 ka)
- Whakapapa Fm. (<15 ka)

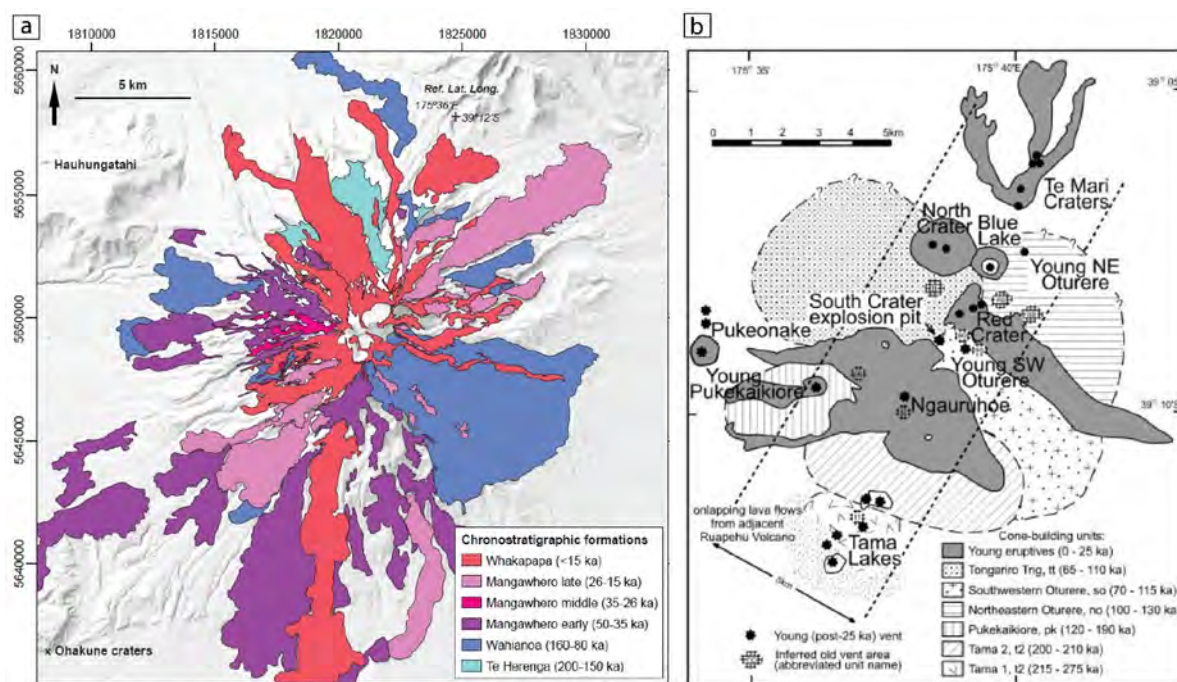


Fig. 7. – a Distribution of cone-building formations at Ruapehu composite cone (Conway et al., 2018) b Cone-building units and eruptive vents (Hobden et al., 2002).

To the North, the Tongariro volcanic complex sits in the Tongariro Graben, which is bounded by the Waihi and Poutu Fault zones (Gómez-Vasconcelos et al., 2017). Eruptive activity at Mt. Tongariro has started about 300 ka and periods of accelerated growth occurred between 210-200, 130-70 and 25 ka to present (Hobden et al., 1996). Young volcanic cones include: Te Maari, Blue Lake, North Crater, Red Crater and Mt. Ngauruhoe (Fig. 7b).

Two smaller composite cones are located at the northern end of the TgVC: Kakaramea and Pihanga. The edifice of Kakaramea has been considerably dissected by erosion and faulting, while the Pihanga structure is more intact with the exception of the lower flank on the NW side, which is intersected by the 1.5 km wide NNE-trending Rotopounamu Graben. The opening of the graben was associated with volcanic activity which formed maars, scoria cones and lava flows (Cole, 1978; Townsend et al., 2017) (Fig. 6). Rocks of

Kakaramea have been dated at 170-220 ka, and Pihanga andesite yielded an age of 125 ka. The morphology of cones the Rotopounamu Graben indicates a significantly younger age than the Pihanga volcano (Fig. 6) (Townsend et al., 2017).

Maungaku and Maungakatote are small, relatively old, poorly-known andesitic cones located at the western margin of the Taupo rift (Fig. 6). There is no direct dating of their rocks available, but stratigraphic observations indicate that their activity just postdates the deposition of the Whakamaru Group ignimbrites and related tephra (Cole, 1978).

The earliest known edifice of the TgVC is the andesitic Hauhungatahi volcano formed about 0.9 Ma, whose remnants are exposed on an upfaulted block of Tertiary marine sediments at the western margin of the Taupo rift (Cameron et al., 2010) (Figs. 3 and 6). The inferred original size of this

structure is comparable with the Kakaramea and Pihanga volcanoes (Hackett, 1985).

Monogenetic/small-volume volcanic activity has occurred at least at four locations outside the area of the axis of the Taupo rift; Rangataua Lakes, Ohakune, Pukeonake and Waimarino along with further two suspected localities (Townsend et al., 2017). Two of these volcanic centres are located on the southern ring plain of Ruapehu near Ohakune township and are both characterised by phreatomagmatic activity. Rangataua Craters/Lakes (also known as the Rangatau, Rangatauanui and Ohakune Lakes) represent the southernmost volcanic activity of the TVZ (Fig. 6), which formed at least two craters associated with phreatomagmatic and Strombolian eruptive styles along an east-west trending fault (Cole, 1978). Due to the lack of outcrops, the evolution and volcanic architecture of this monogenetic volcano remains poorly known. The Ohakune Volcanic Complex (OhVC) (also known as the Ohakune Craters and Rochfort Crater) is another monogenetic cone complex of this area, which is also aligned to an east-west trending fault (for more details of the OhVC, see stop 1.4) (Fig. 6). Pukeonake is located at the west side of the Tongariro massif about 5.5 km from the Ngauruhoe summit that marks the axis of the Taupo rift (Fig. 6). Volcanic activity occurred along a north-south trending fissure, forming a 143 m high scoria cone, a few mounds of agglutinated/welded spatter north from the cone, and a series of lava flows covering about 55 km² of area (Cole, 1978; Hackett, 1985; Hackett and Houghton, 1989).

In contrast with the basic andesitic composition of the above-mentioned small-volume eruptions, the rock type of the Waimarino volcano displays the most primitive characteristics (tholeiitic basalt with low alumina and high Mg/(Mg+Fe²⁺) ratio) within the southern TVZ (Hackett, 1985; Gamble et al., 1990). This volcano has an unusually easterly location compared with other vents of the TgVC, with a distance of 15 km from the axis of the TVZ (Fig. 6). The Waimarino eruption formed a scoria cone and lava flows that advanced 2-2.5 km to the north from the scoria cone (Hackett, 1985; Lee et al., 2011).

The age of the Waimarino eruption post-dates the 25.4 ka Oruanui eruption, whereas the overlying Tongariro Subgroup tephra indicate an age older than ~14 ka (Hackett, 1985; Donoghue et al., 1995a). Stratigraphically, Pukeonake and the two other locations near Ohakune are overlain by the Oruanui tephra, but the absence of paleosols or a major erosional break suggests that these eruptions occurred not much earlier than the deposition of the

Oruanui tephra (Houghton and Hackett, 1984; Hackett, 1985). Additionally, radiometric dating on charred wood from the medial/distal sequence of the OhVC implies an age of ~35 ka (Froggatt and Lowe, 1990; Townsend et al., 2017).

Holocene stratigraphic record of Ruapehu and Tongariro complexes

The extensive ring plain that surrounds Mt. Ruapehu is volumetrically similar to the cone (Hackett and Houghton, 1989). Since the last glacial maximum (23-13 ka), primary medial-distal pyroclastics and secondary reworked material have contributed to its construction (Topping, 1973; Topping, 1974). Five formations were defined: The Te Heuheu Formation (>22.6-14.7 ka), Tangatu Formation (14.7-5.4 ka), Mangaio Formation (4.6 ka), Manutahi Formation (5370-3200 yrs BP, Donoghue and Neall, 2001) and the most recent Onetapu Formation (dated at c. 1850 yrs BP, Fig. 8). The Ring Plain preserves a more complete record of distal explosive products compared to the steep flanks in the proximal cone area which are subjected to erosion and reworking processes, inhibiting clearly identifiable explosive products (Hackett and Houghton, 1989).

Most of Ruapehu's explosively erupted pyroclastics have been deposited on the eastern and northeastern ring plain, due to prevailing westerly to south westerly winds (Donoghue et al., 1995a). Six main tephra formations, sourced from Mt. Ruapehu and Mt. Tongariro can be distinguished here (Topping, 1973; Topping, 1974; Donoghue et al., 1995a). Fig. 8 shows an overview of the formations that can be found in the Ruapehu ring plain, including information on age, individual defined members, the volcanic source and selected external stratigraphic markers.

Eruptive activity at Ruapehu has not been uniform throughout time, neither regarding magnitude nor regarding frequency. The eruptions of the Bullot Formation (27,097±957 to ~10,000 cal. yBP (Pardo et al., 2012b) consist in large Plinian eruptions from Ruapehu's North Crater, with eruption column heights of up to 37 km (Pardo et al., 2012a). These eruptions represent the largest eruptions (VEI 4-5) known from Ruapehu (Pardo et al., 2012a) and relative deposits consist of fall-related pumice lapilli beds, sometimes interbedded with thin pyroclastic density current deposits (Pardo et al., 2012a; Pardo et al., 2012b). Erupted volumes for the five largest eruptions (erupted between ~13.6 and ~10 ka BP) were estimated to at least 0.3 km³ to 0.6 km³ (Pardo et al., 2012a). An approximately coeval equivalent is the Pahoka-

Mangamate sequence (Nairn et al., 1998), whose source is believed to consist in multiple vents (ie., Saddle Cone, Tama Lakes, Half Cone) between Ruapehu and the position of today's Ngauruhoe (proto-Ngauruhoe, Nairn et al., 1998; Auer et al., 2015). This sequence involves six major voluminous ($\sim 1 \text{ km}^3$) andesitic-dacitic sub-Plinian eruptions (Fig. 8) which were erupted during a time span of $\sim 200\text{--}400$ yrs (Nairn et al., 1998; Nakagawa et al., 1998). The overlying Papakai Formation ($\sim 11,000\text{--}3500$ cal. yBP, Topping, 1973; Donoghue et al., 1995a; Moebis, 2010) contains several Ruapehu and Tongariro-sourced tephra, which are poorly studied and of limited dispersal.

The Mangatawai Formation, on the other hand, is considered to be mainly Ngauruhoe-sourced (Gregg, 1960; Topping, 1973; Donoghue et al., 1995a) and consists in sequences of thinly bedded, grey to black ash layers, often containing leaves of the beech *Nothofagus* sp. (Topping, 1973; Moebis, 2010). Studies on glass chemistry show that some of the ash layers are Ruapehu-sourced (Moebis, 2010; Moebis et al., 2011).

The most recent formations overlie the widespread Taupo Pumice (232 AD, Lowe et al., 2013); the Tufa Trig Formation (TTF) groups the Ruapehu-sourced tephra (Donoghue et al., 1997a), while Tongariro and Ngauruhoe-sourced tephra are comprised in the Ngauruhoe Formation (Fig. 8). Generally, this time span is characterised by frequent, small-volume eruptions ($< 0.1 \text{ km}^3$), leading to massive ash-sized tephra sequences, where weathering of individual layers has been slowed down due to frequent activity (Cole et al., 1986). At Ngauruhoe, eruption styles vary from the effusive expulsion of andesitic blocky lava to strombolian, vulcanian or sub-plinian eruptions (Hobden et al., 2002). On the other hand, Ruapehu's late Holocene activity is strongly influenced by the presence of the 10 Mio. m^3 acidic Crater Lake, which fills the current vent system (Christenson and Wood, 1993; Donoghue et al., 1997a; Scott, 2013). This results in predominantly strombolian to sub-Plinian and phreatomagmatic eruption styles and the occurrence of small to very large lahars ($< 10^5$ to $> 10^7 \text{ m}^3$, Lecointre et al., 2004). The latter are defined in the Onetapu Formation which overlies the Taupo Pumice (Donoghue, 1991; Donoghue and Neall, 2001). At least 17 (including 4 historical) lahars of this formation have been identified in the Whangaehu River (Hodgson et al., 2007, and references therein). Lahar-triggering mechanisms and stratigraphic relationships with Tufa Trig tephra are discussed in Lecointre et al. (2004).

Furthermore, Ruapehu's Ring Plain testifies the record of two major debris avalanche events: The

Murimoto Formation (9540 ± 100 yrs BP, Topping, 1973) is deposited on the north western side of Ruapehu and is ascribed to a gravitational collapse (Palmer and Neall, 1989). The youngest debris avalanche is the Mangaio Formation (4600 ± 110 yrs BP, Donoghue and Neall, 2001), which is constrained to the north eastern part of the Rangipo Desert (Donoghue and Neall, 2001).

Historical eruptions

The most recent moderate eruption from Ruapehu was the 2007 phreatomagmatic eruption. It occurred without major precursors (Christenson et al., 2010; Scott, 2013) and was accompanied by several ice-slurry lahars and small surges (Fig. 9a) (Lube et al., 2009) as well as ballistics and minor ash fall (Christenson et al., 2010; Kilgour et al., 2010). Major sustained eruptive episodes at Mt. Ruapehu occurred in 1945 and 1995/1996 (Fig. 7b and c, Johnston et al., 2000; Scott, 2013). The 1995/1996 events started in September 1995 with phreatomagmatic eruptions and ended with gas emissions in September 1996 (Cronin et al., 2003b). An empty Crater Lake was observed in several occasions (e.g. on 11/12 Oct 1995 and 17 June 1996) resulting in more magmatic eruption styles (Johnston and Neall, 1995; Cronin et al., 1997; Cronin et al., 2003b; Scott, 2013). A detailed report on all documented eruptive events and eruptive periods since 1830 can be found in Scott (2013).

Eruption-unrelated dam break lahars occurred on 18th March 2007 and two other events on 24th December 1953 and 13th February 1861 (Scott, 2013). The 1953 event released c. 1.8 Mio. m^3 of water (Hodgson et al., 2007) and led to the collapse of a rail bridge during its course along the Whangaehu River valley. Unfortunately, the driver of the approaching Wellington-Auckland Express was unable to stop in time, leading to the Tangiwai disaster, New Zealand's worst railway accident. 151 lives were lost on this Christmas eve (O'Shea, 1954). The 2007 lahar was triggered by the breakage of an unstable tephra dam deposited by the 1995/1996 eruptions (Manville and Cronin, 2007). The volume of the water released from the Crater Lake was estimated to 1.3 Mio. m^3 with peak discharge rates around $800 \text{ m}^3/\text{s}$ (Manville and Cronin, 2007).

Major historical eruptions from Mt. Tongariro and Mt. Ngauruhoe include the phreatic eruption from Te Maari in 2012 and the eruptions in 1973-1975 and 1954-1955 from Mt. Ngauruhoe. The 1954-55 eruptions were dominated by Strombolian eruptions, accompanied by the emplacement of at least ten lava flows on the NW flank (Hobden et al., 2002). The eruption sequence of the 1973-1975

events culminated in the well documented eruption of the 19th February (Nairn, 1976; Nairn and Self, 1978). Several Vulcanian explosions are described and were accompanied by the ejection of ballistic

blocks and eruptions columns of up to 10 km asl (Nairn and Self, 1978). A series of collapse-related pyroclastic density currents were observed (Fig. 9d) and deposits can be found in the Mangatepopo Valley (Lube et al., 2007).

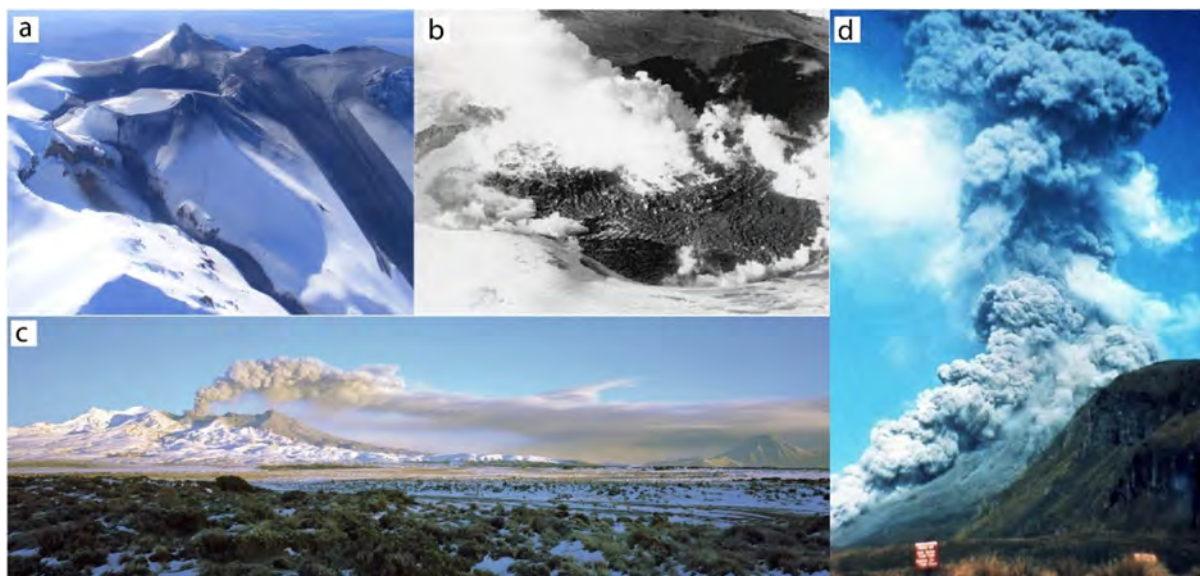


Fig. 9. – a) View of Crater Lake after the September 2007 eruption. Deposits from ash fall, small surges and ice-slurry flows are clearly visible on the snow. Photo: Karoly Nemeth. b) A semi-solid lava tholoid formed within Crater Lake during the 1945 eruption episode. Photo: GNS Science. c) Eruption column June 1996 as seen from the East. Photo: L. Homer, GNS Science. d) Pyroclastic density current during 1975 Ngauruhoe eruption. Photo: Graham Hancox, GNS Science.

Geochemical characterisation of TgVC eruptive products

Existing studies on isotopic and geochemical compositions focus mainly on lava flows from Mts. Ruapehu and Ngauruhoe (i.e. Graham and Hackett, 1987; Gamble et al., 1999; Price et al., 2010; Price et al., 2012; Conway et al., 2018). They suggest complex magmatic systems for both volcanoes, with a significant amount of interaction with the underlying basement, characterised by various degrees of AFC processes (i.e. Price et al., 2012). Furthermore, at Ngauruhoe there are evidences of periodic replenishments by a mantle-derived component (Price et al., 2010). Overall, the dominant compositions are andesitic, although basaltic and dacites compositions occur as well (Price et al., 2010; Price et al., 2012). Petrographic studies indicate a strongly porphyritic character (Hobden, 1997; Nakagawa et al., 1999; Price et al., 2010; Price et al., 2012), with plagioclases, clinopyroxene and orthopyroxene as the dominant phenocryst phases, with rare Fe-Ti oxides (Donoghue et al., 1997a; Hobden, 1997; Gamble et al., 1999; Nakagawa et al., 1999). Ngauruhoe lavas can also contain olivine (Hobden et al., 2002; Price et al., 2010). Xenoliths that are contained in lava flows are of meta-sedimentary and meta-igneous

origin (Graham and Hackett, 1987; Graham et al., 1990). However, type and compositions of xenoliths vary between the two volcanoes, indicating different depth ranges of crustal interactions (Price et al., 2010).

Studies on major element compositions of the TgVC tephra record of the past ~12 ka suggest that Tongariro-sourced tephras are slightly more mafic (basaltic andesite-andesite), compared to the andesite-dacite glasses of Ruapehu-sourced tephras (Donoghue et al., 1997a; Moebis et al., 2011). This fingerprint allows distinguishing the TgVC tephras, based on their K_2O -FeO compositions (Moebis et al., 2011).

Post ~50 ka activity of the Taupo Volcanic Centre

The southern part of the central TVZ is dominated by Lake Taupo, which is the largest lake in New Zealand occupying an area of about 620 km² (Manville et al., 1999). Lake Taupo and its neighbourhood together comprise the Taupo Volcanic Centre (Tp). The broad northern part of the lake represents the depression formed by the caldera-forming Oruanui eruption at 25.4 ka (Vandergoes et al., 2013). The deepest point of the lake at 155 m is located at the eastern part of the

Oruanui caldera, which points to the second caldera collapse having occurred during the 1.8 ka Taupo Pumice eruption (Irwin, 1972; Wilson and Walker, 1985; Davy and Caldwell, 1998; Wilson, 2001; Lowe et al., 2013). Post-Oruanui volcanic activity mostly occurred within the structure of the Oruanui collapse along a NNE-SSW trending lineament

(Fig. 10), and produced $\sim 20 \text{ km}^3$ of volcanic material (without the 35 km^3 volume of Taupo Pumice) by mostly rhyolitic sub-Plinian to Plinian eruptions (Wilson et al., 2009). The two mounds of the Horomatangi Reefs and Waitahanui Bank may represent lava domes that post-date the 1.8 ka

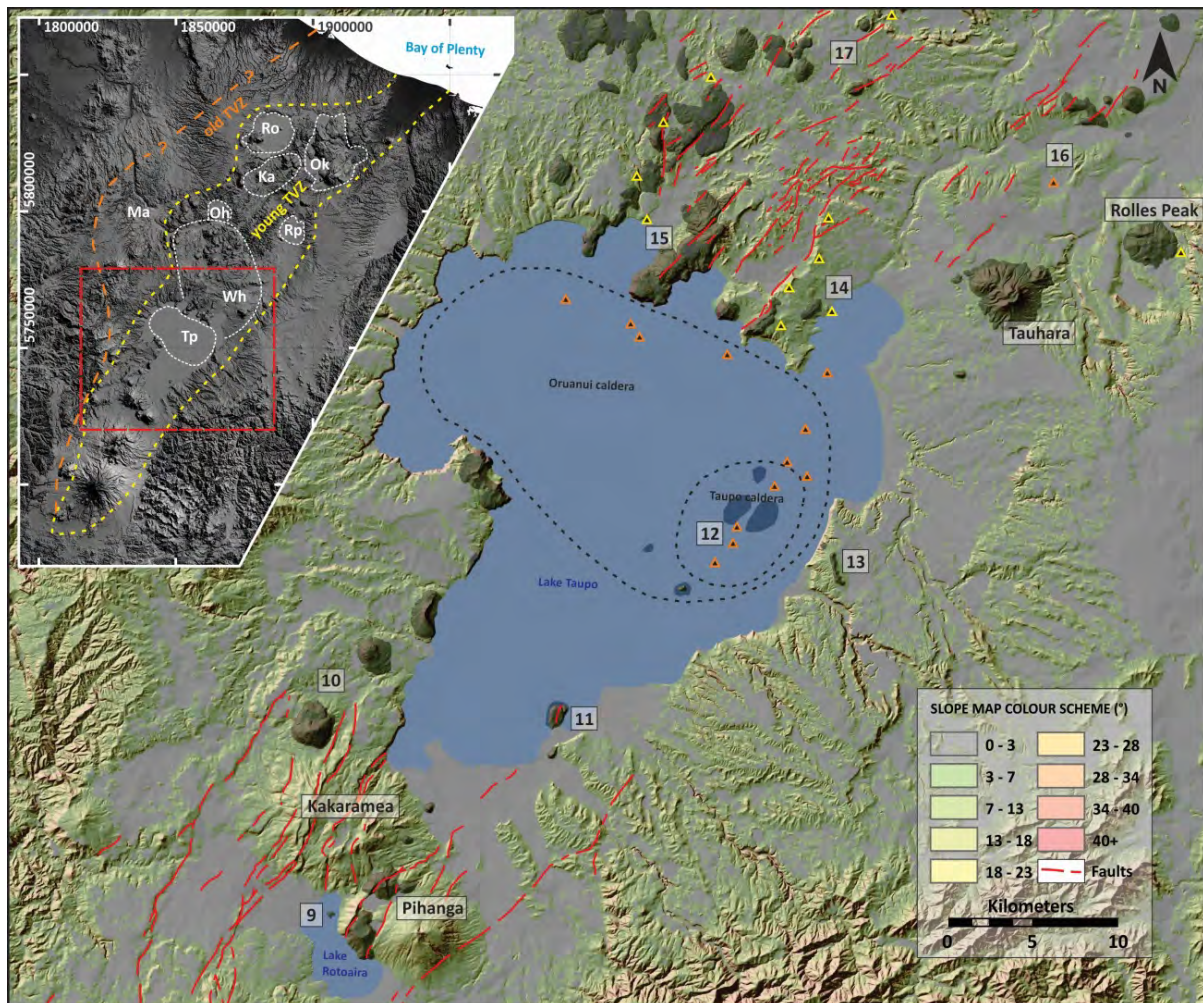


Fig. 10. – Topography of the Taupo Volcanic Centre as displayed on a shaded slope map derived from an 8 m DEM (LINZ – Land Information New Zealand, 2012). The inset map shows its geographic position and extent within the TVZ, coordinates are in NZTM2000. The vent locations mentioned in the text are labelled: 9 – Motuopuhi Island; 10 – Kuharua; 11 – Motuoaapa Peninsula; 12 – inferred post-Oruanui vents related to a NNE-SSW trending lineament; 13 – Ouaha Hills; 14 – Acacia Bay dome; 15 – Kinloch Basalt; 16 – Lake Rotokawa; 17 – PVC and Te Hukui Basalt. Triangles with yellow margins represent basaltic vent locations; with orange margins represent silicic vent locations that characterised by explosive activity. Shaded areas represent silicic domes, and scoria cones of the Rotopounamu Graben

caldera collapse (Fig. 10) (Irwin, 1972; Wilson and Walker, 1985; Wilson et al., 1986; Wilson, 1993; De Ronde et al., 2002; LINZ - Land Information New Zealand, 2013; Barker et al., 2014).

The southern basin of the lake is mostly considered to be a volcanotectonic graben, however it seems that the subsidence characterised by the northward dipping orientation of the pre-Oruanui surface rocks under the lake bed occurred in response to the Oruanui eruption (Davy and Caldwell, 1998), which would qualify the southern basin to be part

of the caldera characterised by trapdoor collapse or subsidence (Wilson, 2001; Cole et al., 2005). The high cliffs of the western and northern lake shores are composed of Whakamaru Group ignimbrites and rhyolitic lava domes (Leonard et al., 2010). Magnetic data indicates that there are numerous lava dome edifices sitting on the Whakamaru sequence within the down-sagged southern basin of Lake Taupo (Davy and Caldwell, 1998). The scalloped shape of the northern lake shore is controlled by the locations of the NNE trending

100-200 ka coalesced domes, with positions defined by the fault system of the Taupo rift. Outside of the limit of Lake Taupo, post-Oruanui volcanic activity is limited to a handful of locations. The eruptions of Acacia Bay (unit D) and Ouaha Hills (unit W) produced lava domes with the ages of 11.4 ka and 2.75 ka, respectively (Fig. 10) (Wilson et al., 2009; Leonard et al., 2010), while Wilson et al. (1986) also proposed a young age (~10 ka) for the Kuharua dome (Fig. 10), and its minimum age was later modified to 13.8 ka due to new stratigraphic observations (Froggatt and Solloway, 1986). Based on geomorphic observations, a post-Oruanui age for the dacite eruptions around the Motuopa Peninsula was also proposed (Fig. 10) (Kósik, 2018). Additionally, the recently examined phreatomagmatic basaltic succession at the lake shore near Kinloch suggests a maximum age of ~9.5 ky (Matheson, 2010). There are two further locations where activities indicate an age coherent with the post-Oruanui activity of the Taupo Volcanic Centre. Volcanic/hydrothermal explosions around Lake Rotokawa occurred at least eight times between 22.6 ka and 3.4 ka, from which the largest explosion produced 11 m thick breccia deposit dispersed within a 12 km² area at ~6 ka (McNamara et al., 2016) (Fig. 10). Despite the lack of juvenile material found, the relatively large-volume, deep excavation (~450 m) and widespread distribution of the deposits suggest some contribution by a magmatic process (Browne and Lawless, 2001). The 16.5 ka Puketerata (or Puketarata) Volcanic Complex (PVC) is located farther north at the southern margin of the Maroa Volcanic Centre (Brooker et al., 1993; Kósik et al., 2017a) (Fig. 10) and is characterised by phreatomagmatic activity together with the formation of two lava domes. A newly-discovered basaltic sequence indicates that maar-forming eruptions occurred earlier at the same location (Kósik et al., 2017b).

Volcanism of the Taranaki Region

The Taranaki Peninsula is composed of the Taranaki Volcanic Lineament (Fig. 5) that trends towards northwest-southeast (Neall, 1979; Neall et al., 1986; King and Thrasher, 1996; Neall, 2003) and expresses the subduction-connected Quaternary volcanism of the western part of North Island. It consists of four individual andesitic volcanoes comprising a chain, that progressively young to NNW-SSE and are distinct from andesitic volcanism of TVZ (Neall et al., 1986): (a) Sugar

Loaf Islands and Paritutu (1.7 Ma), (b) Kaitake Volcano (0.57 Ma), (c) Pouakai Volcano (0.25 Ma). The last member of the trend is Mt. Taranaki (Egmont Volcano; 0.13 Ma), the youngest and most southerly expression of the region (Figs. 4 and 13) (Neall, 1979; Neall et al., 1986).

Mount Taranaki is volumetrically the largest andesitic stratovolcano in New Zealand where volcanic activity started more than 130,000 years ago (Alloway et al., 2005). The almost perfectly shaped edifice made up of lavas and pyroclastic deposits that are younger than 14,000 years (Neall, 1979; Turner et al., 2011).

The nearly symmetric cone is surrounded by an almost circular, volumetrically larger ring-plain containing >150 km³ of volcanoclastic succession, characterised by debris avalanche, mass flow and fluvial deposits (Neall et al., 1986; Procter et al., 2009; Zernack et al., 2011). The ring-plain provides sedimentary records extending back to at least 100,000 years (Neall, 1979; Palmer and Neall, 1991).

Stratigraphy and evolution

The stratigraphy of Mt. Taranaki consists of the modern edifice succession (Figs. 11-12) and the older, ring-plain deposits (see in Fig. 11, Neall, 1979; Neall et al., 1986; Alloway et al., 1995; Alloway et al., 2005; Zernack et al., 2009; Zernack et al., 2011; Damaschke et al., 2017). The present-day edifice of Mt. Taranaki was predominantly constructed over the last 10 ka by effusive, eruptive and dome-building / -collapse events following the deposition of the Warea lahar deposits (debris and hyperconcentrated flows, Neall et al., 1986). Between 12-7 ka, frequent effusive activity produced lava flows interspersed with dome-building episodes and dome-collapse, block-and-ash-flow emplacement on the eastern and western flanks (Neall, 1979; Neall et al., 1986; Platz et al., 2007). Between 10-8 ka, explosive activity resulted in depositing eight tephra beds (Alloway et al., 1995). The Warwick Lavas contain the oldest lava flows (c. 8 ka, Stewart et al., 1996). Emplacement of the Peters Lavas (7-3.3 ka) further built up the edifice (Neall, 2003) and was accompanied by sporadic small to large tephra emission between 8-4.4 ka (Alloway et al., 1995). Two large sub-Plinian eruptions produced widespread tephra at 4.1 ka (Korito Tephra) and 3.6 ka (Inglewood Tephra) as well as at least 3 pyroclastic flows (Neall et al., 1986; Alloway, 1989; Alloway et al., 1995; Torres-Orozco et al., 2017).

Major eruptive activity from the satellite vent Fanthams Peak occurred at c. 3.3 ka and produced several lava flows (Neall et al., 1986; Downey et al., 1994; Alloway et al., 1995) with the latest ones possibly as young as 1.4 ka (Rosenthal, 2005).

Frequent, small to moderate sized eruptions from Fanthams Peak deposited four closely spaced tephra beds at c. 3.1 to 2.8 ka (Alloway et al., 1995; Turner et al., 2008; Torres-Orozco et al., 2017). Subsequently, four lava domes were extruded from subsidiary vents on the lower flanks of Mt. Taranaki: the Dome, Skinner Hill and the Beehives (Neall, 1971; Neall et al., 1986). A period of dome-building and dome-collapse at 2 ka (Neall et al., 1986) was followed by the extrusion of the 1.7 ka Staircase lavas, which partly filled the Opuā amphitheatre (McGlone et al., 1988; Downey et al., 1994; Stewart et al., 1996; Neall, 2003).

The sub-Plinian Kaupokonui eruption at 1.4 ka preceded the construction of the uppermost part of the modern edifice. The youngest lava flows <1.7 ka, which further filled the Opuā amphitheatre, are summarised in the Skeet grouping and the Summit grouping comprising the present summit dome and

the Turtle, a prominent lava coulee on the upper NW flanks (Neall, 2003). The youngest (Maero) eruptive period began around 800 years BP and has been dominated by dome forming and collapse episodes (Maero block-and-ash-flows), several smaller eruptions and the subplinian Burrell eruption (Cronin et al., 2003a; Platz et al., 2007). The Taurangi eruption in AD 1755 was considered as the last known eruptive activity at Mt. Taranaki (Druce, 1966) that produced the Taurangi Ash. Hence, Platz (2007) suggested a later emplacement of the summit dome some time afterwards.

At least 14 large collapse events (destruction phases) occurred within the lifespan of the volcano represented by volcanoclastic debris avalanche (VDA) deposits within the ring-plain record suggesting one major sector collapse or slope failure in every 10-14,000 years (Zernack et al., 2011) with five collapses being happened over the last 30 ka. Construction phases are represented by mass flow deposits in paleo-channel, sheet and overbank lithofacies within interbedded fluvial facies and paleosol-/ peat dominated sequences (Zernack et al., 2009).

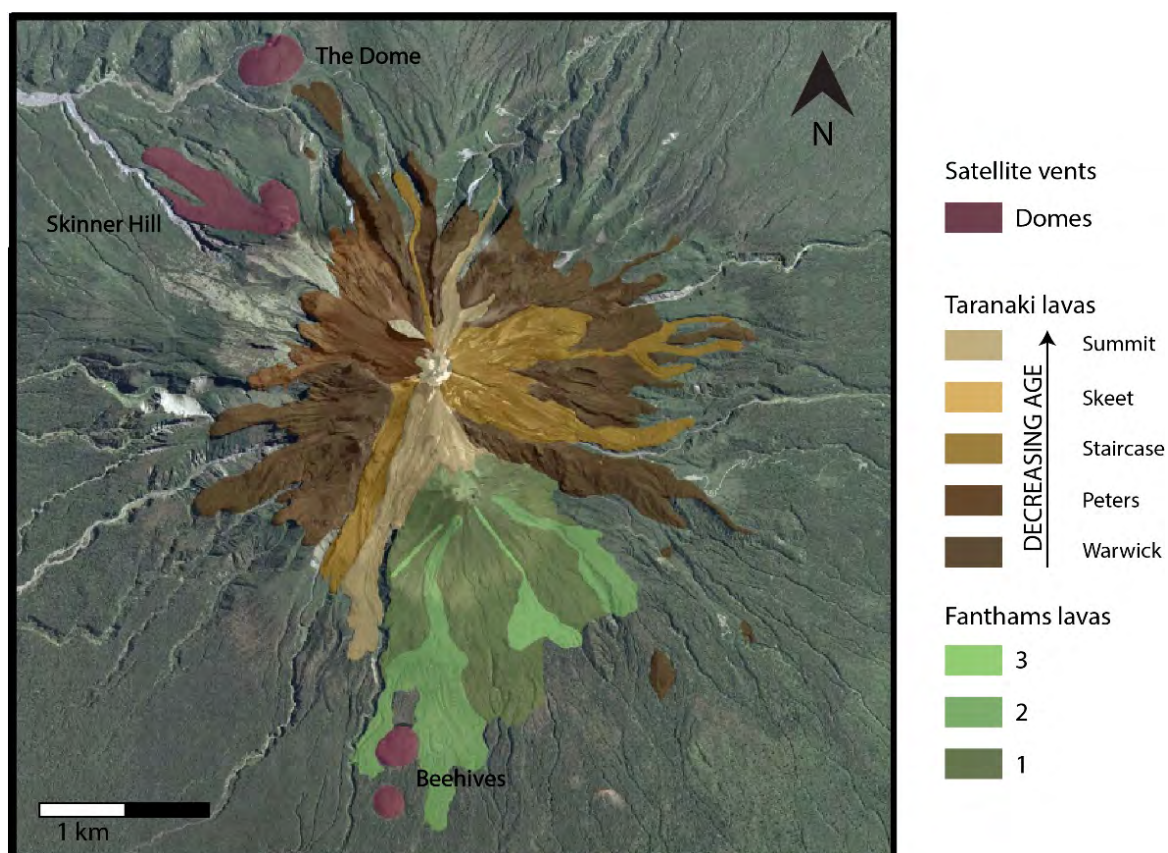


Fig. 12. – Lava flow distribution and stratigraphy of the upper portion of the Mt. Taranaki edifice (modified after Neall, 2003; Zernack, 2008).

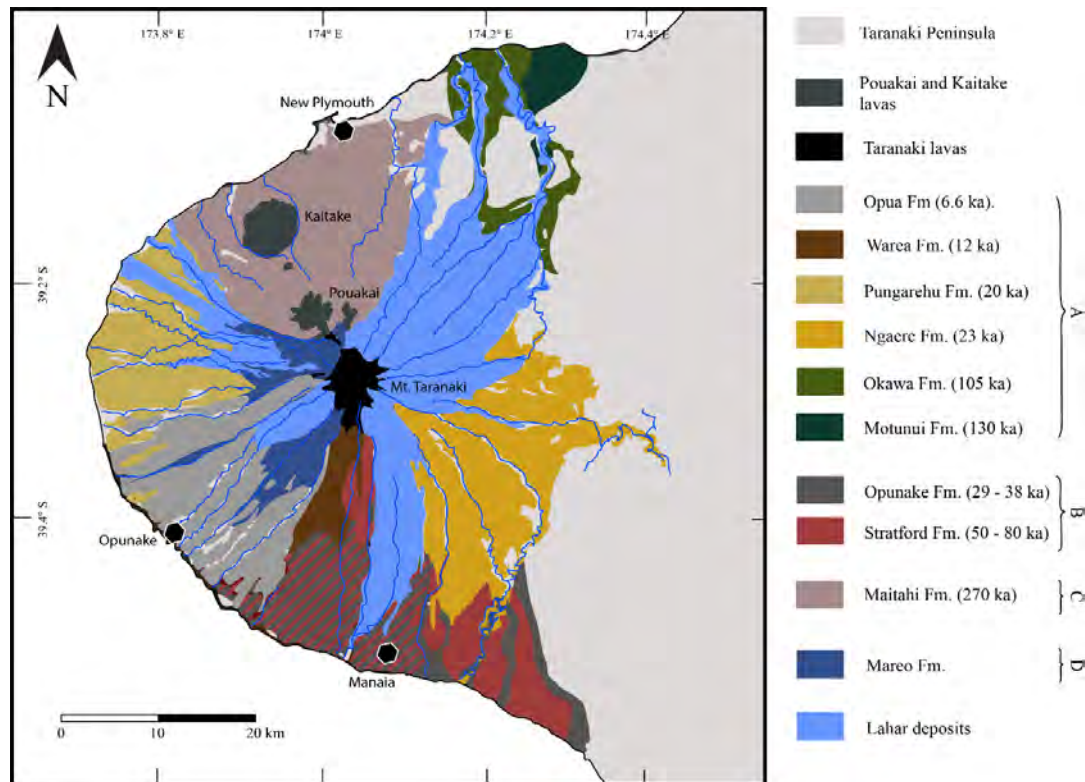


Fig. 13. – Quaternary sedimentology of lava rock formations and mass flow deposits; A: debris avalanche deposits; B: composite formations; C: pre-Taranaki debris avalanche deposit; D: Block-and-ash flow deposit (modified after Neall, 1979; Neall and Alloway, 2004; Alloway et al., 2005)

Petrology and geochemistry of Mt. Taranaki

First classification for Mt. Taranaki rocks were described by Gow (1968) based on ferromagnesian phenocryst assemblages, recognising 5 types of rocks:

- augite andesite;
- augite – hornblende andesite (augite > hornblende);
- augite – hornblende andesite (augite ~ hornblende);
- augite – hornblende andesite (augite < hornblende);
- augite – olivine andesite (modal olivine up to 7%).

Later on, this classification was updated only adding new mineral phases as plagioclase and biotite (Neall et al., 1986; Stewart et al., 1996; Price et al., 1999). Igneous rocks of Mt. Taranaki are mainly andesites, basaltic-andesites with minor basalts (Price et al., 1992). The most common rock type is augite – hornblende andesite (augite>hornblende).

Mostly occurred phenocrysts are plagioclase, clinopyroxene, hornblende, Fe-Ti oxides

(titanomagnetites in majority), minor olivine and orthopyroxene (Neall et al., 1986; Stewart et al., 1996). Accessories, that occur rarely, are apatite and zircon (Neall et al., 1986). Crustal xenoliths are abundant and characterized as peridotite, pyroxenite, amphibolite, gabbro, diorite and meta-sediments mainly originated from the Median Batholith basement (Price et al., 1992; Gruender et al., 2010).

Geochemically, Mt. Taranaki rocks are classified as high-K, low-Si andesites (Fig. 14, Gill, 1981). Taranaki magmas progressively are enriched in potassium and silica in respect of time (Stewart et al., 1996; Price et al., 1999; Price et al., 2005; Price et al., 2016). Taranaki rocks are also highly evolved based on Mg#, that is <53 and have low whole-rock Cr and Ni contents (Price et al., 1999).

Trace elements are characterised by significant enrichment of large ion lithophile elements (LILE; as Rb, Sr, Cs, Ba) and light rare elements (LREE) with lack of high field strength element members (HFSE; Ta, Nb, Zr, Price et al., 1992; Price et al., 1999; Price et al., 2005). Typical arc-signatures as depletion of Nb relative to La, enrichment of Pb and Sr relative to Ce, are characteristic features as well. These signatures are characterised as features of low-degree partial melts of a depleted mantle (Price et al., 1999). Isotopes indicate that Mt.

Taranaki rocks determine a narrow trend of $^{143}\text{Nd}/^{144}\text{Nd}$ and $^{87}\text{Sr}/^{86}\text{Sr}$ ratios (Price et al., 1992; Price et al., 1999; Price et al., 2005). These isotopic compositions are similar to evolved basalts, basaltic andesites from TVZ (Price et al., 1992).

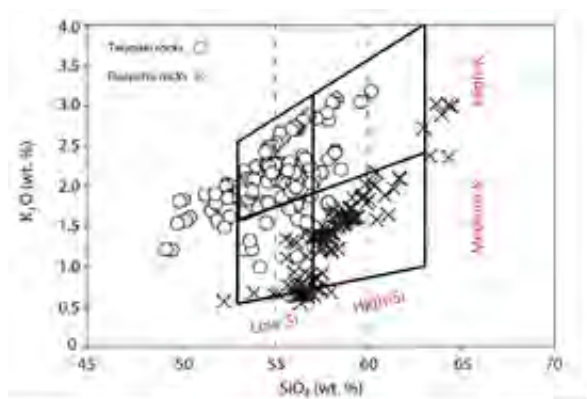


Fig. 14. – Classification of Mt. Taranaki and Mt. Ruapehu rocks after Gill (1981). Modified after Price et al. (1999)

References cited

- Acocella, V., Spinks, K.D., Cole, J.W. and Nicol, A., 2003. Oblique back arc rifting of Taupo Volcanic zone, New Zealand. *Tectonics*, 22(4).
- Alloway, B., McComb, P., Neall, V., Vucetich, C., Gibb, J., Sherburn, S. and Stirling, M., 2005. Stratigraphy, age, and correlation of voluminous debris-avalanche events from an ancestral Egmont Volcano: implications for coastal plain construction and regional hazard assessment. *Journal of the Royal Society of New Zealand*, 35(1-2): 229-267.
- Alloway, B., Neall, V. and Vucetich, C., 1995. Late Quaternary (post 28,000 year BP) tephrostratigraphy of northeast and central Taranaki, New Zealand. *Journal of the Royal Society of New Zealand*, 25(4): 385-458.
- Alloway, B.V., 1989. The late quaternary cover bed stratigraphy and tephrochronology of north-eastern and central Taranaki, New Zealand: a thesis presented in partial fulfillment of the requirements for the degree of Doctor of philosophy in soil science at Massey University, Palmerston North, New Zealand, Unpublished PhD Thesis, Massey University, Palmerston North.
- Ashwell, P.A., Kennedy, B.M., Gravley, D.M., von Aulock, F.W. and Cole, J.W., 2013. Insights into caldera and regional structures and magma body distribution from lava domes at Rotorua Caldera, New Zealand. *Journal of Volcanology and Geothermal Research*, 258: 187-202.
- Auer, A., Martin, C., Palin, J., White, J., Nakagawa, M. and Stirling, C., 2015. The evolution of hydrous magmas in the Tongariro Volcanic Centre: the 10 ka Pahoka-Mangamate eruptions. *New Zealand Journal of Geology and Geophysics*, 58(4): 364-384.
- Ballance, P.F., 1976. Evolution of the upper Cenozoic magmatic arc and plate boundary in northern New Zealand. *Earth and planetary science letters*, 28(3): 356-370.
- Ballance, P.F., Ablaev, A.G., Pushchin, I.K., Pletnev, S.P., Biryulina, M.G., Itaya, T., Follas, H.A. and Gibson, G.W., 1999. Morphology and history of the Kermadec trench-arc-backarc basin-remnant arc system at 30 to 32 S: geophysical profile, microfossil and K-Ar data. *Marine Geology*, 159(1): 35-62.
- Barker, S., Wilson, C., Smith, E.G., Charlier, B., Wooden, J.L., Hiess, J. and Ireland, T., 2014. Post-supereruption magmatic reconstruction of Taupo volcano (New Zealand), as reflected in zircon ages and trace elements. *Journal of Petrology*, 55(8): 1511-1533.
- Barnes, P.M. and Lépinay, B.M., 1997. Rates and mechanics of rapid frontal accretion along the very obliquely convergent southern Hikurangi margin, New Zealand. *Journal of Geophysical Research: Solid Earth*, 102(B11): 24931-24952.
- Beanland, S. and Haines, J., 1998. The kinematics of active deformation in the North Island, New Zealand, determined from geological strain rates. *New Zealand Journal of Geology and Geophysics*, 41(4): 311-323.
- Bibby, H., Caldwell, T., Davey, F. and Webb, T., 1995. Geophysical evidence on the structure of the Taupo Volcanic Zone and its hydrothermal circulation. *Journal of volcanology and geothermal research*, 68(1-3): 29-58.
- Blake, S., Wilson, C., Smith, I. and Walker, G., 1992. Petrology and dynamics of the Waimihia mixed magma eruption, Taupo Volcano, New Zealand. *Journal of the Geological Society*, 149(2): 193-207.
- Boddington, T., Parkin, C. and Gubbins, D., 2004. Isolated deep earthquakes beneath the North Island of New Zealand. *Geophysical Journal International*, 158(3): 972-982.
- Booden, M.A., Smith, I.E., Mauk, J.L. and Black, P.M., 2012. Geochemical and isotopic development of the Coromandel Volcanic Zone, northern New Zealand, since 18Ma. *Journal of Volcanology and Geothermal Research*, 219: 15-32.
- Briggs, R., Houghton, B., McWilliams, M. and Wilson, C., 2005. $^{40}\text{Ar}/^{39}\text{Ar}$ ages of silicic volcanic rocks in the Tauranga-Kaimai area, New Zealand: Dating the transition between volcanism in the Coromandel Arc and the Taupo Volcanic Zone. *New Zealand Journal of Geology and Geophysics*, 48(3): 459-469.
- Brooker, M.R., Houghton, B.F., Wilson, C.J.N. and Gamble, J.A., 1993. Pyroclastic phases of a rhyolitic dome-building eruption: Puketarata Tuff Ring, Taupo Volcanic Zone, New Zealand. *Bulletin of Volcanology*, 55(6): 395-406.
- Cameron, E., Gamble, J., Price, R., Smith, I., McIntosh, W. and Gardner, M., 2010. The petrology, geochronology and geochemistry of Hauhungatahi volcano, SW Taupo Volcanic Zone. *Journal of Volcanology and Geothermal Research*, 190(1-2): 179-191.
- Carroll, L., Gamble, J., Houghton, B., Thordarson, T. and Higham, T., 1997. A radiocarbon age determination for Mount Edgecumbe (Putauaki) volcano, Bay of Plenty, New Zealand.
- Cashman, S.M., Kelsey, H.M., Erdman, C.F., Cutten, H.N. and Berryman, K.R., 1992. Strain partitioning between structural domains in the forearc of the

- Hikurangi subduction zone, New Zealand. *Tectonics*, 11(2): 242-257.
- Charlier, B.L., Wilson, C.J. and Davidson, J.P., 2008. Rapid open-system assembly of a large silicic magma body: time-resolved evidence from cored plagioclase crystals in the Oruanui eruption deposits, New Zealand. *Contributions to Mineralogy and Petrology*, 156(6): 799-813.
- Christenson, B., Reyes, A., Young, R., Moebis, A., Sherburn, S., Cole-Baker, J. and Britten, K., 2010. Cyclic processes and factors leading to phreatic eruption events: Insights from the 25 September 2007 eruption through Ruapehu Crater Lake, New Zealand. *Journal of Volcanology and Geothermal Research*, 191(1): 15-32.
- Christenson, B. and Wood, C., 1993. Evolution of a vent-hosted hydrothermal system beneath Ruapehu Crater Lake, New Zealand. *Bulletin of volcanology*, 55(8): 547-565.
- Cole, J., 1978. Andesites of the Tongariro Volcanic Centre, North Island, New Zealand. *Journal of volcanology and geothermal research*, 3(1-2): 121-153.
- Cole, J., 1981. Genesis of lavas of the Taupo volcanic zone, North Island, New Zealand. *Journal of Volcanology and Geothermal Research*, 10(4): 317-337.
- Cole, J. and Lewis, K., 1981. Evolution of the Taupo-Hikurangi subduction system. *Tectonophysics*, 72(1-2): 1-21.
- Cole, J., Milner, D. and Spinks, K., 2005. Calderas and caldera structures: a review. *Earth-Science Reviews*, 69(1): 1-26.
- Cole, J. and Spinks, K., 2009. Caldera volcanism and rift structure in the Taupo Volcanic Zone, New Zealand. *Geological Society, London, Special Publications*, 327(1): 9-29.
- Cole, J.W., 1990. Structural control and origin of volcanism in the Taupo volcanic zone, New Zealand. *Bulletin of volcanology*, 52(6): 445-459.
- Cole, J.W., Graham, I.J., Hackett, W.R. and Houghton, B.F., 1986. Volcanology and petrology of the Quaternary composite volcanoes of Tongariro volcanic centre, Taupo volcanic zone, Late Cenozoic Volcanism in New Zealand. *Royal Society of NZ Bulletin* 23, pp. 224-250.
- Conway, C.E., Gamble, J.A., Wilson, C.J., Leonard, G.S., Townsend, D.B. and Calvert, A.T., 2018. New petrological, geochemical, and geochronological perspectives on andesite-dacite magma genesis at Ruapehu volcano, New Zealand. *American Mineralogist: Journal of Earth and Planetary Materials*, 103(4): 565-581.
- Conway, C.E., Leonard, G.S., Townsend, D.B., Calvert, A.T., Wilson, C.J., Gamble, J.A. and Eaves, S.R., 2016. A high-resolution 40 Ar/39 Ar lava chronology and edifice construction history for Ruapehu volcano, New Zealand. *Journal of Volcanology and Geothermal Research*, 327: 152-179.
- Cronin, S., Stewart, R., Neall, V., Platz, T. and Gaylord, D., 2003a. The AD1040 to present Maero eruptive period of Egmont volcano, Taranaki, New Zealand. *Geol Soc NZ Misc Publ A*, 116: 43.
- Cronin, S.J., Hedley, M., Smith, R. and Neall, V., 1997. Impact of Ruapehu ash fall on soil and pasture nutrient status 1. October 1995 eruptions. *New Zealand Journal of Agricultural Research*, 40(3): 383-395.
- Cronin, S.J., Neall, V., Lecointre, J., Hedley, M. and Loganathan, P., 2003b. Environmental hazards of fluoride in volcanic ash: a case study from Ruapehu volcano, New Zealand. *Journal of Volcanology and Geothermal Research*, 121(3): 271-291.
- Damaschke, M., Cronin, S.J., Holt, K.A., Bebbington, M.S. and Hogg, A.G., 2017. A 30,000 yr high-precision eruption history for the andesitic Mt. Taranaki, North Island, New Zealand. *Quaternary Research*, 87(1): 1-23.
- Danišák, M., Shane, P., Schmitt, A.K., Hogg, A., Santos, G.M., Storm, S., Evans, N.J., Fifield, L.K. and Lindsay, J.M., 2012. Re-anchoring the late Pleistocene tephrochronology of New Zealand based on concordant radiocarbon ages and combined 238 U/230 Th disequilibrium and (U-Th)/He zircon ages. *Earth and Planetary Science Letters*, 349: 240-250.
- Davey, F., 2010. Crustal seismic reflection measurements across the northern extension of the Taupo Volcanic Zone, North Island, New Zealand. *Journal of Volcanology and Geothermal Research*, 190(1): 75-81.
- Davey, F., Hampton, M., Childs, J., Fisher, M., Lewis, K. and Pettinga, J., 1986. Structure of a growing accretionary prism, Hikurangi margin, New Zealand. *Geology*, 14(8): 663-666.
- Davy, B. and Caldwell, T., 1998. Gravity, magnetic and seismic surveys of the caldera complex, Lake Taupo, North Island, New Zealand. *Journal of volcanology and geothermal research*, 81(1): 69-89.
- De Ronde, C., Stoffers, P., Garbe-Schönberg, D., Christenson, B., Jones, B., Manconi, R., Browne, P., Hissmann, K., Botz, R. and Davy, B., 2002. Discovery of active hydrothermal venting in Lake Taupo, New Zealand. *Journal of Volcanology and Geothermal Research*, 115(3): 257-275.
- Deering, C., Bachmann, O., Dufek, J. and Gravelly, D., 2011. Rift-related transition from andesite to rhyolite volcanism in the Taupo Volcanic Zone (New Zealand) controlled by crystal-melt dynamics in mush zones with variable mineral assemblages. *Journal of Petrology*, 52(11): 2243-2263.
- Deering, C.D., Gravelly, D.M., Vogel, T.A., Cole, J.W. and Leonard, G.S., 2010. Origins of cold-wet-oxidizing to hot-dry-reducing rhyolite magma cycles and distribution in the Taupo Volcanic Zone, New Zealand. *Contributions to Mineralogy and Petrology*, 160(4): 609-629.
- Donoghue, S., 1991. Late Quaternary volcanic stratigraphy of the southeastern sector of the Mount Ruapehu ring plain New Zealand. , Unpublished PhD Thesis, Massey University, Palmerston North.
- Donoghue, S., Neall, V. and Palmer, A., 1995a. Stratigraphy and chronology of late Quaternary andesitic tephra deposits, Tongariro Volcanic Centre, New Zealand. *Journal of the Royal Society of New Zealand*, 25(2): 115-206.
- Donoghue, S., Neall, V., Palmer, A. and Stewart, R., 1997a. The volcanic history of Ruapehu during the past 2 millennia based on the record of Tufa Trig tephra. *Bulletin of Volcanology*, 59(2): 136-146.
- Donoghue, S.L. and Neall, V.E., 2001. Late Quaternary constructional history of the southeastern Ruapehu

- ring plain, New Zealand. *New Zealand Journal of Geology and Geophysics*, 44(3): 439-466.
- Donoghue, S.L., Neall, V.E. and Palmer, A.S., 1995b. Stratigraphy and chronology of late Quaternary andesitic tephra deposits, Tongariro Volcanic Centre, New Zealand. *Journal of the Royal Society of New Zealand*, 25(2): 115-206.
- Donoghue, S.L., Neall, V.E., Palmer, A.S. and Stewart, R.B., 1997b. The volcanic history of Ruapehu during the past 2 millenia based on the record of Tufa Trig tephtras. *Bulletin of Volcanology*, 59: 136-146.
- Downey, W., Kellett, R., Smith, I., Price, R. and Stewart, R., 1994. New palaeomagnetic evidence for the recent eruptive activity of Mt. Taranaki, New Zealand. *Journal of volcanology and geothermal research*, 60: 15-27.
- Downs, D.T., Rowland, J.V., Wilson, C.J.N., Rosenberg, M.D., Leonard, G.S. and Calvert, A.T., 2014a. Evolution of the intra-arc Taupo-Reporoa Basin within the Taupo Volcanic Zone of New Zealand. *Geosphere*, 10(1): 185-206.
- Downs, D.T., Wilson, C.J.N., Cole, J.W., Rowland, J.V., Calvert, A.T., Leonard, G.S. and Keall, J.M., 2014b. Age and eruptive center of the Paeroa Subgroup ignimbrites (Whakamaru Group) within the Taupo Volcanic Zone of New Zealand. *Geological Society of America Bulletin*, 126(9-10): 1131-1144.
- Druce, A., 1966. Tree-ring dating of recent volcanic ash and lapilli, Mt Egmont. *New Zealand journal of botany*, 4(1): 3-41.
- Duncan, A.R., 1970. The petrology and petrochemistry of andesite and dacite volcanoes in eastern Bay of Plenty, New Zealand, Unpublished PhD Thesis, Victoria Univeristy of Wellington, Wellington 316 pp.
- Edbrooke, S., 2001. Geology of the Auckland Area: Scale 1: 250 000. Institute of Geological & Nuclear Sciences.
- Edbrooke, S., 2005. 1: 250 000 Geological Map. Waikato. Institute of Geological & Nuclear Sciences.
- Froggatt, P.C. and Lowe, D.J., 1990. A review of late Quaternary silicic and some other tephra formations from New Zealand: their stratigraphy, nomenclature, distribution, volume, and age. *New Zealand journal of geology and geophysics*, 33(1): 89-109.
- Froggatt, P.C. and Solloway, G.J., 1986. Correlation of Papanetu Tephra to Karapiti Tephra, central North Island, New Zealand. *New Zealand journal of geology and geophysics*, 29(3): 303-313.
- Gamble, J., Smith, I., McCulloch, M., Graham, I. and Kokelaar, B., 1993a. The geochemistry and petrogenesis of basalts from the Taupo Volcanic Zone and Kermadec Island Arc, SW Pacific. *Journal of volcanology and geothermal research*, 54(3-4): 265-290.
- Gamble, J., Wright, I. and Baker, J., 1993b. Seafloor geology and petrology in the oceanic to continental transition zone of the Kermadec-Havre-Taupo Volcanic Zone arc system, New Zealand. *New Zealand Journal of Geology and Geophysics*, 36(4): 417-435.
- Gamble, J.A., Price, R.C., Smith, I.E., McIntosh, W.C. and Dunbar, N.W., 2003. 40 Ar/39 Ar geochronology of magmatic activity, magma flux and hazards at Ruapehu Volcano, Taupo volcanic zone, New Zealand. *Journal of Volcanology and Geothermal Research*, 120(3): 271-287.
- Gamble, J.A., Smith, I.E., Graham, I.J., Kokelaar, B.P., Cole, J.W., Houghton, B.F. and Wilson, C.J., 1990. The petrology, phase relations and tectonic setting of basalts from the Taupo Volcanic Zone, New Zealand and the Kermadec Island Arc-Havre Trough, SW Pacific. *Journal of volcanology and geothermal research*, 43(1-4): 253-270.
- Gamble, J.A., Wood, C.P., Price, R.C., Smith, I.E.M., Stewart, R.B. and Waight, T., 1999. A fifty year perspective of magmatic evolution on Ruapehu Volcano, New Zealand: verification of open system behaviour in an arc volcano. *Earth and Planetary Science Letters*, 170: 301-314.
- Gill, J.B., 1981. Orogenic andesites and plate tectonics. Springer-Verlag.
- Gómez-Vasconcelos, M.G., Villamor, P., Cronin, S., Procter, J., Palmer, A., Townsend, D. and Leonard, G., 2017. Crustal extension in the Tongariro graben, New Zealand: Insights into volcano-tectonic interactions and active deformation in a young continental rift. *GSA Bulletin*, 129(9-10): 1085-1099.
- Gow, A.J., 1968. Petrographic and petrochemical studies of MT Egmont andesites AU - Gow, Anthony J. *New Zealand Journal of Geology and Geophysics*, 11(1): 166-190.
- Graham, I., Cole, J., Briggs, R., Gamble, J. and Smith, I., 1995. Petrology and petrogenesis of volcanic rocks from the Taupo Volcanic Zone: a review. *Journal of volcanology and geothermal research*, 68(1): 59-87.
- Graham, I.J., Blattner, P. and McCulloch, M.T., 1990. Meta-igneous granulite xenoliths from Mount Ruapehu, New Zealand: fragments of altered oceanic crust? *Contributions to Mineralogy and Petrology*, 105(6): 650-661.
- Graham, I.J. and Hackett, W.R., 1987. Petrology of Calc-alkaline Lavas from Ruapehu Volcano and Related Vents, Taupo Volcanic Zone, New Zealand. *Journal of Petrology*, 28(3): 531-567.
- Gravley, D., Deering, C., Leonard, G. and Rowland, J., 2016. Ignimbrite flare-ups and their drivers: A New Zealand perspective. *Earth-Science Reviews*, 162: 65-82.
- Gravley, D.M., Wilson, C.J.N., Leonard, G.S. and Cole, J.W., 2007. Double trouble: Paired ignimbrite eruptions and collateral subsidence in the Taupo Volcanic Zone, New Zealand. *Geological Society of America Bulletin*, 119(1-2): 18-30.
- Gravley, D.M., Wilson, C.J.N., Rosenberg, M.D. and Leonard, G.S., 2006. The nature and age of Ohakuri Formation and Ohakuri Group rocks in surface exposures and geothermal drillhole sequences in the central Taupo Volcanic Zone, New Zealand. *New Zealand Journal of Geology and Geophysics*, 49(3): 305-308.
- Gregg, D., 1960. The geology of Tongariro subdivision. . *New Zealand Geological Survey Bulletin*, 40: 9-152.
- Gruender, K., Stewart, R.B. and Foley, S., 2010. Xenoliths from the sub-volcanic lithosphere of Mt Taranaki, New Zealand. *Journal of Volcanology and Geothermal Research*, 190(1): 192-202.
- Hackett, W.R., 1985. Geology and petrology of Ruapehu volcano and related vents, Unpublished PhD thesis, Victoria University of Wellington, Wellington, 312 pp.

- Hackett, W.R. and Houghton, B.F., 1989. A facies model for a Quaternary andesitic composite volcano: Ruapehu, New Zealand. *Bulletin of volcanology*, 51(1): 51-68.
- Harrison, A. and White, R., 2004. Crustal structure of the Taupo Volcanic Zone, New Zealand: stretching and igneous intrusion. *Geophysical Research Letters*, 31(13).
- Henrys, S., Reyners, M. and Bibby, H., 2003. Exploring the plate boundary structure of the North Island, New Zealand. *Eos, Transactions American Geophysical Union*, 84(31): 289-295.
- Herzer, R.H., 1995. Seismic stratigraphy of a buried volcanic arc, Northland, New Zealand and implications for Neogene subduction. *Marine and petroleum geology*, 12(5): 511-531.
- Hiess, J., Cole, J.W. and Spinks, K.D., 2007. Influence of the crust and crustal structure on the location and composition of high-alumina basalts of the Taupo Volcanic Zone, New Zealand. *New Zealand Journal of Geology and Geophysics*, 50(4): 327-342.
- Hobden, B., Houghton, B., Lanphere, M. and Nairn, I., 1996. Growth of the Tongariro volcanic complex: new evidence from K-Ar age determinations.
- Hobden, B.J., 1997. Modelling magmatic trends in time and space: Eruptive and magmatic history of Tongariro Volcanic Complex, New Zealand, Unpublished PhD Thesis, University of Canterbury, Christchurch.
- Hobden, B.J., Houghton, B.F. and Nairn, I.A., 2002. Growth of a young, frequently active composite cone: Ngauruhoe volcano, New Zealand. *Bulletin of volcanology*, 64(6): 392-409.
- Hochmuth, K. and Gohl, K., 2017. Collision of Manihiki Plateau fragments to accretional margins of northern Andes and Antarctic Peninsula. *Tectonics*, 36(2): 229-240.
- Hodgson, K.A., Lecointre, J.A. and Neall, V.E., 2007. Onetapu formation: the last 2000 yr of laharc activity at Ruapehu volcano, New Zealand. *New Zealand Journal of Geology and Geophysics*, 50(2): 81-99.
- Houghton, B., Wilson, C., Lloyd, E., Gamble, J. and Kokelaar, B., 1987. A catalogue of basaltic deposits within the Central Taupo Volcanic Zone. *NZ Geologic Survey Record*, 18: 95-101.
- Houghton, B.F. and Hackett, W.R., 1984. Strombolian and phreatomagmatic deposits of Ohakune Craters, Ruapehu, New Zealand: a complex interaction between external water and rising basaltic magma. *Journal of Volcanology and Geothermal Research*, 21(3-4): 207-231.
- Houghton, B.F., Wilson, C.J.N., McWilliams, M.O., Lanphere, M.A., Weaver, S.D., Briggs, R.M. and Pringle, M.S., 1995. Chronology and dynamics of a large silicic magmatic system: Central Taupo Volcanic Zone, New-Zealand. *Geology*, 23(1): 13-16.
- Irwin, J., 1972. Lake Taupo Bathymetry 1 : 50 000, Lake Chart Series. New Zealand Oceanographic Institute.
- Jenkins, S.F., Magill, C.R. and McAneney, K.J., 2007. Multi-stage volcanic events: A statistical investigation. *Journal of Volcanology and Geothermal Research*, 161(4): 275-288.
- Johnston, D.M., Houghton, B.F., Neall, V.E., Ronan, K.R. and Paton, D., 2000. Impacts of the 1945 and 1995–1996 Ruapehu eruptions, New Zealand: an example of increasing societal vulnerability. *Geological Society of America Bulletin*, 112(5): 720-726.
- Johnston, D.M. and Neall, V.E., 1995. Ruapehu awakens: the 1945 eruption of Ruapehu. Science Centre and Manawatu Museum.
- Kilgour, G., Manville, V., Della Pasqua, F., Graettinger, A., Hodgson, K. and Jolly, G., 2010. The 25 September 2007 eruption of Mount Ruapehu, New Zealand: directed ballistics, surtseyan jets, and ice-slurry lahars. *Journal of Volcanology and Geothermal Research*, 191(1-2): 1-14.
- King, P.R., 1991. Physiographic maps of the Taranaki Basin-Late Cretaceous to Recent. New Zealand Geological Survey Report, G155.
- King, P.R., 2000. Tectonic reconstructions of New Zealand: 40 Ma to the present. *New Zealand Journal of Geology and Geophysics*, 43(4): 611-638.
- King, P.R. and Thrasher, G.P., 1996. Cretaceous Cenozoic geology and petroleum systems of the Taranaki Basin, New Zealand. Institute of Geological & Nuclear Sciences.
- Kósik, S., 2018. Small-volume volcanism associated with polygenetic volcanoes, Taupo Volcanic Zone, New Zealand, Unpublished PhD thesis, Massey University, Palmerston North, 304 pp.
- Kósik, S., Németh, K., Lexa, J. and Procter, J.N., 2017a. Understanding the evolution of a small-volume silicic fissure eruption: Puketerata Volcanic Complex, Taupo Volcanic Zone, New Zealand. *Journal of Volcanology and Geothermal Research*.
- Kósik, S., Németh, K., Procter, J. and Zellmer, G., 2017b. Maar-diatreme volcanism relating to the pyroclastic sequence of a newly discovered high-alumina basalt in the Maroa Volcanic Centre, Taupo Volcanic Zone, New Zealand. *Journal of Volcanology and Geothermal Research*, 341: 363-370.
- Lecointre, J., Hodgson, K., Neall, V. and Cronin, S., 2004. Lahar-triggering mechanisms and hazard at Ruapehu volcano, New Zealand. *Natural hazards*, 31(1): 85-109.
- Lee, J., Bland, K., Townsend, D. and Kamp, P., 2011. Geology of the Hawke's Bay area, Institute of Geological and Nuclear Sciences 1:250 000 geological map 8. 1 sheet + 93 p. Lower Hutt, New Zealand. GNS Science.
- Leonard, G., Cole, J., Nairn, I. and Self, S., 2002. Basalt triggering of the c. AD 1305 Kaharoa rhyolite eruption, Tarawera volcanic complex, New Zealand. *Journal of Volcanology and Geothermal Research*, 115(3): 461-486.
- Leonard, G.S., 2003. The evolution of Maroa Volcanic Centre, Taupo Volcanic Zone, New Zealand, Unpublished PhD thesis, University of Canterbury, Christchurch, 322 pp.
- Leonard, G.S., Begg, J.G. and Wilson, C.J.N., 2010. Geology of the Rotorua area. Institute of Geological and Nuclear Sciences 1:250,000 geological map 5. sheet + 102 p. Lower Hutt, New Zealand. GNS Science.
- Lewis, J.F., 1968. Tauhara Volcano, Taupo Zone: Part I—Geology and Structure. *New Zealand Journal of Geology and Geophysics*, 11(1): 212-224.

- LINZ - Land Information New Zealand, 2012. NZ 8 m Digital Elevation Model.
- Lowe, D.J., Blaauw, M., Hogg, A.G. and Newnham, R.M., 2013. Ages of 24 widespread tephras erupted since 30,000 years ago in New Zealand, with re-evaluation of the timing and palaeoclimatic implications of the Lateglacial cool episode recorded at Kaipo bog. *Quaternary Science Reviews*, 74: 170-194.
- Lube, G., Cronin, S.J., Platz, T., Freundt, A., Procter, J.N., Henderson, C. and Sheridan, M.F., 2007. Flow and deposition of pyroclastic granular flows: A type example from the 1975 Ngauruhoe eruption, New Zealand. *Journal of Volcanology and Geothermal Research*, 161(3): 165-186.
- Lube, G., Cronin, S.J. and Procter, J.N., 2009. Explaining the extreme mobility of volcanic ice-slurry flows, Ruapehu volcano, New Zealand. *Geology*, 37(1): 15-18.
- Manville, V. and Cronin, S.J., 2007. Breakout lahar from New Zealand's crater lake. *Eos, Transactions American Geophysical Union*, 88(43): 441-442.
- Manville, V., White, J., Houghton, B. and Wilson, C., 1999. Paleohydrology and sedimentology of a post-1.8 ka breakout flood from intracaldera Lake Taupo, North Island, New Zealand. *Geological Society of America Bulletin*, 111(10): 1435-1447.
- Matheson, M.A., 2010. Eruption dynamics and hydrological implications of basaltic volcanic centres at Lake Taupo, Unpublished MSc thesis, The University of Waikato.
- McGlone, M., Neall, V. and Clarkson, B., 1988. The effect of recent volcanic events and climatic changes on the vegetation of Mt Egmont (Mt Taranaki), New Zealand. *New Zealand journal of botany*, 26(1): 123-144.
- McNamara, D.D., Sewell, S., Buscarlet, E. and Wallis, I.C., 2016. A review of the Rotokawa geothermal field, New Zealand. *Geothermics*, 59: 281-293.
- Moebis, A., 2010. Understanding the Holocene explosive eruption record of the Tongariro Volcanic Centre, New Zealand, Unpublished PhD thesis, Massey University, Palmerston North, 381 pp.
- Moebis, A., Cronin, S.J., Neall, V.E. and Smith, I.E., 2011. Unravelling a complex volcanic history from fine-grained, intricate Holocene ash sequences at the Tongariro Volcanic Centre, New Zealand. *Quaternary International*, 246(1-2): 352-363.
- Mortimer, N., 1994. Origin of the Torlesse terrane and coeval rocks, North Island, New Zealand. *International geology review*, 36(10): 891-910.
- Mortimer, N., Campbell, H.J., Stagpoole, M., Wood, R.A., Rattenbury, M.S., Sutherland, R. and Seton, M., 2017. Zealandia: Earth's Hidden Continent. *GSA Today*, 27(3).
- Mortimer, N., Gans, P., Palin, J., Meffre, S., Herzer, R. and Skinner, D., 2010. Location and migration of Miocene-Quaternary volcanic arcs in the SW Pacific region. *Journal of Volcanology and Geothermal Research*, 190(1): 1-10.
- Mortimer, N., Herzer, R., Gans, P., Laporte-Magoni, C., Calvert, A. and Bosch, D., 2007. Oligocene-Miocene tectonic evolution of the South Fiji Basin and Northland Plateau, SW Pacific Ocean: Evidence from petrology and dating of dredged rocks. *Marine Geology*, 237(1): 1-24.
- Nairn, I. and Cole, J., 1981. Basalt dikes in the 1886 Tarawera Rift. *New Zealand Journal of Geology and Geophysics*, 24(5-6): 585-592.
- Nairn, I. and Self, S., 1978. Explosive eruptions and pyroclastic avalanches from Ngauruhoe in February 1975. *Journal of Volcanology and Geothermal Research*, 3(1): 39-60.
- Nairn, I.A., 1976. Atmospheric shock waves and condensation clouds from Ngauruhoe explosive eruptions. *Nature*, 259: 190-192.
- Nairn, I.A., 2002. Geology of the Okataina Volcanic Centre, scale 1: 50 000. Institute of Geological and Nuclear Sciences geological map 25. 1 sheet+ 156 p. Institute of Geological and Nuclear Sciences, Lower Hutt, New Zealand.
- Nairn, I.A., Kobayashi, T. and Nakagawa, M., 1998. The ~ 10 ka multiple vent pyroclastic eruption sequence at Tongariro Volcanic Centre, Taupo Volcanic Zone, New Zealand: Part 1. Eruptive processes during regional extension. *Journal of Volcanology and Geothermal Research*, 86(1): 19-44.
- Nakagawa, M., Nairn, I.A. and Kobayashi, T., 1998. The ~ 10 ka multiple vent pyroclastic eruption sequence at Tongariro Volcanic Centre, Taupo Volcanic Zone, New Zealand: Part 2. Petrological insights into magma storage and transport during regional extension. *Journal of volcanology and geothermal research*, 86(1): 45-65.
- Nakagawa, M., Wada, K., Thordarson, T., Wood, C.P. and Gamble, J.A., 1999. Petrologic investigations of the 1995 and 1996 eruptions of Ruapehu volcano, New Zealand: formation of discrete and small magma pockets and their intermittent discharge. *Bulletin of Volcanology*, 61: 15-31.
- Neall, V.E., 1971. Volcanic domes and lineations in Egmont National Park. *New Zealand Journal of Geology and Geophysics*, 14(1): 71-81.
- Neall, V.E., 1979. Geological Map of New Zealand: Sheets P19, P20, & P21: New Plymouth, Egmont, and Maniaia. Department of Scientific and Industrial Research.
- Neall, V.E., 2003. The volcanic history of Taranaki. Institute of Natural Resources, Massey University.
- Neall, V.E. and Alloway, B., 2004. Quaternary Geological Map of Taranaki, 1: 100 000. Institute of Natural Resources, Massey University.
- Neall, V.E., Smith, I.E. and Stewart, R., 1986. History and petrology of the Taranaki volcanoes. *Royal Society of New Zealand*.
- Nicol, A. and Wallace, L., 2007. Temporal stability of deformation rates: Comparison of geological and geodetic observations, Hikurangi subduction margin, New Zealand. *Earth and Planetary Science Letters*, 258(3-4): 397-413.
- O'Shea, B., 1954. Ruapehu and the Tangiwai disaster. *New Zealand Journal of Science and Technology Bulletin*, 36: 174-189.
- Palmer, B.A. and Neall, V.E., 1989. The Murimotu Formation—9500 year old deposits of a debris avalanche and associated lahars, Mount Ruapehu, North Island, New Zealand. *New Zealand journal of geology and geophysics*, 32(4): 477-486.
- Palmer, B.A. and Neall, V.E., 1991. Contrasting lithofacies architecture in ring-plain deposits related to edifice construction and destruction, the Quaternary Stratford and Opunake Formations,

- Egmont Volcano, New Zealand. *Sedimentary Geology*, 74(1-4): 71-88.
- Pardo, N., Cronin, S., Palmer, A., Procter, J. and Smith, I., 2012a. Andesitic Plinian eruptions at Mt. Ruapehu: quantifying the uppermost limits of eruptive parameters. *Bulletin of volcanology*, 74(5): 1161-1185.
- Pardo, N., Cronin, S.J., Palmer, A.S. and Németh, K., 2012b. Reconstructing the largest explosive eruptions of Mt. Ruapehu, New Zealand: lithostratigraphic tools to understand subplinian-plinian eruptions at andesitic volcanoes. *Bulletin of Volcanology*, 74(3): 617-640.
- Platz, T., Cronin, S.J., Cashman, K.V., Stewart, R.B. and Smith, I.E., 2007. Transition from effusive to explosive phases in andesite eruptions—A case-study from the AD1655 eruption of Mt. Taranaki, New Zealand. *Journal of volcanology and geothermal research*, 161(1): 15-34.
- Price, R., McCulloch, M., Smith, I. and Stewart, R., 1992. Pb-Nd-Sr isotopic compositions and trace element characteristics of young volcanic rocks from Egmont Volcano and comparisons with basalts and andesites from the Taupo Volcanic Zone, New Zealand. *Geochimica et cosmochimica acta*, 56(3): 941-953.
- Price, R.C., Gamble, J.A., Smith, I.E., Maas, R., Waight, T., Stewart, R.B. and Woodhead, J., 2012. The anatomy of an Andesite volcano: a time-stratigraphic study of andesite petrogenesis and crustal evolution at Ruapehu Volcano, New Zealand. *Journal of Petrology*, 53(10): 2139-2189.
- Price, R.C., Gamble, J.A., Smith, I.E.M., Stewart, R.B., Eggins, S. and Wright, I.C., 2005. An integrated model for the temporal evolution of andesites and rhyolites and crustal development in New Zealand's North Island. *Journal of Volcanology and Geothermal Research*, 140(1): 1-24.
- Price, R.C., Smith, I.E.M., Stewart, R.B., Gamble, J.A., Gruender, K. and Maas, R., 2016. High-K andesite petrogenesis and crustal evolution: Evidence from mafic and ultramafic xenoliths, Egmont Volcano (Mt. Taranaki) and comparisons with Ruapehu Volcano, North Island, New Zealand. *Geochimica et Cosmochimica Acta*, 185: 328-357.
- Price, R.C., Stewart, R.B., Woodhead, J.D. and Smith, I.E.M., 1999. Petrogenesis of High-K Arc Magmas: Evidence from Egmont Volcano, North Island, New Zealand. *Journal of Petrology*, 40(1): 167-197.
- Price, R.C., Turner, S., Cook, C., Hobden, B.J., Smith, I.E.M., Gamble, J.A., Handley, H., Maas, R. and Moebis, A., 2010. Crustal and mantle influences and U–Th–Ra disequilibrium in andesitic lavas of Ngauruhoe volcano, New Zealand. *Chemical Geology*, 277(3-4): 355-373.
- Procter, J.N., Cronin, S.J. and Zernack, A.V., 2009. Landscape and sedimentary response to catastrophic debris avalanches, western Taranaki, New Zealand. *Sedimentary Geology*, 220(3-4): 271-287.
- Purves, A., 1990. Landscape ecology of the Rangipo Desert. Unpublished M. Sc. thesis, lodged in the Library, Massey University, Palmerston North, New Zealand.
- Rattenbury M.S. and Isaac M.J., 2012. The QMAP 1:250 000 Geological Map of New Zealand project, New Zealand *Journal of Geology and Geophysics*, 55:4, 393-405
- Reyners, M., 1998. Plate coupling and the hazard of large subduction thrust earthquakes at the Hikurangi subduction zone, New Zealand. *New Zealand Journal of Geology and Geophysics*, 41(4): 343-354.
- Reyners, M., 2013. The central role of the Hikurangi Plateau in the Cenozoic tectonics of New Zealand and the Southwest Pacific. *Earth and Planetary Science Letters*, 361: 460-468.
- Reyners, M., Eberhart-Phillips, D. and Stuart, G., 2007. The role of fluids in lower-crustal earthquakes near continental rifts. *Nature*, 446(7139): 1075-1078.
- Reyners, M., Eberhart-Phillips, D., Stuart, G. and Nishimura, Y., 2006. Imaging subduction from the trench to 300 km depth beneath the central North Island, New Zealand, with Vp and Vp/Vs. *Geophysical Journal International*, 165(2): 565-583.
- Rosenthal, A., 2005. Mapping and characterisation of the eastern Fanthams Peak lavas, Egmont Volcano, Taranaki, New Zealand. Diploma mapping thesis, Technische Universitaet Bergakademie Freiberg.
- Rowland, J. and Sibson, R., 2001. Extensional fault kinematics within the Taupo Volcanic Zone, New Zealand: soft-linked segmentation of a continental rift system. *New Zealand Journal of Geology and Geophysics*, 44(2): 271-283.
- Rowland, J.V., Wilson, C.J.N. and Gravley, D.M., 2010. Spatial and temporal variations in magma-assisted rifting, Taupo Volcanic Zone, New Zealand. *Journal of Volcanology and Geothermal Research*, 190(1-2): 89-108.
- Scott, B., 2013. A revised catalogue of Ruapehu volcano eruptive activity: 1830-2012. 1972192922.
- Shane, P., Martin, S.B., Smith, V.C., Beggs, K.F., Darragh, M.B., Cole, J.W. and Nairn, I.A., 2007. Multiple rhyolite magmas and basalt injection in the 17.7 ka Rerewhakaaitu eruption episode from Tarawera volcanic complex, New Zealand. *Journal of Volcanology and Geothermal Research*, 164(1-2): 1-26.
- Smith, I., Ruddock, R. and Day, R., 1989. Miocene arc-type volcanic/plutonic complexes of the Northland Peninsula, New Zealand. *Royal Society of New Zealand Bulletin*, 26: 205-213.
- Spinks, K.D., Acocella, V., Cole, J.W. and Bassett, K.N., 2005. Structural control of volcanism and caldera development in the transtensional Taupo Volcanic Zone, New Zealand. *Journal of Volcanology and Geothermal Research*, 144(1): 7-22.
- Stern, T. and Davey, F., 1987. A seismic investigation of the crustal and upper mantle structure within the Central Volcanic Region of New Zealand. *New Zealand Journal of Geology and Geophysics*, 30(3): 217-231.
- Stewart, R., Price, R. and Smith, I., 1996. Evolution of high-K arc magma, Egmont volcano, Taranaki, New Zealand: evidence from mineral chemistry. *Journal of Volcanology and Geothermal Research*, 74(3): 275-295.
- Stratford, W. and Stern, T., 2006. Crust and upper mantle structure of a continental backarc: central North Island, New Zealand. *Geophysical Journal International*, 166(1): 469-484.
- Tanaka, H., Kawamura, K.i., Nagao, K. and Houghton, B.F., 1997. K-Ar ages and paleosecular variation of

- direction and intensity from Quaternary lava sequences in the Ruapehu Volcano, New Zealand. *Journal of geomagnetism and geoelectricity*, 49(4): 587-599.
- Timm, C., Davy, B., Haase, K., Hoernle, K.A., Graham, I.J., De Ronde, C.E., Woodhead, J., Bassett, D., Hauff, F. and Mortimer, N., 2014. Subduction of the oceanic Hikurangi Plateau and its impact on the Kermadec arc. *Nature communications*, 5: 4923.
- Topping, W., 1973. Tephrostratigraphy and chronology of late Quaternary eruptives from the Tongariro Volcanic Centre, New Zealand. *New Zealand journal of geology and geophysics*, 16(3): 397-423.
- Topping, W., 1974. Some aspects of quaternary history of Tongariro volcanic centre, Unpublished PhD Thesis, Victoria University of Wellington, Wellington.
- Torres-Orozco, R., Cronin, S.J., Pardo, N. and Palmer, A.S., 2017. New insights into Holocene eruption episodes from proximal deposit sequences at Mt. Taranaki (Egmont), New Zealand. *Bulletin of Volcanology*, 79(1): 3.
- Tost, M. and Cronin, S., 2015. Linking distal volcanoclastic sedimentation and stratigraphy with the development of Ruapehu volcano, New Zealand. *Bulletin of Volcanology*, 77(11): 1-17.
- Townsend, D., Leonard, G.S., Conway, C., Eaves, S.R. and Wilson, C.J.N., 2017. Geology of the Tongariro National Park area, scale 1:60,000, GNS Science geological map 4. 1 sheet + 109 p. . GNS Science.
- Townsend, D.B., Vonk, A. and Kamp, P.J.J., 2008. Geology of the Taranaki area. *Institute of Geological and Nuclear Sciences 1:250 000 geological map 7*. 1 sheet + 77 p. Lower Hutt, New Zealand, GNS Science.
- Turner, M.B., Cronin, S.J., Bebbington, M.S. and Platz, T., 2008. Developing probabilistic eruption forecasts for dormant volcanoes: a case study from Mt Taranaki, New Zealand. *Bulletin of Volcanology*, 70(4): 507-515.
- Turner, M.B., Cronin, S.J., Bebbington, M.S., Smith, I.E. and Stewart, R.B., 2011. Integrating records of explosive and effusive activity from proximal and distal sequences: Mt. Taranaki, New Zealand. *Quaternary International*, 246(1-2): 364-373.
- Vandergoes, M.J., Hogg, A.G., Lowe, D.J., Newnham, R.M., Denton, G.H., Southon, J., Barrell, D.J.A., Wilson, C.J.N., McGlone, M.S., Allan, A.S.R., Almond, P.C., Petchey, F., Dabell, K., Dieffenbacher-Krall, A.C. and Blaauw, M., 2013. A revised age for the Kawakawa/Oruanui tephra, a key marker for the Last Glacial Maximum in New Zealand. *Quaternary Science Reviews*, 74: 195-201.
- Villamor, P. and Berryman, K., 2001. A late Quaternary extension rate in the Taupo Volcanic Zone, New Zealand, derived from fault slip data. *New Zealand Journal of Geology and Geophysics*, 44(2): 243-269.
- Villamor, P., Van Dissen, R., Alloway, B.V., Palmer, A.S. and Litchfield, N., 2007. The Rangipo fault, Taupo rift, New Zealand: An example of temporal slip-rate and single-event displacement variability in a volcanic environment. *GSA Bulletin*, 119(5-6): 529-547.
- Wallace, L.M., Beavan, J., McCaffrey, R. and Darby, D., 2004. Subduction zone coupling and tectonic block rotations in the North Island, New Zealand. *Journal of Geophysical Research: Solid Earth*, 109(B12).
- Wilson, C., 1993. Stratigraphy, chronology, styles and dynamics of late Quaternary eruptions from Taupo volcano, New Zealand. *Philosophical Transactions of the Royal Society of London A: Mathematical, Physical and Engineering Sciences*, 343(1668): 205-306.
- Wilson, C., Houghton, B. and Lloyd, E., 1986. Volcanic history and evolution of the Maroa-Taupo area, central North Island, Late Cenozoic Volcanism in New Zealand. *Royal Society of New Zealand, Bulletin*, pp. 194-223.
- Wilson, C. and Walker, G.P., 1985. The Taupo eruption, New Zealand I. General aspects. *Philosophical Transactions of the Royal Society of London A: Mathematical, Physical and Engineering Sciences*, 314(1529): 199-228.
- Wilson, C.J.N., 2001. The 26.5 ka Oruanui eruption, New Zealand: an introduction and overview. *Journal of Volcanology and Geothermal Research*, 112(1-4): 133-174.
- Wilson, C.J.N., Gravley, D.M., Leonard, G.S. and Rowland, J.V., 2009. Volcanism in the central Taupo Volcanic Zone, New Zealand: tempo, styles and controls. *Studies in Volcanology: The Legacy of George Walker. Special Publications of IAVCEI*, 2: 225-247.
- Wilson, C.J.N., Houghton, B.F., McWilliams, M.O., Lanphere, M.A., Weaver, S.D. and Briggs, R.M., 1995. Volcanic and structural evolution of Taupo Volcanic Zone, New Zealand: a review. *Journal of Volcanology and Geothermal Research*, 68(1-3): 1-28.
- Wright, I.C., 1992. Shallow structure and active tectonism of an offshore continental back-arc spreading system: the Taupo Volcanic Zone, New Zealand. *Marine geology*, 103(1-3): 287-309.
- Zernack, A., Cronin, S., Neall, V. and Procter, J., 2011. A medial to distal volcanoclastic record of an andesite stratovolcano: detailed stratigraphy of the ring-plain succession of south-west Taranaki, New Zealand. *International Journal of Earth Sciences*, 100(8): 1937-1966.
- Zernack, A.V., 2008. Sedimentological and Geochemical Approach to Understanding Cycles of Stratovolcano Growth and Collapse at Mt. Taranaki, New Zealand, Unpublished PhD Thesis, Massey University, 326 pp.
- Zernack, A.V., Procter, J.N. and Cronin, S.J., 2009. Sedimentary signatures of cyclic growth and destruction of stratovolcanoes: a case study from Mt. Taranaki, New Zealand. *Sedimentary Geology*, 220(3-4): 288-305.
- Zhang, G.-L. and Li, C., 2016. Interactions of the Greater Ontong Java mantle plume component with the Osborn Trough. *Scientific reports*, 6: 37561.

Field Excursion to the Tongariro Volcanic Centre

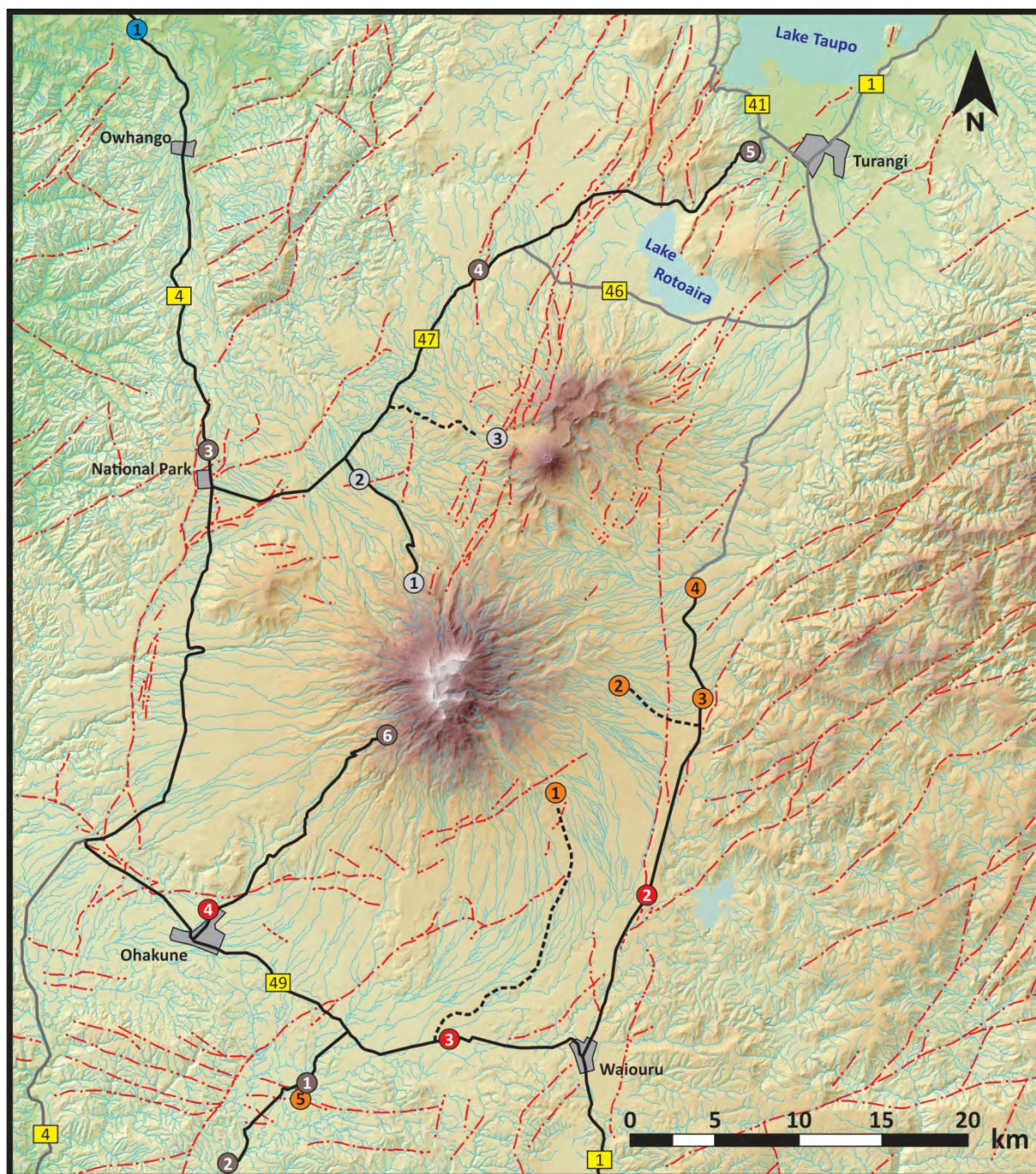
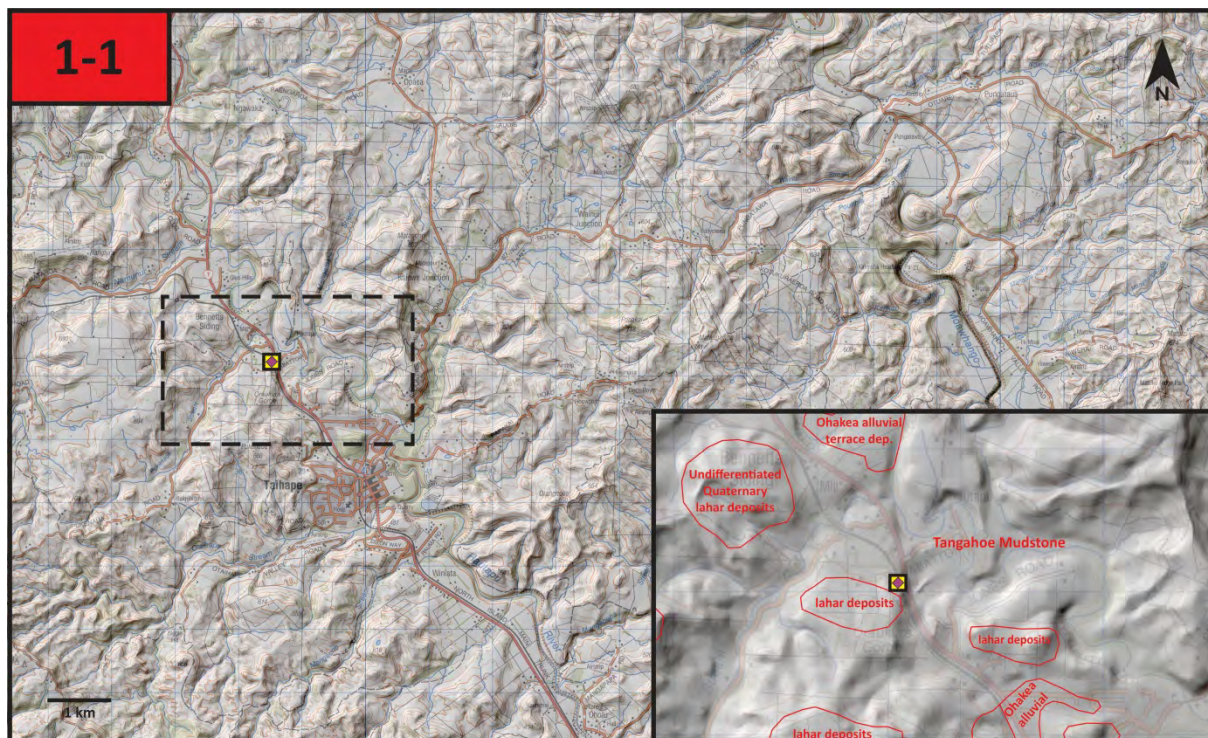


Fig. 15. – Topographic overview over the Tongariro Volcanic Centre dominated by Mt. Ruapehu and Mt. Tongariro with their respective ring plains. Active fault lines are marked by dashed red lines, while townships are indicated in grey. Field stop locations are marked by colour-coded numbers, according to the programme shown in Table 1. The roads followed during the trip are indicated with black continuous line, other main roads are indicated with grey continuous line.

Stop 1-1– Mataroa Formation overview near Taihape



Overview of boulder-covered terraces – highest river terraces in the landscape representing the “Mataroa Formation”:

Exposures of coarse volcanoclastic sediments along the Hautapu River ~50 km southeast of Mount Ruapehu, New Zealand (Fig. 16), show evidence of the largest known collapse event of the stratovolcano, which was followed by a vigorous regrowth phase that produced numerous pyroclastic eruptions and pumice-rich lahars. Cover bed stratigraphy and geochemical correlation of andesitic lava blocks within the debris-avalanche deposit with dated lavas exposed on the cone indicate that deposition occurred between 125 and 150 ka (Fig. 17). The collapse took place during the shift from a glacial to an interglacial climate, when glaciers on the cone were in retreat, and high pore water pressures combined with deep hydrothermal alteration weakened the cone. In addition, collapse may have been accompanied by magmatic unrest. The ~2–3 km³ debris avalanche inundated an area of >260 km² and entered the proto-Hautapu catchment, where it was channelized within the deeply entrenched valley. Mass-wasting events associated with post-collapse volcanism continued to be channeled into the proto-Hautapu River for another ~10 k.y., producing long-runout lahars. Subsequently, the river catchment was isolated from the volcano by incision of the intervening Whangaehu River into the proximal volcanoclastic

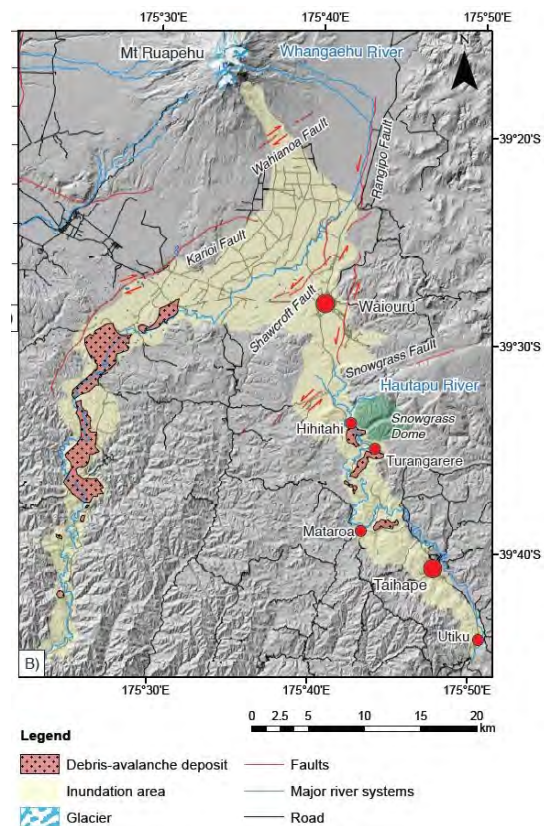


Fig. 16 – Debris avalanche deposits exposed along the Whangaehu and Hautapu River catchments

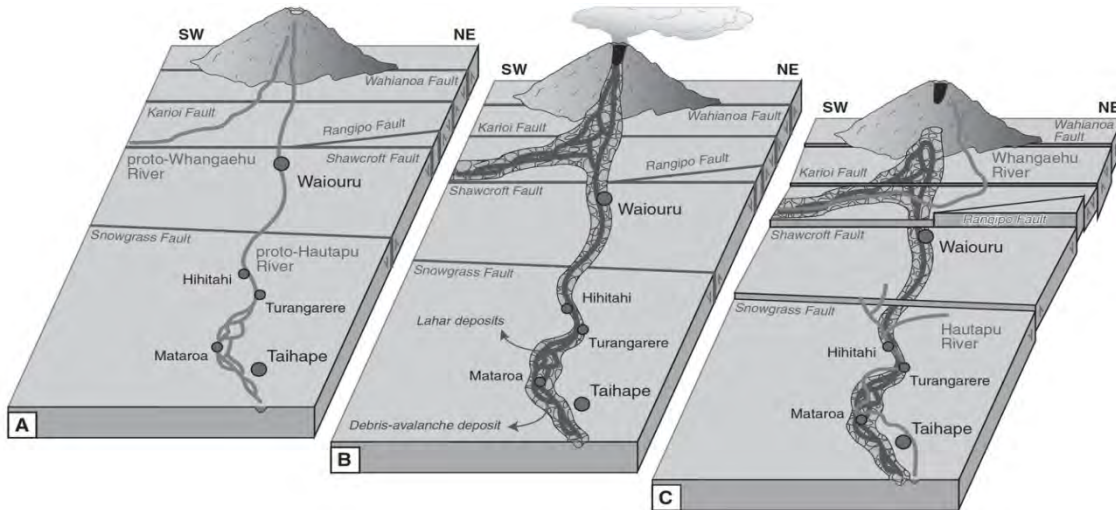


Fig. 17 – Depositional model of the Mataroa Formation. (A) Prior to emplacement of the Mataroa and Lower Whangaehu Formations (>150 ka), the proto-Hautapu River very likely arose either from the flanks of the Mount Ruapehu edifice, or the proximal ring plain. A braided river system developed between Turangarere and Taihape. Origination of the proto-Hautapu River on the volcanic edifice implies the source of a proto-Whangaehu River to be located further southwest than at present. Exposures of volcanoclastic deposits along the Whangaehu River and regional strike-slip faulting indicate that the majority of its course has been consistent over time. (B) Substrate weakening and hydrothermal alteration on the cone resulted in partial collapse of the southeastern Wahianoa flank 125–150 k.y. ago, which produced a debris-avalanche deposit that spilled into the Hautapu (and Whangaehu) River catchment. Subplinian to Plinian eruptions produced vast amounts of pyroclastic material, which was reworked into lahars that descended the volcanic flanks and were emplaced on top of the debris-avalanche deposit. (C) The Whangaehu River emerged at the eastern flank of the volcanic edifice <125 k.y. ago. Its course is dictated by regional strike-slip faulting, especially the Rangipo and Karioi fault, which results in it running southward and incising into the mass-flow deposits of the Mataroa and Lower Whangaehu Formation. At the same time, the proto-Hautapu River was cut off from the proximal Ruapehu ring plain and presently arises from wetlands south of Waiouru.

sediments, accompanied by regional faulting and graben deepening around Ruapehu. At present, the volcanoclastic deposits form a distinctive plateau on the highest topographic elevation within the Hautapu Valley, forming a reversed topography caused by preferred incision of the Hautapu River into softer Late Tertiary sediments concurrent with constant uplift (Fig. 18).

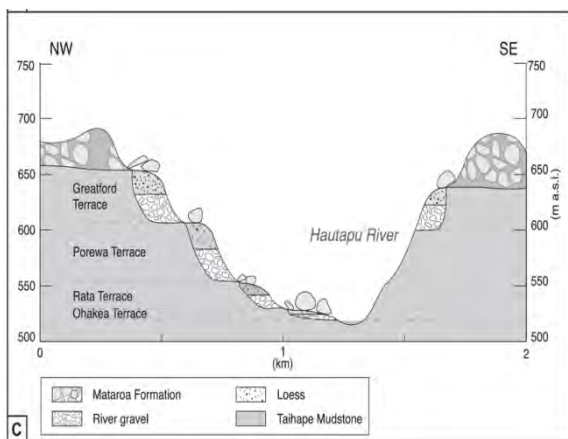


Fig. 18 – Mataroa Formation deposits capping the highest surfaces around the Taihape Town area

Suggested discussion points

- 1) Volcanic edifice to ring plain concept and its applicability for mapping of volcanoes
- 2) Discussion on the interaction between dynamic landscape and volcanism

Further reading

Tost, M. Cronin, S.J., Procter, J.N., Smith, I.E.M., Neall, V.E., Price, R.C. (2015). Impacts of catastrophic volcanic collapse on the erosion and morphology of a distal fluvial landscape: Hautapu River, Mt Ruapehu, New Zealand. *Bulletin of the Geological Society of America* 127: 266-280. DOI:10.1130/B31010.1.

Tost, M. and Cronin, S.J. (2015). Linking distal volcanoclastic sedimentation and stratigraphy with the development of Ruapehu volcano, New Zealand. *Bulletin of Volcanology* 77: 1-17.

Tost, M., Price, R.C., Cronin, S.J. and Smith, I.E.M. (2016): New insights into the evolution of the magmatic system of a composite andesite volcano revealed by clasts from distal mass-flow deposits: Ruapehu volcano, New Zealand. *Bulletin of Volcanology* 78 (5), 1-22.

Tost, M. and Cronin, S.J., (2016). Climate influence on volcano edifice stability and fluvial landscape evolution surrounding Mount Ruapehu, New Zealand. *Geomorphology* 262: 77–90.

Stop 1-2 – Introduction, Whangaehu Valley lahars, fault movements of the Ruapehu Graben

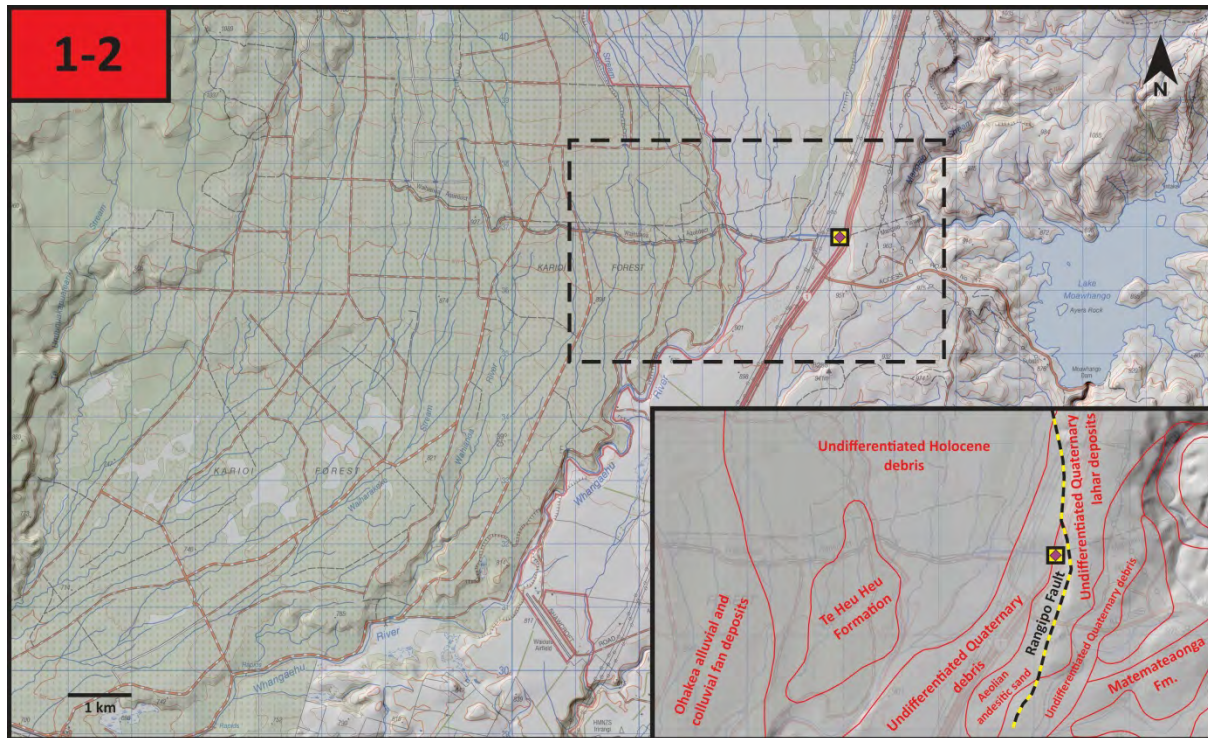


Fig. 19 – Overview SE Ruapehu ring plain showing location of main geomorphological features

This location provides an overview of the medial ring plain of SE Ruapehu and the modern Whangaehu River (Fig. 19). The majority of historical lahars have traveled down this path, including recent flows studied during passage in 1995 (Cronin et al., 1997) and 2007 (Procter et al., 2010).

The NE-striking Rangipo Fault, exposed here, marks the eastern boundary of the Taupo rift and the Ruapehu graben. Slip-rates were calculated to be variable over the past >25.4 cal ka BP (Gómez-

Vasconcelos et al., 2016); elevated slip-rates of 1.8 mm/yr in the time span from >25.4 to 13.6 cal ka BP coincide with the voluminous eruptions of the Ruapehu-sourced Bullot Formation (25 to 11 cal ka BP, Pardo et al., 2012). The present slip-rate has decreased to 0.24 mm/yr since 13.6 cal ka BP (Fig. 20).

The upthrown side of the fault exposes lahar deposits of the Te Heuheu Formation (~14.7 – >22.6 ka BP, Fig. 8), which are buried by younger lahar and pyroclastic deposits on the downthrown

(western) side. In the past, fault activity has changed important geomorphologic features, confining lahar pathways mainly to the SE-E sector of the ring plain after ~15 ka BP (Donoghue & Neall, 2011).

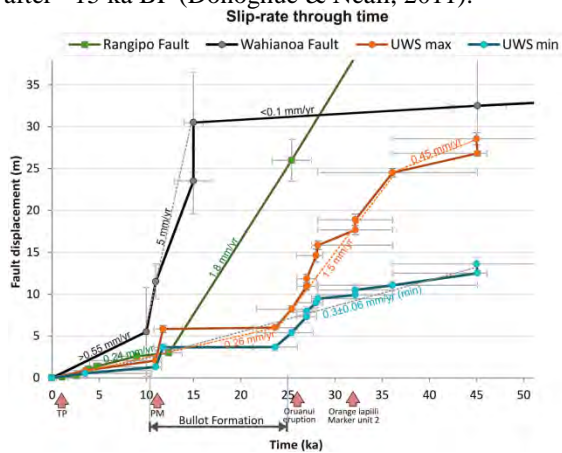


Fig. 20 – Relationship between fault movement and periods of known explosive volcanism from Ruapehu (Gómez-Vasconcelos et al., 2016).

Suggested discussion points

- 1) Discussion of the sector-based growth and deposition around stratovolcanoes
- 2) The relationship of tectonism and deposition
- 3) Discussion on medial facies of lahar deposits and transition from confined to unconfined systems
- 4) Discussion on the transition from the volcanic edifice to the ring plain

- 5) Contrasting the sedimentary environment of the edifice and the ring plain with particular reference to the transition from edifice to ring plain environment
- 6) Introducing the main theme of the workshop such as exploring the sedimentary signatures of ring plain versus edifice accumulation of pyroclasts and coherent lava bodies

Further reading

Cronin, S.J., Neall, V.E., Lecointre, J.A., and Palmer, A.S. (1997). Changes in Whangaehu river lahar characteristics during the 1995 eruption sequence, Ruapehu volcano, New Zealand. *Journal of Volcanology and Geothermal Research* 76: 47-61.

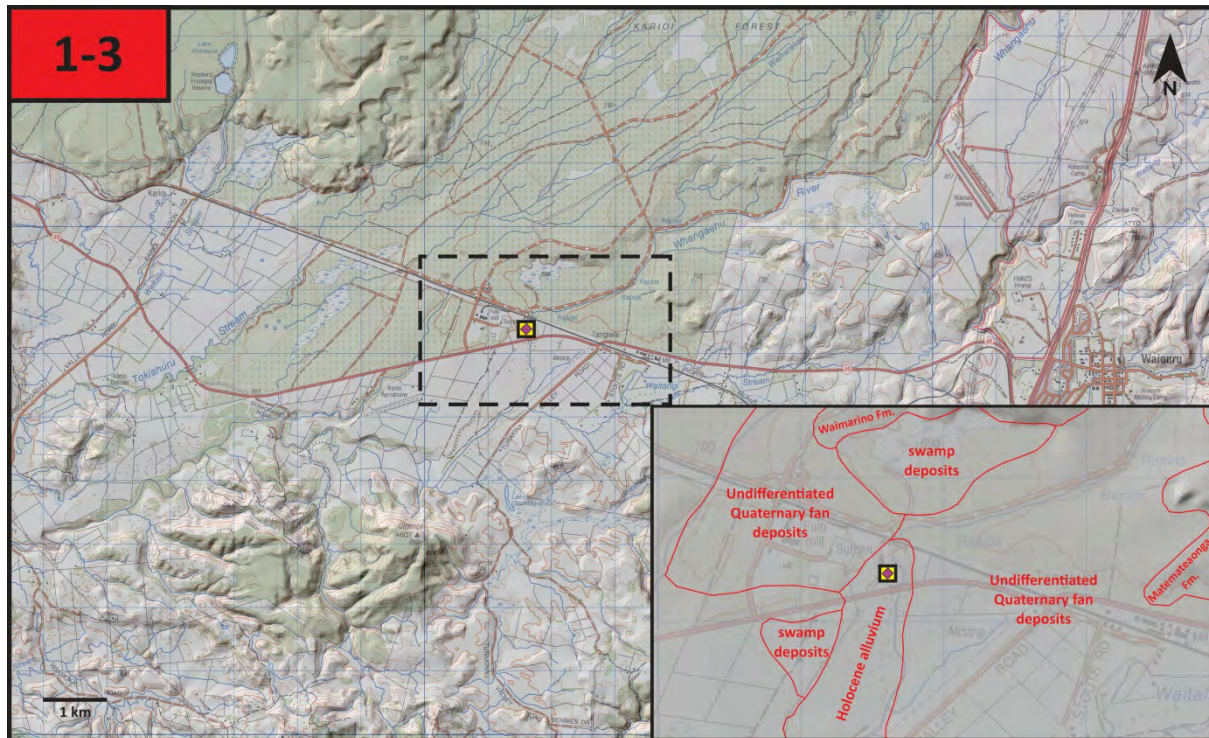
Donoghue, S.L., and Neall, V.E. (2001). Late Quaternary constructional history of the southeastern Ruapehu ring plain, New Zealand. *New Zealand Journal of Geology and Geophysics* 44: 439-466.

Gómez-Vasconcelos, M.G., Villamor, P., Cronin, S.J., Procter, J., Kereszturi, G., Palmer, A., Townsend, D., Leonard, G., Berryman, K., Ashraf, S. (2016). Earthquake history at the eastern boundary of the South Taupo Volcanic Zone, New Zealand. *New Zealand Journal of Geology and Geophysics*: 1-22.

Gómez-Vasconcelos, M.G., Villamor, P., Cronin, S.J., Procter, J.N., Palmer, A.S., Townsend, D., Leonard, G. (2017). Crustal Extension in the Tongariro Graben, New Zealand: Insights into Volcano-Tectonic Interactions and active Deformation in a young Continental Rift. *Geological Society of America Bulletin*, 129 (9-10): 1085-1099.

Procter, J.N., Cronin, S.J., Fuller, I.C., Sheridan, M.F., Neall, V.E., and Keys, H. (2010). Lahar hazard assessment using Titan2D for an alluvial fan with rapidly changing geomorphology: Whangaehu River, Mt. Ruapehu. *Geomorphology* 116: 162-174.

Stop 1-3 – Tangiwai Disaster Memorial and historic lahars of the Whangaehu River (Mt. Ruapehu)



The Whangaehu River drains westwards from Crater Lake at the summit of Ruapehu and then turns south and west around the margin of the Ruapehu ring plain. It is the principal drainage for lahars generated at the summit. Crater Lake is the ultimate source of water involved in lahar formation but Ruapehu also carries substantial snow and ice at high altitude. With substantial volumes of water stored at altitude on an unstable volcanic peak there is a continuous threat of lahars down streams draining from the mountain.

The rail bridge at Tangiwai, which is about 42 km downstream from the Crater Lake source, is the site of New Zealand's last volcanic disaster. 151 people on the overnight train from Auckland to Wellington were killed on Christmas Eve, 1953 when, just before the train arrived, the rail bridge was destroyed by a lahar generated when an ice barrier on the rim of Crater Lake collapsed.

In 1945 a significant eruptive episode of Mt Ruapehu excavated a 300 m deep crater. This filled with water so that by 1953 it was 8 m higher than the 1945 level. It was not generally understood that the upper part of the lake was only held back by a flimsy dam of ice and pyroclastic debris and at 8 p.m. on Christmas Eve 1953, the debris at the outlet of Crater Lake collapsed. The collapse generated a lahar with a volume of 340,000 cubic metres, which

swept down the Whangaehu River valley, bulking up with sand, silt and boulders as it went. It slammed into the concrete piers of the rail bridge at Tangiwai, knocking them out and causing the bridge to partially collapse. At 10.21 p.m. on Christmas Eve 1953, locomotive Ka 949 and its train of nine carriages and two vans plunged into the lahar-flooded Whangaehu River at 65 kph. All 5 second class carriages plunged into the river and four of the five were totally destroyed (Fig. 21). The locomotive driver had applied the emergency brakes some 200



Fig. 21. – Wreckage of train carriages after the 1953 Tangiwai disaster. Image from Galley et al (2004), *The Australasian Journal of Disaster and Trauma Studies*, ISSN: 1174-4707, Volume: 2004-1

metres from the bridge and this action meant that the last three carriages did not fall into the river, saving many lives. The leading first class carriage (Car Z) teetered on the edge before plunging into the river and rolling downstream. Amazingly 21 of the 22 passengers in the carriage survived. Some people had escaped and swam to the banks, but dozens drowned in the tangles of gorse there. Of the 285 passengers and crew on board, 151 died in what became New Zealand's worst railway accident.

On various stations along the main trunk line people waited in vain for loved ones who never arrived. In the days that followed, battered mud-soaked toys and teddy bears were strewn along the banks of the Whangaehu River downstream of Tangiwai.

The 1954 Board of Inquiry concluded that no one was to blame for the disaster and no person or organisation was prosecuted. As a result of the findings of the Board of Inquiry an early warning system was installed upstream on the Whangaehu River. It was a concrete pillar that had a series of lead electrodes up the sides. The acidic, conductive crater lake waters of any lahar outbreak would complete a circuit and trigger an alarm at Ohakune Railway Station. Massive changes to the ownership and management of NZ's railways in the period from 1987 meant that Ohakune became an unmanned station and there was no one to monitor the alarm system. More recently acoustic monitors have been installed on the mountain and these give a much earlier warning. The system was tested by the 2007 lahar breakout event and worked well.

Over the past 15 years, Ruapehu lahars have been intensively studied. During the 1995 eruption of Ruapehu, Crater Lake was emptied of water and over the period 18th September to 12th October 1995 twenty six lahars, with a total volume measured at $10 \times 10^6 \text{ m}^3$ descended the Whangaehu (Cronin et al., 1996, 1997). The 1995/1996 eruptions created an unstable barrier containing the waters of Crater Lake and this subsequently collapsed in 2007 generating the largest lahar (Figs. 2-3) observed in recent New Zealand history (Procter et al., 2010; Lube et al., 2012).

A highly sophisticated monitoring system is in now place along the Whangaehu River and this provides both an early warning function and data for very detailed study of lahar formation and evolution and the erosive effects of lahars on stream morphology (Cronin et al., 1997; Procter et al., 2010; Lube et al., 2012).

An interesting aspect of Ruapehu lahars is that Crater Lake water is highly acid; the pH is in the range 2 to 3. This attribute is useful in studying the behaviour of lahars from Ruapehu because it can be

used as a tracer to study the way in which lahars evolve as they move from source down the Whangaehu.

The Whangaehu River has been the main conduit of lahars from Mt. Ruapehu in the historic record. Lahars are mainly formed by eruptions through and collapses from the highly acidic Crater Lake at 2540 m above sea level. At Tangiwai as well as upstream and downstream, many lahars were observed and sampled during flow to derive new models of how lahars and streamflow interact and how lahars deposit and transport sediment in a conveyor belt like fashion (Fig. 22).

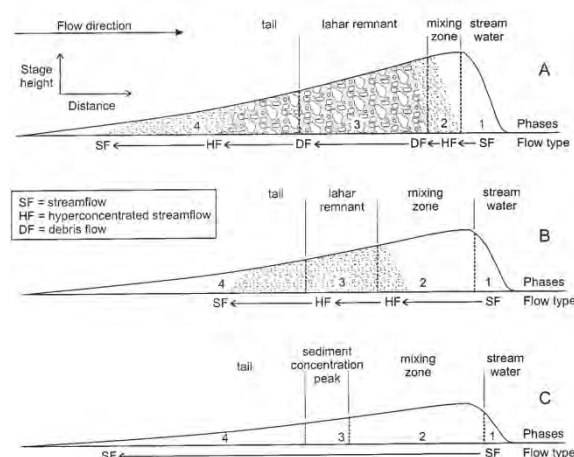


Fig. 22. – Conceptual model of the four phases within a channelized lahar wave and the changes that occur as the wave travels downstream based on the observations and measurements of the Ruapehu lahars. 1 and 2 represent the lahar wave at increasing distances from sources, and 3 represents the stream-flow surge resulting when the lahar has completely transformed.

The lahars of the historical record, including the 1953, 1975, 1995 and 2007 lahars were far smaller than past lahars over the last 2000 years, indicating that some of them must have involved spill of large portions of the Crater Lake of Ruapehu (Fig. 23).

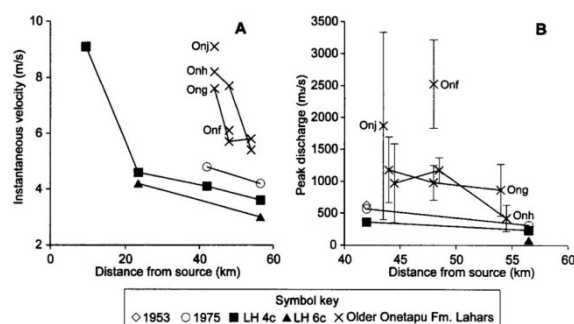


Fig. 23. – Comparison between the prehistoric Onetapu Formation lahars and those of 1953, 1975 and LH4c and LH6c from 1995 (from Cronin et al, 1997)

Suggested discussion points

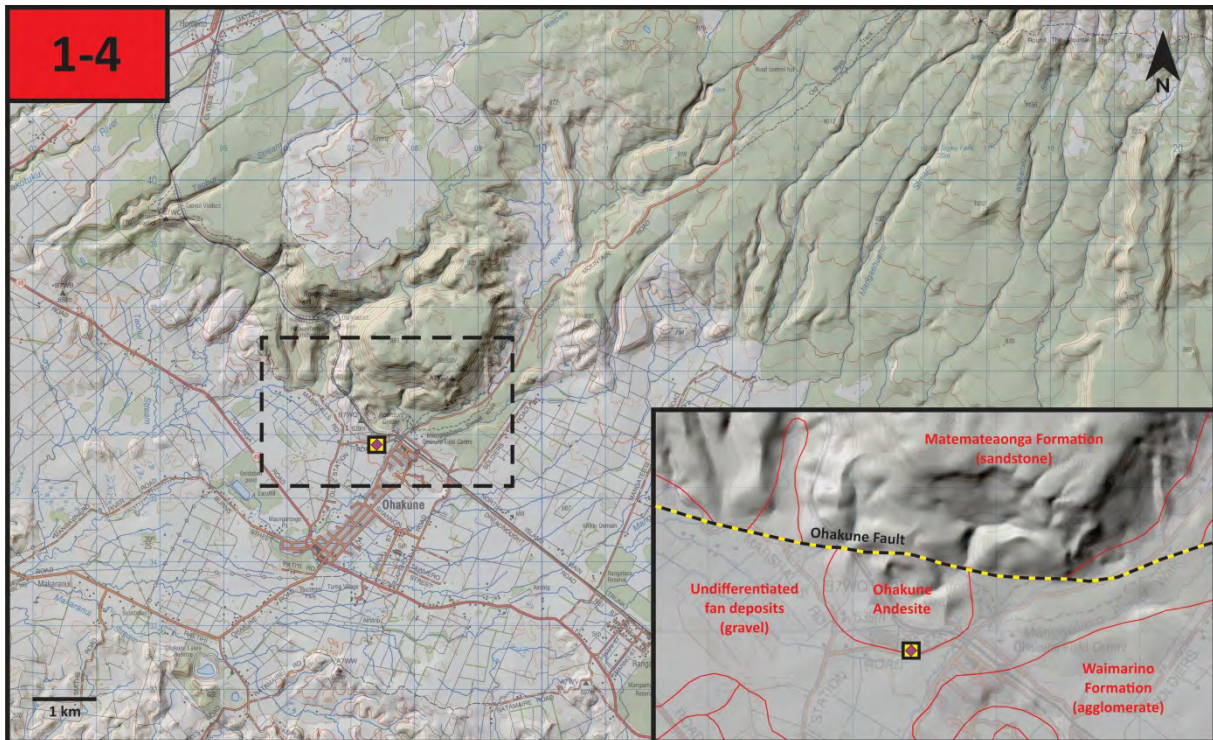
- 1) Discussion on fine scale lahar stratigraphy along an active stream valley
- 2) Preservation potential of thin medial lahar facies along an active stream valley
- 3) Bulking and debulking processes
- 4) Link between channel and overbank facies of laharic deposits
- 5) Discussion on landscape modifying elements of major lahar events
- 6) Discussion on the role of sediment input by lahars to a terrestrial sedimentary system

Further reading

Cronin, S.J., Neall, V.E., Lecointre, J.A. and Palmer, A.S., (1997). Changes in Whangaehu River lahar

- characteristics during the 1995 eruption sequence, Ruapehu volcano, New Zealand. *Journal of Volcanology and Geothermal Research*, 76: 47-61.
- Cronin, S.J., Hodgson, K.A., Neall, V.E., Palmer, A.S., Lecointre, J.A. (1997). 1995 Ruapehu lahars in relation to the late Holocene lahars of Whangaehu River, New Zealand. *NZ Journal of Geology and Geophysics* 40: 507-520.
- Cronin, S.J., Neall, V.E., Lecointre, J.A. and Palmer, A.S., (1999) Dynamic interactions between lahars and stream flow: a case study from Ruapehu volcano, New Zealand. *Geological Society of America Bulletin* 111: 28-38.
- Lecointre, J., Hodgson, K., Neall, V., Cronin, S. (2004). Lahar-triggering mechanisms and hazard at Ruapehu volcano, New Zealand. *Natural Hazards* 31: 85-109.
- Lube, G., Cronin, S.J., Manville, V., Procter, J.N, Cole, S.E & Freundt, A. (2012). Energy growth in laharic mass flows. *Geology* 40, 475-478.
- Procter, J., Cronin, S.J., Fuller, I.C., Lube, G. & Manville, V. (2010). Quantifying the geomorphic impacts of a lake-breakout lahar, Mount Ruapehu, New Zealand. *Geology* 38, 67-70.

Stop 1-4 – Ohakune Volcanic Complex (Mt. Ruapehu)



The history and new results of the investigation of the **Ohakune Volcanic Complex (OhVC)** showed that exposure changes by quarrying can influence dramatically the interpretation of the volcanic history of a single monogenetic volcano (Houghton and Hackett, 1984; Kósik et al., 2016). At the OhVC, the exposed pyroclastic sequence along the quarry walls displays lateral changes of properties of pyroclastic beds accumulated perpendicular and parallel to the main pyroclastic transport direction. The sedimentological features of the pyroclastic beds show the spatial and temporal variations of the activity and illustrate the common unpredictable nature of small-volume volcanism in terms of migration of the eruption locus changes to the corresponding eruption styles.

The OhVC, also known as Ohakune or Rochfort Crater is a late Pleistocene (~35 ka) tuff ring – scoria/spatter cone complex located S-SW of Ruapehu volcano (Fig. 15). This monogenetic or small-volume volcano consists of an outer E-W elongated compound tuff ring edifice, three inner scoria-spatter cones and further volcanic depressions, located on the Ohakune Fault (Fig. 24). The surrounding county rocks are mostly reworked volcanoclastic sediments of Mt. Ruapehu and andesitic to rhyolitic fallout tephra from various sources. Pliocene marine sediments (mostly siltstones and sandstones of the Matemateaonga Formation) underlie the volcanic edifice and

volcanoclastic series, and occasionally crop out as uplifted fault-bounded blocks. The eruptions started in a flat or slightly sloping laharic depositional environment within the unconsolidated reworked volcanoclastic sediments of the 60–15 ka Mangawhero Formation

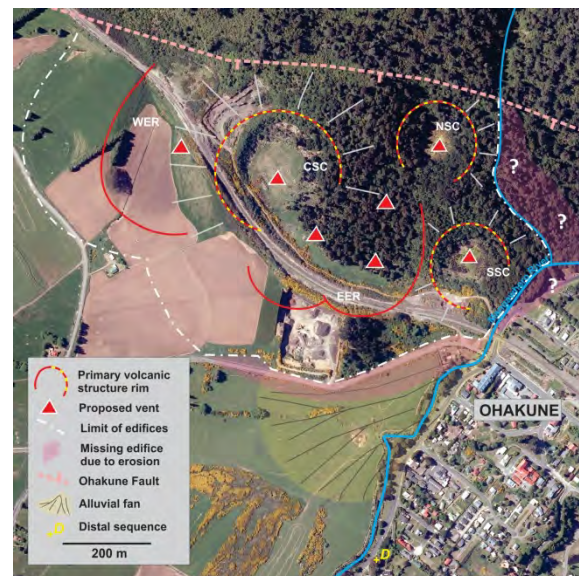


Fig. 24 – Aerial photograph of OVC with its proposed architecture. The main edifices are labeled; West ejecta ring (WER), East ejecta ring (EER), Central scoria cone (CSC), South scoria cone (SSC), North scoria cone (NSC).

The volcanic activity of OhVC initiated with shallow-seated hydrovolcanic eruptions along an at least 600 m eruptive fissure characterized by an almost continuous generation of a low eruptive column, accompanied by wet pyroclastic density currents, together with the ejection of fusiform and cauliflower-shaped juvenile fragments and accidental lithics from the surrounding country rocks (Ab_C beds, fig. 25). Subsequent activity was dominated by a variety of Strombolian eruptions exhibiting differing intensities that were at times disrupted by phreatomagmatic explosions due to the interaction with external water and/or sudden changes in magma discharge rate. At least three major vent-shifting events occurred during the formation of compound tuff ring, which is demonstrated by the truncation of the initial tuff ring and the infilling of the truncated area by several coarse grained surge units (Fig. 25).

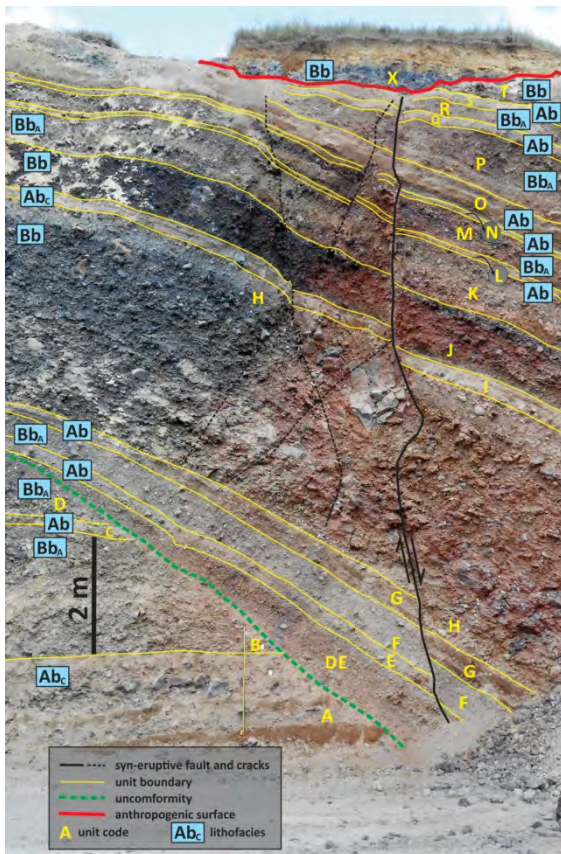


Fig.25 – Stratigraphic sequence of the proximal part of EER at the northwest corner of the quarry. This is one of the locations exhibits the opening of a new vent. Note the oxidation pattern of right hand side of the fault also indicating the vicinity of the vent area.

The frequent vent shifting prevented the long term development of a single edifice. Rather, the products were accumulated at the southern margin of the fissure, forming a multisource ejecta ring structure (EER). This was constructed from Strombolian

bomb beds (Bb , Bb_A beds, fig. 25) alternating with dense and wet pyroclastic surge and fallout deposits (Ab lithofacies). The deposited pyroclasts within the fissure zone were removed by subsequent eruptions leaving a hollow, the smaller pits indicating the area where the dyke intersected the surface.

The late stage evolution was characterized by localization of more stable vents producing Strombolian/Hawaiian fountains due to higher ascent rates and decreased water influence, however the axis of the fissure remained unburied indicating the existence of vent-clearing phreatomagmatic blasts along the other part of the fissure.

Microtexture analysis of beds revealed that the ash fragments from Bb_A beds show identical features with fragments from the ash beds interpreted as having phreatomagmatic origin. Moreover, the examined vesicle microtexture properties of the largest clasts from the Strombolian beds do not exhibit the typical micro-textural characteristics of Strombolian fragments (Fig. 26). The size and shape of their vesicles, as well as the vesicle number density values might reflect an increased degree of cooling and higher viscosities, and interpreted as a result of the influence of magma-water interaction. It seems that throughout the course of the activity water was abundant, which implies the eruptions were unable to permanently dry out the shallow basement.

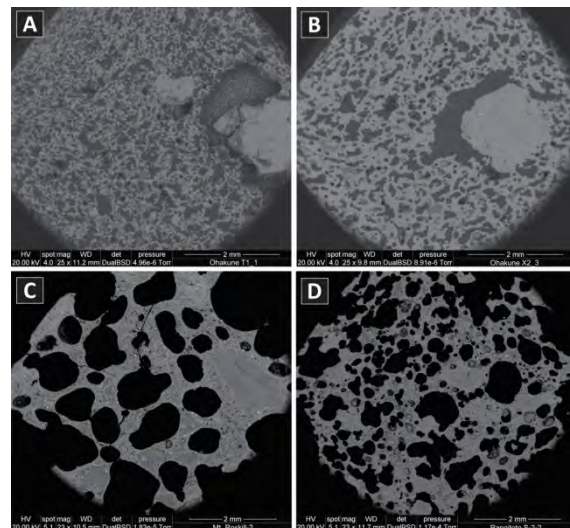


Fig. 26 – SEM images of bombs/blocks (A–B) from OhVC and SEM images of scoria fragments from Mt. Roskill (C) and Rangitoto (D), Auckland Volcanic Field (AVF) for comparison. The two samples from AVF exhibit a Hawaiian and Strombolian (or Violent Strombolian)-style eruptions as the vesicles show mostly spherical or sub-spherical shapes. In contrast, the OhVC samples exhibits completely different textures and are similar to basaltic Plinian eruptions.

Since the activity of OhVC the majority of distal sequences were eroded or buried. The only preserved distal sequence comprises a 1.8-thick

sequence that is situated about 600 m south of the OhVC along a low ridge on the left side of Mangawhero River. The deeply cut channel that separated it from the edifice of OhVC is occupied by an alluvial fan (Fig. 24).

Suggested discussion points

- 1) Preservation potential of phreatomagmatic deposits along the fissure
- 2) The importance of high-resolution geomorphologic mapping in revealing volcanic architecture
- 3) Difficulty of geological mapping in small-volume volcanoes
- 4) Role of phreatomagmatism
- 5) Discussion on linking small volume volcanoes and polygenetic central volcanoes
- 6) Discussion on the interaction between small-volume volcanoes and the sedimentary environment

Further reading

Deering, C., Bachmann, O., Dufek, J. and Gravley, D., 2011. Rift-related transition from andesite to rhyolite volcanism in the Taupo Volcanic Zone (New Zealand) controlled by crystal–melt dynamics in mush zones

with variable mineral assemblages. *Journal of Petrology*, 52(11): 2243-2263.

Hackett, W.R. and Houghton, B.F., 1989. A facies model for a Quaternary andesitic composite volcano: Ruapehu, New Zealand. *Bulletin of volcanology*, 51(1): 51-68.

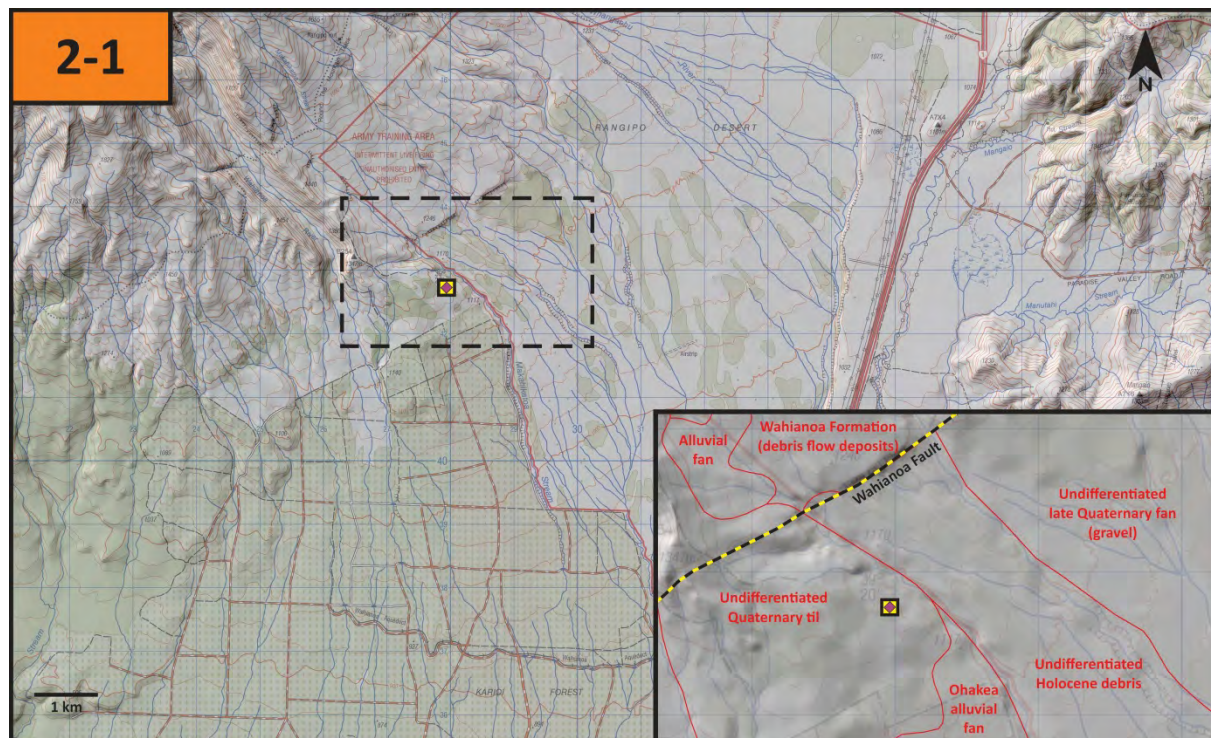
Houghton, B.F. and Hackett, W.R., 1984. Strombolian and phreatomagmatic deposits of Ohakune Craters, Ruapehu, New Zealand: a complex interaction between external water and rising basaltic magma. *Journal of Volcanology and Geothermal Research*, 21(3-4): 207-231.

Kószik, S., Németh, K., Kereszturi, G., Procter, J., Zellmer, G. and Geshi, N., 2016b. Phreatomagmatic and water-influenced Strombolian eruptions of a small-volume parasitic cone complex on the southern ringplain of Mt. Ruapehu, New Zealand: Facies architecture and eruption mechanisms of the Ohakune Volcanic Complex controlled by an unstable fissure eruption. *Journal of Volcanology and Geothermal Research*, 327: 99-115.

Price, R.C., Gamble, J.A., Smith, I.E., Maas, R., Waight, T., Stewart, R.B. and Woodhead, J., 2012. The anatomy of an Andesite volcano: a time–stratigraphic study of andesite petrogenesis and crustal evolution at Ruapehu Volcano, New Zealand. *Journal of Petrology*: egs050.

Townsend, D., Leonard, G.S., Conway, C., Eaves, S.R. and Wilson, C.J.N., 2017. *Geology of the Tongariro National Park area, scale 1:60,000*, GNS Science geological map 4. 1 sheet + 109 p. GNS Science.

Stop 2-1 – Tufa Trig Formation (Mt. Ruapehu)



This location at the northern end of the Karioi Forest (Fig. 15) is the type location of the Ruapehu-sourced Tufa Trig Formation (232 AD–present, Donoghue et al. (1995b); Donoghue et al. (1997b); (Lowe et al., 2013)). Seventeen members (Tf2 to Tf18) are defined here (Fig. 27), overlying the rhyolitic Taupo Pumice or a characteristically bright Taupo-formed soil (Donoghue et al., 1995b; Donoghue et al., 1997b). At this location, native beech vegetation favours good tephra preservation, contrasting to the preservation conditions in Ruapehu’s ring plain, where the most recent tephras are restricted to isolated vegetated pedestals in the Rangipo Desert. Tephra preservation and the completeness of the most recent eruptive record are therefore highly dependent upon pedestal age, stability and the presence or absence of vegetation at time of deposition.

The members appear as discrete tephra layers, interbedded with aeolian Makahikatoa Sands partially altered by soil development (Donoghue et al., 1995b). The stratigraphically lower Makahikatoa Sands contain often reworked material from the underlying Taupo Pumice, while the upper interbedding units contain reworked Ruapehu ash (Purves, 1990; Donoghue et al., 1997b).

The restricted thickness (mm to few cm, often pocketing) and lack of unique features of the individual tephra members makes correlation between locations and an unequivocal identification

often very challenging (Donoghue et al., 1995b).

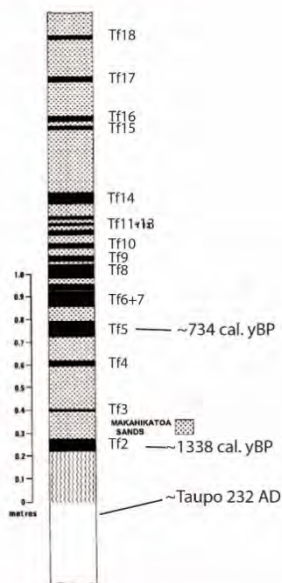


Fig. 27 – Stratigraphic overview over tephra members, defined at the type location. Mod. after Donoghue et al 1997.

Recent detailed studies have shown that the Tufa Trig tephra members can be grouped according to predominant macroscopic sedimentological characteristics, such as grain size, componentry and internal successions (Fig. 28). The combination of these characteristics with further studies on clast morphology, tephra distribution and geochemistry provides a useful tool for tephra correlation, aiding to reconstruct eruption dynamics and mechanisms.

Furthermore, the detailed characterisation of contacts between individual depositional units provides constraints on the time scales involved during the eruption. This results in a more complex record for the past ~1800 yrs, then previously assumed, with important implications for the understanding of existing frequency-magnitude patterns at Mt. Ruapehu.



Fig. 28 – The Ruapehu-sourced Tufa Trig Formation is characterised by different eruption styles. The three main related deposits are shown here; a) single-stage ash unit, b) multi-stage ash sequence and c) pumiceous unit.

This stop provides the opportunity to investigate and to discuss different approaches to decipher the tephrostratigraphy of complex andesitic system.

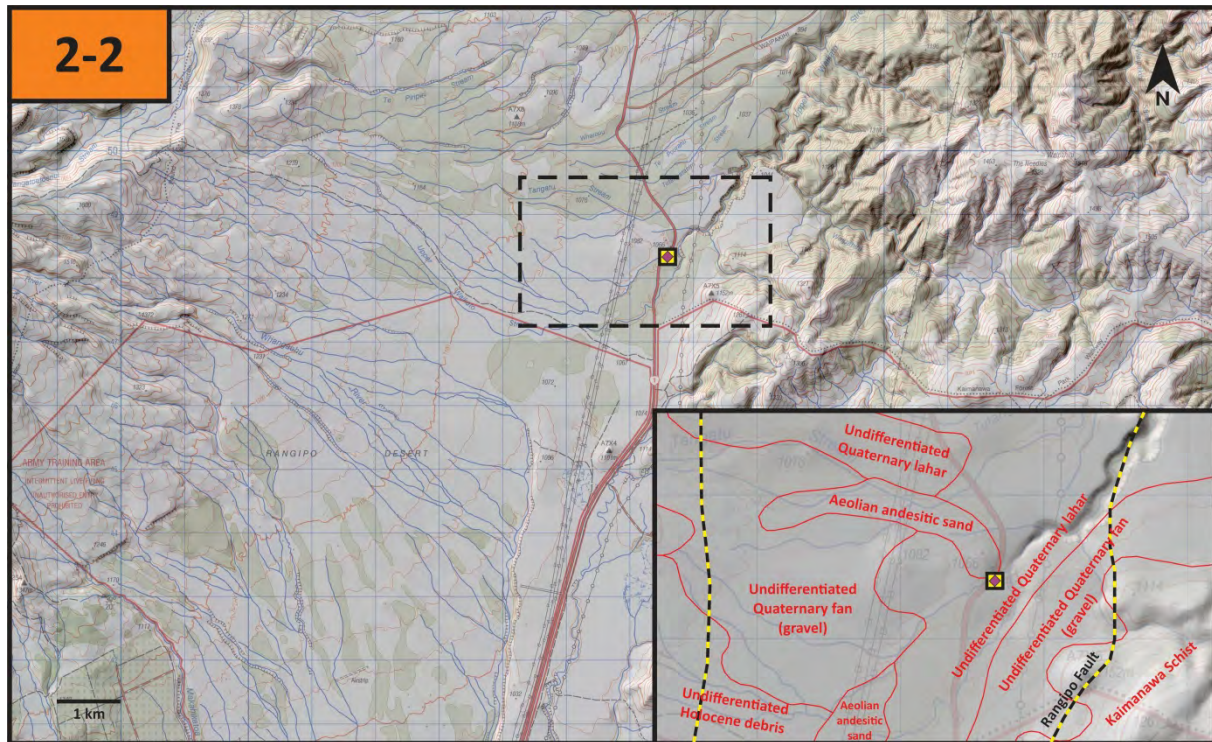
Suggested discussion points

- 1) How can the existing terminology from observed eruptions sequences (e.g., stage vs. event vs. episode from Jenkins et al. (2007)) be applied to geologically preserved tephra deposits?
- 2) How different is the field approach of tephrostratigraphic studies applied to ash-rich small volume andesitic deposits, compared to large volume rhyolitic deposits?
- 3) How important is the influence of the depositional environment on the preservation potential of small volume ash-rich tephtras and how reliable are the measured thicknesses for the reconstruction of eruptive processes?
- 4) How can non-eruptive features such as mm-thick oxidation horizons be used to provide constraints on eruption time scales?
- 5) What is the approach to create a “perfectly” realistic frequency-magnitude record that accounts for small volume eruptions?

Further reading

- Donoghue, S. L., Neall, V. E., and Palmer, A. S. (1995). Stratigraphy and chronology of late Quaternary andesitic tephra deposits, Tongariro Volcanic Centre, New Zealand. *Journal of the Royal Society of New Zealand*, 25(2), 115-206.
- Donoghue, S. L., Neall, V. E., Palmer, A. S., & Stewart, R. B. (1997). The volcanic history of Ruapehu during the past 2 millenia based on the record of Tufa Trig tephtras. *Bulletin of Volcanology*, 59, 136-146.
- Jenkins, S. F., Magill, C. R., and McAneney, K. J. (2007). Multi-stage volcanic events: A statistical investigation. *Journal of Volcanology and Geothermal Research*, 161(4), 275-288.
- Lowe, D. J., Blaauw, M., Hogg, A. G., and Newnham, R. M. (2013). Ages of 24 widespread tephtras erupted since 30,000 years ago in New Zealand, with re-evaluation of the timing and palaeoclimatic implications of the Lateglacial cool episode recorded at Kaipo bog. *Quaternary Science Reviews*, 74, 170-194.
- Purves, A. (1990). Landscape ecology of the Rangipo Desert. Unpublished M. Sc. thesis, lodged in the Library, Massey University, Palmerston North, New Zealand.

Stop 2-2 – A 60 ky slice through the ring plain (Waikato Stream site); sedimentation in relation to volcanic activity and the last glaciation



Continuous exposures along the Upper Waikato Stream (Fig. 15) provide new insights into the north-eastern ring plain of Ruapehu volcano, extending the known stratigraphy beyond 22.6 ka. Time control in the sequence is provided by five rhyolitic tephra units, erupted from central North Island volcanoes, comprising Kawakawa, Okaia, Omataroa, Hauparu, and Rotoehu tephras (e.g. Froggatt and Lowe, 1990; Danišik et al., 2012; Vandergoes et al., 2013). The sequence is dominated volumetrically by diamictons and fluvial deposits resulting both from volcanic events and periods of instability on the flanks of Ruapehu. Within the sequence are > 60 individual andesitic lapilli units, derived primarily from Ruapehu volcano via mostly sub-Plinian eruption mechanisms. An average eruption rate of more than one lapilli eruption per 1000 years is estimated for the ca. 60 ka record (Fig. 29). The style of deposition on the ring plain changes over time and appears to reflect climate change over the Last Glacial period. In periods of severe climatic conditions during marine 81So Stage 4 (Porewan stadial), and the Last Glacial Maximum of marine delta-18 Oxygen Isotope Stage 2 (Ohakean), the north-eastern ring plain aggraded rapidly with deposition of thick continuous diamicton sequences. The other recognized cool period in the southern North Island, the stadial of late delta-18 Oxygen Isotope Stage 3 (Ratan), did not appear to induce

major aggradation on the north-eastern ring plain. During periods of mild climate within the Last Glacial, deposition on the north-eastern ring plain was dominated by fall accession of either tephra or material reworked from other parts of the ring plain by aeolian processes (Cronin et al., 1996a-b).

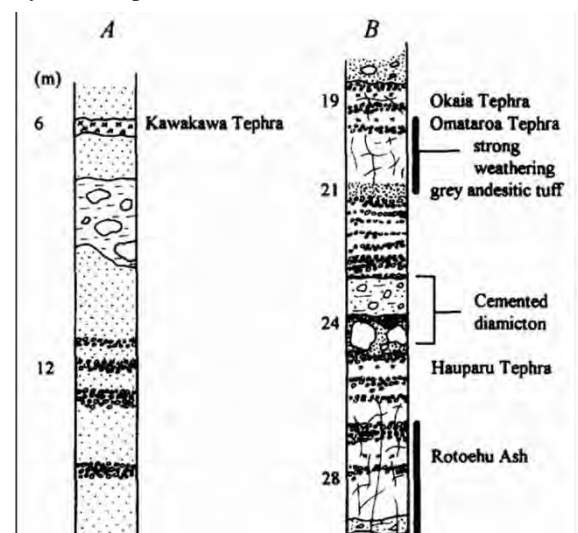


Fig. 29 – Geological history of the north-eastern ring plain of Ruapehu volcano; composite stratigraphic columns of the north-eastern sequence below the regional marker horizon of the Kawakawa/Oruanui tephra Formation (Cronin et al., 1997)

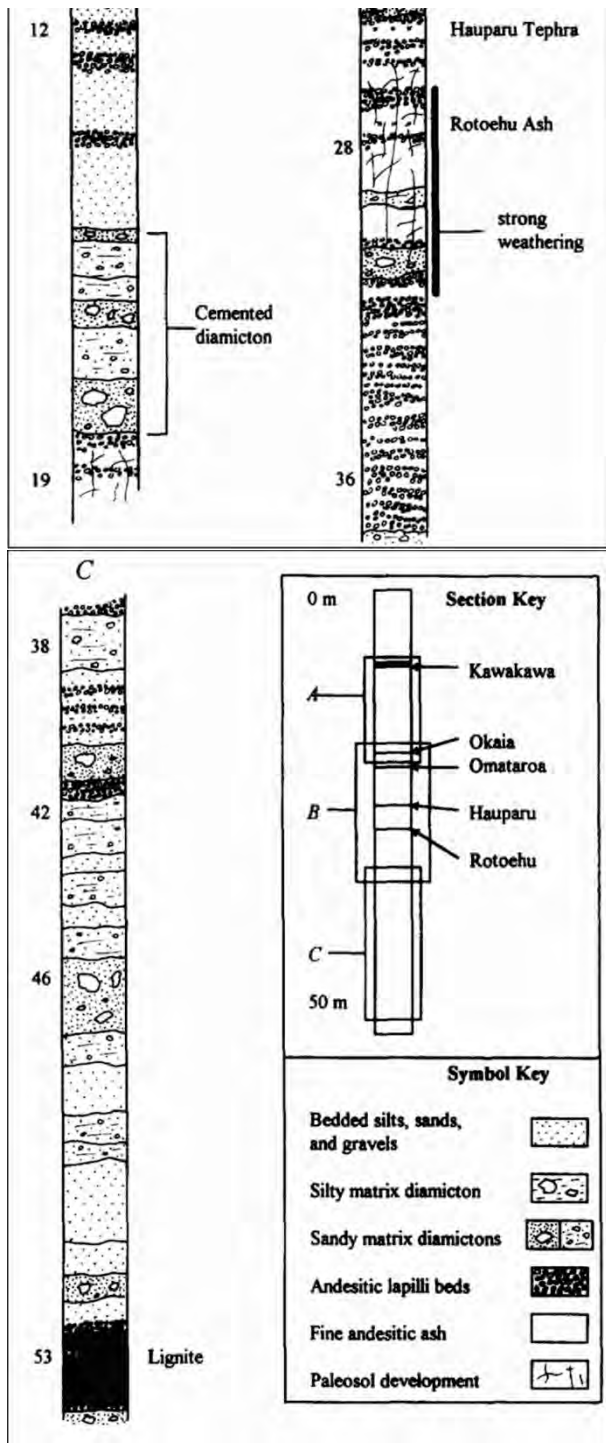


Fig. 29 – Continued

Suggested discussion points

1) How can we use tephrostratigraphy in geological mapping of volcanoes and volcanic terrains

- 2) How can we apply tephrostratigraphy in geological mapping in ancient volcanic terrains; time – scale – scope problem
- 3) How can we link tephra layers and lava flows into a stratigraphy framework that is useful, practical and representative for the volcanic processes contributed to the edifice growth
- 4) What influence the paleoclimate has on the formation of tephra accumulating on the ring plain
- 5) The role of aggradation, river incision and style of pyroclast transport on formation of the pyroclastic assemblages around the volcanoes
- 6) The difficulty of multi-sourced tephra forming a ring plain between edifices; how such succession fit into a conventional stratigraphy framework.

Further reading

Cronin, S.J., Neall, V.E. and Palmer A.S. (1996a). The geological history of the north-eastern ring plain of Ruapehu Volcano, New Zealand. *Quaternary International* 34-36: 21-28.

Cronin, S.J., Neall, V.E. and Palmer, A.S., (1996b). Investigation of an aggrading paleosol developed into andesitic ring plain deposits, Ruapehu volcano, New Zealand. *Geoderma* 69: 119-135.

Cronin, S.J. and Neall, V.E., (1997). A Late Quaternary stratigraphic framework for the northeastern Ruapehu and eastern Tongariro ring plains, New Zealand. *NZ Journal of Geology and Geophysics* 40: 185-197.

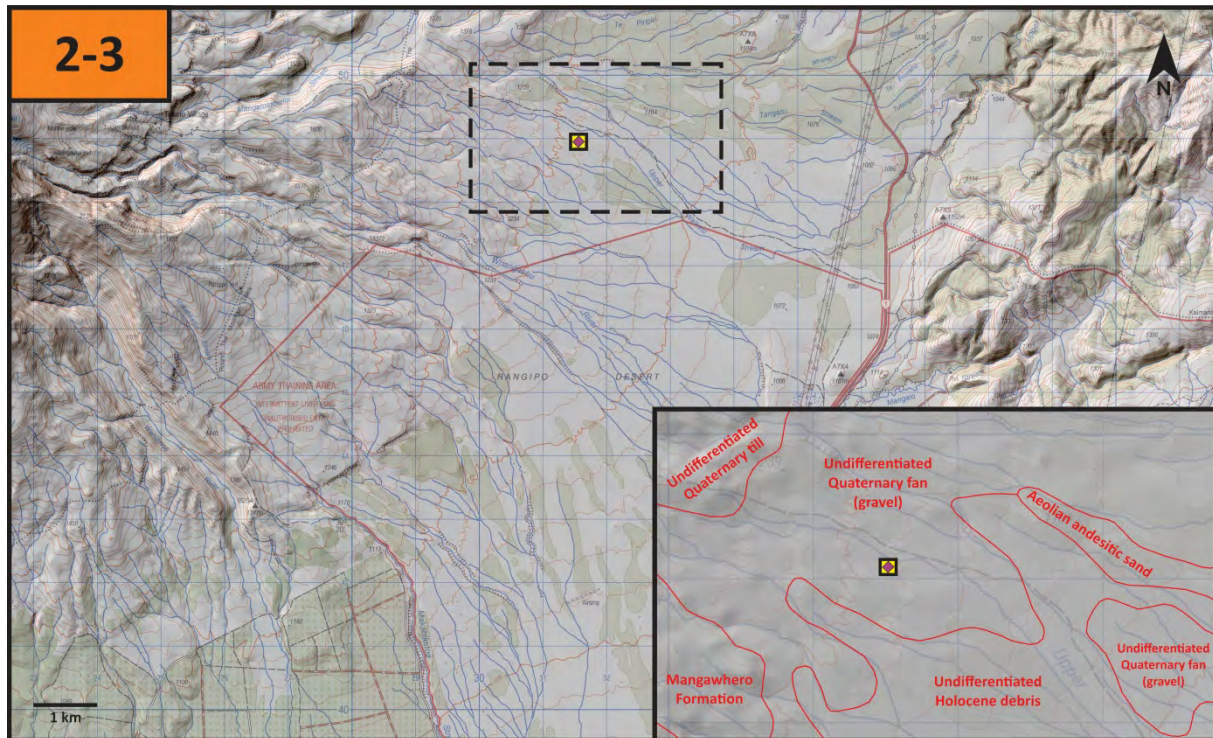
Danišik, M., Shane, P., Schmitt, A.K., Hogg, A., Santos, G.M., Storm, S., Evans, N.J., Fifield, L.K. and Lindsay, J.M., (2012). Re-anchoring the late Pleistocene tephrochronology of New Zealand based on concordant radiocarbon ages and combined ²³⁸U/²³⁰Th disequilibrium and (U–Th)/He zircon ages. *Earth and Planetary Science Letters*, 349: 240-250.

Froggatt, P.C. and Lowe, D.J.. (1990). A review of late Quaternary silicic and some other tephra formations from New Zealand: Their stratigraphy, nomenclature, distribution, volume, and age. *New Zealand Journal of Geology and Geophysics* 33(1): 89-109.

Townsend, D., Leonard, G.S., Conway, C., Eaves, S.R. and Wilson, C.J.N., 2017. *Geology of the Tongariro National Park area, scale 1:60,000*, GNS Science geological map 4. 1 sheet + 109 p. GNS Science.

Vandergoes, M.J., Hogg, A.G., Lowe, D.J., Newnham, R.M., Denton, G.H., Southon, J., Barrell, D.J.A., Wilson, C.J.N., McGlone, M.S., Allan, A.S.R., Almond, P.C., Petchey, F., Dabell, K., Dieffenbacher-Krall, A.C. and Blaauw, M. (2013). A revised age for the Kawakawa/Oruanui tephra, a key marker for the Last Glacial Maximum in New Zealand. *Quaternary Science Reviews*, 74: 195-201.

Stop 2-3 – Bullock Formation type section – major explosive period at Mt. Ruapehu



This eruptive sequence is the latter part of a semi-continuous period of explosive volcanism at Ruapehu that persisted from approximately 40 ka up till ~10 ka B.P. At this point a major collapse from the Northwestern volcano caused a debris avalanche (Murimotu Formation), and shifted subsequent activity into effusive lava flow production on the NW flanks (Whakapapa Formation).

Pardo (2012, 2014) identified several eruption styles (Figs. 30-31) from highly detailed studies of the pumice textures and grain size properties, along with micro-scale sedimentology examination between 27 and 11 cal. ka BP, a transition is observed in Plinian eruptions at Mt. Ruapehu, indicating evolution from non-collapsing (steady and oscillatory) eruption columns to partially collapsing columns (both wet and dry). All eruptions involve andesite to basaltic andesite magmas containing plagioclase, clinopyroxene, orthopyroxene and magnetite phenocrysts. Differences occur in the dominant pumice texture, the degree of bulk chemistry and textural variability, the average microcrystallinity and the composition of groundmass glass. Pumice textures were classified into six types (foamy, sheared, fibrous, micro-vesicular, micro-sheared and dense) according to the vesicle content, size and shape and microlite content. Bulk porosities vary from 19 to 95 % among all textural types. Melt referenced vesicle number density ranges between

1.8×10^2 and $8.9 \times 10^2 \text{ mm}^{-3}$, except in fibrous textures, where it spans from 0.3×10^2 to $53 \times 10^2 \text{ mm}^{-3}$. Vesicle-free magnetite number density

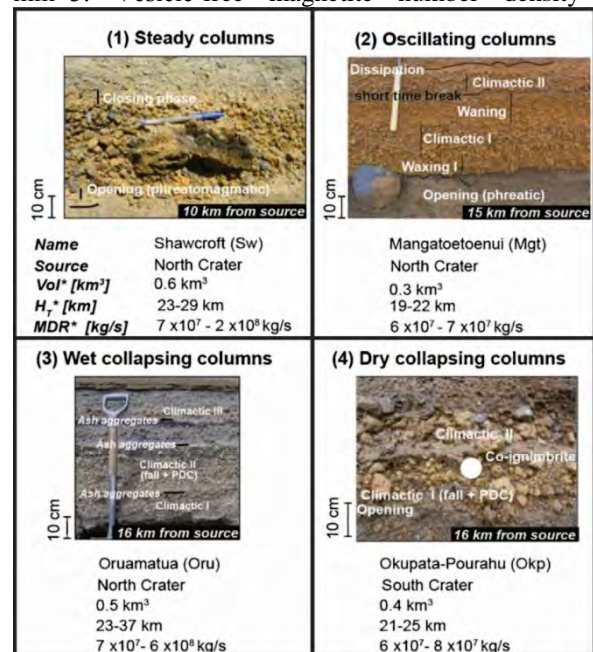


Fig. 30 – Four types of eruption sequences in the Plinian style eruptions that formed the Bullock Formation of Mt. Ruapehu (Pardo et al., 2014).

varies within an order of magnitude from 0.4×10^2 to $4.5 \times 10^2 \text{ mm}^{-3}$ in samples with dacitic groundmass

glass and between 0.0 and $2.3 \times 10^2 \text{ mm}^{-3}$ in samples with rhyolitic groundmass. The data indicate that columns that collapsed to produce pyroclastic flows contained pumice with the greatest variation in bulk composition (which overlaps with but extends to slightly more silicic compositions than other eruptive products); textures indicating heterogeneous bubble nucleation, progressively more complex growth history and shear-localization; and the highest degrees of microlite crystallization, most evolved melt compositions and lowest relative temperatures. These findings suggest that collapsing columns in Ruapehu have been produced when strain localization is prominent, early bubble nucleation occurs and variation in decompression rate across the conduit is greatest. This study shows that examination of pumice from steady phases that precede column collapse may be used to predict subsequent column behavior.

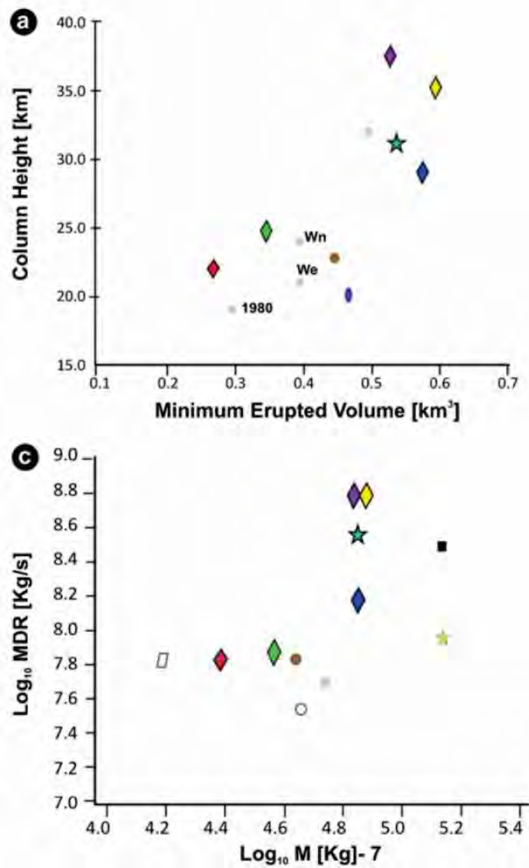
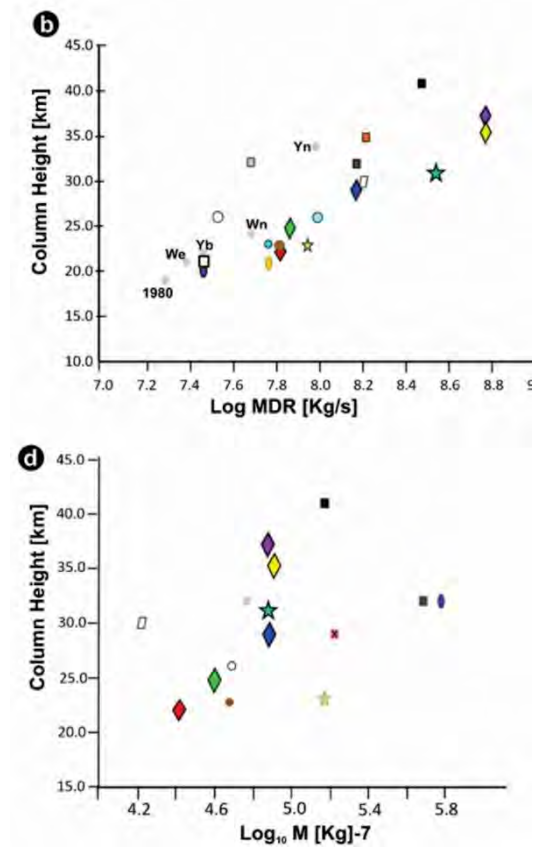


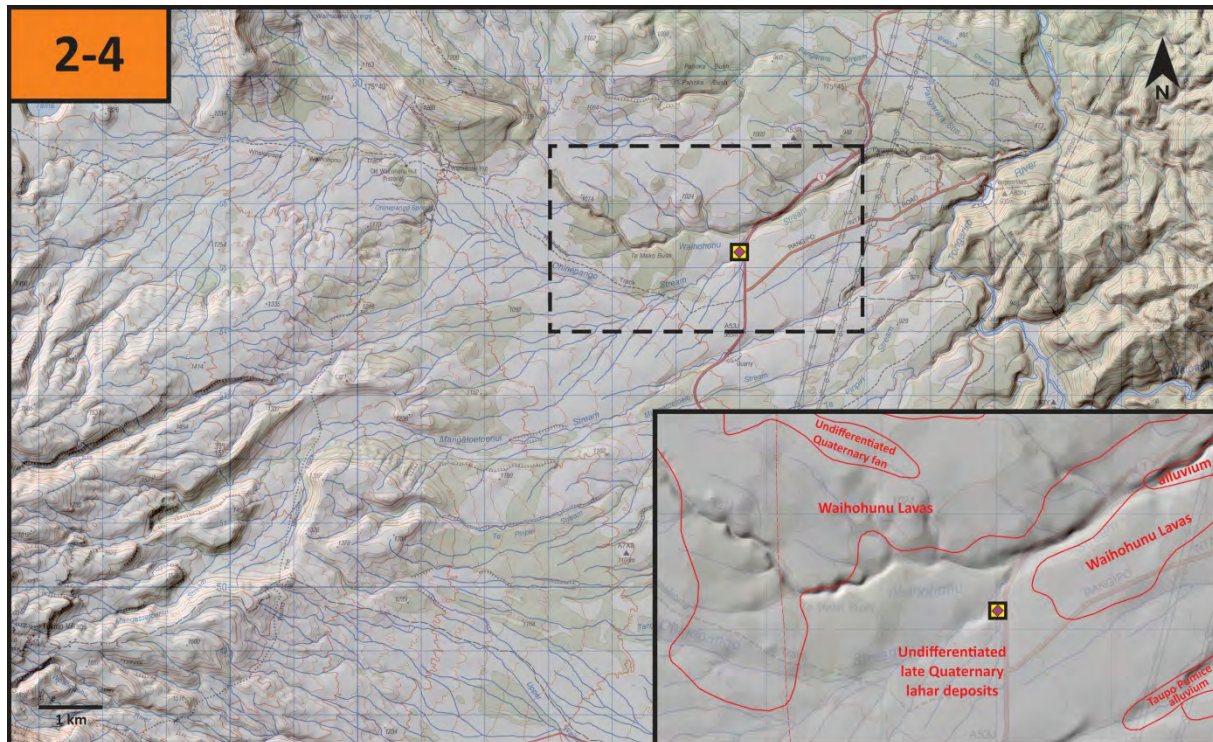
Fig. 31 – Comparison of eruptive parameters with other published for Plinian eruptions at andesitic volcanoes worldwide. Our data indicate: **a** increasing column height with erupted volume as obtained from the whole deposit of each unit and **b** with MRD; **c-d** eruptive intensity (MRD) and column height vs. magnitude ($M = \text{Log}(\text{mass of the deposit in kilograms}) - 7$), with higher intensities (**c**) and column heights (**d**) reached at larger magnitudes



Further reading

Pardo N., Cronin, S.J., Palmer, A.S., Procter, J., Smith, I.E.M., 2012: Andesitic plinian eruptions at Mt Ruapehu: quantifying the uppermost limits of eruptive parameters. *Bulletin of Volcanology* 74: 1161-1185.
 Pardo, N., Cronin, S.J., Palmer, A.S., Nemeth, K., 2012: Reconstructing the largest explosive eruptions of Mt. Ruapehu, New Zealand: lithostratigraphic tools to understand subplinian-plinian eruptions at andesitic volcanoes. *Bulletin of Volcanology* 74: 617-640.
 Pardo, N., Cronin, S.J., Wright, H.M.N., Schipper, C.I., Smith, I.E.M., Stewart, R.B., 2014: Pyroclast textural variation as an indicator of eruption column steadiness in andesitic Plinian eruptions at Mt. Ruapehu. *Bulletin of Volcanology* 76(5): 822.

Stop 2-4 – Waihohonu – Tongariro tephras – a sudden onset of Tongariro eruptions as Ruapehu changed eruption style



The Tongariro Volcanic Complex is an atypical stratovolcano in being centered on an active graben. Extension has hindered formation of a central vent structure and up to seven different vents were active over the last 20 ka B.P., spanning a 13 km-long N-S axis. The eruptive history shows a highly irregular, sporadic occurrence of events with frequent clusters small-scale eruptions of $<0.01 \text{ km}^3$, and rare large eruptions ($0.5\text{-}1 \text{ km}^3$). Six such large eruptions occurred within a ~ 200 yr-long period. This short interval of highly explosive events is unusual in the context of this and similar stratovolcanoes. Here we document new field mapping of pyroclastic deposits (Figs. 32-33) and analysis to identify their eruptive vent areas, eruption column heights and to characterize the range of their explosive eruption styles. Sustained eruption columns characterize the climactic phase of five of the studied eruptions. Two of these most likely produced sub-Plinian to Plinian eruption columns coeval from different vent areas or focal points along an eruptive fissure. One eruption is characterized by pulsating and collapse producing large-scale pyroclastic density currents. Eruption columns ranged between 15 and 22 km in height and erupted volumes of 0.5 to 1.8 km^3 with mass eruption rates of $3 - 7 \times 10^7 \text{ kg/s}$, indicating magnitudes of 4.8 to 5.2. The ~ 200 year paroxysm from Mt. Tongariro began with eruptions in the central and northern parts of the volcanic complex,

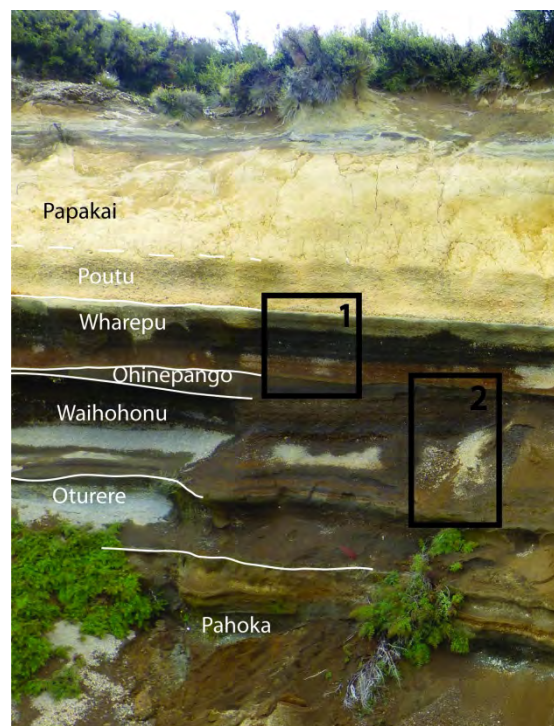


Fig. 32 – Eruptive sequence sourced from different vents of the Tongariro Volcanic Complex

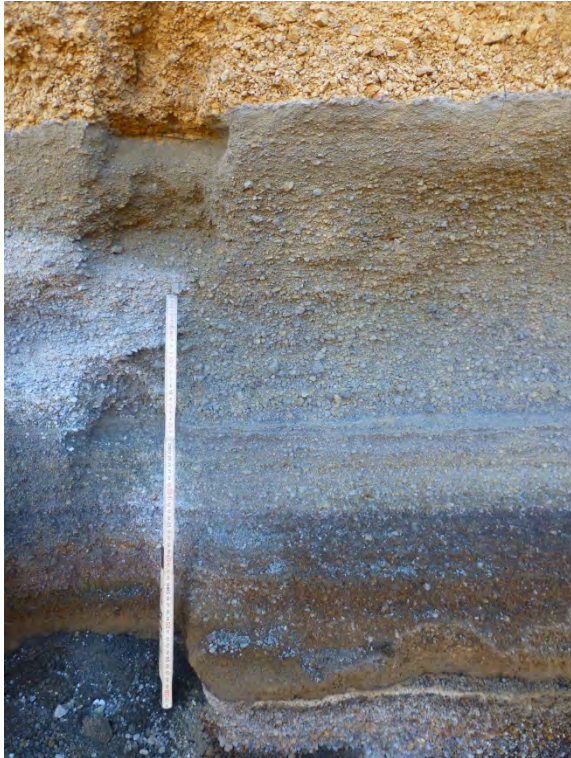


Fig. 33. – Area 1 on Fig. 1 indicates grain size and structural properties of Poutu, Wharepu and Ohinepango tephra.

and these continued to erupt through the period, at time contemporary with later events from the south. Vents in the central and northern complex were most active during the last and largest eruptive phase, which must have lasted several days to produce distinct tephra lobes distributed in four axes, spanning a near 360 degrees range (Fig. 34). This study highlights that extreme hazard scenario of successive large scale eruptions are possible at this and similar volcanoes and also shows how diverse eruptive scenarios may occur from different vent areas or fissures along a single volcanic complex including contemporaneous activity of two or more areas along an extended fissure system.

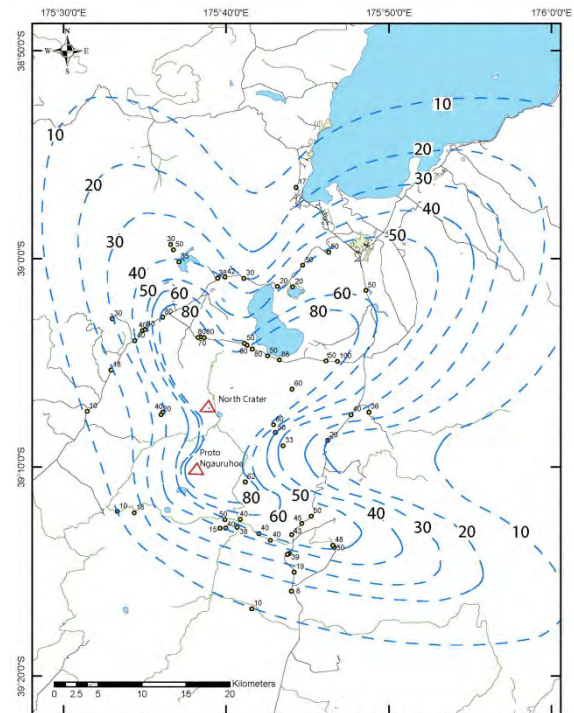


Fig. 34 – The unusually broad distribution of the Poutu Tephra, where several overlapping lobes appear to have formed during different phases of eruption, possibly from different vent areas along the axis of Mt. Tongariro. From Heinrich et al., (in prep).

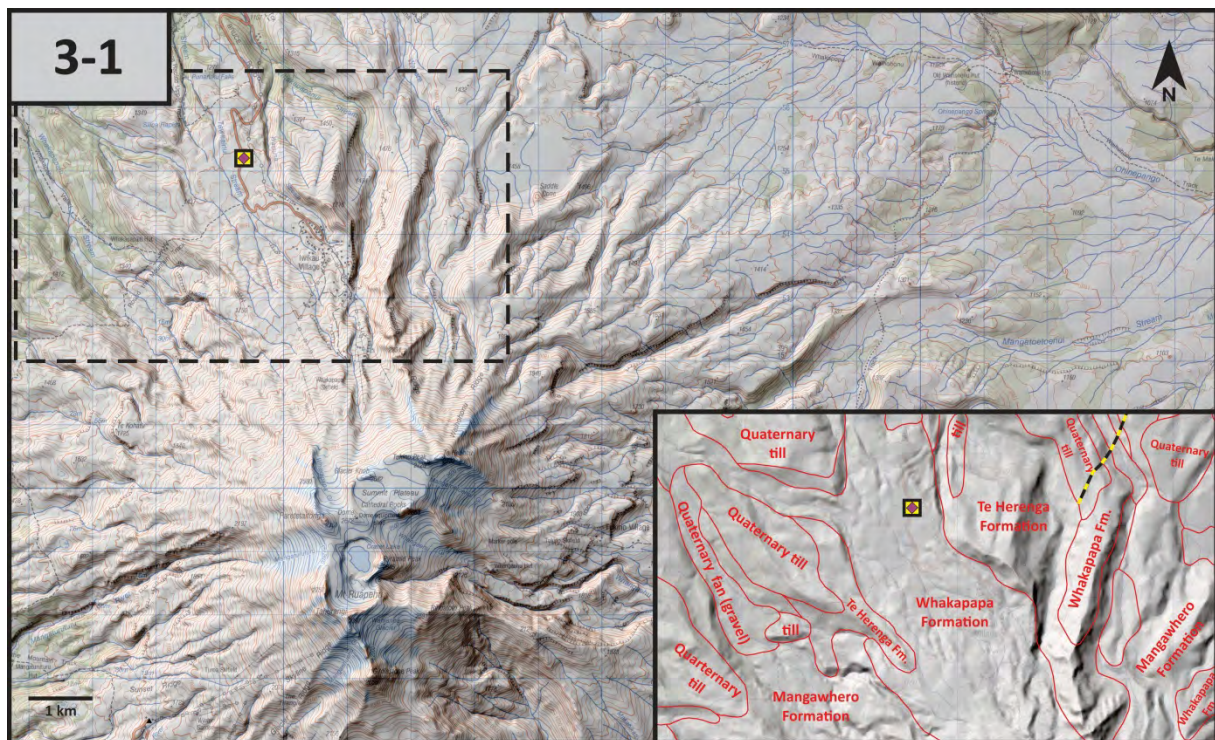
Suggested discussion points

- 1) Discussion on the effect of multi-sourced eruptions providing tephra to the ring plain
- 2) Discussion on the controlling parameters on air fall distribution patterns and their implications to resolve stratigraphy problems
- 3) Style of eruptions and mode of deposition
- 4) How mapping techniques used in active and young volcanoes can be adapted to ancient volcanic terrains.

Further reading

- Heinrich, M., Cronin, S., Pardo, N., (in prep): Understanding multi-vent Plinian eruptions at Mt. Tongariro, New Zealand. To be submitted to BV.
- Townsend, D., Leonard, G.S., Conway, C., Eaves, S.R. and Wilson, C.J.N., (2017). Geology of the Tongariro National Park area, scale 1:60,000, GNS Science geological map 4. 1 sheet + 109 p. GNS Science

Stop 3-1 – Whakapapa Skifield – Scoria Flat and Pinnacle Ridge



At this stop the main idea of the discussion focuses on the volcano edifice collapse and associated volcanic debris avalanches that commonly form an unconformity. In addition in this stop the participants can observe the rocks of the Whakapapa Formation that represent an increased lava flow emitting period at Ruapehu as the volcano changed its eruptive and sedimentary regime.



Fig. 34. – View to the Scoria Flat (with buildings) and the Pinnacle Ridge (Te Herenga Formation) from the upper northern flank of Mt. Ruapehu. Note the steep margins of the descending Whakapapa lavas on the left.

At 2797 m, Ruapehu is the highest point in the North Island and the largest volcanic edifice in the Tongariro Volcanic Centre, representing about 40% of known andesitic eruptive products of the TVZ. It is composed of 110 km³ of cone-building lavas and pyroclastic rocks surrounded by a ring plain of similar volume. The volcano has been continually

active for the last two thousand years with small volume (<0.1 km³) eruptions from the present vent, modified by eruption through a crater lake. Late Quaternary to Holocene magma output has been varied with high magma outputs at ~ 130 ka, 26 ka and 10 ka, interspersed with periods of low but continuous activity.

The styles of eruptive activity at Ruapehu have varied. Most of the andesitic eruptions fall into one of the following:

1. Small phreatomagmatic eruptions from summit, flank and satellite vents
2. Strombolian eruptions from the same vents
3. Voluminous aa and block flows from the summit and flank vents
4. Emplacement and collapse of summit and possibly flank vent domes
5. Infrequent sub-Plinian eruptions

In addition, rare eruptions of andesitic to dacitic pyroclastic flows are also known.

Ruapehu volcano has been built in a series of effusive cone building events interspersed with periods of erosion and sector collapse. Four major lava flow formations have been identified (Hackett, 1985; Hackett and Houghton, 1989) and the general distribution of these is shown in Fig. 7a. The older formations have been dated by the Ar-Ar method

(Tanaka et al., 1997; Gamble et al., 2003) and the youngest by indirect, stratigraphy-based methods (see below). From oldest to youngest the principal formations are: **Te Herenga**, **Wahianoa**, **Mangawhero** and **Whakapapa** (for ages of formations see the general description of Ruapehu volcanism).

The geochemistry and petrology of Ruapehu lavas are described in detail by Graham and Hackett (1989) and Price et al. (2012). Samples from the most recent events (1945–1996) were described by Gamble et al. (1999) and Nakagawa et al. (1999).

The most extensive lava fields assigned to the Whakapapa Formation are found on the Whakapapa skifield. They were erupted from vents near the present day summit and they partially fill an amphitheater between Pinnacle Ridge and the Whakapapaiti stream (Fig. 34). Their emplacement has been postulated to have followed a sector collapse event which deposited the Murimotu Formation, a debris avalanche and lahar deposit on the north western ring plain (Palmer and Neall, 1989). The Murimotu Formation has been dated by the ^{14}C method at $9,540 \pm 100$ (Topping, 1973).

Flows making up Whakapapa Formation are too young to be dated by the Ar-Ar method but tephra sequences preserved on the ring plain that surrounds the mountain (Donoghue et al., 1995) and on top of lavas higher on the volcano can be used to constrain ages. Many tephra have been dated by the ^{14}C method and others by using their stratigraphic positions relative to ^{14}C -dated rhyolitic tephra from the TVZ caldera volcanoes to the north.

Since the eruption of the Taupo Pumice around 1850 years ago, eruptions at Ruapehu have been low volume ($<0.05 \text{ km}^3$) but frequent (25 – 30 years) and they have taken place through a crater lake at the summit (Donoghue et al., 1995, 1997).

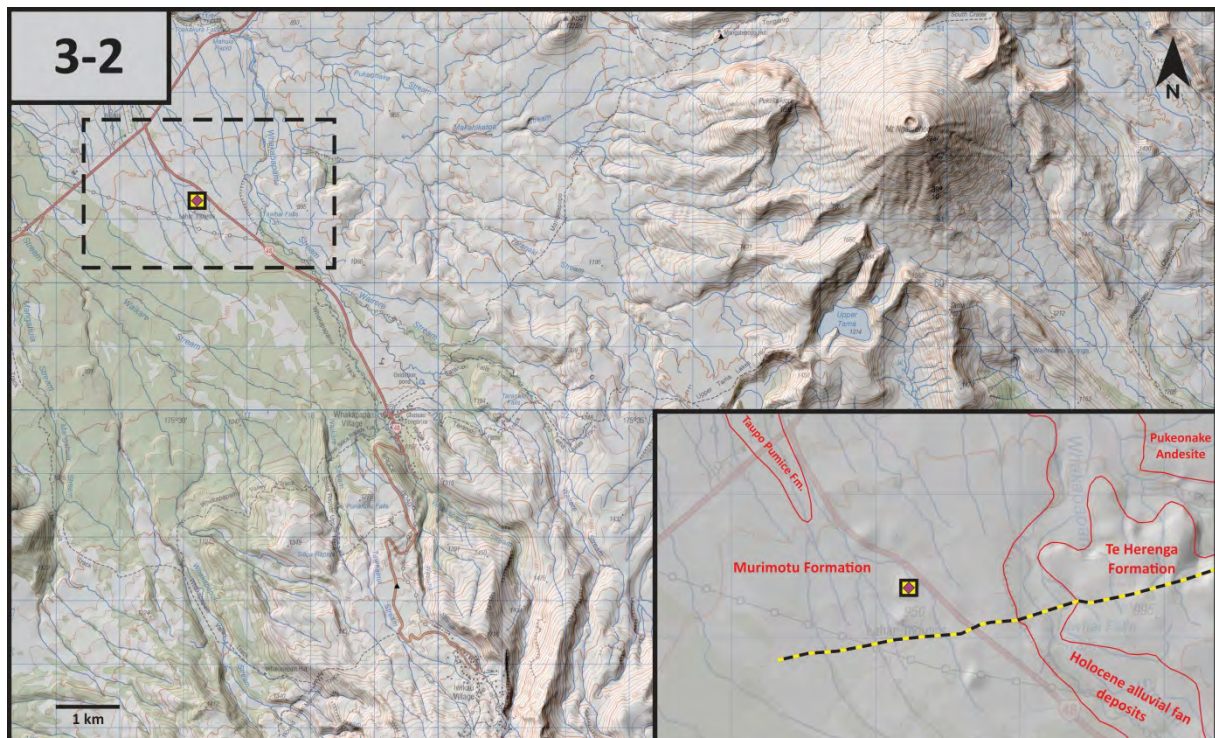
Suggested discussion points

- 1) Edifice-building lava versus tephra succession
- 2) The role of phreatomagmatism on explosive activity on a glaciated and/or crater lake controlled volcano
- 3) Preservation potential of tephra fall in proximal regions and their correlation potential to tephra successions accumulated in the ring plain.

Further reading

- Donoghue, S., Neall, V. and Palmer, A., 1995. Stratigraphy and chronology of late Quaternary andesitic tephra deposits, Tongariro Volcanic Centre, New Zealand. *Journal of the Royal Society of New Zealand*, 25(2): 115-206.
- Donoghue, S., Neall, V., Palmer, A. and Stewart, R., 1997. The volcanic history of Ruapehu during the past 2 millennia based on the record of Tufa Trig tephra. *Bulletin of Volcanology*, 59(2): 136-146.
- Gamble, J.A., Price, R.C., Smith, I.E., McIntosh, W.C. and Dunbar, N.W., (2003). 40 Ar/39 Ar geochronology of magmatic activity, magma flux and hazards at Ruapehu Volcano, Taupo volcanic zone, New Zealand. *Journal of Volcanology and Geothermal Research*, 120(3): 271-287.
- Graham, I.J. and Hackett, W.R., (1987). Petrology of Calc-alkaline Lavas from Ruapehu Volcano and Related Vents, Taupo Volcanic Zone, New Zealand. *Journal of Petrology*, 28(3): 531-567.
- Hackett, W.R., (1985). Geology and petrology of Ruapehu volcano and related vents, Unpublished PhD thesis, Victoria University of Wellington, Wellington, 312 pp.
- Hackett, W.R. and Houghton, B.F., (1989). A facies model for a Quaternary andesitic composite volcano: Ruapehu, New Zealand. *Bulletin of volcanology*, 51(1): 51-68.
- Nakagawa, M., Wada, K., Thordarson, T., Wood, C.P. and Gamble, J.A. (1999). Petrologic investigations of the 1995 and 1996 eruptions of Ruapehu volcano, New Zealand: formation of discrete and small magma pockets and their intermittent discharge. *Bulletin of Volcanology*, 61: 15-31.
- Palmer, B.A. and Neall, V.E. (1989). The Murimotu Formation—9500 year old deposits of a debris avalanche and associated lahars, Mount Ruapehu, North Island, New Zealand. *New Zealand Journal of Geology and Geophysics*, 32(4): 477-486.
- Price, R.C., Gamble, J.A., Smith, I.E., Maas, R., Waight, T., Stewart, R.B. and Woodhead, J., (2012). The anatomy of an Andesite volcano: a time-stratigraphic study of andesite petrogenesis and crustal evolution at Ruapehu Volcano, New Zealand. *Journal of Petrology*, 53(10): 2139-2189.
- Tanaka, H., Kawamura, K.i., Nagao, K. and Houghton, B.F., (1997). K-Ar ages and paleosecular variation of direction and intensity from Quaternary lava sequences in the Ruapehu Volcano, New Zealand. *Journal of geomagnetism and geoelectricity*, 49(4): 587-599.
- Topping, W., (1973). Tephrostratigraphy and chronology of late Quaternary eruptives from the Tongariro Volcanic Centre, New Zealand. *New Zealand journal of geology and geophysics*, 16(3): 397-423.
- Townsend, D., Leonard, G.S., Conway, C., Eaves, S.R. and Wilson, C.J.N. (2017). Geology of the Tongariro National Park area, scale 1:60,000, GNS Science geological map 4. 1 sheet + 109 p. . GNS Science.

Stop 3-2 – Mounds walk, deposits of the Murimotu debris avalanche



At this locality, the road cuts through a volcanic debris avalanche mound that is part of the Murimotu debris avalanche deposit of Palmer and Neall (1989) (Fig. 35). In the past, these mounds have been interpreted as drumlins and lahars deposits but the currently accepted hypothesis is that they are part of a debris avalanche deposit formed by a collapse of the western sector of Ruapehu around 9,500 years ago.



Fig. 35. – Mounds of the Murimotu Formation with the misty Mt. Ruapehu at the background. Pinnacle Ridge just visible under the clouds.

Hornblende bearing dacite blocks occur at this exposure, which is unusual; amphibole is very rare in Ruapehu rocks. Alternative explanations include derivation from a source in the vicinity of Tama Lakes (Hackett, 1985) or from a dacite dome on the

northwest side of Ruapehu (Hackett and Houghton, 1989).

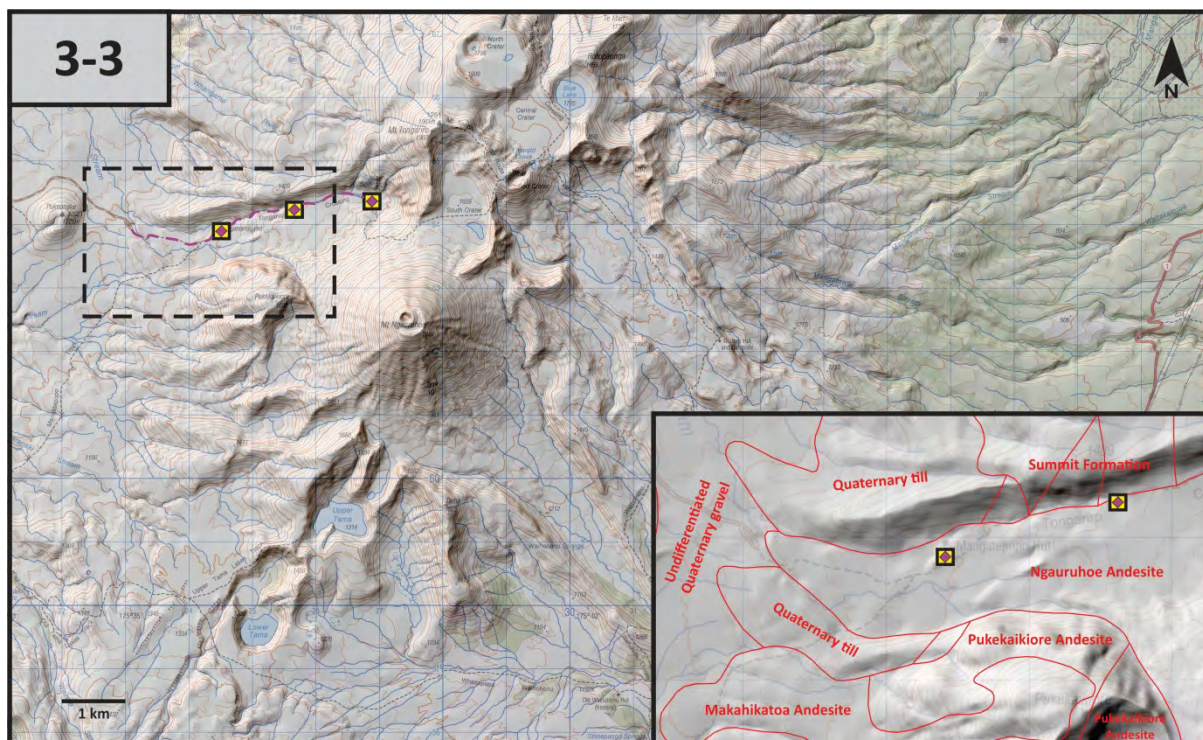
Suggested discussion points

- 1) How can we distinguish volcanic debris avalanche mounds from coarse-grained laharic deposits?
- 2) On the continuum between volcanic debris avalanche and laharic deposits
- 3) How can volcanic debris avalanche mounds form and what is their significance in geological mapping of volcanic terrains?

Further reading

- Hackett, W.R., (1985). Geology and petrology of Ruapehu volcano and related vents, Unpublished PhD thesis, Victoria University of Wellington, Wellington, 312 pp.
- Hackett, W.R. and Houghton, B.F., (1989). A facies model for a Quaternary andesitic composite volcano: Ruapehu, New Zealand. *Bulletin of volcanology*, 51(1): 51-68.
- Palmer, B.A. and Neall, V.E. (1989). The Murimotu Formation—9500 year old deposits of a debris avalanche and associated lahars, Mount Ruapehu, North Island, New Zealand. *New Zealand Journal of Geology and Geophysics*, 32(4): 477-486.

Stop 3-3 – Eruptive styles and glacial history of the Tongariro volcano, growth of Mt. Ngauruhoe



Stop A: Glacial history, older volcanic structures at the west side of Tongariro volcano

The Mangatepopo Valley is a broad glacial valley flanked by paired moraine ridges (Fig. 36). The interval 13 – 23 ka is regarded as the Last Glacial Maximum in the central North Island (Pillans et al., 1993). Such glacial features occur elsewhere on Tongariro, and glacial erosion of deep valleys reveals the internal stratigraphy of the six older cone centres. Erosion of the pre-glacial cones has been softened to a certain extent by post-glacial cone building and infilling of valleys with young lava flows. For example, the cone of Ngauruhoe has from c.2.5 ka grown to bury the intersection point of several older cones of the Tongariro volcanic complex (Figure 8) including Pukekaikiore, (190-120 ka), Tongariro Trig cone (110-65 ka), and Tama 2 (210-200 ka) and SW Oturere (115-65 ka) cones to the south and east. From the track we can observe thick (<100 m) lavas outcropping on Pukekaikiore, ranging from regular sub-columnar-jointed flows (north margin) to coulee-like ponded lava flows with massive, distorted columnar-slabby radiating jointing (east margin).

Stop B: Ngauruhoe sectorial cone growth and historical eruption chronology (1300 m)

The symmetrical cone of Ngauruhoe has grown rapidly with constant modification of the summit of

the cone. Numerous youthful andesitic aa to block lava flows are preserved around all sectors of the cone. The best-constrained sequence of flows occurs here in the Mangatepopo Valley. This sequence is taken to be broadly representative of the evolution of the cone, showing the sectorial growth pattern, and the relationships between successive flows as they follow depressions which flank their predecessors, or reoccupy old channels. Lava flow paths were constrained by the cliffs of the eroded older cone of Pukekaikiore, adjacent to which they stopped and banked up in thick piles, or were diverted along the base of the cliffs in either direction. Other 1954 Ngauruhoe flows (eg. the large 30 June flow) contain small elongate windows into the underlying surface caused by temporary branching out of flow lobes around higher relief of older lava flows.

Ngauruhoe has been nearly continuously active in historical times (Gregg, 1960; Cole and Nairn, 1975), with tephra eruptions every two or three years on average. The more than 60 significant eruptive episodes recorded from Ngauruhoe since 1839 represent a diverse range of styles including effusion of aa and block lava flows (e.g. 1870, 1949, 1954), Strombolian fire-fountaining to form scoria cones (e.g. 1954), and Vulcanian-style explosions generating block and ash flows and pyroclastic falls (e.g. 1974-75). Figure 11 shows the historical flows preserved in Mangatepopo Valley, which comprise

two lava flows from 1870 (viewed at Stop 3), one lava flow and two pyroclastic avalanches from 1949, at least ten lava flows from 1954, and at least 5 pyroclastic avalanches from 1975 (main deposit examined at Stop 3). The darkest gray lava flows were erupted over a four-month period during 1954. Each lava flow formed relatively quickly, reaching its maximum length in 1-2 days, with observed flows advancing at rates of up to ~300 metres per hour (Gregg, 1956).



Fig. 36. – The glacial Mangatepopo valley with descending lava flows of Ngauruhoe volcano. The grey areas on the top of the brownish-colored lavas represent PDC deposits.

On the basis of detailed stratigraphic sampling, petrography, radiocarbon dating and glass chemistry, Möbis (Möbis et al., 2008; Möbis, 2010) modified earlier stratigraphic interpretations (e.g. Donoghue et al., 1995) and subdivided the tephra stratigraphy of Ngauruhoe into four chronological stages. Stages 1 to 3 predate the Taupo Pumice, which was emplaced 1.85 ka B.P. (Wilson, 1993). Stage 1 is placed within the Papakai Formation and was erupted between 3.5 and 5 ka B.P. Stage 2 is contained within the Mangatawai Formation, which includes tephra erupted during the earliest stages of construction of the present day cone, 3.5 to 2.7 ka before present day. Stage 3, commencing at ~2.7 ka B.P. was the start of the main cone building phase and Stage 4 includes all eruptive activity post-dating the emplacement of the Taupo Pumice.

Mapping and detailed geochemical and petrographic investigation of Ngauruhoe lava flows provided Hobden (1997) with the basis for constructing a flow stratigraphy for the present day cone. The flow sequence was divided into five stratigraphic groups (Hobden et al., 2002). For a number of reasons correlation of tephra and lava flow stratigraphy is challenging. Flows tend to be restricted to the upper slopes of the volcano and older flows are commonly concealed under younger lavas. Most of the older flows have been eroded on the unstable and steep upper slopes of the active volcano. Consequently, older flows that would be correlative with older tephra of Möbis's Stages 1 and 2 are not well represented in the flow stratigraphy. In addition, the geochemistry of tephra and flows cannot be directly compared; tephra are generally glassy fragments of relatively evolved melt or magma and their

compositions are not directly comparable with less evolved, crystal-rich andesitic magmas represented by lava flows.

The oldest of the five flow groupings identified by Hobden et al. (2002) was emplaced before the Taupo pumice (1.85 ka). These Group 1 lava flows, which are exposed on the eastern and north western flanks of the volcano are very likely to be time equivalents of tephra Stage 2 (see above). They are olivine-bearing basaltic andesites. Group 2 lavas were erupted down the north western slopes. Some are older and some younger than the Taupo Pumice and they could therefore be time equivalents of tephra Stage 3 or Stage 4. Like Group 1 eruptives they are olivine-bearing basaltic andesites. Groups 3, 4 and 5 were emplaced during tephra Stage 4 (post Taupo Pumice to the present day). Group 3 includes three long (3-4 km) lava flows on the southern slopes of the volcano. Group 4 lavas were erupted down the southern slopes but at least one flow descended the north western flank. Group 5 includes all lava and block and ash flows erupted between 1870 and 1975 AD and consequently it is the group that has been most intensively sampled; these younger flows have covered and concealed many of the older eruptives on the upper slopes of the volcano. Group 5 flows are olivine-bearing basaltic andesites and andesites showing considerable compositional variability. Most of these flows were emplaced on the northern flanks or higher eastern slopes of the volcano.

Stop C: 1975 Ngauruhoe pyroclastic avalanche deposit (1380 m)

We will briefly detour from the track to examine the lobate flow front of the main pyroclastic avalanche deposit erupted on 19 February 1975. The most recent eruptions from Ngauruhoe occurred in 1974-75 when violent Vulcanian-style explosions and ash eruptions generated several pyroclastic avalanches, or block and ash flows, down the northwest slopes of the cone and a thin widespread fall deposit (Fig. 37). The eruption of 19 February 1975 was observed closely and began with voluminous gas-streaming, followed by violent cannon-like explosions which ejected ballistic blocks up to 2.8 km from the vent, accompanied by atmospheric shock waves and condensation clouds (Nairn, 1976; Nairn and Self, 1978). Dense eruption columns up to 10 km high underwent partial collapse to form pyroclastic avalanches (of both fresh magmatic and older lithic blocks) down the flanks of the cone (Nairn and Self, 1978). Near to Ngauruhoe the fall deposit comprised 3-4 cm of scoria-ash, and thinned to 1 mm of ash at 21 km along the dispersal axis (Nairn and Self, 1978). Maximum initial ejecta velocities of around 400 m s⁻¹ (Nairn, 1976) were linked to high explosion gas pressures caused by magmatic intrusions rapidly heating meteoric water confined

beneath a solidified lava cap (Nairn and Self, 1978; Self et al., 1979).

The deposits comprise a sequence of overlapping, inter-digitating tongues of dark grey basaltic andesite, with thin (1-1.5 m) lobate fronts. The surface of the deposit features conspicuous flow channels and marginal levées, indicating high yield strength during the flow. The deposit is coarse-grained and very poorly sorted; fine ash and dense blocks and bombs are concentrated in the channels, whereas scoriaceous blocks up to 1 m in diameter dominate the levées and flow fronts. Some bombs have smooth, ropy surfaces, others are vesiculated, breadcrusted or cauliflower-shaped. Dense, massive blocks lack any signs of plastic deformation, indicating that they were rigid when ejected. Some blocks have prismatic joints caused by stress release during cooling, showing that they were hot when ejected (temperatures of blocks in the deposit varied from $>900^{\circ}\text{C}$ to cold, Nairn and Self, 1978). Altered orange-white lithic blocks are also a component of the pyroclastic avalanche deposit. Quartzite xenoliths present in the lava contain a thin, irregular, closely-spaced layering of calc-silicates between the quartz grains which is interpreted to represent the original structure of calcite/dolomite-quartz veins within the Mesozoic Torlesse metasedimentary crustal basement. Glass along the grain boundaries is evidence for partial melting of these quartzite xenoliths, suggestive of their involvement in crustal contamination of Tongariro magmas.

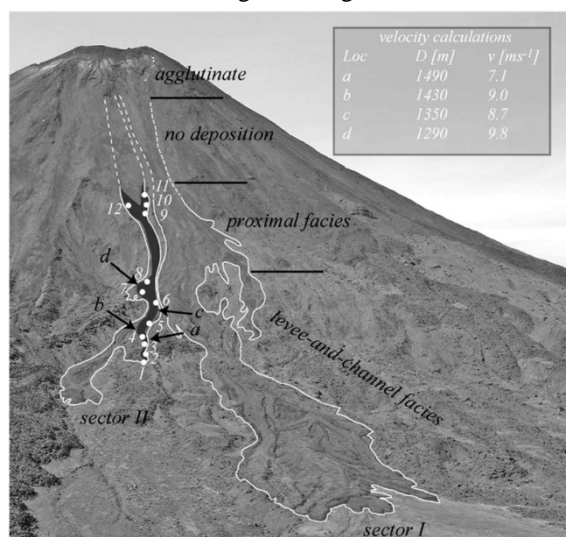
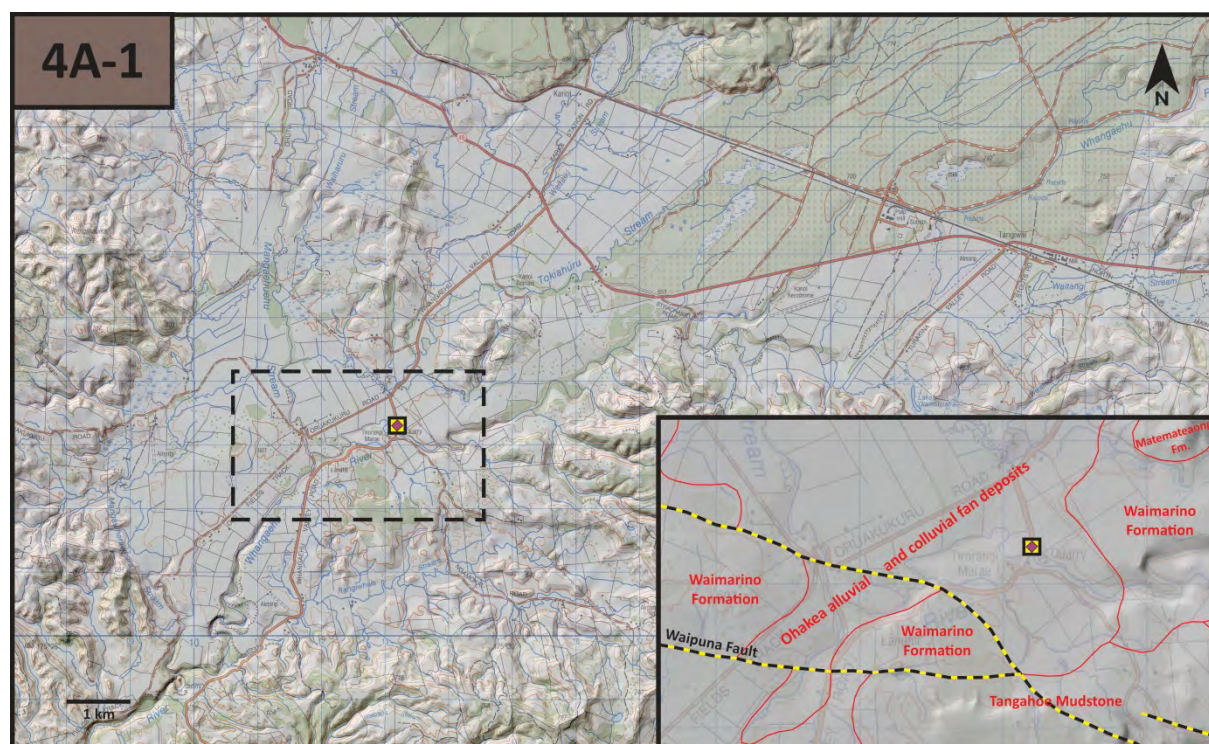


Fig. 37. – 1975 pyroclastic flow deposits, Mt. Ngauruhoe, with velocity estimates from flow run-up properties

Further reading

- Donoghue, S., Neall, V. and Palmer, A. (1995). Stratigraphy and chronology of late Quaternary andesitic tephra deposits, Tongariro Volcanic Centre, New Zealand. *Journal of the Royal Society of New Zealand*, 25(2): 115-206.
- Gregg, D., (1956). Eruption at Ngauruhoe 1954-1955. *NZ J. Sci. Technol.*, B, 37: 675-688.
- Hackett, W.R. (1985). Geology and petrology of Ruapehu volcano and related vents, Unpublished PhD thesis, Victoria University of Wellington, Wellington, 312 pp.
- Hackett, W.R. and Houghton, B.F. (1989). A facies model for a Quaternary andesitic composite volcano: Ruapehu, New Zealand. *Bulletin of volcanology*, 51(1): 51-68.
- Hobden, B.J. (1997). Modelling magmatic trends in time and space: Eruptive and magmatic history of Tongariro Volcanic Complex, New Zealand, Unpublished PhD Thesis, University of Canterbury, Christchurch.
- Hobden, B.J., Houghton, B.F. and Nairn, I.A. (2002). Growth of a young, frequently active composite cone: Ngauruhoe volcano, New Zealand. *Bulletin of volcanology*, 64(6): 392-409.
- Lube, G., Cronin, S.J., Platz, T., Freundt, A., Procter, J.N., Henderson, C.J., Sheridan, M.J. (2007). Flow and deposition of pyroclastic granular flows: a type example from the 1975 Ngauruhoe eruption, New Zealand. *Journal of Volcanology and Geothermal Research* 161: 165-186.
- Möbis, A. (2010). Understanding the Holocene explosive eruption record of the Tongariro Volcanic Centre, New Zealand. Unpublished PhD thesis, Massey University, Palmerston North, New Zealand.
- Möbis, A., Cronin, S.J., Lube, G., Neall, V.E. and Németh, K. (2008). History of Ngauruhoe volcano, New Zealand Geological Society of New Zealand Miscellaneous Publication 124A, 188.
- Nairn, I.A. (1976). Atmospheric shock waves and condensation clouds from Ngauruhoe explosive eruptions. *Nature* 259, 190-192
- Nairn, I. and Self, S. (1978). Explosive eruptions and pyroclastic avalanches from Ngauruhoe in February 1975. *Journal of Volcanology and Geothermal Research*, 3(1): 39-60.
- Pillans, B., McGlone, M., Palmer, A., Mildenhall, D., Alloway, B. and Berger, G., (1993). The last glacial maximum in central and southern North Island, New Zealand: a paleoenvironmental reconstruction using the Kawakawa Tephra Formation as a chronostratigraphic marker. *Palaeogeography, Palaeoclimatology, Palaeoecology*, 101(3): 283-304.
- Self, S., Wilson, L. & Nairn, I.A. (1979). Vulcanian eruption mechanisms. *Nature* 277, 440-443.
- Wilson, C. (1993). Stratigraphy, chronology, styles and dynamics of late Quaternary eruptions from Taupo volcano, New Zealand. *Philosophical Transactions of the Royal Society of London A: Mathematical, Physical and Engineering Sciences*, 343(1668): 205-306.

Stop 4A-1 – Lahars of Mt. Ruapehu, Onetapu Formation



Mt. Ruapehu is well recognized for producing lahars with laharic activity being associated with events in 1861, 1895, 1945, 1953, 1969, 1975, 1995 and 2007. All of these lahars have been contained to two main catchments the western Whakapapa/Whakapapaiti Rivers and the eastern Whangaehu River. Lahars have generally been triggered through explosive activity through the Crater Lake, however the 1953 and 2007 lahars were related to small collapses of the rim of the crater. The 2007 lahar was recorded in detail through a variety of sensors and used as a case study to improve mass flow modelling.

The lahars associated with the 1995/1996 eruptions of Ruapehu were intensively studied (e.g. Cronin et al., 1997; Hodgson and Manville, 1999). Eruption began in September 1995 with activity consistent with that predicted from interpretation of the Tufa Trig Formation deposits. On the 25 September, five large lahars were initiated (LH4a to LH4e) over a period of more than 12 hours. They reached a total volume of flow $>5 \times 10^6 \text{ m}^3$, corresponding to the release of c. 1/3 of Crater Lake waters. All of these lahar events while they have been destructive and fatal have generally been geomorphically contained to existing river channels (Fig. 38). Mapping and investigation of older Holocene lahars have shown similar trigger mechanisms yet much larger volumes have been released depositing large volumes of material across the landscape.

The Onetapu Formation represents the aggradation of deposits left by lahars that inundated the Whangaehu River catchment following the emplacement of the 232 AD Taupo ignimbrite (Palmer et al., 1993; Donoghue and Neall, 2001). The formation includes at least 14 prehistoric units (Hodgson, 1993; Cronin et al., 1997b). The Onetapu Formation is well exposed along the main channel of the Whangaehu River, reaching distal sites located up to 134 km from source with volumes $>4 \times 10^7 \text{ m}^3$. However, the geological record of aggradational laharic sequences should be seen as incomplete, reflecting the selective preservation of deposits left mainly by the largest events (Cronin et al., 1997b). Some of the lahar deposits are readily identified by their sedimentological and lithological characteristics.

The Onetapu Formation covers a complete range of lithofacies from indurated, clay-rich, matrix-supported diamictites to fluviually reworked, coarse sands and gravels (Palmer et al., 1993; Hodgson, 1993; Donoghue and Neall, 2001). Using the accepted terminology for lahars, they correspond to a sporadic succession of avalanche-induced, cohesive debris flows (Lecointre et al., 2002), and non-cohesive debris flows to dilute, hyperconcentrated stream flows. Correlations between proximal and distal outcrops are made on the basis of (1) the chronostratigraphy of the

deposits (lahars, interbedded tephra and soils), (2) the lithology of the diamictons (both matrix and clasts), and (3) the geochemistry of the juvenile components. Understanding the stratigraphy of these

units and their trigger mechanisms allows us to link those processes to eruptive sequences and processes (Fig. 39).

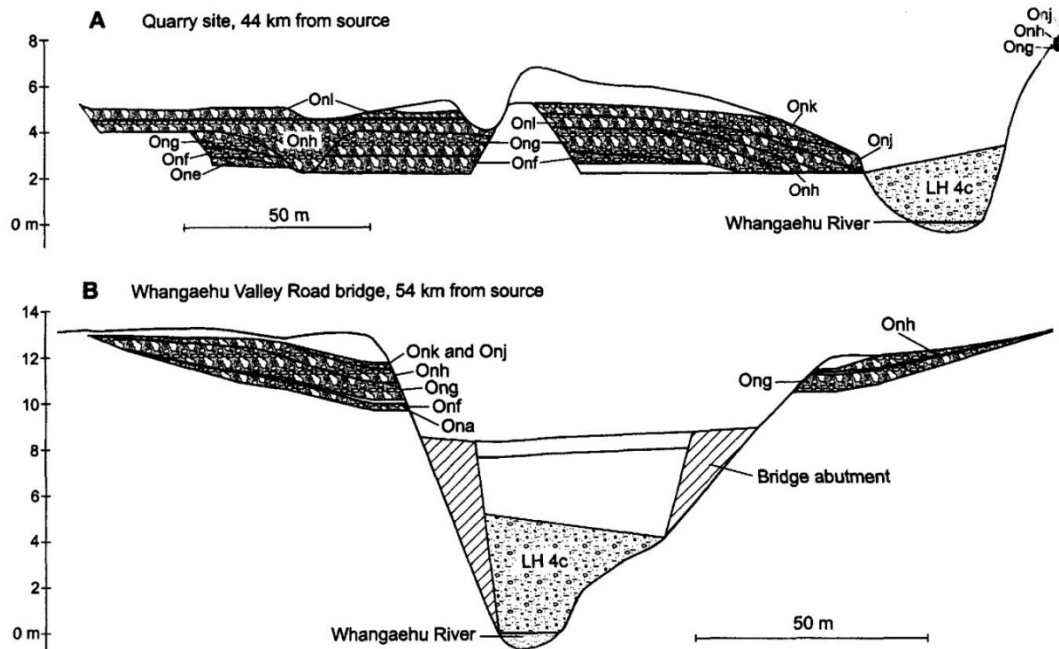


Fig. 38. – Comparison of the 1995 lahar LH4c with the older Onetapu lahars at (A) 44 km from the source and (B) 54 km from the source (Cronin et al., 1997b).

TIME SCALE	LAHAR UNIT	TEPHRA UNIT	LAHAR-TRIGGERING MECHANISM	LAHAR SIZE	CRATER LAKE
2001 AD					45% full (January 2002)
1996 AD	Ono-6	TT 19	• Rain triggered • Eruption-driven	**	Empty
1995 AD	Ono-5		• Eruption-driven	**	
1975 AD	Ono-4		Ice-dam collapse	**	
1953 AD		TT 18	Plinian eruption / Growth of lava dome	NO MAJOR LAHAR RECORDED	Partial break-out Lake displaced slowly
1945 AD					
1861 AD	Ono-3		• Eruption-triggered	**	
200 BP		TT 17			
300 BP	Ono-2 Ono-1	TT 15		*	Reconstruction of the crater wall
400 BP	Ono-3		• Eruption-triggered • Crater wall collapse	****	Break-out
500 BP	Ono-1	TT 13 to 9	• Eruption triggered ?	****	Break-out Lake filled
600 BP		TT 8			
700 BP					
800 BP					
900 BP		TT 7			NO LAHARS RECORDED
1000 BP					Construction of the crater wall
1100 BP					
1200 BP	Ono (4 sub-units)	TT 6	← Phreatomagmatic eruption followed by plinian eruption ? • Eruption-triggered	****	
1300 BP					
1400 BP					
1500 BP	Onb	TT 5	← Phreatomagmatic eruption	***	
1600 BP	Ono-4	TT 4	• Collapse of Crater rim ?	***	Progressive development of a proto-Crater Lake
1700 BP	Ono-3 Ono-2	TT 3	• Slumping from Pyramid Peak area • Slumping from Pyramid Peak area	+	
1800 BP	Ono-1	TT 2	Cone collapse from hydrothermally altered source area (Pyramid Peak)	***	
2000 BP	TAUPO TEPHRA	TT 1	← Strombolian eruptions		NO CRATER LAKE

Fig. 39. – Correlation between laharic and eruptive events over the last 2000 years highlighting the role the Crater Lake and water plays in both eruption style and hazard.

Further reading

Cronin, S. J., Neall, V. E., Lecoindre, J. A., and Palmer, A. S.: (1997a) Changes in Whangaehu river lahar characteristics during the 1995 eruption sequence, Ruapehu volcano, New Zealand, *J. Volcanol. and Geotherm. Res* 76, 47–61.

Cronin, S. J., Hodgson, K. A., Neall, V. E., Palmer, A. S. and Lecoindre, J. A.: (1997b). 1995 Ruapehu lahars in relation to the late Holocene lahars of Whangaehu River, New Zealand, *New Zealand J. Geol. and Geophys.* 40, 507–520.

Donoghue, S. L. and Neall, V. E.: (2001). Late Quaternary constructional history of the southeastern Ruapehu ring plain, New Zealand, *New Zealand J. Geol. and Geophys.* 44: 439–466.

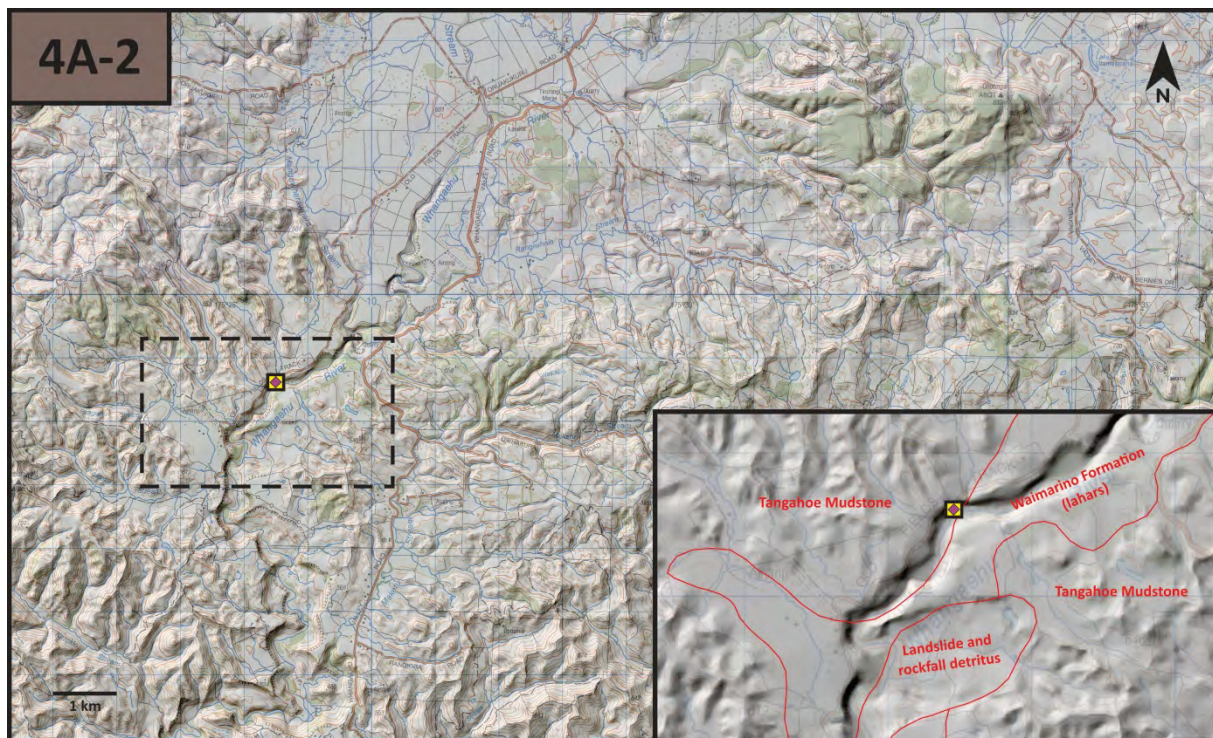
Hodgson, K. A.: (1993). Late Quaternary lahars from Mount Ruapehu in the Whangaehu River Valley, North Island, New Zealand, unpublished PhD thesis, Massey University, New Zealand.

Hodgson, K. A. and Manville, V. R.: (1999). Sedimentology and flow behavior of a rain-triggered lahar, Mangatoetoe Stream, Ruapehu volcano, New Zealand, *GSA Bull.* 111, 743–754.

Lecoindre, J.A., Neall, V.E., Wallace, R.C. and Prebble, W.M. (2002). The 55- to 60-ka Te Whaiiu Formation: a catastrophic, avalanche-induced, cohesive debris flow deposit from Proto-Tongariro Volcano, New Zealand *Bulletin of Volcanology* 63: 509-525.

Palmer, B. A., Purves, A. M., and Donoghue, S. L. (1993). Controls on accumulation of a volcanoclastic fan, Ruapehu composite volcano, New Zealand, *Bull. Volcanol.* 55: 176–189.

Stop 4A-2 – Whangaehu Valley Formation



The Whangaehu Formation (Hodgson, 1993; Keigler et al., 2011) provides a record of the proto-Ruapehu massifs as those earlier cone building deposits are not preserved on the present Mt. Ruapehu cone. The Formation in the middle course of the Whangaehu River Valley comprises three principal stratigraphic units representing an estimated volume of c. 1 km³. The **Lower Member** comprises a coarse, clast-supported, ungraded, megaclast-rich breccia, with oblique to sub-horizontal fractures indicating that shearing occurred at its base. The Lower Member also contains rip-up clasts from the underlying Tertiary siltstones. An indurated and sheared clast mixture of angular to subangular cobbles and pebbles supports large boulders at the base of the breccias, with fracturing concentrated near the base of this stratum (Fig. 40). Pockets of shattered clasts representing monolithological domains, and boulders showing jigsaw fractures indicate collision effects during transportation from source. The breccia is interpreted as a debris-avalanche deposit resulting from a collapse of the southern flank of Ruapehu between 180 ka and 45 ka. The **Middle Member** suggests fluvial reworking of the debris-avalanche deposit interspersed with post-collapse lahar deposits on the ancestral Ruapehu ring plain. The **Upper Member** reflects an aggradation phase on the southern ring plain, with deposition of lahars associated with volcanic activity, as shown by reworked tephra. The catastrophic debris avalanche represented by the Whangaehu Fm. Lower Member

illustrates a significant hazard to the surrounds of Mt. Ruapehu that has been previously underestimated.



Fig. 40 – Selected photographs of sedimentary features of the Lower Member of Whangaehu Formation from Keigler et al. (2011).

Suggested discussion points

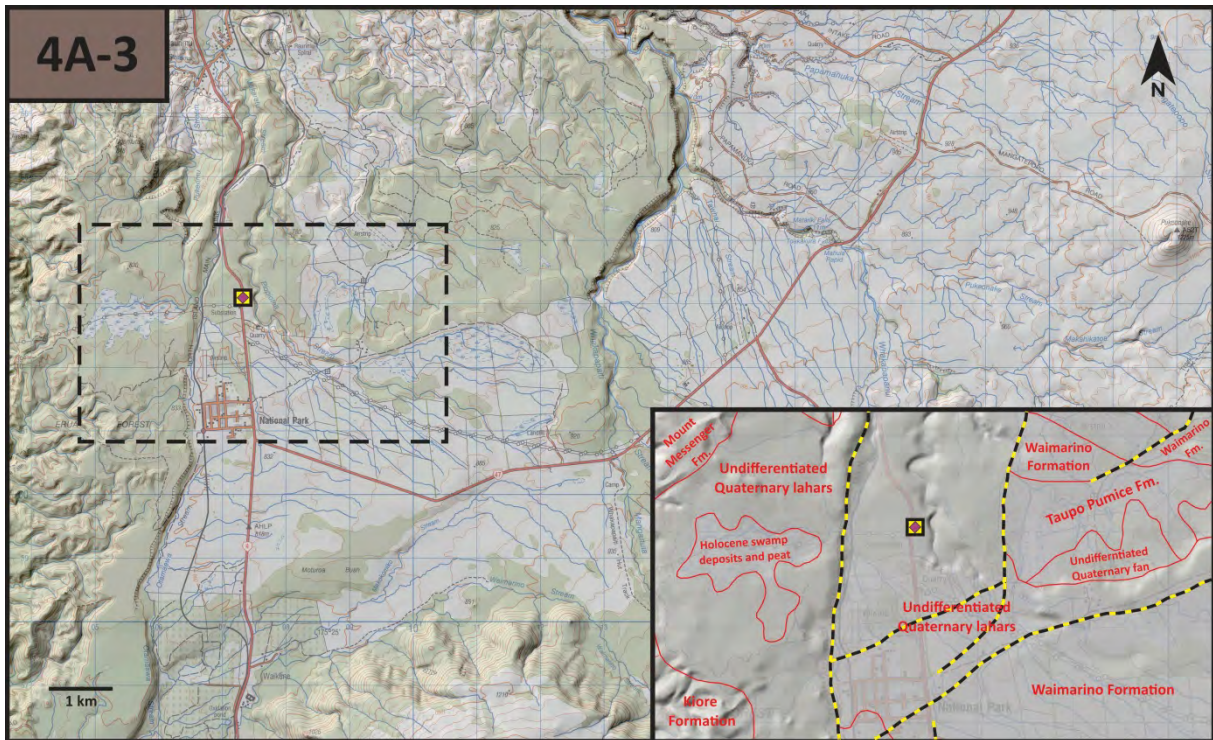
- 1) Discussion on the stratigraphical framework of volcanic debris avalanches and their potential to landscape-scale correlation
- 2) Volcanic debris avalanche stratigraphy versus geological mapping units
- 3) The significance of volcanic debris avalanche deposits in geological mapping of volcanic terrains

- 4) Discussion on the interlink between normal sedimentary systems with volcanic debris avalanche and laharic systems from lithostratigraphy point of view
- 5) Discussion on the transition processes and resulting sediments between volcanic debris avalanches, laharic deposits and fluvial sediments
- 6) Discussion on the role of volcanic debris avalanche deposits in volcanoclastic successions in ancient settings in the light of the lessons we learned from Ruapehu

Further reading

- Hodgson, K. A.: (1993). Late Quaternary lahars from Mount Ruapehu in the Whangaehu River Valley, North Island, New Zealand, unpublished PhD thesis, Massey University, New Zealand.
- Keigler, R., Thouret, J. C., Hodgson, K. A., Neall, V. E., Lecointre, J. A., Procter, J. N., and Cronin, S. J. (2011). The Whangaehu Formation: Debris-avalanche and lahar deposits from ancestral Ruapehu volcano, New Zealand. *Geomorphology*, 133(1-2), 57-79.
- Tost, M. (2015). Linking distal volcanoclastic sedimentation and stratigraphy with the growth and development of stratovolcanoes, Ruapehu volcano, New Zealand, Unpublished PhD thesis, Massey University, Palmerston North
- Tost, M., Cronin, S.J., Procter, J.N. (2014). Transport and emplacement mechanisms of channelised long-runout debris avalanches, Ruapehu volcano, New Zealand *Bulletin of Volcanology* 76: 881.

Stop 4A-3 – Raurimu Spiral road section



The roadcuts along State Highway 4 expose old Ruapehu-sourced volcanic debris avalanches in the base of the section covered by several old lahar deposits sourced also from Ruapehu (Figs 41-42).

Radiometric ages (~180 ka) of these deposits correspond to the Te Herenga cone building episode (Tost, 2015).



Fig 41. – Basalt debris avalanche deposit of the Piriaka Formation is unconformably overlain by two hyperconcentrated-flow deposits.



Fig 42. – The c. 10 m thick sequence of hyperconcentrated-flow deposits of the Piriaka Formation

Table 3 – Approximate runout and apparent coefficient of friction of the confined Ruapehu debris avalanches considering spreading of the mass within a v-shaped valley

	V [km ³]	L _{max} [km]	H [km]	A [km ²]	L ^a [km]	H/L ^a
Mataroa Formation	2.9	64.0	2.1	256	16.00	0.13
Pukekahu Formation	1.56	56.0	2.4	120	14.00	0.17
Oreore Formation	3	80.0	2.3	200	20.00	0.12
Piriaka-A Formation	1.35	72.0	2.5	225	18.00	0.14
Piriaka-B Formation	1.4	75.0	2.5	260	18.75	0.13
Lower Whangaehu Formation	2.4	60.0	2.3	120	15.00	0.15

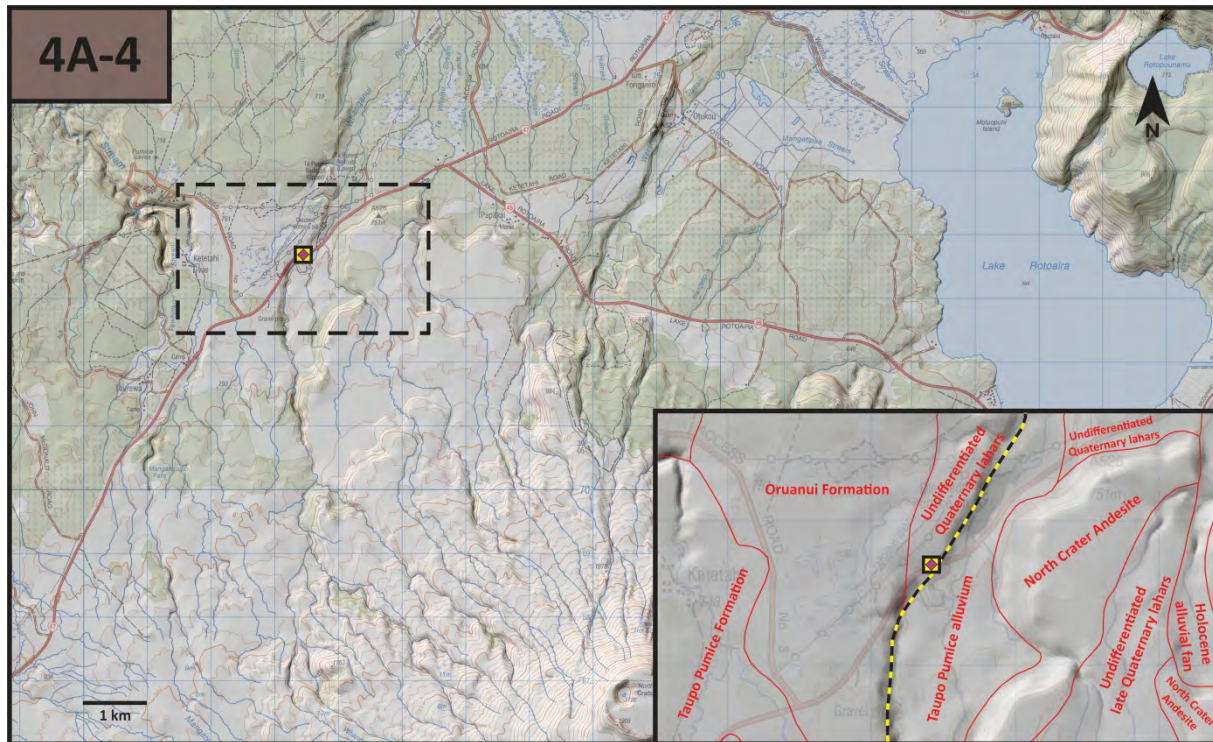
Suggested discussion points

- 1) Landscape evolution through an area influenced by volcanic debris avalanches in the early stage of the Ruapehu volcano
- 2) Explore the role of understanding landscape elements such as terraces, their relative elevation to various volcanic debris avalanche and lahar deposit horizons to derive a time and space framework to see the influence of volcanism on a fluvial network and its sedimentation
- 3) To explore the scale of sedimentary processes act on the shaping of valley formation and sediment distribution

Further reading

- Tost, M. (2015). Linking distal volcanoclastic sedimentation and stratigraphy with the growth and development of stratovolcanoes, Ruapehu volcano, New Zealand, Unpublished PhD thesis, Massey University, Palmerston North
- Tost, M., Cronin, S.J., Procter, J.N. (2014). Transport and emplacement mechanisms of channelised long-runout debris avalanches, Ruapehu volcano, New Zealand *Bulletin of Volcanology* 76: 881.
- Townsend, D., Leonard, G.S., Conway, C., Eaves, S.R. and Wilson, C.J.N., 2017. Geology of the Tongariro National Park area, scale 1:60,000, GNS Science geological map 4. 1 sheet + 109 p. GNS Science

Stop 4A-4 – Te Whaiiau debris avalanche and valley-ponded facies of the Taupo Pumice Formation



The area bordering the Mangamingi/Otamangakau Stream was extensively surveyed in the late 1960's for the development of the Tongariro Power Scheme (Whanganui, Te Whaiiau and Otamangakau dams and canals). Boreholes and trenches revealed a thick and extensive layer of "outwash debris" and an upper "clayey-silt formation" underlying andesitic cover beds and Taupo Pumice (Prebble, 1967; 1969). At this locality, which is the type section (Lecointre et al., 2002), the Te Whaiiau Formation occurs as a massive, poorly sorted, clay-rich diamicton which contains angular blocks of various altered andesites (Fig. 43). Clays identified in the matrix include smectites (montmorillonite), kandites (kaolinite + halloysite) and iron sulfide particles. Pyrite and marcasite have been detected in the sand fraction. The mineralogical assemblage points towards an alteration process due to acid geothermal fluids percolating through material forming the source area of the deposit (Lecointre et al., 2002).

A period of erosion followed the emplacement of Te Whaiiau Formation. Below the Te Whaiiau Formation, the 65 ka-old, Okataina-sourced Rotoehu Tephra has been found over a sequence of tephra-rich sands which include peat and paleosol horizons correlated to the Otamangakau interstadial (McGlone and Topping, 1983). As a consequence of

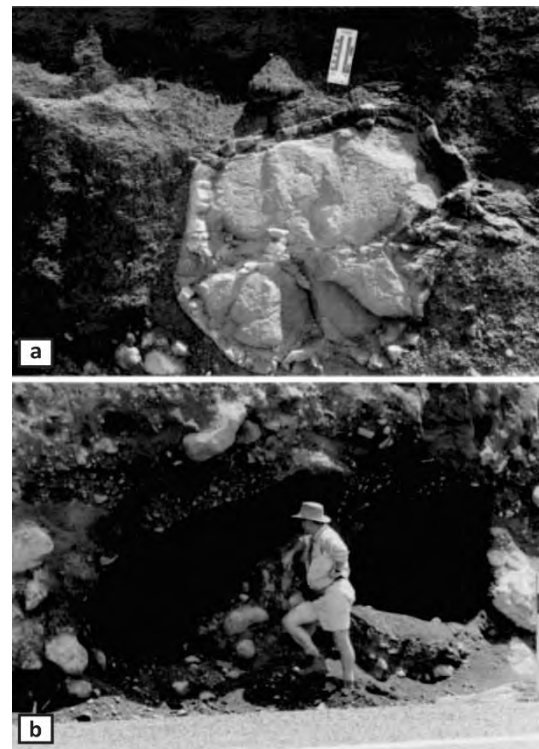


Fig. 43 Type section of deposits of the Te Whaiiau Formation, a A typical andesite boulder with distinct, fractured, outer margin, b Large cavities previously occupied by >2-m boulders of fresh andesite. (after Lecointre et al., 2002)

this stratigraphic succession, the emplacement of the Te Whaiiau Formation is estimated at c. 55-60 ka (Lecointre et al., 2002). The Formation is argued to have been generated by a sector collapse event on the north-western flank of the proto- Tongariro edifice (Lecointre et al., 2002). A large segment of the volcano failed generating a water saturated debris avalanche, which transformed downstream into a cohesive debris flow. The flow spread laterally filling stream channels on the western sector of the Tongariro ring plain up to 15 km from source.

At this locality there is also an excellent exposure of the valley pond facies of the 232 AD Taupo eruption sequence. These are deposits of the final phase of the paroxysmal eruption of Taupo volcano, which devastated the central part of the North Island in what is now recognised as the most violent eruption worldwide in recent times.

Suggested discussion points

- 1) Textural and facies variations of valley-confined pumiceous flow deposits
- 2) Facies transition of valley filling and overbank deposits of large volume pumiceous flow deposits
- 3) Discussion on the emplacement processes of ignimbrites

- 4) Discussion on the remobilisation potential of sudden input of primary pumiceous deposits into the fluvial systems
- 5) Discussion on the preservation potential of large volume pumiceous flow deposits
- 6) Link between ancient and modern pumiceous flow deposits and the role of welding
- 7) Textural characteristics of non-welded ignimbrites and their potential to use their facies variations for geological mappings.

Further reading

- Lecointre, J.A., Neall, V.E., Wallace, R.C. and Prebble, W.M. (2002). The 55- to 60-ka Te Whaiiau Formation: a catastrophic, avalanche-induced, cohesive debris flow deposit from Proto-Tongariro Volcano, New Zealand. *Bulletin of Volcanology* 63: 509-525.
- McGlone, M.S. & Topping, W.W. (1983). Late Quaternary vegetation, Tongariro region, central North Island, New Zealand. *New Zealand Journal of Botany* 21, 53-76.
- Prebble, W.M. (1967). Tongariro Power Development. Western diversions. Report on the geology of Otamangakau upper dam site. New Zealand Geological Survey, Wellington. 8 pages.
- Prebble, W.M. (1969). Tongariro Power Development. Engineering geology of the Te Whaiiau dam site. A report on the geological investigations. New Zealand Geological Survey, Wellington. 10 pages.

Stop 4A-5 – An overview of the silicic volcanism of central TVZ, Te Ponanga Lookout, eastern slope of Kakaramea volcano

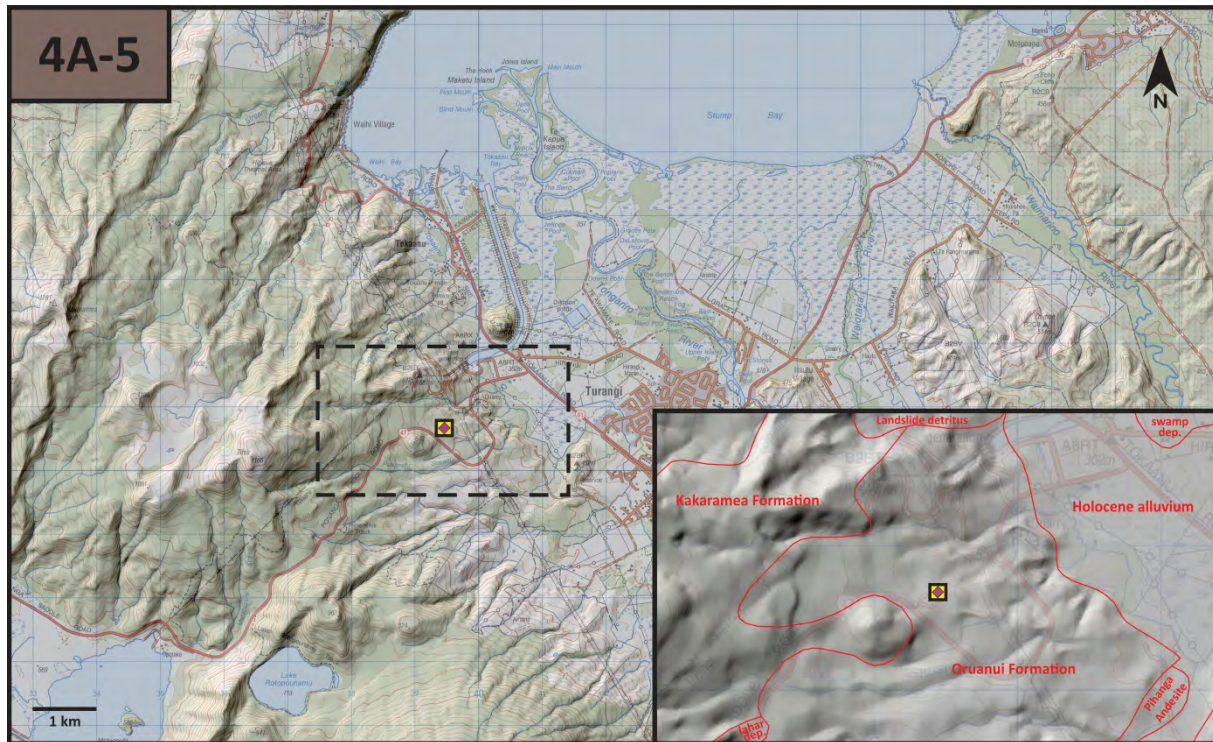


Fig. 44 – View from the eastern slopes of Kakaramea volcano to the Taupo Volcanic Centre mostly occupied by Lake Taupo. **a** Maunganamu (Mosquito Hill), **b** Rangitukua, **c** Karangahape, **d** Kaiapo Fault, **e** Tauhara, **f** Motuoapa Peninsula, **g** Korohe

The lookout is situated in the vicinity of a barely known monogenetic cone on the eastern slope of the ~220 ka Kakaramea andesitic volcano. The most recent activity of this area was occurred along the Rotopouname Graben hosting andesitic maars and scoria cones (Townsend et al. 2017). In good weather conditions the dome complex of Tarawera

may visible from here, which hosted the most recent basaltic and rhyolitic eruptions of the central TVZ in 1886 and 1314 AD, respectively (Nairn, 2002; Leonard et al., 2002). In an average day only the Lake Taupo and surrounding small-volume silicic and mafic volcanic centres can be observed along with the Tongariro delta located behind the dacitic

Maunganamu dome. The northern basin of Lake Taupo was the source of the two most recent caldera-forming eruptions of the TVZ. The deposits of the 25.4 ka Oruanui eruption (530 km³, DRE) form ignimbrite plateaus on the eastern and northern sides of the lake. The high cliff on the western side is composed of the ~350 ka Whakamaru Formation (Leonard et al. 2010). The 232 AD caldera-forming event of the Taupo volcano produced 35 km³ DRE volcanic material, which volumetrically mostly deposited as valley-ponded ignimbrites around Lake Taupo (Wilson and Walker, 1985). Subsequent barely-known activity was documented with lava dome formation and minor explosive activity at the bed of the newly forming lake postdating the climactic Taupo eruption by several decades (van Lichtan et al., 2016). Most of the small-volume silicic eruptions predate the Oruanui eruption, except Acacia dome, located on the ridge east from the Kaiapo Fault, and Ouaha Hills represent a fissure eruption sits on the top of the Oruanui ignimbrite plateau between f and g (Fig. 44) (Wilson et al. 2009). Kuharua and the dacite dome of Motuoapa Peninsula and Korohe may also postdate the Oruanui event (Figs. 10 and 44) (Kósik, 2018).

Suggested discussion points

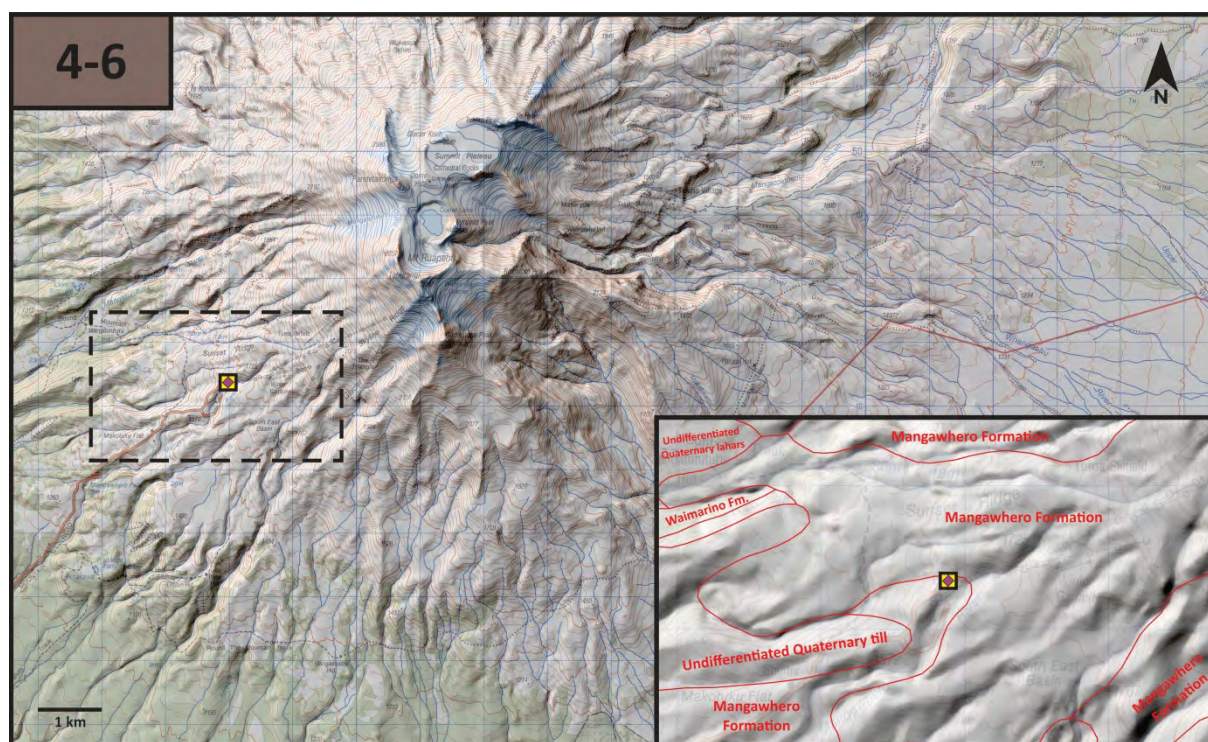
- 1) Discussion on the relative role of small-to-medium volume silicic eruptions in the total magmatic output of the central Taupo Volcanic Zone
- 2) Discussion on the variety of lava dome features associated with a large caldera-dominated volcanotectonic graben
- 3) Discussing the environmental impact of caldera-forming events in the terrestrial basins
- 4) Discussing of the relative lake level changes over short period of time and their impact on the terrestrial sedimentation of the region
- 5) Discussion on the lava dome morphology and their potential link to eruptive processes

- 6) Discussion on the potential geoenvironments lava domes can form between major caldera-forming eruptions
- 7) Discussion on the total sedimentary environment influenced by large caldera-forming events and lava dome eruptions of various styles.

Further reading

- Kósik, S., (2018). Small-volume volcanism associated with polygenetic volcanoes, Taupo Volcanic Zone, New Zealand, Unpublished PhD thesis, Massey University, Palmerston North, 304 pp.
- Leonard, G., Cole, J., Nairn, I. and Self, S., 2002. Basalt triggering of the c. AD 1305 Kaharoa rhyolite eruption, Tarawera volcanic complex, New Zealand. *Journal of Volcanology and Geothermal Research*, 115(3): 461-486.
- Leonard, G.S., Begg, J.G. and Wilson, C.J.N., 2010. Geology of the Rotorua area. Institute of Geological and Nuclear Sciences 1:250,000 geological map 5. sheet + 102 p. Lower Hutt, New Zealand. GNS Science.
- von Lichtan, I., White, J., Manville, V. and Ohneiser, C., (2016). Giant rafted pumice blocks from the most recent eruption of Taupo volcano, New Zealand: Insights from palaeomagnetic and textural data. *Journal of Volcanology and Geothermal Research*, 318: 73-88.
- Wilson, C.J.N. (2001). The 26.5 ka Oruanui eruption, New Zealand: an introduction and overview. *Journal of Volcanology and Geothermal Research*, 112(1-4): 133-174.
- Wilson, C.J.N., Gravley, D.M., Leonard, G.S. and Rowland, J.V., 2009. Volcanism in the central Taupo Volcanic Zone, New Zealand: tempo, styles and controls. *Studies in Volcanology: The Legacy of George Walker*. Special Publications of IAVCEI, 2: 225-247.
- Wilson, C.J.N., Houghton, B. and Lloyd, E., 1986. Volcanic history and evolution of the Maroa-Taupo area, central North Island, Late Cenozoic Volcanism in New Zealand. *Royal Society of New Zealand, Bulletin*, pp. 194-223.
- Wilson, C.J.N. and Walker, G.P.L., (1985). The Taupo eruption, New Zealand I. General aspects. *Philosophical Transactions of the Royal Society of London A: Mathematical, Physical and Engineering Sciences*, 314(1529):199-228.

Stop 4-6 – Turoa Skifield – recapping the Ruapehu experience



The SW sector of the edifice of Ruapehu is dominated by the lavas of Mangawhero Formation (Hackett, 1985) (Fig. 45). The lavas of this formation lie unconformably on the Te Herenga and Wahiano Formations and are intercalated with glacial deposits (Townsend et al., 2017). The formation at the cone consists of lava and monolithologic breccias, individual flows are between 1 and 100 m thick (Conway et al., 2015). Emplacement of Mangawhero lavas began at ~50 ka, following an apparent 30 ky hiatus in lava effusion at Ruapehu volcano (Conway et al., 2016).



Fig. 45. – Ski season on Mt Ruapehu (Turoa Skifield)

This location serves as a viewpoint to the Ruapehu central edifice as well as from the edifice toward the further ring plain region. Looking to the west, there is a good view to the summit of the Haungatahi volcano representing the oldest edifice in the southern TVZ (Fig. 46) (Cameron et al. 2010).

In this location, the participants will discuss and share the field trip experiences they gained from Mt. Ruapehu.

Suggested points for discussion

- 1) Discuss the sedimentary facies relationship between edifice building successions to medial to distal volcanic facies zones
- 2) Define and refine the definition of a ring plain in the context of the visited sites in and around Ruapehu
- 3) Share knowledge from other sites to compare with the visited sites at Ruapehu
- 4) Discuss the guideline of volcanic stratigraphy and geological mapping in active stratovolcanic terrains and refine their link to ancient settings
- 5) Discuss the volcanic core complex definition and define it



Fig. 46. – View to the ~900 ka andesitic Hauhungatahi volcano from Turoa. Note that the steep-sided base of this volcano is the late Miocene mudstone of Matemateaonga Formation

- 6) Discuss the volcanic edifice forming lava flows and their role in the total volcanic budget of a stratovolcano
- 7) Discuss the steps needed to follow to establish volcanic stratigraphy of lava flow dominated versus pyroclastic succession dominated volcanoes on the basis of their edifice building successions
- 8) Explore other sedimentary processes contribute to shape a stratovolcano in high altitude
- 9) Compare Ruapehu experience with other large stratovolcanoes and define end-member edifice architecture, sedimentary environment and erosion processes that play key roles in the edifice development
- 10) Discuss the link between proximal to distal fall out tephra units and how to define the boundary of a ring plain

Further reading

- Cameron, E., Gamble, J., Price, R., Smith, I., McIntosh, W. and Gardner, M. (2010). The petrology, geochronology and geochemistry of Hauhungatahi volcano, SW Taupo Volcanic Zone. *Journal of Volcanology and Geothermal Research*, 190(1-2): 179-191
- Conway, C.E., Leonard, G.S., Townsend, D.B., Calvert, A.T., Wilson, C.J., Gamble, J.A. and Eaves, S.R. (2016). A high-resolution $^{40}\text{Ar}/^{39}\text{Ar}$ lava chronology and edifice construction history for Ruapehu volcano, New Zealand. *Journal of Volcanology and Geothermal Research*, 327: 152-179.
- Conway, C.E., Townsend, D.B., Leonard, G.S., Wilson, C.J.N., Calvert, A.T. and Gamble, J.A. (2015). Lava-ice interaction on a large composite volcano: a case study from Ruapehu, New Zealand. *Bulletin of Volcanology*, 77(3): 21.
- Hackett, W.R. (1985). *Geology and petrology of Ruapehu volcano and related vents*, Unpublished PhD thesis, Victoria University of Wellington, Wellington, 312 pp.
- Townsend, D., Leonard, G.S., Conway, C., Eaves, S.R. and Wilson, C.J.N., 2017. *Geology of the Tongariro National Park area*, scale 1:60,000, GNS Science geological map 4. 1 sheet + 109 p. GNS Science.

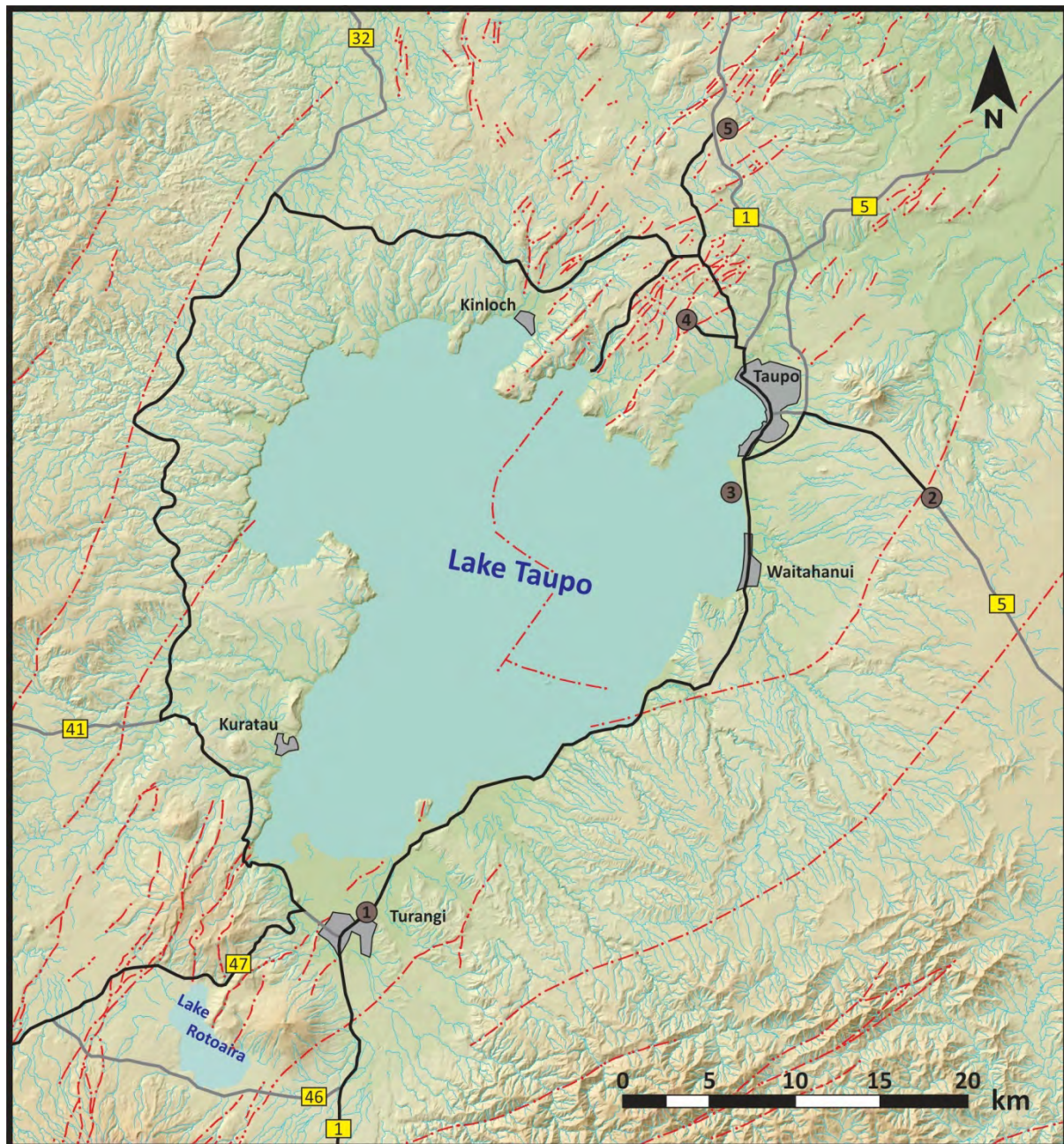
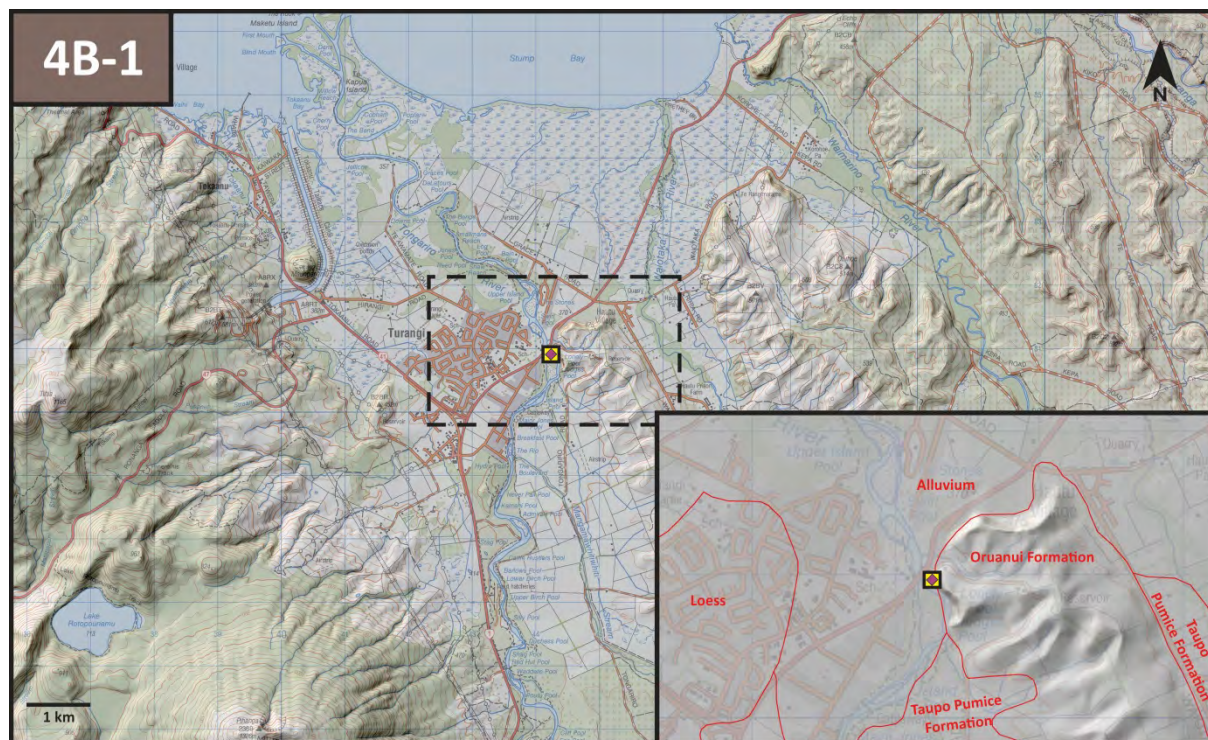
Field excursion to the central Taupo Volcanic Zone

Fig. 46 – Topographic overview of the Taupo Volcanic Centre. Active fault lines are represented by dashed red lines, while townships are shown by grey areas. Field stop locations are marked by colour-coded numbers, according to the programme shown in Table 1. The roads followed during the trip are indicated with black continuous line, other main roads are indicated with grey continuous line.

Stop 4B-1 – Oruanui Formation; accretionary lapilli-bearing ignimbrite section, Turangi (Taupo Volcanic Centre)



The 25.4 ka Oruanui eruption was the largest caldera-forming eruption of New Zealand since the ~350 ka Whakamaru event. It produced 530 km³ DRE volcanic materials characterised by extremely large dispersal (Table 2, Fig. 47) (Wilson 2001; Vandergoes 2013). The Oruanui event is divided into 10 Plinian phases based on nine mappable fall units and a further, poorly preserved, but volumetrically dominant fall unit. Fall units 1-9 individually range from 0.8 to 85 km³ and display a wide range of depositional features, from dry to

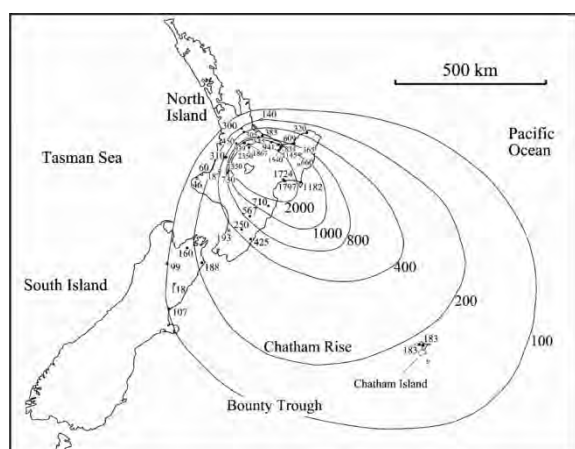


Fig. 47. – Reconstructed isopach map for the total Oruanui fall deposits, modified after Wilson (2001).

water saturated, reflecting different locations of source vents and resulting varied magma-water ratios. Multiple bedding and normal grading of the deposits of phase 1-3 indicate short-lived but intense burst of activity that were separated by time breaks from minutes up to several weeks to months. The widely dispersed fall deposits of the Oruanui eruption originally present over most of New Zealand and jointly form a distal marker horizon variously called Aokautere Ash, Kawakawa Tephra or Oruanui tephra. The Oruanui deposits were extensively reworked by central North Island rivers and strong winds during the last glacial maximum to form part of the fluvial Hinuera Formation or the wind-blown Mokai Sand Formation, respectively.

Dilute and concentrated pyroclastic density currents (PDC) were common during the entire eruptive episode, but the latter being volumetrically dominant (>90 %). Deposits of PDCs range from mm-to cm thick veneer enclosed within fall to 200 m-thick ignimbrite in proximal localities. The volume of PDC deposits was estimated to be 740 km³ including intracaldera successions (Davy and Caldwell, 1998; Wilson, 2001).

The eruptive vents were located within the area now occupied by the northern basin of Lake Taupo (Wilson, 2001), which area might have been similar

to the present day Okataina Volcanic Centre with remnants of the Lake Huka that was subdivided by lava dome complexes (Leonard et al. 2010).

The visited outcrop exposes a relatively proximal sequence of Oruanui ignimbrite with gas-segregation pipes and accretionary lapilli along the right bank of Tongariro River located about 25 km from the source (Figs. 48-49).



Fig. 48. – Tongariro River photographed from the bridge of State Highway 1. The cliffs on the left side expose the Oruanui Formation with accretionary lapilli up to 2 cm in size.

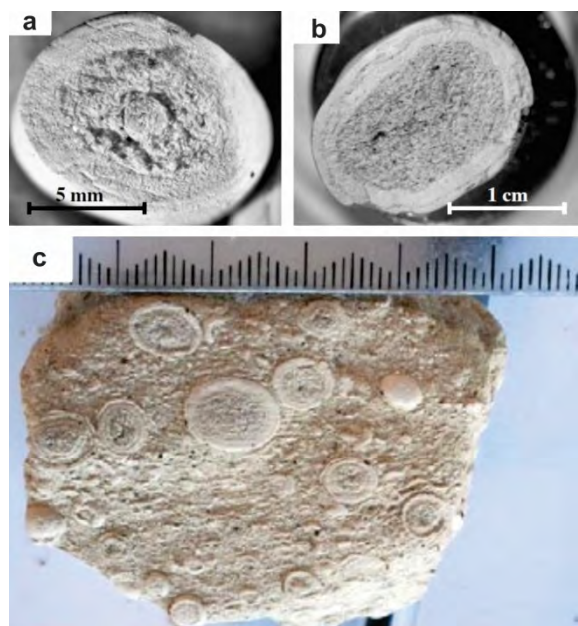


Fig. 49. – Examples for ultrafine rim-type accretionary lapilli (a, b) and aggregates floating in a matrix of individual particles and fragmented aggregates from the Oruanui ignimbrite proximal facies (Van Eaton and Wilson, 2013)

Suggested discussion points

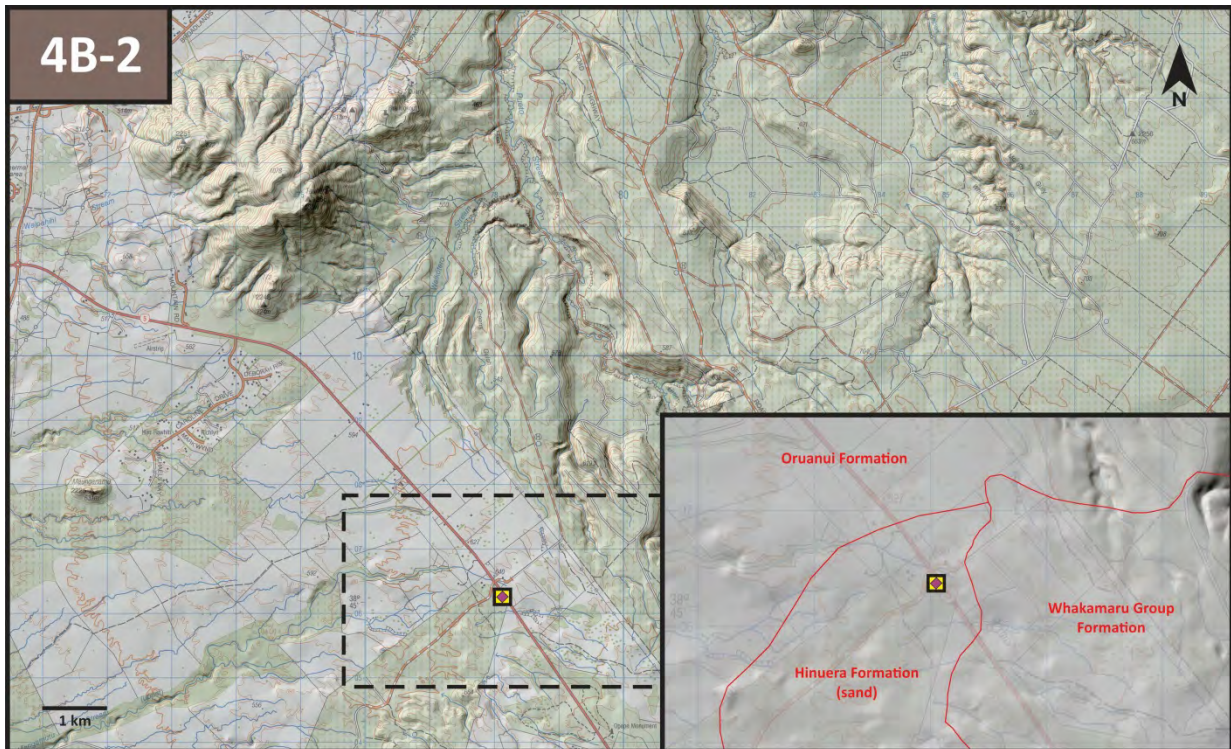
- 1) Discussion on the origin of ash aggregates through Phreatoplinian eruptions
- 2) The role of external water in ash aggregation
- 3) The role of meteorological conditions in ash aggregation

- 4) The role of the fragmentation energy in ash aggregation
- 5) Discussion on the mechanism of gas escape pipe formation
- 6) Discussion on the usage of large volume and laterally extensive non-welded ignimbrites in geological mapping
- 7) Discussion on the correlation problems between ignimbrite and associated fall out tephra, the role of new dating techniques
- 8) Discussion on the landscape building effects of large ignimbrite forming eruptions

Further reading

- Allan, A.S., Morgan, D.J., Wilson, C.J. and Millet, M.-A., (2013). From mush to eruption in centuries: assembly of the super-sized Oruanui magma body. *Contributions to Mineralogy and Petrology*, 166(1): 143-164.
- Davy, B. and Caldwell, T., (1998). Gravity, magnetic and seismic surveys of the caldera complex, Lake Taupo, North Island, New Zealand. *Journal of volcanology and geothermal research*, 81(1): 69-89.
- Manville, V. and Wilson, C.J.N., 2004. The 26.5 ka Oruanui eruption, New Zealand: a review of the roles of volcanism and climate in the post-eruptive sedimentary response. *New Zealand Journal of Geology and Geophysics*, 47(3): 525-547.
- Leonard, G.S., Begg, J.G. and Wilson, C.J.N. (2010). *Geology of the Rotorua area. Institute of Geological and Nuclear Sciences 1:250,000 geological map 5. sheet + 102 p. Lower Hutt, New Zealand. GNS Science.*
- Van Eaton, A.R. and Wilson, C.J.N. (2013). The nature, origins and distribution of ash aggregates in a large-scale wet eruption deposit: Oruanui, New Zealand. *Journal of Volcanology and Geothermal research* 250: 129-154.
- Vandergoes, M.J., Hogg, A.G., Lowe, D.J., Newnham, R.M., Denton, G.H., Southon, J., Barrell, D.J.A., Wilson, C.J.N., McGlone, M.S., Allan, A.S.R., Almond, P.C., Petchey, F., Dabell, K., Dieffenbacher-Krall, A.C. and Blaauw, M. (2013). A revised age for the Kawakawa/Oruanui tephra, a key marker for the Last Glacial Maximum in New Zealand. *Quaternary Science Reviews*, 74: 195-201.
- Vucetich, C.t. and Pullar, W., 1969. Stratigraphy and chronology of late Pleistocene volcanic ash beds in central North Island, New Zealand. *New Zealand Journal of Geology and Geophysics*, 12(4): 784-837.
- Wilson, C.J.N. (2001). The 26.5 ka Oruanui eruption, New Zealand: an introduction and overview. *Journal of Volcanology and Geothermal Research*, 112(1-4): 133-174.

Stop 4B-2 – Taupo Pumice Formation (Taupo Volcanic Centre)



The 232 AD caldera-forming eruption of Taupo Volcanic Centre was the most violent and complex rhyolitic eruption world-wide in the last 5000 years (Hogg et al., 2011, Smith and Houghton, 1995). Most of the Taupo Pumice Formation (TPF) by volume is a typically tens of metres thick valley-ponded ignimbrite. In many places near the source, the ignimbrite forms a terrace in valleys eroded into the older ignimbrite plateaus of the Oruanui Formation. The ignimbrite is usually poorly-consolidated with light-coloured ash and low-density pumice fragments (Leonard et al. 2010).

The Taupo-Napier Road section provides a comprehensive overlook of the different phases of the youngest Taupo eruption located in a high ground. The landscape is dominated by the primary and reworked deposits of Taupo Pumice eruption forming a plateau. Only the ~60 ka Tauhara dacite lava dome complex rises to the sky with block-and-ash flow fans along State Highway 1 (Lewis 1968).

The complete pyroclastic sequence of TPF comprises seven units erupted over six contrasting phases of activity (Wilson and Walker, 1985). (Fig. 50). The sequence includes phreatomagmatic deposits emplaced during three phases (units 1, 3, and 4), deposits of Plinian phases (units 2 and 5), an intra-Plinian ignimbrite unit (unit 6) emplaced during phase 5, and a final caldera-forming phase

involving violent emplacement of ignimbrite (unit 7) over a very wide area.

The initial ash (Unit 1) represents minor phreatomagmatic activity in the opening stages of the eruption (Wilson and Walker, 1985).

Unit 2 (Hatepe lapilli) is a mostly uniform, well-sorted, moderately-sized Plinian fall deposit (Walker, 1980).

The Hatepe ash (Unit 3) represents a period of large-scale phreatomagmatic activity when abundant external water gained access to the actively vesiculating magma (Walker, 1980). There is abundant evidence throughout this deposit of water-aided deposition and it has been described as an archetypal Phreatoplinian deposit. Over a significant part of its dispersal area, the top of the Hatepe ash is intensively eroded and it is inferred that the water for this gullying was ejected from the lake (Walker 1980).

The Rotongaio ash (Unit 4) has been interpreted as the product of large-scale phreatomagmatic activity, however it is quite different to the Hatepe ash. It is strikingly fine grained with little material coarser than 1 mm, even in the most proximal exposures, and it is composed mainly of poorly to non-vesicular juvenile material. The unit is typically plane-parallel bedded on a mm-to-cm scale, and beds consist mostly of a range of small

(1-3mm) ash aggregates or show vesicular ash textures. Also, the unit contains numerous intra-formational gullies and rills produced by syn-eruptive erosion. Many thin beds have adhered to steep slopes indicating accumulation as cohesive ash, but thicker beds have typically slumped as a mobile ash-slurry.



Fig. 50. – Stratigraphy of the 232 AD Taupo eruption sequence

Unit 5 (Taupo Plinian pumice/Taupo lapilli) records the sudden return to a magmatic fragmentation involving rapid discharge of very gas-rich magma and fallout of pumice lapilli over a very wide area (Walker, 1980). This unit is notable for its extremely wide dispersal and the very low rate of thinning with distance from vent, and was termed 'ultraplinian' by Walker (1980).

Isopach maps of this unit and orientation of logs in unit 7 (Taupo ignimbrite) were used to first suggest Horomatangi Reefs as a vent location for the Taupo Pumice eruption. Taupo ignimbrite (Unit 7) was emplaced as the climactic phase of the eruption triggered by a caldera collapse. Deposits of Unit 7 travelled radially outwards for at least 80 km and up to 300 m/s. The unit is spread very thinly and exhibits considerable lateral facies variation due to the deposition from a relatively dilute and turbulent current.

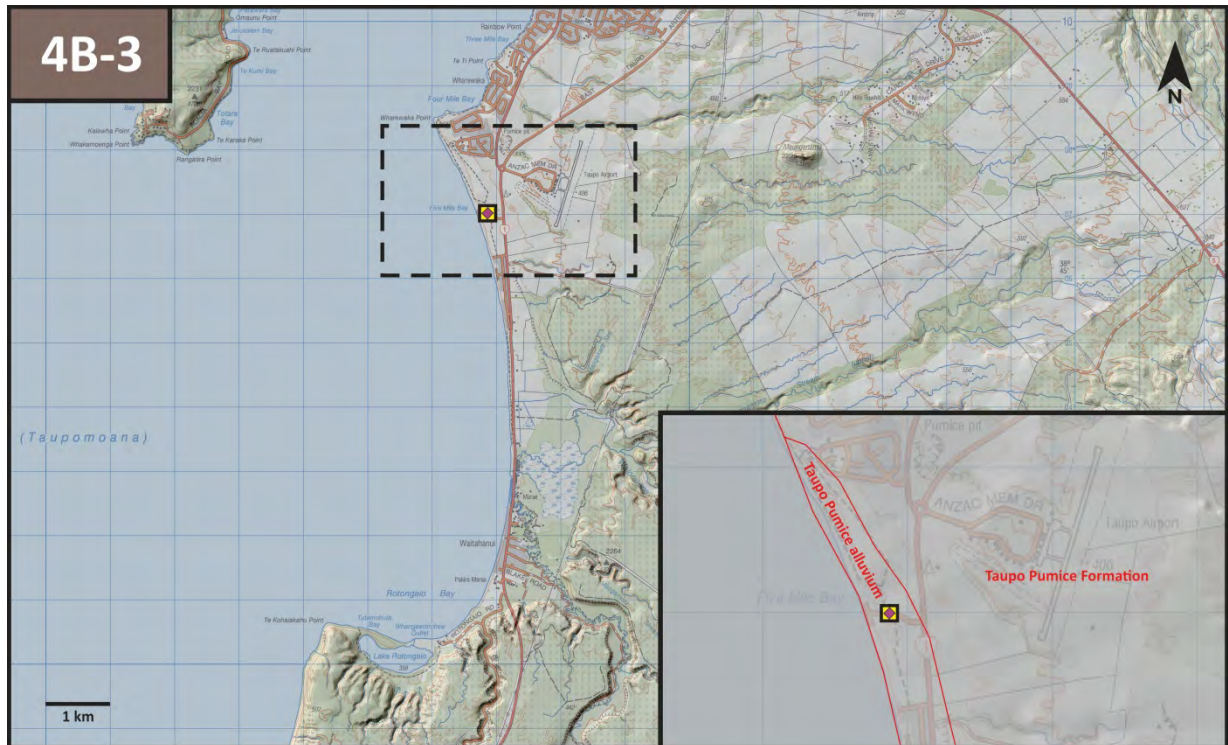
Suggested discussion points

- 1) How can we trace depositional breaks in the volcanic activity in a sequence that formed by highly unstable eruptive processes
- 2) What is the timeframe of the deposition of such a complex eruptive sequence and how that can be supported
- 3) Identifying the relative role of phreatomagmatic fragmentation in pyroclast formation in large pumiceous, caldera-forming eruptions
- 4) How can we distinguish or identify depositional sequences related to large-volume silicic eruptions from those forming successive small- to medium-volume explosive eruptions dominated by lava dome associated processes.
- 5) How confidently possible to correlate individual eruptive units across a complicated landscape morphology

Further reading

- Froggatt, P.C. (1981). Stratigraphy and nature of Taupo Pumice Formation, *New Zealand Journal of Geology and Geophysics* 24(2): 231-248.
- Hogg, A., Lowe, D.J., Palmer, J., Boswijk, G. and Ramsey, C.B., (2011). Revised calendar date for the Taupo eruption derived by ¹⁴C wiggle-matching using a New Zealand kauri ¹⁴C calibration data set. *The Holocene*: 0959683611425551.
- Lewis, J.F., (1968). Tauhara Volcano, Taupo Zone: Part I—Geology and Structure. *New Zealand Journal of Geology and Geophysics*, 11(1): 212-224.
- Rosenberg, M.D., (2017). Volcanic and tectonic perspectives on the age and evolution of the Wairakei-Tauhara geothermal system, Unpublished PhD thesis, Victoria University of Wellington, Wellington
- Smith, R.T. and Houghton, B.F. (1995). Delayed deposition of plinian pumice during Phreatoplinian volcanism: the 1800-yr-B.P. Taupo eruption, *New Zealand Journal of Volcanology and Geothermal Research* 67: 221-226.
- Walker, G.P.L. (1980) The Taupo pumice; Product of the most powerful known (ultraplinian) eruption? *Journal of Volcanology and Geothermal Research* 8: 69-94.
- Walker, G.P.L., Wilson, C.J.N. and Froggatt, P.C. (1981). An ignimbrite veneer deposit: the trail-marker of a pyroclastic flow *Journal of Volcanology and Geothermal Research* 9: 409-421.
- Wilson, C.J.N. and Walker, G.P.L., (1985). The Taupo eruption, *New Zealand I. General aspects. Philosophical Transactions of the Royal Society of London A: Mathematical, Physical and Engineering Sciences*, 314(1529):199-228.
- Wilson, C.J.N., 1985. The Taupo eruption, *New Zealand II. The Taupo Ignimbrite. Philosophical Transactions of the Royal Society of London A: Mathematical, Physical and Engineering Sciences*, 314(1529): 229-310.

Stop 4B-3 – Formation of lake terraces and post-eruption lacustrine sedimentation (Five Mile Bay, Taupo Volcanic Centre)



After the 232 AD Taupo eruption the caldera collapse structures and volcanotectonic depression at the southern basin of the present day Lake Taupo subsequently were refilled from precipitation runoff. The post-1.8 ka high stand of the lake was at ~34 m above its present level (390 m asl.). Estimates of the time necessary for the lake to refill to 390 m asl. based on hypsometry and estimated precipitation runoff vary from 15 to 40 yr. Then the lake rapidly fell back to the modern level as the confining dam at the lake outlet catastrophically failed and was eroded away (Manville et al., 1999, Manville, 2002) discharging ~23 km³ of water in total.

The cliffs located near the shore of Five Mile Bay formed during the regression of lake shore from its maximum extent consist of pumiceous sand and gravels and giant pumiceous fragments (Fig. 51). The bedded lacustrine deposits laid down as the lake level was rising, whereas the large highly vesicular blocks formed as a carapace of lava domes most likely at the Horomatangi Reef and Waitahanui Bank. Explosive activity of dome extrusion broke off fragments from the carapace, where the most vesicular parts floated to the lake surface and were driven ashore by the prevailing westerly winds (Wilson and Walker, 1985; von Lichten, 2016). Most of the large pumiceous blocks display polygonal joints generated by contraction during

rapid cooling and often characterised by the same paleomagnetic alignment indicating that the interior of the blocks was remained above the Curie point when they stranded.



Fig. 51. – Highly-vesicular block of lava from the carapace of subaqueous lava domes.

From the beach, there is a good view to the 5.3 ka fissure vents of Ouaha Hill located south from the Five Mile Beach on the top of the Oruanui

ignimbrite plateau, as well as to the other side of the Acacia bay, where the highest points of the distant long ridge represent the mafic monogenetic centres will be visited during the next stop.

Suggested discussion points

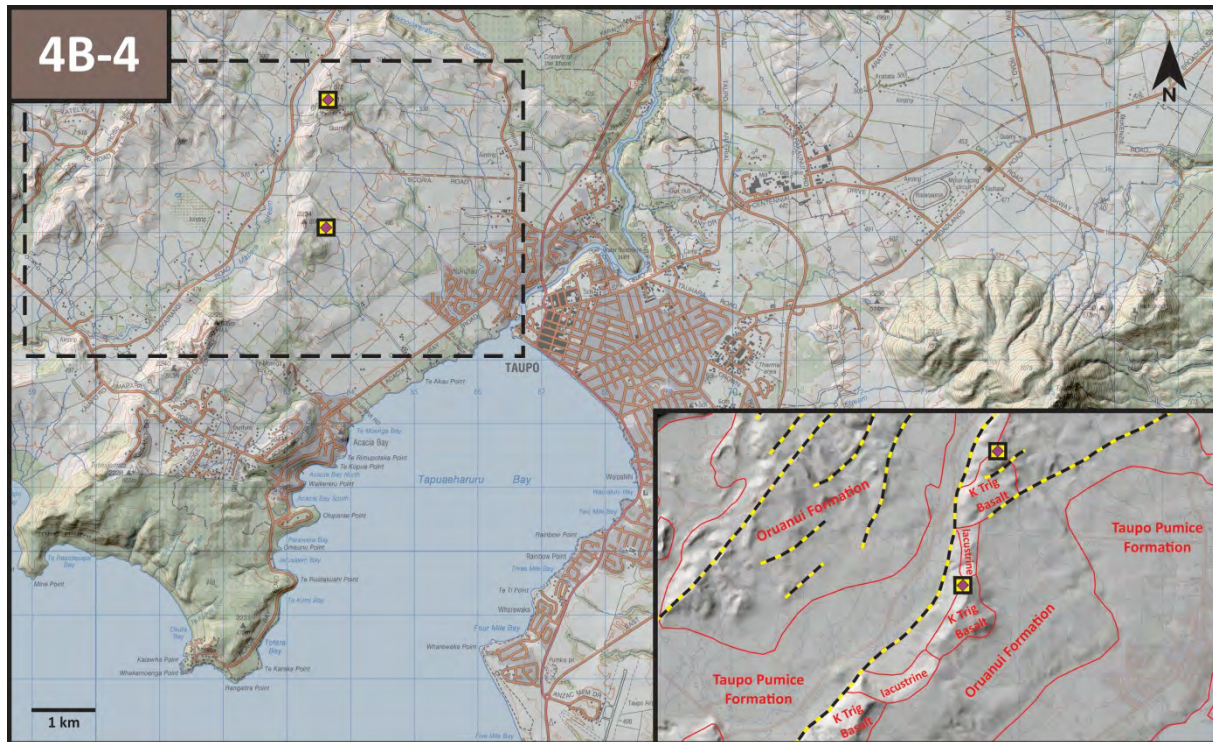
- 1) Discussion on the formation of lacustrine terraces as indicators for the evolution and volcanic activity of large silicic systems (e.g. surface deformation, lake level changes)
- 2) Discussion on the landscape modifying effect of large volume silicic eruptions
- 3) Discussion on the variety of sedimentary environment can be produced by large volume silicic eruptions and the time frame the landscape reset to its original conditions
- 4) Discussion on the drainage pattern disturbance a large scale silicic explosive eruption can cause
- 5) Discussion over the natural hazard aspects of large scale silicic eruptions
- 6) Discussion over the total addition of pumiceous fragments to the total sedimentary budget of a terrestrial to marine setting influenced by frequent volcanic eruptions.

- 7) Discussion over the sudden and abrupt variations of geo-environments large scale silicic eruptions can produce in what subsequent volcanism take place.

Further reading

- Manville, V. (2002). Sedimentary and geomorphic responses to ignimbrite emplacement: readjustment of the Waikato River after the AD 181 Taupo eruption, New Zealand. *The Journal of Geology*, 110(5): 519-541.
- Manville, V., White, J.D.L., Houghton, B. and Wilson, C.J.N, (1999). Paleohydrology and sedimentology of a post-1.8 ka breakout flood from intracaldera Lake Taupo, North Island, New Zealand. *Geological Society of America Bulletin*, 111(10): 1435-1447.
- von Lichten, I., White, J., Manville, V. and Ohneiser, C., (2016). Giant rafted pumice blocks from the most recent eruption of Taupo volcano, New Zealand: Insights from palaeomagnetic and textural data. *Journal of Volcanology and Geothermal Research*, 318: 73-88.
- Wilson, C.J.N. and Walker, G.P.L., (1985). The Taupo eruption, New Zealand I. General aspects. *Philosophical Transactions of the Royal Society of London A: Mathematical, Physical and Engineering Sciences*, 314(1529):199-228.

Stop 4B-4 – Punatekahi Complex – small-volume mafic volcanism of the Taupo Volcanic Centre



Basaltic volcanic eruptions along the Taupo Volcanic Zone are volumetrically minor however represent great diversity of volcano type formation from maars, tuff rings, tuff cones and scoria cones (Wilson and Smith, 1985; Brown et al., 1994; Hiess et al., 2007; Sable et al., 2009). Punatekahi Complex formed along a NE-SW trending normal fault system just NW of the present day Taupo Lake. The eruptive products overlay a complex stratigraphy of the Whakamaru Ignimbrite (~350 ka) covered by complex volcanoclastic succession of lacustrine units that are part of the Waiora Formation (~350-200 ka) and covered by the sub-horizontal lacustrine beds of the Huka Falls Formation (~200-25 ka). K/Ar dating of the products of these basaltic eruptions (K-Trig Basalt) yields an age of ~140 ka.

Extensive explosive phreatomagmatism that resulting in the formation of the K-trig basaltic tuff cone is known just about 3 km to the SW from the Punatekahi Complex. The Punatekahi Complex is well exposed due to active quarrying in two chains of open pit scoria quarries providing accessible half section of scoria cones. In the northern side of the basaltic cones excavation reached the deep level of the former volcanic craters exposing numerous unconformity surfaces marking the 3D architecture of the former cones. In this sections agglomeratic scoria, clastogenic spatter and rheomorphic lava flows forming individual lumps of coherent-like

rock bodies inferred to be ponded in local vents of the growing cones (Fig. 52). In this succession, non-welded scoria forms loose, grain-supported moderately vesicular layers.



Fig. 52. – Red scoria grading into clastogenic lava flows in the centre of the scoria cone

Vesicle shapes are in most of the scoriaceous deposits indicate vesicle collapses, chilled margins around larger lapilli and some limited volume of accidental volcanic lithics indicating some effect of external water during the magmatic gas-driven explosive fragmentation of pyroclasts. In addition, the successions expose a laterally continuous dm-to-m thick unit that is very rich in cauliflower shape bomb and lapilli. These fragments show typical

chilled margins, cauliflower shapes and additional exotic lithic accumulations (Fig. 53).



Fig. 53. – . Cauliflower bomb from the middle of the scoria cone proximal setting

This specific unit in the middle of the half section of the cone inferred to be the product of sudden access of external water to the active fountain feeding conduit causing contractions, chilling and quench fragmentation (Fig. 54).



Fig. 54. – Cauliflower bomb from the middle of the scoria cone proximal setting

In the SW vents scoriaceous successions show bedded characters with some low to moderately vesicular ash and lapilli suggesting more steady state fragmentation where mild external water influence is inferred. The demonstrated architecture is coherent with the syn-eruptive paleoenvironment and also highlight the prospect of more explosive phases even in random or unexpected fashion to interfere with otherwise normal Strombolian style explosive eruption phases if basaltic magma would erupt in areas where the shallow subsurface rock units are porous and potentially influenced by ground water tables effected by the nearby large water mass of any

lacustrine system such as the present day Lake Taupo (Fig. 55).



Fig. 55. – Overview of the exposed diatreme of the Punatekahi scoria cone complex with pumiceous cover beds over the top of the eroded scoria cone

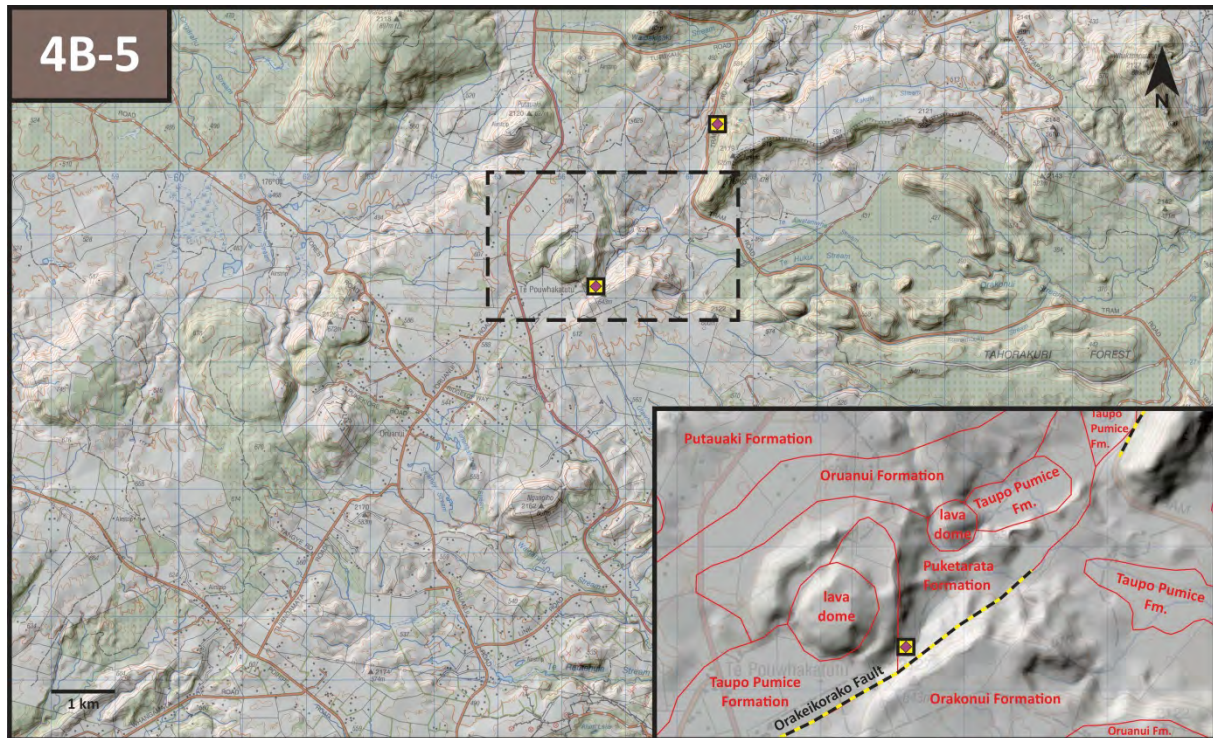
Suggested discussion points

- 1) Role of phreatomagmatism in the growth of an otherwise dry small-volume volcano (scoria cone)
- 2) Preservation potential of small-volume basaltic volcanoes in a silicic eruption-dominated volcanic system
- 3) Formation of cauliflower bombs
- 4) Diatremes and feeder systems of small-volume mafic volcanoes
- 5) Sedimentary history locked in cover beds and their meaning

Further reading

- Brown, S., Smith, R., Cole, J. and Houghton, B.F. (1994). Compositional and textural characteristics of the strombolian and surtseyan K-Trig basalts, Taupo Volcanic Centre, New Zealand: Implications for eruption dynamics. *New Zealand Journal of Geology and Geophysics*, 37(1): 113-126.
- Hiess, J., Cole, J.W. and Spinks, K.D., 2007. Influence of the crust and crustal structure on the location and composition of high-alumina basalts of the Taupo Volcanic Zone, New Zealand. *New Zealand Journal of Geology and Geophysics*, 50(4): 327-342.
- Sable, J., Houghton, B., Wilson, C. and Carey, R., 2009. Eruption mechanisms during the climax of the Tarawera 1886 basaltic Plinian eruption inferred from microtextural characteristics of the deposits. *Studies in volcanology. The legacy of George Walker*. Geological Society, London: 129-154.
- Wilson, C.J.N. and Smith, I.E.M., (1985). A basaltic phreatomagmatic eruptive centre at Acacia Bay, Taupo volcanic centre. *Journal of the Royal Society of New Zealand*, 15(3): 329-337.

Stop 4B-5 – Small-volume silicic volcanism in the central TVZ (tuff rings, maars and lava domes at Puketerata, Maroa Volcanic Centre)



The Puketerata (or Puketarata) Volcanic Complex (PVC) formed as a result of a series of rhyolitic eruptions along a 2.5 km long NE-trending eruptive fissure at the southern margin of Maroa Volcanic Centre (Whakamaru caldera) at ~16 ka. Initial deep-seated explosions were excavated and widen the pre-existing volcanic structures associated to earlier basaltic activity (Kósik et al., 2017b). The subsequent emplacement of two lava domes and associated shallow-seated phreatomagmatic activity produced a widespread tephra blanket characterized by alternating surge and fall dominated pyroclastic

units. The silicic magma erupted during the Puketerata activity was highly degassed, where explosive fragmentation was driven only by the interaction with external water. The lava domes and ejecta ring makes up more than two-thirds ($98 \times 10^6 \text{ m}^3$ DRE) of the total eruptive volume ($\sim 143 \times 10^6 \text{ m}^3$ DRE). The compound ring structures surrounding the larger dome totally overlap the underlying volcanic landforms that formed during the initial phase (Figs. 55-56). The ejecta ring around the larger dome represents a complex landform, which predominantly consists of outwardly thinning

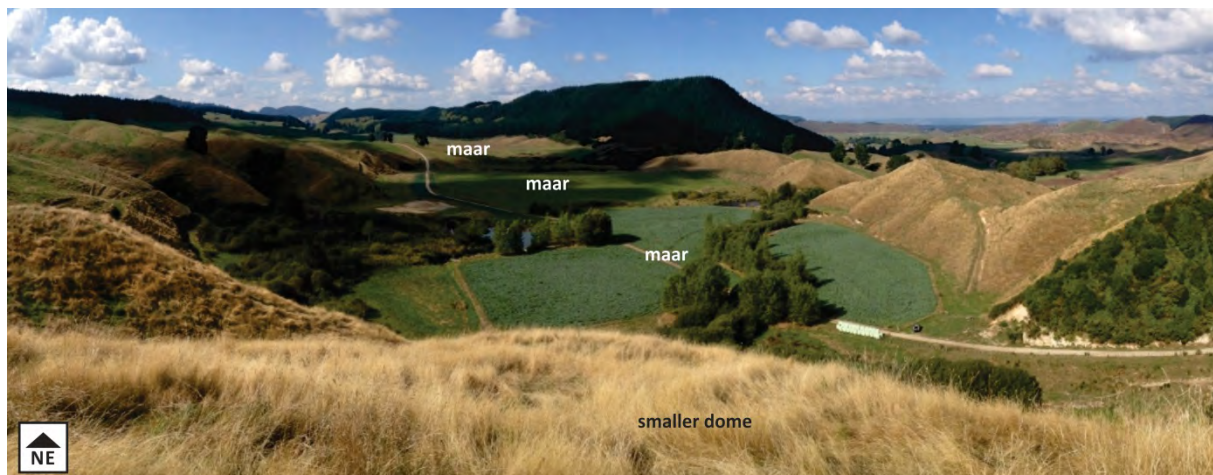


Fig. 55. – View from the summit of the smaller dome to chain of the coalesced maar craters at the NE end of the fissure.



Fig. 56. – Panoramic view of the larger dome and the surrounding ejecta ring from the top of the scarp of the Orakeikorako Fault

pyroclastic breccias forming of outwardly thinning pyroclastic breccias forming fan-shape bodies relating to the series of destruction of the larger dome (Fig. 57). Despite the relatively large combined

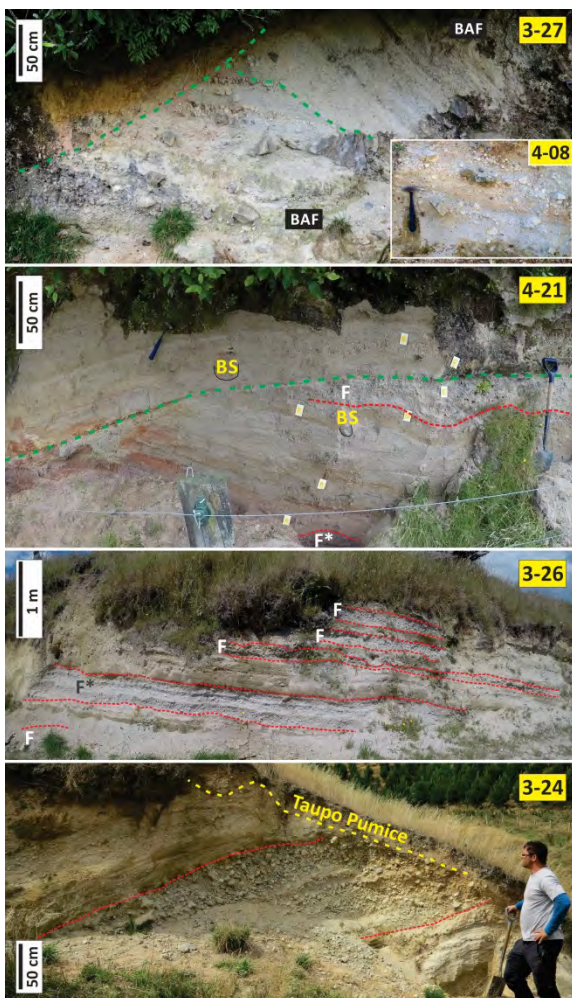


Fig. 57. – Key outcrops are locating at proximal locations. Fall beds (F) are delimited by red dashed lines, internal disconformities by green dashed lines indicate.

dispersal area of the pyroclastic deposits generated by the entire activity (235 km^2), the volume of single fall beds suggest that individual explosive events was not exceeding VEI 2-3 magnitudes.

Understanding the volcanic processes operated at PVC it was essential to examine the internal stratigraphy and sedimentological properties of PVC deposits along with the physical and textural properties (Fig. 58) of their pyroclastic fragments. Moreover, the geomorphic observations and DEM-based analysis also contributed to the clarification of volcanic history of this monogenetic volcano.

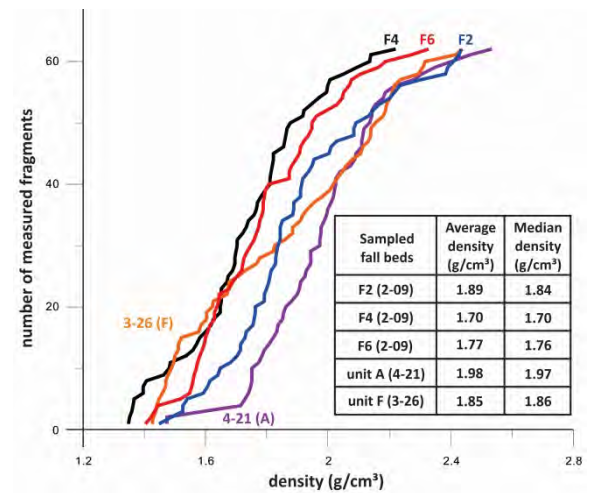


Fig. 58. – Density distribution of essential clast from selected major fallout beds.

The PVC also provides a good example for laterally quickly changing facies characteristics especially between proximal and medial sections (Figs. 57 and 59) as well as for the evolution of landscape in response to the different facies of locally distributed deposits of small-volume eruptions and ignimbrites sourced from large caldera-forming eruptions. The area of Puketerata is dominated by dissected overlapping ignimbrite plateaus forming sequences

of the Orakonui and Oruanui ignimbrites. The patchy appearance of Puketerata deposits indicates dynamic erosion during the late Quaternary affecting the area characterized by re-incision of two paleovalleys exposing the sequence between the ejecta ring and a smaller dome and at the eastern side of the tuff ring nearby the Orakeikorako Fault. The last major surface forming event affecting this area was the 232 AD Taupo eruption, whose products mantled and smoothed the landscape. The depressions of maar craters and valleys were filled up with thick ignimbrite deposits resetting the landscape.



Fig. 59. – Main outcrops at the road cut of State Highway 1. Major fall beds (F1 to F8) are delimited by red dashed line, block-and-ash flow units (BAF) delimited by black dashed line with yellow background. BS: bomb sags. Yellow dashed lines indicate the boundary between the basement, Puketerata and the subsequent Taupo Pumice deposits. Blue dashed and dotted lines indicate faults and related displacements.

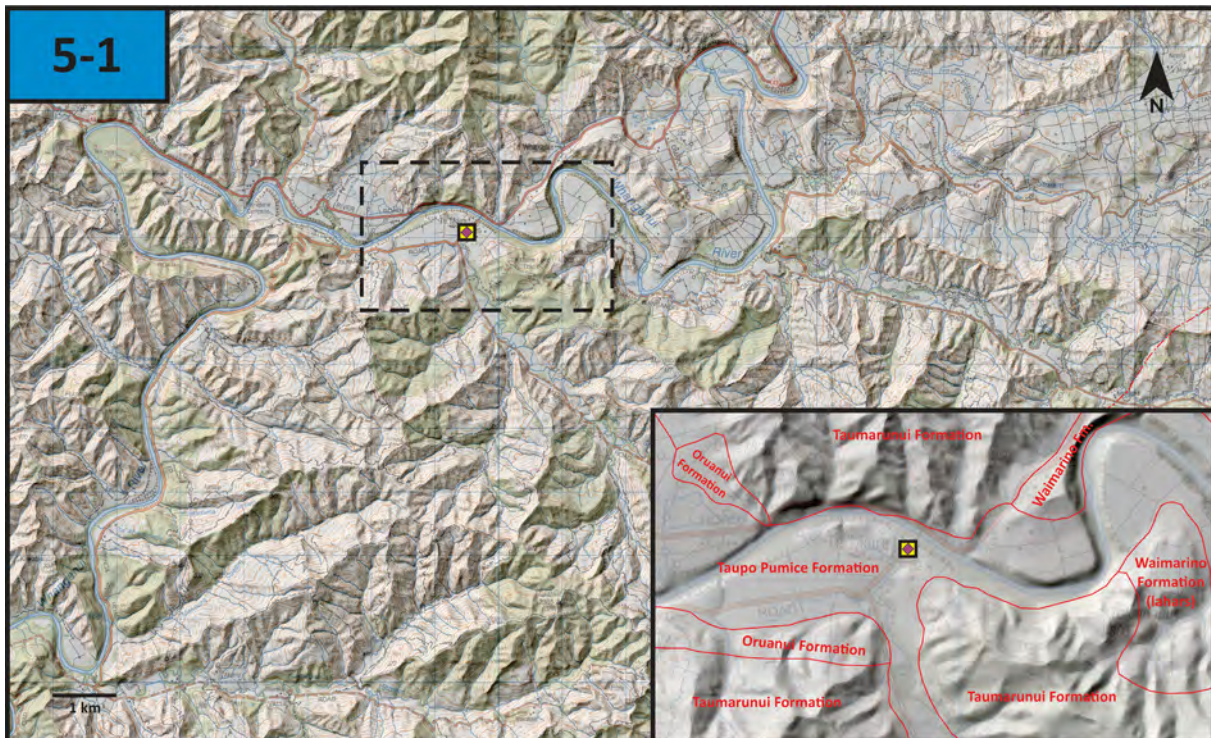
Suggested discussion points

- 1) Role of lava dome growth, eruption and erosion in the total sedimentary budget of silicic caldera-dominated systems
- 2) Challenges of mapping of volcanic units of small-volume localized and large volume laterally extensive eruptive products in buried and re-incised paleovalleys
- 3) Discussion on the link of various volcanic facies associated with the central lava domes and the surrounding pyroclastic rim
- 4) Discussion on the eruptive mechanism of silicic fissure eruptions
- 5) Discussion on the magma mingling and mixing along regionally controlled structural zones
- 6) Discussion on the volcanic hazards a fissure eruption can cause between major silicic, caldera-forming events
- 7) Discussion on the link between small volume mafic and large volume silicic eruptions in the TVZ and elsewhere

Further reading

- Brooker, M.R., Houghton, B.F., Wilson, C.J.N. and Gamble, J.A. (1993). Pyroclastic phases of a rhyolitic dome-building eruption: Puketerata Tuff Ring, Taupo Volcanic Zone, New Zealand. *Bulletin of Volcanology*, 55(6): 395-406.
- Kósik, S., Németh, K., Lexa, J. and Procter, J.N. (2017a). Understanding the evolution of a small-volume silicic fissure eruption: Puketerata Volcanic Complex, Taupo Volcanic Zone, New Zealand. *Journal of Volcanology and Geothermal Research*.
- Kósik, S., Németh, K., Procter, J.N. and Zellmer, G.F. (2017b). Maar-diatreme volcanism relating to the pyroclastic sequence of a newly discovered high-alumina basalt in the Maroa Volcanic Centre, Taupo Volcanic Zone, New Zealand. *Journal of Volcanology and Geothermal Research*, 341: 363-370.
- Lloyd, E.F. (1972). *Geology and hot springs of Orakeikorako, New Zealand*. Department of Scientific and Industrial Research.
- Shane, P., Smith V.C., Lowe D.J. and Nairn I. (2003). Re-identification of c. 15 700 cal yr BP tephra bed at Kaipo Bog, eastern North Island: Implications for dispersal of Rotorua and Puketerata tephra beds, New Zealand *Journal of Geology and Geophysics* 46(4): 591-596.

Stop 5-1 – Landscape response to ignimbrite deposition; valley-ponded ignimbrite facies of Taupo Pumice Formation



In this location the participants can enjoy a vista to a deeply incised fluvial valley of Whanganui River that exposes lahar deposits sourced from the Ruapehu volcano and valley-ponded facies of the Taupo Pumice Formation (Fig. 60). For more detail about Taupo Pumice Formation see Stop 4B-2.



Fig. 60 – Panoramic view to the meandering Whanganui River.

The Whanganui River, the second longest in the North Island, rises on the western side of the TVZ with the highest parts of its catchment on the western flanks of Mt. Ruapehu. After leaving the ring plain the river turns to southwards in a steep-walled gorge cut through uplifted and deeply dissected Miocene–Pleistocene marine sediments of the Wanganui Basin (Manville et al. 2009).

The river catchments of central North Island were strongly effected by the ignimbrite deposition followed the 232 AD Taupo eruption (Wilson, 1985; Wilson and Walker, 1985).

Valley-ponded ignimbrites forms a flat-topped terrace nearly all the valleys and depressions out to 70 km from the vent(s) of Taupo eruption. The thickness of ponds vary in thickness from less than 1 m to 70 m. Predominantly valley ponds comprise a single flow unit. At the side of the valleys or depressions the facies transforms to veneer deposits marked by several features, such as sub-horizontal upper surface changes to being sub-parallel to the pre-ignimbrite surface, decreasing size of pumice clast, and grainsize startification become visible. The transition may occur with 2 metres, where the local slope is steeper than 20°, whereas at low angle local slopes the transition takes tens to hundreds of meters (Wilson, 1985).

Near to the headwaters of fluvial systems, such as our current location, the characteristic process was the erosion of the ignimbrite and formation of river terraces (Fig. 61).

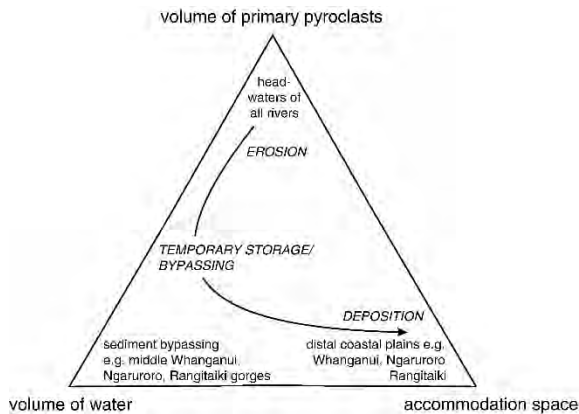


Fig. 61 – Ternary diagram representing the relative roles of pyroclastic volume, river discharge, and accommodation space in governing the style of landscape response in the catchments impacted by the 232 AD Taupo eruption (from Manville et al. 2009).

Suggested discussion points

- 1) Discussion on the interaction between normal background (fluvial) sedimentation and sudden input of volcanoclastic material due to laharcic events, pyroclastic flows or volcanoclastic debris avalanches
- 2) The role of valley filling “flow” type volcanoclastic deposits in building a volcanostratigraphy framework for a volcanism-influenced terrain

- 3) How can we trace valley-filling volcanoclastic successions in ancient volcanic terrains and how can we use them to establish volcanic history of a region
- 4) Aggradational terrace formation and volcanoclastic mass flow deposits
- 5) Landscape evolution and fluvial processes
- 6) How can we see the effect of volcanism in a broad terrain by using volcanoclastic sediments.

Further reading

Manville, V., Segschneider, B., Newton, E., White, J.D.L., Houghton, B.F. and Wilson, C.J.N., 2009. Environmental impact of the 1.8 ka Taupo eruption, New Zealand: Landscape responses to a large-scale explosive rhyolite eruption. *Sedimentary Geology*, 220(3-4): 318-336.

Wilson, C.J.N. and Walker, G.P.L., (1985). The Taupo eruption, New Zealand I. General aspects. *Philosophical Transactions of the Royal Society of London A: Mathematical, Physical and Engineering Sciences*, 314(1529):199-228.

Wilson, C.J.N., 1985. The Taupo eruption, New Zealand II. The Taupo Ignimbrite. *Philosophical Transactions of the Royal Society of London A: Mathematical, Physical and Engineering Sciences*, 314(1529): 229-310.

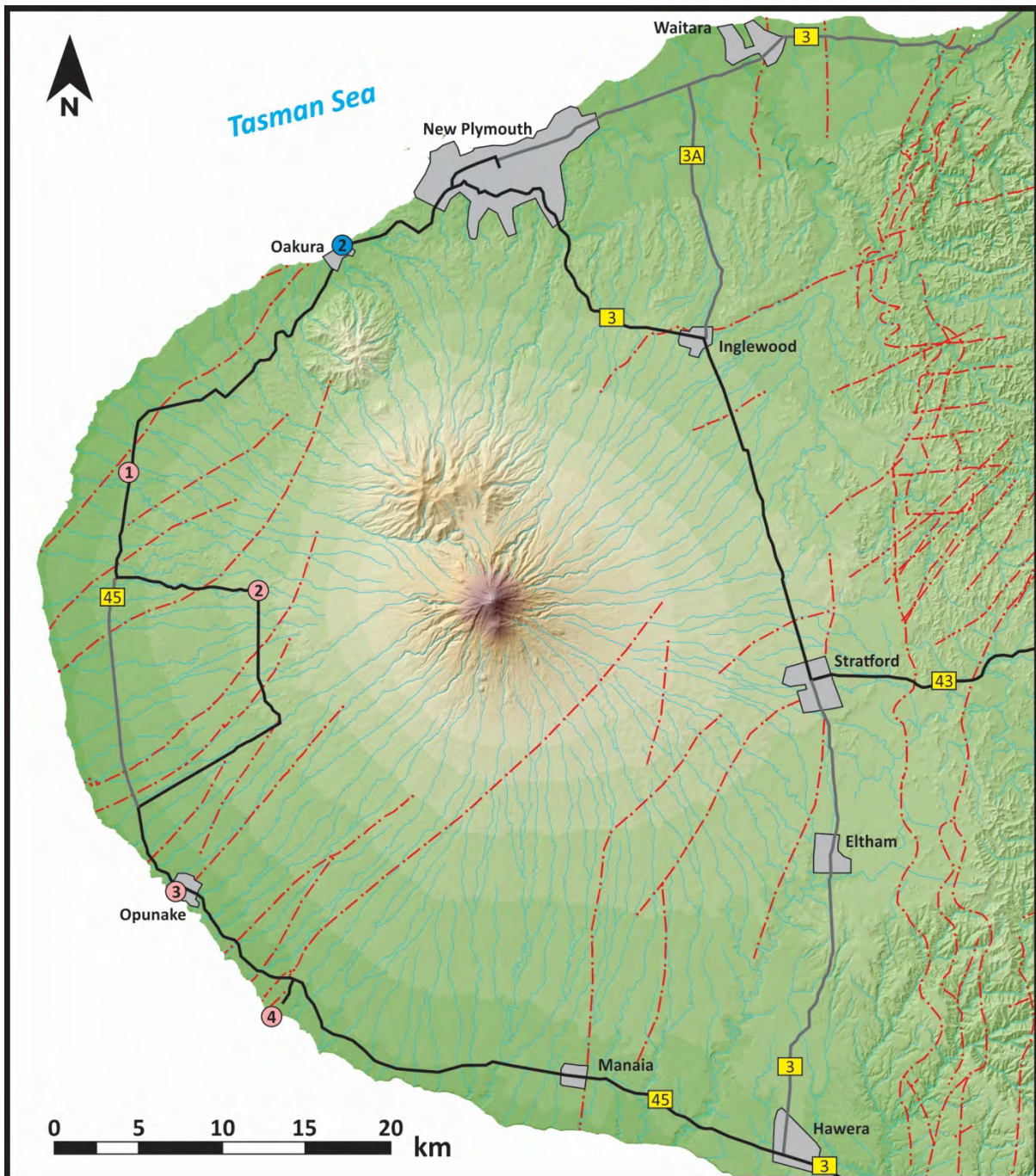
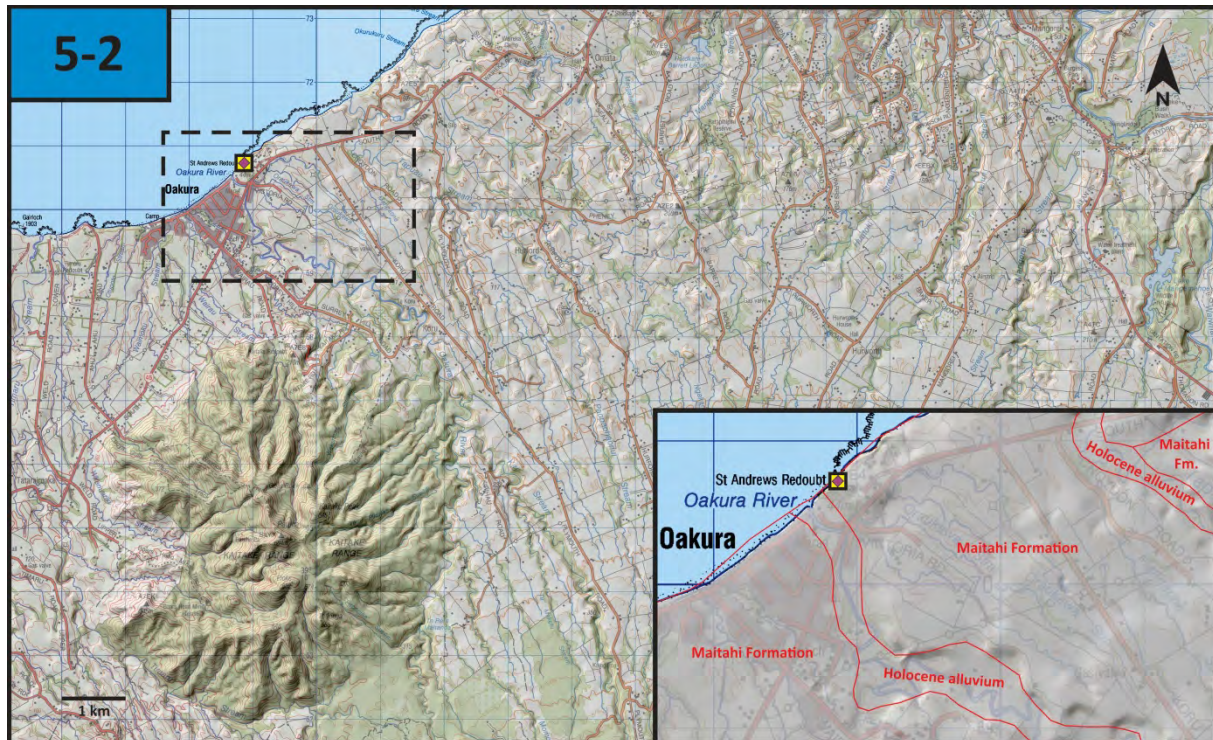
Field excursion to the Taranaki Peninsula

Fig. 62 – Topographic overview over the Taranaki Peninsula. Active fault lines are marked by dashed red lines, while townships are indicated in grey. Field stop locations are marked by colour-coded numbers, according to the programme shown in Table 1. The roads followed during the trip are indicated with black continuous line, other main roads are indicated with grey continuous line.

Stop 5-2 – Maitahi debris avalanche



Maitahi Formation was originally defined by Neall (1979) for a debris avalanche exposed in coastal sections near Oakura. It comprises both matrix-rich and matrix-poor facies and large megablocks of volcanoclastic origin as well as large rip-up clasts of sedimentary origin. The megaclasts comprise a range of lithologies which include lava flow material and also intact sequences of tephra. The sedimentary rocks are mudstones and sandstones from the underlying Tertiary units of the area. The interclast matrix is often rich in up to cm-sized hornblende crystals. The Maitahi debris avalanche deposit is thought to have been derived from an edifice collapse of nearby c. 250 ka old Pouakai volcano, based on field studies and lithostratigraphic relationships (Figs. 63-64) (Neall, 1979; Neall and Alloway, 2004). Subsequent detailed field work has shown that the Maitahi deposits have resulted from debris avalanches that have transformed laterally into debris flows, or lahars. Ar/Ar dates on hornblendes cluster are 670 ka, close to the assumed age of Kaitake Volcano at 580 ka, while two other dates are c. 270 ka and 360 ka (Gaylord et al., 1997). Three scenarios suggested by this data are;

- A source from Pouakai volcano;
- A source from Kaitake volcano;
- Sequential accumulation from both volcanoes

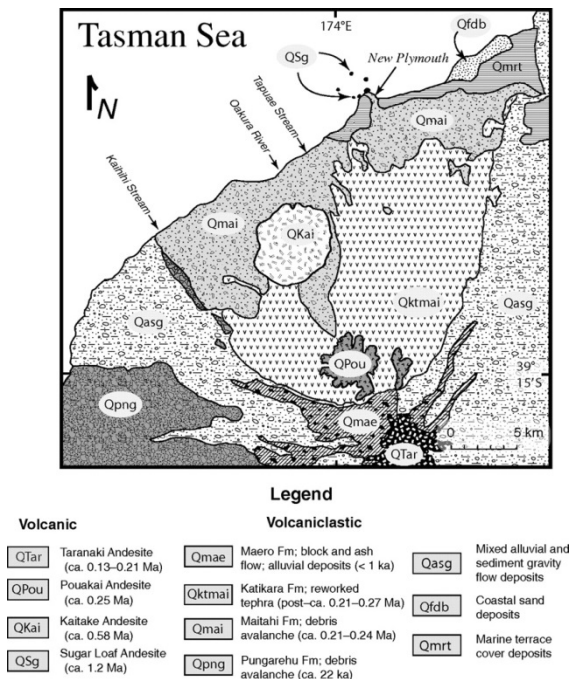


Fig. 63 – The distribution of the Maitahi Formation (from Gaylord and Neall, 2012)

Stratigraphic continuity with the former Pouakai vent and lack of stratigraphic continuities led Gaylord and Neall (2012) to conclude that the most likely source was Pouakai and that the megaclasts were derived from older parts of the edifice or

scoured from the terrain over which the debris avalanche passed.

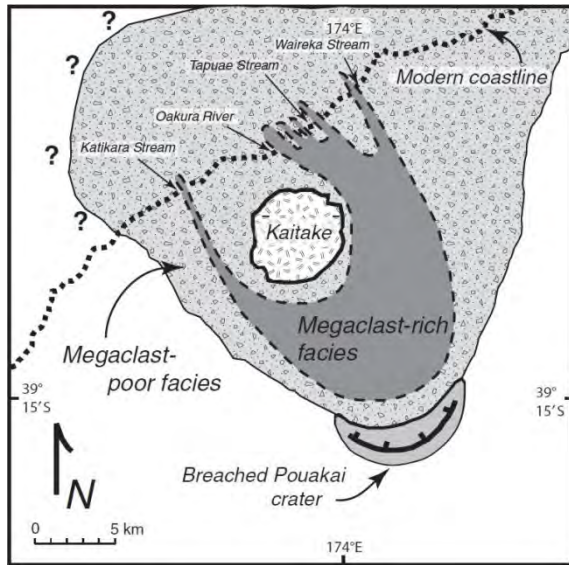


Fig.64 – Inferred distribution of megaclast-rich (solid gray) and megaclast-poor (breccia pattern) facies within the Maitahi Formation (from Gaylord and Neall, 2012)

This stop at Oakura Beach is a superb example of the axial facies of a large debris avalanche (Fig. 65). As we progress north along the cliffs, we pass into what was a channel down which megaclasts were concentrated. Note the range of megaclast fabrics, including intricate deformation within bedded sedimentary clasts that reflects the deforming forces they were subjected to.



Fig. 65 – Maitahi Formation, axial a facies at Oakura Beach

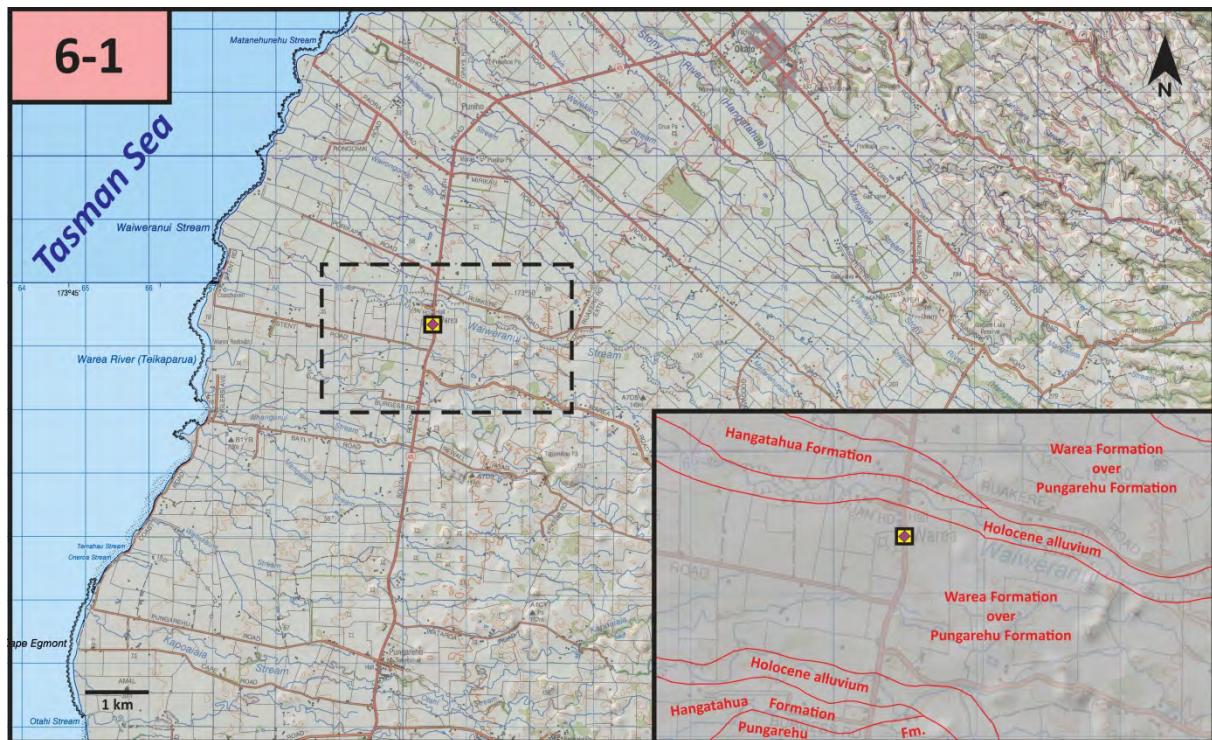
Suggested discussion points

- 1) Pitfalls in recognizing megablocks in volcanic debris avalanche deposits
- 2) Discussion on the stratigraphy significance of volcanic debris avalanches as major “event” deposits
- 3) The landscape modifying role of volcanic debris avalanches
- 4) Reworking volcanic debris avalanche deposits
- 5) Facies analysis of volcanic debris avalanche deposits
- 6) Discussion on the role of volcanic debris avalanche deposits to re-establish original volcano stratigraphy

Further reading

- Gaylord, D.R. and Neall, V.E., (2012). Subedifice collapse of an andesitic stratovolcano: The Maitahi Formation, Taranaki Peninsula, New Zealand. *Bulletin*, 124(1-2): 181-199.
- Neall, V.E., (1979). *Geological Map of New Zealand: Sheets P19, P20, & P21: New Plymouth, Egmont, and Manaia*. Department of Scientific and Industrial Research.
- Neall, V.E. and Alloway, B. (2004). *Quaternary Geological Map of Taranaki, 1: 100 000*. Institute of Natural Resources, Massey University.
- Zernack, A.V., Procter, J.N. and Cronin, S.J. (2009). Sedimentary signatures of cyclic growth and destruction of stratovolcanoes: a case study from Mt. Taranaki, New Zealand. *Sedimentary Geology*, 220(3-4): 288-305.

Stop 6-1 – Nomenclature of Taranaki lahars, Warea Formation



The Indonesian term “*lahar*” is commonly used to describe a volcanic mudflow originating from the steep flanks of the volcanic edifice. Usually the event is triggered by volcanic heat melting snow and ice, dam break from a crater lake or rainfall runoff remobilizing or eroding deposited volcanoclastics (Scott, 2009). Smith and Fritz (1989) define the term as “*a rapidly flowing mixture of rock debris and water (other than normal streamflow) from a volcano.*” Pierson and Costa (1987) recognize that lahars consist of water and sediment with the proportions of the two being highly variable in various settings with the rheological characteristics of a lahar being strongly influenced by other factors such as grain size, velocity, topography and temperature.

The term lahar does however create a broad generalized category of two-phase (water and sediment) volcanic flows. Generally, lahars are grouped into two categories, hyperconcentrated flows and debris flows. Beverage and Culbertson (1964) first used the term hyper-concentrated flow to differentiate between normal floods and floods containing a higher sediment concentration between 20-60% sediment. Pierson (2005b) generally defines these terms as spectrum from floods (hyper-concentrated flows), that contain 4% by volume or 10% by weight of suspended sediment, to debris flows that contain 60% by volume or 80% by

weight of sediment with approximately 50% of rock clasts larger than sand size. However, most classifications of lahars (hyperconcentrated flow – debris flow) are rheological classifications based on the flowing sediment/water mass. Rheologically, Pierson and Costa (1987) define the difference between the two end members as hyperconcentrated flows having a yield strength being dominated by fluid flow with constrained sediment moving in a turbulent motion. Debris flows are described as being more of a plastic mass, with high yield strength with the sediment being more buoyant due to dispersive forces and intergranular collision. Despite these rheological concepts, classification and definitive description of related deposits are highly variable. In general Pierson (2005a) provides a practical description for both;

Debris Flow deposits

- Sand and fine gravel grains typically angular to subangular (hillslope source)
- Non-stratified, extremely poorly sorted (= massive diamictons)
- Normal and/or inverse grading common in vertical sections
- Matrix filling all voids except at margins or where washed out

- Coherent, semi-indurated consistency; difficult to dig - outcrops break off in small chunks when struck
- Multiple flow units commonly indistinguishable stratigraphically
- Coarse clast distribution fairly random in centres of deposit surfaces but more concentrated at deposit margins; deposit surfaces commonly convex upward
- Clasts oriented randomly except at flow margins

Hyperconcentrated flow deposits (HCFD)

- Most grains (all sizes) are rounded to subrounded (stream bed source)
- Flood deposits sediments usually stratified – distinct laminae and beds, commonly with cross-bedding; HCFDs show faint horizontal to massive bedding with outsized individual gravel clasts and lenses sometimes appear as massive but poorly consolidated diamictons
- In flood deposits, abrupt changes in mean grain size in vertical sections; sorting moderate to good within individual bedding units; coarser clasts may be imbricated
- In HCFDs, sorting usually poor to very poor; textural changes usually not abrupt
- Voids common between larger clasts (openwork texture) in water-flow deposits, not in HCFDs
- Flood deposits consistency is loose and friable when dry (easy to dig), although HCFDs slightly more consolidated
- Flood deposits surfaces commonly have longitudinal bars (usually armoured with coarse clasts), dunes, and/or ripples; abrupt changes in mean grain size between bars and channel axes are typical

Changes in channel morphology, flow discharge and inclusion of water can dramatically and rapidly change mechanisms required for deposition (Pierson, 2005b), therefore changing the characteristics and textures of the related deposits. These transitions can be seen in a variety of stratigraphically equivalent lateral and longitudinal sections in the Taranaki ring-plain with the most common changes resulting in textures of either clast-rich/-supported or matrix-rich/- supported deposits. These changes can be seen clearly as overbank, HCFDs directly grading out from the paleochannel or grading directly from the central debris flow facies of the flow. Transitions from debris flow to hyper-concentrated flow can also be seen in

longitudinal or downstream change in grain size. The most obvious change is the deposit becoming thinner and inundating a wider area with clasts being deposited and grain size becoming finer.

Mt Taranaki and the surrounding ring-plain have not been inundated by lahars in historic times and no lahars have been witnessed by the surrounding community; yet the stratigraphic record shows re-occurring periods of frequent large lahar events. The most recognisable lahar deposits on the ring-plain (Fig. 66) are those of the 13-22500 yr B.P Warea Formation (Neall, 1979). Other identified lahar deposits are the Kahui Debris Flows (7000-12000 yr B.P.) and the Maero Debris Flows (<1000 yr B.P.) (Neall, 1979). However, these formations are not single events but represent time periods of activity and are more recognised as chrono-stratigraphic units. Further volcanoclastic diamictons on the Taranaki ring plain that may be related to laharcic or flood activities are the Holocene Hangatuhua Gravels and sections of the Opunake Formation (30000-38000 yr B.P).

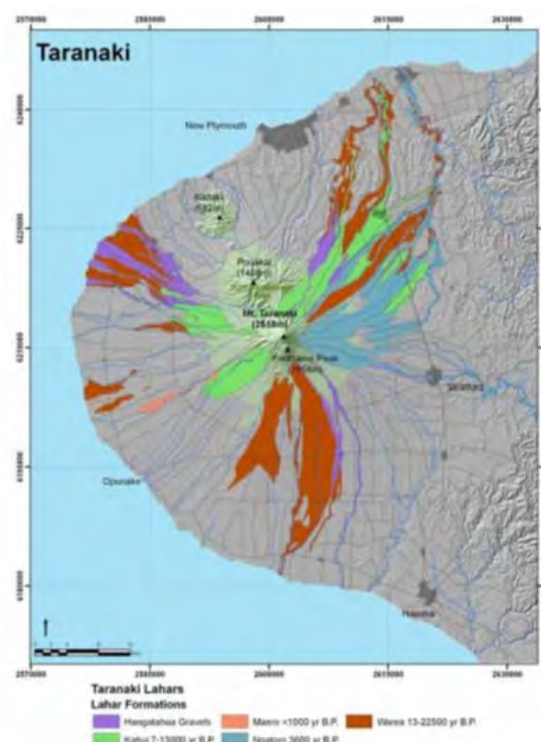


Fig. 66. – Distribution and age of lahar formations in Taranaki

The Warea Formation can be found in the field between the township of Warea and the Stony River in western Taranaki. The deposit is recognised on the landscape as large flat areas between and around the debris avalanche mounds of older deposits. Neall and Alloway (2004) identified a number of lobes originating from the cone in several directions and grouped all lahar deposits as one chrono-

stratigraphic unit. In general, the Warea Formation is described as being a laharic conglomerate, breccia and sandstone that spans a large time period from 13000-22500 years B.P., the age being primarily derived from over- and underlying tephra and soil layers. The type locality of this deposit shows a coarse sandy matrix containing poorly sorted, dense, sub-angular, black andesitic clasts which range in size from 1cm to 10cm. The unique characteristic of this deposit is its strong lithification and the abundance of large (~30cm) radial fractured, breadcrusted volcanic bombs. This deposit was interpreted to be a warm lahar generated from eruptive processes or possibly the distal parts or run-out phase of a pyroclastic flow that has interacted with snow or water.

However, recent field mapping of the Warea Formation shows a complex system of landscape readjustment and reaction after deposition of the Pungarehu debris avalanche that inundated vast areas of the ring-plain. This complex system shows areas of braided river channels with flood deposits redistributing already erupted material, the transport of freshly erupted material and large confined debris flows that fill channels.

The Warea Formation can then be divided into 6 very different spatial groups (Fig. 1) defined by stratigraphy and distribution along specific river catchments;

- Stony River (16 ka – 22.5 ka),
- Matanehunu Stream (14826 +/- 77 B.P.),
- Waiweranui Stream (<22.5 ka),
- Kapoaiaia Stream (<22.5 ka),
- Oanui Stream (17 702 +/-82 B.P.),
- Mangawhero Stream (1.8 ka – 7 ka).

All areas show a maximum of three individual episodes separated by time represented by soil development. Within each major episode there are a number of pulses of different flows shown by changes in grain size, sorting, bedding features and occasionally a thin silt layer which represents a period of ponding or settling of water on the top of the flow. All deposits typically show features characteristic of debris flows such as poor sorting, matrix support, angular clasts or fragments and lateral/longitudinal transition into hyperconcentrated flows which display better sorting and smaller clast size.

Recent work by Lerner et al. (2018) near the Waiweranui Stream on younger sequences of the Warea Formation highlights that these deposits are pyroclastic flow deposits. New methods of examining remnant magnetism through consolidating and sampling oriented blocks of

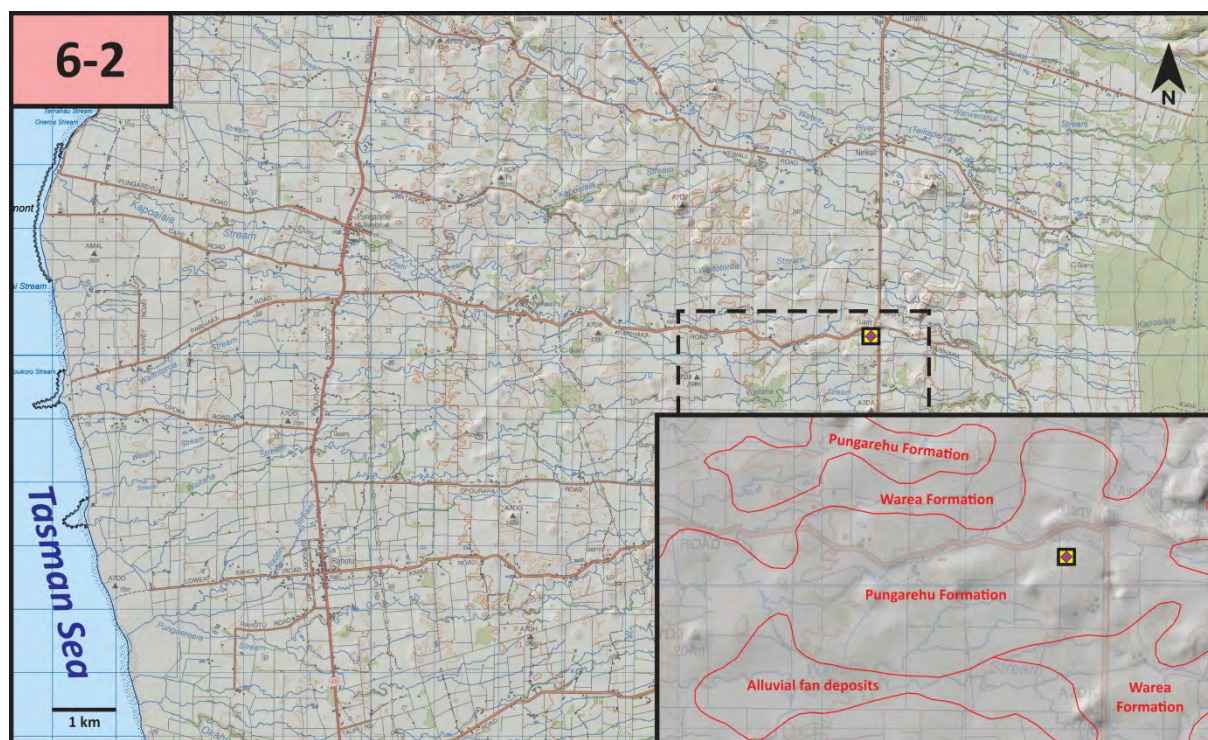
friable ash material with a strengthening compound were examined using paleomagnetism. This method was used to show that a >25 km runout mass-flow deposit was emplaced as a hot PDC, contrary to an earlier a cold lahar interpretation. We corroborate the results from ash with data from clast samples at some sites and show that the matrix was emplaced at temperatures of at least 250°C, while clasts were deposited at up to 410°C.

This study shows how the paleomagnetic study of unconsolidated matrix ash material in volcanoclastic deposits can be used to identify hot pyroclastic density current deposits where alternative methods fail. This is especially important when defining hazard zones for deadly PDCs in the outer ring plains of stratovolcanoes, 15-25 km from source. This also highlights that a previously mapped lahar deposit at Mt. Taranaki was formed by a PDC emplaced as part of a sub-Plinian eruption at ~11500 cal. yr. B.P.

Further reading

- Beverage J.P., Culbertson J.K. (1964). Hyper-concentrations of suspended sediment. *Journal of the Hydraulics Division, American Society of Civil Engineers* 90: 117-126.
- Lerner, G., Cronin, S.J., and Turner, G.M. (2018). Assessing high-temperature hazards associated with block-and-ash flows at Mt. Taranaki, New Zealand. In: Corsaro, R.A et al., 2018 (Eds.) Abstracts Volume of the International meeting “Cities on Volcanoes 10”, Millenia of Stratification between Human Life and Volcanoes: strategies and coexistence, *Miscellanea INGV* 43, Naples, Italy. 31: 85-109.
- Neall, V.E., 1979. *Geological Map of New Zealand: Sheets P19, P20, & P21: New Plymouth, Egmont, and Maniaia*. Department of Scientific and Industrial Research.
- Neall V.E., Alloway B.E. (2004). *Quaternary Geological Map of Taranaki*. INR, Massey University, Dep. Soil Sci. Occ. Pub No.4.
- Pierson T.C. (2005a). Distinguishing between Debris Flows and Floods from Field Evidence in Small Watersheds U.S. Geological Survey Fact Sheet 2004-3142.
- Pierson T.C. (2005b). Hyper-concentrated flow - transitional process between water flow and debris flow. In Jakob M., and Hungr O., (eds) (2005). *Debris-flow Hazards and Related Phenomena*. Praxis. Springer Berlin Heidelberg.
- Pierson T.C., Costa J.E. (1987). A rheologic classification of subaerial sediment-water flows. *Geological Society of America, reviews in engineering geology* VII: 1-12.
- Scott K.M., Macías J.L., Naranjo JA, Rodriguez S, McGeehin JP (2001). *Catastrophic Debris Flows Transformed from Landslides in Volcanic Terrains: Mobility, Hazard Assessment and Mitigation Strategies*: U.S. Geological Survey Professional Paper 1630.
- Smith G.A., Fritz WJ (1989). Volcanic influences on terrestrial sedimentation. *Geology* 17: 375-376.

Stop 6-2 – Pungarehu debris avalanche mounds



In Taranaki, three late Quaternary laharic breccia deposits (Fig. 13) extending west and south-west from Egmont Volcano were mapped by Neall, (1979).

The main internal structure of debris avalanche deposits comprises two major components: 1) fragmental rock clasts (hereafter referred to as “FRCs”), and 2) matrix. A FRC is defined as a fragmented or deformed piece of lava or layered volcanoclastic material commonly preserving stratification and/or intrusive contacts formed within the original volcanic edifice (Alloway et al., 2005). In Taranaki, the most commonly recognised FRC is andesitic lava that is commonly brecciated forming a diamicton of homogeneous composition. The FRC sizes are classified as: boulder (0.256 - 10 m), megaboulder (10 - 100 m), block (100 - 1000 m) and megablock (1 - 10 km), according to the scheme of Sundell and Fisher (1985), with the addition of a gravel-sized class of FRCs (0.002 - 0.256 m). Matrix is referred to as inter-clast matrix and is defined as all the material within the deposit surrounding the FRCs and less than 0.002 m in diameter. It should not be confused with the matrix of a FRC, which is here termed intra-clast matrix (Alloway et al., 2005). Inter-clast matrix includes all blended, unsorted, and unstratified parts of the deposit and consists of material ranging in size from clay to very coarse sand. Inter-clast matrix also contains rip-up clasts of plastically distorted soil, peat and tephra layers,

clasts with variable rounding, and wood fragments derived from the terrain beneath. Inter-clast matrix is more abundant in inter-mound areas and is predominant in the distal and lateral margins of the deposit. The lithology and ratio of inter-clast matrix to FRCs varies within each debris-avalanche deposit and between the deposits. These variations are influenced not only by the composition of the original volcanic edifice and type and scale of the initial volcanic event, but also by topographic features such as ridges, channel systems and lowlands. Where FRCs predominate, expressed by the development of hummocky surfaces, the debris avalanche was mapped as axial facies by Neall (1979) and as block facies by Crandell et al. (1984). Inter-clast matrix-dominated areas were mapped as marginal facies by Neall (1979), as matrix facies by Crandell et al. (1984), as main facies by Mimura et al. (1982), and matrix mixture by Ui (1983). In eastern Taranaki, an adaptation of axial and marginal facies nomenclature was considered more appropriate since it distinguishes the mapping units from sedimentological descriptions (Fig. 67).

Three facies are recognised; axial a, axial b, and marginal facies (Alloway 1989; Palmer et al. 1991; Alloway et al., 2005). Axial a facies is defined as a mappable area where fragmental rock clasts dominate, with <30% inter-clast matrix and where the surface topography is dominated by a concentrated area of steep sloping hills and mounds

up to 50 m high and basal diameters as much as 500 m. Axial b facies is defined as an area where the proportion of inter-crest matrix is sub-dominant to dominant (30-90%) relative to FRCs and where the surface physiography is dominated by sparsely

distributed mounds and hills up to 10 m high with basal diameters < 25 m. This facies corresponds with the mixed block and matrix facies of Glicken (1986). Marginal facies is defined as an area where the proportion of inter-crest matrix is dominant (>90%) relative to FRCs and where the surface physiography is without mounds or hills.

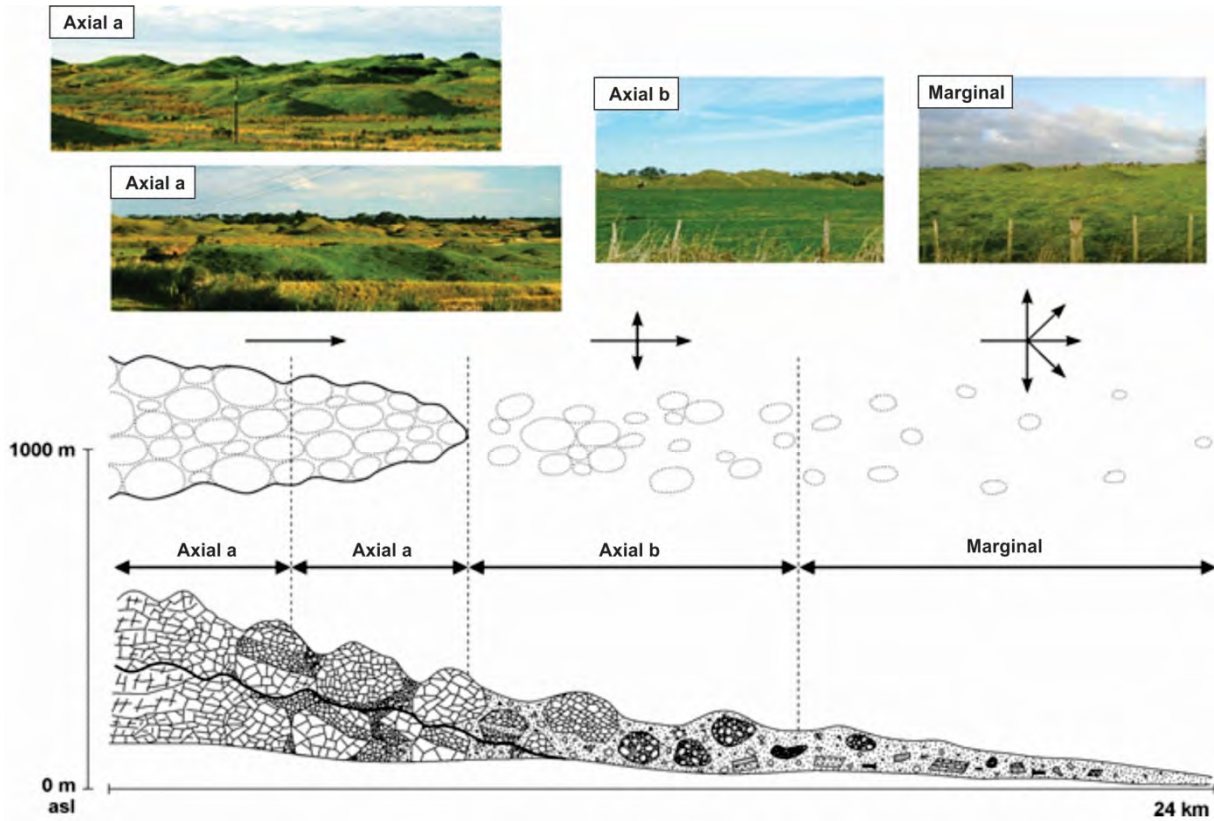


Fig. 67. – Sketch and photos of the dominant landscapes in relation to each of the identified facies. Lower sketch shows a longitudinal cross-section of a debris avalanche deposit (modified from Palmer et al., 1991; Zernack, 2009). Upper sketch displays the plan view and distribution of mounds. Arrows indicate preferred flow direction.

The Mt. Taranaki edifice is geomorphically the dominant feature of the peninsular yet the related near circular ring plain expanding up to 30 km from in distance from the volcano contains volcanoclastics that are volumetrically more significant and consists of a range of deposits that record numerous mass flow events that exhibit sedimentological features recoding a spectrum of rock-water rheologies. The most distinctive features are the surface mounds that were originally called conical hills and initially thought to be individual volcanic blisters of lava flows or related to glacial outwash deposits (Grange, 1931).

In Taranaki, three late Quaternary laharic breccia deposits extending west and south-west from Egmont Volcano were mapped by Neall, (1979). These deposits with their characteristic mounds or “conical hills” (Morgan & Gibson 1927), were named Opuā, Warea and Pungarehu formations;

later to be identified as debris-avalanche deposits. The most spectacular of these is the Pungarehu Formation, which has an estimated minimum volume of 7.5 km³.

The Pungarehu Formation (Neall, 1979) is the best-exposed debris avalanche deposit of the Taranaki volcanic ring plain which dominates the landscape with distinctive mounds ranging in average height from 5 m near the coast to 30 m at 300 m altitude (Neall 1979). The deposit overlies the 25.4 ka Kawakawa Tephra and inundated 200-250 km² of the western ring plain. Its offshore extent is thought to be at least 8 km west of Cape Egmont (Neall 1979) and bathymetric maps show the occurrence of debris avalanche mounds on the seafloor to a depth of about 60 m (Shell, BP and Todd Oil Services Ltd. 1974). To the south, its extent is obscured due to the progressive overlapping of the younger Warea and Opuā Formations. The deposit thickness exceeds 60

m in proximal locations and 16 m near its main dispersal axis at medial coastal outcrops.

Neall (1979) first identified the Pungarehu Formation as a large laharcic mass flow that later was identified as specifically as a debris avalanche. The main internal structure of debris avalanche deposits comprises two major components: 1) fragmental rock clasts, and 2) matrix. A fragmental rock clast is defined as a fragmented or deformed piece of lava or layered volcanoclastic material commonly preserving stratification and/or intrusive contacts formed within the original volcanic edifice (Alloway et al., 2005). The internal structure of Taranaki debris avalanche deposits is characterised by fragmental rock clasts (FRC) and matrix. The matrix is unsorted and unstratified and may contain rip - up clasts of plastically distorted soil, peat and tephra layers as well as wood fragments derived from the terrain beneath. Intra - clast matrix is a separate entity that occurs within or between fragmental rock clasts and megaclasts of the original lithologies from the edifice (Alloway et al., 2005). Scott et al. (2001) and Palmer et al. (1991) define megaclasts as being >1 m in diameter. These can be large coherent fragments of rock, intact portions of the original edifice strata, fragmented clasts that have been partially disaggregated and those that have completely disaggregated to form a “ domain ” of rock fragments that are recognisably related and could represent a jigsaw puzzle (Gaylord and Neall, 2012). The lithology and ratio of matrix to FRCs can vary within each debris - avalanche deposit depending on the characteristics of the source area, related volcanic activity, as well as flow rheology and interaction with paleo-physiography.

Debris avalanche deposits are distinguished from diamictons with similar textural characteristics by their content of mega - clasts (Neall, 1979, Palmer et al., 1991; Scott et al., 2001), which are single (encased) definable fragments of lithologically or stratigraphically coherent material derived from the original edifice. Other diagnostic features include jig - saw fragmented clasts, major zones of strongly sheared and deformed soft clasts and sheared basal margins with common rip - up clasts (Siebert et al., 1987; Glicken, 1981; Ui et al., 2000; Scott et al., 2001). The content of clay and/or clay-sized particles is also a diagnostic feature of debris avalanche deposits and can provide information on source areas, initiation and emplacement processes. Wet debris avalanches and clay - rich (cohesive) debris flows are typically associated with the collapse of fluid - saturated portions of a volcanic edifice (Vallance and Scott, 1997). The available water, pore-water and alteration or weakness of the pre - avalanche mass contributes to the rapid

transformation from debris avalanche to clay-rich debris flow.

Ui et al. (1986) provided one of the first studies examining or quantifying the variations in block or clast size and jigsaw fractures within the deposit and spatial across the extents of the deposit. The data showed a pattern of decreasing blocks size with distance and as a result of collision and transportation while in contrast the jigsaw fractures were determined to be created closer to source. It was also noted that abrasion and other clast-to-clast contact resulted in distinctive impact features.

Common features observed (under scanning electron microscope; SEM) in debris avalanche samples (coarse sand <2 mm) fraction are the presence of micro cracks (lateral displacement separations and intersecting relations) and hackly (concave fracture) surfaces. These features have been described as being diagnostic of debris avalanches and originating during their initiation by Komorowski et al. (1991) and Belousov et al. (1999). Procter (2009) examined rock fragments, pyroxene and hornblende crystals within the Opuia Formation (debris avalanche deposit) matrix that typically showed micro cracks from impacts and splitting of the particles. The rock fragments were subrounded to subangular with curved conjugate pairs of micro cracks visible at 90 to 350× magnification, yet very little jointing was observed or evidence was of surface friction or scratching from other grains with only a small number of grains exhibiting hackles in one or two locations on the grain. Micro cracks that were present were typically one or two large cracks that have migrated across the entire shard. The greatest impacts on the surfaces of glass shards may not be attributed to a decompression or explosion during initiation of the debris avalanche but rather to the relative softness of the glass. Procter (2009) suggested that since hackles are concentrated in localized areas (on the grain) that they result from grain to grain contact during flow. The most striking examples of impact scouring, indentations, micro cracking/shear fractures and discrete plumose hackles occur on pyroxene and hornblende crystals. Procter (2009) also determined that the proportion of fragments displaying micro cracks in samples from longitudinal and lateral cross - sectional showed few consistent variations or a spatial pattern of distribution. Overall, axial deposits show the highest proportions of micro cracked crystal grains compared to those from marginal areas of the deposit. The more recent study of Roverato et al., (2014) showed similar spatial distribution patterns of micro-cracks throughout the Pungarehu Formation. However, Roverato et al., (2015) also identified clusters of fractured clasts and micro cracks within the deposits and attributed this chaotic distribution to

be more related to megaclasts or shear zones within the flowing mass. It is considered that the more regular occurrence of the matrix at distal locations is a result of collisional and frictional regimes influencing transport and emplacement.

Suggested discussion points

- 1) The role of volcanic debris avalanche deposits in volcano stratigraphy
- 2) Volcanic debris avalanche deposits in formal stratigraphy frameworks
- 3) On the processes forming volcanic debris avalanches
- 4) Cyclic growth and destruction of large polygenetic volcanoes and their implication to volcanic stratigraphy

Further reading

- Alloway, B.V. (1989). Late Quaternary cover-bed stratigraphy and tephrochronology of northeastern and central Taranaki Region, New Zealand. Unpublished PhD thesis, Massey University, Palmerston North, New Zealand.
- Alloway, B., McComb, P., Neall, V., Vucetich, C., Gibb, J., Sherburn, S. and Stirling, M. (2005). Stratigraphy, age, and correlation of voluminous debris - avalanche events from an ancestral Egmont Volcano: implications for coastal plain construction and regional hazard assessment. *Journal of the Royal Society of New Zealand*, 35(1-2): 229-267.
- Belousov A, Belousova M, Voight B. (1999). Multiple edifice failures, debris avalanches and associated eruptions in the Holocene history of Shiveluch volcano, Kamchatka, Russia. *Bull Volcanol* 61: 324-342.
- Crandell, D. R.; Miller, D. D.; Glicken, H. X.; Christiansen, R. L.; Newhall, C. G. (1984) Catastrophic debris-avalanche from ancestral Mount Shasta Volcano, California. *Geology* 12: 143-146.
- Gaylord, D.R. and Neall, V.E., (2012). Subedifice collapse of an andesitic stratovolcano: The maitahi formation, Taranaki Peninsula, New Zealand. *Bulletin*, 124(1-2): 181-199.
- Glicken, H.X. (1986): Rockslide avalanche of May 18 1980, Mt. St. Helens volcano. Unpublished PhD. thesis, University of California, Santa Barbara, California.
- Glicken, H. X.; Voight, B.; Janda, R. J. (1981). Rockslide-debris-avalanche of May 18, 1980, Mount St. Helens volcano (abstr.) IAVCEI Symposium Arc Volcanism, Tokyo and Hakone, 109-110.
- Komorowski, J. C., Glicken, H. X., & Sheridan, M. F. (1991). Secondary electron imagery of microcracks and hackly fracture surfaces in sand-size clasts from the 1980 Mount St. Helens debris-avalanche deposit: Implications for particle-particle interactions. *Geology*, 19(3): 261-264.
- Mimura, K.; Kawachi, S.; Fijimoto, U.; Taneichi, M.; Hyuga, T.; Ichikawa, S.; Koizumi, M. (1982) Debris-avalanche hills and their natural remnant magnetisation – Nirasaki debrisavalanche, central Japan. *Journal Geological Society of Japan* 88: 653-663.
- Morgan, P.G., Gibson, W. (1927): The geology of the Egmont subdivision, Taranaki. *New Zealand Geological Bulletin* 29: 92p.
- Neall, V.E., (1979). Geological Map of New Zealand: Sheets P19, P20, & P21: New Plymouth, Egmont, and Manaia. Department of Scientific and Industrial Research.
- Neall V.E., Alloway B.E. (2004). Quaternary Geological Map of Taranaki. INR, Massey University, Dep. Soil Sci. Occ. Pub No.4.
- Palmer, B. A.; Alloway, B. V.; Neall, V. E. (1991). Volcanic debris-avalanche deposits in New Zealand - lithofacies organisation in unconfined, wet avalanche flows In: *Sedimentation in Volcanic Settings*. SEPM Special Publication No. 45. Edited by R. V. Fisher and G. A. Smith. Tulsa, Oklahoma, U.S.A.
- Procter, J.N. (2009). Towards improving volcanic mass flow hazard assessment at New Zealand stratovolcanoes. Unpublished PhD Thesis, INR, Massey University, New Zealand.
- Roverato, M., Cronin, S., Procter, J. and Capra, L. (2015). Textural features as indicators of debris avalanche transport and emplacement, Taranaki volcano. *Bulletin*, 127(1-2): 3-18.
- Scott K.M., Macías J.L., Naranjo JA, Rodriguez S, McGeehin JP (2001). Catastrophic Debris Flows Transformed from Landslides in Volcanic Terrains: Mobility, Hazard Assessment and Mitigation Strategies: U.S. Geological Survey Professional Paper 1630.
- Sundell, K.; Fisher, R. V. (1985). Very coarse grained fragmental rocks: A proposed size classification. *Geology* 13: 692-695
- Ui, T. (1983). Volcanic debris-avalanche deposits – Identification and comparison with nonvolcanic debris stream deposits. *Journal of Volcanology and Geothermal Research* 18: 135-150.
- Ui, T.; Kawachi, S.; Neall, V. E. (1986). Fragmentation of debris-avalanche material during flowage – evidence from the Pungarehu Formation, Mount Egmont, New Zealand. *Journal of Volcanology and Geothermal Research* 27: 255-264.
- Vallance J.W., Scott K.M. (1997). The Osceola Mudflow from Mount Rainier; sedimentology and hazard implications of a huge clay-rich debris flow. *GSA Bulletin* 109: 143-163.

Stop 6-3 – Middleton Bay, Opunake paleo-river system



Cyclic volcanoclastic sedimentation

The >200 ka volcanic history of Mt. Taranaki is characterised by alternating phases of edifice growth and large-scale failures. In contrast to other volcanoes with similar cyclic behavior, an almost complete stratigraphic record of distal ring plain successions is exposed here due to continuous coastal erosion and tectonic uplift. The volcanoclastic sequences along the southern coast represent a cross-section through diverse sedimentological settings and lithofacies. Volcanoclastic flow facies include debris-avalanche (DA), cohesive debris-flow (DF), hyperconcentrated-flow (HF), channelised debris-flow (CH), floodplain/ overbank (FP) and localised fluvial (Flu) deposits as well as transitions between them. These facies are related to specific periods within a repeating pattern of deposition that was used to develop a model of cyclic volcanoclastic sedimentation in distal areas of stratovolcanoes (Zernack et al. 2009).

A generalised volcanic cycle at Taranaki begins with edifice re-growth following collapse, which is characterised by small-scale pyroclastic eruptions and localised lava flows with no long-runout mass-flows being produced. Distal areas accumulate thick paleosols of medial ash and/or lignite with interbedded tephra layers reflecting the proximal activity. Once the cone has grown to a size at which

pyroclastic activity starts generating long-runout mass-flows, distal accumulation is characterised by massive sequences of pebbly sand-dominated, mainly monolithologic DF and HF deposits that intercalate with tephra beds, paleosols, dune sands, and local fluvial sediments. The main body of these flows seems to be confined to pre-existing channels forming CH deposits that grade into more wide-spread, unconfined overbank-type (FP) deposits.

Edifice growth is limited to a critical point at which it fails. The cycle is closed with a major sector or cone collapse, in distal areas represented by cohesive DF and DA deposits. At least 15 DA-producing events have been identified in the Taranaki ring plain, ranging from small-scale flank collapse to catastrophic edifice failures with volumes from 0.1 to >7.5 km³ (Zernack et al. 2010, 2012).

Ring plain locations show 3 types of sequences: (1) Areas where DA deposition is followed by distal quiescence, marked by paleosol/lignite formation and their preservation. (2) Areas repeatedly buried by DAs with little (preserved) accumulation between collapse events. (3) Areas frequently inundated by DF, HF and CH deposits. Erosive and transitional contacts to the underlying DA deposit imply that its surface was rapidly reworked.

The ring plain record shows that while debris avalanche events represent the greatest hazard from



Fig. 68 – Wide channel filled by a coarse debris-flow deposit (DFD) that grades into finer-grained, better sorted hyperconcentrated-flow overbank deposits (OF).

this stratovolcano, long-runout mass flows generated during growth phases are far more frequent and can also extend >30 km from the volcano.

Ringplain morphology and drainage systems

The nature of the drainage pattern around Mt. Taranaki seems to have been similar throughout its history. The gently dipping ring plain was only weakly incised by a network of small, shallow streams that originated from the edifice. This is reflected in the frequent occurrence of relatively localised, cross-bedded fluvial deposits throughout the succession. Even though the character of stream channels continuously changed in response to varying sediment influx from syn- and inter-eruptive volcanic mass flows, their position shifted only slightly (cf. Major et al. 1996; Rodolfo 1996 et al.; Pierson 2005). Following periods of ring-plain aggradation, incision of new channels occurred along or near the margins of previous, infilled ones. The typically tabular, laterally widespread geometry of hyperconcentrated-flow deposits throughout the sequence confirms the existence of broad coastal or near-coastal plains.

Large river channels that were deeply incised into the easily erodible volcanoclastic debris are also common throughout the volcanic record. They typically consist of a central channel area that provided flow paths for the most voluminous and sediment-rich volcanic mass flows (Fig. 68). Once these were infilled, only more dilute and less confined hyperconcentrated flows inundated the increasingly shallower channel and adjacent floodplain as indicated by accumulation of more widespread, finer-grained HF deposits towards the top of the channel sequences. Individual channels of the Taranaki ring plain succession extend 15-30 m laterally, are as deep as 10 m and often characterised by steep slopes. Facies transitions from coarse channel fill to fine-grained overbank facies occur abruptly at the steep channel margins. Activity along these channels typically ceased after their filling or burial by later debris-avalanche deposits.

Subsequent channels often formed in similar locations, i.e. adjacent to previous settings or cut into the deposit sequence that filled the previous channel.

Two large paleo-river systems near Opunake township and Puketapu Road (“Lizzie Bell”) are an exception.

The Opunake paleo-river system

The location of these two large paleo-river systems is possibly related to nearby fault lines with tectonic activity leading to continuous re-establishment of river channels in the same area even after rapid filling or burial by large debris-avalanche deposits. These long-lived river systems are characterised by a laterally extensive network of overlapping channels that provided primary lahar paths over a long time-span and thus contain a more complete record of events than minor or shorter-lived channels (cf. Palmer et al. 1993). Repeated debris-flow events led to incremental infilling and lateral shifting of active channels. These are typically cut by more dilute and erosive flows as indicated by hyperconcentrated-flow deposits underlying younger coarser debris-flow units. Evidence of channel migration, i.e. lateral channel widening through bank erosion and burial of low-lying areas, is a common process in low-gradient channels during aggradational phases (Rodolfo et al. 1996; Pierson 2005) and was also observed. These laterally eroded channels are typically rectangular in cross-section due to undercutting and the formation of near-vertical banks in unconsolidated volcanoclastic deposits (cf. Fig. 69).

Continuous aggradation, channel shifting and lateral migration resulted in a complicated network of overlapping channels, which cut into and eroded the underlying strata, often just preserving lenses of older lahar and fluvial deposits that formed in previous channels. Hence, it is often impossible to laterally trace and correlate individual flow units further than a few metres from the channel margins. Due to a lack of preserved paleosols or other marker beds no accurate age control, other than

chronostratigraphic estimates, could thus far be established for the formation of individual channels.

An approximate age range of c. 33-13 ka for the Opunake river system is given by the stratigraphic position of channels and associated deposits. The

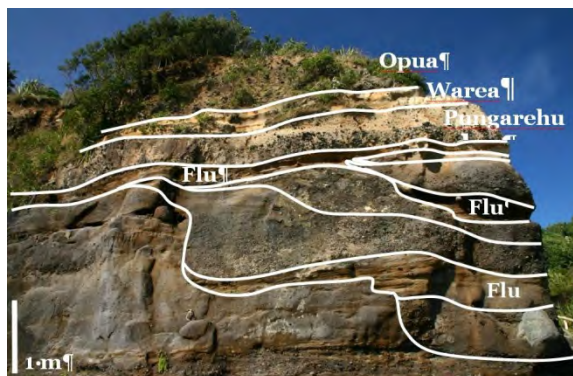


Fig. 69 – Middleton Bay section where small channels were cut in the same location as previous ones and were subsequently filled with coarse hyperconcentrated-flow deposits, separated by fluvial sediments (Flu).

lowermost channel fill units cut into and in some areas erode the top of the underlying 33-35 ka Hihiwera Peat but were not found below it. Only lenses of the Te Namu and Pungarehu debris-avalanche deposits were found within the network of channels (Fig. 70), indicating that they were almost completely reworked within the river system. The channel sequences are capped by a set of hyperconcentrated-flow deposits of the Warea Formation, which thicken in remaining shallow channels. The river system ceased to exist after these last flows were deposited and is overlain by the Opua DAD (Fig. 69). The lateral extent of the Opunake river system in coastal cross-section is c. 1.8 km.

At the **Middleton Bay location**, the upper part of the Opunake River system is exposed. The cliff section comprises a range of volcanoclastic and fluvial facies that reflect the above described erosion and sedimentation processes observed in Taranaki river systems, including lateral facies transitions of flow deposits and channel morphologies. At this location, stratigraphic control is provided by distal correlatives of the Opua, Warea and Pungarehu Formation providing chronostratigraphic markers at the top of the sequence (Fig. 69) and the Hihiwera Peat at the bottom, placing the deposition of mass-flow deposits to between 34-24.8 cal. yr BP. The Kawakawa Tephra was also found preserved in a small paleosol lense a few meters below the Pungarehu DAD. In the cliff face on the southern side of the promontory the Te Namu DAD is exposed, overlying older, channelised mass flow deposits (Fig. 70).

Stratigraphic markers at this location include;

- Opua DAD (c. 7.5 cal. yr BP)
- Pungarehu DAD (c. 24.8 cal. yr BP)
- Kawakawa T. (c. 25.4 cal. yr BP)
- Te Namu DAD (c. 34 cal. yr BP)
- Hihiwera Peat (c. 34-36.9 cal. yr BP)
- Ihaia DFD (c. 36.9 cal. yr BP)

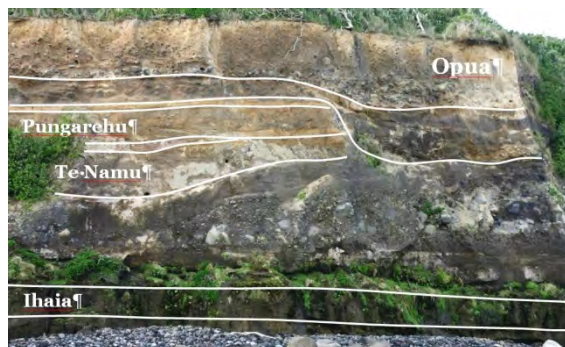


Fig. 70 – The older part of the Opunake river system at Opunake Beach. Here, the Te Namu DAD directly underlies the Pungarehu, providing further age control.

Suggested discussion points

- 1) What influences the frequency and size of volcano collapse - factors leading to edifice instability and trigger mechanisms
- 2) Longitudinal and lateral facies transitions in Taranaki debris-avalanche deposits
- 3) Controls on the long-term evolution of volcanoclastic ring plains

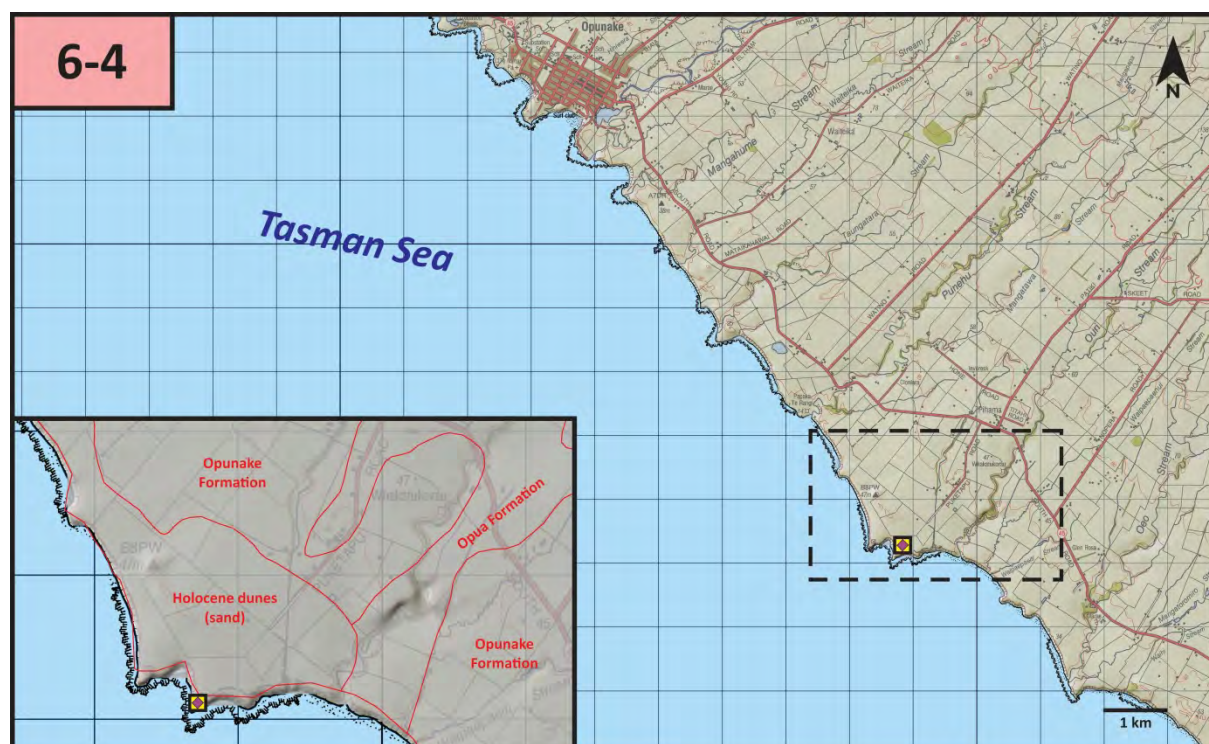
Further reading

- Palmer, B.A., Purves, A.M., Donoghue, S.L., (1993). Controls on accumulation of a volcanoclastic fan, Ruapehu composite volcano, New Zealand. *Bulletin of Volcanology* 55: 176-189.
- Pierson, T.C., (2005). Hyperconcentrated flow - transitional process between water flow and debris flow. In: Jakob M, Hungr O (Eds.) *Debris-flow Hazards and Related Phenomena*, Springer, Heidelberg, p. 159-202.
- Rodolfo, K.S., Umbal, J.V., Alonso, R.A., Remotique, C.T., Paladio-Melosantos, M.L., Salvador, J.H.G., Evangelista, D., Miller, Y., (1996). Two years of lahars on the western flank of Mount Pinatubo: Initiation, flow processes, deposits, and attendant geomorphic and hydraulic changes. In: Newhall CG, Punongbayan RS (Eds.) *Fire and mud: Eruptions and lahars of Mount Pinatubo*, Philippines. Philippine Inst of Volcanology and Seismology, Quezon City and University of Washington Press, Seattle, pp. 989-1013.
- Zernack, A.V., Procter, J.N., Cronin, S.J., (2009). Sedimentary signatures of cyclic growth and destruction of stratovolcanoes: A case study from Mt. Taranaki, NZ. *Sedimentary Geology* 220: 288-305.

Zernack, A.V., Cronin, S.J., Neall, V.E., Procter, J.N., (2011). A medial to distal volcanoclastic record of an andesite stratovolcano: Detailed stratigraphy of the ring-plain succession of south-west Taranaki. *International Journal of Earth Sciences* 100: 1936-1966.

Zernack, A.V., Cronin, S.J., Bebbington, M., Price, R., Smith, I.E.M., Stewart, R.B., Procter, J.N., (2012). Forecasting catastrophic stratovolcano collapse: A model based on Mt. Taranaki, New Zealand. *Geology* 40: 983-986.

Stop 6-4 – Lizzie Bell paleochannel system



Litho- versus chronostratigraphic mapping

Previous work divided the southern Taranaki ring plain into two chronostratigraphic units, i.e. the 80-50 ka Stratford and 50-30 ka Opunake Formations (Palmer and Neall 1991). More recently, Zernack et al. (2011) suggested a combined chrono-lithostratigraphic framework based on the identified cyclic nature of sedimentation, where a chronozone represents one full volcanic cycle and consists of deposits representing edifice growth and collapse.

As a next step, a current project is conducting a more detailed lithostratigraphic investigation of the deposits produced during growth phases to better understand the past eruptive activity of Mt. Taranaki. The volcanoclastic succession contains the only preserved and accessible record of past primary products and thus provides a unique opportunity to study the volcano's long-term eruptive behaviour. Lithologies within these volcanoclastic deposits are being used to assess the origin and frequency of long-runout mass flows in relation to eruptive activity. Their geochemical composition provides insights into the nature of the magmatic system and eruptive activity at the time. In addition, sedimentary features are used to classify the deposits within the fluvial-hyperconcentrated-debris flow spectrum and help identify time breaks between individual flow events or series of events related to the same eruptive episodes.

Lizzie Bell: A representative site for growth - phase characterization at Mt. Taranaki

27.7 km away from the modern edifice of Mt. Taranaki, the Lizzie Bell paleochannel system (see lateral distribution in Fig. 71) is a representative site where the well-exposed coastal-cliff successions reveal stratigraphic markers and characteristic mass flow deposits (in stratigraphic order):

- aeolian deposits (*Punehu Sands*; massive sequence of paleo-sand dunes) indicating coastal environment (60 – 80 ka)
- debris avalanche deposit deputizing a collapse event (*Otakeho DAD*; 55 ka)
- extremely erosive debris flow deposit outlining a paleochannel system (*Lizzie Bell debris flow*; 55 – 35 ka)
- mass-flow deposit sequences (c. 55 – 35 ka) that are separated by thick tephric soil layers indicating alternating edifice growth and quiescence periods

The coastal successions provide cross-sections of the mass flow deposits that were deposited perpendicular to their transportation axis. Lizzie Bell paleochannel was filled by mass flow pulses producing a ~500 m wide paleochannel.

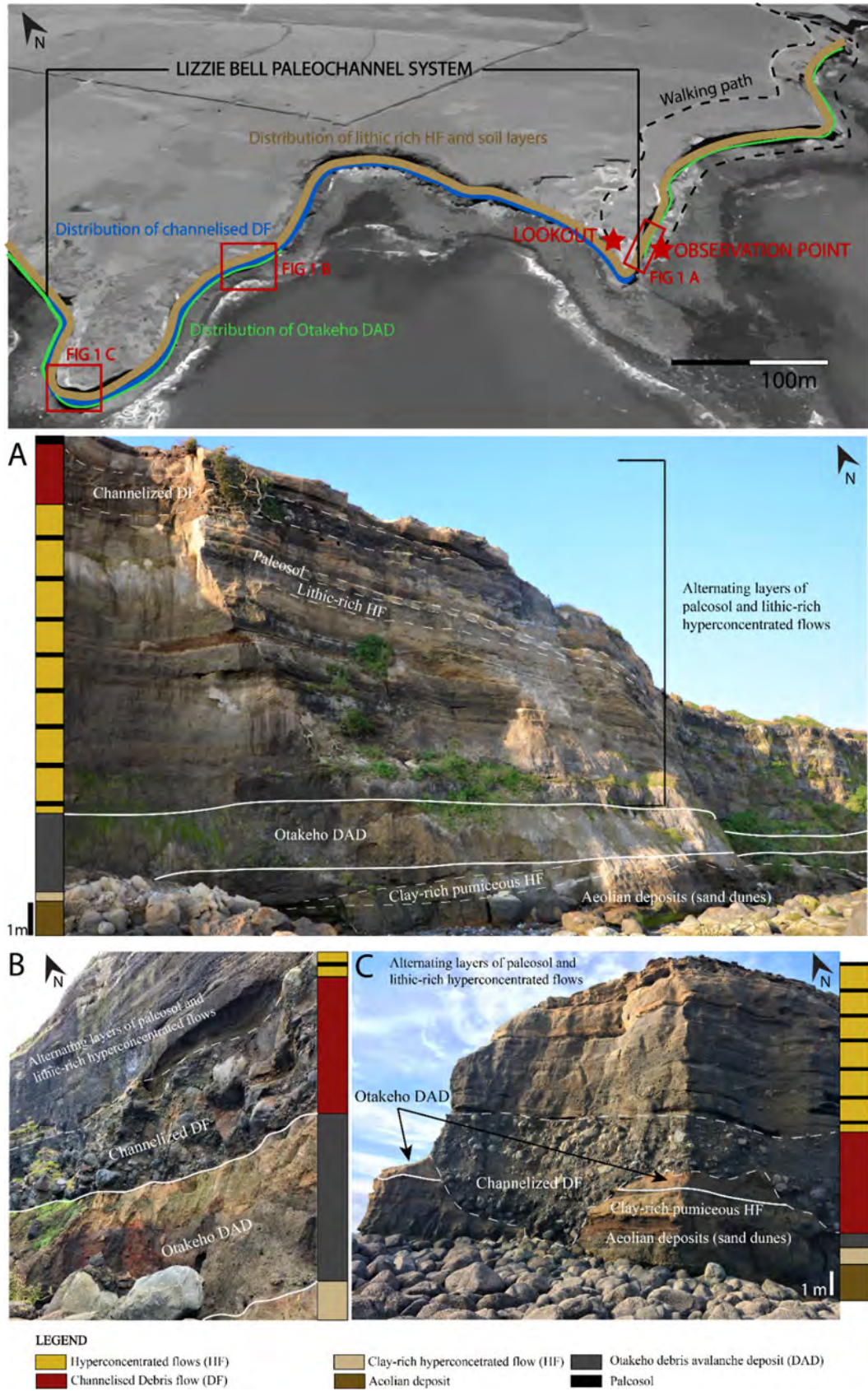


Fig. 71. – Top figure: Overview of the Lizzie Bell Paleochannel System showing the distribution of the main deposits and the location of the taken photos and their longitudinal connection. Find explanatory of deposits in the description part..

The age-range of the up-filling is ca. 35 – 55 thousand years based on the dated Otakeho debris avalanche deposit (DAD), as a marker, which can be spotted at the bottom of the sequence (Fig. 71A-C). In this location, the thickness of the debris avalanche deposit is approx. 1, 5 – 3, 5 meters. The upper light-brown and bottom light-grey appearance of the DAD can be easily distinguished in the north-western part of the Lizzie Bell system (Fig. 71B).

The DAD overlies an up to 10 m-thick sequence of well-sorted, cross-stratified dune sands. These so-called Punehu Sands accumulated in near-coastal environments during high sea-level stands between c. 60-80 ka (Zernack et al. 2011). These sands are interbedded with fluvial reworked deposits that often contain pumiceous components that are mostly coarse-ash to medium-lapilli sized rounded pumice clasts.

Stratigraphically, above the sand dune suits, clay-rich pumiceous hyperconcentrated-flow deposit suggests eruptive activity connected mass flow events. The investigated most bottom deposit in this sequence is considered as a debris flow deposit composed of clay-rich matrix containing high amount of tree logs.

Above the Otakeho DAD, several meter thick debris flow deposit (DFD) is present that filled up the paleochannel system (note the extremely erosive boundary between Otakeho DAD and the DFD in Fig. 71C).

The channelized erosive DFD is overlain by several lithic-rich HFDs with interbedded paleosol layers that deplete the upper part of the sequence (Fig. 71A, C). Their thickness and frequency differ across the Lizzie Bell river system. Their textures vary according to the physiography conditions of the terrain. On coastal plains, they show a massive or graded texture (Fig. 71A), whereas they exhibit transitional, more chaotic textures in overbanks or channels (Fig. 71C). These hyperconcentrated-flow deposits represent eruptive episodes of Mt. Taranaki during its growth phase. In contrast, the interbedded tephricsoils indicate relatively cold

climate that formed during periods of quiescence at this location with regards to sedimentary processes and eruptive activity.

Suggested discussion points

- 1) Lithic-rich mass flow deposits: What type of processes could trigger widely distributed mass flow deposits containing high amount of pumice?
- 2) Stratigraphical solution for hiatus determination in medial coastal-cliff cross-sections
- 3) Frequency determination of mass flow events in relation to the interbedded paleosol layers
- 4) What could be the origin of erosive, widely distributed (hundreds of meters) channelized debris flow deposits?

Further reading

- Palmer, B.A., Neall, V.E., (1991) Contrasting lithofacies architecture in ring plain deposits related to edifice construction and destruction, The Quaternary Stratford and Opunake Formations, Egmont Volcano, New Zealand – *Sedimentary Geology* 74: 71-88
- Smith, G.A., (1991) Facies Sequences and Geometries in Continental Volcaniclastic Settings. In: Fisher R.V., Smith, G.A., (Eds.) – *Sedimentation in Volcanic Settings*, SEPM Special Publication 45: 109-121
- Vallance, J.W., (2000) Lahars – In: Sigurdsson H, Houghton B, McNutt S, Rymer H, Stix J (Eds.) *Encyclopedia of Volcanoes*, Academic Press, San Diego, p. 601-616
- Zernack, A.V., Procter, J.N., Cronin, S.J., 2009. Sedimentary signatures of cyclic growth and destruction of stratovolcanoes: A case study from Mt. Taranaki, New Zealand – *Sedimentary Geology* 220: 288-305
- Zernack, A.V., Cronin, S.J., Neall, V.E., Procter, J.N., 2011. A medial to distal volcaniclastic record of an andesite stratovolcano: detailed stratigraphy of the ring-plain succession of south-west Taranaki, New Zealand – *International Journal of Earth Sciences* 100: 1937-1966







3rd International Congress on Stratigraphy
strati 2019
 2-5 July 2019, Milano, Italy

Second Circular

Following the first edition of this congress, held in Lisbon (Portugal) in 2013 and the second edition organized in Graz (Austria) in 2015, the third edition of STRATI will be held in **Milano (Italy), 2-5 July 2019**. As in previous editions, the congress will also host meetings of the ICS and of its Subcommissions to debate topics and problems in updating and improving the geological time scale.

VENUE

The congress will be held in the prestigious venue of the Università degli Studi di Milano, Via Festa del Perdono 7, located in the old “Ca’ Granda” (literally “the Big House”). It is a striking historical complex in the heart of the city, located only a seven-minute walk from the famous Piazza del Duomo and easily reachable by public transportation. The University’s main campus, a former hospital built between 1456 and 1472, is one of the most historically and artistically significant buildings in Milano.

LOCATION

Milano is a city with an eclectic spirit that can please everyone: those who seek for art and those who prefer food, recreation or business. Located in North Italy, Milano is often referred to as the Italian “capital of industry, commerce, finance, fashion and design”. The history of the town dates back to Roman times. Such a long history is well documented by monuments and churches. Milano was also visited by several artists, especially during the Middle Age and the Renaissance, whose masterpieces are preserved in several Museums. The most representative monument is the Duomo, the highest expression of the Italian Gothic. The quality of accommodation and tourist attraction in Milano and the excellent transport links with most Italian and European towns, will make this event very interesting for the international audience.

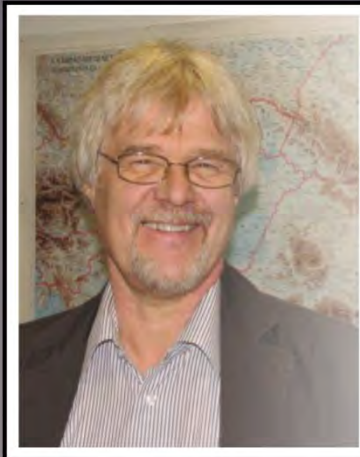




ILP2019
SEDIMENTARY BASINS
INTERNATIONAL LITHOSPHERE
PROGRAM TASK FORCE VI



A CONFERENCE IN MEMORY OF FRANK HORVÁTH (1944 - 2018)



UNDERSTANDING THE MULTI-SCALE FORMATION AND EVOLUTION OF OROGENS AND SEDIMENTARY BASINS

THIS FOUR DAY CONFERENCE AND FIELD EXCURSION WILL COMMEMORATE THE LIFE AND WORK OF FRANK HORVÁTH, WHO WAS PROFESSOR AT EÖTVÖS UNIVERSITY, BY BRINGING TOGETHER EXPERTS FROM THE FIELDS HE HELPED TO SHAPE.

1. Dynamics of sedimentary basins and the underlying lithosphere
2. Tectonic control of sedimentation and dynamics of landscape evolution
3. Links between orogens and sedimentary basins
4. Volcanism and related processes at all scales
5. Analogue and numerical modelling - crustal and lithospheric processes
6. Groundwater flow modelling
7. Mineral-, hydrocarbon- and geo-thermal resources
8. Geohazards

+ **Field excursion**

Early registration before 26th April

Industry experts	295 €
Academic researchers	250 €
Students	120 €

Organizing Committee

László Fodor lasz.fodor@yahoo.com Szilvia Kövér koversz@yahoo.com Attila Balázs abalazs@uniroma3.it

HUNGARY, BALATON HIGHLAND, HÉVÍZ
16-19 OCTOBER, 2019

1er CONGRESO ASOCIACIÓN LATINOAMERICANA DE VOLCANOLOGÍA

ALVO

3 al 7 de Noviembre de 2019

www.1ercongresoalvo.com

“Volcanología en y para Latinoamérica”

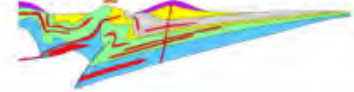


Universidad Católica del Norte, Antofagasta, Chile

LASI

VI

Neuquén Basin



Laccoliths, sills and dykes (LASI6): The physical geology of subvolcanic systems

25-29 November 2019, Malargüe, Argentina

More information: www.lasi6.org and : LASI6Malargue

Contact: olivier.galland@geo.uio.no

Themes

- Emplacement processes of dykes, sills, laccoliths, plutons
- Volcanic plumbing systems in active volcanic areas
- Field observations, geophysics, laboratory, numerical and theoretical modelling
- Magma-sediment interactions: contact aureoles, magma contamination, phreatomagmatic activity and hydrothermal venting, and climate implications
- Economic geology of subvolcanic systems: hydrocarbons, shale gas, water and ore deposits
- The plumbing systems of mud volcanoes and their analogies to igneous plumbing systems



Organizing Committee

Olivier Galland	- The Njord Centre, University of Oslo, Norway
José Mescua	- CONICET, Mendoza, Argentina
Karen Mair	- The Njord Centre, University of Oslo, Norway
Octavio Palma	- CONICET/Y-TEC, La Plata, Argentina
Héctor A. Leanza	- Museo Argentino de Ciencias Naturales, Buenos Aires, Argentina

Scientific Committee

Patricia Sruoga	- CONICET, Mendoza, Argentina
Sverre Planke	- VBPR/CEED, University of Oslo, Norway
Steffi Burchardt	- University of Uppsala, Sweden
Dougal Jerram	- DougalEarth, UK/CEED, University of Oslo, Norway

